

MECÁNICA DE ROCAS APLICADA A LA MINERÍA

(del 10 al 15 de abril, 1978)

FECHA	HORARIO	TEMA	PROFESOR
10 de abril	9 a 13 h	CLASIFICACION DE ROCAS CON FINES INGENIERILES (clases)	Dr. M. Ashraf Mahtab
	13 a 14 h	COMIDA	
	15 a 16 h	COLECCION DE DATOS GEOLOGICOS (demostración)	Dr. M. Ashraf Mahtab
	17 a 18 h	COLECCION DE DATOS GEOLOGICOS (clase)	Dr. M. Ashraf Mahtab
11 de abril	9 a 11 h	COLECCION DE DATOS GEOLOGICOS (clase)	Dr. M. Ashraf Mahtab
	11 a 13 h	ANALISIS DE DATOS GEOLOGICOS	Dr. M. Ashraf Mahtab
	13 a 14 h	COMIDA	
	15 a 18 h	PRACTICAS DE CLASIFICACION DE ROCAS (En la Mina Real del Monte)	
12 de abril	9 a 11 h	ANALISIS DE DATOS GEOLOGICOS (clase)	Dr. M. Ashraf Mahtab
	11 a 13h	TALLER DE ANALISIS DE DATOS	Dr. M. Ashraf Mahtab
	13 a 14 h	COMIDA	

12 de abril	15 a 18 h	LEVANTAMIENTO DE DATOS GEOLOGICO ESTRUCTURALES (en la Mina Real del Monte)	Dr. M. Ashraf Mahtab
13 de abril	9 a 12 h	ESFUERZOS IN-SITU (clase)	" " "
	12 a 13 h	PRESENTACION DE EJEMPLOS	" " "
	13 a 14 h	COMIDA	
	15 a 18 h	ANALISIS DE DATOS GEOLOGICOS (En el Centro de Computación)	" " "
14 de abril	9 a 12 h	DETERMINACION DE ESFUERZOS IN-SITU (clase)	" " "
	12 a 13 h	TALLER DE ESFUERZOS IN-SITU	" " "
	13 a 14 h	COMIDA	
	15 a 18 h	ANALISIS DE DATOS GEOLOGICOS (En el Centro de Computación)	" " "
15 de abril	9 a 11 h	INFLUENCIA DEL AGUA EN LAS MASAS ROCOSAS	" " "
	11 a 12 h	TALLER	" " "
	12 a 13 h	DISCUSIÓN GENERAL	
	13 a 14 h	CLAUSURA	
		CONVIVIO	

DIRECTORIO DE PROFESORES

MECANICA DE ROCAS APLICADA A LA MINERIA

ING. DAVID GOMEZ RUIZ
GERENTE ADMINISTRATIVO DE
INDUSTRIAL MINERA MEXICO, S.A.
BAJA CALIFORNIA No. 200- 7^a PISO
MEXICO 7, D.F.
TEL: 564.70.6

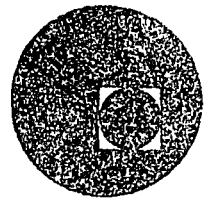
M. ASHRAF MAHTAB
SENIOR ROCK MECHANICS ENGINEER
ACRES CONSULTING SERVICES LTD
5259 DORCHESTER ROAD
NIAGARA FALLS, ONT. CANADA L2E6W1
TEL: (416) 354-3831

ING. VICTOR M. NAVARRO
PROFESOR DE TIEMPO COMPLETO
UNIVERSIDAD AUTONOMA DE ZACATECAS
LOPEZ VELARDE No. 603
ZACATECAS, ZACS.
TEL: 91 - 492 - 2 - 08 - 27
ó 2- 39- 80

'pmc.



centro de educación continua
división de estudios superiores
facultad de ingeniería, unam



MECANICA DE ROCAS APLICADA A LA MINERIA

CLASIFICACION INGENIERIL DE LAS ROCAS

ABRIL, 1978.

TABLE 2-10
References to Some Engineering
Classification Systems for Rock

Object	For general purpose	For a special purpose
Rock Material	Coates (1964) Coates and Parsons (1966) Deere and Miller (1966) and Deere et al (1967) Underwood (1967) - shales	Bergh-Christensen and Selmer-Olsen (1970) - resistance to blasting Selmer-Olsen and Blindheim (1970) - drillability
Rock Mass	John (1962) Onodera (1970) Iida et al (1970) Muller and Hoffman (1970) Franklin et al (1971)*	Terzaghi (1946) - tunnels Lauffer (1958) - tunnels Bieniawski (1974) - tunnels Barton et al (1975) - tunnels Kruse et al (1969) - tunnel liner design Ege (1968) - tunnels in granitic rocks Obert and Duvall (1967) - mining Goodman and Duncan (1971) - rock slopes Caterpillar Tractor Co. (1966) rippability

* Best applied to rippability classification.

2-10). The rock strength is to be determined either by unconfined compressive strength tests or by the point load index, previously discussed. This approach can be useful for organizing case experiences.

A number of workers have considered the specific problem of rock mass classification for tunnel excavation and supports. Barton,

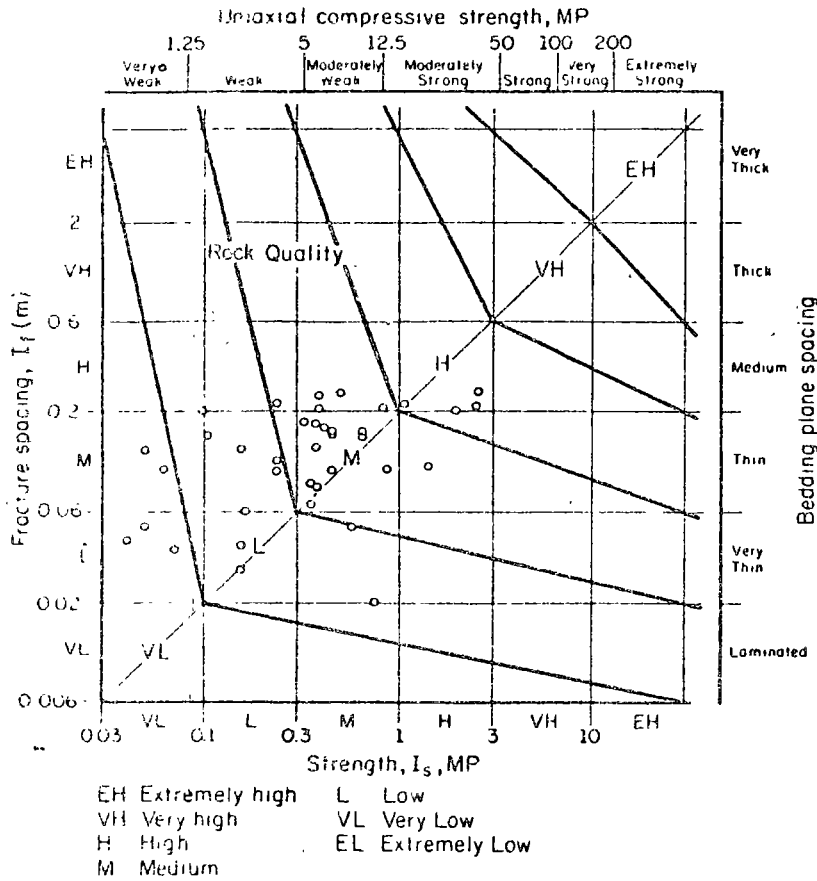


Figure 2-10. Franklin's rock quality classification; Franklin et al. (1971). The strength I_s is the point load index.

Lien and Lunde (1975), for example, adjusted six parameters by means of detailed study of 200 underground case histories, in proposing a single numerical tunneling index -- Q.

$$Q = \frac{RQD}{J_n} \cdot \frac{J_r}{J_a} \cdot \frac{J_w}{SRF} \quad (5)$$

RQD refers to the percent modified core recovery (Deere, et al., 1967), calculated from drilling logs by deleting from the "recovered" category all pieces of core less than four inches long*. A minimum

* Barton, Lien and Lunde state that Norwegian Geotechnical Institute geologists have found they can estimate RQD values in jointed, hard, clay-free rocks from field estimates of the number of joints per cubic meter (J_v). RQD = 115 - 3.3 J_v ; (RQD ≤ 100)

RQD of 10 is used in evaluating Q. The other terms in Equation 5 evaluate the number of joint sets and the roughness, alteration, water and stress conditions according to Table 2-11.

TABLE 2-11

Values of the Parameters
in Barton, Lien, and Lunde's Classification

A.	<u>Number of sets of discontinuities</u>	<u>Jn</u>
	massive	0.5
	one set	2.0
	two sets	4.0
	three sets	9.0
	four or more sets	15.0
	crushed rock	20.0
B.	<u>Roughness of discontinuities</u>	<u>Jr*</u>
	non-continuous joints	4.0
	rough, wavy	3.0
	smooth, wavy	2.0
	rough, planar	1.5
	smooth, planar	1.0
	slick, planar	0.5
	"filled" discontinuities	1.0
	* add 1.0 if mean joint spacing exceeds 3 meters	
C.	<u>Filling and wall rock alteration</u>	<u>Ja</u>
	a) <u>essentially unfilled</u>	
	healed	0.75
	staining only; no alteration	1.0
	silty or sandy coatings	3.0
	clay coatings	4.0
	b) <u>filled</u>	
	sand or crushed rock filling	4.0
	stiff clay filling <5 mm thick	6.0
	soft clay filling <5 mm thick	8.0
	swelling clay filling <5 mm thick	12.0
	stiff clay filling >5 mm thick	10.0
	soft clay filling >5mm thick	15.0
	swelling clay filling >5 mm thick	20.0

Table 2 11 (continued)

D. <u>Water conditions</u>	<u>Jw</u>
dry	1.0
medium water inflow	0.66
large inflow with unfilled joints	0.5
large inflow with filled joints which wash out	0.33
high transient inflow	0.2 - 0.1
high continuous inflow	0.1 - 0.05

E. <u>Stress reduction class</u>	<u>SRF*</u>
loose rock with clay-filled discontinuities	10.0
loose rock with open discontinu- ities	5.0
rock at shallow depth (<50m) with clay-filled discontinuities	2.5
rock with tight, unfilled dis- continuities under medium stress	1.0

* Barton et al also define SRF values corresponding to degrees of bursting, squeezing, and swelling rock conditions.

TABLE 2-12

After Barton, Lien, and Lunde (1975)

<u>Q</u>	<u>Rock mass quality for tunneling</u>
<0.01	exceptionally poor
0.01 - 0.1	extremely poor
0.1 - 1.0	very poor
1.0 - 4.0	poor
4.0 - 10.0	fair
10.10 - 40.0	good
40.0 - 100.0	very good
100.0 - 400.0	extremely good
>400.0	exceptionally good

Barton's analysis of case histories yielded a relationship for the maximum safe span (D) for an unsupported underground opening as a function of Q:

$$D = 2.1 (Q)^{0.387} \quad (6)$$

where D is in meters, and Q is in the range $0.001 \leq Q \leq 1,000$. Other functions of Q are given to select supports for different types of openings.

For example, consider the rock masses in Figures 2-9c and 2-9e with respect to tunneling at 40 meters depth. In the former case, assume the RQD is found to equal 30% and in the latter 75%. Assuming there will be no water inflow, we might estimate Q for each case as follows. For the rock of figure 2-9c:

$$Q = \frac{30}{9} \cdot \frac{1.0}{2.0} \cdot \frac{1.0}{2.0} = 0.83 \quad (7)$$

According to Table 2-12, this classifies as very poor rock; the maximum unsupported span according to (6) is about two meters. For the rock of figure 2-9e:

$$Q = \frac{75}{15} \cdot \frac{1.5}{1.0} \cdot \frac{1.0}{1.5} = 5 \quad (8)$$

This qualifies as fair rock; the maximum unsupported span is about four meters.

Barton's classification scheme has considerable potential for engineering for underground works as well as for generalization of experiences in other areas of engineering. A somewhat similar classification, developed by Bieniawski (1974) is presented in Table 2-13. Of course, no classification system can assign a name as generally informative as a careful description of the geological environment, the rock material, the weathering profile, and the system of discontinuities. Table 2-14 summarizes those factors appropriate in a geotechnical description of a rock mass. Table 2-15

is a standardized data sheet developed by the South African Central Scientific and Industrial Research Organization (CSIRO) and is useful for providing input for Bieniawski's classification.

TABLE 2-13
Geomechanics Classification of Jointed Rock Masses

A. CLASSIFICATION PARAMETERS AND THEIR RATINGS

1	Strength of intact rock material	Point load strength index or Uniaxial compressive strength	8 MPa	4 - 8 MPa	2 - 4 MPa	1 - 2 MPa	Use of uniaxial compressive test preferred				
			200 MPa	100 - 200 MPa	50 - 100 MPa	25 - 50 MPa	10-25 MPa	3 to 10 MPa	1-3 MPa		
	Rating		15	12	7	4	2	1	0		
2	Drift loss per 10m	RQD	90% - 100%	75% - 90%	50% - 75%	25% - 50%	25%				
			Rating	20	17	13	8	3			
3	Spacing of joints	J m	1 - 3 m	0.3 - 1 m	50 - 300 mm	50 mm					
			Rating	30	25	20	10				
4	Condition of joints	Very rough surfaces Not continuous No separation Hard joint wall rock	Slightly rough surfaces Separation < 1 mm Hard joint wall rock	Slightly rough surfaces Separation < 1 mm Soft joint wall rock	Slickensided surfaces OR Gouge < 5 mm thick OR Joints open < 5 mm Continuous joints	Soft gouge < 5 mm thick OR Joints open < 5 mm Continuous joints					
						Rating	25	20	12	8	0
5	Ground water	Inflow per 10m cave length	None			25 litres/min	25 - 125 litres/min	125 litres/min			
			Hard OR General conditions	OR			OR	OR	OR		
				0			0.0 - 0.2	0.2 - 0.5	0.5		
			Completely dry			Moist only (interstitial water)		Water under moderate pressure		Several water profiles	
	Rating		10	7	4	0					

B. ADJUSTMENT FOR JOINT ORIENTATIONS

Orientation	Type of structure	Very favourable	Favourable	Fair	Unfavourable	Very unfavourable
		Rating				
Vertical	Tunnels	0	2	5	-10	-12
	Excavations	0	2	7	-15	-25
	Slopes	0	5	25	-50	-60

C. ROCK MASS CLASSES AND THEIR RATINGS

Class No	I	II	III	IV	V
Description	Very good rock	Good rock	Fair rock	Poor rock	Very poor rock
Rating	100 - 30	90 - 70	70 - 50	50 - 25	25

D. MEANING OF ROCK MASS CLASSES

Class No	I	II	III	IV	V
Average stand up time	10 years for 5 m span	6 months for 3 m span	1 week for 3 m span	5 hours for 1.5 m span	10 minutes for 0.5 m span
Compressive strength of the rock mass	300 kPa	200 - 300 kPa	150 - 200 kPa	100 - 150 kPa	100 kPa
Friction angle of the rock mass	45°	40 - 45°	35° - 40°	30° - 35°	30°
Case history of use	Very poor	Will not be used readily Large openings	Fair	Will cave readily Good fragmentation	Very poor

TABLE 2-14

Some Factors to be Considered in
a Geotechnical Description of a Rock Mass

A. Rock material

Petrologic description -- rock name, texture, fabric, principal and accessory minerals; nature of cement; alteration effects. Presence of alterable minerals such as gypsum, pyrrhotite, etc. should especially be noted.

Classification as "rock"; "weathered rock" or "soil-like rock" according to results of simple tests (see Table 2-1).

Weatherability according to slake-durability or other test.

Mechanical properties according to an index test -- e.g. Schmidt hammer, point load test, or scratch hardness.

Degree of weathering according to laboratory index tests or mineralogic criteria.

State of fissuring, determined from polished sections or thin sections or by results of wave velocity measurements, tension tests, volumetric compression, or radial permeability tests.

Micro structures in the hand specimen -- bedding, foliation, etc.

B. Weathering Profiles

Description and classification of all the intermediate weathering products and their spatial arrangement together with results of laboratory tests indicative of their mechanical properties.

Description of joint properties in the different stages of weathering.

C. Discontinuities

Preferred orientations and spacings of each set, structural name, (e.g. bedding, joint) for each set; roughness angles versus wave length and description of wall rock as wavy, rough, smooth, or slickensided; note roughness anisotropy.

Wall rock scratch hardness expressed by a standard terminology, or strength as measured by Schmidt hammer.

Table 2-14 (continued)

Filling material: thickness; completeness of filling; compactness; composition; % clay and soil properties; classification as: swelling, erodible, soluble, or or stable.

interlocking and tightness of fit: healed, close, open, cavernous (or loosened).

Other features: estimate of relative extent; chemistry of water; will rock alteration.

TABLE 2-15

Input Data Form:
Geomechanics Classification of Jointed Rock Masses

Name of project		INPUT DATA FORM GEOMECHANICS CLASSIFICATION OF JOINTED ROCK MASSES								
Site of survey	Conducted by	Date	STRUCTURAL REGION	ROCK TYPE AND ORIGIN			CONDITION OF JOINTS			
							CONTINUITY	Set 1	Set 2	Set 3
DRIFE CORE QUALITY RQD			WEATHERING			Not continuous, no gouge with gouge				
Very poor quality 50-100%			Unweathered			Continuous, no gouge with gouge				
Good quality 75-90%			Slightly weathered			SEPARATION				
Fair quality 50-75%			Moderately weathered			Very tight joints Less than 0.1 mm				
Poor quality 25-50%			Highly weathered			Tight joints 0.1-1 mm				
Very poor quality 25%			Completely weathered			Moderately open joints 1-5 mm				
Rock Quality Designation			STRENGTH OF INTACT ROCK MATERIAL			Open joints More than 5 mm				
Correlate with the method of DeGruyter			Uniaxial compressive strength			ROUGHNESS				
SHEDDING WEATHER			Point load strength index			Very rough surfaces				
FOLLOW per 10 m			Very high Over 200 MPa 8 MPa			Rough surfaces				
of tunnel length			High 100-200 MPa 4-8 MPa			Slightly rough surfaces				
or			Medium 50-100 MPa 2-4 MPa			Smooth surfaces				
WATER PRESSURE kPa			Low 25-50 MPa 1-2 MPa			Slack-sided surfaces				
or			Very low 10-25 MPa 1 MPa			JOINT WALL ROCK				
GENERAL CONDITIONS (completely dry, moist or water under pressure, severe problems)			3-10 MPa			Hard rock				
			1-3 MPa			Medium hard rock				
						Soft rock				
SPACING OF JOINTS						NOTE Provide data for each joint set				
Very wide Over 3 m			Set 1 Set 2 Set 3 Set 4			MAJOR FAULTS OR FOLDS				
Wide 1-3 m										
Moderately close 0.3-1 m						Describe major faults and folds specifying their locality, nature and orientations				
Close 50-300 mm						GENERAL REMARKS AND ADDITIONAL DATA				
Very close 50 mm						If gouge is present specify its type, thickness, continuity and consistency				
NOTE: These values are obtained from a joint survey and not from borehole logs			STRIKE AND DIP ORIENTATIONS			Describe waviness of joints				
Provide data for each joint set			Strike (direction) Dip (angle) (direction)			Assess regional stresses				
Set 1 Strike (direction) Dip (angle) (direction)										
Set 2 Strike (direction) Dip (angle) (direction)										
Set 3 Strike (direction) Dip (angle) (direction)										
Set 4 Strike (direction) Dip (angle) (direction)										
NOTE: Provide data for each joint set. Refer all directions to magnetic north						NOTE: The data on this form constitute the minimum required for Engineering design. The geologist should, however, supply any further information which he considers essential.				

TABLE 13

REQUIRED INTACT ROCK AND ROCK MASS PROPERTIES
WITH APPROPRIATE INVESTIGATION TECHNIQUES

<u>Important Intact Rock and Rock Mass Properties Required</u>	<u>Appropriate Direct Investigation Techniques</u>	<u>Appropriate Geophysical Investigation Techniques</u>	<u>Comments</u> (A) Good data obtainable (B) Some uncertainties but no major adverse implications
Lithology, Stratigraphy	Core recovery and inspection. Borehole camera or television.	Numerous, including spontaneous or natural potential, resistivity,) caliper log, sonic velocity.) Nuclear probe, i.e. natural gamma, neutron-neutron, neutron-gamma, gamma-gamma.	- Open borehole. - Open or cased borehole - Core inspection more reliable. (A)
Fissure, joint and bedding plane frequency (RQD)	Core recovery and inspection. Borehole camera or television.	Resistivity, caliper log, some velocity, seisviewer.	Direct methods and seisviewer most useful. Seisviewer can be used in mud-filled hole. (A)
Fissure, joint and bedding plane orientations	Borehole camera or television. Oriented core (Corex).	Caliper log.	(A)
Fissure, joint and bedding plane roughness and undulation	Core recovery and inspection.	None applicable.	Good assumption can be made in competent rock. (B)
Fissure, joint and bedding plane filling and condition	Mineralogical and petrographic examination (indirect)	Natural gamma (clay or shale content of adjacent rock).	Caution should be used in design if high clay content identified. (B)
Fissure widths	Borehole camera or television. Core recovery and inspection.	Caliper log Seisviewer.	Fine fissures - core, integral sampling, seisviewer, caliper. Wide fissures - all methods except core. (A)
Location and extent of weak zones	Core recovery and inspection. Borehole camera or television.	Numerous, as lithology and stratigraphy, plus seisviewer.	(A)
Mineral content of weak zones	Mineralogical and petrographic examination of core. Borehole camera or television.	Natural gamma (clay or shale content).	May be some difficulty in recover- ing V. weak material due to effects of drilling wash. (A)
Mass Permeability	Packer tests, drill stem tests, borehole camera or television (highly permeable zones).	As for fissure widths and frequencies.	Packer and drill stem tests best direct methods. Other methods should indicate presence of very permeable zones. (B)

Table 13 (cont'd)

Required Intact Rock and Rock Mass Properties
With Appropriate Investigation Techniques - 2

<u>Important Intact Rock and Rock Mass Properties Required</u>	<u>Appropriate Direct Investigation Techniques</u>	<u>Appropriate Geophysical Investigation Techniques</u>	<u>Comments</u> (A) Good data obtainable (B) Some Uncertainties but no major adverse implications
Porosity and bulk density	Core recovery and testing.	Spontaneous or natural potential. Neutron-neutron, neutron-gamma, gamma-gamma and seismic velocity.	(A)
Water levels (pressures)	Piezometers.	Spontaneous potential, resistivity, neutron-gamma, gamma-gamma.	(A)
In-situ state of stress	Hydraulic fracturing.	None applicable.	Other methods available but not for use at great depth. Hydrofract of limited use if $\sigma_H > \sigma_v$. (B)
Unconfined compressive and tensile strength of intact rock	Core recovery and testing.	None applicable.	Standard lab tests, no problems foreseen. (A)
Mineralogical composition of rock	Mineralogical and petrographic examination of core.	Some available, but redundant if core is recovered.	(B)
Groundwater chemistry	Mechanical baler with opening and closing hatch at depth.	Calibrated fluid resistivity. Neutron chloride logging. - Measure ion concentration and salinity.	Baler may need some minor development. (A)
Modulus of elasticity of intact rock or rock mass	Core.	Sonic velocity.	Modulus determinations not of major significance, but useful. (B)
Rock temperature	None.	Temperature probe.	(A)
Source and movement of groundwater in hole	None.	Flowmeter (could be considered as direct technique, but performed by geophysical exploration company).	(B)
Borehole directional survey	Dipmeter. Multi-shot photographic directional inclinometer.	See comments.	Hole direction can be surveyed during drilling and/or with geophysical logging. (A)
Overall geologic structure	Lithological and stratigraphic correlations between drill holes.	Various geophysical techniques at ground surface. Lithological and stratigraphic correlations between boreholes.	(A)



centro de educación continua
división de estudios superiores
facultad de ingeniería, unam



MECANICA DE ROCAS APLICADA A LA MINERIA

COLECCION DE DATOS GEOLOGICOS

ABRIL, 1978

Table 7. Estimated costs for borehole viewing equipment and services (1975)

Instrument	Maximum range in ft (m)	Direction of view	Transmission of image	Maximum diameter of instrument	Approximate borehole size	Cost (\$)		Remarks
						purchase	lease	
Borescope	10 (3)	at right angles to borescope	2 telescoping tubes	1.25 in. (3.2 cm)	-	360	-	
Borescope	25 (8)	at right angles to borescope	series of coupled extension tubes	1.31 in. (3.3 cm)	-	430	-	
Periscope	110 (33)	at right angles to periscope	coupled extension tubes	2.20 in. (5.6 cm)	2.5 in. (6.4 cm)	27000	250/wk	
Camera	1000 (300)	parallel to probe axis	record image on film	2.75 in. (7.0 cm)	3.0 in. (7.6 cm)	30000	-	cost includes camera + 1000 ft (300 m) cable and winch
Television	1000 (300)	parallel to probe axis	power and transmission cable	3.0 in. (7.6 cm)	4.0 in. (10.2 cm)	-	300/day	cost includes probe with 1000 ft of cable, monitoring unit, truck technician and all facilities except mobilization and interpretation
Television	1000 (300)	at right angles to probe axis	power and transmission cable	2.48 in. (6.3 cm)	3.0 in. (7.6 cm)	46000	-	cost includes all equipment with 1000 ft (300 m) of cable, monitoring unit etc

Note: Costs given are those for new units; used equipment is considerably cheaper. Delivery time for periscope, camera or television is approximately 5 months. Range is limited by the amount of cable with unit and by the water pressure on the probe: the probes given here are only rated to withstand 750 psi (5MPa).

It includes compass orientation and depth on the 16 mm film. Analysis involves projecting the doughnut-like picture onto a 360° groundglass screen, using a conical mirror. A special transparent overlay sheet is used to make the necessary structural interpretations (6).

116. The borehole television camera (7) uses a closed-circuit television system and consists of a probe containing the television camera, a lowering device, drum of coaxial cable, control console, and monitoring unit as shown in Fig 10. Dirty water is a drawback and must be removed. Minimum

TABLE 1

PRELIMINARY SUMMARY OF COMMON CORING TECHNIQUES
IN HEAVILY JOINTED AND POORLY CONSOLIDATED ROCK

<u>Method</u>	<u>Supplier</u>	<u>Description</u>
Triple Tube Wire- line System	Longyear	Wire-line core barrel with split tube liner for retention of sample. Variations: Drill with mud in poor ground; use with basket-type "Full Closure" lifter; plastic liner for inner tube; chrome plated inner tube.
Denison Sampler	Acker & Others	Basically a thin walled core barrel capable of retrieving large diameter (in relation to hole dia.) cores.
Craelius Sampler	Atlas Copco Craelius	Similar to above, with split tube liner option.
Hydra-Flex Core Barrel	Diamond Oil Well Drilling Co. (Texas)	Thick walled core barrel (4-1/2" O.D./NX Core) incorporating nylon reinforced rubber liner which envelopes core to prevent disturbance.
Core Barrel Flow Control Valve	Acker	Device fitted to core barrel to decrease fluid flow in soft zones, thus preventing washing of sample.
Cryo-Coring	Various	Pre-freezing poor ground prior to drilling.

TABLE 2-13

Geomechanics Classification of Jointed Rock Masses

A. CLASSIFICATION PARAMETERS AND THEIR RATINGS

1	Strength of intact rock material	Point load strength index	8 MPa	4 - 8 MPa	2 - 4 MPa	1 - 2 MPa	Use of uniaxial compressive test preferred		
		Uniaxial compressive strength	200 MPa	100 - 200 MPa	50 - 100 MPa	25 - 50 MPa	10-25 MPa	3 to 10 MPa	1-3 MPa
	Rating	15	12	7	4	2	1	0	
2	Drill core quality ROD		90% - 100%	75% - 90%	50% - 75%	25% - 50%	25%		
	Rating		20	17	13	8	3		
3	Spacing of joints		> 3 m	1 - 3 m	0.3 - 1 m	50 - 300 mm	50 mm		
	Rating		30	25	20	10	5		
4	Condition of joints		Very rough surfaces Not continuous No separation Hard joint wall rock	Slightly rough surfaces Separation 1 mm Hard joint wall rock	Slightly rough surfaces Separation 1 mm Soft joint wall rock	Slickensided surfaces OR Gouge - 5 mm thick OR Joints open 1-5 mm Continuous joints	Gouge - 5 mm thick OR Joints open 5 mm Continuous joints		
	Rating		25	20	12	6	0		
5	Ground water	Inflow per 10m tunnel length	None		25 litres/min	25 - 125 litres/min	125 litres/min		
		Ratio $\frac{\text{joint water pressure}}{\text{major principal stress}}$	OR		OR	OR	OR		
		General conditions	Completely dry		Moist only (interstitial water)	Water under moderate pressure	Severe water problems		
	Rating		10		7	4	0		

B. ADJUSTMENT FOR JOINT ORIENTATIONS

Strike and dip orientations of joints		Very favourable	Favourable	Fair	Unfavourable	Very unfavourable
Ratings	Tunnels	0	-2	-5	-10	-12
	Foundations	0	-2	-7	-15	-25
	Slopes	0	-5	-25	-50	-60

C. ROCK MASS CLASSES AND THEIR RATINGS

Class No	I	II	III	IV	V
Description	Very good rock	Good rock	Fair rock	Poor rock	Very poor rock
Rating	100 ← 90	90 ← 70	70 ← 50	50 ← 25	25

D. MEANING OF ROCK MASS CLASSES

Class No	I	II	III	IV	V
Average stand-up time	10 years for 5 m span	6 months for 4 m span	1 week for 3 m span	5 hours for 1.5 m span	10 minutes for 0.5 m span
Cohesion of the rock mass	300 kPa	200 - 300 kPa	150 - 200 kPa	100 - 150 kPa	100 kPa
Friction angle of the rock mass	45°	40° - 45°	35° - 40°	30° - 35°	10°
Caveability of ore	Very poor	Will not cave readily Large fragments	Fair	Will cave readily Good fragmentation	Very good

MUESER, RUTLEDGE, WENTWORTH & JOHNSTON CONSULTING ENGINEERS
415 MADISON AVE., NEW YORK, N.Y. 10017

SHEET 2 OF 3
FILE NO. 3279-G
BORING NO. A-21

PROJECT Rapid Transit System - Washington D.C.
LOCATION Rockville Route RES ENGR. Val. V. Tepordei

DAILY PROG.	CORE				ROCK TYPE	WEATH.	FABRIC FOL. DIP	DISCONTINUITIES			DRILL TIME	REMARKS
	NO.	DEPTH	DISC.	REC/ROF				JT/FT	DIP	COND.		
Oct. 3, 1974 Partly Cloudy, 50°-65° Drilling Time 7 1/2 hrs.	6C	55'0"		40/10	Light Brown (weath.) to Light Gray Quartz Biotite Schist to Gneiss w. occasional Quartz augens	Dec	Low Recov. No Dist. Fol.					
	7C	59'5"		25/10		Dec. to HiW						61.0' - 61.7' HiW & Bkn. - S.Z.?
	8C	64'0"		45/15		HiW		5/1'			2m	67.0' - 68.0' HiJ Zone
	9C	68'5"	HiJ	80/35		MdW		4/1'	HiJ		3m	71.5' - 72.5' Bkn Z. Pass S.Z.
	10C	73'0"	50° 50°	80/45		SIW		4/1'	Bkn.		15m/1'	J75° at 76.8' J60° at 77.0'
Oct. 4, 1974 Sunny & mild, 55°-65° Drilling Time 8 1/2 hours.	11C	78'0"	77.5° 160° 30°	90/75	Light Brown (weath.) to Light Gray Quartz Biotite Schist to Gneiss w. occasional Quartz augens	UnW ExJts	Fine to Medium Grain Size Poor to Moderate Foliation, sometimes irregular foliation @ 60° to 70°	6/1'	1/1'		3m	J75° at 76.8' J60° at 77.0'
	12C	83'0"		75/60		SIW		3/1'	2/1'		4m	J15° x F at 84.2' 87.5' - 88.0' Bkn. Z. large frag. w. Horiz. Jts
	13C	88'0"	360° 360°	95/35		UnW Ex Jts		3/1'	3/1'		4m	J60° at 88.7' J60° at 90.1'
	14C	93'0"		90/45				4/1'	3/1'		6m	2x J55° & 65° at 90.5' J35° RF irreg. & rough at 91.5'
	15C	98'0"		95/90		UnW Ex Jts		1/2'			8m	J50° F w red clay & silt at 98.3'

BORING NO. A-21
SURFACE ELEV. 321.7'

FIGURE 1. Field copy of a rock core log and form derived by Meuser, Rutledge, Wentworth & Johnston. (Log, courtesy of Washington Metropolitan Area Transit Authority).

STRUCTURAL CORE LOG

Drilling Company		Site Description				Borehole No.			
						Sheet No.			
						Job No.			
Drilling Method					Logged by				
					Identification				
Corr. Elev.	Northing		Easting		Azimuth	Incl.	Length	Sec. Obs.	Ref. Dn.
Number	Distance from Collar	Disc. Type	Dip Direction	Dip	Spacing	Infilling	Lithology	Strength	Symbolic Log
									Miscellaneous: Diameter, Recovery, RQD, Penetrometer, Point Load, Schmidt Hammer, Weathering

STRUCTURAL CORE LOG

Ref. Dn.	Sec. Obs.	Job No.		Borehole No.		Sheet No.			
Number	Distance from Collar	Disc. Type	Dip Direction	Dip	Spacing	Infilling	Lithology	Strength	Symbolic Log
									Miscellaneous: Diameter, Recovery, RQD, Penetrometer, Point Load, Schmidt Hammer, Weathering.

Fig B-2 - Structural core log.

FIGURE 1 - SIMPLIFIED LOG OF WEST VALLEY WELL NO. NPS CH1

Depth, ft.	Description	Modulus E (10 ⁶ psi)	Other
0	Glacial Drift		
100			
200	Weathered shale	?	
Top of vert. frac.	Silty shale & siltstone mod. fissile to mass., prof. frac. at shale-silt contacts		300
WESTFIELD SHALE			
400	Silty shale, seams of silt, fissile, some sharpstone	5.5	400
Vert. frac. 001. to 101 ft. long	Silty shale & shaley siltstone cross-bedded shale & siltstone fractured silty shale	4.5	500
500	Shale with thin beds of siltstone, sharpstone cong., mass. individual beds with frac. along contacts.		
IN CANADAWAY		5.1	
600	Thick beds of shaley siltstone & silty shale, calcareous zone at 635 ft		
Weathered vert. frac.			700
700	Silty shale, slightly calcareous & petroliferous	4.5	760
Vert. frac.			
800	Dunkirk transition zone occasionally calcareous, pyritic & cross-bedded structure	5.5	850
Vert. frac.			
900	Petroliferous & pyritic shale with siltstone layers & frac. parallel to bedding	4.8	HORIZON 1 910
Vert. frac.			
1000	Interbedded shale and siltstone with sharpstone cong	6.5	1030
	Shale interbedded with siltstone with some sharpstone cong.	5.3	1100
1100	Shale with beds of siltstone & pyrite, one 5-ft long vert. frac. with base at 1159 ft	5.5	1170
Vert. frac.			
1200	Shale with silt & pyrite seams & occasional fossils		HORIZON 2 1250
	Shale with fossils, occasionally petroliferous, several vert. joints filled with calcite, 1 vert. frac. 4.7 ft long with base at 1316 ft	4.8	
1300	Vert. frac.		
1400	Shale with silt, pyrite & pet. several vertical joints up to 12-in. long		
1500			1500

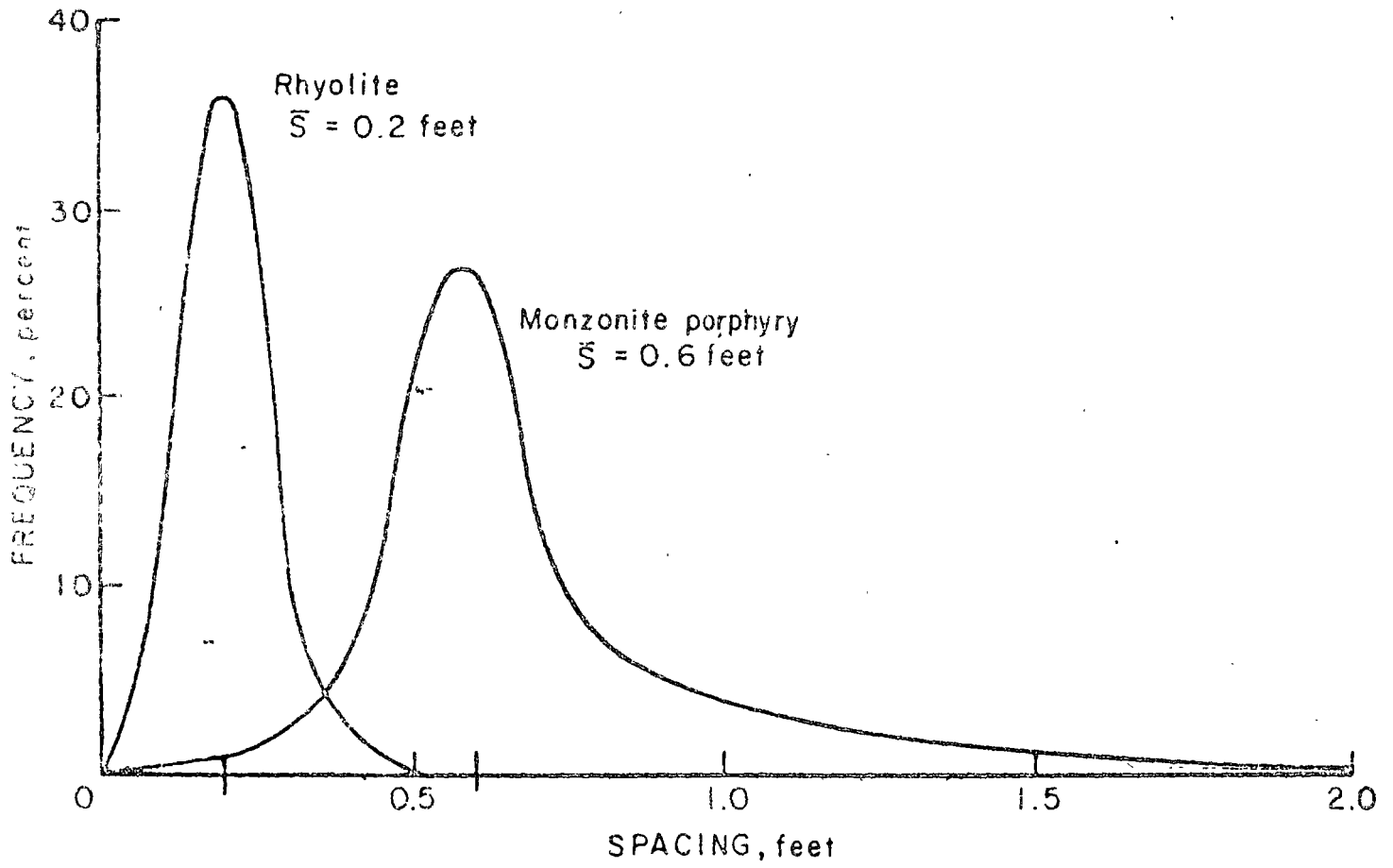
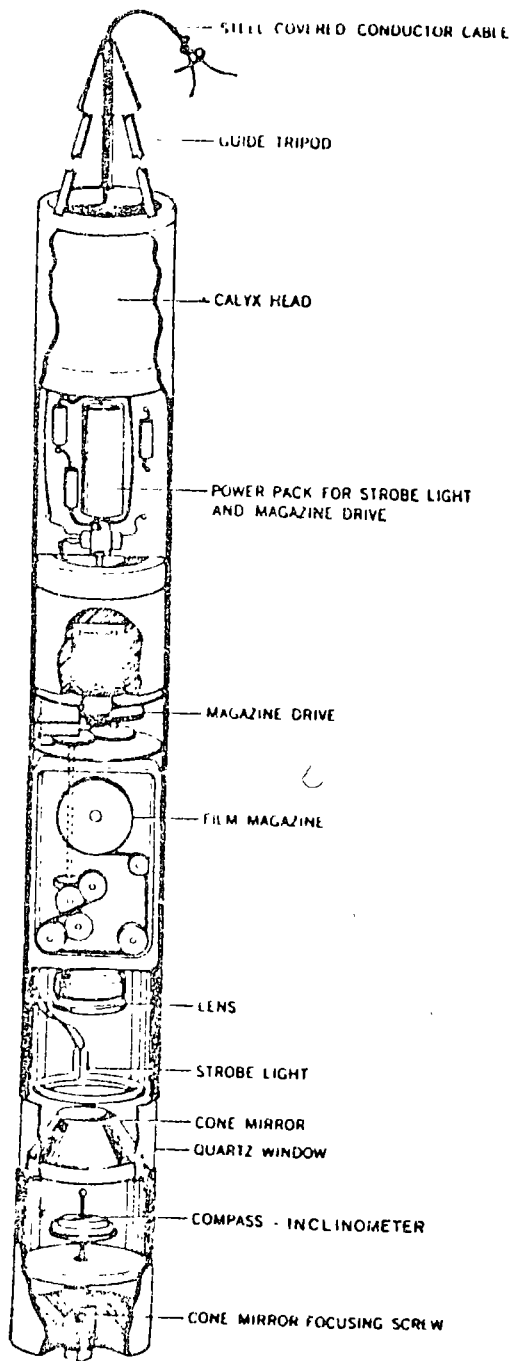


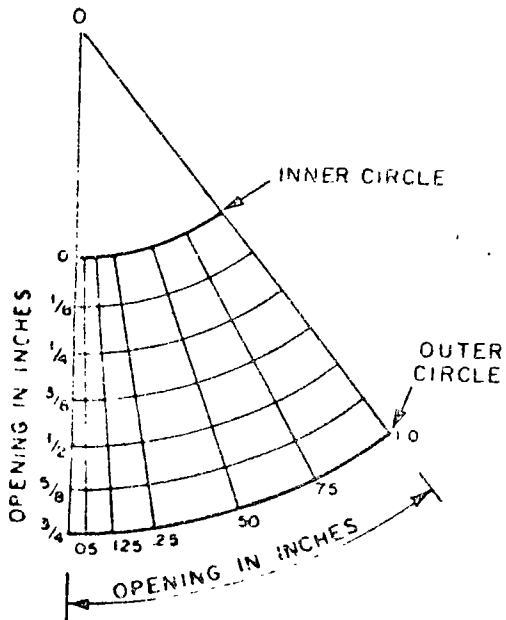
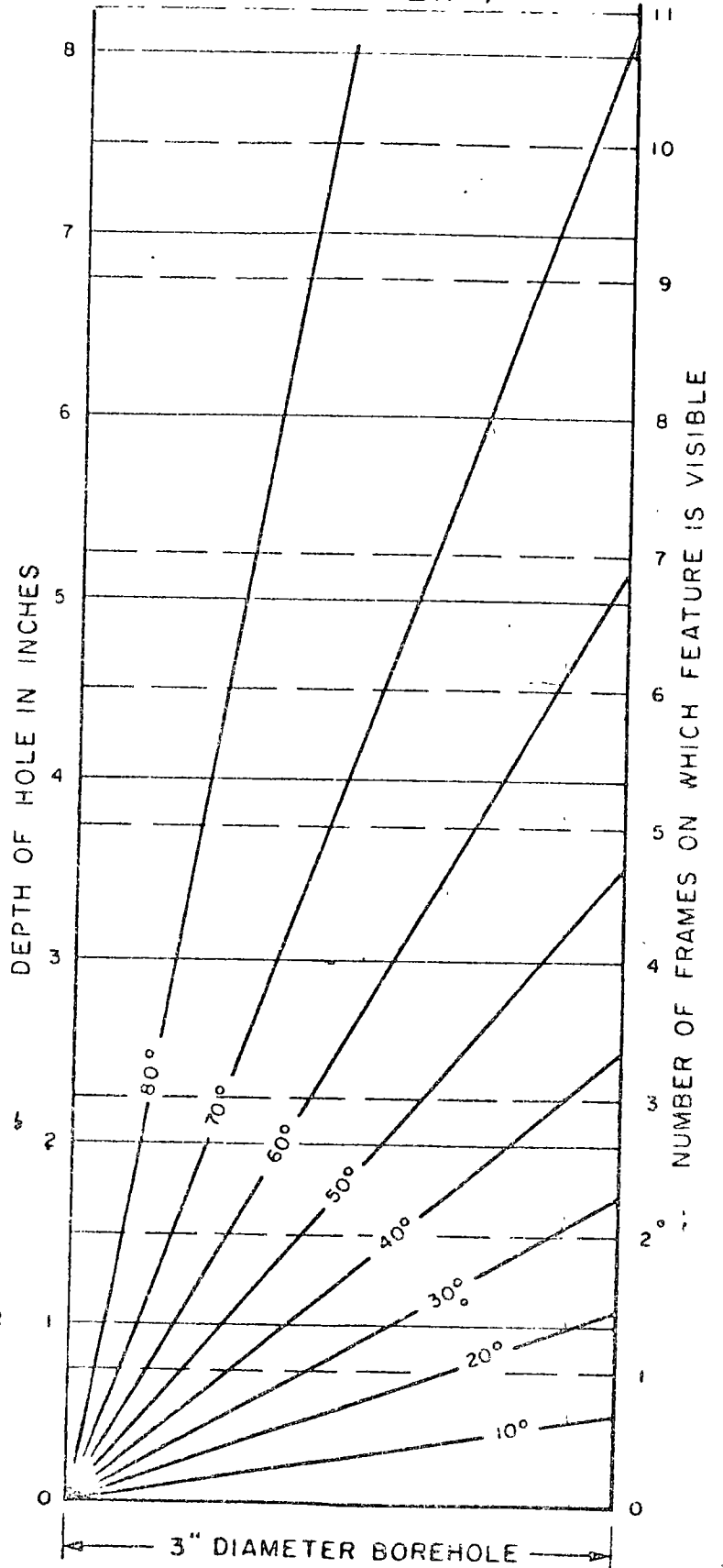
FIGURE 4.-Plot of Spacing Versus Frequency For One of Three Fracture Sets, San Manuel.



DEPTH GUIDE

NUMBER OF FRAMES ON FILM	CORRESPONDING DEPTH - INCHES
0	0
1	0.75
2	1.50
3	2.25
4	3.00
5	3.75
6	4.50
7	5.25
8	6.00
9	6.75
10	7.50
11	8.25
12	9.00
13	9.75
14	10.50
15	11.25
16	12.00
<hr/>	
32	2 FT
48	3 FT
64	4 FT
80	5 FT

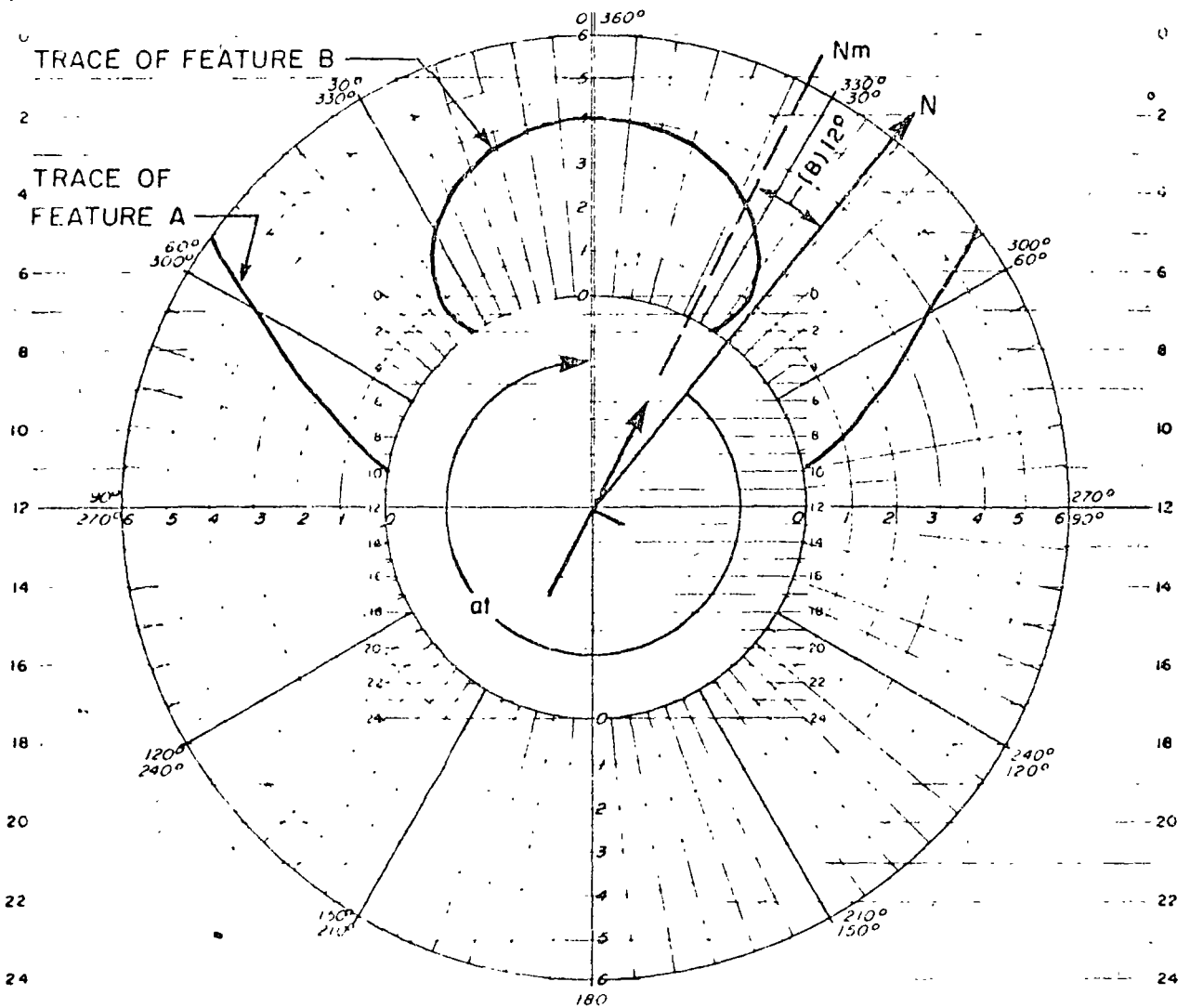
ESTIMATING ANGLE OF DIP (OR APPARENT DIP)



JOINT OPENING GUIDE

VERTICAL HOLE

FIG.



ACRES CONSULTING SERVICES LIMITED

BOREHOLE PHOTOGRAPHY - INTERPRETATION SHEET A

PROJECT	ARNPRIOR GENERATING STATION	DATE	JULY 6, 1973
MAGNETIC DECLINATION (B)	N 12° W	HOLE No.	MD-34A
INCLINATION	0°	FILM ROLL	2
AZIMUTH OF HOLE	a1	DEPTH	572 FT.
ANGLE OF APPARENT DIP DIRECTION OF FEATURE 1	321° (TRUE DIP DIRECTION 1 FOR VERTICAL HOLE)	STRIKE (VERTICAL HOLE ONLY)	231° or S 51° W
PLANAR FEATURE	A - TIGHT JOINT ; B - FOLIATION		

FEATURE A	CALCULATION OF APPARENT DIP	FEATURE B
METHOD I	METHOD II	
INTERSECT INNER CIRCLE AT left 10.1 right 9.9 av 10.0	INTERSECT 30° AT left 2.5 right 2.3 av 2.4	
INTERSECT OUTER CIRCLE AT left 4.9 right 5.1 av 5.0	INTERSECT 0°/360° AT 4.0	
INTERSECTION DIFFERENCE (POSITIVE) I 5.0	INTERSECTION DIFFERENCE II 1.6	
	ANGLE DIFFERENCE II 30°	

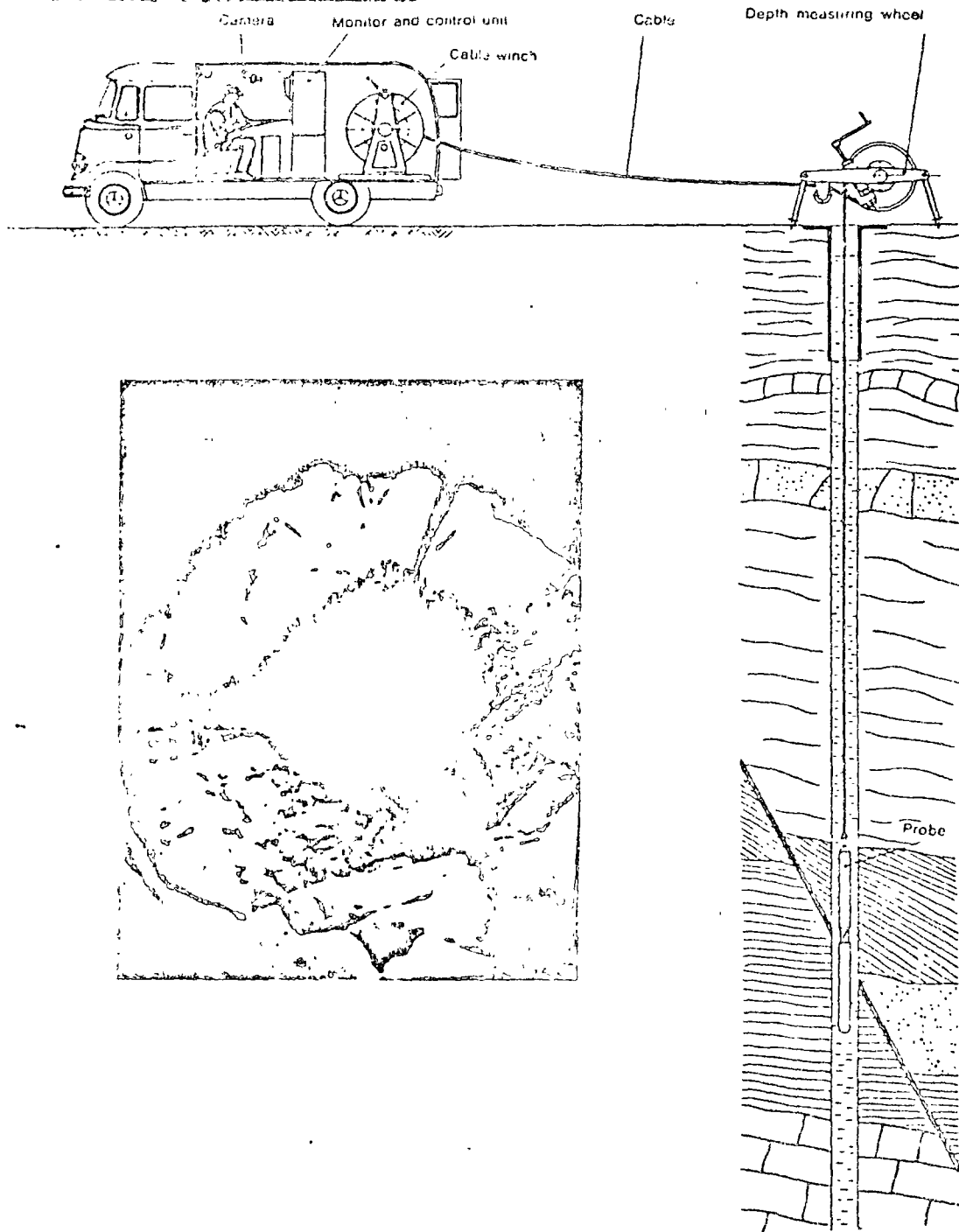


Fig 10 - Borehole viewing with a television probe (7).

hole size required is about 2.0 in. (5 cm).

117. The borehole television camera delivers a direct view of the drillhole and allows observation of interesting detail. It can be oriented such that a fracture plane shows as a straight line on the screen, and the angle of dip

and strike can readily be determined. Photographing the television picture is possible, but lacks the clarity of direct photographs of the borehole wall.

118. The borehole periscope is the least expensive tool for borehole viewing and combines the

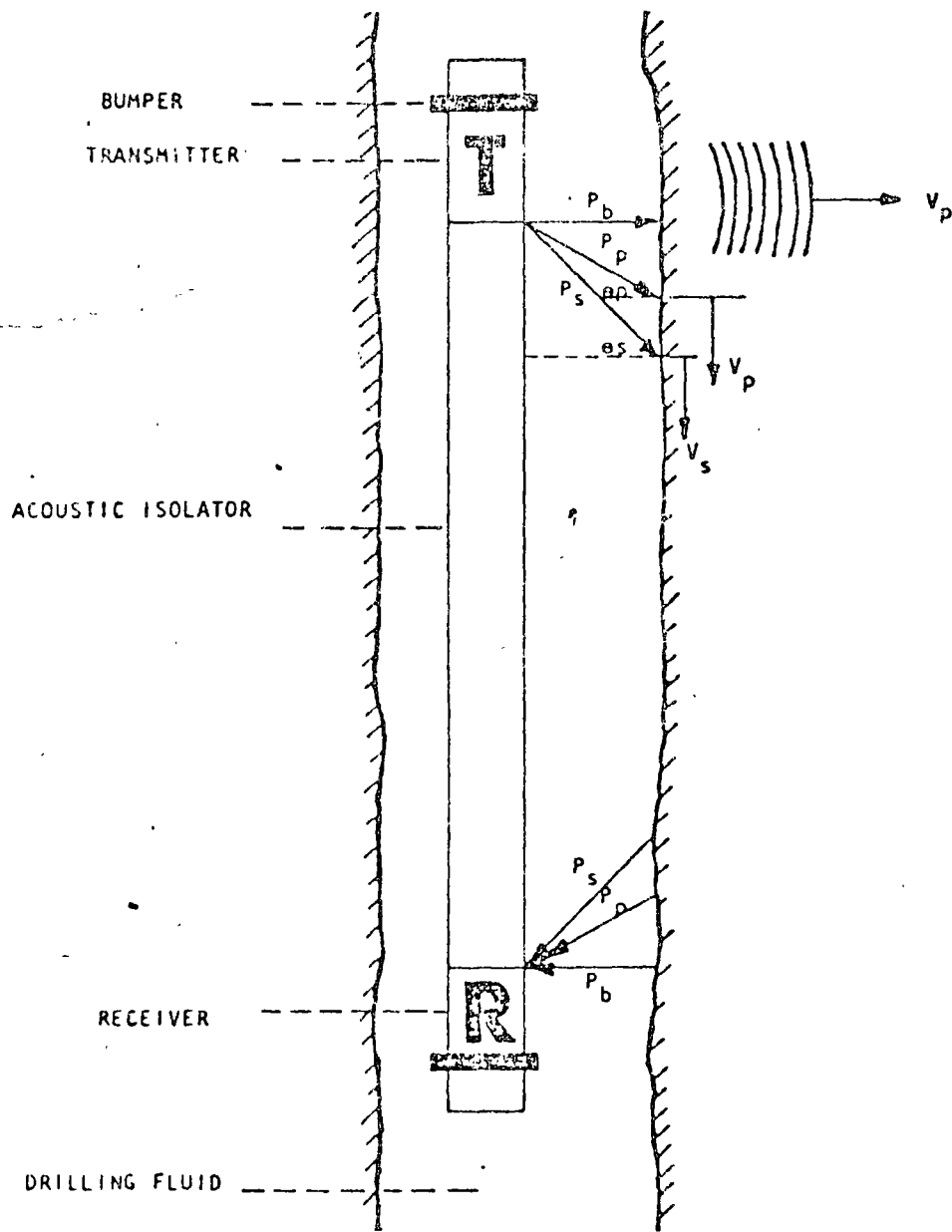


Figure 9. Diagram of 3-D Velocity Tool

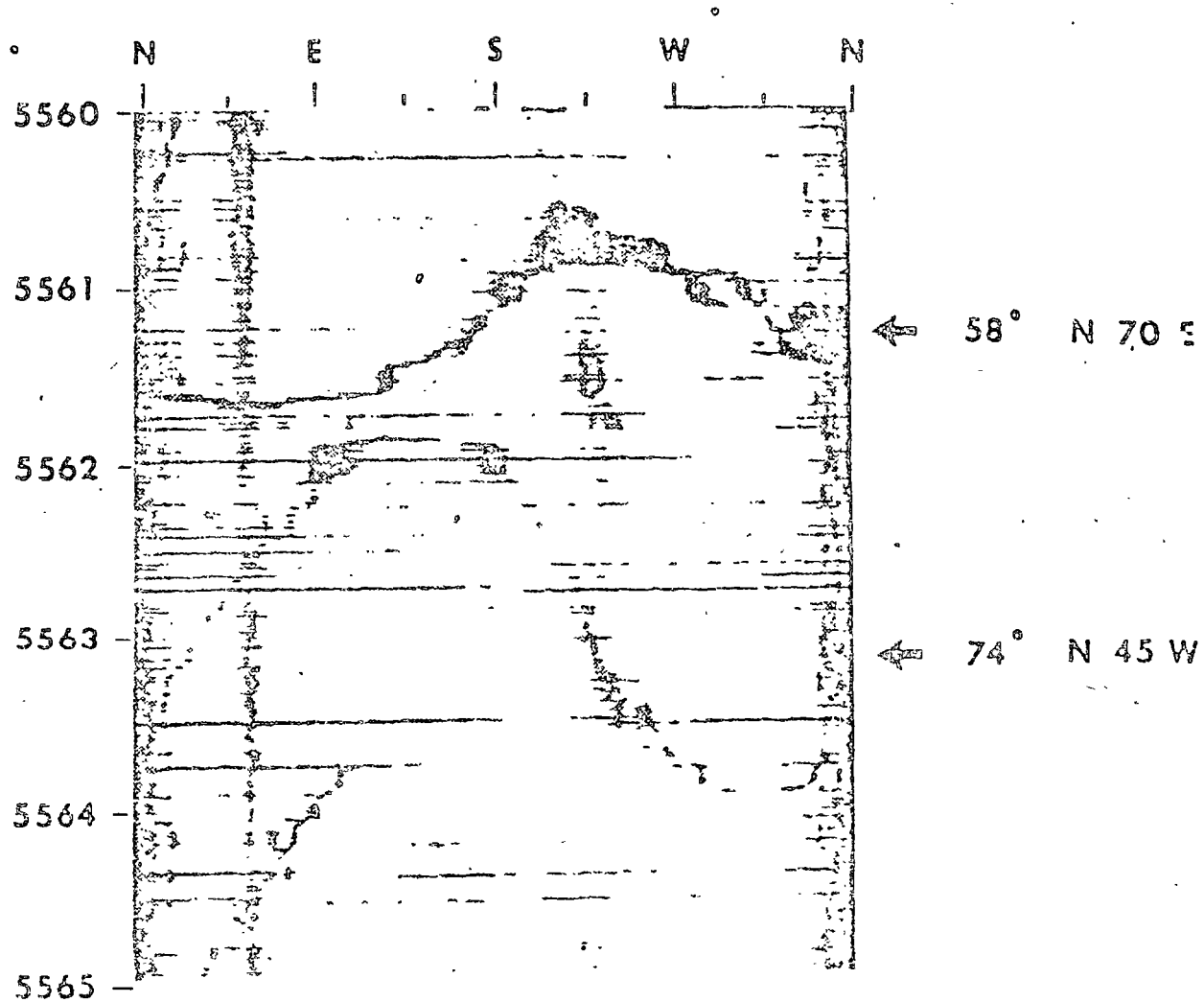
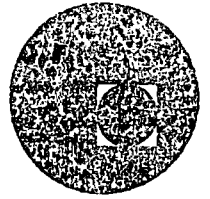


Figure 8. High Angle Fractures Intersecting Near Borehole



centro de educación continua
división de estudios superiores
facultad de ingeniería, unam



MECANICA DE ROCAS APLICADA A LA MINERIA

ANALISIS DE DATOS GEOLOGICOS ESTRUCTURALES

ABRIL, 1978.

DETERMINATION OF ATTITUDES OF JOINTS SURVEYED WITH A BORESCOPE IN INCLINED BOREHOLES

by

M. A. Mahtab,¹ D. D. Bolstad,² and R. R. Pulse³

ABSTRACT

This report describes the procedures used by the Bureau of Mines for obtaining attitudes of joints surveyed with a borescope in inclined boreholes. An algorithm for computing the dips and azimuths of the observed joints is presented. The algorithm is used to solve an example problem. A computer program based on the algorithm is listed. It is hoped that the procedures described here will be useful in treating large quantities of data obtained from comprehensive borehole surveys.

INTRODUCTION

A borescope (also called a borehole periscope or a stratascope) is an optical instrument used for visual inspection of boreholes. Important subsurface geologic information can be readily obtained by a borescope examination of small-diameter, short (less than 100 ft) boreholes. During the past few years, the Bureau of Mines has frequently surveyed boreholes for obtaining the geometry (that is, spacing, orientation, and aperture) of fractures in underground mines. A computerized scheme was devised in 1970 for determining attitudes (dips and azimuths of dip) of the joints surveyed in inclined boreholes with a borescope. This scheme has proved useful in reducing the field data from many comprehensive borehole surveys of joint orientations. The purpose of this report is to state the procedures used by the Bureau in determining attitudes of joints surveyed in inclined boreholes.

The solution for dip and azimuth of dip (or equivalently, the strike) of joint surfaces surveyed in inclined boreholes with a borescope has not (to the author's best knowledge) been reported before. The relatively simple problem of finding attitudes of joints surveyed in horizontal boreholes has been treated by Cooper (2).⁴ The more interesting problem of inclined boreholes has been solved by Dakhnov (3) for borehole surveys made with a

¹Physical scientist.

²Geologist.

³Physical research scientist.

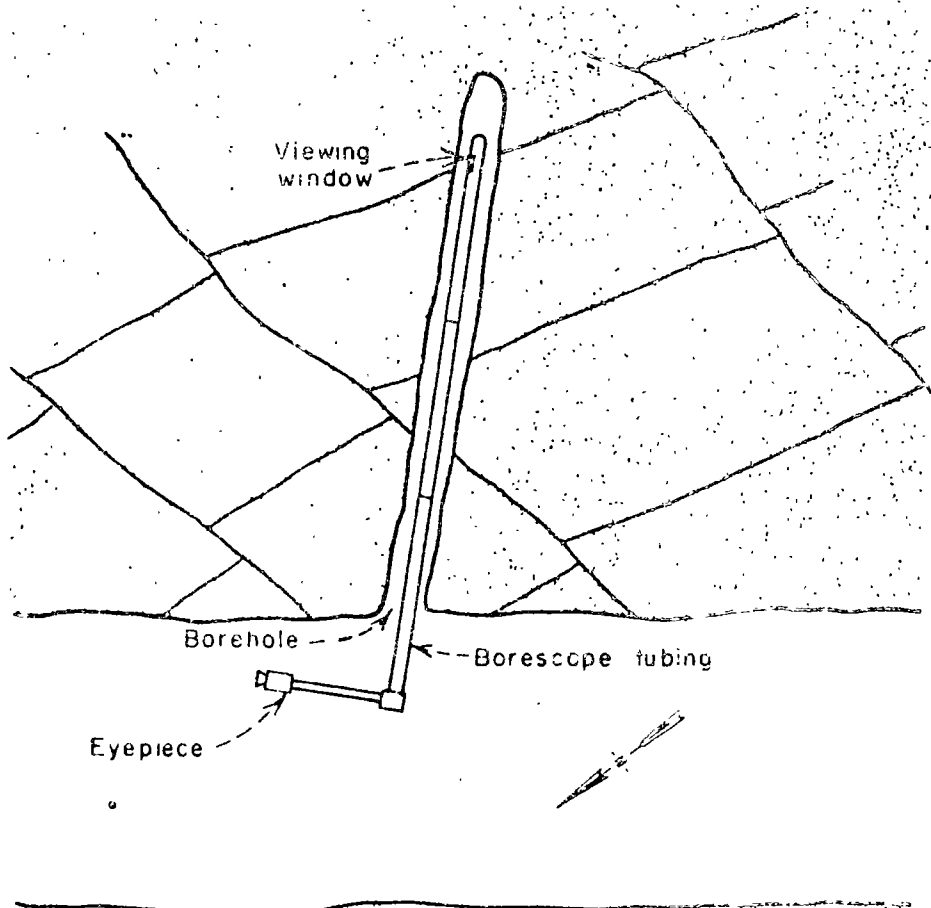
⁴Underlined numbers in parentheses refer to items in the list of references at the end of this report.

three-electrode sonde. A modified Dakhnov solution would, however, be suitable only for a borehole with a diameter equal to that of the borescope. In addition to this limitation, Dakhnov's solution would require a greater computational effort than would the scheme presented in this report.

The next section of this report describes the procedures used for collecting and recording the borescope data. The algorithm used for determining the attitude of an observed joint is described in a subsequent section. Another section of the report lists the computer program for determining attitude of the surveyed joints.

DATA COLLECTION PROCEDURES

The essential optical features of a borescope are shown in figure 1. A light source is housed at the bottom end (farthest from the viewer) of the borescope. A picture window near the bottom end of the borescope transmits the picture of the object to a prism that refracts the image and transmits it



through a sequence of lenses to another prism near the eyepiece. Several extension tubes (of lengths 2 ft to 6 ft) can be assembled to reach a desired depth in the hole. A winch (or a tripod) is normally required for supporting and guiding the borescope in upholes (or downholes) that are longer than about 15 ft. The viewing direction in the hole is determined by the pin in the first (eyepiece) tube, which is in alignment with the pins on all the other (extension) tubes.

Bore-scope surveying for joint attitudes consists of

FIGURE 1. - Essential features of a borescope (plan view).

Project: San Manuel - Boreoscope surveying of joints

Study site: 2015 Level, Drift 22

Borehole: Hole No. EX2, \perp to Joint Set 3

Azimuth of hole = 134°

Inclination of hole with the horizon = 12° (inclined up)

Diameter of hole = 1.5 in.; diameter of boreoscope = 1.0 in.

Observer: R. Palat

Recorder: R. Palat

Date: May 1, 1970

Joint No.	Distance from a collar to eyepiece, ft			Length of tubing removed, ft	Remarks
	Right	Top	Left		
1	0.80	0.99	0.75		Initial length of tubing = 15.05 ft Open joint ($\frac{1}{8}$ " wide, $\frac{1}{8}$ " deep)
2	1.44	1.33	1.39		Partially open, $\frac{1}{8}$ " wide, pyrite filling
—					
—					
21	6.00	5.96	5.99	6.00	Open joint, $\frac{1}{8}$ " wide, one 6 ft extension removed
22	0.22	0.20	0.23		Open on left, $\frac{1}{8}$ " wide
—					
—					
37	5.69	5.77	5.74	6.00	Open, $\frac{1}{4}$ " wide, calcite filling one 6 ft extension removed
38	0.16	0.19	0.17		Open, $\frac{1}{16}$ " wide
—					
—					
44	2.60	2.52	2.59		Deeply open, $\frac{1}{8}$ " wide, last observation in this hole

FIGURE 2. - Example data sheet for recording boreoscope observations of joints.

measuring the axial distances from the collar of the borehole to three points on the observed joint plane. Two of these points, the "right" and the "left" points, are located at the intersections of the midheight borescope diameter with the borehole perimeter. The third point is located at the crown of the borehole. Unless the joint plane is normal to the axis of the borehole, the borescope has to be moved back (or forth) between the right and the top and between the top and the left points. An example data sheet for recording borescope observations is shown in figure 2. Note that the distances from the borehole collar to the eyepiece are recorded in the data sheet. The actual distances from the collar to the three points on the joint plane are simply obtained by subtracting the recorded distances from the known total length of the borescope tubing. Note also that the observations are begun at the joint farthest from the collar of the hole; successive lengths of the borescope tubing are removed as the bottom end of the borescope is brought closer to the collar.

DETERMINATION OF ATTITUDE OF A JOINT

The attitude of a joint plane is defined by two angles; namely, the dip ϕ (downward inclination of the joint with the horizon) and the azimuth of dip θ (clockwise horizontal angle from north) to the directed dip line. The choice of azimuth of dip, instead of "strike" (angle with north of a horizontal line on the joint plane), was made for convenience in using the existing computer techniques (4) for analyzing joint orientations.

The Algorithm

As mentioned in the previous section, a borescope measures the axial distances from the collar of the borehole to three points (1 = right, 2 = top, and 3 = left): Figure 3 shows the location of these points in a local (X' , Y' , Z') system and the global (X , Y , Z) system. Notice that the Y' Z' plane is given by rotating the $Y Z$ plane around the X (or X') axis by angle γ ; that is, the axis of the hole (Y') is inclined up at angle γ . The two coordinate systems are related as follows:

$$\begin{Bmatrix} X \\ Y \\ Z \end{Bmatrix} = \begin{Bmatrix} 1 & 0 & 0 \\ 0 & \cos \gamma & -\sin \gamma \\ 0 & \sin \gamma & \cos \gamma \end{Bmatrix} \begin{Bmatrix} X' \\ Y' \\ Z' \end{Bmatrix} \quad (1)$$

Note that for a hole inclined down from the horizon, a negative sign should be used in front of γ in equation 1.

For convenience in computation, the origin of the $X' Y' Z'$ system can be shifted by a distance Y' , along Y' such that

$$\begin{Bmatrix} X \\ Y \\ Z \end{Bmatrix} = \begin{Bmatrix} 1 & 0 & 0 \\ 0 & \cos \gamma & -\sin \gamma \\ 0 & \sin \gamma & \cos \gamma \end{Bmatrix} \begin{Bmatrix} X' \\ Y'' \\ Z' \end{Bmatrix} \quad (2)$$

where $Y'' = Y' - Y_1'$.

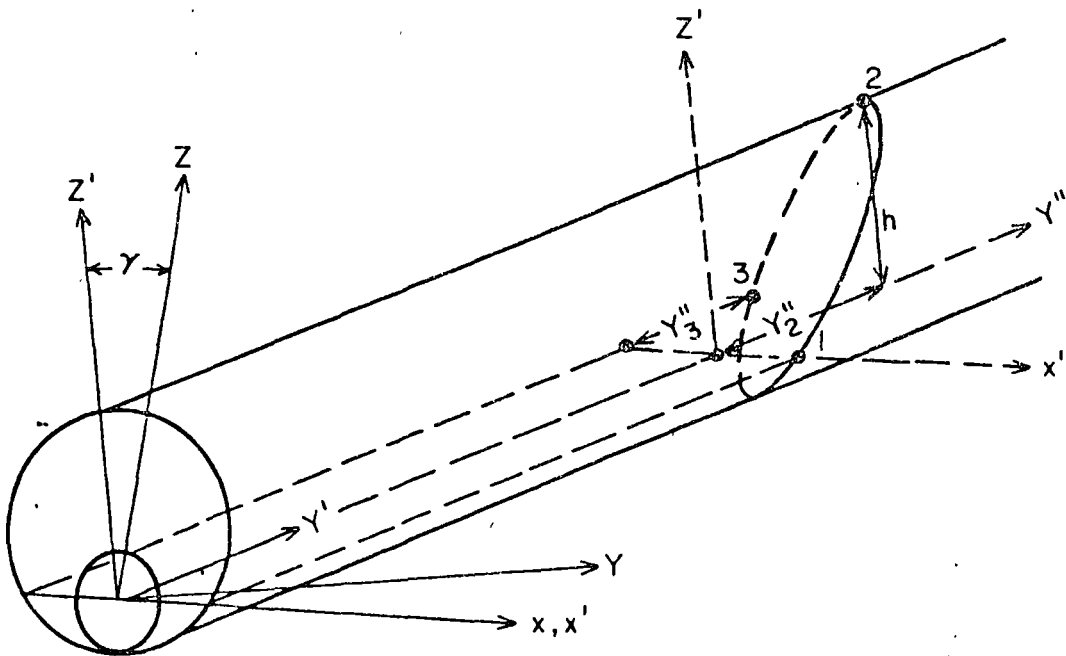
Figure 4 shows a cross section of the borehole in the $X'Z'$ plane and gives the X' and Z' coordinates of the points 1, 2, and 3. Now, using equation 2, the X , Y , and Z coordinates of the three points are

$$X_1 = a, X_2 = 0, X_3 = -a;$$

$$Y_1 = 0, Y_2 = Y_2'' \cos\gamma - h \sin\gamma, Y_3 = Y_3'' \cos\gamma;$$

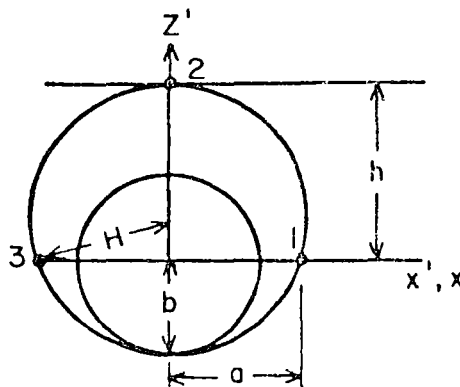
and

$$Z_1 = 0, Z_2 = Y_2'' \sin\gamma + h \cos\gamma, Z_3 = Y_3'' \sin\gamma.$$



NOTE: X, Y, Z are global coordinates, and X', Y', Z' are local coordinates. $Y_2'' = Y_2' - Y_1'$; $Y_3'' = Y_3' - Y_1'$; $\gamma =$ angle between YZ and $Y'Z'$ planes

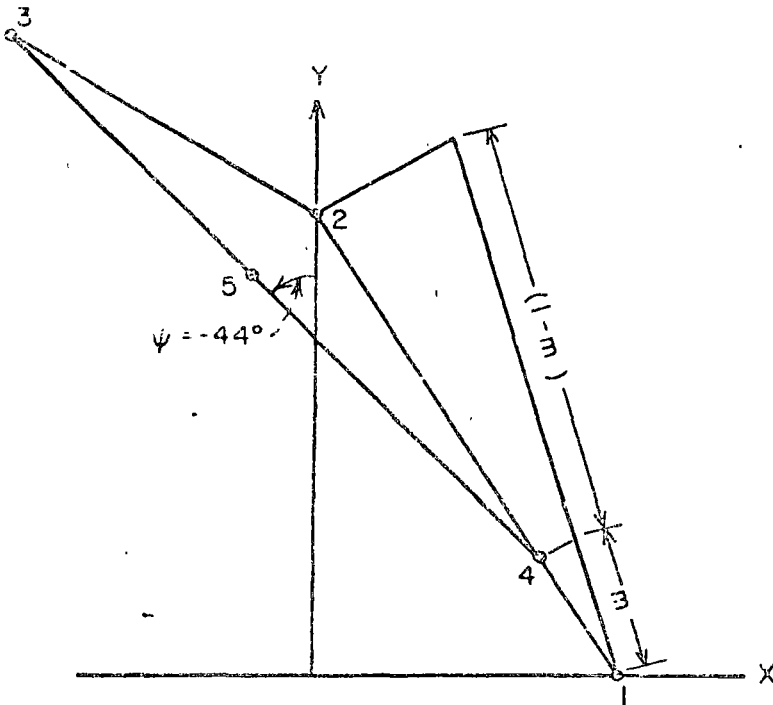
FIGURE 3. - Coordinates of three points on a joint surveyed with a borescope.



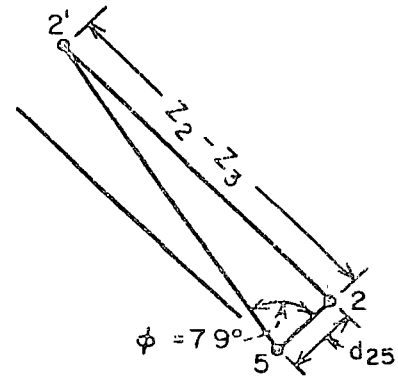
$H =$ Borehole radius
 $b =$ Borescope radius
 $h = Z_2' - Z_1' = 2H - b$
 $a = x_1' = (bh)^{\frac{1}{2}}$

FIGURE 4. - Section of borehole normal to borehole axis.

The well-known principles of the graphic solution (fig. 5) to the "three-point problem" can now be used to solve for the attitude of a joint plane. The solution is carried out in three steps: (1) The angle between Y-axis and a



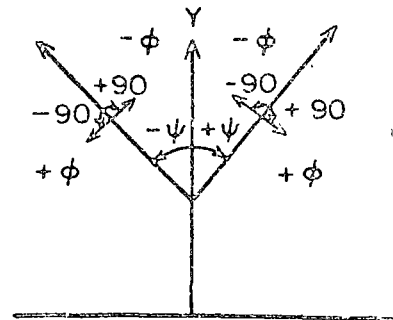
A. Solution for ψ



B. Solution for dip, ϕ

	1	2	3
X	0.059	0	-0.059
Y	0	0.089	0.130
Z	0	0.104	0.028

C. Global coordinates (ft) of three points on the joint plane



D. Sign convention for dip azimuth
 $\theta = \text{Azimuth of } Y \pm \psi \pm 90(\text{deg})$

FIGURE 5. - Graphical solution for attitude of a joint plane (adapted from Billings (1), p. 560).

horizontal line in the plane of the joint is obtained, (2) the dip of the joint is computed, and (3) the azimuth of dip is computed from the results of the previous two steps.

To obtain the angle (with the Y-axis) of a horizontal line in the joint plane 123, the position of point 4 (lying in the horizontal plane containing point 3) is first defined (fig. 5A). Since point 4 lies on a line through points 1 and 2 and at the elevation of 3,

$$X_4 = (1 - m) X_1,$$

and

$$Y_4 = m Y_2,$$

$$\text{where } m = \frac{Z_3}{Z_2}.$$

Let $\Psi (0^\circ \leq \Psi \leq 90^\circ)$ be the angle between the level line 34 and Y, then

$$\cos \Psi = \frac{|Y_3 - Y_4|}{d_{34}} = \frac{|Y_3 - mY_2|}{d_{34}}, \quad (3)$$

$$\text{where } d_{34} = [(Y_3 - Y_4)^2 + (X_3 - X_4)^2]^{1/2} = [(Y_3 - mY_2)^2 + a^2(m-2)^2]^{1/2},$$

and where $|Y_3 - Y_4|$ is the absolute difference between Y_3 and Y_4 .

The angle Ψ is considered positive (negative) when it is measured clockwise (counterclockwise) from the Y-axis; that is, the angle Ψ assumes the sign of the ratio $(Y_3 - Y_4)/(X_3 - X_4)$. The graphical solution for Ψ for an example problem is shown in figure 5A.

The dip $\phi (-90 \leq \phi \leq 90)$ of the joint plane (fig. 5B) is given by the relation

$$\tan \phi = \frac{Z_2 - Z_3}{d_{25}}, \quad (4)$$

where d_{25} , the horizontal distance between point 2 and the level line 34, is given by

$$d_{25} = \frac{2A}{d_{34}}. \quad (5)$$

In equation 5, A is the area of triangle 234, and its value is obtainable from

$$2A = \det \begin{bmatrix} 1 & X_2 & Y_2 \\ 1 & X_3 & Y_3 \\ 1 & X_4 & Y_4 \end{bmatrix} = a(1-m)(2Y_2 - Y_3). \quad (6)$$

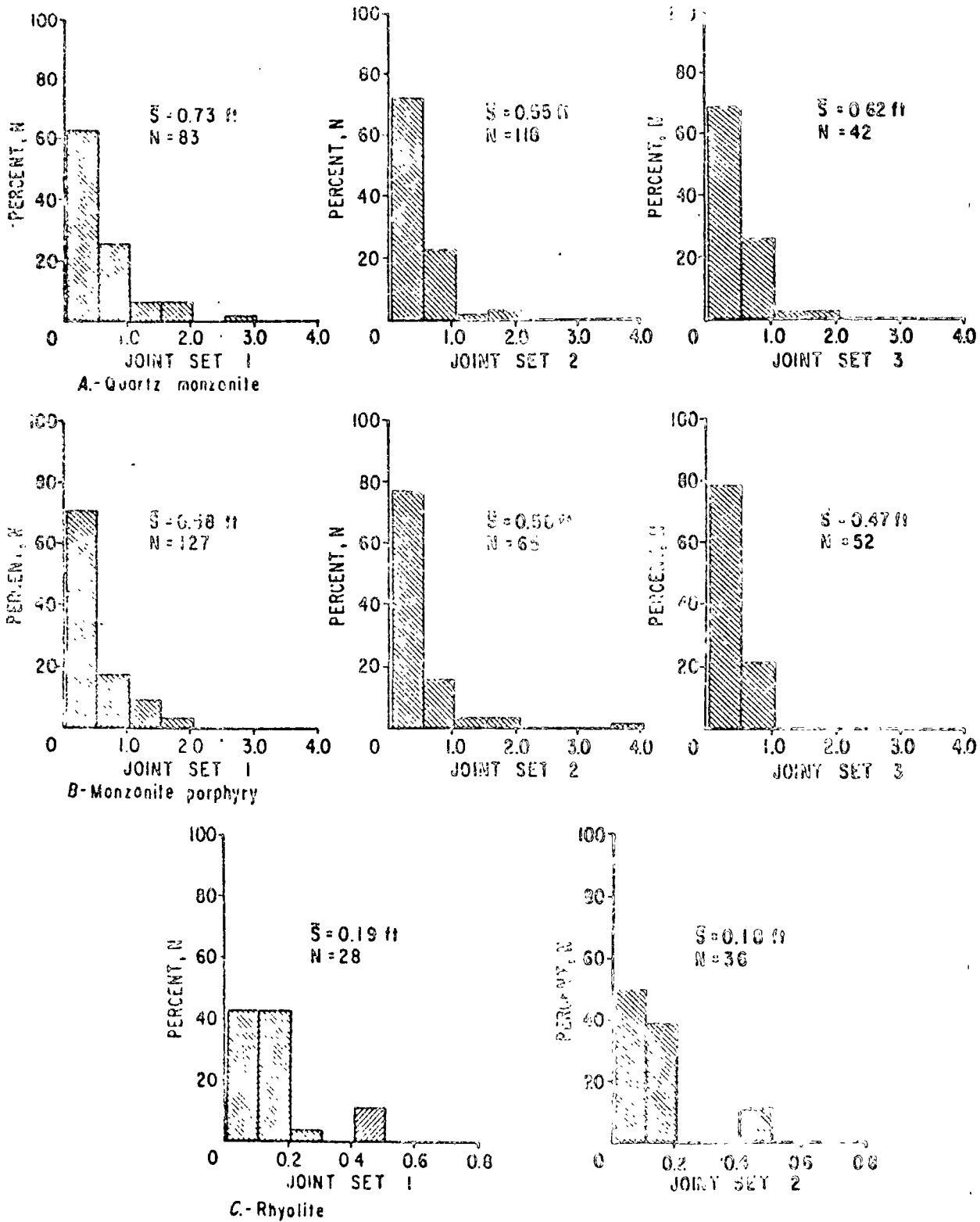


FIGURE 12. - Spacings (Feet) of the Three Most Prominent Fracture Sets in Study Area on 2015 Level by Rock Type. \bar{S} = mean spacing, N = number of observations. The scale of abscissa for rhyolite is changed to accommodate the smaller range of values.

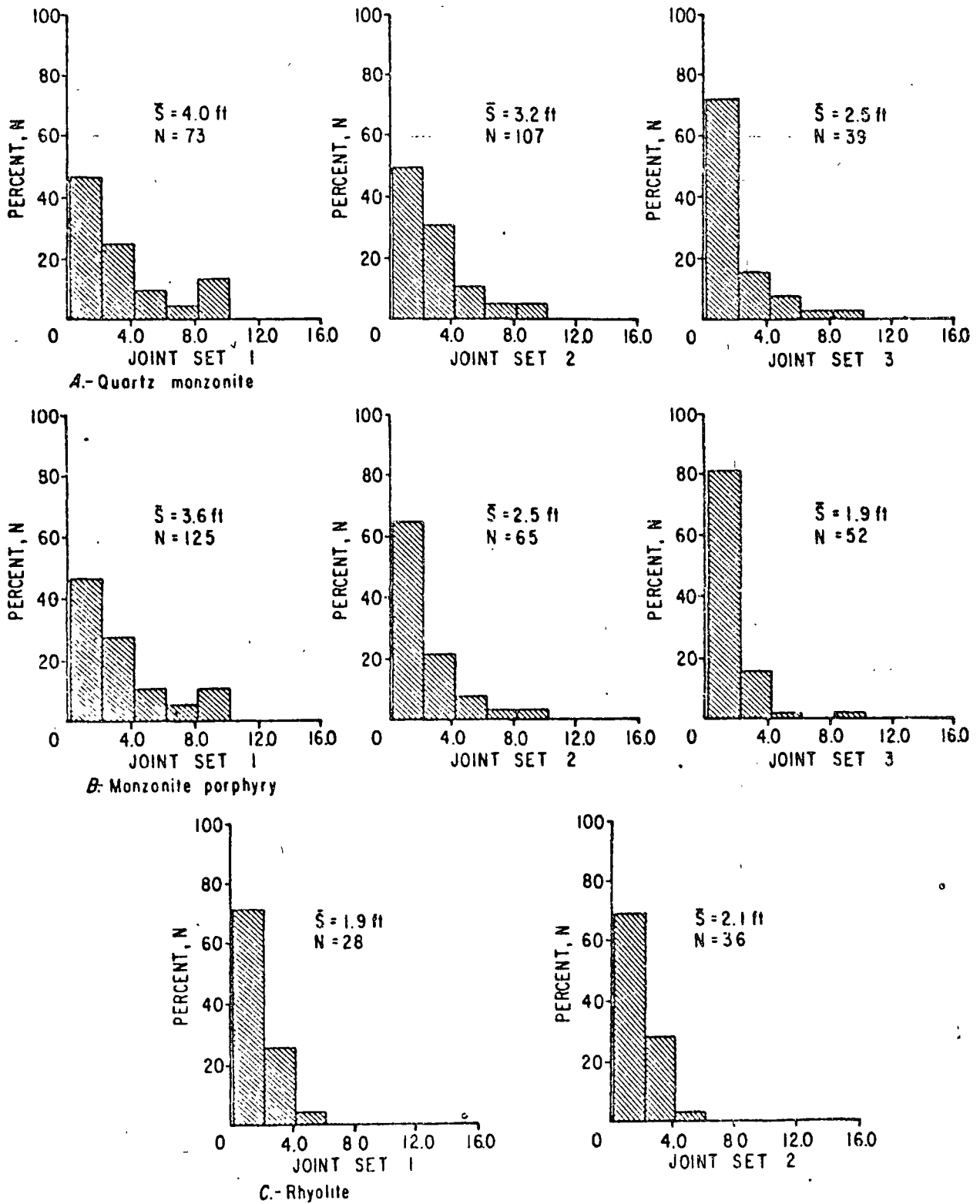


FIGURE 13. - Extents (Feet) of the Three Most Prominent Fracture Sets in Study Area on 2015 Level by Rock Type. \bar{x} = mean extent, N = number of observations.

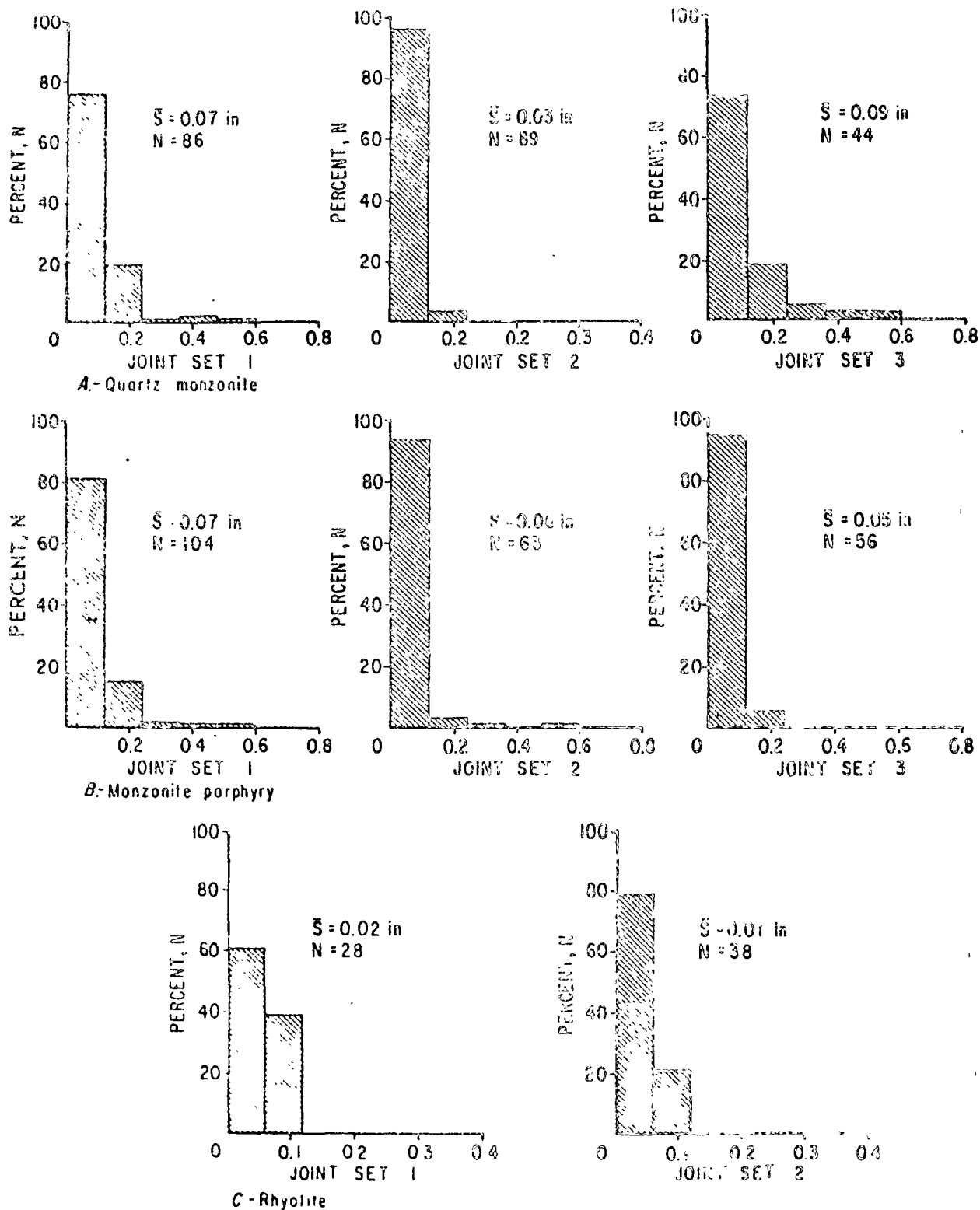


FIGURE 14. - Apertures (Inches) of the Three Most Prominent Fracture Sets in Study Area on 2015 Level by Rock Type. \bar{S} = mean aperture, N = number of observations. The scale of abscissa for rhyolite is changed to accommodate the smaller range of values.



centro de educación continua
división de estudios superiores
facultad de ingeniería, unam



MECANICA DE ROCAS APLICADA A LA MINERIA

ANALISIS DE DATOS GEOLOGICOS

II PARTE

ABRIL, 1978

Chapter 3: Graphical presentation of geological data

Introduction

The dominant role of geological discontinuities in rock slope behaviour has already been emphasised and few engineers or geologists would question the need to base stability calculations upon an adequate set of geological data. But what is an adequate set of data? What type of data and how much detailed information should be collected for a stability analysis?

This question is rather like the question of which came first - the chicken or the egg? There is little point in collecting data for slopes which are not critical but critical slopes can only be defined if sufficient information is available for their stability to be evaluated. The data gathering must, therefore, be carried out in two stages as suggested in Figure 6.

The first stage involves an examination of existing regional geology maps, air photographs, easily accessible outcrops and the core recovered during exploration drilling. A preliminary analysis of this data will indicate slopes which are likely to prove critical and which require more detailed analysis.

The second stage involves a much more detailed examination of the geological features of these critical regions and may require the drilling of special holes outside the ore body, excavation of trial pits or adits and the detailed mapping and testing of discontinuities.

An important aspect of the geological investigations, in either the first or second stages, is the presentation of the data in a form which can be understood and interpreted by others who may be involved in the stability analysis or who may be brought in to check the results of such an analysis. This means that everyone concerned must be aware of precisely what is meant by the geological terms used and must understand the system of data presentation.

The following definitions and graphical techniques are offered for the guidance of the reader who may not already be familiar with them. There is no implication that these are the best definitions or techniques available and the reader who has become familiar with different methods should certainly continue to use those. What is important is that the techniques which are used in any study should be clearly defined in documents relating to that study so that errors arising out of confusion are avoided.

Definition of geological terms

Rock Material or intact rock, in the context of this discussion, refers to the consolidated and cemented assemblage of mineral particles which form the intact blocks between discontinuities in the rock mass. In most hard igneous and metamorphic rocks, the strength of the intact rock is one or two orders of magnitude greater than that of the rock mass and failure of this intact material is not generally involved in the processes of slope failure. In softer sedimentary rocks, the intact material may be relatively weak and failure of this material may play an important part in slope failure.

Rock mass is the *in-situ* rock which has been rendered discontinuous by systems of structural features such as joints, faults and bedding planes. Slope failure in a rock mass is generally associated with movement on these discontinuity surfaces.



An ordered structural pattern in slate.

Waste rock or broken rock refers to a rock mass which has been disturbed by some mechanical agency such as blasting, ripping or crushing so that the interlocking nature of the *in-situ* rock has been destroyed. The behaviour of this waste or broken rock is similar to that of a clean sand or gravel, the major differences being due to the angularity of the rock fragments.

Discontinuities or weakness planes are those structural features which separate intact rock blocks within a rock mass. Many engineers describe these features collectively as *joints* but this is an over-simplification since the mechanical properties of these features will vary according to the process of their formation. Hence, faults, dykes, bedding planes, cleavage, tension joints and shear joints will all exhibit distinct characteristics and will respond in different ways to applied loads. A large body of literature dealing with this subject is available and the interested reader is referred to this for further information^{34, 35, 36}. For the purposes of this discussion, the term *discontinuity* will generally be used to define the structural weakness plane upon which movement can take place. The type of discontinuity will be referred to when the description provides information which assists the slope designer in deciding upon the mechanical properties which will be associated with a particular discontinuity.

Major discontinuities are continuous planar structural features such as faults which may be so weak, as compared with any other discontinuity in the rock mass, that they dominate the behaviour of a particular slope. Many of the large failures which have occurred in open pit mines have been associated with faults and particular attention should be paid to tracing these features.

Discontinuity sets refers to systems of discontinuities which have approximately the same inclination and orientation. As a result of the processes involved in their formation³⁴, most discontinuities occur in families which have preferred directions. In some cases, these sets are clearly defined and easy to distinguish while, in other cases, the structural pattern appears disordered.

Continuity. While major structural features such as faults may run for many tens of feet or even miles, smaller discontinuities such as joints may be very limited in their extent. Failure in a system where discontinuities terminate within the rock mass under consideration will involve failure of the intact rock bridges between these discontinuities. Continuity also has a major influence upon the permeability of a rock mass since this depends upon the extent to which discontinuities are hydraulically connected.

Continuity or persistence is the most difficult geological parameter to define and, as far as the author is aware, no satisfactory system for reliable evaluation of continuity is available. Jennings and his co-workers in South Africa^{37, 38, 39} have attempted to measure continuity and to



An apparently disordered structural pattern in hard rock.

use these measurements to estimate the cohesive strength of potential failure planes. This author does not believe that continuity can be quantified in this way and prefers to err on the side of safety - if in doubt, assume that all discontinuities are continuous. Cohesive strength is estimated by other methods which will be described later.

Gouge or infilling is the material between two faces of a structural discontinuity such as a fault. This material may be the debris resulting from the sliding of one surface upon another or it may be material which has been precipitated from solution or caused by weathering. Whatever the origin of the infilling material in a discontinuity, its presence will have an important influence upon the shear strength of that discontinuity. If the thickness of the gouge is such that the faces of the discontinuity do not come into contact, the shear strength will be equal to the shear strength of the gouge. If the gouge layer is thin so that contact between asperities on the rock surfaces can occur, it will modify the shear strength of the discontinuity but will not control it⁴⁰.

Roughness. Patton^{41,42} emphasised the importance of surface roughness on the shear strength of structural discontinuities in rock. This roughness occurs on both a small scale, involving grain boundaries and failure surfaces, and on a large scale, involving folds and flexures in the discontinuity. The mechanics of movement on rough surfaces will be discussed in the chapter dealing with shear strength.

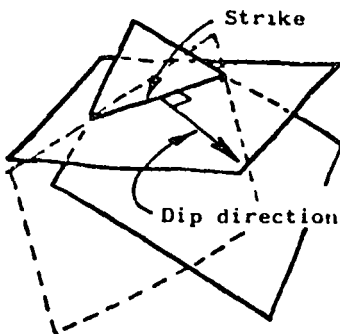
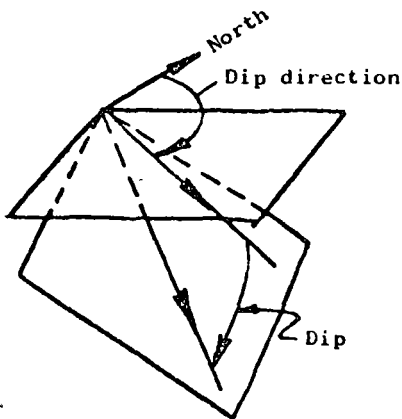
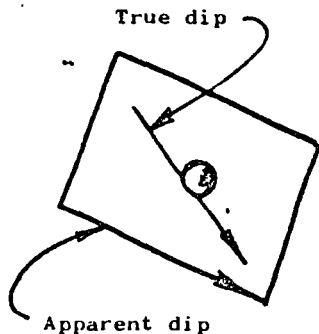
Definition of geometrical terms

Dip is the *maximum* inclination of a structural discontinuity plane to the horizontal. It is sometimes very difficult, when examining an exposed portion of an obliquely inclined plane, to visualise the *true dip* as opposed to the *apparent dip* which is the inclination of an arbitrary line on the plane. The apparent dip is always smaller than the true dip.

One of the simplest models which can be used in thinking about the definition of the dip of a plane is to consider a ball rolling down an obliquely inclined plane. The path of the ball will always lie along the line of maximum inclination which corresponds to the true dip of the plane.

Dip direction or dip azimuth is the direction measured clockwise from North, of the horizontal trace of the line of dip. In terms of the ball rolling down the oblique plane, it is the angle, measured clockwise in degrees on the compass dial, which the direction of rolling would take from true North.

Strike is the trace of the intersection of an obliquely inclined plane with a horizontal reference plane and it is at right angles to the dip and dip direction of the oblique plane. The practical importance of the strike of a plane is that it is the visible trace of a discontinuity which is seen on the horizontal surface of a rock mass. The disadvantage of using this term in slope analysis is that there are in fact *two* planes with the same dips and strikes as shown on the sketch opposite and, unless a strict convention is adopted in terms of the direction in which the strike is measured, confusion can easily arise.



For this reason, the term *strike* when it is used in this book, will always be defined as:

$$\text{Strike} = (\text{dip direction} - 90^\circ)$$

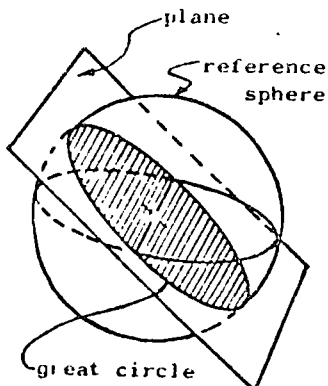
Preferred terms. In order to avoid the confusion which can arise from using strike, particularly when a number of engineers and geologists are involved in analysing the same set of data, many slope designers have turned to using dip and dip direction as the preferred terms for the presentation of all structural data. The same system has been adopted by the author and all the examples presented in this book are in terms of dip and dip direction.

Graphical techniques for data presentation

One of the most important aspects of rock slope analysis is the systematic collection and presentation of geological data in such a way that it can easily be evaluated and incorporated into stability analyses. Experience has shown that spherical projections provide a convenient means for the presentation of geological data. The engineer or geologist, who is not familiar with this technique, is strongly advised to study the following pages carefully. A few hours invested in such a study can save many hours of frustration and confusion later when the reader becomes involved in studying designs and reading reports in which these methods have been used.

Many engineers shy away from spherical projection methods because they are unfamiliar and because they appear complex, bearing no recognisable relationship to more conventional engineering drawing methods. For many years the author regarded these graphical methods in the same light but, faced with the need to analyse three-dimensional rock slope problems, an effort was made, with the aid of a patient geologist colleague, and the mystery associated with these techniques was rapidly dispelled. This effort has since been repaid many times by the power and flexibility which these graphical methods provide for the rock engineer.

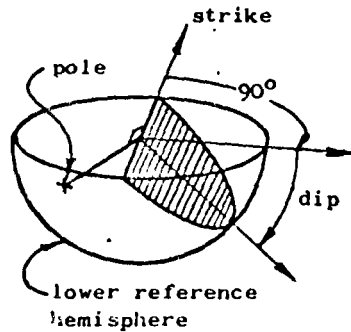
Several types of spherical projection can be used and a comprehensive discussions on these methods have been given by Phillips⁴³, Turner and Weiss³⁶, Badgley⁴⁴ and Friedman⁴⁵. The projection which is used exclusively in this book is the *equal area projection*, sometimes called the Lambert projection or the Schmidt net.



Equal-area projection

The Lambert equal area projection will be familiar to most readers as the system used by geographers to represent the spherical shape of the earth on a flat surface. In adapting this projection to structural geology, the traces of planes on the surface of a reference sphere are used to define the dips and dip directions of the planes. Imagine a reference sphere which is free to move in space but which is *not* free to rotate in any direction; hence any radial line joining a point on the surface to the centre of the sphere will have a fixed direction in space. If this sphere is now moved so that its centre lies on the plane under consideration, the great circle which is traced

out by the intersection of the plane and the sphere will uniquely define the inclination and orientation of the plane in space. Since the same information is given on both upper and lower parts of the sphere, only one of these need be used and, in engineering applications, the *lower reference hemisphere* is used for the presentation of data.



In addition to the great circle, the inclination and orientation of the plane can also be defined by the *pole* of the plane. The pole is the point at which the surface of the sphere is pierced by the radial line which is normal to the plane.

In order to communicate the information given by the great circle and the position of the pole on the surface of the lower reference hemisphere, a two dimensional representation is obtained by projecting this information onto the horizontal or equatorial reference plane. The method of projection is illustrated in Figure 12a and 12b, illustrates the polar and equatorial projections of a sphere.

Polar and equatorial equal-area nets are presented in Figure 13 for use by the reader. Good undistorted copies or photographs of these nets will be useful in following the examples given in this chapter and later in the book.

The most practical method of using the stereonet for plotting structural information is to mount it on a base-board of $\frac{1}{4}$ inch thick plywood as shown in Figure 14. A sheet of clear plastic film of the type used for drawing on for overhead projection, mounted over the net and fixed with *sellotape* around its edges, will keep the stereonet in place and will also protect the net markings from damage in use. The structural data is plotted on a piece of tracing paper or film which is fixed in position over the stereonet by means of a carefully centred pin as shown. The tracing paper must be free to rotate about this pin and it is essential that it is located accurately at the centre of the net otherwise significant errors will be introduced into the subsequent analysis.

Before starting any analysis, the North point must be marked on the tracing so that a reference position is available.

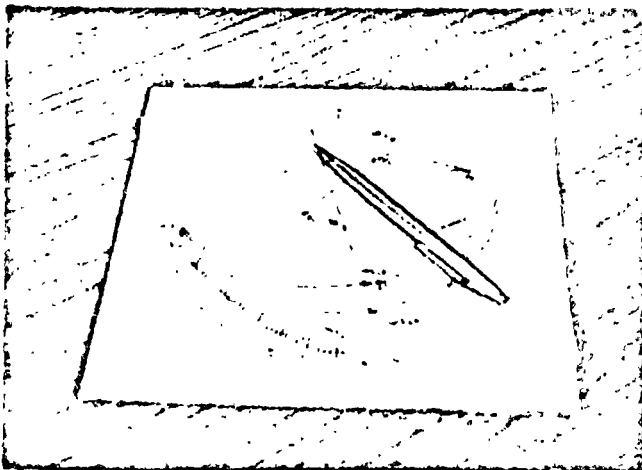


Figure 14:

Geological data is plotted and analysed on a piece of tracing paper which is located over the centre of the stereonet by means of a centre pin as shown. The net is mounted on a base-board of plywood or similar material.

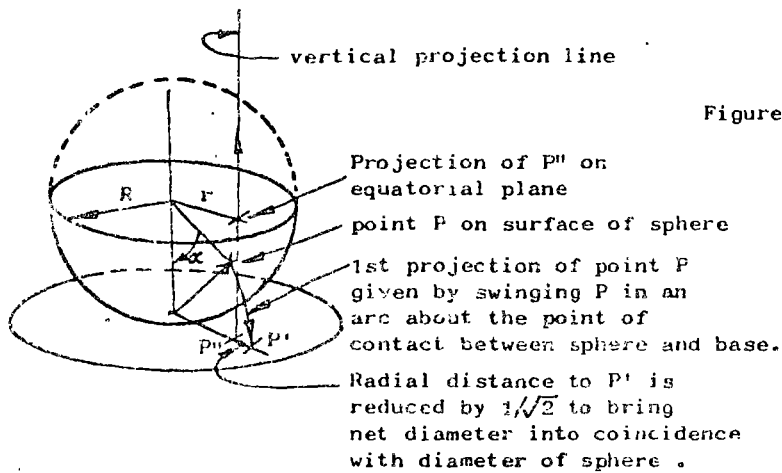


Figure 12a : Method of construction of an equal-area projection.

The radial distance r of the projected point P'' on the stereonet is given by :

$$r = \sqrt{2} \cdot R \sin \frac{\alpha}{2}$$

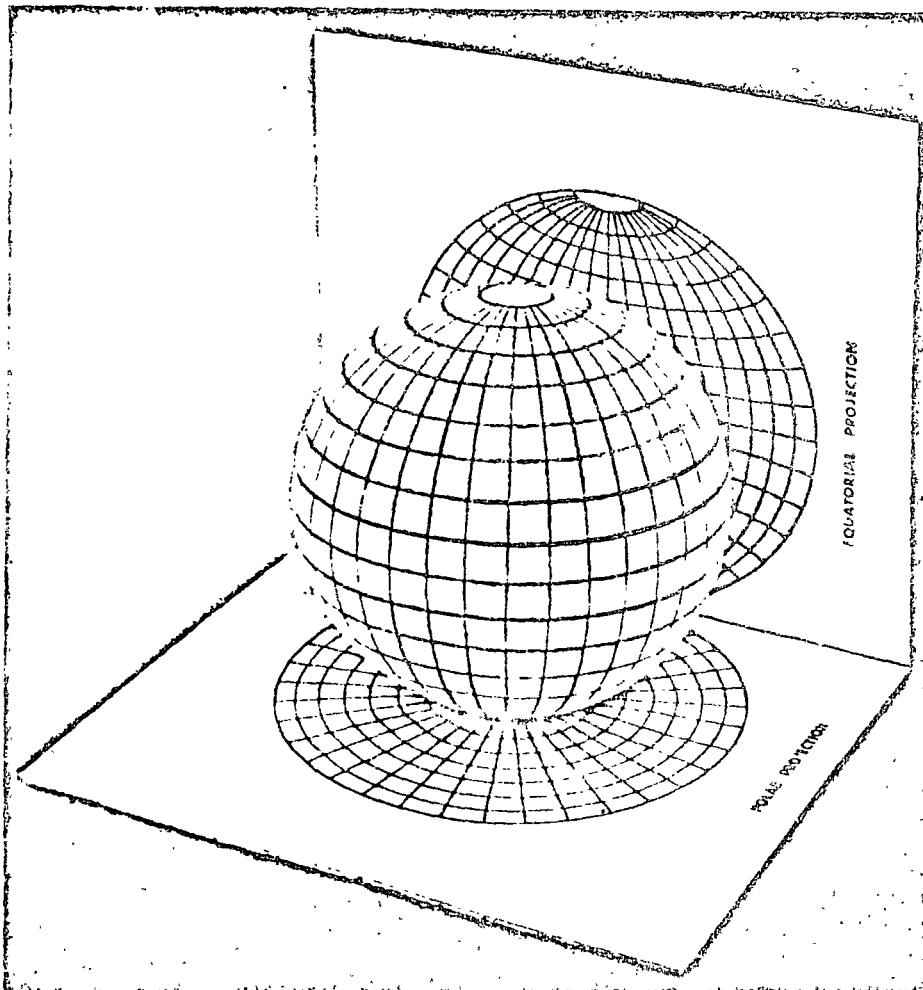


Figure 12b: Polar and equatorial projections of a sphere.

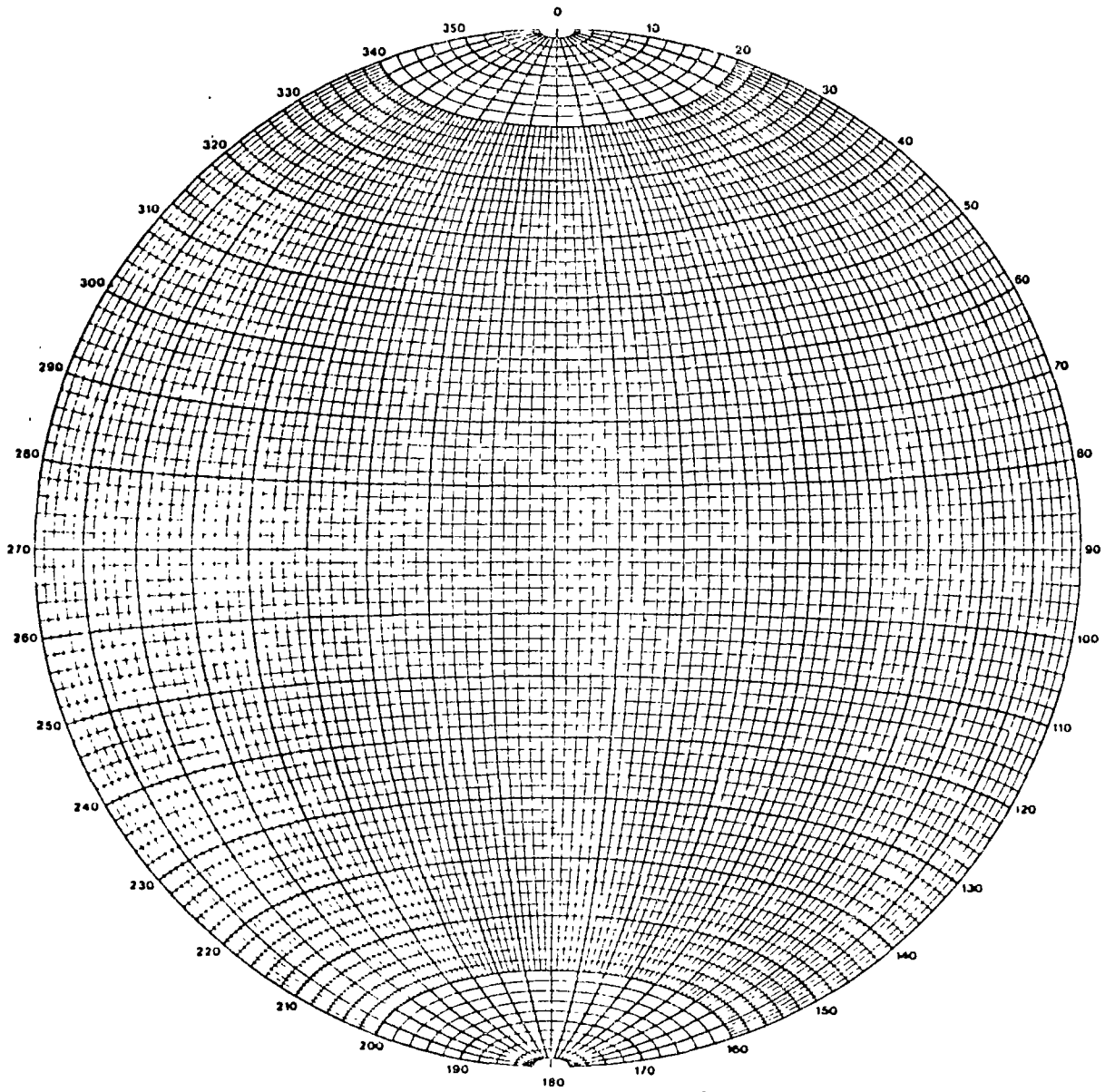


Figure 13a : Equatorial equal-area stereonet marked in 2° intervals. This net is most useful for the construction of great circles during the analysis of structural data.

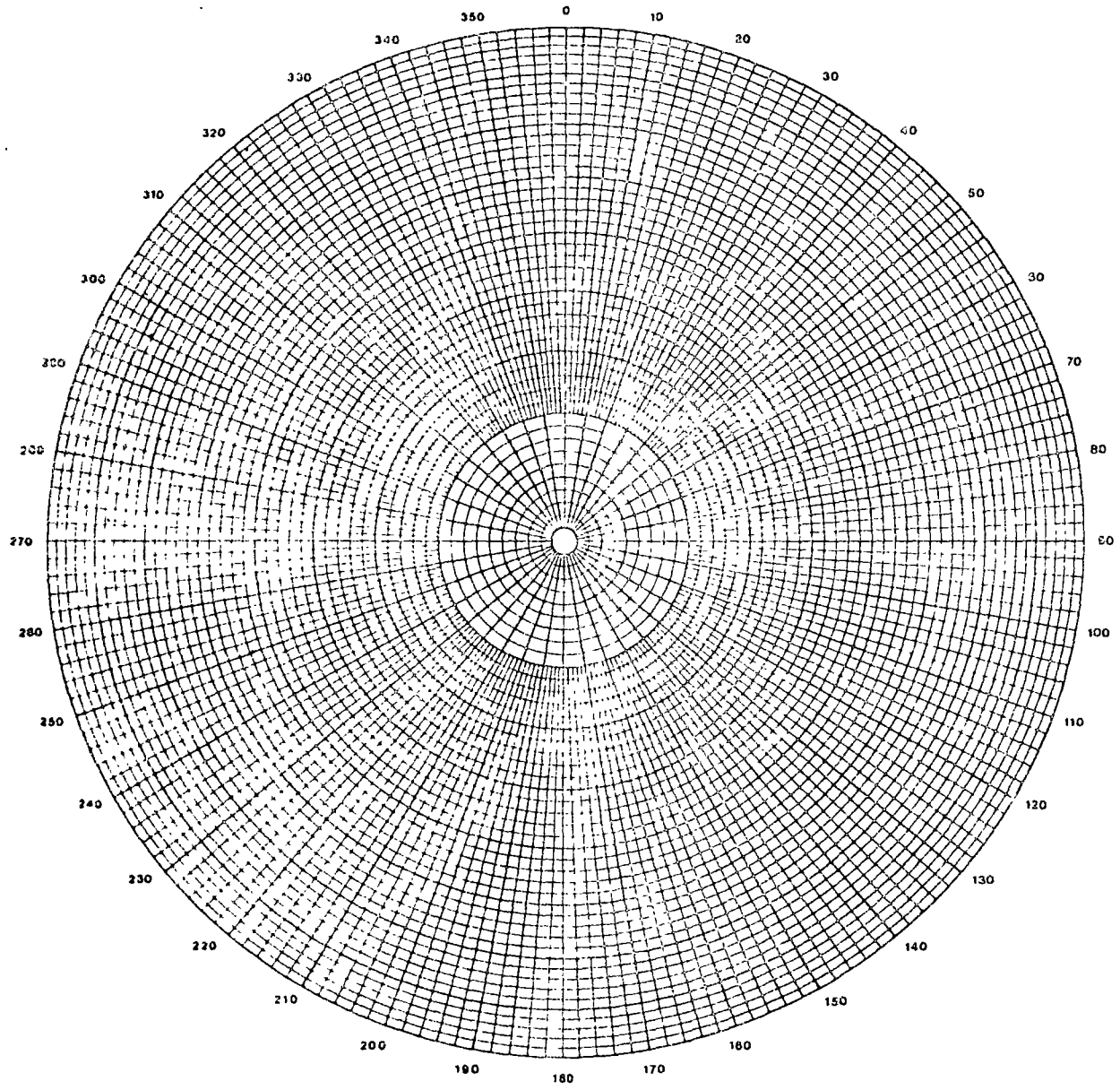
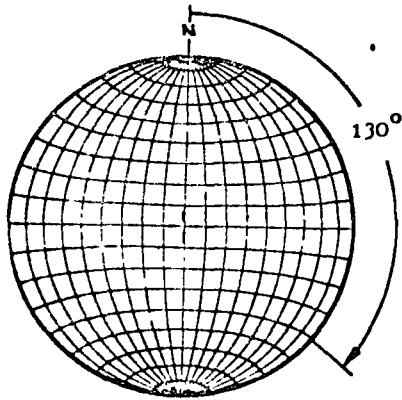


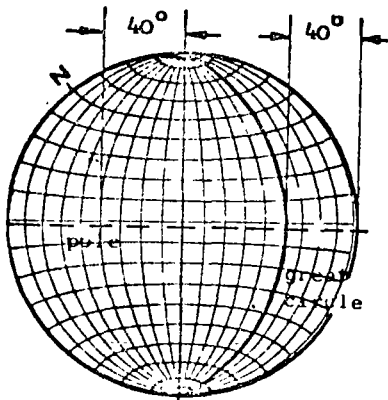
Figure 13b : Polar equal-area stereonet marked in 2° intervals.
This net is used for plotting poles of planes during
the analysis of structural data.



Construction of a great circle and a pole representing a plane.

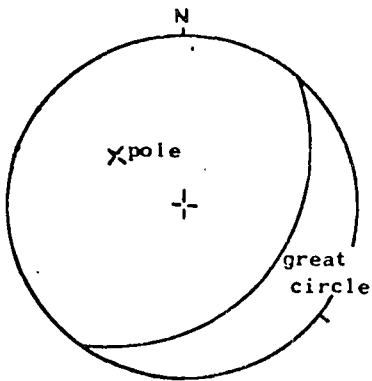
Consider a plane dipping at 40° in a dip direction of 130° . The great circle and the pole representing this plane are constructed as follows:

Step 1: With the tracing paper located over the stereonet by means of the centre pin, trace the circumference of the net and mark the north point. Measure off the dip direction of 130° clockwise from north and mark this position on the circumference of the net.

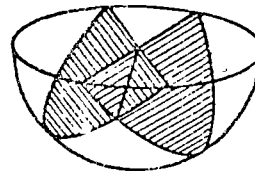


Step 2: Rotate the tracing about the centre pin until the dip direction mark lies on the W-E axis of the net, i.e. the tracing is rotated through 40° . Measure off 40° from the outer circle of the net and trace the great circle which corresponds to a plane dipping at this angle.

The position of the pole, which has a dip of $(90^\circ - 40^\circ)$, is found by measuring off 40° from the centre of the net as shown or, alternatively, 50° from the outside of the net. The pole lies on the projection of the dip direction line which, at this stage in the construction, is coincident with the W-E axis of the net.

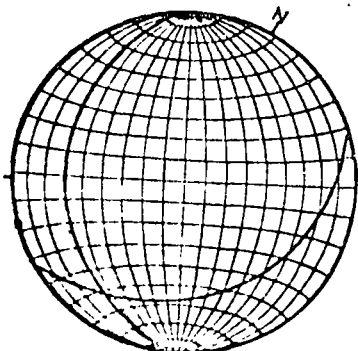


Step 3: The tracing is now rotated back to its original position so that the north mark on the tracing coincides with the north mark on the net. The final appearance of the great circle and the pole representing a plane dipping at 40° in a dip direction of 130° is as illustrated.

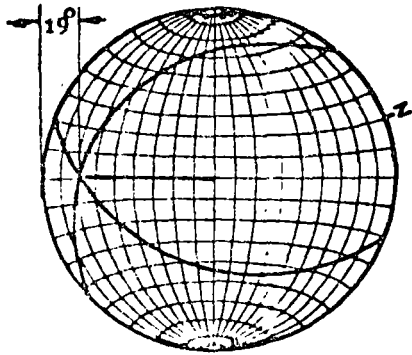


Determination of the line of intersection of two planes

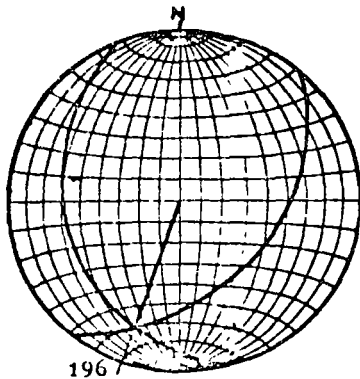
Two planes, having dips of 40° and 30° and dip directions of 130° and 250° respectively, intersect. It is required to find the dip and dip direction of the line of intersection.



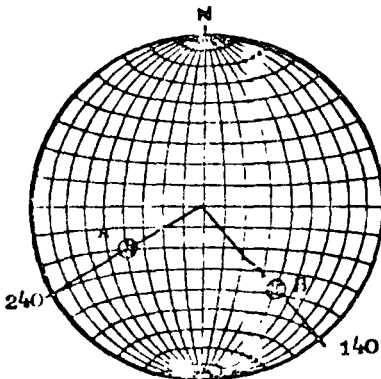
Step 1: One of these planes has already been described above and the great circle defining the second plane is obtained by marking off the 250° dip direction on the circumference of the net, rotating the tracing until this mark lies on the W-E axis and tracing the great circle corresponding to a dip of 30° .



Step 2: The tracing is now rotated until the intersection of the two great circles lies along the W-E axis of the stereonet and the dip of the line of intersection is measured as 19° .



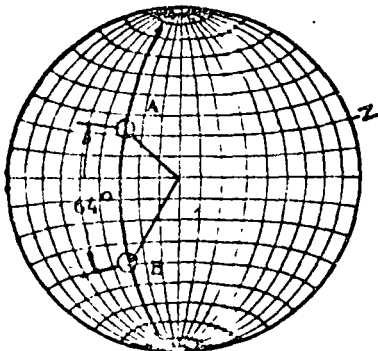
Step 3: The tracing is now rotated until the north mark coincides with the north point on the stereonet and the dip direction of the line of intersection is found to be 196° .



To determine the angle between two specified lines.

Two lines in space, e.g. lines of intersection or normals to planes, are specified by dips of 54° and 40° and dip directions of 240° and 140° respectively. It is required to find the angle between these lines.

Step 1: The points A and B which define these lines are marked on the stereonet as described under the procedure for locating the pole.

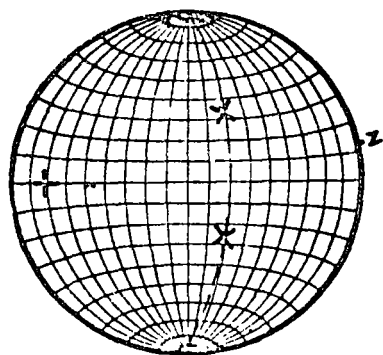
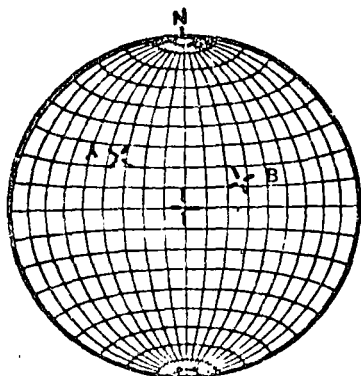


Step 2: The tracing is now rotated until these two points lie on the same great circle on the stereonet and the angle between the lines is determined by counting the small circle divisions between A and B, along the great circle. This angle is found to be 64° .

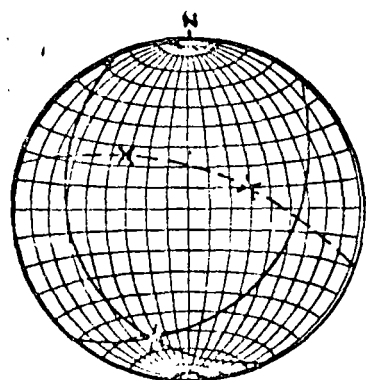
The great circle on which A and B lie defines the plane which contains these two lines and the dip and dip direction of this plane are found to be 60° and 200° respectively.

Alternative method for finding the line of intersection of two planes.

Two planes, dipping at 40° and 30° in dip directions of 130° and 250° respectively are defined by their poles A and B as shown. The line of intersection of these two planes is defined as follows:



Step 1: Rotate the tracing until both poles lie on the same great circle. This great circle defines the plane which contains the two normals to the planes.

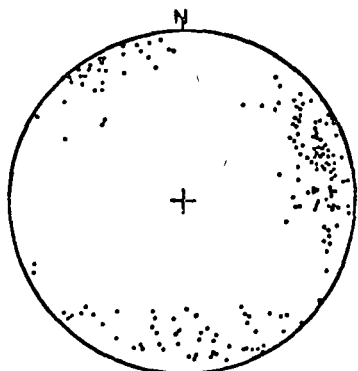


Step 2: Find the pole of this plane by measuring off the dip on the W-E axis of the stereonet. This pole P defines the normal to the plane containing A and B and, since this normal is common to both planes, it is, in fact, the line of intersection of the two planes.

Hence, the pole of a plane which passes through the poles of two other planes defines the line of intersection of those planes.

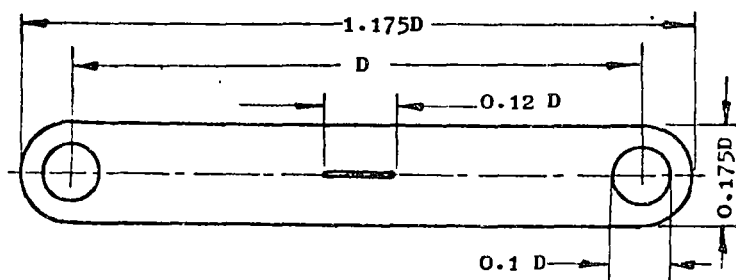
Determination of preferred orientations of discontinuity sets.

In plotting field observations of dip and dip direction, it is convenient to work in terms of poles rather than great circles since, when the number of observations exceeds about 10, the plot of great circles can be very confusing. Even when the information is plotted in terms of poles, using a polar stereonet, the overall picture, as shown opposite, can be confusing and requires additional interpretation.



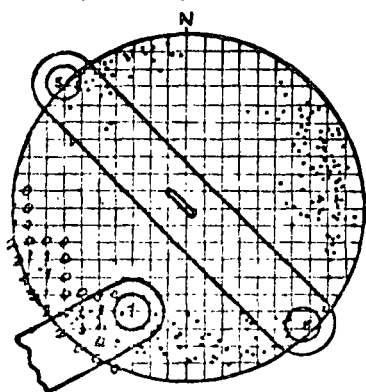
In order to identify the preferred orientations of systems of structural discontinuities from a pole plot such as that shown, a number of contouring techniques are available. One of these techniques will be described and the reader requiring further details on these methods is referred to texts such as that by Turner and Weiss³⁶.

Schmidt or grid method

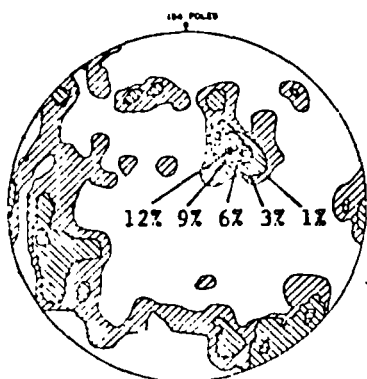


Schmidt point counter machined from 1.5 mm thick perspex sheet. Dimensions are given in multiples of D, the diameter of the stereonet.

The basic tool required for this contouring method is a transparent counter such as that illustrated above. These counters are not commercially available but can easily be machined from a sheet of perspex or similar material. The dimensions of the counter are given in terms of the stereonet diameter which, for this application, would normally be 15 to 20 cms. The centre slot is end-milled or cut with a fret-saw and should be approximately 1 mm wide.



The tracing, on which the poles have been plotted, is placed over a grid with lines spaced at one-twentieth of the grid diameter (i.e. a 1 cm grid for a 20 cm stereonet). With the centre of one of the circular holes at the end of the counter centred on a grid intersection, the number of poles falling within the circle is counted and this number is written on the grid intersection. The counting circle is moved to successive grid points and the count noted at each point. Where poles fall very close to the periphery of the stereonet, the counter is located with its centre slot over the centre pin of the stereonet and poles falling within both circles are counted as shown. The total number of poles in the two circles is noted at both intersection points.



Once the counting has been completed and all the counts noted at intersection points, contouring is carried out by joining intersection points having the same number written over them. The contour values are determined from the individual pole counts divided by the total number of poles on the stereonet. Hence, in the example given, the total number of poles is 134 and the line joining intersections with 8 poles represents the 6% contour. Similarly, 16 poles corresponds to 12% and 4 poles to 3%. The contour intervals are normally shaded as shown in order to assist the user in rapid identification of significant pole concentrations.

Evaluation of potential slope problems

Different types of slope failure are associated with different geological structures and it is important that the slope designer should be able to recognise potential stability problems during the early stages of a project. Some of the signs which should be watched for when examining stereoplots of the structural data are outlined on the following pages and a test for the possibility of sliding on one or more discontinuity is described.

Figure 15 shows the four main types of failure considered in this book and gives the appearance of typical stereoplots of geological conditions likely to lead to such failures. Note that in assessing stability, the cut face of the slope must be included in the stereoplot since sliding can only occur as a result of movement towards the free face created by the cut.

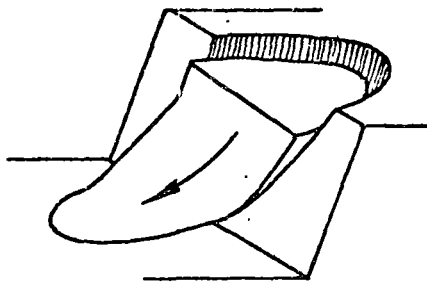
The diagrams given in Figure 15 have been simplified for the sake of clarity. In an actual rock slope, combinations of several types of geological structures may be present and this may give rise to additional types of failure. For example, presence of discontinuities which can lead to toppling as well as planes upon which wedge sliding can occur could lead to the sliding of a wedge which is separated from the rock mass by a "tension crack".

In a typical field study in which structural data has been plotted on stereonets, a number of significant pole concentrations may be present. It is useful to be able to identify those which represent potential failure planes and to eliminate those which represent structures which are unlikely to be involved in slope failures. John⁴⁶, Panet⁴⁷ and McMahon²³ have discussed methods for identifying important pole concentration but the author prefers a method recently developed by Markland⁴⁸.

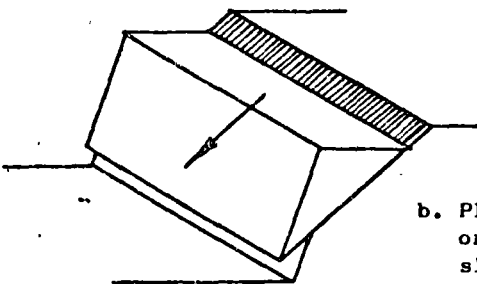
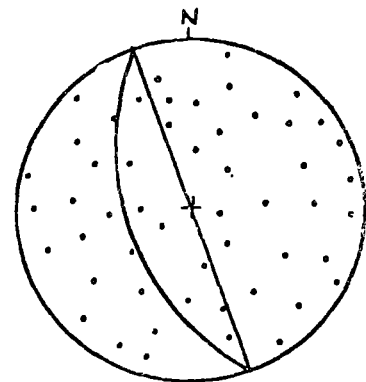
Markland's test, described hereunder, is to establish the possibility of a wedge failure in which sliding takes place along the line of intersection of two planar discontinuities as illustrated in Figure 15c. Plane failure, Figure 15b, is also covered by this test since it is a special case of wedge failure. If contact is maintained on both planes, sliding can only occur along the line of intersection and hence this line of intersection must "daylight" in the slope face. In other words, the dip of the line of intersection must be less than the dip of the slope face, measured in the direction of the line of intersection as shown in Figure 16a.

As will be shown in the chapter dealing with wedge failure, the factor of safety of the slope depends upon the dip of the line of intersection, the shear strength of the discontinuity surfaces and the geometry of the wedge. The limiting case occurs when the wedge degenerates to a plane, i.e. the dips and dip direction of the two planes are the same, and when the shear strength of this plane is due to friction only. As already discussed, sliding under these conditions occurs when the dip of the plane exceeds the angle of friction ϕ and hence, a first approximation of wedge stability is obtained by considering whether the dip of the line of intersection exceeds the friction angle for the rock surfaces. Figure 16b shows that the slope is potentially unstable when the point defining the line of intersection of the two planes falls within the area included between the great circle defining the slope face and the circle defining an infinite series of planes (a cone) all dipping at the angle of friction ϕ .

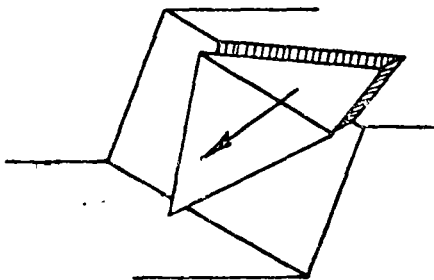
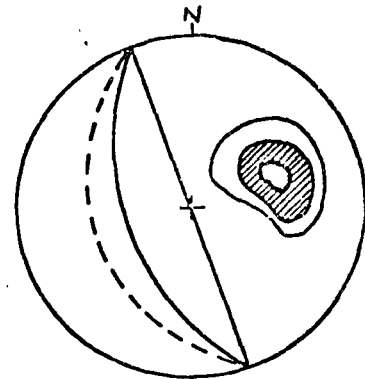
The reader who is familiar with wedge analysis will argue that this area can be further reduced by allowing for the influence of "wedging" between the two discontinuity planes. On the other hand, the stability may be decreased if water is present in the slope. Experience suggests that these



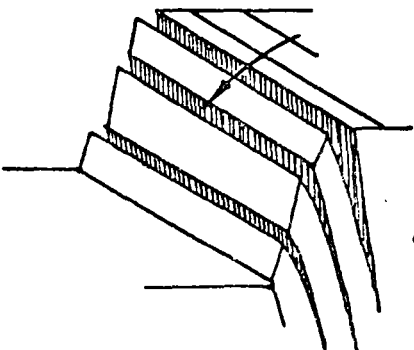
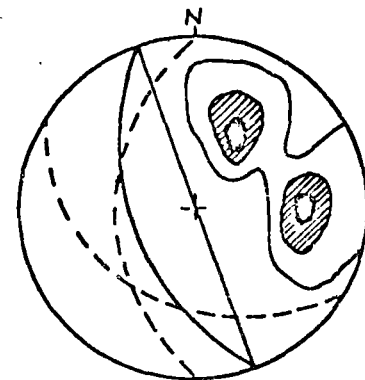
a. Circular failure in overburden soil, waste rock or heavily fractured rock with no identifiable structural pattern.



b. Plane failure in highly ordered structure such as slate.



c. Wedge failure on two intersecting discontinuities.



d. Toppling failure in hard rock which can form columnar structures separated by steeply dipping discontinuities.

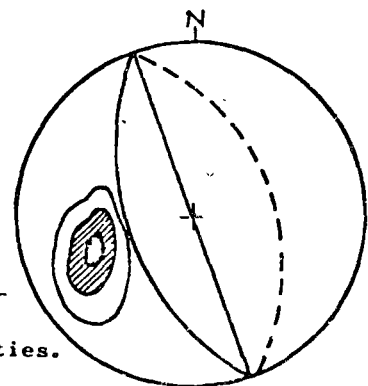


Figure 15 : Main types of slope failure and appearance of stereoplots of structural conditions likely to give rise to these failures.

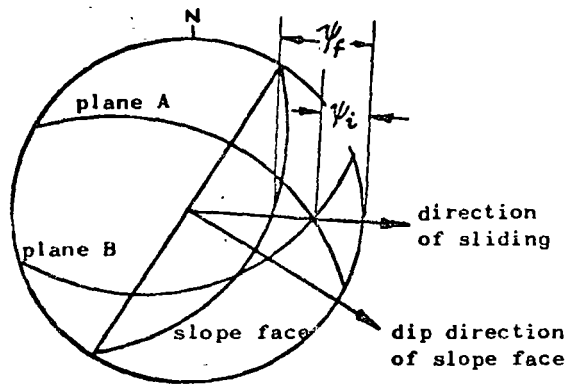


Figure 16a : Sliding along the line of intersection of planes A and B is possible when the dip of this line is less than the dip of the slope face, measured in the direction of sliding, i.e. $\psi_f > \psi_i$.

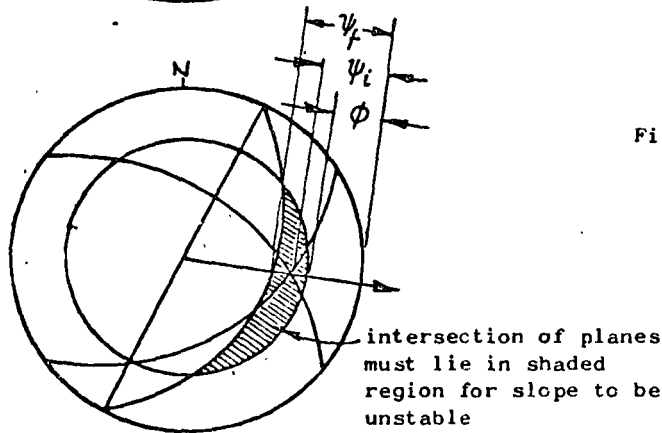


Figure 16b : Sliding is assumed to occur when the dip of the line of intersection exceeds the angle of friction, i.e. when $\psi_f > \psi_i > \phi$.

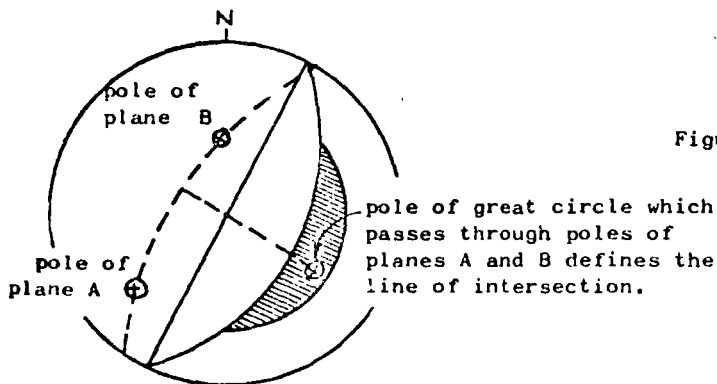


Figure 16c : Representation of planes by their poles and determination of the line of intersection by the pole of the great circle which passes through these poles.

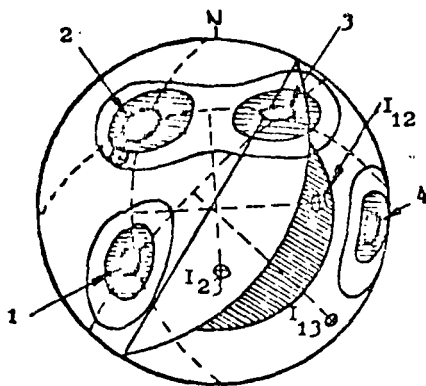
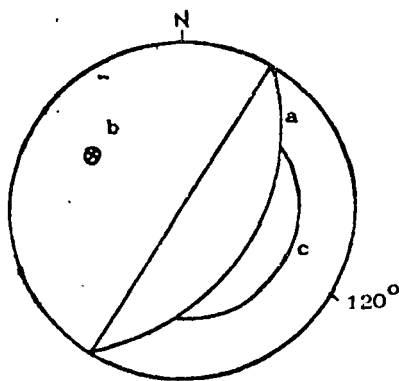


Figure 16d : Preliminary evaluation of the stability of a 50° slope in a rock mass with 4 sets of structural discontinuities.

two factors will tend to cancel one another in typical wedge problems and that the crude assumption used in deriving Figure 16b is adequate for most practical problems. It should be remembered that this test is designed to identify critical discontinuities and, having identified them, a more detailed analysis would normally be necessary in order to define the factor of safety of the slope.

Figures 16a and 16b show the discontinuity planes as great circles but, as has been discussed on the previous pages, field data on these structures is normally plotted in terms of poles. In Figure 16c the two discontinuity planes are represented by their poles and, in order to find the line of intersection of these planes, the method described on page 47 is used. The tracing on which the poles are plotted is rotated until both poles lie on the same great circle. The pole of this great circle defines the line of intersection of the two planes.



Overlay for checking possibility of wedge failures .

As an example of the use of this test consider the contoured stereoplot of poles given in Figure 16d. It is required to examine the stability of a slope face with a dip of 50° and dip direction of 120° . A friction angle of 30° is assumed for this analysis. An overlay is prepared on which the following information is included:

- a. The great circle representing the slope face
- b. The pole representing the slope face
- c. The friction circle.

This overlay is placed over the contoured stereoplot and the two are rotated together over the stereonet to find great circles passing through pole concentrations. The lines of intersection are defined by the poles of these great circles as shown in Figure 16d. From this figure it will be seen that the most dangerous combination of discontinuities is that represented by the pole concentrations numbered 1 and 2. The intersections I_{23} and I_{13} both fall outside the critical area and are not likely to give rise to instability. The pole concentration numbered 4 will not be involved in sliding but, as shown in Figure 15d, it could give rise to toppling or the opening of tension cracks.

In the example described above, it would be necessary to examine this slope, and particularly discontinuities 1 and 2, in more detail to establish whether the critical conditions suggested by this preliminary analysis do indeed exist or whether there are other factors which increase the stability of the slope.

In cases where only one major pole concentration occurs as in Figure 15b, plane failure is possible if this concentration lies close to the pole of the slope face. In the example given in Figure 16d, pole concentration 2 lies sufficiently close to the pole of the slope face for two dimensional sliding to be considered a possibility and to justify a more detailed examination of this possibility.

Suggested method of data presentation and analysis for open pit planning.

During the early feasibility studies on a proposed open pit mine, an estimate of safe slope angles is required for the calculation of ore to waste ratios and for the preliminary pit layout. The only structural data which is likely to be available at this stage is that which has been obtained by logging cores drilled for mineral evaluation purposes and by mapping surface outcrops. Scanty as this data is, it does provide a basis for a first estimate of potential slope problems and the author suggests that this data should be treated in the manner illustrated in Figure 17.

On an outline plan of the proposed open pit, contoured stereoplots of whatever structural data is available are drawn. These plots are drawn at the location of the field observations and should, where possible, be evenly spaced around the pit perimeter. It is particularly important that areas of major faulting or areas in which changes of rock type occur should be mapped.

An overlay is prepared as described earlier and, in Figure 17, it has been assumed that the stability of 45° slopes is to be checked. Where the geological mapping has indicated the presence of faults or clay seams, a friction angle of 20° should be used to define the friction circle. Where no such structures appear to be present, a friction angle of 30° is more realistic and this is the value used in Figure 17.

The eastern side of the hypothetical porphyry-copper pit illustrated in Figure 17 does not contain structures which are unfavourable to stability and, since porphyry is a good hard rock, steepening of these slopes can be considered. Figure 7 on page 20 can be used as a guide to the maximum permissible slope angle for a given pit depth.

Note that the structures which occur in the south-eastern part of the pit could give rise to toppling failure if steep slopes are created (see Figure 15d). This possibility should be kept in mind as the pit planning progresses and a further analysis carried out if required.

The structures in the south-western part of the pit are not critical but there are bound to be local discontinuities which will cause small wedge slides on individual benches. This would be particularly true for the porphyry/slate contact. Since flattening of the slate slopes is essential, it would be wise to start this flattening in the south-western corner of the pit.

The most critical area in this particular pit will be the western slopes where the slate dips into the pit at about the same angle as the slopes (note that the pole concentration coincides with the pole of the slope face - a critical limiting condition for two-dimensional sliding). It would be essential to carry out further investigations in this part of the pit. Additional drilling to check the extent of the slate, groundwater studies and shear testing of discontinuity planes would all be necessary. A detailed stability analysis, using methods described in later chapters, would have to be carried out to establish the safe slope angles for this part of the pit.

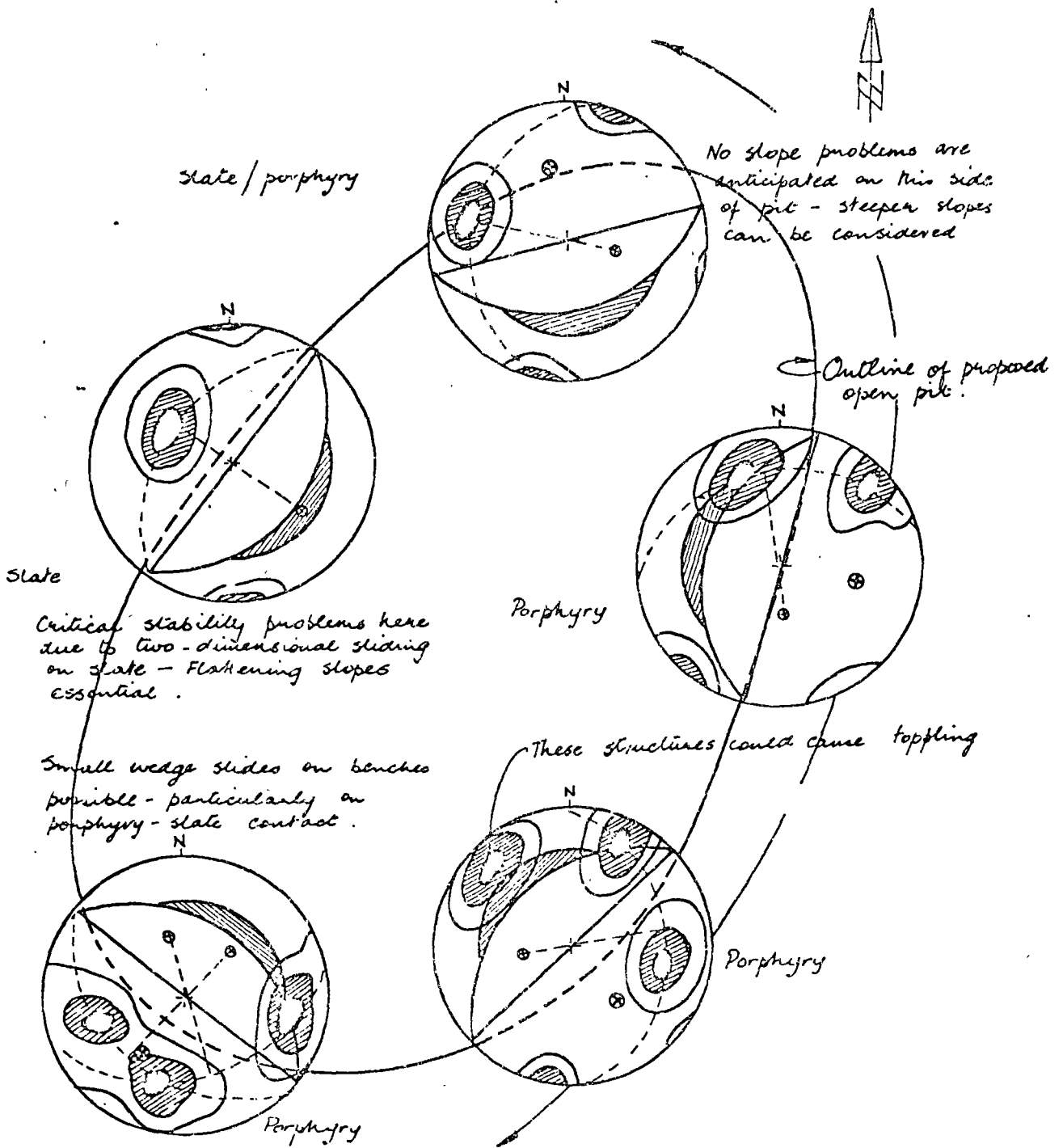


Figure 17 : Presentation of geological data and preliminary analysis of slope stability for feasibility study on hypothetical open pit mine.



centro de educación continua
división de estudios superiores
facultad de ingeniería, unam



MECANICA DE ROCAS APLICADA A LA MINERIA

LEVANTAMIENTO DE DATOS GEOLOGICOS-ESTRUCTURALES

ABRIL, 1978.

Palacio de Minería

Calle de Tacuba 5,

primer piso.

México 1, D. F.

PROCEDURES USED FOR SAMPLING FRACTURE ORIENTATIONS IN AN UNDERGROUND COAL MINE

by

D. D. Bolstad,¹ J. R. Alldredge,² and M. A. Mahtab³

ABSTRACT

The Bureau of Mines has developed procedures for sampling the geometry of fractures in underground coal mines. Stratified cluster sampling and the unit area concept are applied to the collection of fracture orientation data. The use of unit area mapping, stratification, and site delineation is made to assure collection of representative data. The procedures developed here help to isolate sources of variability in the fracture patterns.

INTRODUCTION

Fractures are planes of weakness in a rock mass, and very often their geometric patterns (attitude, spacing, extent, and aperture) influence the mechanical behavior of excavated structures in the fractured medium. During the past decade, numerical techniques have been increasingly and successfully employed for stability analyses of engineered structures in fractured media. The sophistication of the numerical techniques has increased the need for quantitative and reliable input information regarding fracture geometry. Some appropriate schemes for quantifying the geometric characteristics of fractures have recently become available (2).⁴ However, no systematic and acceptable procedures are available for sampling fracture patterns in subsurface excavations.

As part of the Bureau's investigation of the influence of fractures on coal mine roof behavior, the Bureau developed and used procedures for sampling fracture orientations in selected underground coal mines. One of the several mines selected for the roof behavior study was Duquesne Light Co. Warwick mine Portal No. 3, Greensboro, Pa. The objective of sampling fracture orientations in this mine was limited to correlating natural fracture⁵ orientations with roof falls. To meet this objective, sampling procedures were

¹Geologist.

²Mathematical statistician.

³Physical scientist.

⁴Underlined numbers in parentheses refer to items in the list of references at the end of this report.

⁵Natural fractures are defined as recurrent planar geologic discontinuities having spacings of from tenths of a foot to tens of feet.

devised (1) to extract information on fracture orientations from a relevant (small) portion of the mine (called the study area) and (2) to provide a statistical background for estimating the mean fracture orientations in the study area. This report discusses the procedures used by the Bureau for sampling fracture orientations in Warwick mine Portal No. 3.

ACKNOWLEDGMENTS

The authors wish to thank the management of Duquesne Light Co., Pittsburgh, Pa., for permission to collect data on geometry of fractures in their Warwick mine Portal No. 3.

GENERAL SAMPLING PROCEDURES

Three main steps were followed in the development of the sampling procedures: (1) Defining the factors that might affect the sample, (2) obtaining and analyzing a preliminary sample, and (3) obtaining and analyzing the final sample and presenting the results in a form useful for engineering analysis. (In this example the analysis involved correlating fracture orientations with roof falls.) The general procedures followed in this study are illustrated in the flowsheet shown in figure 1. These procedures may be readily interpreted to fit the objectives of other problems involving sampling of attitudes, spacings, extents, and apertures of fractures in underground mines; for example, a recent Bureau of Mines study (3) described application of these procedures in an underground copper porphyry mine in Arizona. The methods of sampling may also be applied to problems relating to other planes of weakness, such as fault traces, blasting fracture patterns, and bedding plane partings.

This report emphasizes the following sampling concepts:

1. Cluster sampling, where a cluster consists of all the fractures in a small division of the study area. The clusters will be referred to as unit areas.
2. Stratified sampling, where the study area is separated into blocks or strata. The term strata is used here in a statistical rather than a geological sense.

The concepts of cluster sampling and stratified sampling are combined to result in a stratified cluster sampling plan. This is a common sampling plan used in many other fields of study.

RECONNAISSANCE

This section outlines the geologic setting of the Warwick mine Portal No. 3 and describes the geologic and layout factors recognized during a short reconnaissance of the mine (one engineer and one geologist spent a day visiting the mine). The objective of the reconnaissance was to select several areas for preliminary sampling on the basis of the observed differences in their geologic and engineering characteristics.

The Warwick mine Portal No. 3 is located within a region of gently dipping NNE-trending anticlines and synclines composed of sandstones, shales,

and coal seams of Pennsylvanian-Permian age. Major faulting is lacking in this region.

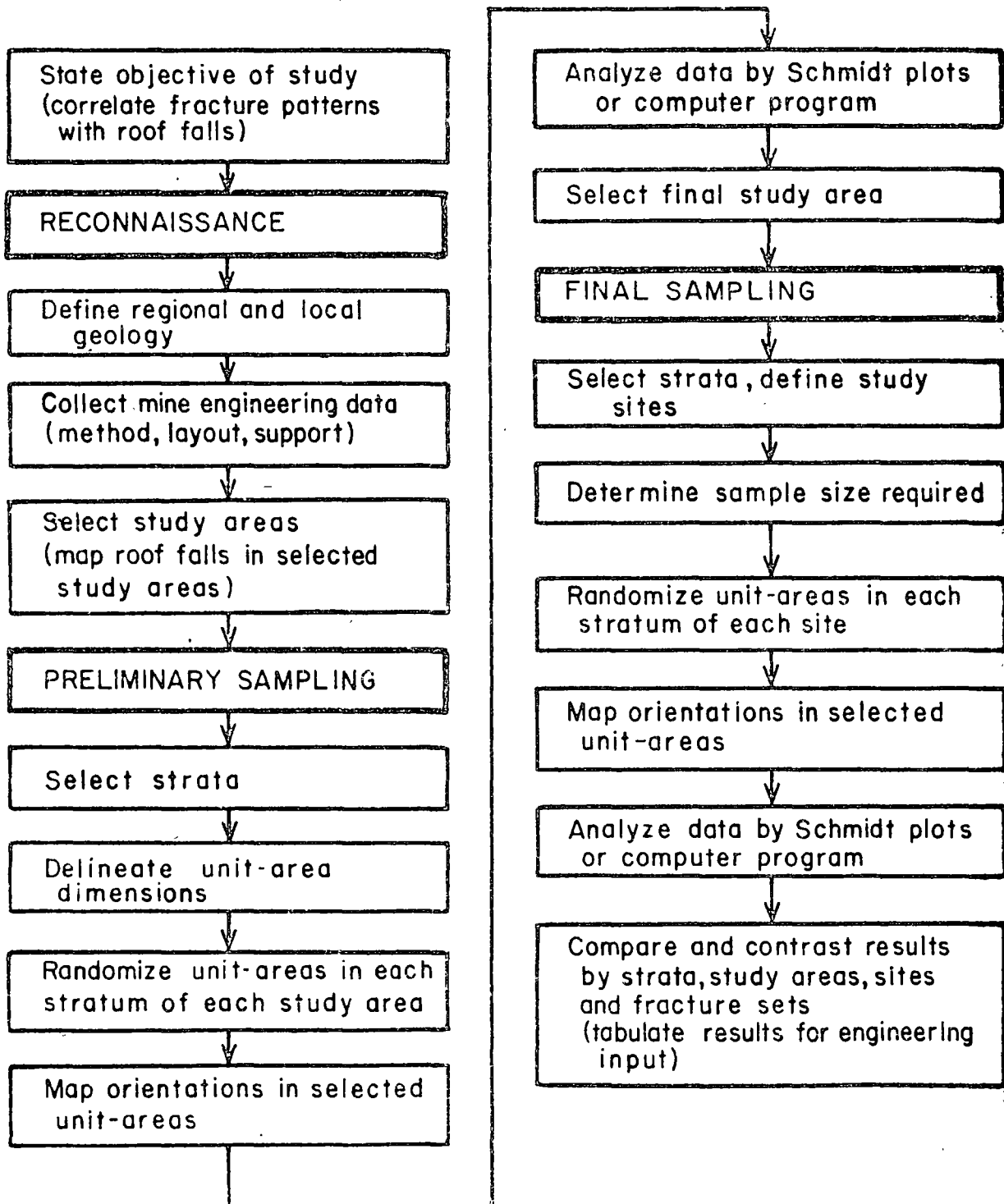


FIGURE 1. - Procedures followed for sampling fracture orientations in an underground coal mine.

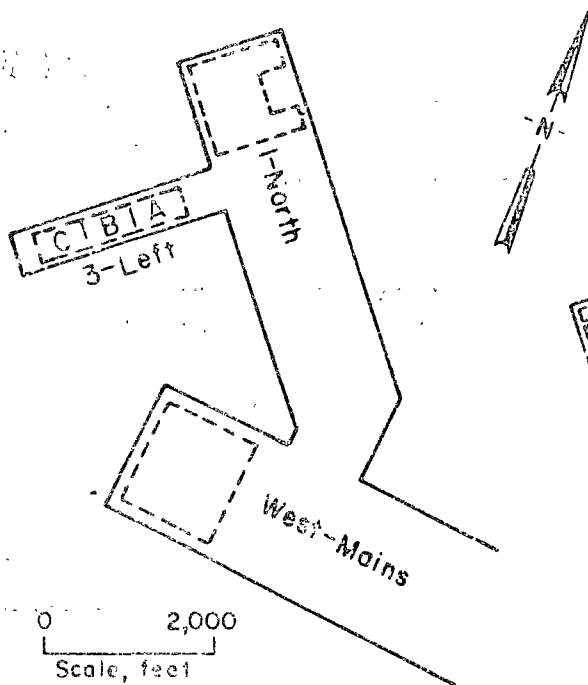


FIGURE 2. - General plan of Warwick mine Portal No. 3.

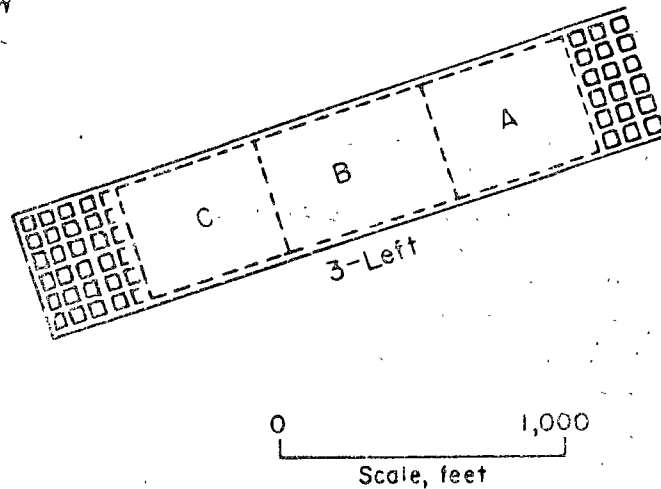


FIGURE 3. - Division of the study area into sites.

A nearly orthogonal system of vertical roof fractures was observed throughout the Warwick mine Portal No. 3. The shale roof appeared to have no major observable structural or lithologic discontinuities. The coal cleat system paralleled the roof fracture system and had well-defined face and butt cleats. Three major mining areas were active (fig. 2); they were the 1-North, 3-Left, and West-Mains entry systems. Since the objective of the fracture orientation mapping study was to correlate roof falls with the patterns of natural fractures, the three active areas were selected for preliminary sampling, as these areas would afford a greater probability of observing natural fractures than would the inactive areas.

PRELIMINARY SAMPLING

The purpose of the preliminary sampling was to supply information about the geometry of the fracture patterns and to provide measures of the natural variability present within and between selected areas. This information was then used to design the final sampling plan. This section describes the design of the preliminary sampling plan and reports results of the preliminary sampling.

Design of the Preliminary Sampling Plan

Prior to mapping the fractures, the factors that might influence the results of the study were identified, and a sampling plan was designed to take account of these factors. For example, the effect of relative location, study-area sizes, ferromagnetic influences, difference in rock type, variability

of roof-fall areas, and operator bias were considered in designing the sampling plan.

Each study area (1-North, 3-Left, West-Mains) was defined on the basis of equivalent size and quantity of available entries and crosscuts. These study areas were sampled and analyzed independently to examine the effect of relative location on fracture orientations. Each study area encompassed 70 to 80 pillars, exclusive of return airways and actual working faces. The entries and crosscuts were approximately 20 ft wide and were driven on 70-ft centers. The general absence of ferromagnetic influences within the study areas allowed the use of a standard Brunton compass for orientation measurements.

Each study area was divided into (statistical) strata based on rock type and unsupported span dimensions. The three strata were (1) coal ribs, (2) shale roof between ribs, and (3) shale roof at intersections. This is an application of stratified sampling. However, since unit areas (clusters) are being sampled, this plan is referred to as stratified cluster sampling. A cluster, as defined in this study, consists of all the fractures within a unit area. In the unit area technique each (statistical) stratum is divided into many small areas. In this study, 5-ft-square unit areas⁶ were delineated on all coal ribs, and 20-ft-square unit areas were delineated in the shale roof between the ribs and in the shale roof at intersections. The unit area technique was used in preference to the line of traverse method because the latter method is biased against the fractures paralleling the line. In addition, the unit area technique allows a comparison of fracture-set geometries between individual areas and groups of areas.

In this study the unit areas in each stratum within the study areas were numbered for identification on mine maps. A random-number table was used to select two roof-intersection unit areas, four roof-between-the-ribs unit areas, and four coal-rib unit areas for mapping in each study area. This sample size was based on the time available for mapping during the preliminary phase. The unit areas were randomized to insure that an unbiased and representative sample of the area under study was obtained.

Results of the Preliminary Sampling

After mapping, fracture sets were identified from the data and their mean attitudes were calculated using a computer program (2). Table 1 lists the results of an analysis of preliminary sample. Two major fracture sets were prevalent throughout the three study areas. No major differences in the mean attitudes of fracture sets were found in a comparison of the three study areas. Because of this, it was decided to concentrate the final sampling efforts in just one study area. Since the 1-North study area contained a large air shaft whose effect on the neighboring fracture patterns was unknown, and since the access within the West-Mains study area was impaired, the final sampling was conducted in the 3-Left study area. The final sampling (and

⁶The choice of a square shape was convenient. The side of a square unit area was given by the height (5 ft) or width (20 ft) of the entries.

analysis) of the fracture orientations in the 3-Left study area are discussed in the next section.

TABLE 1. - Summary of fracture orientations obtained during preliminary sampling

Fracture set	Study area								
	West-Mains			3-Left			1-North		
	Azimuth, degrees	Dip, degrees	C, ¹ degrees	Azimuth, degrees	Dip, degrees	C, ¹ degrees	Azimuth, degrees	Dip, degrees	C, ¹ degrees
Set 1:									
Coal ²	203	88	-	25	87	1.8	202	88	1.6
Roof ³	197	88	3.2	09	90	2.3	192	88	2.6
Intersection ⁴	193	89	5.4	191	86	4.0	195	87	3.5
Set 2:									
Coal.....	113	89	-	116	83	3.1	116	87	3.9
Roof.....	115	90	9.8	(⁵)	(⁵)	(⁵)	110	88	5.5
Intersection	(⁵)	(⁵)	(⁵)	98	89	14.2	120	88	14.1

¹Apex angle of the cone around the sample mean (as its axis) such that the cone will contain the true mean with 95-percent confidence--valid only for hemispherically normally distributed data.

²Surface of ribs away from intersections, four 5-ft-square unit areas.

³Roof away from intersections, four 20-ft-square unit areas.

⁴Roof at intersections, two 20-ft-square unit areas.

⁵Insufficient data to delineate a fracture set.

FINAL SAMPLING

The purpose of the final sampling was to define the parameters of the fracture sets within each stratum of the 3-Left study area in a form useful for engineering analysis, particularly for a study of any correlation between roof falls and fracture orientations. This section describes the design of the final sampling plan, including sample size determination and further stratification of the study area, and gives the results of analysis of the final sample.

Design of the Final Sampling Plan

Here, as in the preliminary sampling plan, the factors that might influence the results of the study must be identified and the final sampling plan designed accordingly. For the final sampling plan the 3-Left study area was stratified into coal ribs, shale roof between ribs, and shale roof at intersections. In addition, since the objective of the sampling was to correlate roof falls with the geometry of natural fractures, the study area was divided into three sites (A, B, and C) based on roof condition. Figure 3 illustrates this division. Sites A and C contained few roof falls, whereas site B had a strong concentration of roof falls.

The unit area technique was used for mapping and, as in the preliminary sampling, the selection of the unit areas to be mapped was made through the use of the random number table (thus reducing the possibility of operator bias in the selection).

The approximate number of fractures, N_t , to be mapped in each stratum, was determined by applying the following formula:

$$N_t = \sum_{i=1}^n N_i, \quad (1)$$

where n = number of fracture sets delineated in the preliminary sample of the stratum.
 N_i is determined for fracture set i by the relation

$$N_i = 1 + \frac{\log_e (1/P)}{\log_e [1 + (k - 1)(1 - \cos c)]} \quad (2)$$

The derivation of equation 2 follows from confidence interval relationships for the Fisher distribution on the sphere (1). The values of k, which is a measure of the tightness of the data points in a fracture set around its mean attitude, were obtained from the computer analysis (2) of the preliminary sample for each stratum. The probability, P, was set at the 95-percent level of confidence, and c, the confidence radius around the mean, was given a value of 1°. In other words, the sample mean was required to be within 1° of the true mean with 95-percent confidence. During the preliminary sampling, an average of 15 fractures was mapped in a unit area in a 15-minute time allotment. The allotment of 15 minutes, though arbitrary, appeared to yield adequate coverage of each unit area and a sufficiently large preliminary sample. The number of unit areas to be mapped in a stratum during the final sampling was therefore $N_i/15$.

Results of the Final Sampling

The final sample was analyzed by the computer program (2). The results of the analysis are listed in Table 2. Two fracture sets (sets 1 and 2) occur throughout the study area; that is, in each of the three strata (coal, roof, and intersection) in each of the three sites (A, B, and C). Two additional fracture sets were identified: Set 3 occurs in the roof of sites B and C, whereas set 4 appears in the roof of site B only. (It is noted here that the frequency of roof falls observed in the study area was greatest for site B.) The division of the 3-Left study area into strata and into sites exposes the variability in the fracture patterns. If this had not been done, large variations within fracture sets would have obscured any fine-scale interpretation.

TABLE 2. - Summary of fracture orientations obtained during final sampling

Fracture set	Site								
	A			B			C		
	Azimuth, degrees	Dip, degrees	C, ¹ degrees	Azimuth, degrees	Dip, degrees	C, ¹ degrees	Azimuth, degrees	Dip, degrees	C, ¹ degrees
Set 1:									
Coal ²	16.9	89.7	-	19.1	88.7	-	198.9	89.1	1.0
Roof ³	4.0	89.7	-	186.1	89.9	-	181.5	89.3	2.8
Intersection ⁴	180.2	89.3	-	184.9	89.8	-	181.3	89.2	-
Set 2:									
Coal.....	108.5	85.9	2.5	111.5	84.1	-	113.8	86.5	2.6
Roof.....	96.5	86.9	4.3	292.0	89.7	5.1	82.4	89.8	8.7
Intersection	97.3	87.3	-	278.7	89.9	-	278.7	88.0	4.5
Set 3:									
Coal.....	-	-	-	-	-	-	-	-	-
Roof.....	-	-	-	123.8	84.2	5.9	302.3	85.3	8.0
Intersection	-	-	-	-	-	-	-	-	-
Set 4:									
Coal.....	-	-	-	-	-	-	-	-	-
Roof.....	-	-	-	70.4	88.3	9.7	-	-	-
Intersection	-	-	-	-	-	-	-	-	-

¹Apex angle of the cone around the sample mean (as its axis) such that the cone will contain the true mean with 95-percent confidence--valid only for hemispherically normally distributed data.

²Surface of ribs away from intersections, 5-ft-square unit areas.

³Roof away from intersections, 20-ft-square unit areas.

⁴Roof at intersections, 20-ft-square unit areas.

SUMMARY

This report develops and applies a stratified cluster sampling procedure for sampling fracture orientations in an underground coal mine with the objective of correlating roof falls with fracture orientations. The use of the sampling plan provides a statistical basis for calculating mean orientation values for fracture sets. Application of this plan involves three steps: (1) Reconnaissance to define the strata by their engineering and geologic properties, (2) preliminary sampling to obtain initial quantitative information about the patterns of fracture orientations and to provide the necessary data for computation of the sample size for final sampling, and (3) final sampling in a portion of the mine to obtain statistical estimates of the parameters of fracture orientation sets for application to an engineering analysis.

The sampling procedures employed in this study were organized around the idea that the collection of representative data was necessary for an accurate analysis of the effect of fracture geometry on roof stability. The use of unit area mapping, stratification, and site delineation contributed to the collection of representative data.

REFERENCES

1. Fisher, R. A. Dispersion on a Sphere. Proc. Royal Soc. (London), Ser. A., v. 217, 1953, pp. 295-305.
2. Mahtab, M. A., D. D. Bolstad, J. R. Alldredge, and R. J. Shanley. Analysis of Fracture Orientations for Input to Structural Models of Discontinuous Rock. BuMines RI 7669, 1972, 76 pp.
3. Mahtab, M. A., D. D. Bolstad, and F. S. Kendorski. Analysis of the Geometry of Fractures in San Manuel Copper Mine, Arizona. BuMines RI 7715, 1973, 24 pp.

A BUREAU OF MINES DIRECT-READING AZIMUTH PROTRACTOR

by

D. D. Bolstad¹ and M. A. Mahtab²

ABSTRACT

This report describes the construction and use of a direct-reading azimuth protractor (DRAP) by the Bureau of Mines for measuring fracture orientations in mines, tunnels, or other excavations having a magnetic environment. The DRAP allows a rapid and simultaneous measurement of dip and azimuth of dip of a fracture plane. The instrument is rugged, lightweight, and easily constructible from standard hardware items. The DRAP can measure dip to within $\pm 0.5^\circ$ and azimuth of dip to within $\pm 5^\circ$ of corresponding values obtained with a Brunton compass.

INTRODUCTION

This report describes the direct-reading azimuth protractor (DRAP) developed by the Bureau of Mines for mapping fracture orientations in mines, tunnels, or other excavations where the existing magnetic fields affect the accuracy of measurements made with a magnetic compass. The DRAP is a modified version of an instrument originally developed by E. D. Wilson³ for mapping fracture orientations in the San Manuel copper mine, Arizona. Wilson's device consisted of three components: A compass card, a strike board, and a handle. Strike azimuths can be read directly with Wilson's device. However, the measurement of dip requires the use of an additional instrument, such as the Brunton compass. By the addition of a compass card to Wilson's device, DRAP has been made capable of simultaneously measuring the dip azimuth and the dip of a fracture plane. The color coding of the dip scales in DRAP provides a "fail-safe" means of obtaining the proper dip direction. The addition of a bubble level has also increased the accuracy of the observations.

The device (DRAP) in its present state allows the collection of data in a form suitable for statistical processing on digital computers. Instead of measuring the strike of a joint plane, the azimuth of its dip is measured.

¹Geologist.

²Physical scientist.

³Wilson, E. D. Geologic Factors Related to Block Caving at San Manuel Copper Mine, Pinal County, Ariz. Progress Report, April 1954-March 1956. BuMines RI 5336, 1957, 78 pp.

The dip and the azimuth of dip then completely define the attitude of a fracture in spherical coordinates.

ACKNOWLEDGMENTS

The authors wish to express their gratitude to L. A. Thomas, chief geologist, Magma Copper Co., San Manuel Div., San Manuel, Ariz., for independent evaluation of DRAP and to F. S. Kendorski, (presently geological engineer, Climax Molybdenum Co., Climax, Colo.), for extensive field testing of DRAP at the San Manuel mine during 1971. Special thanks are due J. C. Bean, engineering draftsman, Denver Mining Research Center, for introducing modifications in the detail drawings of DRAP components to facilitate machining.

CONSTRUCTION OF DRAP

The basic device as illustrated in figures 1 and 2 was machined from aluminum plate and thick-wall brass pipe for durability and low weight. The complete device weighs 2-1/4 lb. Any lightweight, moderately inexpensive

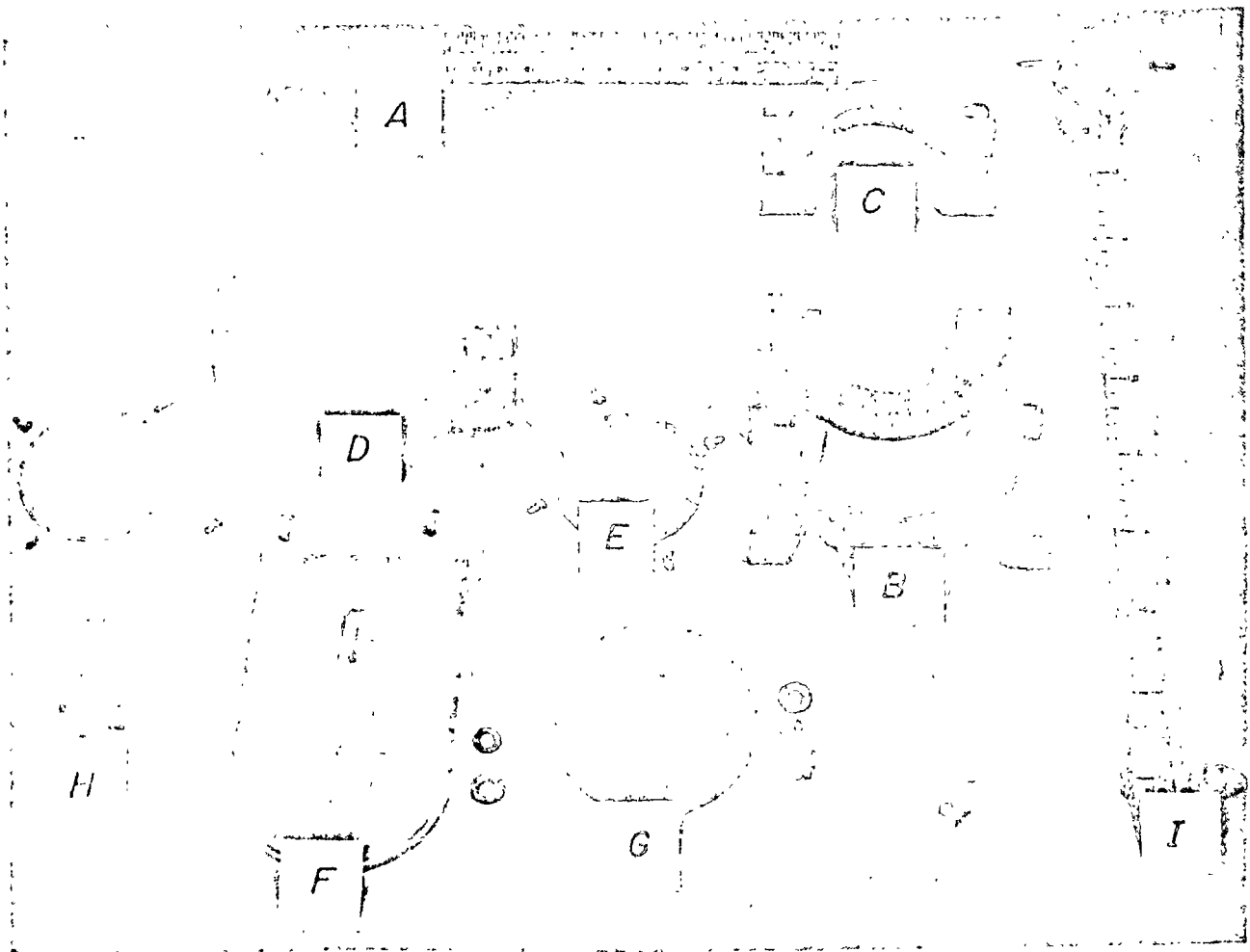


FIGURE 1. - DRAP component parts.

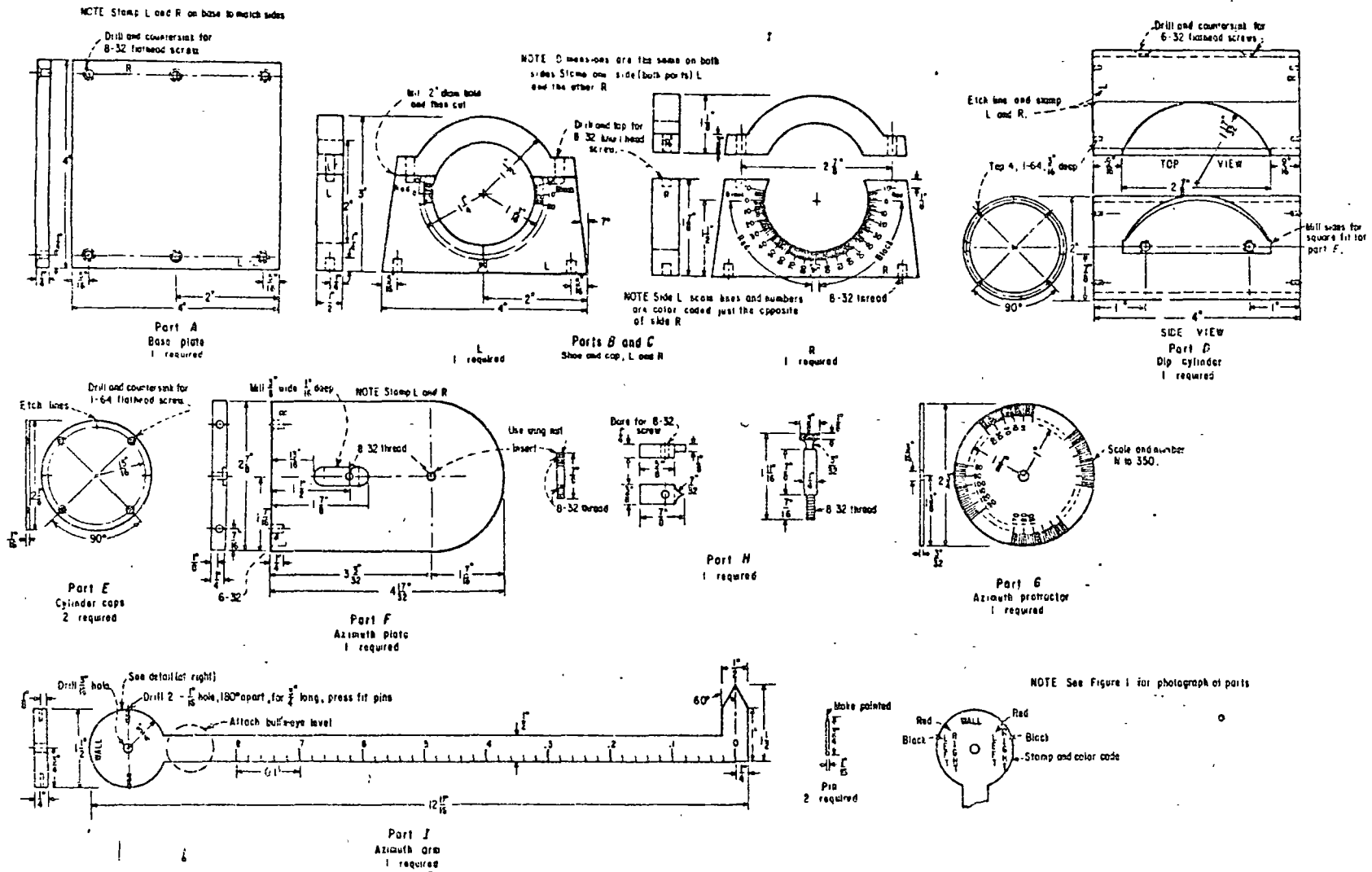


FIGURE 2. - Detail drawing of DRAP components.

material could be used in construction of the device. All bolts, screws, and nuts were standard hardware items. Figure 1 illustrates the components of DRAP, figure 2 provides a detail drawing⁴ of the components, and figure 3 illustrates the complete assembly. The individual parts are described in the following sections.

Base Plate A⁵.--This is a 1/4 in-thick aluminum plate measuring 4 in by 4 in; it provides a flat surface to lay the device on the fracture surface.

Base Shoes B.--These are machined from 1/2-in aluminum plate, are attached to edges of the base plate A, and provide the bearing surfaces for the rotating dip cylinder D. Two dip scales, graduated from 0° to 90°, are provided on each shoe. The graduations are scribed in increments of 1° and numbered every 10°. The dip scales are color coded in red and black. Red numbers are the light-toned numbers illustrated in figures 1 and 3; black numbers appear in a darker tone. Additional markings of 0° to 15° are scribed beyond either end of the 0° to 90° scales to provide greater ease in mapping nearly horizontal fractures. Note that in figure 3, the base shoes are positioned such that the red (light-tone) numbers are closed to the azimuth arm I than are the black numbers.

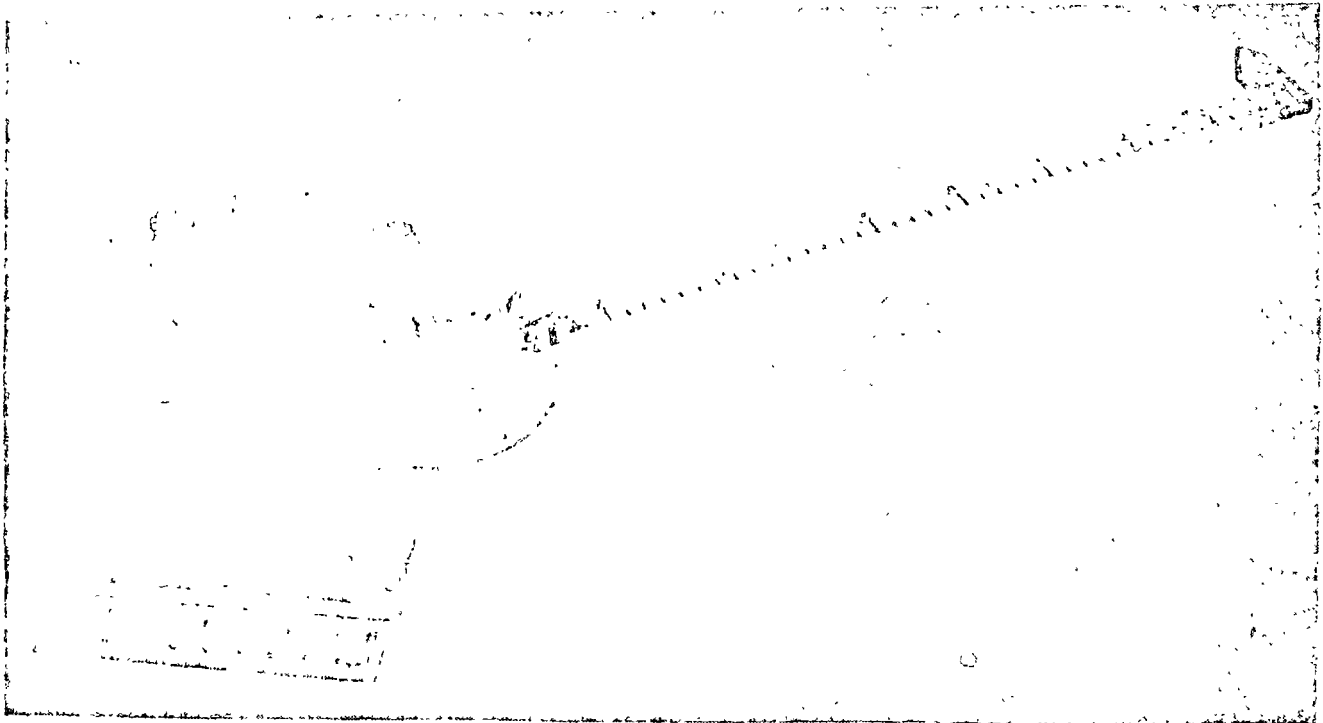


FIGURE 3. - DRAP assembly.

⁴Note that figure 2 contains some modifications (in design) to simplify machining of parts.

⁵Underlined letters refer to individual components illustrated in figures 1 and 2.

End Caps C. --These caps are machined from 1/2-in aluminum plate and provide a means of dust-sealing the dip cylinder D. Each cap is drilled to allow thumbscrews to be inserted into threaded holes in the corresponding base shoe B.

Dip Cylinder D. --The cylinder was cut from a piece of brass pipe having 2-in OD and 1-7/8-in ID. The 4-in-long cylinder provides a rotating unit that fits within the base shoes B. Each end of the cylinder is capped with a 2-1/8-in-diam round plate E to prevent lateral movement. The cylinder is slotted to accept the azimuth plate F, which is then screwed to the back of the cylinder D.

Azimuth Plate F. --This plate provides a surface for mounting the azimuth protractor G and the locking thumbscrew H. The azimuth plate was machined from 1/4-in aluminum stock and measures 3 in by 4-1/2 in with one end rounded to a 1-3/8-in radius to reduce weight.

Azimuth Protractor G. --The protractor was cut from 1/8-in-thick aluminum and is scribed in 2° increments proceeding clockwise from 0° azimuth (north) to 360° azimuth (north). The 2-3/4-in-diam protractor G provides a means of setting the proper drift azimuth value by using the drift azimuth pointer lock H to fasten the protractor firmly to the azimuth plate F. The protractor is also used in obtaining the azimuth of dip of a fracture.

Azimuth Arm I. --The 1/4-in-thick aluminum arm is bolted to the azimuth plate F through a center hole in the azimuth protractor G. A thumbscrew provides a friction lock on the free-turning arm. No threads are required in the center hole of the azimuth arm I as the arm must move freely during the mapping process. A simple (30 min) bull's eye level is fastened to the arm and allows the arm and cylinder unit to be leveled prior to taking azimuth and dip readings. A scale (graduated in tenths of a foot) is scribed on the arm to allow measurement of apertures and spacing of fractures. The pointer on the end of the arm does not correspond to a specific direction to be used, rather it provides a 90° angle useful for alignment with steel sets (or other supports) in the drift being mapped.

The circular portion of the arm is scribed with color-coded "right" and "left" markings. Note, again, that the light-toned letters represent red color, and the darker letters represent black color, as illustrated in figure 1, I. Two pointers are placed at 90° to the long axis of the arm and at 180° apart.

USE OF DRAP

In a magnetic environment, the azimuth measurements made with a magnetic compass are not reliable. This difficulty is overcome by using DRAP, which measures the azimuth of dip of a fracture with reference to a known direction, for example, the azimuth of a drift axis. The accuracy of observations, therefore, depends on the ability of the observer in positioning the azimuth arm I of DRAP at 90° to the reference line. The authors have consistently been able to reproduce DRAP measurements of dip to within $\pm 0.5^\circ$ and azimuth of dip to

within $\pm 5^\circ$ of the corresponding measurements made (in a nonmagnetic environment) with a Brunton compass. In addition, DRAP has allowed a slightly greater speed of measuring these angles as compared with a Brunton compass. Another important advantage of DRAP over a Brunton compass is that DRAP makes available much larger measuring surface (base plate A). The 16-sq-in surface tends to average over the protrusions, crystal growths, and other rough features on fracture surfaces, thus giving truer dip and azimuth readings. On the other hand, the approximately 0.75-sq-in surface (edge) of a Brunton compass sometimes yields false dip and strike values due to localized asperities on fracture surfaces.

The following paragraphs describe the various steps involved in using DRAP to obtain the orientations of fractures in underground mines.

Setting Drift Azimuth.--Before any measurements can be made with DRAP, it is necessary to set, on the protractor G, the azimuth of the (reference) axis of the drift that is being mapped. The azimuth values for the drifts to be mapped are determined from the mine maps. Each drift axis will have two azimuths, such as 044° and 224° , as illustrated in figure 4. If the operator travels northeasterly down the drift (044°) this value is set on DRAP by rotating the azimuth protractor G until 044° is aligned with the drift azimuth pointer lock H. The protractor G is locked into place by tightening the lock H. If the operator reverses direction, the new azimuth of 224° would have to be reset on the protractor.

Note that the azimuth setting determines the rib's right and left directions, in relation to the direction of travel of the operator.

Alinement of DRAP.--To map a fracture, the base plate A of DRAP is placed on the fracture surface and is shifted around while rotating the dip cylinder D until the level-bubble is centered. The azimuth arm I is now rotated until it is at 90° to the axis of the drift. This right angle must be visually estimated. With practice, however, a good ($\pm 5^\circ$) estimate of this angle is easily made. As mentioned earlier, the pointer on the end of the azimuth arm also provides a means of sighting-in along the steel sets or other supports to maintain accuracy.

Dip Angle Reading.--The angle of dip of the fracture is read directly from either side of the base shoes B. One of the scribe lines on the cylinder caps E will be aligned with a degree marking on the base shoes B. This degree value is color coded either red (light tone) or black (dark tone).

Azimuth of the Dip Reading.--The pointers, on either side of the circular portion of the azimuth arm I have color-coded (red and black) "right" and "left" markings (for each pointer). These markings refer to the rib (wall) being mapped. Note that in a previous step entitled "Alinement of DRAP", an initial drift azimuth setting of 044° was used. Therefore, the "right" and "left" walls correspond to the operator's right and left as he is facing 044° . In this example the operator is mapping the left wall and has obtained a black color-coded dip reading of 14° . Therefore, the pointer on the side of the azimuth I, which is marked "left" and is colored black, will correspond to an

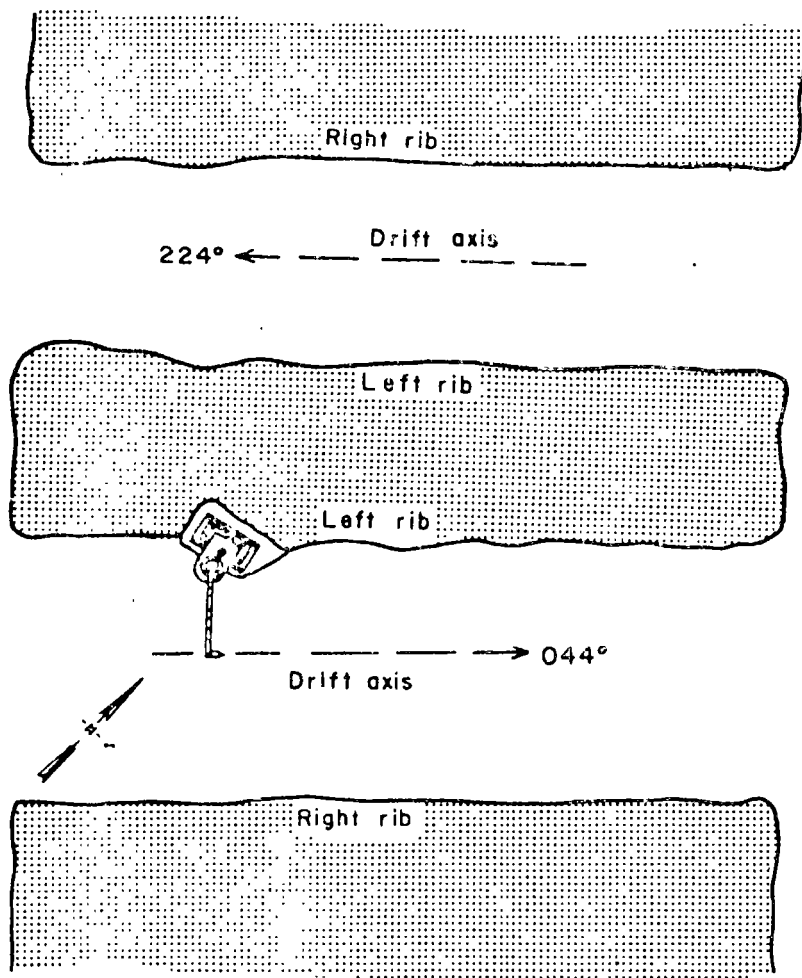


FIGURE 4. - Drift axis direction and rib designation (plan view).

azimuth of dip value marked on the azimuth protractor G. Note that in figure 2, the side marked black "left" is also marked red "right." For this example a reading of 166° represents the azimuth of the dip valve. This corresponds to a strike of $N 76^\circ W$ (or $S 76^\circ E$). To directly read strike values a new azimuth protractor G would have to be scribed with quadrant markings (N,S, E,W). However, dip values would now have to be read in quadrants also, thus complicating procedures more than is necessary for rapid data collection.

SUMMARY

The direct-reading azimuth protractor, DRAP, provides a rapid means of mapping fracture orientations in geologic environments where magnetic influences affect compass measurements. The device is easily constructed and is designed to eliminate operator error in mapping by the use of color-coded dip and azimuth of the

dip markings. The DRAP is constructed from aluminum plate and brass pipe to maintain low weight; it uses standard hardware items to reduce machining cost.

Adeptness in the use of DRAP is readily acquired in less than 1 hr of practice in the field. Comparisons of accuracy can be made by mapping surface faces with a Brunton compass and DRAP in a nonmagnetic environment. The DRAP can measure dip to within $\pm 0.5^\circ$ and azimuth of dip to within $\pm 5^\circ$ of the corresponding values obtained with a Brunton compass.

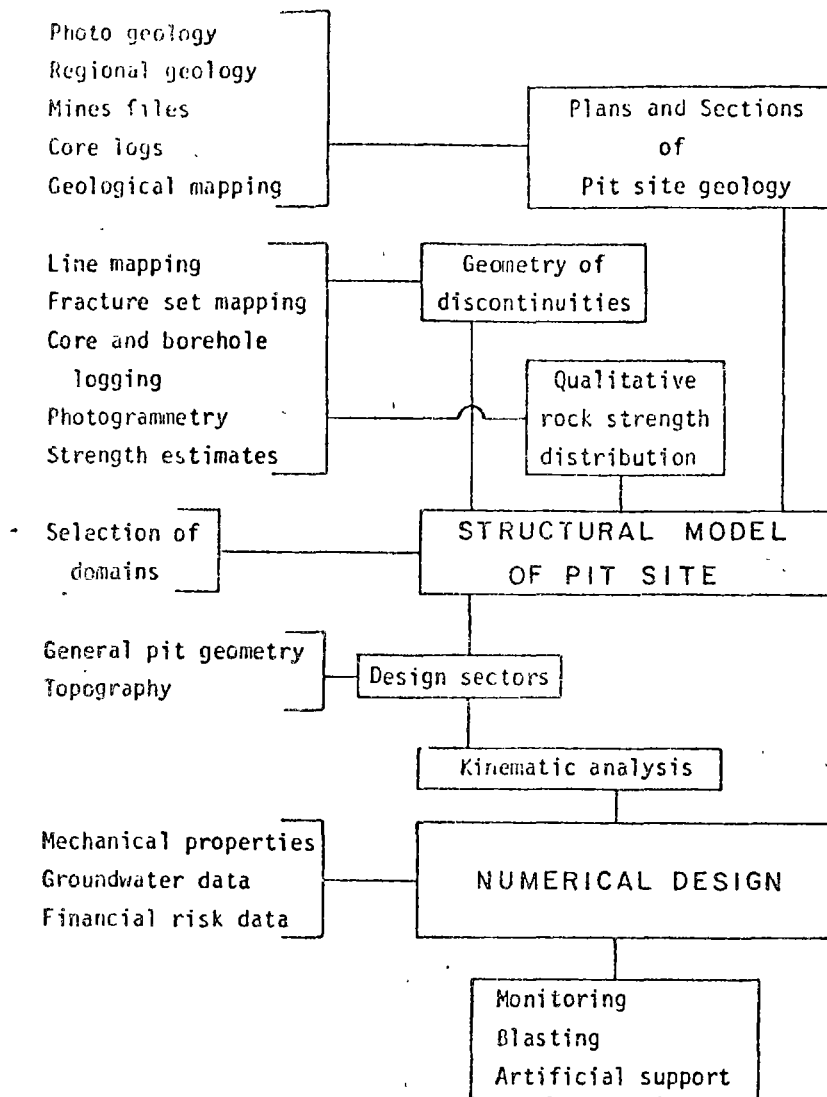


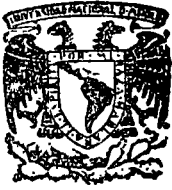
Fig 3 - Flow of geological data for the design of pit slopes.

REGIONAL AND MINE SCALES

24. As indicated above, the site location alone might allow anticipation of potential slope problems if open pit mining experience or data on natural slopes are available for the area. To develop a good understanding of the geology at the pit site, an integration of the local geology into the regional geological pattern is vital. Regional geological data are available from maps by the Geological Survey of Canada and provincial Departments of Mines. Other relevant sources of information are quoted in paragraph 196.

DETAILED MAPPING FOR PIT DESIGN

25. The general geological map of the pit site provides essential background information but is insufficient for geotechnical assessments. Rock types should not only be known by geological names, but an estimate of strength with simple hardness tests is the minimum required to identify areas where instability could occur due to a weak rock substance. The same applies for the discontinuities which have to be described in more detail than is the case in general geological mapping.



centro de educación continua
división de estudios superiores
facultad de ingeniería, unam



MECANICA DE ROCAS APLICADA A LA MINERIA

LEVANTAMIENTO DE DATOS GEOLOGICOS-ESTRUCTURALES

ABRIL, 1978.

PROCEDURES USED FOR SAMPLING FRACTURE ORIENTATIONS IN AN UNDERGROUND COAL MINE

by

D. D. Bolstad,¹ J. R. Alldredge,² and M. A. Mahtab³

ABSTRACT

The Bureau of Mines has developed procedures for sampling the geometry of fractures in underground coal mines. Stratified cluster sampling and the unit area concept are applied to the collection of fracture orientation data. The use of unit area mapping, stratification, and site delineation is made to assure collection of representative data. The procedures developed here help to isolate sources of variability in the fracture patterns.

INTRODUCTION

Fractures are planes of weakness in a rock mass, and very often their geometric patterns (attitude, spacing, extent, and aperture) influence the mechanical behavior of excavated structures in the fractured medium. During the past decade, numerical techniques have been increasingly and successfully employed for stability analyses of engineered structures in fractured media. The sophistication of the numerical techniques has increased the need for quantitative and reliable input information regarding fracture geometry. Some appropriate schemes for quantifying the geometric characteristics of fractures have recently become available (2).⁴ However, no systematic and acceptable procedures are available for sampling fracture patterns in subsurface excavations.

As part of the Bureau's investigation of the influence of fractures on coal mine roof behavior, the Bureau developed and used procedures for sampling fracture orientations in selected underground coal mines. One of the several mines selected for the roof behavior study was Duquesne Light Co. Warwick mine Portal No. 3, Greensboro, Pa. The objective of sampling fracture orientations in this mine was limited to correlating natural fracture⁵ orientations with roof falls. To meet this objective, sampling procedures were

¹Geologist.

²Mathematical statistician.

³Physical scientist.

⁴Underlined numbers in parentheses refer to items in the list of references at the end of this report.

⁵Natural fractures are defined as recurrent planar geologic discontinuities having spacings of from tenths of a foot to tens of feet.

devised (1) to extract information on fracture orientations from a relevant (small) portion of the mine (called the study area) and (2) to provide a statistical background for estimating the mean fracture orientations in the study area. This report discusses the procedures used by the Bureau for sampling fracture orientations in Warwick mine Portal No. 3.

ACKNOWLEDGMENTS

The authors wish to thank the management of Duquesne Light Co., Pittsburgh, Pa., for permission to collect data on geometry of fractures in their Warwick mine Portal No. 3.

GENERAL SAMPLING PROCEDURES

Three main steps were followed in the development of the sampling procedures: (i) Defining the factors that might affect the sample, (2) obtaining and analyzing a preliminary sample, and (3) obtaining and analyzing the final sample and presenting the results in a form useful for engineering analysis. (In this example the analysis involved correlating fracture orientations with roof falls.) The general procedures followed in this study are illustrated in the flowsheet shown in figure 1. These procedures may be readily interpreted to fit the objectives of other problems involving sampling of attitudes, spacings, extents, and apertures of fractures in underground mines; for example, a recent Bureau of Mines study (3) described application of these procedures in an underground copper porphyry mine in Arizona. The methods of sampling may also be applied to problems relating to other planes of weakness, such as fault traces, blasting fracture patterns, and bedding plane partings.

This report emphasizes the following sampling concepts:

1. Cluster sampling, where a cluster consists of all the fractures in a small division of the study area. The clusters will be referred to as unit areas.
2. Stratified sampling, where the study area is separated into blocks or strata. The term strata is used here in a statistical rather than a geological sense.

The concepts of cluster sampling and stratified sampling are combined to result in a stratified cluster sampling plan. This is a common sampling plan used in many other fields of study.

RECONNAISSANCE

This section outlines the geologic setting of the Warwick mine Portal No. 3 and describes the geologic and layout factors recognized during a short reconnaissance of the mine (one engineer and one geologist spent a day visiting the mine). The objective of the reconnaissance was to select several areas for preliminary sampling on the basis of the observed differences in their geologic and engineering characteristics.

The Warwick mine Portal No. 3 is located within a region of gently dipping NNE-trending anticlines and synclines composed of sandstones, shales,

and coal seams of Pennsylvanian-Permian age. Major faulting is lacking in this region.

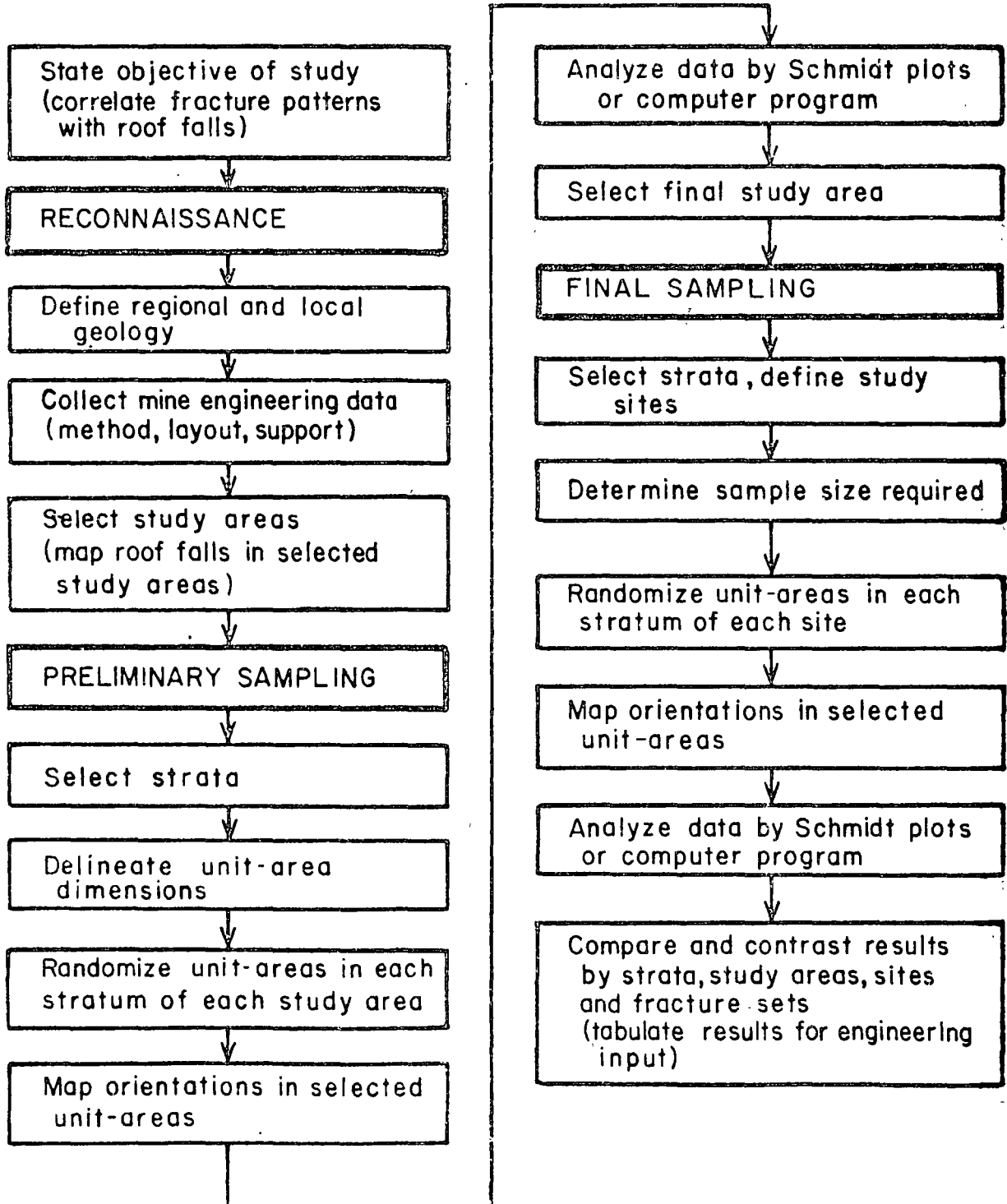


FIGURE 1. - Procedures followed for sampling fracture orientations in an underground coal mine.

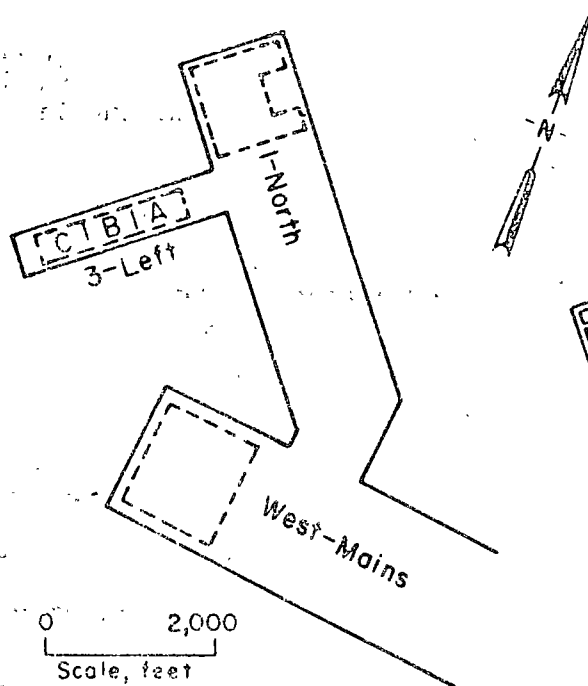


FIGURE 2. - General plan of Warwick mine Portal No. 3.

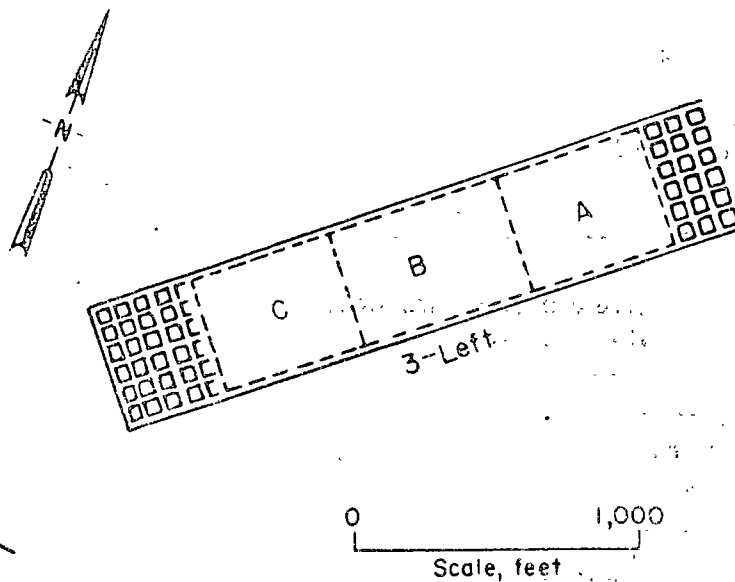


FIGURE 3. - Division of the study area into sites.

A nearly orthogonal system of vertical roof fractures was observed throughout the Warwick mine Portal No. 3. The shale roof appeared to have no major observable structural or lithologic discontinuities. The coal cleat system paralleled the roof fracture system and had well-defined face and butt cleats. Three major mining areas were active (fig. 2); they were the 1-North, 3-Left, and West-Mains entry systems. Since the objective of the fracture orientation mapping study was to correlate roof falls with the patterns of natural fractures, the three active areas were selected for preliminary sampling, as these areas would afford a greater probability of observing natural fractures than would the inactive areas.

PRELIMINARY SAMPLING

The purpose of the preliminary sampling was to supply information about the geometry of the fracture patterns and to provide measures of the natural variability present within and between selected areas. This information was then used to design the final sampling plan. This section describes the design of the preliminary sampling plan and reports results of the preliminary sampling.

Design of the Preliminary Sampling Plan

Prior to mapping the fractures, the factors that might influence the results of the study were identified, and a sampling plan was designed to take account of these factors. For example, the effect of relative location, study-area sizes, ferromagnetic influences, difference in rock type, variability

of roof-fall areas, and operator bias were considered in designing the sampling plan.

Each study area (1-North, 3-Left, West-Mains) was defined on the basis of equivalent size and quantity of available entries and crosscuts. These study areas were sampled and analyzed independently to examine the effect of relative location on fracture orientations. Each study area encompassed 70 to 80 pillars, exclusive of return airways and actual working faces. The entries and crosscuts were approximately 20 ft wide and were driven on 70-ft centers. The general absence of ferromagnetic influences within the study areas allowed the use of a standard Brunton compass for orientation measurements.

Each study area was divided into (statistical) strata based on rock type and unsupported span dimensions. The three strata were (1) coal ribs, (2) shale roof between ribs, and (3) shale roof at intersections. This is an application of stratified sampling. However, since unit areas (clusters) are being sampled, this plan is referred to as stratified cluster sampling. A cluster, as defined in this study, consists of all the fractures within a unit area. In the unit area technique each (statistical) stratum is divided into many small areas. In this study, 5-ft-square unit areas⁶ were delineated on all coal ribs, and 20-ft-square unit areas were delineated in the shale roof between the ribs and in the shale roof at intersections. The unit area technique was used in preference to the line of traverse method because the latter method is biased against the fractures paralleling the line. In addition, the unit area technique allows a comparison of fracture-set geometries between individual areas and groups of areas.

In this study the unit areas in each stratum within the study areas were numbered for identification on mine maps. A random-number table was used to select two roof-intersection unit areas, four roof-between-the-ribs unit areas, and four coal-rib unit areas for mapping in each study area. This sample size was based on the time available for mapping during the preliminary phase. The unit areas were randomized to insure that an unbiased and representative sample of the area under study was obtained.

Results of the Preliminary Sampling

After mapping, fracture sets were identified from the data and their mean attitudes were calculated using a computer program (2). Table 1 lists the results of an analysis of preliminary sample. Two major fracture sets were prevalent throughout the three study areas. No major differences in the mean attitudes of fracture sets were found in a comparison of the three study areas. Because of this, it was decided to concentrate the final sampling efforts in just one study area. Since the 1-North study area contained a large air shaft whose effect on the neighboring fracture patterns was unknown, and since the access within the West-Mains study area was impaired, the final sampling was conducted in the 3-Left study area. The final sampling (and

⁶The choice of a square shape was convenient. The side of a square unit area was given by the height (5 ft) or width (20 ft) of the entries.

analysis) of the fracture orientations in the 3-Left study area are discussed in the next section.

TABLE 1. - Summary of fracture orientations obtained during preliminary sampling

Fracture set	Study area								
	West-Mains			3-Left			1-North		
	Azimuth, degrees	Dip, degrees	C, ¹ degrees	Azimuth, degrees	Dip, degrees	C, ¹ degrees	Azimuth, degrees	Dip, degrees	C, ¹ degrees
Set 1:									
Coal ²	203	88	-	25	87	1.8	202	88	1.6
Roof ³	197	88	3.2	09	90	2.3	192	88	2.6
Intersection ⁴	193	89	5.4	191	86	4.0	195	87	3.5
Set 2:									
Coal.....	113	89	-	116	83	3.1	116	87	3.9
Roof.....	115	90	9.8	(⁵)	(⁵)	(⁵)	110	88	5.5
Intersection	(⁵)	(⁵)	(⁵)	98	89	14.2	120	88	14.1

¹Apex angle of the cone around the sample mean (as its axis) such that the cone will contain the true mean with 95-percent confidence--valid only for hemispherically normally distributed data.

²Surface of ribs away from intersections, four 5-ft-square unit areas.

³Roof away from intersections, four 20-ft-square unit areas.

⁴Roof at intersections, two 20-ft-square unit areas.

⁵Insufficient data to delineate a fracture set.

FINAL SAMPLING

The purpose of the final sampling was to define the parameters of the fracture sets within each stratum of the 3-Left study area in a form useful for engineering analysis, particularly for a study of any correlation between roof falls and fracture orientations. This section describes the design of the final sampling plan, including sample size determination and further stratification of the study area, and gives the results of analysis of the final sample.

Design of the Final Sampling Plan

Here, as in the preliminary sampling plan, the factors that might influence the results of the study must be identified and the final sampling plan designed accordingly. For the final sampling plan the 3-Left study area was stratified into coal ribs, shale roof between ribs, and shale roof at intersections. In addition, since the objective of the sampling was to correlate roof falls with the geometry of natural fractures, the study area was divided into three sites (A, B, and C) based on roof condition. Figure 3 illustrates this division. Sites A and C contained few roof falls, whereas site B had a strong concentration of roof falls.

The unit area technique was used for mapping and, as in the preliminary sampling, the selection of the unit areas to be mapped was made through the use of the random number table (thus reducing the possibility of operator bias in the selection).

The approximate number of fractures, N_t , to be mapped in each stratum, was determined by applying the following formula:

$$N_t = \sum_{i=1}^n N_i, \quad (1)$$

where n = number of fracture sets delineated in the preliminary sample of the stratum.
 N_i is determined for fracture set i by the relation

$$N_i = 1 + \frac{\log_e (1/F)}{\log_e [1 + (k - 1)(1 - \cos c)]} \quad (2)$$

The derivation of equation 2 follows from confidence interval relationships for the Fisher distribution on the sphere (1). The values of k, which is a measure of the tightness of the data points in a fracture set around its mean attitude, were obtained from the computer analysis (2) of the preliminary sample for each stratum. The probability, P, was set at the 95-percent level of confidence, and c, the confidence radius around the mean, was given a value of 1°. In other words, the sample mean was required to be within 1° of the true mean with 95-percent confidence. During the preliminary sampling, an average of 15 fractures was mapped in a unit area in a 15-minute time allotment. The allotment of 15 minutes, though arbitrary, appeared to yield adequate coverage of each unit area and a sufficiently large preliminary sample. The number of unit areas to be mapped in a stratum during the final sampling was therefore $N_i/15$.

Results of the Final Sampling

The final sample was analyzed by the computer program (2). The results of the analysis are listed in table 2. Two fracture sets (sets 1 and 2) occur throughout the study area; that is, in each of the three strata (coal, roof, and intersection) in each of the three sites (A, B, and C). Two additional fracture sets were identified: Set 3 occurs in the roof of sites B and C, whereas set 4 appears in the roof of site B only. (It is noted here that the frequency of roof falls observed in the study area was greatest for site B.) The division of the 3-Left study area into strata and into sites exposes the variability in the fracture patterns. If this had not been done, large variations within fracture sets would have obscured any fine-scale interpretation.

TABLE 2. - Summary of fracture orientations obtained during final sampling

Fracture set	Site								
	A			B			C		
	Azimuth, degrees	Dip, degrees	C, ¹ degrees	Azimuth, degrees	Dip, degrees	C, ¹ degrees	Azimuth, degrees	Dip, degrees	C, ¹ degrees
Set 1:									
Coal ²	16.9	89.7	-	19.1	88.7	-	198.9	89.1	1.0
Roof ³	4.0	89.7	-	186.1	89.9	-	181.5	89.3	2.8
Intersection ⁴	180.2	89.3	-	184.9	89.8	-	181.3	89.2	-
Set 2:									
Coal.....	108.5	85.9	2.5	111.5	84.1	-	113.8	86.5	2.6
Roof.....	96.5	86.9	4.3	292.0	89.7	5.1	82.4	89.8	8.7
Intersection	97.3	87.3	-	278.7	89.9	-	278.7	88.0	4.5
Set 3:									
Coal.....	-	-	-	-	-	-	-	-	-
Roof.....	-	-	-	123.8	84.2	5.9	302.3	85.3	8.0
Intersection	-	-	-	-	-	-	-	-	-
Set 4:									
Coal.....	-	-	-	-	-	-	-	-	-
Roof.....	-	-	-	70.4	88.3	9.7	-	-	-
Intersection	-	-	-	-	-	-	-	-	-

¹Apex angle of the cone around the sample mean (as its axis) such that the cone will contain the true mean with 95-percent confidence--valid only for hemispherically normally distributed data.

²Surface of ribs away from intersections, 5-ft-square unit areas.

³Roof away from intersections, 20-ft-square unit areas.

⁴Roof at intersections, 20-ft-square unit areas.

SUMMARY

This report develops and applies a stratified cluster sampling procedure for sampling fracture orientations in an underground coal mine with the objective of correlating roof falls with fracture orientations. The use of the sampling plan provides a statistical basis for calculating mean orientation values for fracture sets. Application of this plan involves three steps: (1) Reconnaissance to define the strata by their engineering and geologic properties, (2) preliminary sampling to obtain initial quantitative information about the patterns of fracture orientations and to provide the necessary data for computation of the sample size for final sampling, and (3) final sampling in a portion of the mine to obtain statistical estimates of the parameters of fracture orientation sets for application to an engineering analysis.

The sampling procedures employed in this study were organized around the idea that the collection of representative data was necessary for an accurate analysis of the effect of fracture geometry on roof stability. The use of unit area mapping, stratification, and site delineation contributed to the collection of representative data.

REFERENCES

1. Fisher, R. A. Dispersion on a Sphere. Proc. Royal Soc. (London), Ser. A., v. 217, 1953, pp. 295-305.
2. Mahtab, M. A., D. D. Bolstad, J. R. Alldredge, and R. J. Shanley. Analysis of Fracture Orientations for Input to Structural Models of Discontinuous Rock. BuMines RI 7669, 1972, 76 pp.
3. Mahtab, M. A., D. D. Bolstad, and F. S. Kendorski. Analysis of the Geometry of Fractures in San Manuel Copper Mine, Arizona. BuMines RI 7715, 1973, 24 pp.

A BUREAU OF MINES DIRECT-READING AZIMUTH PROTRACTOR

by

D. D. Bolstad¹ and M. A. Mahtab²

ABSTRACT

This report describes the construction and use of a direct-reading azimuth protractor (DRAP) by the Bureau of Mines for measuring fracture orientations in mines, tunnels, or other excavations having a magnetic environment. The DRAP allows a rapid and simultaneous measurement of dip and azimuth of dip of a fracture plane. The instrument is rugged, lightweight, and easily constructible from standard hardware items. The DRAP can measure dip to within $\pm 0.5^\circ$ and azimuth of dip to within $\pm 5^\circ$ of corresponding values obtained with a Brunton compass.

INTRODUCTION

This report describes the direct-reading azimuth protractor (DRAP) developed by the Bureau of Mines for mapping fracture orientations in mines, tunnels, or other excavations where the existing magnetic fields affect the accuracy of measurements made with a magnetic compass. The DRAP is a modified version of an instrument originally developed by E. D. Wilson³ for mapping fracture orientations in the San Manuel copper mine, Arizona. Wilson's device consisted of three components: A compass card, a strike board, and a handle. Strike azimuths can be read directly with Wilson's device. However, the measurement of dip requires the use of an additional instrument, such as the Brunton compass. By the addition of a compass card to Wilson's device, DRAP has been made capable of simultaneously measuring the dip azimuth and the dip of a fracture plane. The color coding of the dip scales in DRAP provides a "fail-safe" means of obtaining the proper dip direction. The addition of a bubble level has also increased the accuracy of the observations.

The device (DRAP) in its present state allows the collection of data in a form suitable for statistical processing on digital computers. Instead of measuring the strike of a joint plane, the azimuth of its dip is measured.

¹Geologist.

²Physical scientist.

³Wilson, E. D. Geologic Factors Related to Block Caving at San Manuel Copper Mine, Pinal County, Ariz. Progress Report, April 1954-March 1956. BuMines RI 5336, 1957, 78 pp.

The dip and the azimuth of dip then completely define the attitude of a fracture in spherical coordinates.

ACKNOWLEDGMENTS

The authors wish to express their gratitude to L. A. Thomas, chief geologist, Magma Copper Co., San Manuel Div., San Manuel, Ariz., for independent evaluation of DRAP and to F. S. Kendorski, (presently geological engineer, Climax Molybdenum Co., Climax, Colo.), for extensive field testing of DRAP at the San Manuel mine during 1971. Special thanks are due J. C. Bean, engineering draftsman, Denver Mining Research Center, for introducing modifications in the detail drawings of DRAP components to facilitate machining.

CONSTRUCTION OF DRAP

The basic device as illustrated in figures 1 and 2 was machined from aluminum plate and thick-wall brass pipe for durability and low weight. The complete device weighs 2-1/4 lb. Any lightweight, moderately inexpensive

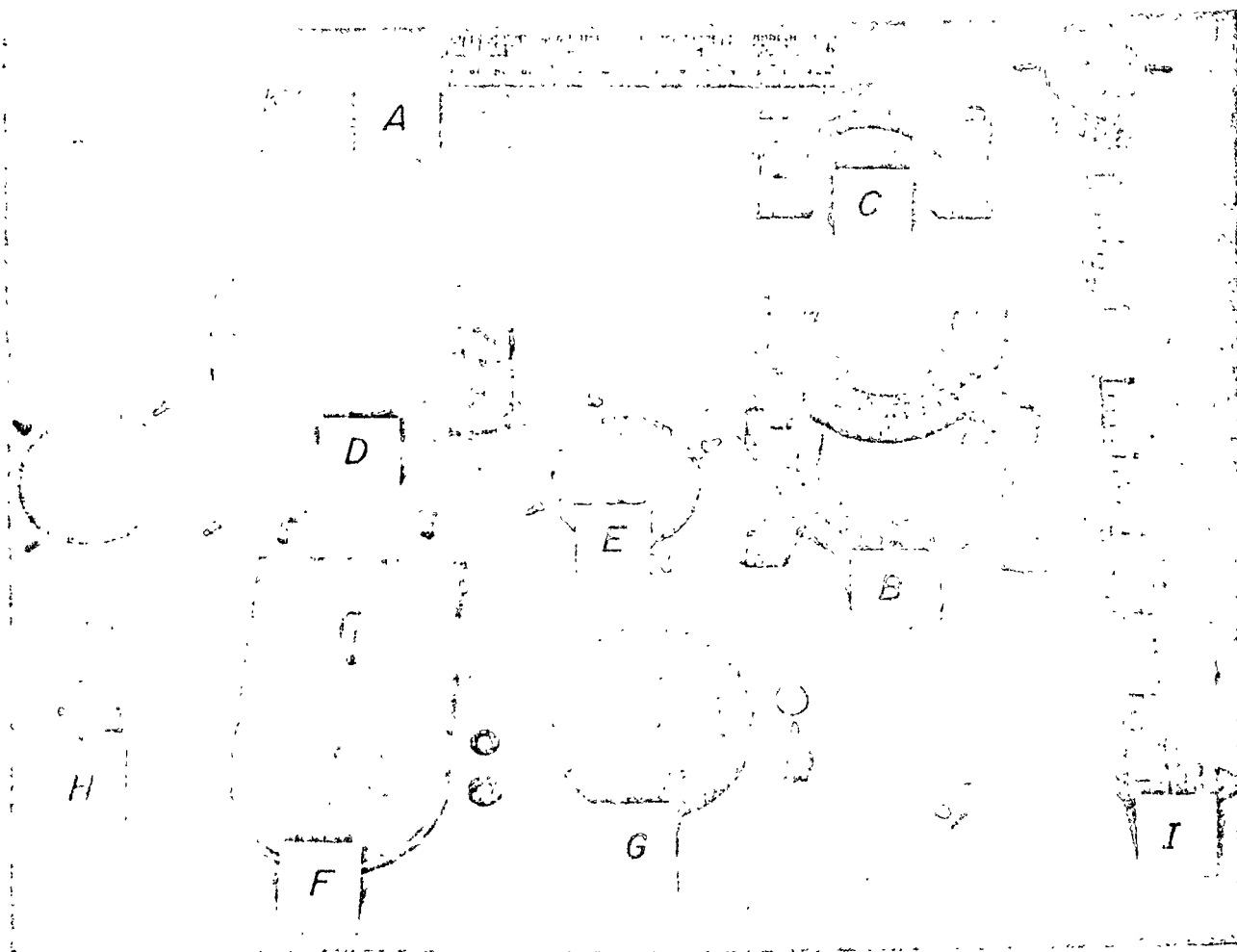


FIGURE 1. - DRAP component parts.

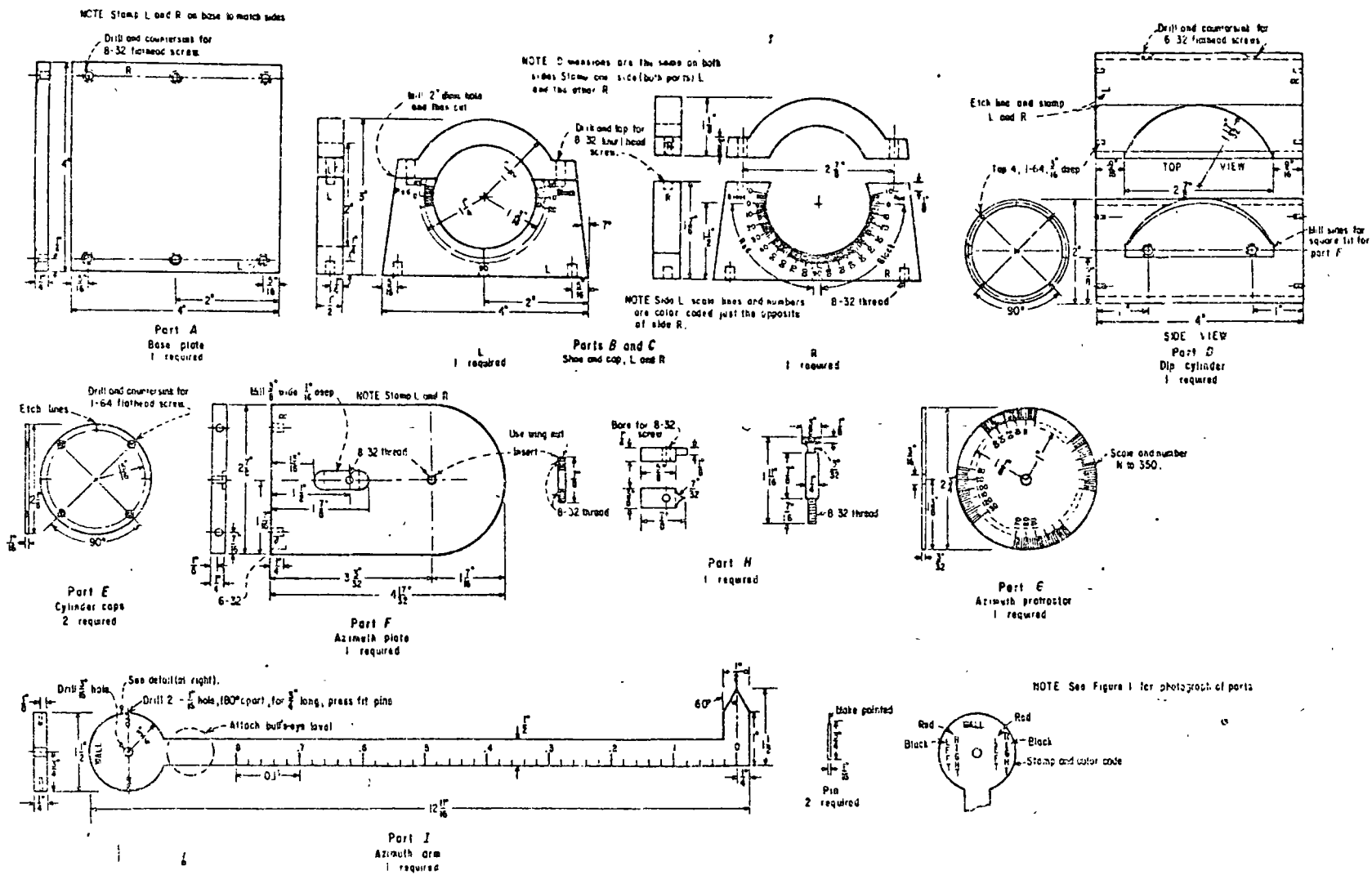


FIGURE 2. - Detail drawing of DRAP components.

material could be used in construction of the device. All bolts, screws, and nuts were standard hardware items. Figure 1 illustrates the components of DRAP, figure 2 provides a detail drawing⁴ of the components, and figure 3 illustrates the complete assembly. The individual parts are described in the following sections.

Base Plate A⁵.--This is a 1/4 in-thick aluminum plate measuring 4 in by 4 in; it provides a flat surface to lay the device on the fracture surface.

Base Shoes B.--These are machined from 1/2-in aluminum plate, are attached to edges of the base plate A, and provide the bearing surfaces for the rotating dip cylinder D. Two dip scales, graduated from 0° to 90°, are provided on each shoe. The graduations are scribed in increments of 1° and numbered every 10°. The dip scales are color coded in red and black. Red numbers are the light-toned numbers illustrated in figures 1 and 3; black numbers appear in a darker tone. Additional markings of 0° to 15° are scribed beyond either end of the 0° to 90° scales to provide greater ease in mapping nearly horizontal fractures. Note that in figure 3, the base shoes are positioned such that the red (light-tone) numbers are closed to the azimuth and I that are the black numbers.

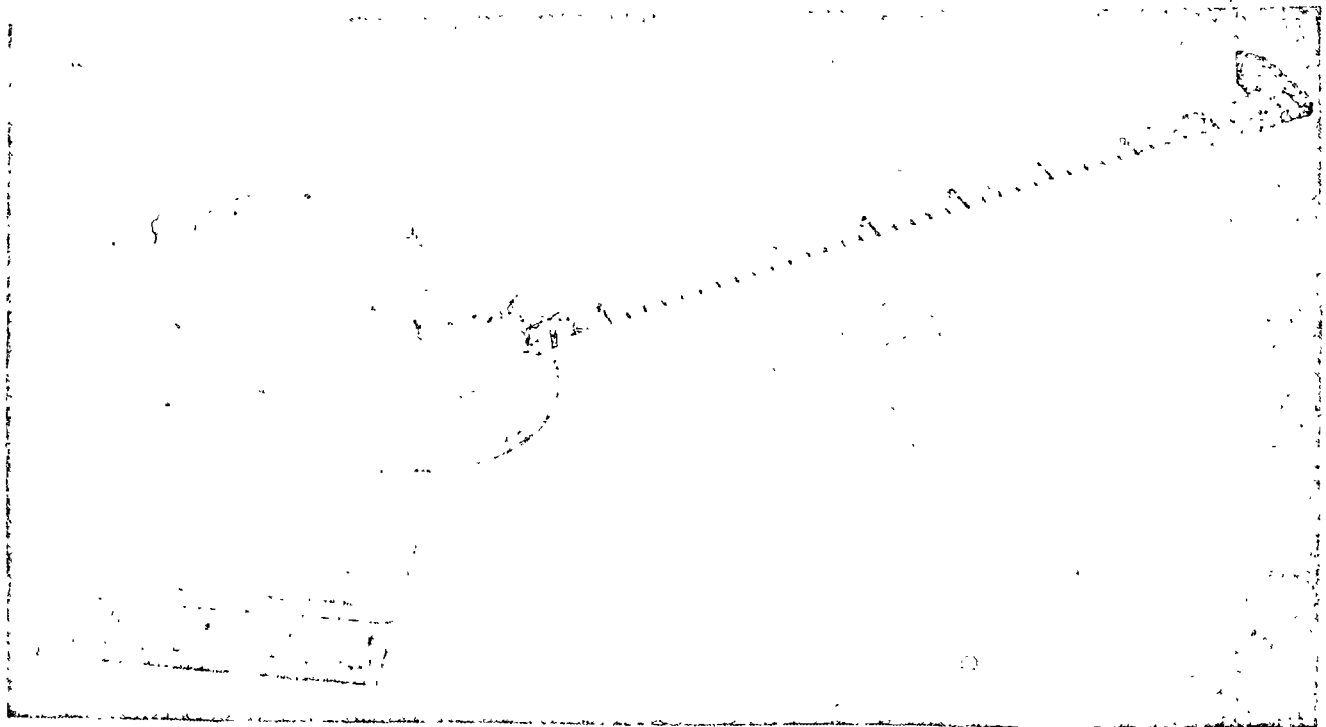


FIGURE 3. - DRAP assembly.

⁴Note that figure 2 contains some modifications (in design) to simplify machining of parts.

⁵Underlined letters refer to individual components illustrated in figures 1 and 2.

End Caps C. --These caps are machined from 1/2-in aluminum plate and provide a means of dust-sealing the dip cylinder D. Each cap is drilled to allow thumbscrews to be inserted into threaded holes in the corresponding base shoe B.

Dip Cylinder D. --The cylinder was cut from a piece of brass pipe having 2-in OD and 1-7/8-in ID. The 4-in-long cylinder provides a rotating unit that fits within the base shoes B. Each end of the cylinder is capped with a 2-1/8-in-diam round plate E to prevent lateral movement. The cylinder is slotted to accept the azimuth plate F, which is then screwed to the back of the cylinder D.

Azimuth Plate F. --This plate provides a surface for mounting the azimuth protractor G and the locking thumbscrew H. The azimuth plate was machined from 1/4-in aluminum stock and measures 3 in by 4-1/2 in with one end rounded to a 1-3/8-in radius to reduce weight.

Azimuth Protractor G. --The protractor was cut from 1/8-in-thick aluminum and is scribed in 2° increments proceeding clockwise from 0° azimuth (north) to 360° azimuth (north). The 2-3/4-in-diam protractor G provides a means of setting the proper drift azimuth value by using the drift azimuth pointer lock H to fasten the protractor firmly to the azimuth plate F. The protractor is also used in obtaining the azimuth of dip of a fracture.

Azimuth Arm I. --The 1/4-in-thick aluminum arm is bolted to the azimuth plate F through a center hole in the azimuth protractor G. A thumbscrew provides a friction lock on the free-turning arm. No threads are required in the center hole of the azimuth arm I as the arm must move freely during the mapping process. A simple (30 min) bull's eye level is fastened to the arm and allows the arm and cylinder unit to be leveled prior to taking azimuth and dip readings. A scale (graduated in tenths of a foot) is scribed on the arm to allow measurement of apertures and spacing of fractures. The pointer on the end of the arm does not correspond to a specific direction to be used, rather it provides a 90° angle useful for alignment with steel sets (or other supports) in the drift being mapped.

The circular portion of the arm is scribed with color-coded "right" and "left" markings. Note, again, that the light-toned letters represent red color, and the darker letters represent black color, as illustrated in figure 1, I. Two pointers are placed at 90° to the long axis of the arm and at 180° apart.

USE OF DRAP

In a magnetic environment, the azimuth measurements made with a magnetic compass are not reliable. This difficulty is overcome by using DRAP, which measures the azimuth of dip of a fracture with reference to a known direction, for example, the azimuth of a drift axis. The accuracy of observations, therefore, depends on the ability of the observer in positioning the azimuth arm I of DRAP at 90° to the reference line. The authors have consistently been able to reproduce DRAP measurements of dip to within $\pm 0.5^\circ$ and azimuth of dip to

within $\pm 5^\circ$ of the corresponding measurements made (in a nonmagnetic environment) with a Brunton compass. In addition, DRAP has allowed a slightly greater speed of measuring these angles as compared with a Brunton compass. Another important advantage of DRAP over a Brunton compass is that DRAP makes available much larger measuring surface (base plate A). The 16-sq-in surface tends to average over the protrusions, crystal growths, and other rough features on fracture surfaces, thus giving truer dip and azimuth readings. On the other hand, the approximately 0.75-sq-in surface (edge) of a Brunton compass sometimes yields false dip and strike values due to localized asperities on fracture surfaces.

The following paragraphs describe the various steps involved in using DRAP to obtain the orientations of fractures in underground mines.

Setting Drift Azimuth.--Before any measurements can be made with DRAP, it is necessary to set, on the protractor G, the azimuth of the (reference) axis of the drift that is being mapped. The azimuth values for the drifts to be mapped are determined from the mine maps. Each drift axis will have two azimuths, such as 044° and 224° , as illustrated in figure 4. If the operator travels northeasterly down the drift (044°) this value is set on DRAP by rotating the azimuth protractor G until 044° is aligned with the drift azimuth pointer lock H. The protractor G is locked into place by tightening the lock H. If the operator reverses direction, the new azimuth of 224° would have to be reset on the protractor.

Note that the azimuth setting determines the rib's right and left directions, in relation to the direction of travel of the operator.

Alinement of DRAP.--To map a fracture, the base plate A of DRAP is placed on the fracture surface and is shifted around while rotating the dip cylinder D until the level-bubble is centered. The azimuth arm I is now rotated until it is at 90° to the axis of the drift. This right angle must be visually estimated. With practice, however, a good ($\pm 5^\circ$) estimate of this angle is easily made. As mentioned earlier, the pointer on the end of the azimuth arm also provides a means of sighting-in along the steel sets or other supports to maintain accuracy.

Dip Angle Reading.--The angle of dip of the fracture is read directly from either side of the base shoes B. One of the scribe lines on the cylinder caps E will be aligned with a degree marking on the base shoes B. This degree value is color coded either red (light tone) or black (dark tone).

Azimuth of the Dip Reading.--The pointers, on either side of the circular portion of the azimuth arm I have color-coded (red and black) "right" and "left" markings (for each pointer). These markings refer to the rib (wall) being mapped. Note that in a previous step entitled "Alinement of DRAP", an initial drift azimuth setting of 044° was used. Therefore, the "right" and "left" walls correspond to the operator's right and left as he is facing 044° . In this example the operator is mapping the left wall and has obtained a black color-coded dip reading of 14° . Therefore, the pointer on the side of the azimuth I, which is marked "left" and is colored black, will correspond to an

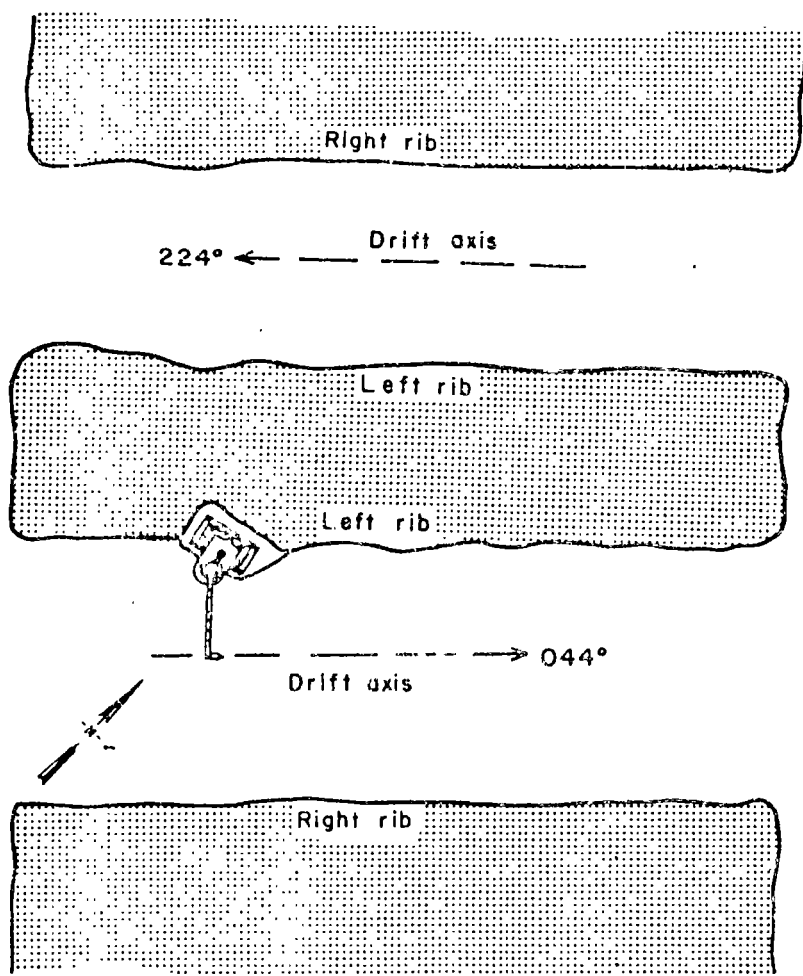


FIGURE 4. - Drift axis direction and rib designation (plan view).

dip markings. The DRAP is constructed from aluminum plate and brass pipe to maintain low weight; it uses standard hardware items to reduce machining cost.

Adeptness in the use of DRAP is readily acquired in less than 1 hr of practice in the field. Comparisons of accuracy can be made by mapping surfaces with a Brunton compass and DRAP in a nonmagnetic environment. The DRAP can measure dip to within $\pm 0.5^\circ$ and azimuth of dip to within 15° of the corresponding values obtained with a Brunton compass.

azimuth of dip value marked on the azimuth protractor G. Note that in figure 2, the side marked black "left" is also marked red "right". For this example a reading of 166° represents the azimuth of the dip value. This corresponds to a strike of $N 76^\circ W$ (or $S 76^\circ E$). To directly read strike values a new azimuth protractor C would have to be scribed with quadrant markings (N,S, E,W). However, dip values would now have to be read in quadrants also, thus complicating procedures more than is necessary for rapid data collection.

SUMMARY

The direct-reading azimuth protractor, DRAP, provides a rapid means of mapping fracture orientations in geologic environments where magnetic influences affect compass measurements. The device is easily constructed and is designed to eliminate operator error in mapping by the use of color-coded dip and azimuth of the

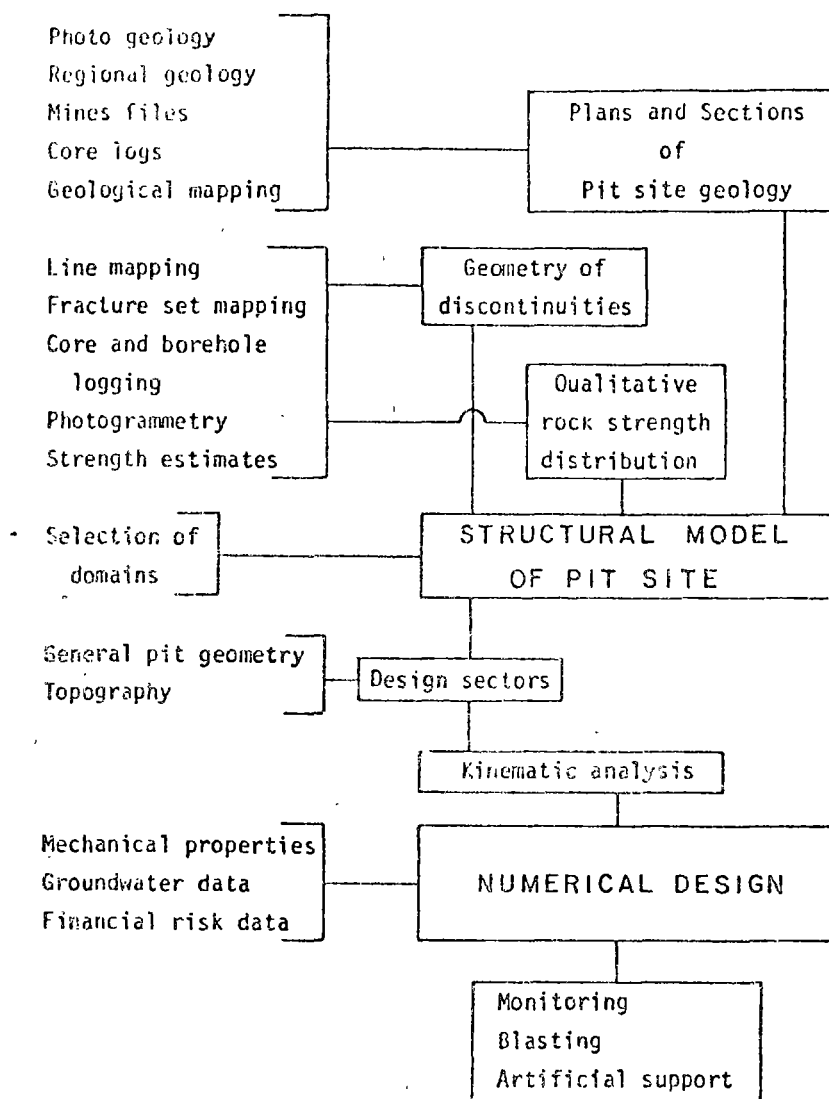


Fig 3 - Flow of geological data for the design of pit slopes.

REGIONAL AND MINE SCALES

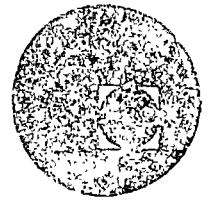
24. As indicated above, the site location alone might allow anticipation of potential slope problems if open pit mining experience or data on natural slopes are available for the area. To develop a good understanding of the geology at the pit site, an integration of the local geology into the regional geological pattern is vital. Regional geological data are available from maps by the Geological Survey of Canada and provincial Departments of Mines. Other relevant sources of information are quoted in paragraph 196.

DETAILED MAPPING FOR PIT DESIGN

25. The general geological map of the pit site provides essential background information but is insufficient for geotechnical assessments. Rock types should not only be known by geological names, but an estimate of strength with simple hardness tests is the minimum required to identify areas where instability could occur due to a weak rock substance. The same applies for the discontinuities which have to be described in more detail than is the case in general geological mapping.



centro de educación continua
división de estudios superiores
facultad de ingeniería, unam



MECANICA DE ROCAS APLICADA A LA MINERIA

TEMA: DETERMINACION DE ESFUERZOS IN SITU

ABRIL, 1978.

OVERCORING EQUIPMENT AND TECHNIQUES USED IN ROCK STRESS DETERMINATION

by

Verne E. Hooker¹ and David L. Bickel²

ABSTRACT

Stress-relief techniques and instrumentation have been developed through many years of research in the Federal Bureau of Mines and successfully used to determine the in situ state of stress in rock. This paper describes the drilling equipment and accessories for use with the Federal Bureau of Mines three-component deformation borehole gage. Operation and calibration procedures for the deformation gage are discussed in detail. Site selection and overcoring procedures are included to provide a complete working knowledge for surface or underground applications.

INTRODUCTION

The Bureau of Mines three-component (measures three diameters 60° apart) borehole deformation gage, which has all sensing elements in the same plane, is designed to measure diametral deformations of a 1½-inch borehole during overcoring stress relief. The process essentially consists of the following three steps: (1) Drilling a 1½-inch-diameter gage hole (pilot hole) with a diamond bit and reamer, (2) positioning the borehole gage in the gage hole, and (3) drilling over the gage with a 6-inch-diameter thin-walled diamond bit. Deformation readings are taken at the start, during, and at the end of the overcoring. After overcoring, the borehole gage is removed and the drilled core is broken and retrieved. The orientation of the core and the position of the borehole gage in the core are marked on the core.

The marked core is tested in a biaxial chamber (2)³ to determine the physical properties of the rock. The physical properties and the deformation measurements from each overcore are used to calculate the secondary principal stresses and their orientation in the plane normal to the axis of the borehole. The effects of anisotropy can be included in the calculation (1). If borehole deformation measurements are obtained from at least three nonparallel holes, a three-dimensional representation of the average ground stress components can be determined (4).

¹ Supervisory geophysicist.

² Engineering technician.

³ Underlined numbers in parentheses refer to items in the list of references preceding the appendixes.

DRILLING EQUIPMENT

The following drilling equipment should be employed for in situ stress measurements:

1. A drill with a chuck speed ranging down to 120 rpm and a penetration rate of $\frac{1}{2}$ inch per 35 to 50 seconds using a 6-inch-diameter overcoring bit, the chuck and quill large enough to take EW⁴ drill rod. See figure A-1. (Note.--Since drills do not normally have chuck speeds as low as 120 rpm, a change in gear ratio is necessary. For the CP-65 air drill the recommended rotation speed is 0 to 1,000 rpm and feed ratios are 200, 300, 500, and 800 revolutions/inch).

2. An EWX⁵ double-tube swivel-type core barrel--one 5 feet and one 7 feet in length, and an EWX single tube core barrel 2 feet in length. See figure A-2.

3. EX diamond bits.

4. A reamer to use with the EX bit for the $1\frac{1}{2}$ -inch-diameter pilot gage hole.

5. EW drill rod in the following lengths: six 5-foot pieces, four 2-foot pieces, and two 1-foot pieces.

6. Two stabilizers (5-7/8 inches in diameter by 8 inches long) on a 2-foot length of EW drill rod. (Note.--The stabilizer can be made from a used 6-inch-diameter core barrel cut 8 inches long.) See figure A-3.

7. Some BX wireline drill rod in the following lengths: three 5-foot pieces, four 2-foot pieces, and two 1-foot pieces. BX wireline is the drill rod that has been found to be the most satisfactory to perform overcore drilling. The inside diameter of the drill rod is large enough for the borehole gage and placement tool to pass through the drill rod. The wire line drill rod is light in weight, yet, it has the strength to meet our drilling requirements. Four threads per inch on the rod are desirable to provide fast coupling.

8. Two stabilizers (5-7/8 inches in diameter by 8 inches long) on 2-foot length of BX wire line drill rod.

9. An adapter sub (EW box to BX wireline pin) for EW drill rod in the chuck and quill to BX wire line drill rod.

10. A water swivel to fit the EW⁴ drill rod in the drill with a 1/2-inch hole for the borehole gage cable to go through and a plug to fit when the cable is not used. See figure A-4. (Note.--The EW pins at the water swivel and at the chuck must be drilled out to at least 9/16 inch for cable and water to go through.)

⁴E, EW, B, and N denote diameter or size.

⁵X denotes manufacturer's series of equipment.

11. Expander head to fit BX wire line drill rod and a 6-inch-OD diamond overcoring bit. See figure A-5.

12. Six-inch-diameter thin-wall masonry overcoring bits long enough to obtain 2 feet of overcore 5-5/8 inches in diameter. See figure A-6.

13. A 6-inch-diameter starter barrel 1 foot in length rigged with a detachable 1½-inch-diameter pilot shaft in the center. The pilot shaft should extend approximately 5 inches beyond the diamonds of the starter barrel. This barrel is used to center the 6-inch-diameter hole over an initial 1½-inch-diameter hole at the face. See figures 2 and A-7.

14. An EW core barrel to replace the detachable pilot shaft. This barrel should be cut to extend 1 inch beyond the starter barrel. When the bit and reamer are attached, the unit is used to drill a 1½-inch-diameter starter hole 4 inches deep in the bottom of a 6-inch-diameter horizontal hole.

15. A centering stabilizer for starting the 5-foot or 7-foot EWX core barrel into the 4-inch horizontal starter hole or for centering the EWX core barrel in the bottom of a 6-inch-diameter vertical hole. See figure A-8.

16. A steel ring 2 inches OD, 1.448 inches ID, and 3/4 inch wide placed on the EWX core barrel in front of the centering stabilizer for retrieving the centering stabilizer. See figure 8.

17. A core breaker to fit the EW rod. The core breaker should be at least 2½ inches wide and hardened. See figure A-9.

18. A 6-inch core shovel to fit an EW rod for retrieving the core from a horizontal hole. See figure A-9.

19. A 6-inch core puller approximately 18 inches in length to fit an EW drill rod for retrieving core from a vertical hole. See figure A-9. The back end of the barrel has an approximate 5/8-inch-thick steel plate welded to the barrel with an EW box welded in the center of the plate. Three 1-1/2-inch-diameter holes on 120° centers are drilled into the plate to allow water to pass through when the core puller is lowered into the 6-inch-diameter hole. On the front end of the barrel are four U cuts 90° apart. These rectangular sections of metal are pushed in slightly to hold the 6-inch core when lifting the core from the vertical hole. (Note.--The shovel and core puller should be made from a used 6-inch core barrel.)

INSTRUMENTATION

The following instruments are required for calibration, testing the drilled core, and measurement of the deformations during the overcoring:

1. Three-component borehole gage and accessories (including special pliers, 0.005-inch and 0.015-inch thick brass washers, and silicone grease). See figures A-11 and B-1.

2. Three Budd⁶ Model P-350 or equivalent strain indicators. (Note.-- If other indicators are used and gage factor (G.F.) of 0.40 cannot be obtained, then calibration at G.F. of 1.5 or other nominal G.F. is necessary.)

3. Orientation and placement tools for the borehole gage. See figures A-12 and B-2.

4. Calibration device for calibrating the three-component borehole gage. See figures A-13 and B-3.

5. Biaxial chamber to determine the modulus of elasticity of the rock. See figures A-14 and B-4.

SITE SELECTION

In order to calculate the complete stress ellipsoid, deformation measurements must be obtained in at least three nonparallel holes. Typical systems of boreholes and directions of measurement are shown in figure 1. Three orthogonal boreholes provide the best configuration of three boreholes for determining all six stress components with uniform precision (fig. 1A). It is possible, however, to obtain very good results from configurations 1B and 1C where the angle between the horizontal holes has been minimized to reduce drilling depths in the horizontal holes. Deformation measurements should be made outside the zone of influence of the mined opening. This distance is usually taken to be one diameter of the mine opening. Borehole configurations 1A, 1B, and 1C require

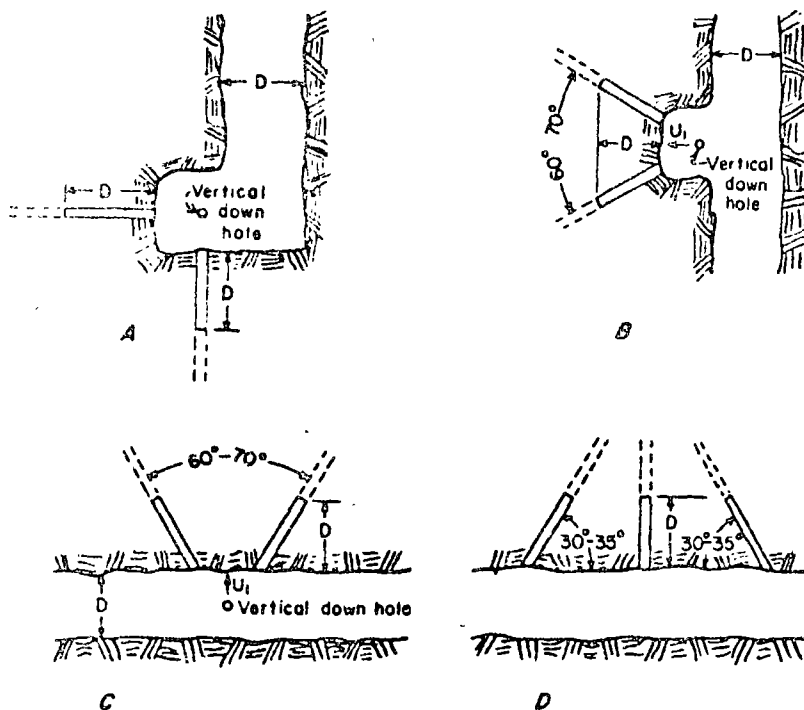


FIGURE 1. - Drill hole configuration (D indicates diameter of mine opening).

only one drill setup. Geologic or structural conditions may require that the zone of stress measurement be confined to a small area. The configuration of 1D will provide good engineering estimates of the stress components except that a high standard deviation will exist for any calculated principal stress component having an orientation parallel or nearly parallel to the axis of any of the holes of the borehole configuration. This configuration requires three drill setups.

⁶Reference to specific company or brand names is made to facilitate understanding and does not imply endorsement by the Bureau of Mines.

Horizontal holes should be started 5° upward from horizontal to facilitate removal of water and drill cuttings from the hole. The drill site should be selected in competent rock where lengths of core of 1 or 2 feet can be obtained. Sometimes it may be advisable to drill NX holes in the proposed overcore configuration to determine if cores of sufficient length can be obtained.

OVERCORING PROCEDURE

If the stress distribution is to be studied near the mine opening, the following procedures should be used:

1. Drill 7 feet of EX pilot hole. The distance of 7 feet has been experimentally determined to be the usual limit of pilot-hole depth before overcoring off centers the pilot hole to such a degree that cores cannot be tested for Young's modulus. The deformation readings will not be effected if the pilot hole does not remain concentric with the 6-inch-diameter hole. However, to determine Young's modulus, the pilot hole should stay 1-1/2 inches or more from the circumference of the 5-5/8-inch-diameter core which is drilled by the 6-inch-diameter thin-wall diamond bit.
2. The 6-inch-diameter starter barrel should be used to drill $\frac{1}{2}$ inch to $1\frac{1}{2}$ inches or enough kerf so that the overcoring barrel can be started. See figure 2.
3. Uncouple the starter barrel from the drill rod near the chuck and remove the starter barrel.
4. Open the drill to make room for borehole gage placement and retrieval tool.
5. String the borehole gage cable (which has had its end taped) through the adapter sub, EX drill rod, and water swivel. See figure 3.
6. Remove tape from the borehole gage cable and hook the cable to the three strain indicators as shown in figure 4 or 5. The six pistons are pulled from the gage with the special pliers and kept in order. A zero deformation reading is taken for each component and recorded on the field data sheet (fig. 7) in the row labeled, "zero," and in the three columns labeled, "U₁," "U₂," and "U₃." (Note.--When only one indicator is available, use a switching and balancing unit or just a switching unit. With no switching unit, hook up the indicator as shown, take a reading, U₁, and replace the white and red wire with the yellow and orange wire. Take another reading, U₂, and replace the yellow and orange wire with the brown and blue wire. Read U₃.) The pistons are greased and replaced in their proper place in the gage. Material can be removed from the O-ring by a toothbrush if a piston is accidentally dropped. (Note.--Always grease the piston O-ring before putting it back into the borehole gage.) Each diameter should be checked by applying slight finger pressure on the pistons to insure that the correct diameter is connected to the selected indicator and is working properly. The respective indicator needles will move as the pressure is applied to a piston.

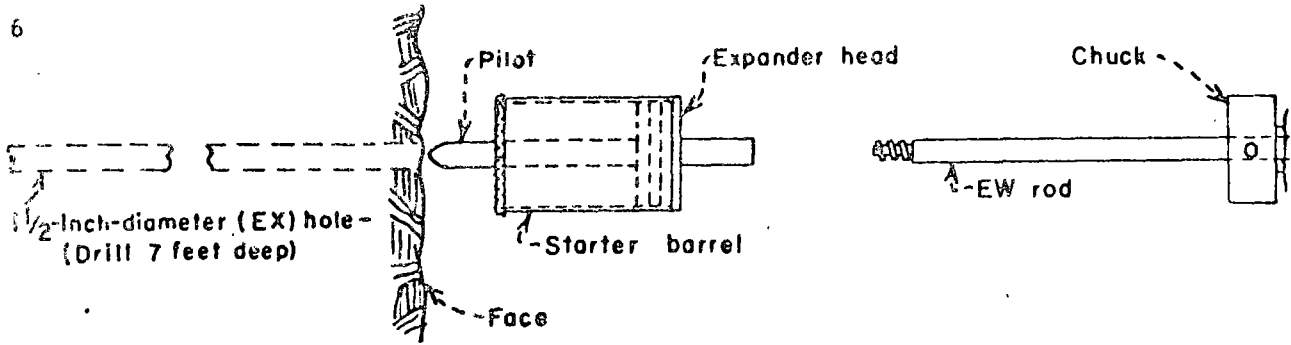


FIGURE 2. - Starting the 6-inch-diameter overcoring hole.

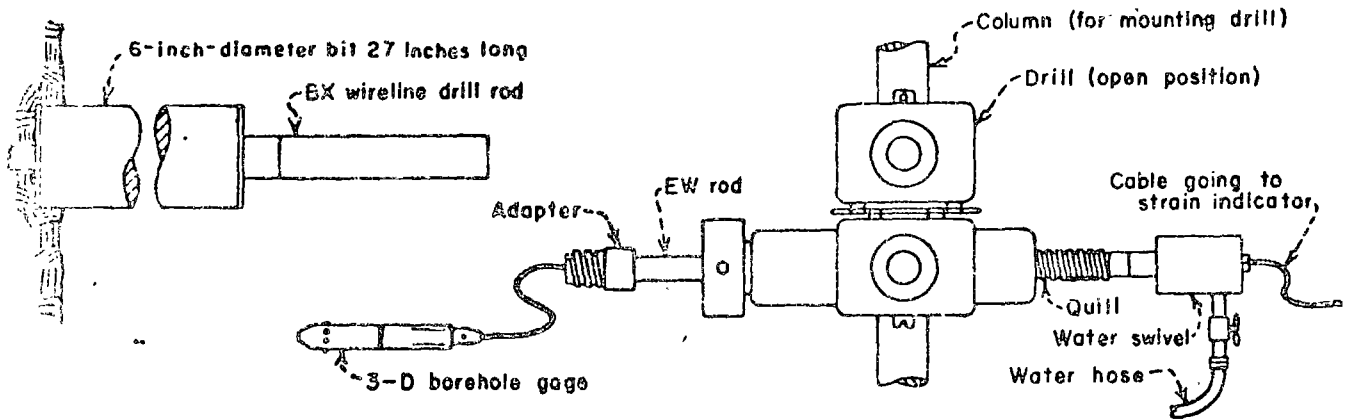
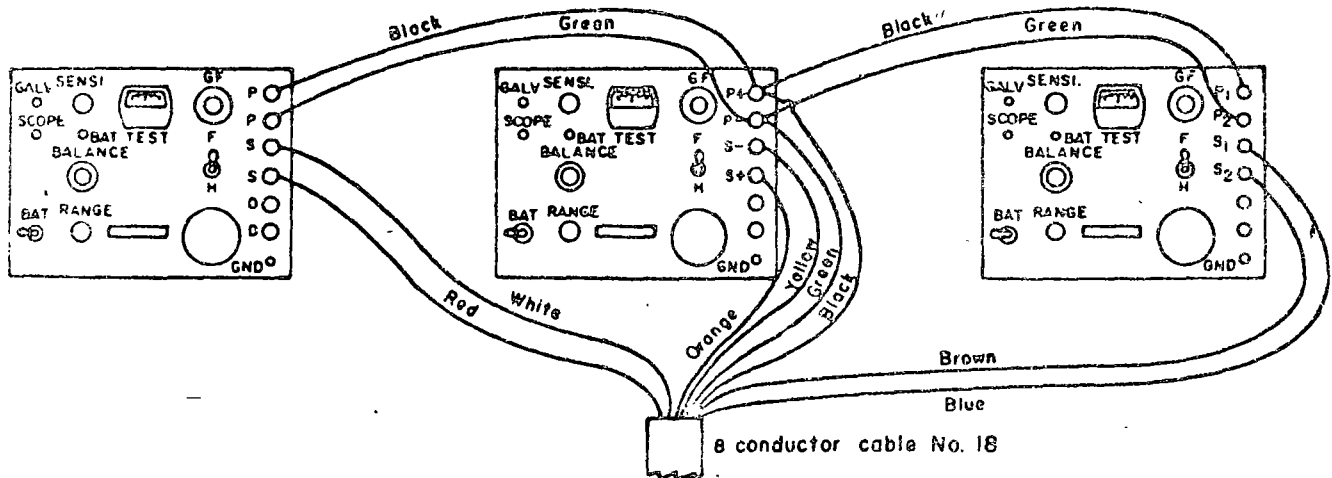


FIGURE 3. - Setup for the three-component (3-D) borehole gage placement.

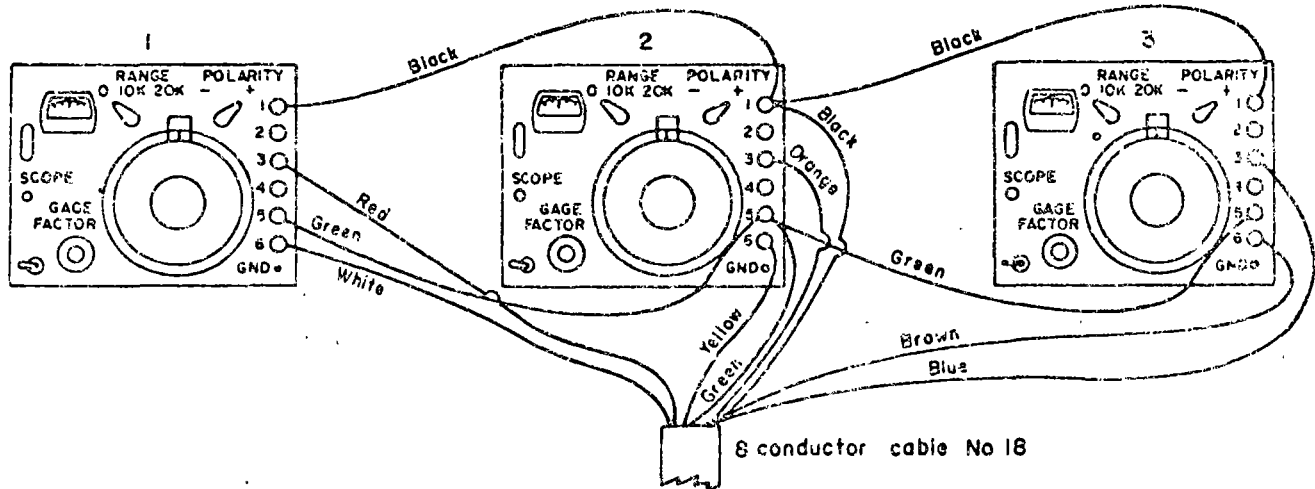
Sensitivity knob: turn full clockwise.
 Balance knob: put mid-range (5 turns of the 10-turn potentiometer).
 Bridge switch: Switch to full (F).



Note. Hook black and green wires to Indicator No. 2 and use two other wires (No. 18 or No. 20) to common P+ and P- (or P₁ and P₂) of all three indicators.

FIGURE 4. - Wire hookup to model P-350 strain indicators.

Gage factor =1.50 (lowest gage factor this indicator will go).



On the BLH Model N strain indicators, the terminal marked B on all three indicators are hooked together as are the terminals marked G. The black and green wires coming from the 8 conductor cable are hooked to these terminals.

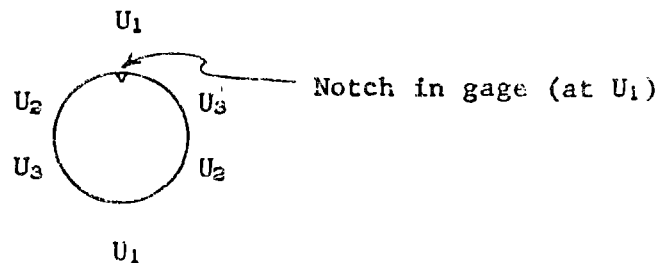
FIGURE 5. - Wire hookup to model HW-1 strain indicators.

Examine the case screws of this borehole gage and tighten them if necessary.

7. Place the 6-inch-diameter core barrel into the hole made by the starter barrel.

8. Holding the borehole gage (notch up), engage the orientation pins (see fig. B-1) of the borehole gage with the placement and retrieval tool using a clockwise motion and secure the cable with the wire clip (see fig. B-2). For correct alignment, the cable groove in the placement and retrieval tool should be aligned with the notch in the gage case that indicates U_1 (component 1). The notch is filed in front of the piston in the borehole gage case.

POSITION OF COMPONENTS



Looking from rear of gage

This placement and retrieval tool is designed to set and orient the gage with clockwise motion. Since U_1 (a notch in the gage) is perpendicular to the

orientation handle, a small level can be used on the handle for orientation in horizontal holes.

9. With the placement rod, put the borehole gage through the 6-inch core barrel and into the EX hole 9 inches past the 6-inch-diameter kerf and orient the gage. See figure 6.

10. Check the bias of the gage on the strain indicators. (See section on Procedure for Operating the Three-Component Borehole Gage for amount of bias needed and for changing bias on the gage.)

11. Turn the placement tool counterclockwise (approximately 60°) to free the placement tool from the gage. Similarly, when retrieving the gage, the tool is slipped onto the gage and rotated clockwise until the tool stops against the orientation pins of the borehole gage. (Note.--If the gage is oriented too far clockwise, a counterclockwise motion of about 120° will allow the gage to be moved counterclockwise, then reoriented correctly on the clockwise motion.)

12. Remove the placement and retrieval tool from the hole.

13. Close the drill.

14. Pull all excess cable through the drill.

15. Couple the drill rod that is in the chuck to the BX wire line-drill rod extending out of the drill hole.

16. Hold or tie the cable behind the water swivel.

17. Turn on water. Allow approximately 10 minutes from the time the gage is set for the gage, drill water, and rock to come to temperature equilibrium.

18. Start the overcore with a chuck speed of approximately 120 rpm and a penetration rate of $\frac{1}{2}$ inch per 40 seconds; 120 rpm gives very satisfactory bit life and will lessen the chance of damaging the gage if the core should break during an overcore relief. Each $\frac{1}{2}$ -inch penetration should be signaled to the

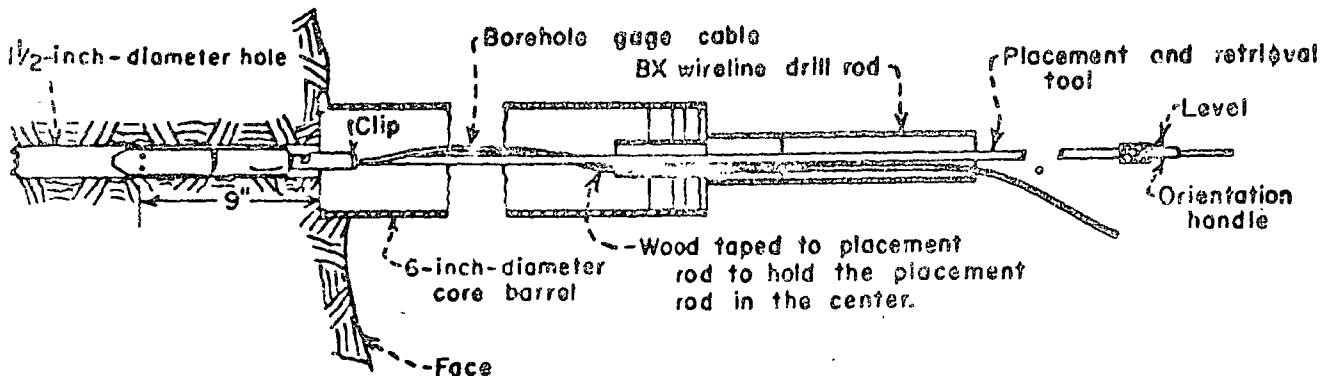


FIGURE 6. - Positioning the three-component (3-D) borehole gage with the placement rod through the 6-inch-diameter core barrel and drill rod.

indicator reader and the indicator readings (deformation measurements) recorded on the field data sheet (fig. 7). The rate of penetration of

Hole No. _____ Date _____ Orientation: U_1 _____
 Gage No. _____ Calibration Factor U_1 _____
 Gage factor _____ U_2 _____
 True Bearing of Hole _____ U_3 _____

DEPTH			DEFORMATION			TIME			TEMP.		REMARKS
Gage	Hole (+)		INDICATOR READING			Gage Set	Overcore Start	Deformation Read	Rock	Water	
			U_1	U_2	U_3						
		Zero									
9"	Face	Bias									
	1/2"										
	1"										
	1 1/2"										
	2"										
	2 1/2"										

	7"										
	7 1/2"										
	8"										
	8 1/2"										
Pistons	9"										
	9 1/2"										
	10"										
	10 1/2"										
	11"										

	13"										
	13 1/2"										
	14"										
	14 1/2"										
	15"										
	15 1/2"										
	16"										
	16 1/2"										
	17"										
	17 1/2"										
	18"										

Note. Next relief would start at 18 inches and go to 36 inches and gage would be orientated at a depth of 27 inches.

FIGURE 7. - Field data sheet.

40 seconds allows just enough time for the data observer to record the three diametral readings. Overcoring should proceed for a total of 18 inches which is 9 inches beyond the plane of measurement for a complete overcore. If readings are taken each $\frac{1}{2}$ inch, 36 sets of readings are recorded.

Modifications of the length of overcore can be reduced as low as 6 and 6 or a total of a 12-inch run with good results still obtainable. (Note.--If the core breaks during overcoring, this breakage will be noticed by the indicators fluctuating or the cable twisting through the drill rod. If this happens, the drill should be shut down immediately and the gage and broken core retrieved.)

19. Upon completion of the overcore or when the core breaks prematurely, uncouple the EX wire line-drill rod at the adapter sub.

20. Pull a little slack in the cable so the drill can be opened.

21. Retrieval tool is hooked onto the borehole gage cable by the wire clip, and then inserted through the BX wire line-drill rod to retrieve the gage. This procedure is described in step 11.

22. Remove the core barrel and drill rod from the hole.

23. Use the core breaker to break core.

24. Retrieve this core with the core shovel. In a vertical hole retrieve the core with the core puller. Mark an orientation on the core after the core is brought to the collar of the 6-inch-diameter hole. Be careful not to rotate the core puller when retrieving core from a vertical hole.

25. Place the core barrel and drill rod back in the 6-inch-diameter hole.

26. Repeat steps 8 through 25 for each additional relief in the remaining EX pilot hole. Do not position the borehole gage pistons closer than 12 inches to the bottom of the pilot hole.

Overcores should be tested in a biaxial chamber as soon as conveniently possible after recovery to determine the modulus of elasticity.

The 7 feet of EX hole allows for approximately four complete overcores before drilling out the last foot or so of EX and recentering and drilling the next 7 feet of EX hole for more determinations. Stabilizers are inserted in the drill stem generally at 10-foot-rod intervals.

In all drilling, the pilot EX hole should be cored with a double tube barrel so that the core can be obtained for observation. This core indicates the fractures and/or if core dinking is occurring so that the gage can be placed in the competent zones. Dinking areas or highly fractured areas should be drilled out prior to gage emplacement.

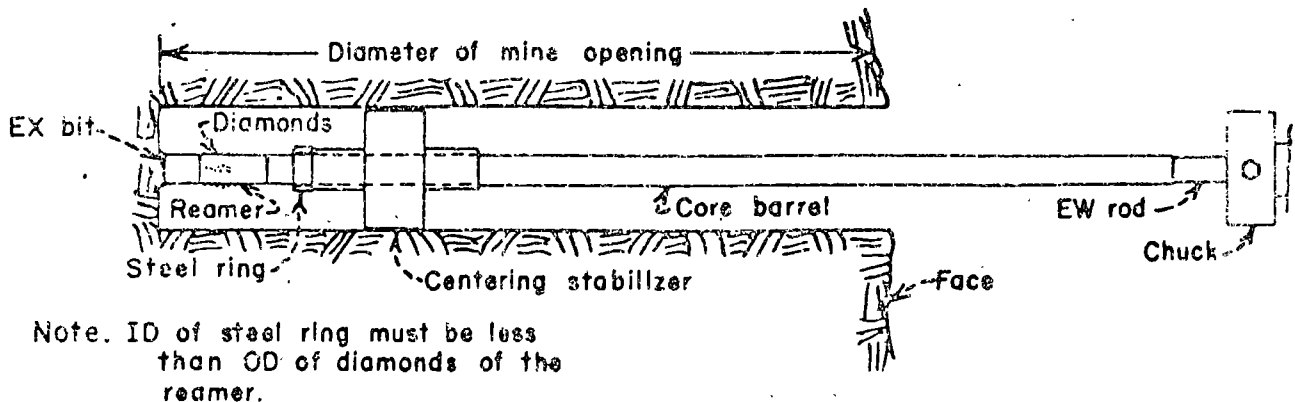


FIGURE 8. - Starting the 1½-inch-diameter hole in the bottom of the 6-inch-diameter hole.

Providing the only interest is to determine the stress field outside the influence of the mine opening, time can be saved by drilling the 6-inch-diameter hole without instrumentation. Then, centered in the bottom of the 6-inch-diameter hole, approximately 7 feet of EX hole is drilled for gage emplacement and subsequent overcore determinations. See figure 8. At this distance of one diameter from the opening, at least three good sets of readings should be obtained from each hole for a good statistical determination of the average ground stress components.

PROCEDURE FOR OPERATING THE THREE-COMPONENT BOREHOLE GAGE

The procedures described in the section have been developed through use of the gage over a long period of time. It is important that the details be followed closely in order to minimize any chance of damage to the gage and provide for the most reliable acquisition of data.

1. Hook the gage to the indicators, as shown in figure 4 or 5, or to the switching unit and one indicator.
2. Remove all the pistons from the gage with special pliers. See figure A-11. The special pliers are made by brazing a piece of brass 1/2-inch-by-3/8-inch-long (round stock preferred) to the jaws of a standard pair of pliers. An 11/32-inch-diameter hole is drilled parallel to the jaws of the pliers in the center of the brass. The pliers are opened by sawing through the brass along the diameter perpendicular to the handles of the pliers. The outside edges are filed to fit inside the 1/2-inch-wide milled flats of the borehole gage case.
3. Record the zero deformation reading for each of the three components. Label them U_1 , U_2 , and U_3 zero reading.
4. Grease the O-ring on all the pistons and insert the pistons back into the gage.

5. Place the gage in the $1\frac{1}{2}$ -inch hole or into the test specimen if the work is done in the lab. Caution.--Do not force the gage into the $1\frac{1}{2}$ -inch hole if it fits very tightly. Instead, remove any washers that may be on the pistons, as follows:

- a. First remove one piston at a time with the special pliers.
- b. Hold the piston with both pliers and screw it apart, being careful not to grab the O-ring with the pliers.
- c. Remove the washer and screw the piston firmly back together.
- d. Grease the O-ring and insert the piston into the gage.
- e. Do this to only one piston in each diametral pair (U_1 , U_2 , and U_3) and reset the gage in the EX hole. If the gage is still very tight, remove a washer from the remaining three pistons as stated in steps a-d. If the gage is very loose inside the $1\frac{1}{2}$ -inch hole, remove the pistons one at a time and put on a washer using steps a-d.

6. If the gage offers some resistance when placing it into the $1\frac{1}{2}$ -inch hole, position the gage in the desired orientation.

7. Read all three components (U_1 , U_2 , and U_3).

When relieving stress as in field overcoring stress relief, the bias set on each component should be between 10,000 and 15,000 indicated units ($\mu\text{in/in}$) with a gage factor of 0.40. When stress is applied to a specimen as in the lab, or in the biaxial chamber, a bias set on each of the components should be between 4,000 and 8,000 indicated units ($\mu\text{in/in}$) for a gage factor of 0.40. Using a gage factor of 1.50 the bias should be between 2,300 and 3,400 indicated units ($\mu\text{in/in}$) for overcoring stress relief and between 900 and 1,800 indicated units ($\mu\text{in/in}$) for lab testing. The following tabulation shows typical zero readings and calibration factors for the two gage factors mentioned:

For a gage factor of 0.40:

Zero readings (pistons out):

$$U_1 \approx -4000$$

$$U_2 \approx +3100$$

$$U_3 \approx +4100$$

Calibration factors:

$$U_1 \quad 1.00 \mu\text{in per } \mu\text{in/in}$$

$$U_2 \quad 1.00 \mu\text{in per } \mu\text{in/in}$$

$$U_3 \quad 1.04 \mu\text{in per } \mu\text{in/in}$$

For a gage factor of 1.50:

Zero readings (pistons out):

$$U_1 \approx -930$$

$$U_2 \approx +670$$

$$U_3 \approx +960$$

Calibration factors:

$$U_1 \quad 4.35 \mu\text{in per } \mu\text{in/in}$$

$$U_2 \quad 4.39 \mu\text{in per } \mu\text{in/in}$$

$$U_3 \quad 4.36 \mu\text{in per } \mu\text{in/in}$$

Care must be taken to not overload the transducers. Maximum load on any component should not exceed 20,000 indicated units ($\mu\text{in/in}$) using a gage factor of 0.40; and 4,560 indicated units ($\mu\text{in/in}$) using a gage factor of 1.50.

Lowering the gage factor increases sensitivity. A gage factor of 0.40 gives a readout of one indicator unit ($\mu\text{in/in}$) for 1 microinch deformation.

Using any other gage factor besides the two mentioned, the workable range in indicated units must be determined as must the calibration factors.

BOREHOLE GAGE CALIBRATION

The following steps describe the procedure for calibrating the three-component borehole gage. Calibration should be done before the borehole gage is used in situ or in the laboratory. It is a good practice to calibrate the borehole gage after it has been used. This will concur that no damage has occurred to the borehole gage during its use.

1. Grease all pistons.
2. Put them into the gage.
3. Place the gage into the calibration jig.
4. Position the gage so that the pistons for component one are visible through the micrometer holes.
5. Tighten the three wing nuts.
6. Install the two micrometer heads and lightly tighten the set screws.
7. Set the strain indicator on "Full Bridge," center the balance knob if there is one, and set the gage factor at 0.40 or any gage factor desired. (Note.--The gage factor setting must be the same for calibration as used in the field for overcoring and for biaxial testing.)
8. Hook the wires for component one (black, green, white, and red) to the indicator as shown in figure 4 or 5 and balance it.
9. Turn one micrometer in, until the needle of the indicator just starts to move. The micrometer is now in contact with the pistons.
10. Do the same with the opposite micrometer.
11. Rebalance the indicator if necessary.
12. Record this no load reading (zero displacement).
13. Turn in each micrometer 0.0160 inch (a total of 0.0320 inch displacement for component one). (Note.--The micrometer is read to a ten-thousandths of an inch.)
14. Balance the indicator.

15. Record the reading.
16. Wait 2 minutes to check that the combined creep for the two transducers making up the component is not excessive. (For 2 minutes the creep should not exceed 20 $\mu\text{in/in}$).
17. Record the new reading.
18. Back off each micrometer 0.0040 inch (a total of 0.0080 inch for the component).
19. Balance and record.
20. Continue this procedure until you are back to the starting point on the micrometers. (Note.--This zero displacement reading will also be the zero displacement reading for a second run.)
21. Repeat steps 13 through 20 for the second cycle.
22. Loosen the wing nuts and rotate the gage clockwise to line up component two with the micrometers.
23. Retighten the wing nuts.
24. Hook up the wires for component two (black, green, yellow, and orange) to the strain indicator.
25. Proceed with steps 9 through 21.
26. Calibrate component three in similar manner.

CALIBRATION DATA ANALYSIS

Subtract the zero displacement strain indicator reading (last reading of each run) from all your other indicator readings to establish the differences. These values are in microinch per inch. Because of friction between the O-ring around the piston and the wall of the holes in the borehole gage case, the last subtracted value (6,860 $\mu\text{in/in}$ at 0.0080 inch displacement) is subtracted from the largest displacement difference (30,535 $\mu\text{in/in}$ at 0.0320 inch). This difference (23,675) in microinch per inch is divided into the deformation difference for this given range, which is 0.0240 inch or 24,000 microinches per inch. The resulting amount is the calibration factor. Do this again for the second run and average these two calibration factors for the calibration factor used for component one.

Repeat the above procedure to determine the calibration factors for component two and component three.

The following is a sample of two runs for one component, calibrated at a gage factor of 0.40:

Displacement, inches	Indicator reading	Difference
RUN 1 ¹		
0	-693	-
.0320	+30,140	Wait 2 minutes
.0320	30,055	30,535 μ in/in
.0240	21,920	22,400 μ in/in
.0160	14,040	14,520 μ in/in
.0080	6,380	6,860 μ in/in
0	-480	-
RUN 2 ¹		
0	-480	-
.0320	+30,034	Wait 2 minutes
.0320	29,980	30,430 μ in/in
.0240	21,914	22,364 μ in/in
.0160	13,975	14,425 μ in/in
.0080	6,335	6,785 μ in/in
0	-450	-

¹ Calibration factor: $\frac{\text{Known displacement } (\mu\text{in})}{\text{Indicator units}} = \mu\text{in/indicator unit.}$

Thus, for run 1

$$\frac{24,000}{23,675} = 1.014; \text{ and}$$

for run 2

$$\frac{24,000}{23,645} = 1.015.$$

Use a calibration factor of 1.01 for the component.

The above method is a faster means and is within 1 percent of the least squares method for determining the calibration factor. However, if desired, a least squares determination can be made from a plot of micrometer displacement versus indication units.

IDENTIFICATION OF SOURCE OF MALFUNCTION OF BOREHOLE GAGE

If Balance on One or More of the Indicators Is Not Achieved

Recheck the wiring hookup to see that the hookup is in accordance with the wiring diagrams in figure 4 or 5 and that all connections are tight. If balancing is still not achieved, the problem may be due to the plug-in cable connection in the borehole gage. This is checked by removing all of the screws from the placement end of the gage, removing this end, turning off the knurled clamping nut, and pushing in the cable to insure good plug-in connection. With the indicator set to the zero reading for each component and when good connection is made, the indicators will balance. Screw back the knurled clamping nut very tightly and replace the end. (Note.--Nonbalance may occur when too much pull has been exerted on the cable accidentally or intentionally

during gage retrieval after overcoring. Sometimes in a vertical hole, cuttings or broken rock drop into the $1\frac{1}{2}$ -inch hole impeding the gage retrieval tool from hooking onto the orientation pins of the gage. A tendency always exists to attempt to retrieve the gage by pulling the cable. A better way to retrieve the gage is to remove the drilling rod and the 6-inch-diameter core barrel and break off the core with the gage still inside. Remove the borehole gage cable from the drill, 6-inch-diameter core barrel, and drill rod. String the cable through one of the holes in the end of the core puller. Then retrieve both core and gage with the 6-inch core puller.)

One or More Elements Become Insensitive on Indicator

If elements become insensitive to deflection of the pistons or nonresponsive to the turning of the indicator dial, the probability exists that water or moisture has somehow entered through the gage into the connecting plug or cable. In this case do the following:

1. Remove the pistons and the borehole gage case to check for water. If water is present, check the piston O-rings for a possible cut that may have occurred from gripping the O-ring with pliers. Grease the O-rings and replace the case.

2. Remove the placement end as stated previously. Check the grommet seal. If water is found inside the gage or in the cable connecting plug, dry out completely, regrease the cable where it passes through the grommet and tighten the knurled nut firmly. Replace the placement end.

One Component Does Not Balance Anywhere on the Indicator Dials or Balances Intermittently

This situation indicates a disconnected wire or possibly a cold solder joint. Remove the borehole gage case and check all wires going to this component including the plug-in cable connector. Solder where needed and replace the gage case.

Indicators Are Sensitive When Being Touched

This sensitivity generally occurs after the instruments are used for a period of time in very humid conditions. Use plastic or other insulating material underneath the indicators during the working day. Each night the indicators should be brought out of the mine and allowed to dry.

REFERENCES

1. Becker, Robert M., and Verne E. Hooker. Some Anisotropic Considerations in Rock Stress Determination. BuMines RI 6965, 1967, 23 pp.
2. Fitzpatrick, John. Biaxial Device for Determining the Modulus of Elasticity of Stress-Relief Cores. BuMines RI 6128, 1962, 13 pp.
3. Obert, Leonard. Triaxial Method for Determining the Elastic Constants of Stress Relief Cores. BuMines RI 6490, 1964, 22 pp.
4. Panek, Louis A. Calculation of the Average Ground Stress Components From Measurements of the Diametral Deformation of a Drill Hole. BuMines RI 6732, 1966, 41 pp.

APPENDIX A.--PHOTOGRAPHS OF THE DRILLING EQUIPMENT,
BOREHOLE GAGE, AND ACCESSORIES

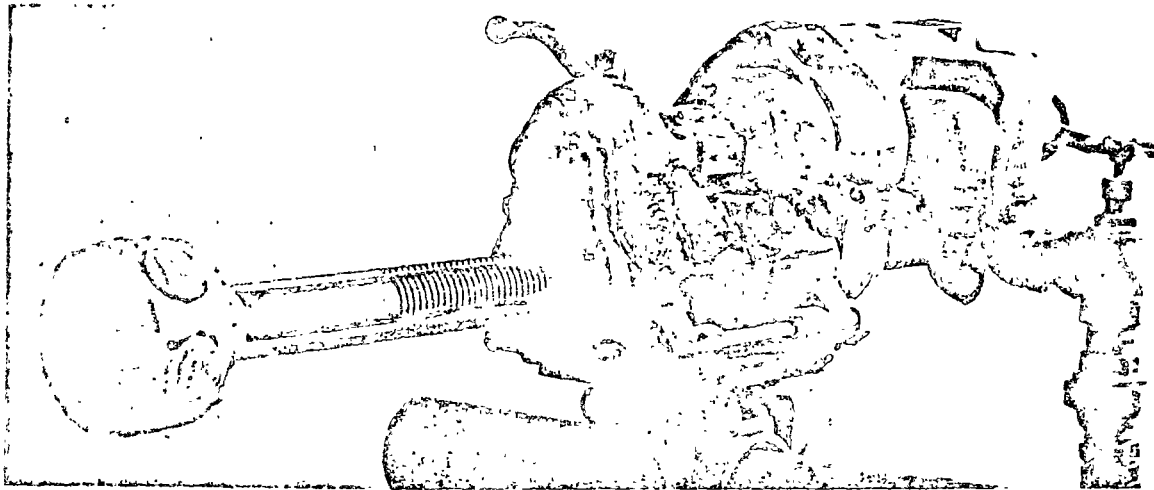


FIGURE A-1. - Type CP-65 air drill.

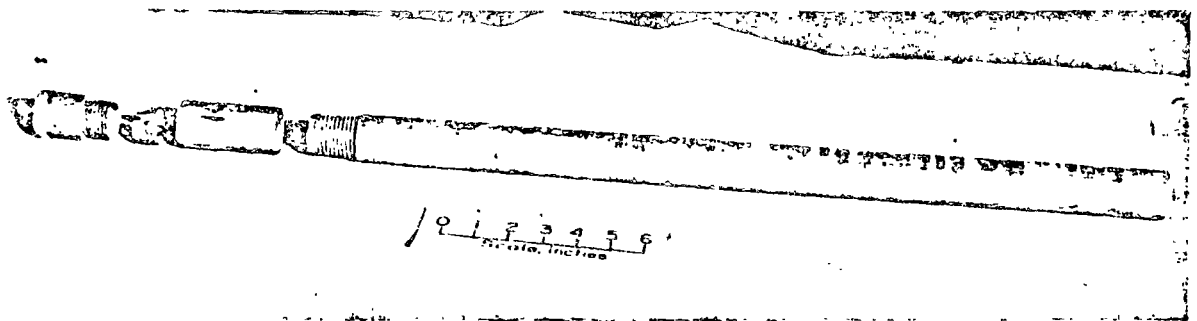


FIGURE A-2. - EX size bit with core spring, reamer, and 2-foot EWX core barrel.

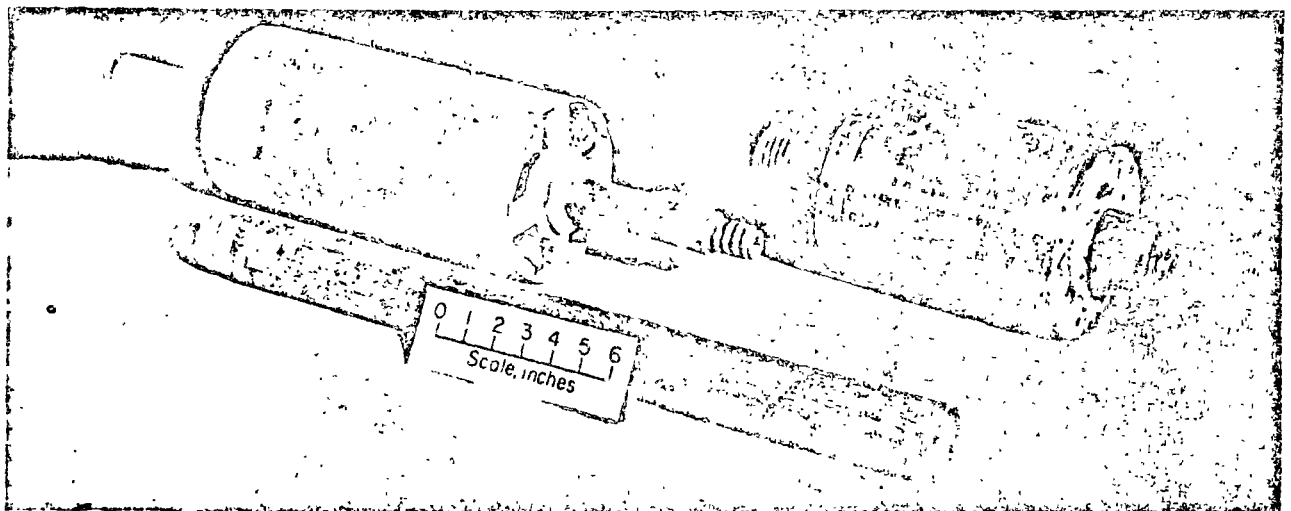


FIGURE A-3. - Stabilizer on a 2-foot section of EW drill rod (upper left), stabilizer on a 1-foot section of BX wire line drill rod (upper right), and a 2-foot piece of BX wire line drill rod (foreground).

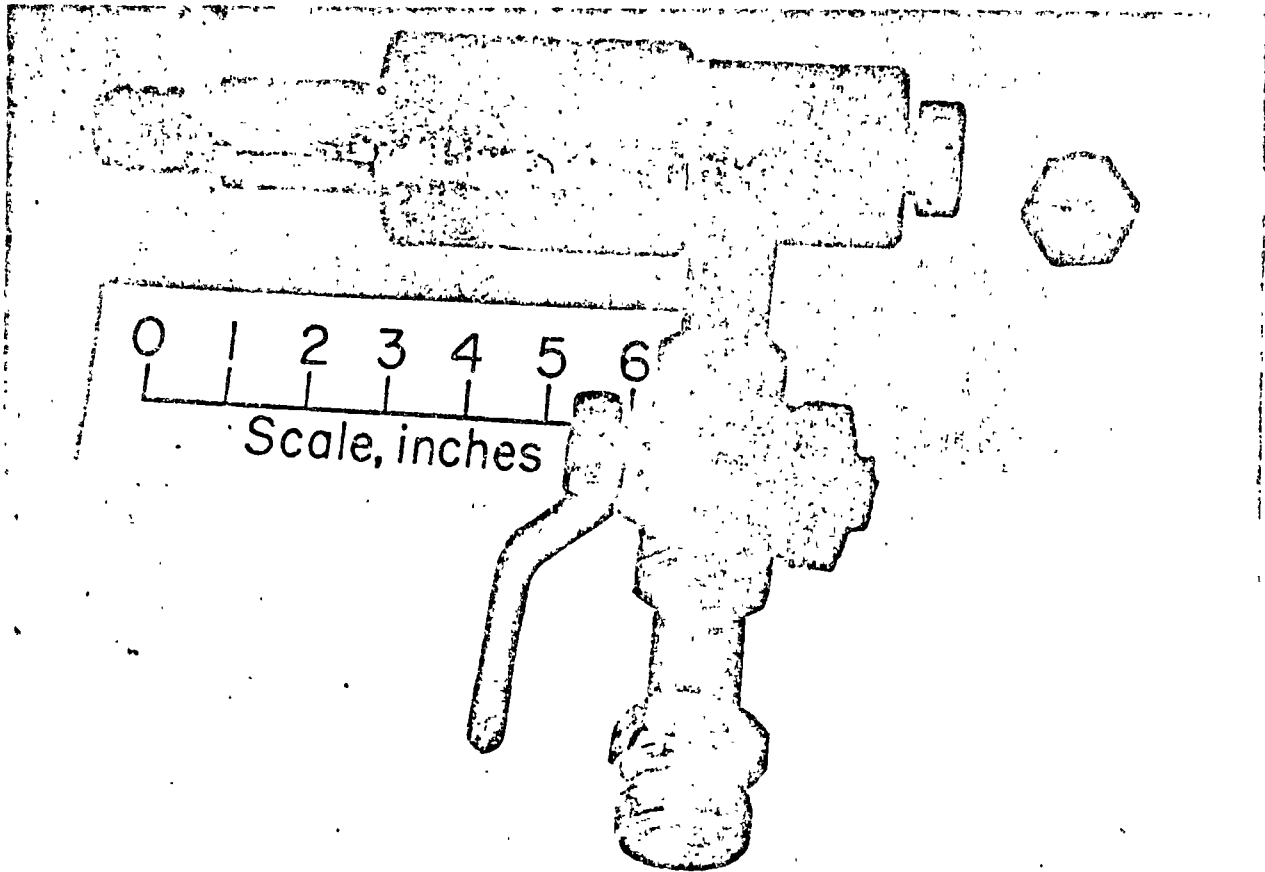


FIGURE A-4. - Water swivel with solid plug. Plug at right used during overcoring.

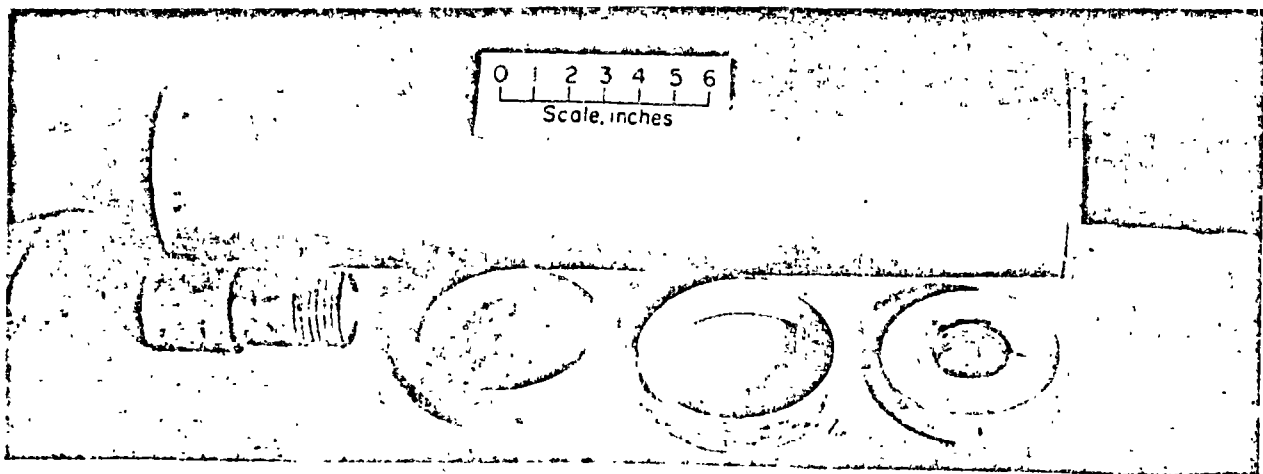


FIGURE A-5. - 6-inch-diameter core barrel 27 inches long (referred to as a 2-foot core barrel) and disassembled expander head.

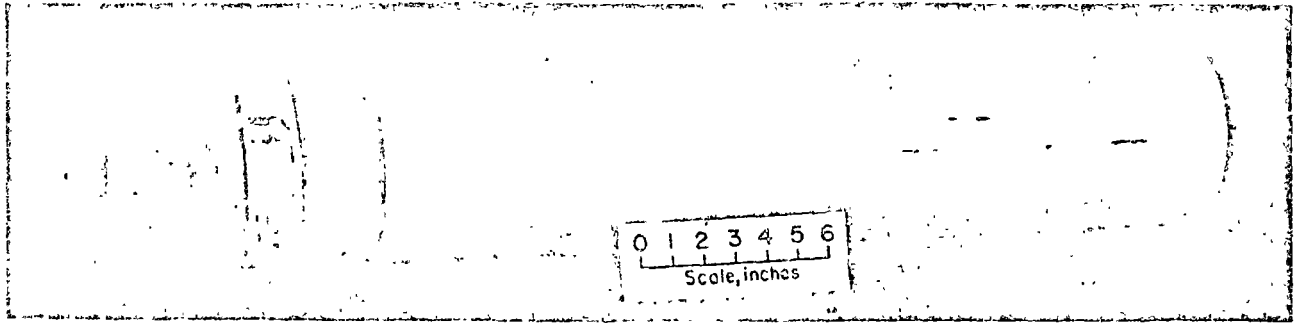


FIGURE A-6. - Expander head assembled (adapted for BX wire line drill rod) and 6-inch-diameter core barrel.

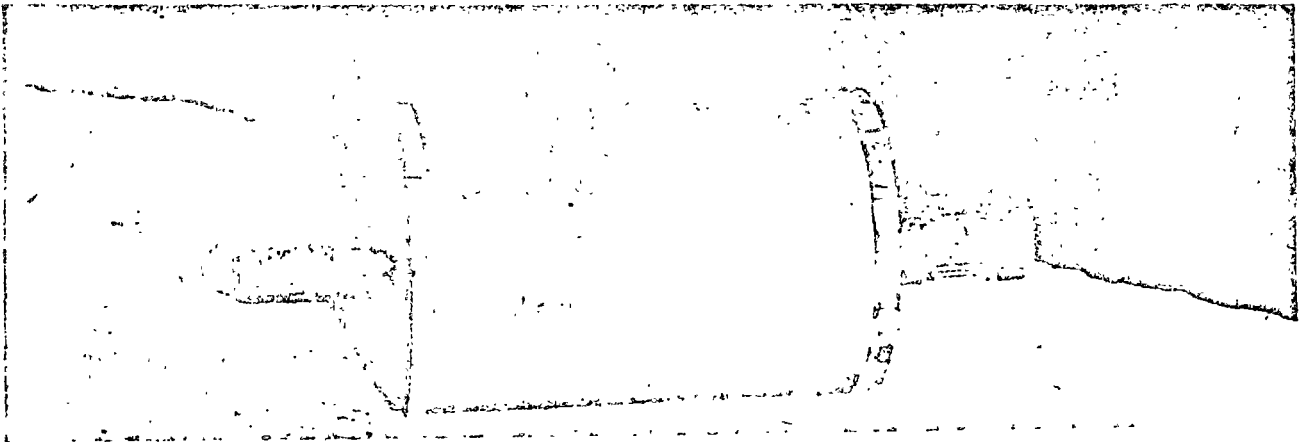


FIGURE A-7. - 6-inch-diameter starter barrel with pilot and expander head adapted for EW drill rod.

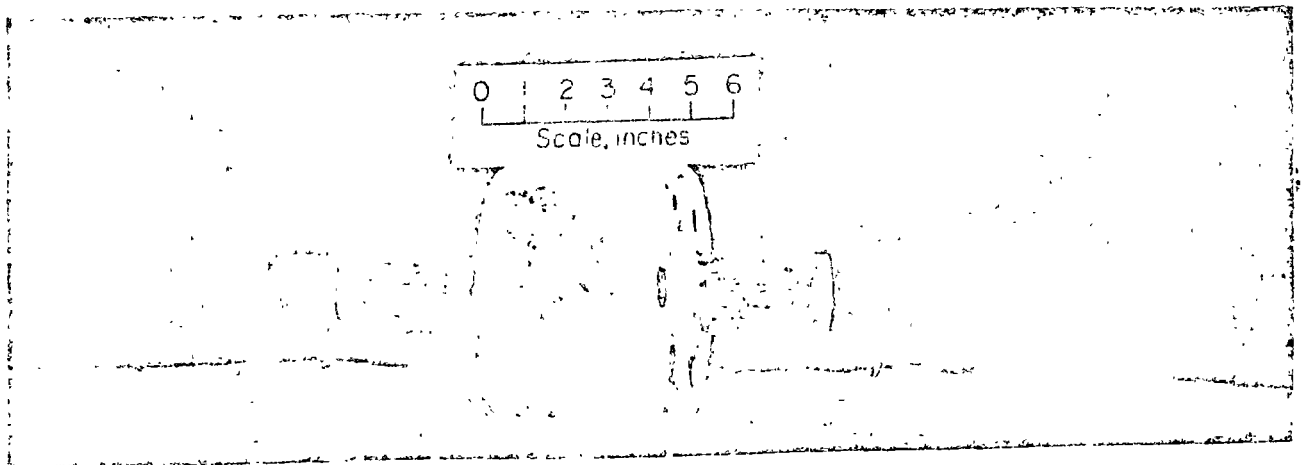


FIGURE A-8. - Centering stabilizer.

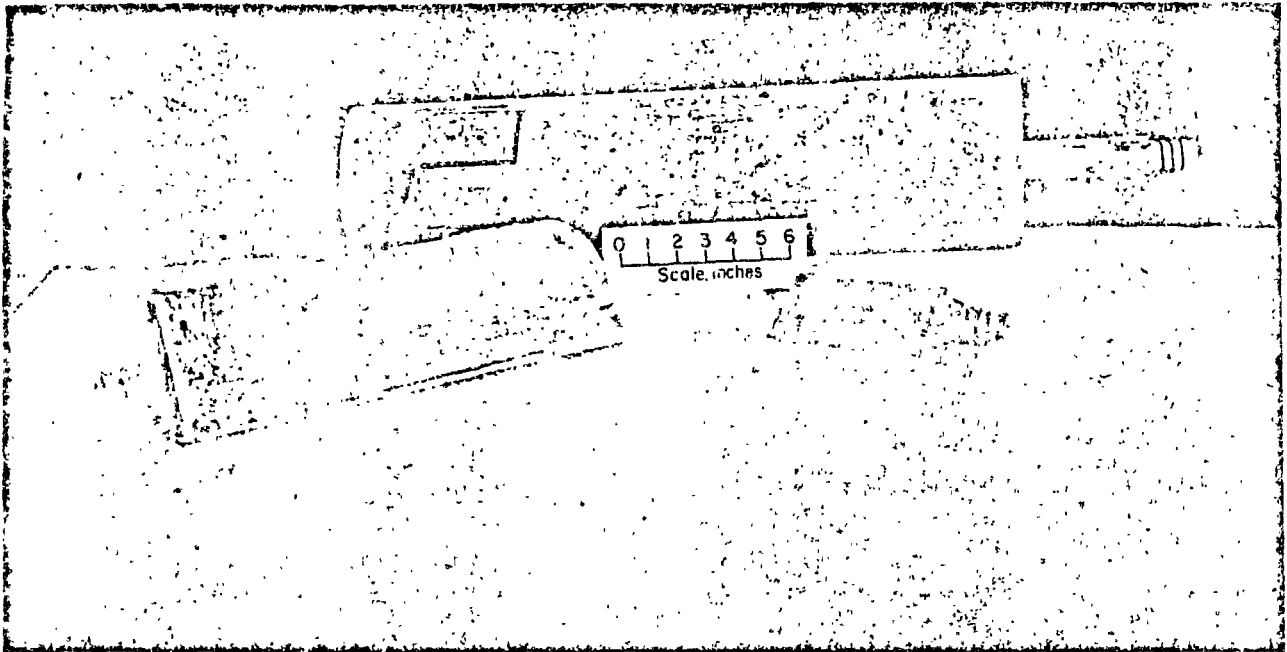


FIGURE A-9. - Core breaker (lower right), core shovel (lower left), and core puller (center).

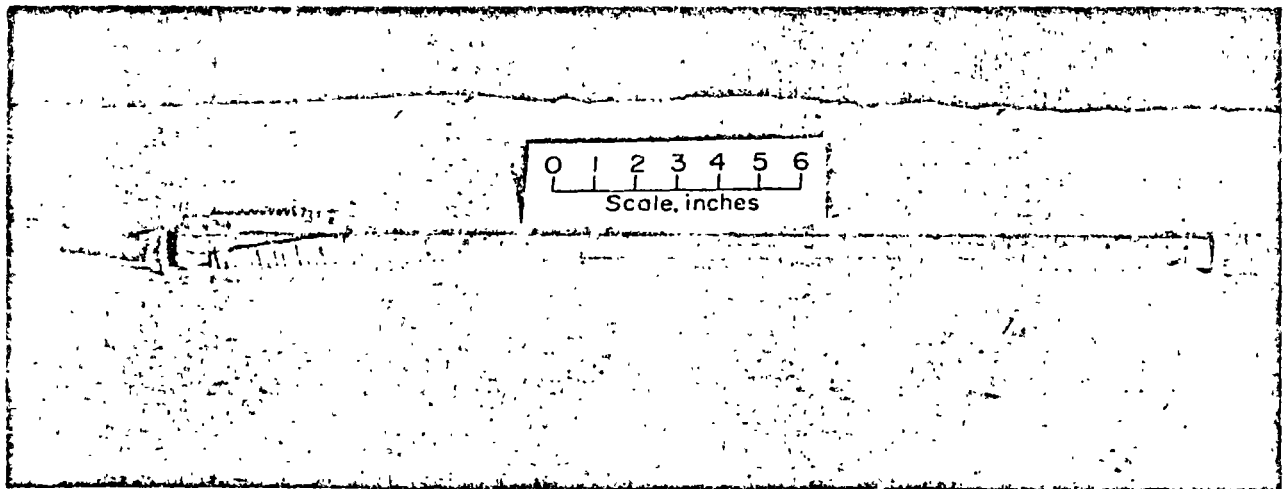


FIGURE A-10. - Retrieval tool used in place of the core puller to retrieve 6-inch-diameter core from a vertical hole that has a 1½-inch-diameter hole through the core.

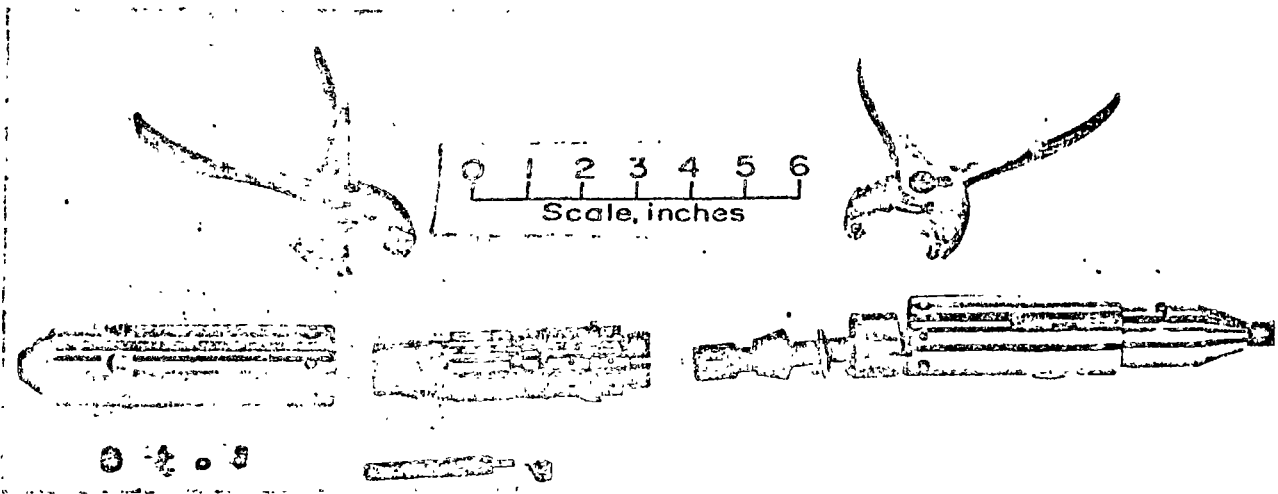


FIGURE A-11. - Special pliers, the Bureau of Mines three-component borehole gage, a piston, disassembled piston and washer, and a transducer with nut.

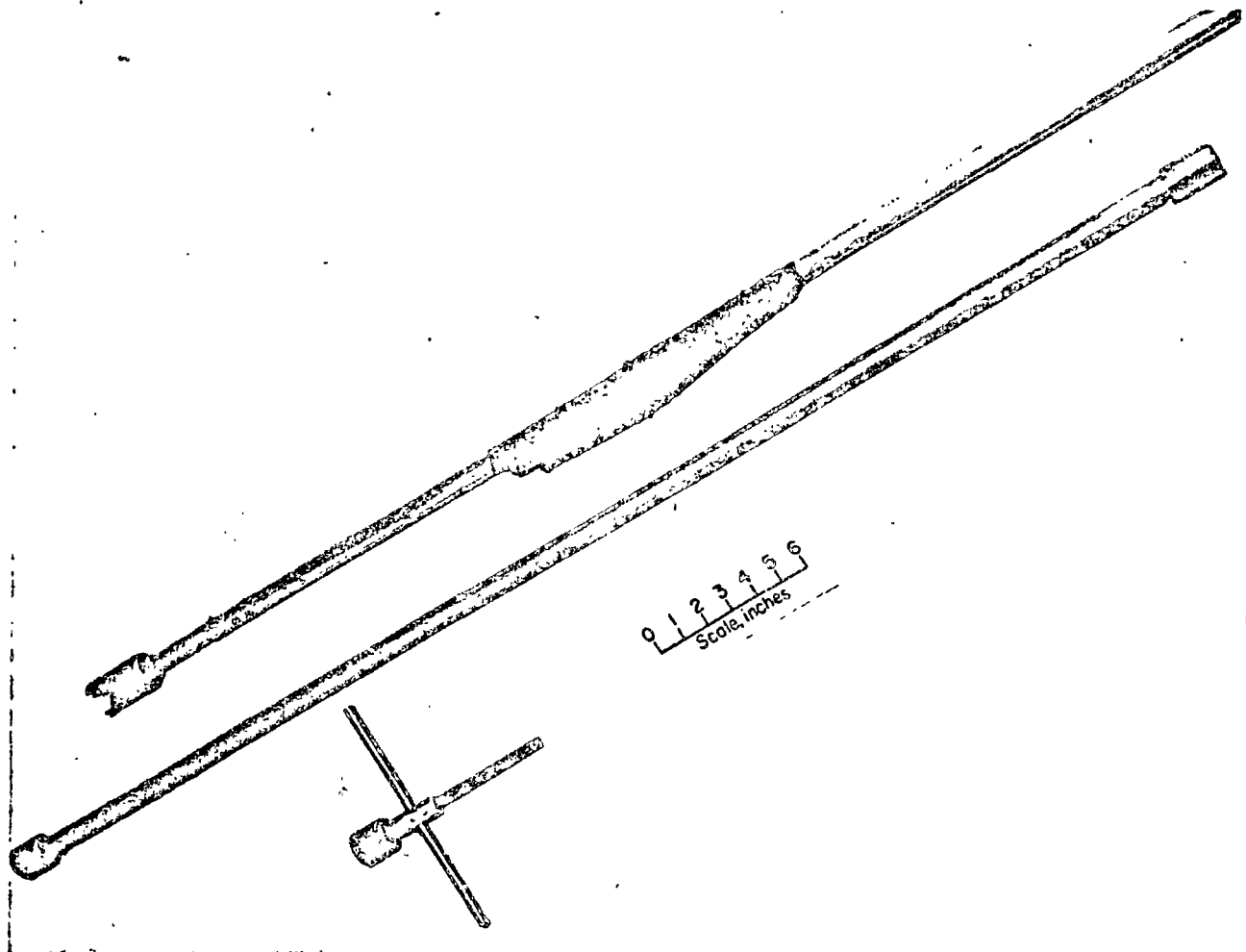


FIGURE A-12. - Placement and retrieval tool.

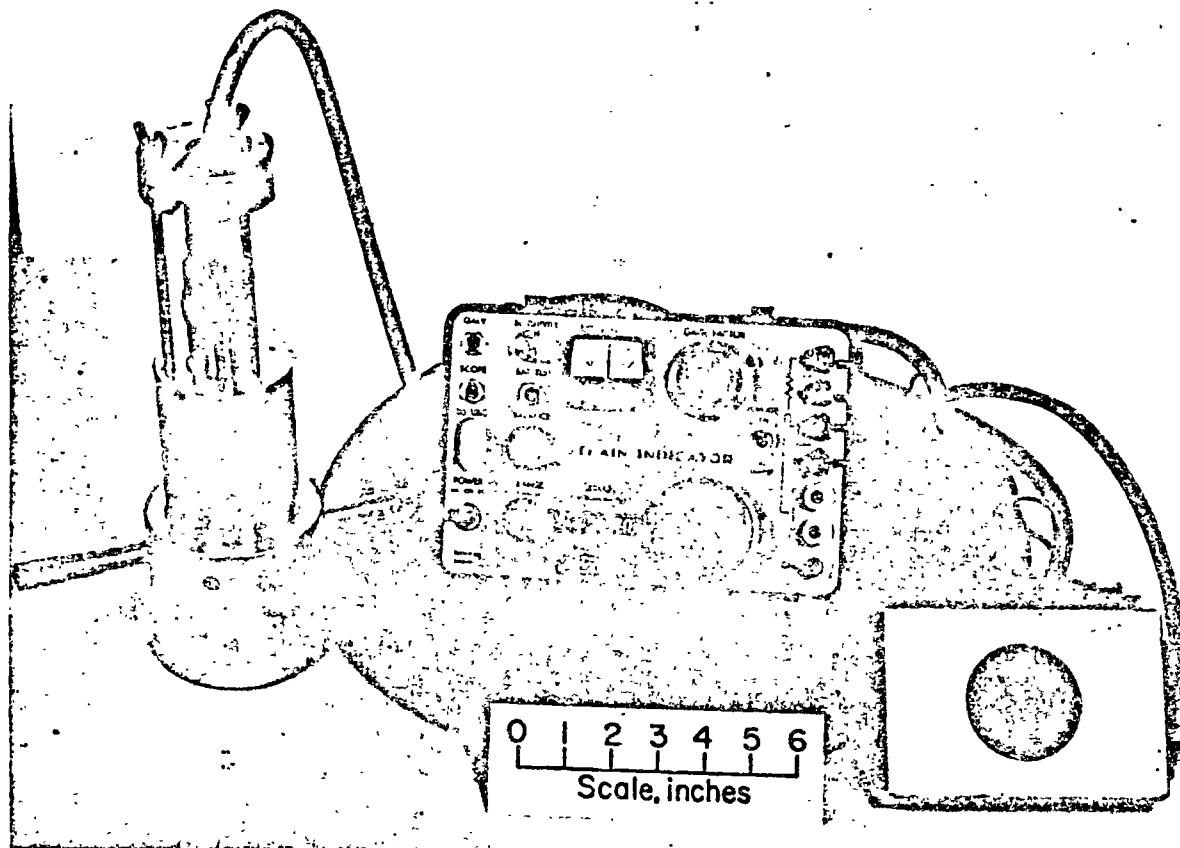


FIGURE A-13. - The calibration device (left side) and a switching unit (right side).

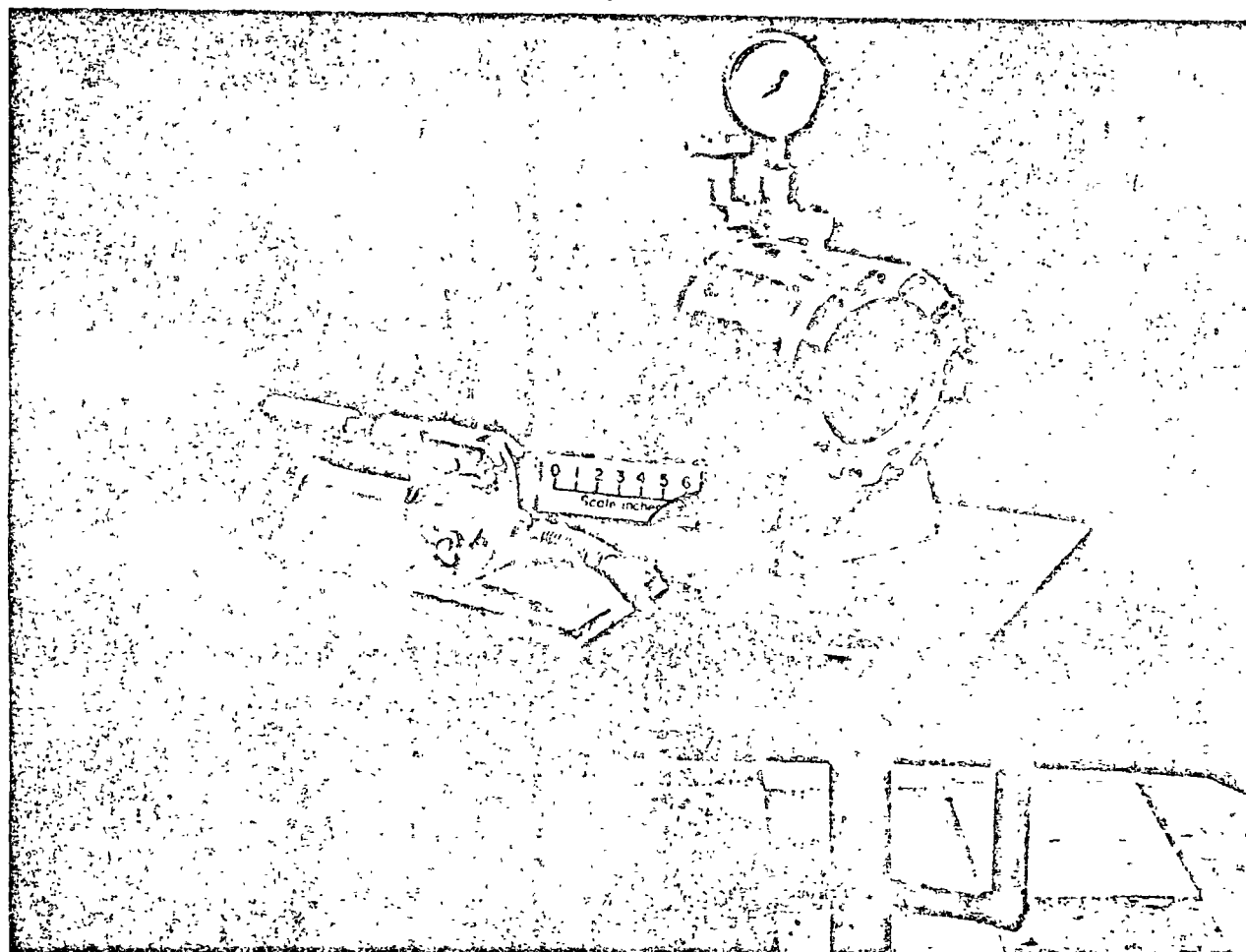


FIGURE A-14. - Biaxial chamber and pump (2).

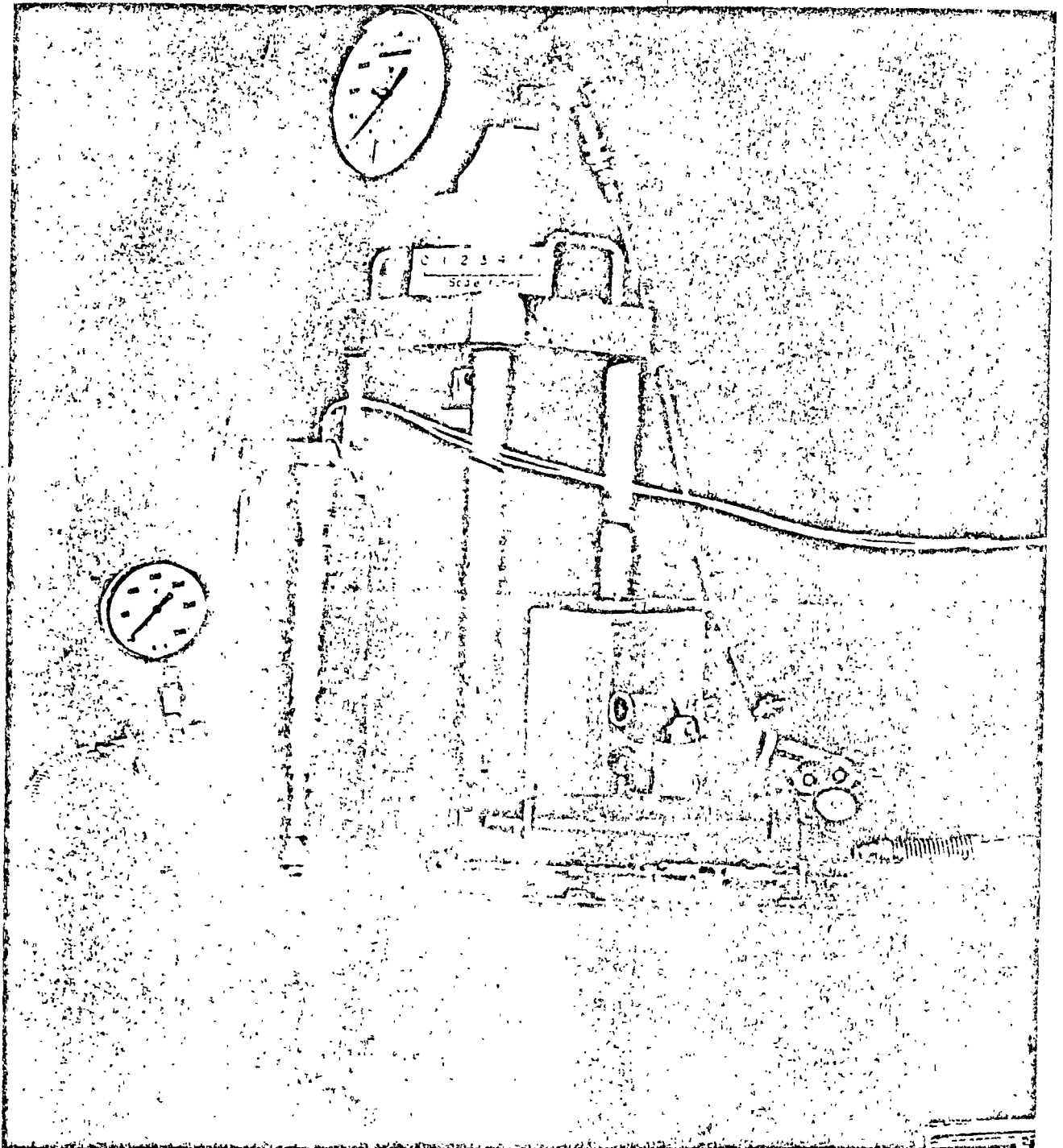


FIGURE A-15. - Triaxial chamber, press, and pump (3).

APPENDIX B.--DIAGRAMS OF THE BOREHOLE GAGE, PLACEMENT AND RETRIEVAL TOOL,
CALIBRATION JIG, AND BIAXIAL AND TRIAXIAL PRESSURE CHAMBERS

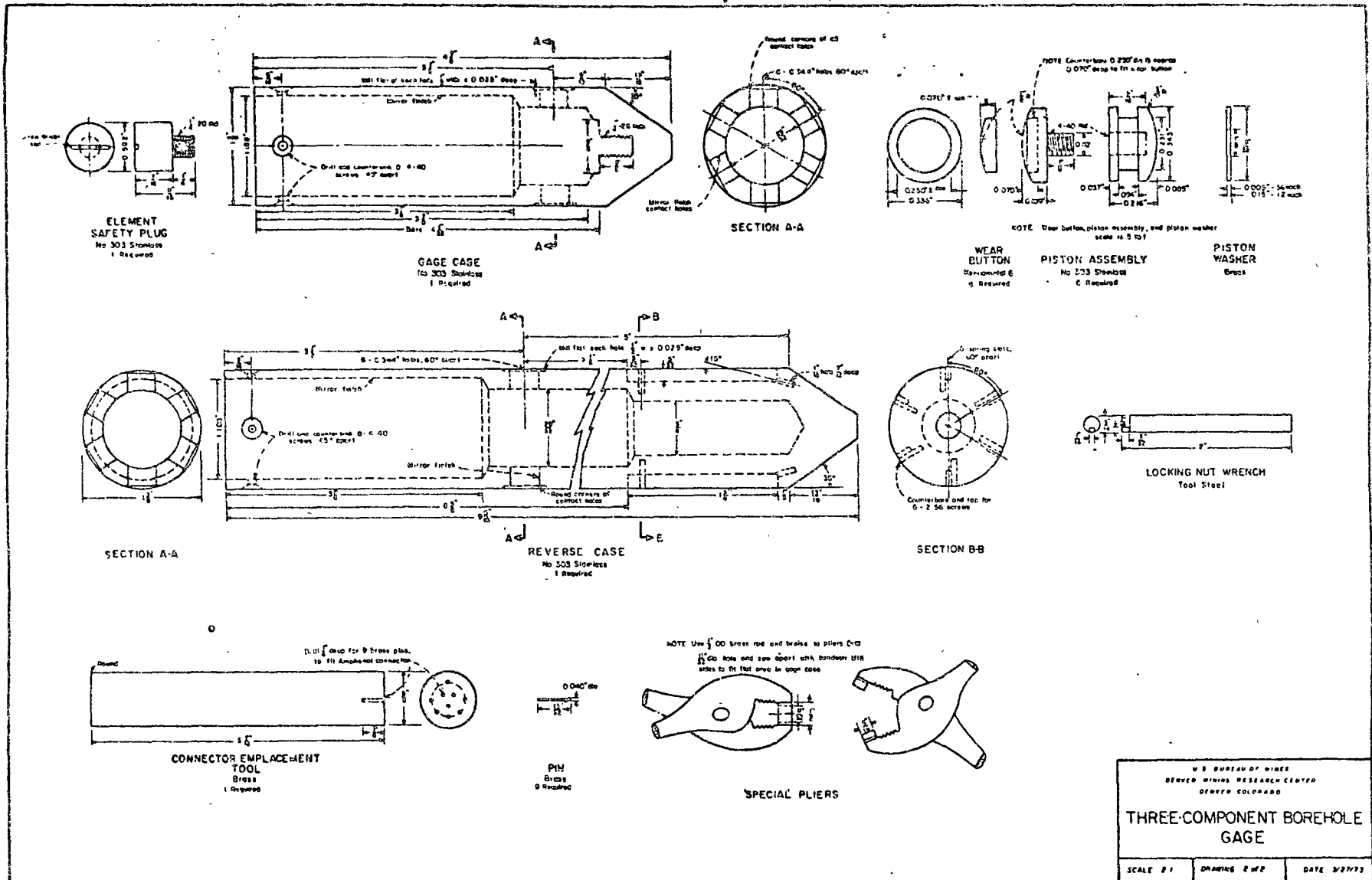


FIGURE B-1. - Three-component (3-D) borehole gage.

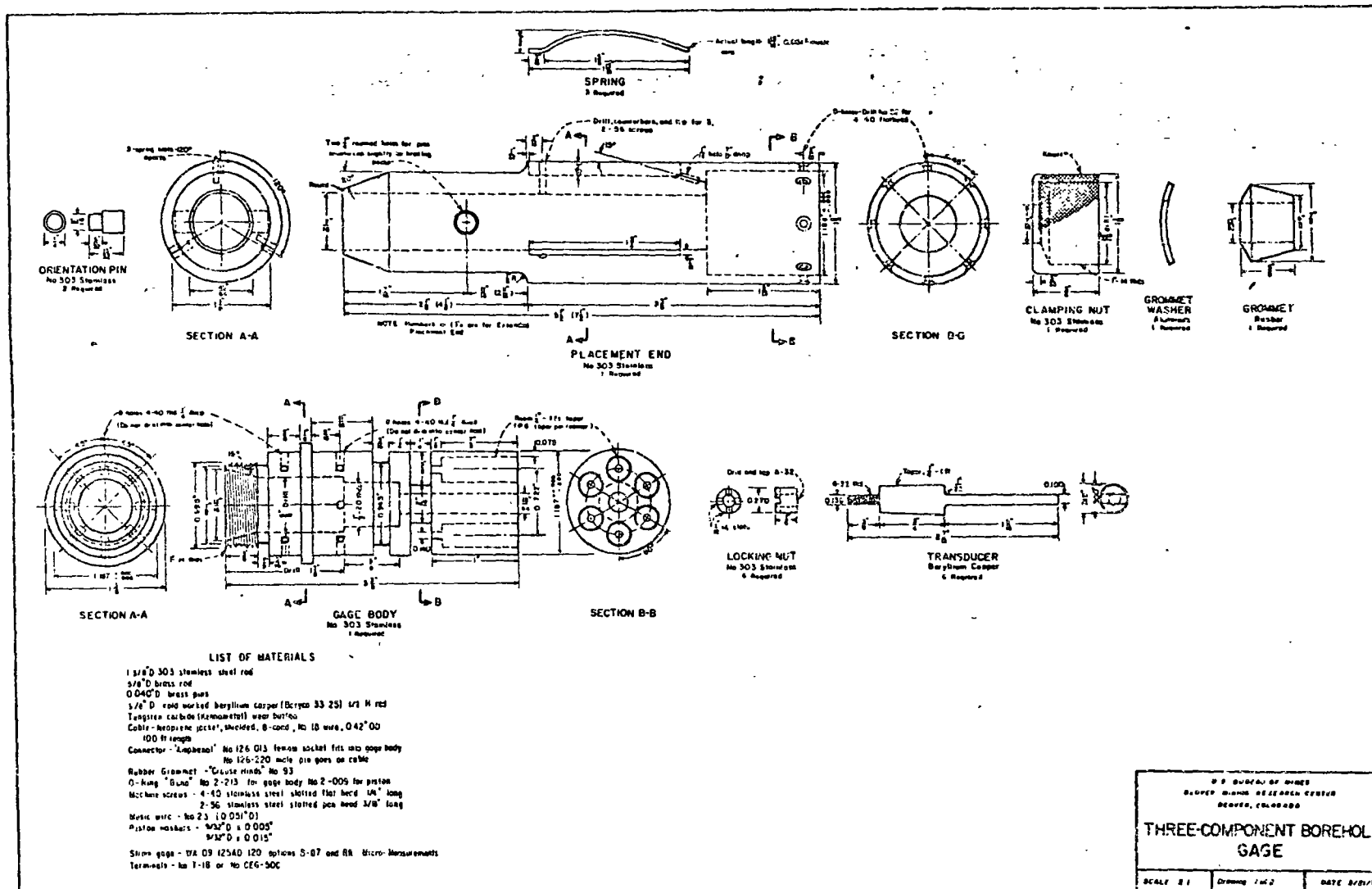


FIGURE B-1. - Three-component (3-D) borehole gage.—Continued

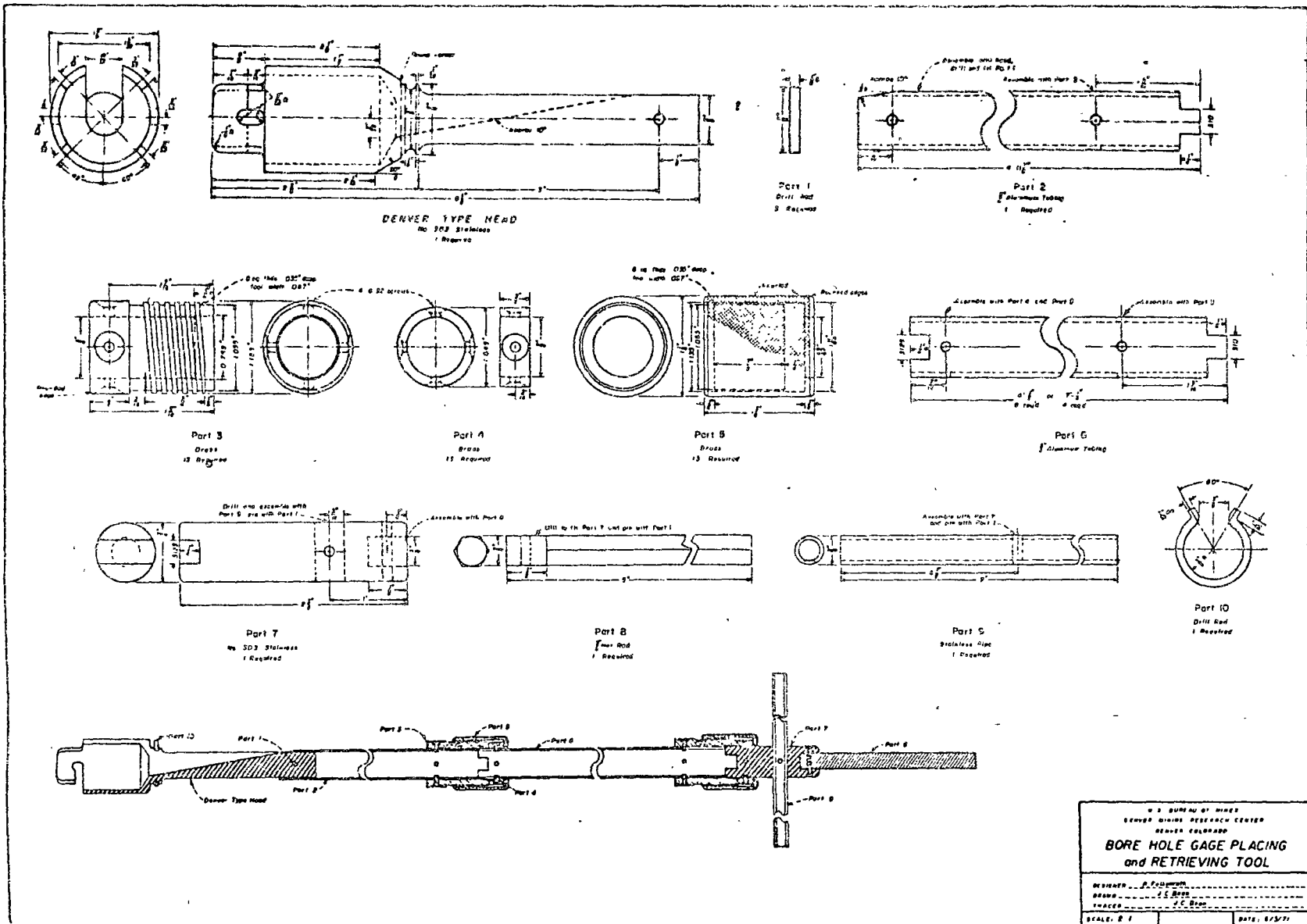


FIGURE B-2. - Borehole gage placing and retrieving tool.

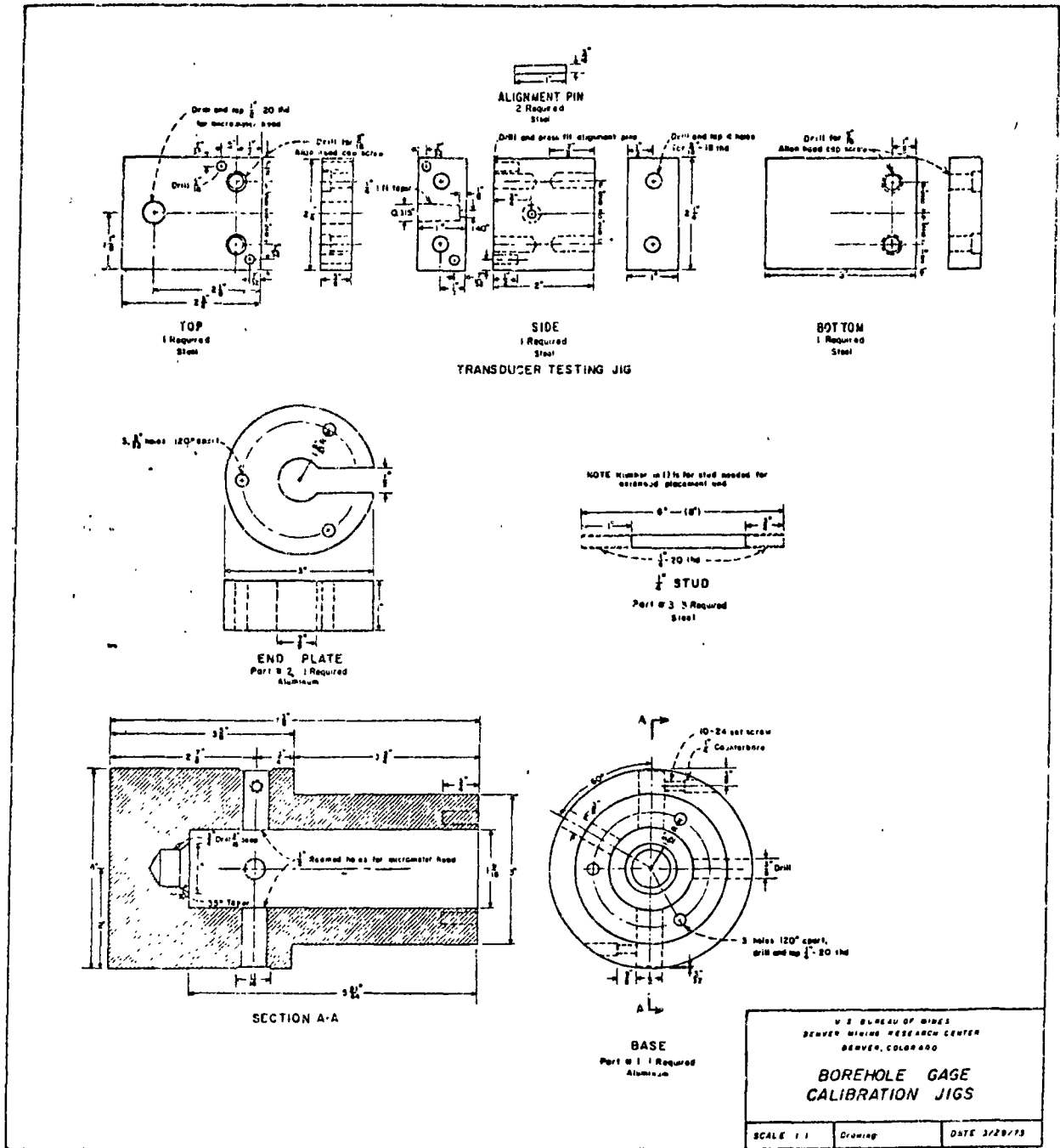


FIGURE B-3. - Calibration jig and transducer testing jig.

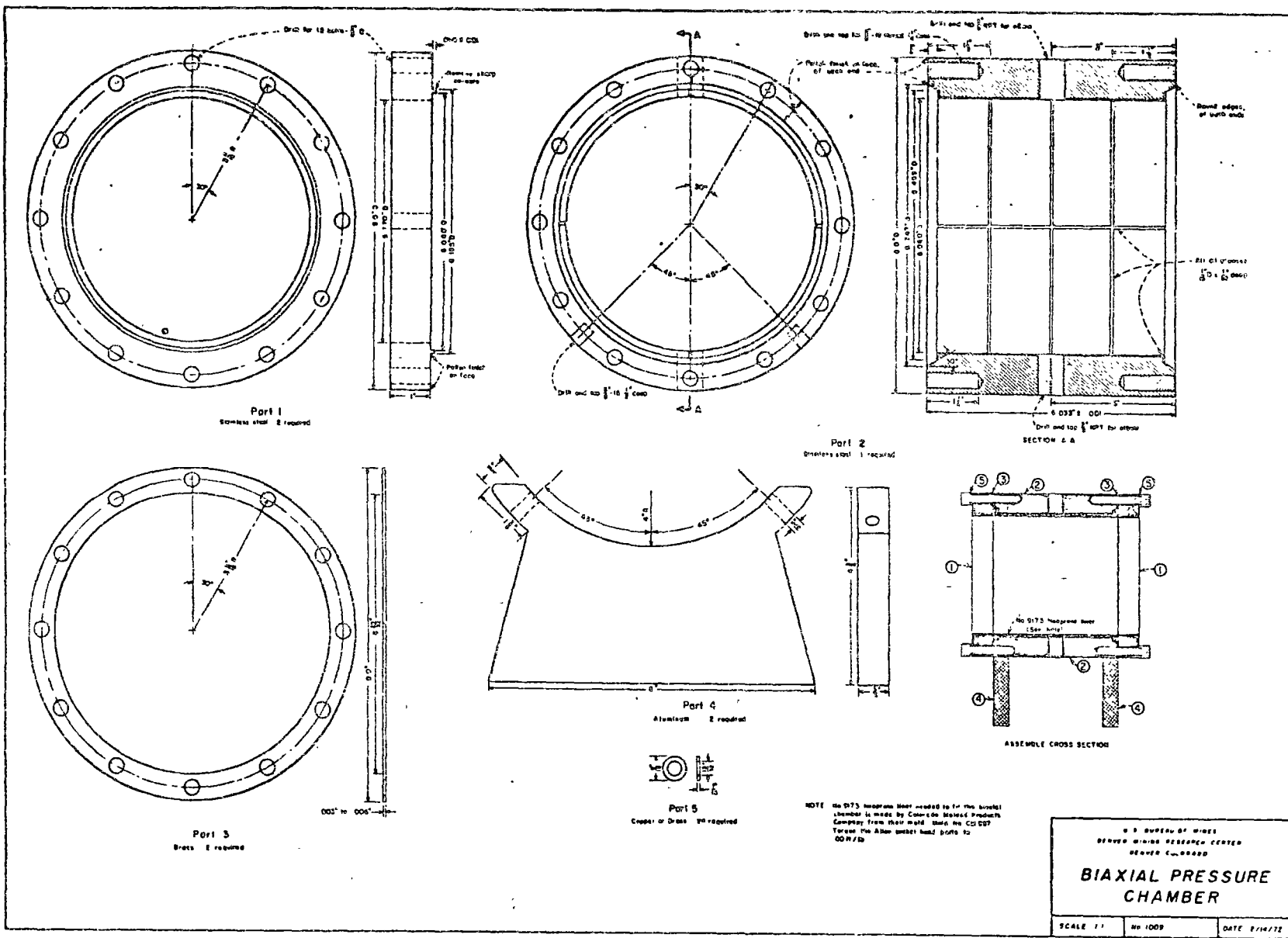


FIGURE B-4. - Biaxial pressure chamber.

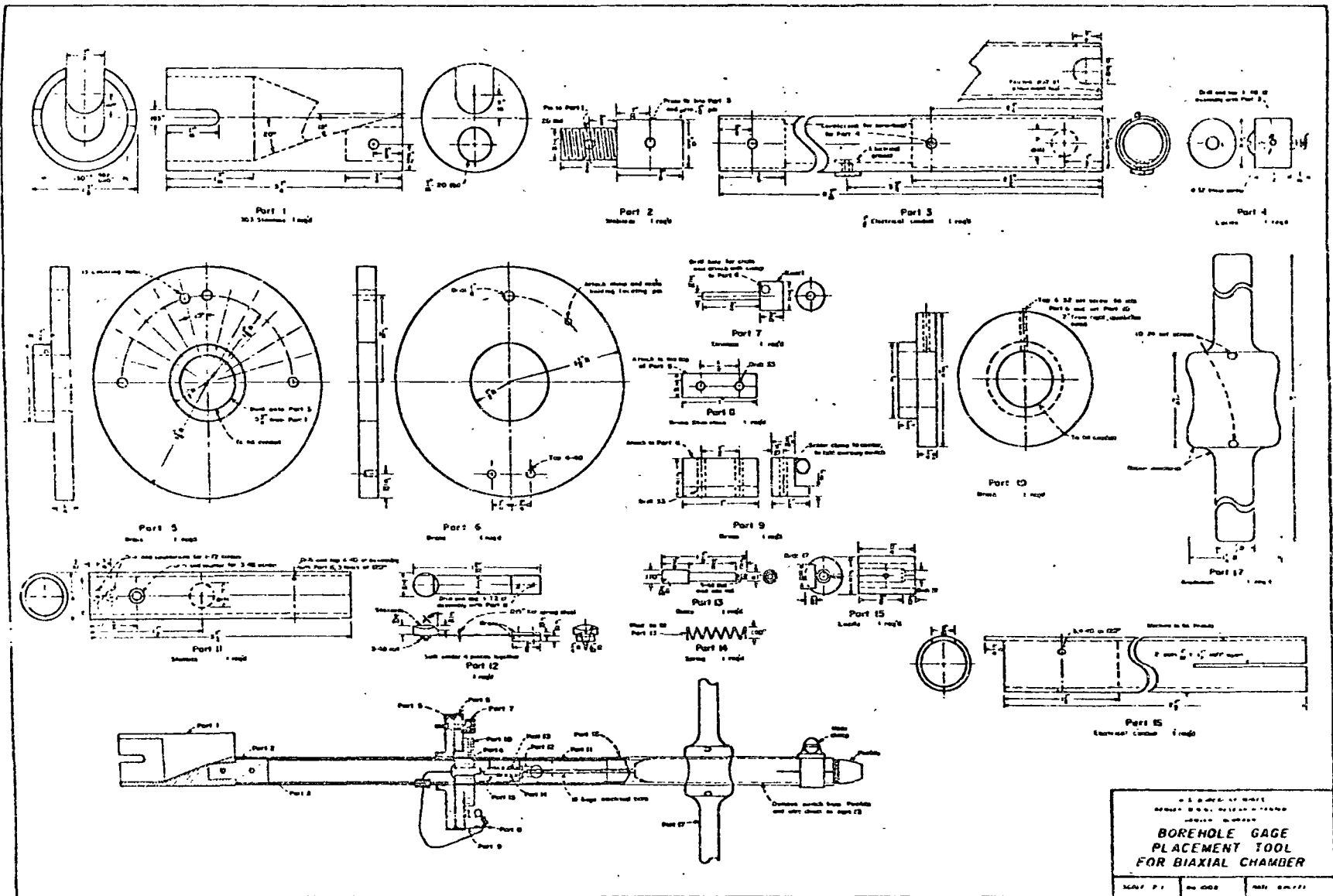


FIGURE B-5. - Borehole gage placement tool for biaxial chamber.

La medida de tensiones y deformaciones en macizos rocosos.

A. Roberts

6.1 Introducción

El objeto fundamental de la Mecánica de Rocas es el estudio del comportamiento mecánico de las rocas y macizos rocosos frente a solicitaciones estáticas y dinámicas. Trataremos aquí la determinación de las tensiones y la medida de las deformaciones. Puede aducirse que el ingeniero ocupado en obras de minería, cimentaciones o geología de obras civiles se enfrenta en el terreno con las propiedades generales de los macizos rocosos, en lugar de con el material rocoso en sí. Con todo debemos conocer las propiedades de todos los elementos de que se compone un macizo rocoso, así como las del conjunto, si queremos llegar a entender los problemas particulares que pueden presentarse en cualquier instante. En algunos de nuestros problemas los factores predominantes son los que dependen de las propiedades del material base, mientras que otras veces el factor crítico puede ser alguna propiedad del macizo rocoso.

En el desarrollo de la Mecánica de las Rocas en los últimos años, ningún problema ha encontrado mayor dificultad de solución que la determinación del estado tensional *in situ* de un macizo rocoso. Sin embargo, a pocos problemas se les ha prestado tanta atención. Son innumerables los aparatos y técnicas desarrollados con este fin y cada reunión de Mecánica de Rocas hace surgir otros nuevos. El que esto suceda quiere decir que hasta el momento no se ha encontrado una técnica aceptable en general, tanto desde el punto de vista práctico como teórico. Muchos equipos y métodos no han pasado de la fase de prototipo y bastantes investigadores han expresado la opinión de que sería mucho más útil emplear el tiempo y el dinero en otras vías de investigación en lugar de intentar medir el estado tensional *in situ*. Se ha sugerido que los ingenieros de Mecánica de Rocas deberían expresarse en términos de deformaciones en lugar de en tensiones, ya que aquéllas se pueden observar y medir. «Debemos preguntarnos a qué grado de distorsión perderá el material su estabilidad y bajo qué deformación se romperá»*.

La medida de la magnitud y velocidad del cierre de cavidades y de la deformación de los macizos rocosos en los que se han excavado, han constituido siempre un aspecto fundamental de la técnica de control de estratos en minería.

Tales medidas incluyen la observación de los movimientos entre puntos

* Dr. Leopold Müller, discurso de introducción al I Congreso de la Sociedad Internacional de Mecánica de Rocas, Lisboa, 1966.

de referencia establecidos en la bóveda y solera o a lo largo de las paredes laterales. Los aparatos empleados pueden ser sencillos o sofisticados, en función principalmente de la sensibilidad de medida deseada y de la necesidad de un registro o control remoto.

Principios de medida análogos pueden aplicarse a las paredes de la excavación, colocando varillas o cables en sondeos, anclándolos en un extremo y estableciendo algún sistema para medir su longitud en el otro.

Colocando varios cables en un sondeo, cada uno de ellos anclado a diferente longitud dentro del mismo, pueden medirse los movimientos relativos entre los estratos a diferentes profundidades. Las deformaciones de un macizo se observan entre puntos de referencia colocados con la separación deseada y situados, por ejemplo, en sondeos perforados entre excavaciones adyacentes o con medidas entre puntos de referencia a distancia considerable según la pared de una excavación.

Sin embargo, mientras no podamos determinar el estado tensional en la corteza terrestre y en los macizos donde se ubican nuestras excavaciones, la ingeniería de rocas seguirá siendo un arte. Si la Mecánica de Rocas se ha de desarrollar como una ciencia con aplicaciones prácticas en ingeniería, debemos poner a punto métodos adecuados para la medida de tensiones *in situ*. Sin poder hacer tales medidas, gran parte del trabajo realizado en los últimos años habrá sido de interés académico únicamente; tal es el caso, por ejemplo, del desarrollo de criterios de rotura para rocas y de la evolución de métodos racionales para el proyecto de excavaciones subterráneas. Investigadores de muchos países han propuesto que la rotura de una roca bajo carga puede expresarse en función de la teoría de rotura frágil, habiendo ampliado la teoría para tener en cuenta los estados de tensión triaxiales, el efecto del cierre de las grietas a compresión y la existencia de presiones intersticiales en el interior de la roca. Pero la aplicación de cualquiera de estas teorías presupone el conocimiento del estado tensional *in situ*. Esto implica un conocimiento, no sólo del estado original de tensiones en la roca, sino también de la distribución completa de tensiones en cada fase del proceso de rotura. En el momento actual estamos muy lejos de tal grado de conocimiento.

La estabilidad de una excavación en roca depende de la resistencia de la roca frente a las tensiones que se le imponen en las proximidades de la excavación. Si la excavación va a ser sostenida desde el interior, por ejemplo mediante el revestimiento de un túnel, necesitamos conocer las fuerzas que debe resistir el revestimiento si se quiere seguir un método racional de proyecto. Estos métodos, por ejemplo el descrito por Horvath¹, hacen una hipótesis sobre el estado de tensiones *in situ*, a partir del cual se calcula la capacidad portante del revestimiento. Se requieren medidas de los empujes de los estratos y las cargas soportadas para comprobar la validez de tales métodos de proyecto. Otro método consiste en la medida de cargas y empujes en estructuras existentes y en el entorno de las mismas, acumulando datos reales sobre los que se puedan basar futuros proyectos en circunstancias comparables.

6.1.1 Tensiones en la corteza terrestre

El estado tensional en la corteza terrestre, en un cierto instante y emplazamiento, se debe a fuerzas de distintos orígenes y características. Se conviene en denominar estado tensional virgen o *natural* al que existe antes de realizar cualquier obra de ingeniería. Este estado tensional es alterado por la construcción de terraplenes, excavaciones y estructuras que dan lugar a una nueva

función de tensiones inclinadas en las rocas de la corteza. En estas tensiones laterales están incluidas las gravitatorias, debidas al peso de la cobertura rocosa y el efecto de las tensiones latentes, algunas de las cuales se han originado en procesos de cristalización, metamorfismo, sedimentación, consolidación y desecación, según los distintos tipos de rocas, mientras que otras proceden de fuerzas tectónicas y movimientos de la corteza terrestre.

El concepto de tensiones gravitatorias supone, de forma convencional, que la roca se comporta como un material elástico con deformación lateral totalmente impedida, en cuyo caso el estado tensional a la profundidad H viene definido por:

Tensión principal vertical

$$\sigma_1 = Hw \quad (\text{donde } w = \text{peso por unidad volumen}) \quad (6.1)$$

Tensión principal lateral

$$\sigma_2 = \sigma_3 = \frac{\nu}{1-\nu} Hw \quad (\nu = \text{módulo de Poisson})$$

La relación tensión lateral-tensión vertical es en este caso

$$C = \frac{\nu}{1-\nu}$$

Si el confinamiento lateral no es completamente rígido, C alcanzará otros valores. Si la roca se comporta como un material plástico ideal, alcanzará un estado hidrostático en el que $C = 1$. Investigadores de diversos laboratorios han establecido la existencia de fases elásticas y plásticas para ciertos materiales rocosos, según las condiciones de confinamiento y el estado tensional. Horvath postula que para una roca con ciertas características tensión de fluencia, peso específico y módulo de Poisson, existe una profundidad límite por encima de la cual las tensiones laterales pueden calcularse a partir de la teoría elástica, pero para mayores profundidades la tensión principal horizontal debe deducirse de un criterio de fluencia plástica como el siguiente:

$$\sigma_2 = Hw - \sigma_F \quad (\sigma_F = \text{tensión de fluencia}) \quad (6.2)$$

Seagar² también describe un caso en el que una roca puede comportarse elásticamente, siempre que la diferencia entre las tensiones principales sea inferior a una tensión tangencial de fluencia, y deformándose después plásticamente al seguir aumentando la carga. Al suprimir la carga el material debería comportarse de nuevo elásticamente cuando la diferencia de tensiones quedara debajo del límite de fluencia. Cabe imaginar que se produzca un ciclo de este tipo si los estratos, de situación profunda, se dejan al descubierto parcialmente. Si estratos adyacentes tienen diferentes límites de fluencia los cálculos de Seagar indican que pueden estar sometidos a diferentes presiones laterales si no hayan sufrido la misma historia de carga.

Un estrato de roca resistente puede no haber cedido bajo carga, mientras que un estrato más débil se puede haber deformado más, dando lugar a un empuje lateral. De acuerdo con la hipótesis de Seagar, el empuje lateral puede ser superior al calculado a partir de la elasticidad pura, y fácilmente puede superar en magnitud a la presión vertical.

Si el material de un punto de un estrato es elástico, además de las producidas por las cargas aplicadas, el estado tensional puede ser elástico y superior a las verticales, dando de esperar unas condiciones de orientación preferencial. Algunos autores, sin embargo, sostienen que la fluencia bajo cargas mantenidas a un nivel de tiempos geológicos ha podido eliminar las tensiones diferenciales, dando lugar a un sistema de tensiones hidrostático. Everling³, al describir los resultados generales de los estudios realizados sobre el estado tensional *in situ* de los sedimentos carboníferos de Europa Central, señala: «De todas las hipótesis referentes a la presión horizontal, la más probable es la de igualdad de presiones en todas las direcciones.»

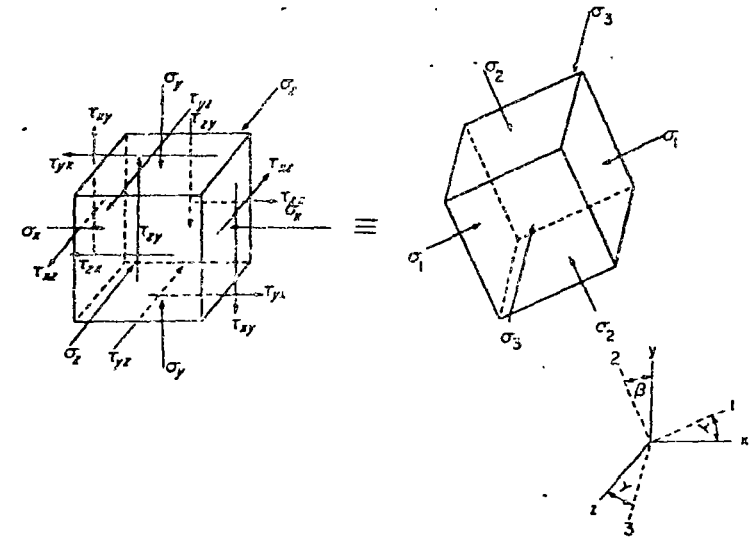


Figura 6.1 Representación de las tensiones en un punto de un sólido (Leeman)

La existencia de fallas y la producción de terremotos constituyen, sin embargo, una clara evidencia de la capacidad de los estratos rocosos para soportar tensiones diferenciales a una escala de tiempos geológica.

6.1.2 Distribución de tensiones en torno a excavaciones en roca

Al considerar el estado natural de tensiones en problemas de Mecánica de Rocas conviene referirse a las tensiones principales en tres direcciones ortogonales, una de ellas vertical. De hecho, estas son tensiones principales secundarias que sirven para identificar las primarias, desconocidas en magnitud y dirección. Se pueden determinar las tensiones principales si se conocen las 9 componentes de tensión que actúan sobre un cubo elemental (Fig. 6.1). Estas componentes son función de seis variables independientes.

Sin embargo el estado natural de tensiones está alterado en las rocas en torno a excavaciones y cavidades así como en la proximidad de la cimentación de estructuras. Se produce una redistribución que da lugar a concentración de tensiones, unas de compresión y otras de tracción, en distintos puntos de las

rocas adyacentes a las obras de ingeniería. Este nuevo estado tensional inducido es tridimensional y ampliamente variable en magnitud y dirección. Todo lo más que sabemos es que las tensiones inducidas pueden alcanzar una magnitud varias veces superior a la de las tensiones naturales. La determinación de la situación probable y de la magnitud de las concentraciones de tensiones resulta, sin embargo, de importancia primordial.

Se puede obtener un conocimiento detallado de la naturaleza de las concentraciones de tensiones en torno a excavaciones, en un material elástico ideal bajo un estado de carga dado, a partir de métodos numéricos* o mediante estudios en modelo fotoelástico, como los empleados por Hiramatsu y Oka⁴ (Fig. 6.2) u otros análogos. Estudios semejantes pueden ampliarse para materiales rocosos reales o simulados, como los descritos en las referencias (5) y (6).

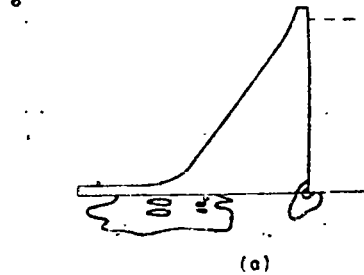


Figura 6.2 Isostáticas en modelos fotoelásticos de un túnel de carretera bajo carga vertical, horizontal y oblicua⁴

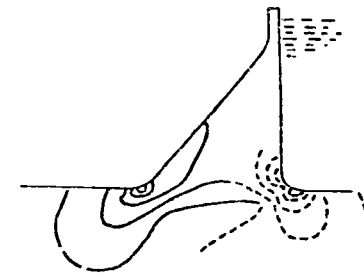
donde se ha visto que la heterogeneidad y anisotropía tienen una influencia considerable sobre la distribución de tensiones, a veces con escasa semejanza con el caso ideal (Fig. 6.3). Los modelos suelen ser bidimensionales y sometidos a sistemas tensionales conocidos y constantes. La situación real es tridimensional y comprende componentes dinámicas. Cuando el terreno cede, la zona de concentración de tensiones se deforma hasta una profundidad desconocida en el interior de la roca. La deformación puede ser elástica y la roca permanece intacta hasta llegar a la rotura al aumentar las tensiones, o puede ser función del tiempo y la excavación se va cerrando paulatinamente bajo carga constante. En rocas elásticas duras, la rotura puede producirse a partir de concentraciones de tensiones en torno a discontinuidades o grietas del material rocoso y no solamente en torno a la periferia de la excavación. Durante la realización de obras de ingeniería, como excavaciones en rocas, perforación de túneles y voladuras, las tensiones inducidas variarán al progresar la excavación y, en cualquier caso, las rocas de la corteza terrestre están constantemente sometidas a las variaciones diurnas de tensiones producidas por las fuerzas de marea terrestres.

El ingeniero que se enfrente con la determinación de las tensiones *in situ* debe, por tanto, valorar una magnitud que varía en el espacio y en el tiempo y que no se puede predecir en un punto y en un instante dados. Únicamente puede intentar medirlas en las condiciones presentes.

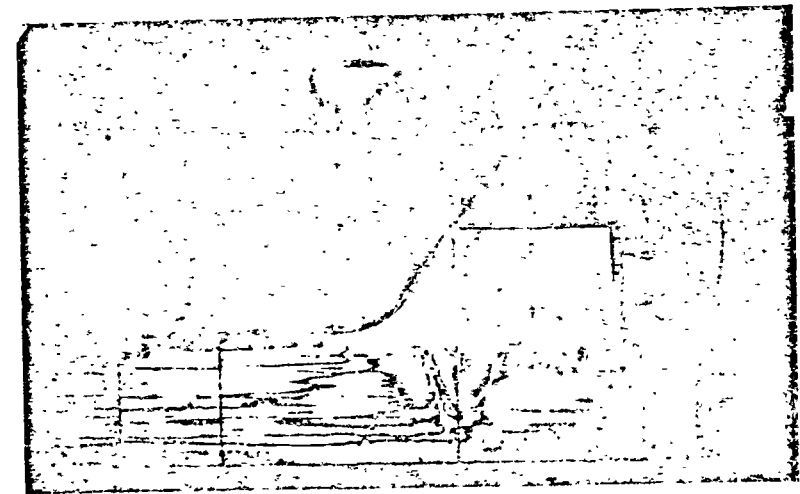
* Véase el capítulo 8.



(a)



(b)



(c)

Figura 6.3 Estudio en modelo fotoelástico de la distribución de tensiones en la roca de cimentación de una presa de gravedad*

* McCubben: (1), (2), (3).

6.1.3 Características tensión-deformación de las rocas

Es imposible medir tensiones directamente, pero podemos definir las en la forma de una fuerza por unidad de superficie y deducirlas midiendo la fuerza aplicada para establecer un estado de equilibrio. Por otro lado, podemos determinar las tensiones midiendo alguna otra propiedad física si se conoce la relación entre esa propiedad y las tensiones. Entre esas propiedades podemos incluir la velocidad acústica, la resistividad eléctrica y la deformación. Los extensómetros (*strain gauges*) son con mucho los dispositivos más generalmente utilizados para el estudio de tensiones en materiales elásticos. Sin embargo en la Mecánica de Rocas, aunque puede esperarse que algunas rocas como las ígneas y metamórficas se comporten elásticamente, otras, en especial las evaporitas y los sedimentos porosos, no lo hacen así. Muchas rocas presentan características marcadas de anisotropía y son conjuntos heterogéneos de varios materiales de propiedades mecánicas muy diferentes.

La justificación para ampliar la aplicación de la teoría elástica a rocas diferentes de las ígneas y metamórficas, por ejemplo a las areniscas y otras rocas sedimentarias, es que, después de ciclos sucesivos de carga-descarga, bien durante ensayos *in situ* a gran escala, como los de carga con placa, o en ensayos de laboratorio sobre pequeñas muestras, se puede apreciar una relación tensión-deformación la cual, aunque raramente es lineal en todo el intervalo de observación, puede frecuentemente aproximarse por una relación lineal en un intervalo de carga limitado. El «módulo» obtenido a partir de tales ensayos viene determinado principalmente por la forma en que las discontinuidades y poros se cierran por compresión en la zona de influencia de las placas de carga o gatos en los ensayos *in situ*, y por la máquina de ensayo a compresión, en la muestra de laboratorio con cargas bajas. Con cargas elevadas pueden obtenerse a veces en laboratorio resultados reproducibles en cierta extensión y con un lazo de histéresis muy cerrado, pero el ensayo *in situ* no da una información que describa las propiedades físicas del macizo rocoso en términos absolutos. Los resultados de tales ensayos sólo se pueden aplicar al lugar y a las circunstancias en que se han obtenido y no puede esperarse que exista una correlación sencilla con los ensayos de laboratorio sobre muestras del material rocoso.

En los últimos años se han empleado los conceptos de la reología para caracterizar las propiedades de distintos materiales rocosos. Los modelos reológicos, formados por elementos como muelles elásticos y amortiguadores viscosos, representan las propiedades de elasticidad y viscosidad por medio de las cuales pueden describirse las características de deformación del material en carga y descarga y de las que se pueden deducir ecuaciones básicas tensión-deformación y deformación-tiempo.

6.2 Principios de la medida de tensiones en rocas

Consideraremos dos tipos de medidas:

- a) La determinación del estado tensional absoluto,
- b) La medida de tensiones relativas, es decir variaciones de tensiones.

Existe una amplia variedad de aparatos y métodos para ambos tipos de medidas.

En las rocas que muestran un comportamiento elástico, la medida de tensiones absolutas puede requerir la aplicación de un método de liberación de tensiones en el que el elemento rocoso donde se ha introducido el aparato de medida se descarga de las tensiones ejercidas por la roca circundante. A continuación se mide la deformación a que ha dado lugar esta eliminación de tensiones y la conversión de la misma en tensión se hace a partir relaciones, conocidas o supuestas, de tensión-deformación para la roca estudiada. Las tensiones relativas pueden determinarse midiendo las tensiones absolutas al principio y al final de un intervalo de tiempo dado, pero esto no es siempre necesario y mientras sea posible no se utilizan para medir tensiones relativas las técnicas de liberación de tensiones, que son caras y lentas. Hablando en general, los instrumentos empleados en ambos tipos de medidas son semejantes pero aunque cualquier instrumento proyectado para la medida de tensiones absolutas medirá también tensiones relativas, algunos aparatos que son de diseño sencillo e ideados para medidas relativas, no pueden aplicarse sin cierta modificación para medidas absolutas.

6.2.1 El método de liberación de tensiones (*stress-relief*)

En este método, el instrumento de medida debe adherirse a la superficie de la roca expuesta en la excavación. A continuación la zona de roca a la que se ha unido el instrumento se separa del entorno, bien cortando unas ranuras en cuadro mediante una sierra o perforando una corona de taladros secantes en torno a la misma. En otros casos la parte de roca y el instrumento asociado se recortan mediante una corona de perforación hueca de diámetro apropiado. A continuación se miden las deformaciones registradas en la roca independizada.

Entre los instrumentos empleados de esta forma se encuentran los extensómetros que miden la deformación superficial según tres direcciones, las rosetas de extensómetros y los medidores fotoelásticos biaxiales. Los resultados permiten identificar la tensión principal secundaria, en un estado biaxial, en el plano de la pared de la excavación. En este caso la tercera tensión principal es nula.

La determinación del estado tensional natural requiere la realización de medidas más allá de la zona de influencia de la excavación. Esto puede conseguirse perforando un sondeo en el frente de excavación y colocando el medidor en el fondo del mismo. A continuación se realiza la sobreperforación* en toda la longitud del sondeo original (Fig. 6.4).

También en este caso los resultados proporcionan las tensiones principales secundarias en un plano normal al eje del sondeo. Como se quiere estudiar el estado de tensiones triaxial, es necesario medir seis deformaciones principales, según tres planos ortogonales, para obtener una solución. Hasta el momento esto no se ha conseguido casi nunca. Lo más corriente ha sido realizar medidas en un único sondeo, introduciendo hipótesis simplificadoras sobre la dirección de la tercera tensión principal. Dos hipótesis hechas corrientemente son que una tensión principal es de dirección vertical (en cuyo caso el sondeo se perfora horizontalmente en la pared rocosa) o (si el sondeo no es horizontal) la tercera tensión principal tiene la dirección del eje del sondeo.

* Elegimos esta palabra para traducir la inglesa «overcoring», o parece de equivalente en castellano. (N. del T.)

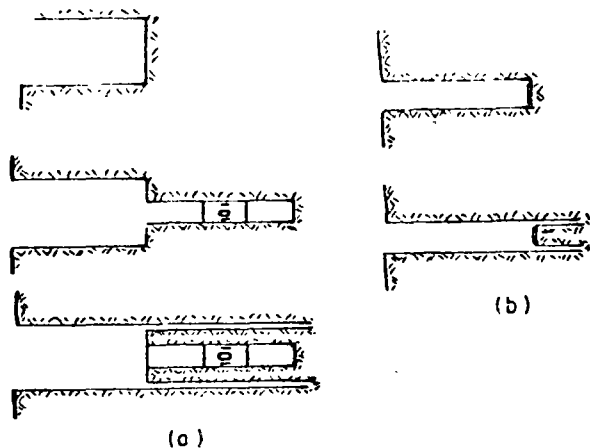


Figura 6.4 Método de liberación de tensiones. (a) Utilizando un medidor de deformación transversal o la célula múltiple de Lecman. (b) Empleando una célula de bandas extensométricas

Se han empleado tres tipos diferentes de medidores de deformaciones en sondeos. Pueden clasificarse como 7 «medidores de deformación transversal», «tensímetros de inclusión» y «células de deformación».

6.3 Medidores de deformación transversal (Borehole deformation meters)

Estos aparatos miden las variaciones en las dimensiones transversales de un taladro realizado en roca, cuando éste se deforma como resultado de la variación de tensiones. Las tensiones se calculan por la teoría elástica.

La ecuación general de la deformación plana es

$$\Delta D = \frac{\alpha_1 D}{E} \{ (1 + K) - \nu L + 2(1 - K)(1 - \nu^2) \cos 2\theta_1 \} \quad (6.3)$$

$$\Delta D = \frac{D}{E} \{ (\sigma_1 + \sigma_2) - \nu \sigma_3 + 2(\sigma_1 - \sigma_2)(1 - \nu^2) \cos 2\theta_1 \} \quad (6.4)$$

y para el estado plano de tensiones:

$$\Delta D = \frac{D}{E} \{ (\sigma_1 + \sigma_2) + 2(\sigma_1 - \sigma_2) \cos 2\theta \} \quad (6.5)$$

donde ΔD = variación de longitud del diámetro que forma un ángulo θ_1 con la dirección de la tensión principal σ_1 ,

D = longitud inicial del diámetro,

$$K = \frac{\sigma_2}{\sigma_1},$$

$$L = \frac{\sigma_3}{\sigma_1}$$

Si se miden los corrimientos según tres diámetros diferentes y se conoce el módulo de elasticidad y el módulo de Poisson, puede calcularse la magnitud y dirección de las tensiones.

En la figura 6.5:

$$\sigma_1 + \sigma_2 = \frac{E}{3D(1 - \nu^2)} (U_1 + U_2 + U_3) \quad (6.6)$$

$$\sigma_1 - \sigma_2 = \frac{\sqrt{2}E}{6D(1 - \nu^2)} [(U_1 - U_2)^2 + (U_2 - U_3)^2 + (U_1 - U_3)^2]^{1/2} \quad (6.7)$$

donde U_1 , U_2 y U_3 son los corrimientos medidos.

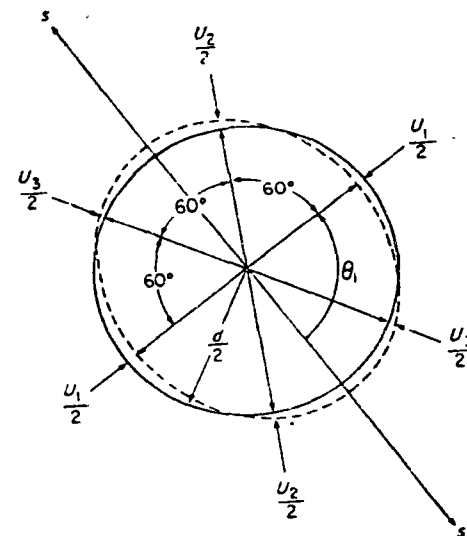


Figura 6.5 Deformación de un orificio circular en una placa sometida a un estado de tensiones biaxial. Roseta de 60° (medidor de deformación transversal del U. S. B. M.)

El ángulo que forma σ_1 con la dirección según la cual se mide el corrimiento U_1 vale

$$\operatorname{tg} 2\theta_1 = \frac{\sqrt{3}(U_2 - U_3)}{2U_1 - U_2 - U_3} \quad (6.8)$$

Si los corrimientos medidos forman ángulos de 45°

$$\sigma_1 + \sigma_2 = \frac{E(U_1 + U_3)}{2D(1 - \nu^2)} \quad (6.9 a)$$

$$\sigma_1 - \sigma_2 = \frac{E[(U_1 - U_2)^2 + (U_2 - U_3)^2]^{1/2}}{2D\sqrt{2}(1 - \nu^2)} \quad (6.9 b)$$

$$\operatorname{tg} 2\theta_1 = \frac{-2(U_2 - U_1 - U_3)}{U_1 - U_3} \quad (6.9 c)$$

Merrill y Peterson⁸ dan las siguientes reglas para la determinación de θ_1 :
Para una roseta con ejes a 60° :

1. Si $U_2 > U_3$, θ_1 está comprendido entre $+90^\circ$ y $+180^\circ$ ó entre 0° y -90° .
2. Si $U_2 < U_3$, θ_1 está comprendido entre 0° y $+90^\circ$.
3. Si $U_2 = U_3$ y si
 - a) $U_1 > U_2$, $\theta_1 = 0^\circ$,
 - b) $U_1 < U_2$, $\theta_1 = \pm 90^\circ$;

y para una roseta con ejes a 45° :

1. Si $U_2 > (U_1 + U_3)/2$, θ_1 está comprendido entre $+90^\circ$ y 180° o entre 0° y -90° .
2. Si $U_2 < (U_1 + U_3)/2$, θ_1 está comprendido entre 0° y $+90^\circ$.
3. Si $U_2 = (U_1 + U_3)/2$, y si
 - a) $U_1 > U_3$, $\theta_1 = 0^\circ$,
 - b) $U_1 < U_3$, $\theta_1 = 90^\circ$.

Uno de los primeros medidores de deformación transversal empleado con éxito en Europa y Africa del Sur es la célula de Maihak^{7,9,10}. En este instrumento el elemento sensible es un medidor de cuerda vibrante conectado a un vástago que se hace salir mediante un mecanismo de tornillo hasta que entra en contacto con las paredes del taladro. Se requieren diferentes colocaciones sucesivas del aparato para obtener una solución, ya que sólo se registra un corrimiento diametral. Posteriormente se han desarrollado en otros países aparatos que miden simultáneamente los corrimientos según dos diámetros, permitiendo además un registro continuo. De este tipo son los medidores de deformación Marks I y II desarrollados por el C. S. I. R. (Africa del Sur) que emplean como mecanismo sensible extensómetros de resistencia eléctrica en anillos que se deforman bajo la acción de vástagos que entran en contacto con las paredes del taladro o transformadores diferenciales lineales conectados directamente a tales vástagos, respectivamente^{11,12}.

Los aparatos empleados en Europa Central para investigaciones de Mecánica de Rocas han sido descritos por Cibek¹³, quien ha proyectado un medidor de deformación que registra las variaciones diametrales según dos direcciones ortogonales. En este aparato los vástagos de contacto actúan sobre una palanca mecánica haciendo variar la resistencia eléctrica de un sencillo potenciómetro.

Uno de los medidores empleados con más éxito en el mundo de habla inglesa es el del U. S. Bureau of Mines, presentado por Merrill y otros en 1962^{8,14}. Este aparato proyectado para su introducción en un taladro de tamaño EX (1,5 pulgadas de diámetro) se muestra en la figura 6.6. El elemento sensible es una chapa en ménsula de cobre-berilio a la que están conectadas cuatro bandas extensométricas formando un puente de Wheatstone. El aparato tiene una sensibilidad de aproximadamente $20 \mu\text{cm}$, por cm , que corresponde a una precisión en las tensiones de aproximadamente $0,95 \text{ kg/cm}^2$ para una roca de $E = 210.000 \text{ kg/cm}^2$.

La instalación del aparato U. S. B. M. y la realización de medidas comprenden la siguiente serie de operaciones:

Se perfora un sondeo de 6 pulgadas (15 cm) de diámetro (mediante una corona de diamante de $5\frac{1}{2}$ " de diámetro exterior) en la pared rocosa, a una distancia suficiente para traspasar la zona fracturada exterior. Se extrae el testigo y se coloca un cable en el sondeo para centrar una batería y corona de perforación de tamaño EX. Con ella se perfora hasta una profundidad de 3 o más metros más allá del final del sondeo de 6 pulgadas.

Se coloca el aparato en el taladro de diámetro EX a una profundidad no inferior a 15-25 cm, según la naturaleza de la roca. El medidor se orienta para realizar medidas según el diámetro vertical del sondeo y los cables se llevan a través del varillaje hasta un puente de medida. Después de tomar una lectura inicial, se comienza la sobreperforación, tomando lecturas a intervalos regulares hasta que se termina la operación. Se ve que la deformación medida por el instrumento, tal como la aprecia el puente de medida, se produce más o menos gradualmente al pasar la corona de sobreperforación por los vástagos

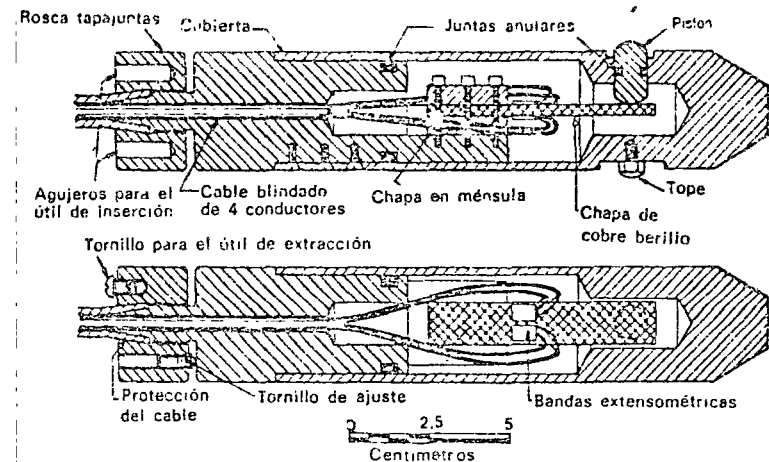


Figura 6.6 Medidor de deformación transversal del U. S. Bureau of Mines

que transmiten la deformación a la placa en ménsula (que ejerce una presión de 4,5 a 14 kg sobre la pared del sondeo). Cuando la corona ha pasado 2 a 5 cm de ese punto, se suele haber producido la liberación de tensiones. Se toma una lectura final y se extrae el testigo que contiene el aparato para realizar otros ensayos con objeto de determinar los módulos elásticos de la roca. A continuación se extrae el medidor y se le vuelve a colocar en el sondeo de diámetro EX para medir corrimientos en otra dirección (ver la figura 6.4 a).

El aparato se calibra desplazando la placa una magnitud conocida, registrada con un micrómetro, y anotando la medida correspondiente en el puente extensométrico. Como las medidas U_1 , U_2 y U_3 no se hacen en el mismo plano es necesario interpolar entre los valores medidos sucesivamente. Esto es un inconveniente que limita la utilidad del aparato en los puntos donde son de esperar elevados gradientes de tensiones, como por ejemplo en zonas de concentración de tensiones en torno a una excavación. Para estos casos se han proyectado medidores múltiples en los Estados Unidos, principalmente por Grosvenor y Griswold¹⁵ y más recientemente por Crouch y Hurst¹⁶.

6.5.1 El «doorstopper» de Leeman

Los primeros intentos para sobreperforar aparatos con bandas extensométricas colocados en el fondo de un taladro tropezaron con problemas, debidos principalmente a la dificultad de aislar las bandas y sus conexiones al sistema eléctrico, del agua introducida en torno a la corona en las perforaciones realizadas en roca dura.

Leeman³² resolvió este problema de manera eficaz empotrando las conexiones eléctricas de las bandas en un taco de caucho de silicona de 35 mm de diámetro, en cuya cara frontal estaba montada una roseta rectangular de bandas extensométricas que, en la célula original, quedaba protegida por una película de araldita de 0,6 mm de espesor. Los cables procedentes de la roseta estaban unidos a cuatro bornas de cobre en una ficha de conexión aislada (fig. 6.16). El equipo puede emplearse en un taladro perforado con el diámetro standard BX (60 mm).

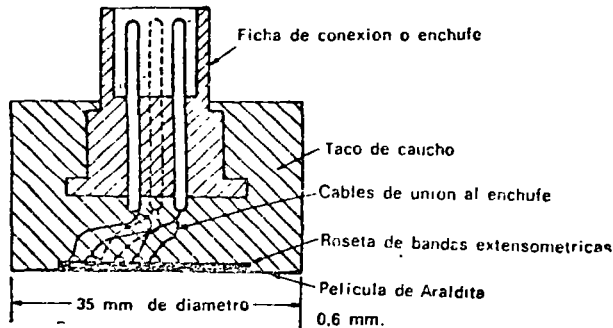


Figura 6.16 «Doorstopper» de Leeman

Puede emplearse un aparato para colocar la célula, orientándola para medir deformaciones en las direcciones vertical, horizontal y a 45°. El aparato introductor se mantiene acoplado hasta que la célula queda fija a la roca, extrayéndole entonces para comenzar la sobreperforación.

Si las diferencias de lectura de las bandas extensométricas en las direcciones vertical, a 45° y horizontal, antes y después de la sobreperforación son respectivamente ϵ_v , ϵ_{45} y ϵ_h , las deformaciones principales ϵ_1 y ϵ_2 de la roca en el extremo del taladro son:

$$\epsilon_1 \text{ o } \epsilon_2 = \{(\epsilon_h + \epsilon_v) \pm \sqrt{2\epsilon_{45}^2 - (\epsilon_h + \epsilon_v)^2 + (\epsilon_h - \epsilon_v)^2}\} \quad (6.12)$$

Las direcciones de ϵ_1 y ϵ_2 son θ_1 y θ_2 , medidas en sentido contrario a las agujas del reloj respecto a la dirección de ϵ_h y vienen dadas por:

$$\left. \begin{aligned} \operatorname{tg} \theta_1 &= \frac{2(\epsilon_1 - \epsilon_h)}{2\epsilon_{45} - (\epsilon_h + \epsilon_v)} \\ \operatorname{tg} \theta_2 &= \frac{2(\epsilon_2 - \epsilon_h)}{2\epsilon_{45} - (\epsilon_h + \epsilon_v)} \end{aligned} \right\} \quad (6.13)$$

Las tensiones principales en la roca en el extremo del taladro son:

$$\left. \begin{aligned} \sigma_1 &= \frac{E}{1 - \nu^2} (\epsilon_1 + \nu\epsilon_2) \\ \sigma_2 &= \frac{E}{1 - \nu^2} (\epsilon_2 + \nu\epsilon_1) \end{aligned} \right\} \quad (6.14)$$

6.5.2 La célula biaxial fotoelástica

Hawkes y Moxon han descrito el empleo de una célula fotoelástica biaxial para determinación de tensiones absolutas por la técnica de liberación de tensiones³³ (fig. 6.17). La célula está formada por un cilindro de resina epoxy de 44 mm de diámetro y 3 mm de espesor, con un agujero central. La base de la célula está pintada con una película reflectante que deja un reborde bien

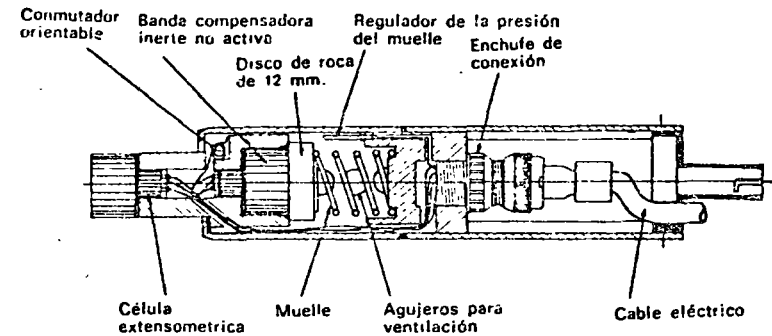


Figura 6.17 Elemento de inserción de la célula de Leeman

diferenciado en el cilindro. Este se adhiere a la roca por el reborde mediante un cemento de fraguado rápido. La secuencia de operaciones se muestra en la figura 6.18.

La célula se observa con un polariscopio de reflexión (fig. 6.19), cuyas señales ópticas son semejantes a las descritas para el tensímetro de vidrio. Sin embargo, la célula biaxial se calibra en términos de deformación utilizando unas bandas extensométricas colocadas en cruz (fig. 6.20).

Como en el tensímetro fotoelástico, las direcciones de deformación principal vienen dadas automáticamente por los ejes de simetría del sistema de franjas observado y la relación ϵ_1/ϵ_2 por la medida de la distancia entre puntos isotrópicos del eje ϵ_1 . La célula se calibra de forma que el número de orden de las franjas proporcione directamente ϵ_1 . La sensibilidad teórica del tipo de célula empleado actualmente³⁴ es de 440×10^{-6} deformaciones por franja. La sensibilidad determinada experimentalmente en estados de tensión biaxiales es de 440 microdeformaciones por franja (fig. 6.21). El límite de medida utilizando el analizador manual es del 2 al 3% de una franja. La medida con números de orden de franja bajos (menores de media franja) requiere cierta habilidad y por tanto la célula fotoelástica es preferible en rocas bajo cargas elevadas que desarrollan una recuperación elástica considerable en el proceso de liberación de tensiones.



centro de educación continua
división de estudios superiores
facultad de ingeniería, unam



MECANICA DE ROCAS APLICADA A LA MINERIA

TEMA: ANALISIS DE DATOS GEOLOGICO-ESTRUCTURALES

PARTE II

ABRIL, 1978.

ANALYSIS OF FRACTURE ORIENTATIONS FOR INPUT TO STRUCTURAL MODELS OF DISCONTINUOUS ROCK

by

M. A. Mahtab,¹ D. D. Bolstad,² J. R. Alldredge,³ and R. J. Shanley⁴

ABSTRACT

This report presents a new procedure for analyzing the orientations of rock fractures in an engineering site. This procedure, coded in a computer program, identifies clusters or groupings among the fracture orientations and calculates (1) the mean orientation of the fractures within each cluster and (2) the dispersion or scatter among these fracture orientations. Data points are represented by intersections of joint normals with the upper hemisphere, which is divided into 100 equal-area quadrilateral patches. The points in adjacent patches where the Poisson distribution test shows significant concentrations are assigned to a single cluster. For a cluster whose fracture orientations follow Arnold's hemispherical normal distribution, a confidence interval for the fracture orientation mean is calculated by applying Fisher's estimates. The technique is applied to the treatment of three examples.

INTRODUCTION

The mechanical behavior of loaded structures in rock mass is strongly influenced by the geometric and mechanical parameters of the prevailing geologic planes of weakness, such as joints and fractures, which may be defined as recurrent planar geologic discontinuities having spacings of from tenths of a foot to tens of feet. Throughout this report the words joint and fracture are used synonymously.

As a result of the availability of large computers and owing to the recent advances made in finite-element analysis techniques, boundary-value problems in jointed rock have become increasingly tractable. For mathematical modeling of these problems, the orientations of the discontinuities are important input parameters. Additional geometric parameters, such as spacing and character of joint surfaces, as well as the mechanical parameters

¹Physical scientist.

²Geologist.

³Mathematical statistician.

⁴Mathematician.

All authors are with the Rock Mass Behavior Group.

of joints, are equally important considerations in modeling a rock mass. This report will, however, be restricted to a treatment of data on joint orientations.

Very often the attitudes of fractures in a site are observed to be non-randomly distributed, and in most of these instances, it is possible to group the fractures into sets such that the elements of each set have a statistically preferred attitude.

When constructing models of discontinuous rock containing sets of joints it is essential to estimate a single direction for each set and to obtain a measure of precision of this estimate so that the corresponding precision can be computed in the output of the structural analyses that employ these models.

The available techniques for defining preferred directions of sets in orientation data consist in visual selection of the means (or modes) from a planar projection of the hemispherical distributions. However, errors occur in these quantities owing to the inherent distortions in the planar projections. These errors may prove to be important in an engineering analysis. Furthermore, since the form of the distribution of the data points cannot be tested against a known distribution, no estimates of precision of the mean attitudes can be formulated. Consequently, the engineer is faced with the alternative of treating the orientations as univariates of dip and azimuth. However, as pointed out by Pincus (8),⁶ this alternative is valid for the study of nearly vertical surfaces only, since one of the variables is now a constant (that is, dip $\approx 90^\circ$).

The problem consists of devising an efficient scheme for quantifying the preferred (or mean) directions of clusters in a sample of joint orientations. It is necessary to test and illustrate the form of the distribution of points in each cluster and to give an estimate of the population mean in the case of a hemispherical normal distribution.

This Bureau of Mines report describes a new technique of obtaining significantly tight groupings of points, or clusters, of intersections of joint normals with the hemisphere. An efficient computer program is developed to treat multiple clusters as well as antipodal clusters in the sample. Clusters of bivariate data points are compared with the hemispherical normal distribution by applying the chi-square test. Confidence intervals are then assigned to the means of the clusters whose data follow the hemispherical normal distribution.

ACKNOWLEDGMENTS

The authors wish to express their gratitude to K. J. Arnold for his kind permission to use materials from his unpublished dissertation. The assistance of the management and personnel of Magma Copper Co. during collection of

⁶Underlined numbers in parentheses refer to items in the list of references preceding the appendixes.

prophyry fracture orientation data at San Manuel, Ariz., is gratefully acknowledged. The authors also wish to thank F. S. Kendorski, Climax Molybdenum Co., for his assistance during collection of data at San Manuel. Several helpful suggestions were received from G. S. Koch, Jr., University of Georgia.

METHOD OF ANALYSIS

The method of analysis is presented here in two convenient steps: (1) Identifying significant concentrations, or clusters, which occur in the data; and (2) determining attitudes of joint sets (or clusters); both steps involve the application of statistical principles.

Definition of Clusters

In the past, the generally accepted technique for defining mean orientations of joint sets (or clusters) has been the use of planar projections of a hemisphere. Lambert azimuthal equal-area (or Schmidt) projection is most commonly employed. The projection of the traces of the joint normals, called a point diagram, is displayed on the equal-area net. Point concentrations (expressed as percentages of the total points that occupy 1-percent areas of the hemisphere) are obtained by manually counting the points in 1-percent-area circles centered on intersections of a grid that is superimposed on the projection. (There are several variations of this basic counting technique. The following arguments are, however, applicable to all of these techniques.) Some recently developed computer programs, for example, Jeran and Mashey (3), have reduced the effort involved in counting of points and subsequent plotting of contours of point concentrations on the planar projection.

The azimuthal projection of a 1-percent-area circle on the sphere is circular only if the pole (defined here as the vertical projection of the center on the upper hemisphere) of the sphere forms the center of the circle. The equal-area projections of all other circles on the hemisphere will be elliptical, with the distortions being most pronounced for the equatorial areas. Point concentrations obtained by counting points in a specified circular area in the projection are, therefore, inaccurate. Consequently, any attempts to find mean values for joint sets will result in quantities which cannot be used with confidence in an engineering analysis of structures in jointed rock. This report does not use projections in defining joint sets and, therefore, avoids introducing distortions inherent in the projection techniques.

Joint orientations are best expressed as the orientations of the joint normals which are directions without sense; that is, a joint normal can be directed in the positive or the negative sense along an axis normal to the joint plane. However, the sense of a joint normal can be fixed by defining it as being normal to the directed dip line in a left-handed Cartesian frame. Thus, if the dip, ϕ_1 ($0 \leq \phi_1 \leq 90^\circ$), and the azimuth of dip, θ_1 ($0 \leq \theta_1 \leq 360^\circ$), of the joint plane, 1, are observed in the field, the joint normal originating from the center of a unit sphere will be directed toward the upper hemisphere. The angular coordinates of the joint normal can then be specified by its colatitude, ϕ_1 , and its longitude, θ_1 (figs. 1 and 4).

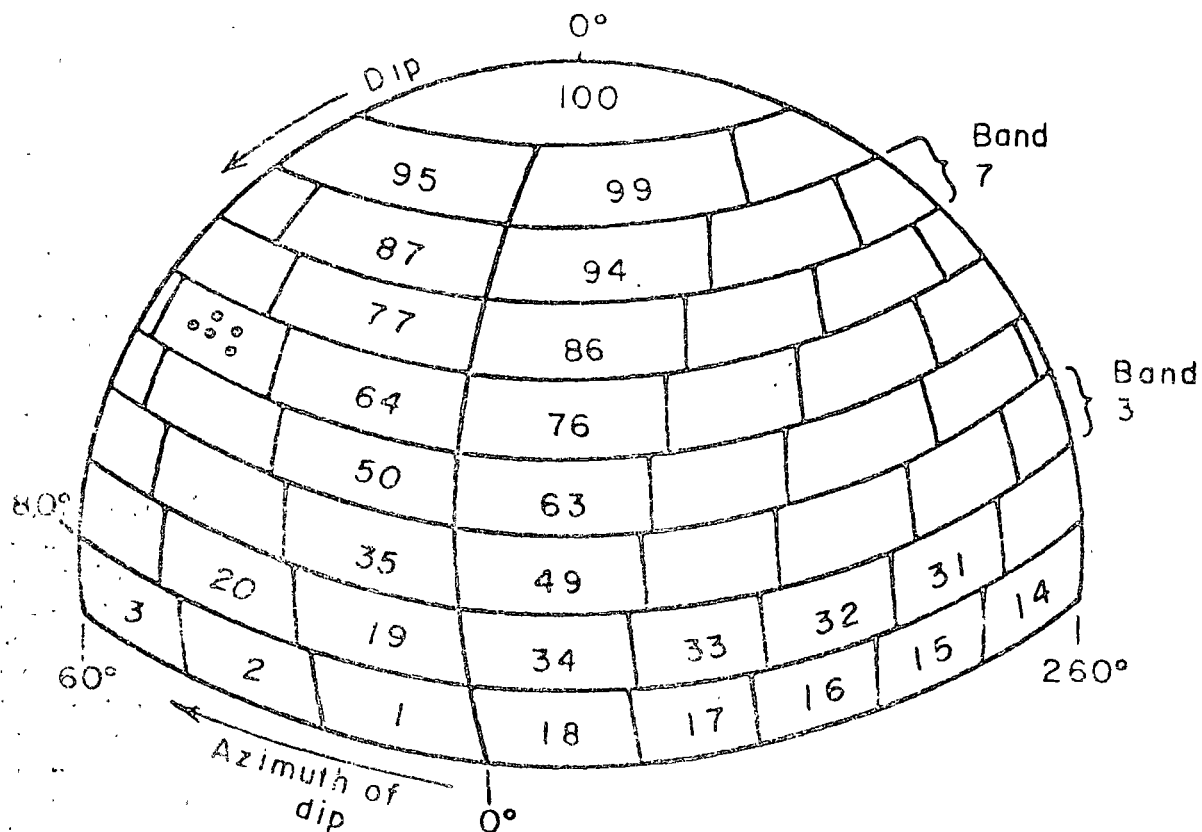


FIGURE 1. - Division of Hemispherical Surface Into 100 Equal-Area Patches.

The approach adopted in this study for defining densities of traces of joint normals was the use of 100 equal-area cells (or patches) which cover the hemispherical surface. Any shape of unit patches (that is, circular, elliptical, or a quadrilateral patch) could be used for this purpose. However, many more unit circles or unit ellipses would be required to cover the entire hemispherical surface than the number of unit quadrilateral patches. The 100 quadrilateral patches used in this study (fig. 1) were designed through the following procedure:

The hemispherical surface was divided into nine coaxial bands such that band 1 contained the equator and band 9 contained the pole of the hemisphere. It was decided to include the following percentages of the hemispherical surface in the bands numbered 1 to 9: 18, 16, 15, 14, 13, 10, 8, 5, and 1; these percentages also represent the number of unit patches to be assigned to the corresponding bands. The next step involved the assignment of colatitude ϕ (or dip) values to the boundaries of each band. Suppose that with reference to figure 1 ϕ_l^j and ϕ_u^j are the dips corresponding to the lower and upper boundaries of band number j (where $j = 1, 2, \dots, 9$) such that

$$0 \leq \phi_l^j \leq \phi_u^j \leq 90^\circ,$$

then the percentage of the hemispherical surface S^j contained in band j is given by

$$S^j = 100 (\cos \phi_u^j - \cos \phi_l^j).$$

Now, for band 1, $S^1 = 18$ and $\phi_l^1 = 90^\circ$. The above equation then yields

$$\phi_u^1 = 79.63^\circ.$$

The azimuth range for each of the 18 patches in band 1 is given by $(360/18)^\circ$, or 20° . The first patch in band 1 is bounded by longitudes (or azimuths) of 0° and 20° , and the rest of the patches in the band are numbered consecutively in the increasing direction of θ ; for example, the azimuth ranges for patches 1, 2, 3, etc., in band 1 are, respectively, $0^\circ \leq \theta \leq 20^\circ$, $20^\circ < \theta \leq 40^\circ$, $40^\circ < \theta \leq 60^\circ$, etc.

Proceeding in the above manner, the dip ranges of the other eight bands and the azimuth ranges for patches in each of these bands are obtained. The dip ranges for bands 1 to 9 are as follows:

Band 1.....	$90^\circ \geq \phi \geq 79.63^\circ$
Band 2.....	$79.63^\circ > \phi \geq 70.12^\circ$
Band 3.....	$70.12^\circ > \phi \geq 60.66^\circ$
Band 4.....	$60.66^\circ > \phi \geq 50.95^\circ$
Band 5.....	$50.95^\circ > \phi \geq 40.54^\circ$
Band 6.....	$40.54^\circ > \phi \geq 30.68^\circ$
Band 7.....	$30.68^\circ > \phi \geq 19.95^\circ$
Band 8.....	$19.95^\circ > \phi \geq 8.11^\circ$
Band 9.....	$8.11^\circ > \phi \geq 0^\circ$

Notice that the range of azimuth for patches in a given band is a function of the band number and increases nonlinearly with the increasing band number (fig. 2). For example, the azimuth range for a patch in band 1 is 20° , whereas the azimuth range for a patch in band 8 is 72° . Now, for a constant instrument error in measuring the azimuth of a joint plane, there will be an error introduced in the measured azimuth which Muller (7) has shown to be a geometric function of the dip of the plane. A graph of the error in measured azimuth as a function of dip is shown in figure 3 for an instrument error of 5° . A close qualitative similarity can be noted between figures 2 and 3, indicating that the scheme of subdivision of the hemisphere in figure 1 adopted for this study appropriately exploits the error in measured azimuth, thus producing an efficient design of the 100 patches.

Referring to figure 1, the density of a patch is given by the number of observations that plot in it; for example, patch 65 has a density of 5. In order to define significant concentrations, some kind of randomness test is required to indicate the acceptable level of significance, or "threshold" density. Clusters are then defined as collections of all points in adjacent patches, where each patch possesses a density that exceeds the threshold value. The Poisson distribution model (see Stauffer, 9), provides a means of obtaining the threshold density. The Poisson model states that the probability of occurrence of a random density D ($D \leq x$) is given by

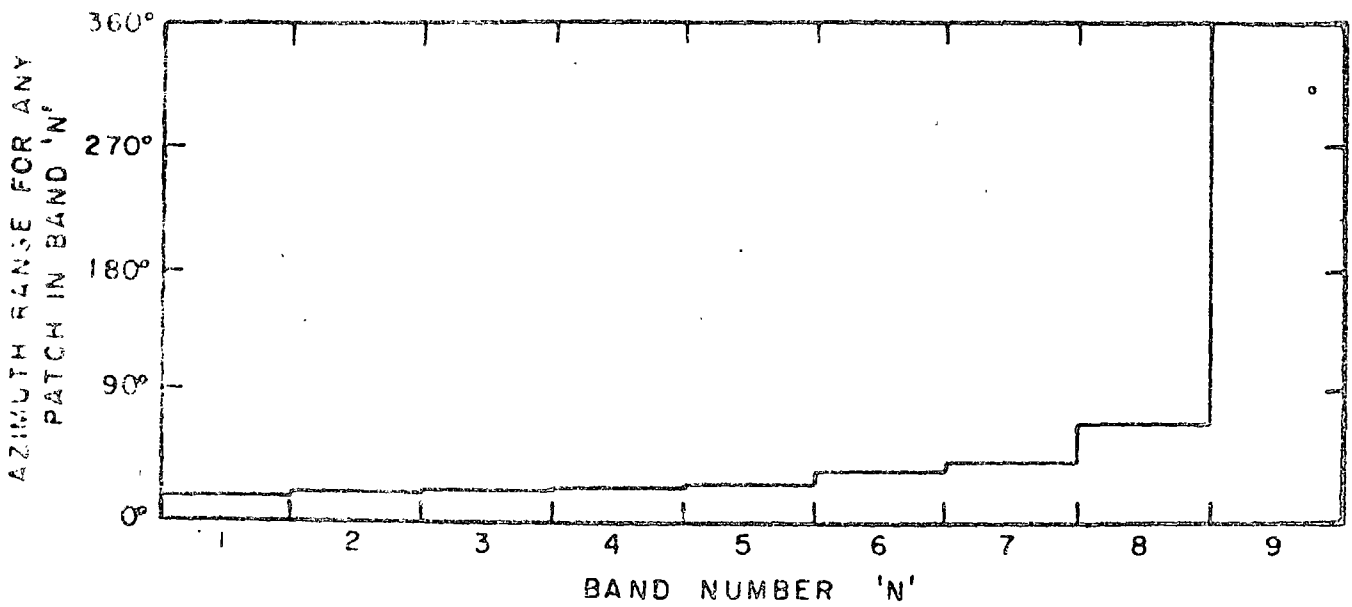


FIGURE 2. - Azimuth Range for Patches as a Function of Band Number. (See fig. 1.)

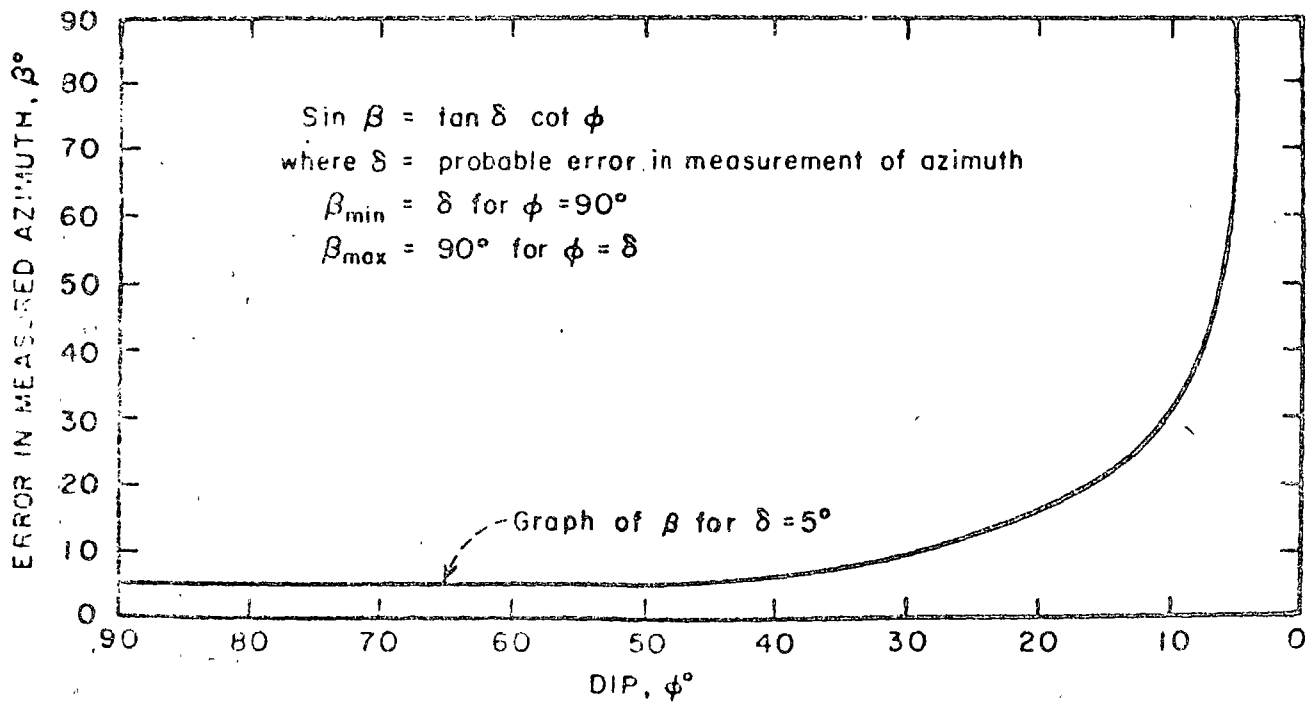


FIGURE 3. - Error in Measured Azimuth (of Dip) as a Function of Dip.

$$P(D > x) = 1 - \sum_{j=0}^x \frac{e^{-m} m^j}{j!}, \quad (1)$$

where m is the average density over all the 100 patches.

For the purpose of this report, the largest value of integer x satisfying

$$P(D > x) \leq 0.05$$

was selected as the threshold density.

Clusters in the data points are defined according to the above procedure by the computer program PATCH, which is listed in appendix B. One particular operation in the program merits comment here: While scanning the first band, it is possible to discover diametrically opposite or antipodal patches, each having a density above the threshold density. The program will combine the pair of clusters to which such patches belong on the assumption that the points encountered therein belong to a single joint set with a mean dip of approximately 90° .

Analysis of Clusters

The data of many clusters follow the hemispherical normal distribution. For this reason, the present section will indicate how to calculate statistics, such as the mean and the measure of dispersion for the hemispherical normal distribution. In addition, the relationship between the angular deviation from the mean, the measure of dispersion, and the probability level for the hemispherical normal distribution will be examined.

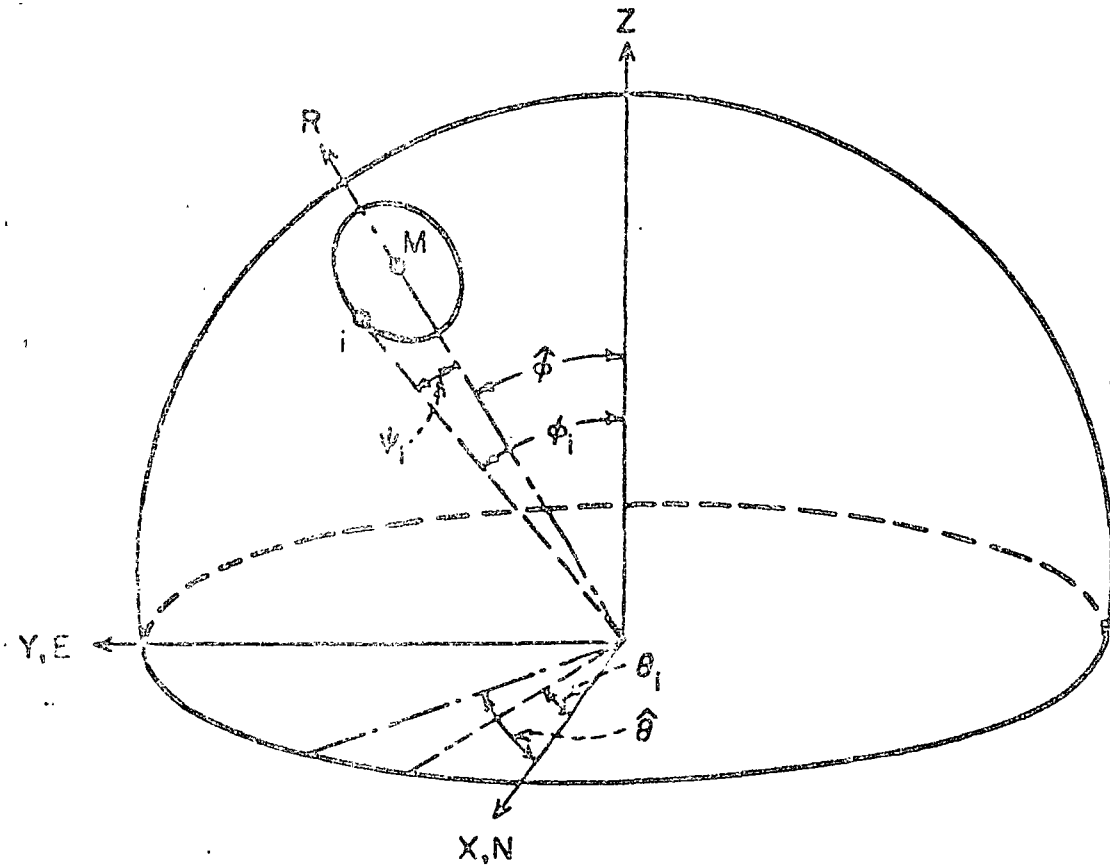
In the previous section the angular coordinates of the normal to joint plane i were defined as its colatitude ϕ_i and its longitude θ_i . In this section i takes on values from 1 to N , where N is the total number of data points in the cluster being analyzed. Referring to figure 4, a left-handed rectangular coordinate frame can be defined such that the x -axis indicates zero azimuth. Then the direction cosines of the unit vector representing observation i are given by

$$\begin{aligned} \ell_i &= \sin \phi_i \cos \theta_i \\ m_i &= \sin \phi_i \sin \theta_i \\ n_i &= \cos \phi_i \end{aligned} \quad (2)$$

where $i = 1, 2, \dots, N$.

The resultant, \vec{R} , of N of these observed unit vectors passes through the center of gravity of the cluster. The magnitude of the resultant is given by

$$|R| = [(\sum \ell_i)^2 + (\sum m_i)^2 + (\sum n_i)^2]^{1/2}, \quad (3)$$



$$X_i = l_i = \sin \phi_i \cos \theta_i; \quad Y_i = m_i = \sin \phi_i \sin \theta_i$$

$$Z_i = n_i = \cos \phi_i$$

M = Intersection of mean vector (colatitude $\hat{\phi}$, longitude $\hat{\theta}$) with the hemisphere.

ψ_i = Angle between the mean and observation i

FIGURE 4. - Rectangular Coordinates (or Direction Cosines) of a Point i (With Colatitude = ϕ_i and Longitude = θ_i) on a Unit Sphere.

where $i = 1, 2, \dots, N$. The direction of \vec{R} is that of the vector sum of the unit vectors representing the normals to the observed joints. The angular coordinates of the resultant are obtained as follows:

$$\hat{\phi} = \tan^{-1} \frac{[(\sum l_i)^2 + (\sum m_i)^2]^{1/2}}{\sum n_i} \quad (4)$$

and

$$\hat{\theta} = \tan^{-1} \frac{\sum m_i}{\sum l_i} \quad (5)$$

These coordinates estimate the coordinates of the mean orientation vector of the joint set under study.

If the direction cosines of the mean orientation vector are defined as l , m , and n , the angle ψ_i between the mean orientation vector and the i^{th} observation is given by

$$\cos(\psi_i) = ll_i + mm_i + nn_i \quad (6)$$

Arnold (1) has shown the hemispherical distribution to have the following form (for details, refer to appendix D):

$$U(\psi, k) = \frac{k}{4\pi(e^k - 1)} e^{k \cos \psi} \quad (7)$$

where ψ is a random variable which assumes values ψ_i defined in equation 6, and k is a measure of dispersion. This is apparent since when k is large, the distribution is confined to a small portion of the hemisphere in the neighborhood of the mean orientation vector, and when k is zero, the distribution is uniform over the hemispherical surface. The maximum likelihood estimate of k , denoted by \hat{k} , satisfies the following equation which is derived in appendix D:

$$\frac{|R|}{N} = \frac{e^{\hat{k}}}{e^{\hat{k}} - 1} - \frac{1}{\hat{k}} \quad (8)$$

Now, in the analysis of the many groups of orientation data⁶ examined by the authors (including the examples cited in table 1), the value of \hat{k} was found to be greater than 6. It is reasonable to assume that the data points in joint sets (defined through application of the Poisson test) will not occupy a sizable portion of the hemispherical surface. Large values of \hat{k} are, therefore, assured. Assuming $k \geq 6$, equation 8 reduces to the following form:

$$\frac{|R|}{N} = 1 - \frac{1}{\hat{k}}, \quad (9)$$

which can be rewritten as

$$\hat{k} = \frac{N}{N - |R|} \quad (10)$$

⁶This includes 39 independent groups of coal cleat and shale joint data from a Pennsylvania coal mine, 13 independent groups of data on joints and faults in an underground copper mine, and the data for surface joints in a Precambrian granite in Arizona.

This provides a convenient formula for estimating the measure of dispersion of a set of orientation data.

The radial coordinate \hat{a} of the center of gravity of the cluster of points on the hemisphere is expressed by the left-hand side of equation 8; that is

$$\hat{a} = \frac{|R|}{N}. \quad (11)$$

This too is an excellent indicator of the scatter of the data points. For example, when \hat{a} approaches unity, the data points will bunch about a single direction. Pincus (8, p. 506) discusses the relationship between \hat{a} and R for the hemispherical normal distribution.

Arnold (1) has also tabulated the probability integral for the hemisphere. This integral is represented by the area on the hemisphere cut by a cone whose vertex lies at the center of the sphere. Arnold (1, table VIII) gives the probability, P , of an observation lying within an (angular) distance ψ of the mean for several values of k . The relationship is as follows:

$$P = \frac{1 - e^{-k(1 - \cos \psi)}}{1 - e^{-k}}. \quad (12)$$

When k is greater than 6, this equation reduces to

$$\cos \psi = 1 + \frac{1}{k} \log_e (1-P). \quad (13)^7$$

⁷Note here that equations 10 and 13 are identically derivable for $k \geq 3$ from the spherical normal distribution formulated first by Arnold (1) and later by Fisher (2). In the spherical normal distribution

$$U_0(\psi, k) = \frac{k}{4\pi \sinh k} e^{k \cos \psi}$$

The value of k is expressed by

$$\coth k - \frac{1}{k} = \frac{|R|}{N};$$

for $k \geq 3$, we have

$$\hat{k} = \frac{N}{N - |R|}. \quad (10A)$$

The probability of finding an observation within displacement ψ of the mean of a spherical normal distribution is expressed by

$$P = \frac{1 - e^{-k(1 - \cos \psi)}}{1 - e^{-2k}}. \quad (12A)$$

For $k \geq 3$, equation 12A reduces to

$$\cos \psi = 1 + \frac{1}{k} \log_e (1-P). \quad (13A)$$

Equation 13 is illustrated graphically in figure 5 which has been fashioned after Watson and Irving (10, fig. 1). These curves should further clarify the meaning of k .

In this section it was indicated how the resultant vector, \vec{R} , is calculated. Also, an approximate estimate for the measure of dispersion, k , is provided. The relationship between ψ , the angular deviation from the mean orientation vector; P , the probability level for the hemispherical normal distribution; and k , a measure of dispersion, is reviewed.

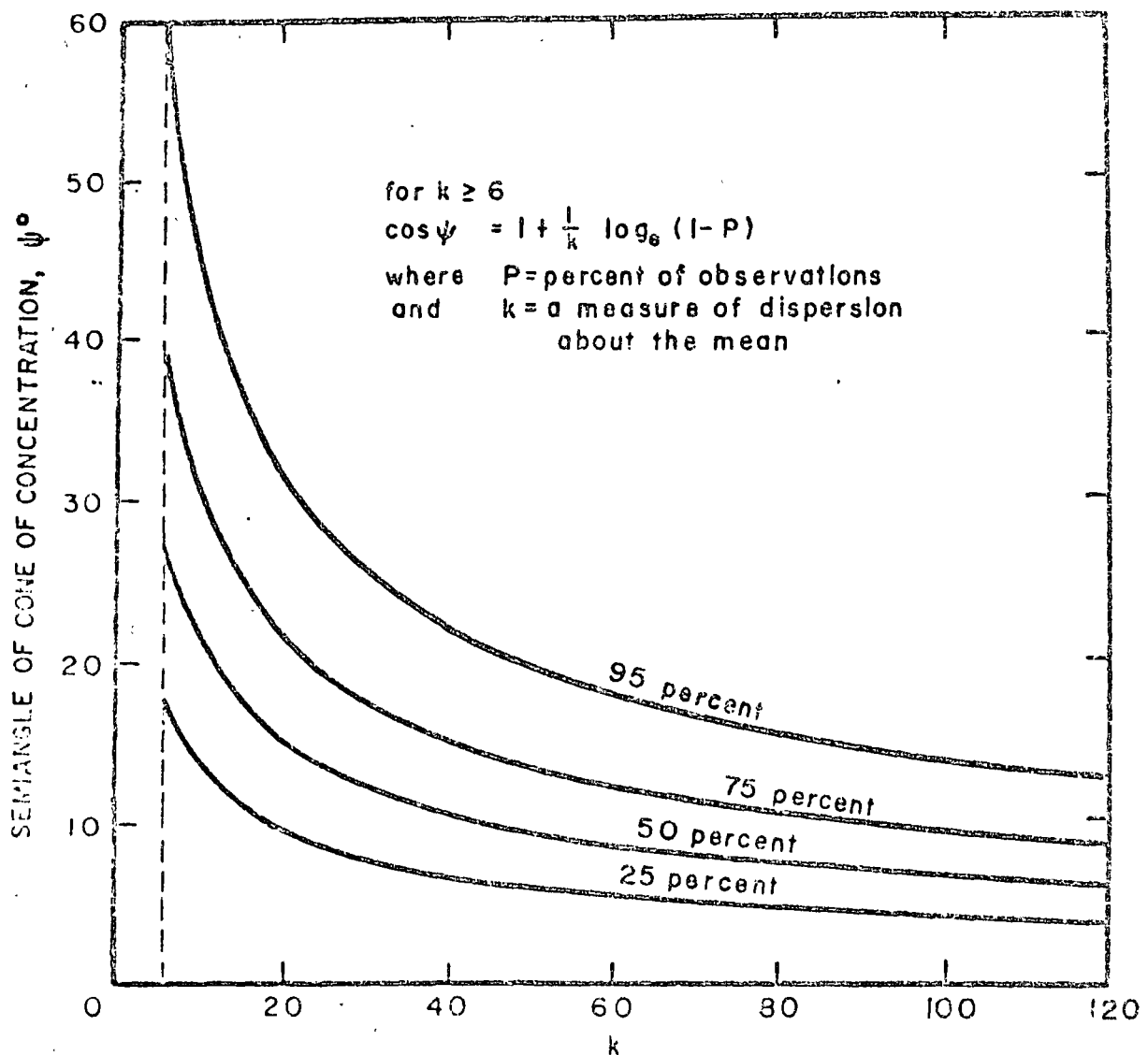


FIGURE 5.- Semiangle of Cone of Concentration, ψ° , as a Function of k (10). Curves represent percent of observations that fall within ψ° of the mean direction.

Confidence Interval for the Mean of a Hemispherical
Normal Distribution

In the section on "Definition of Clusters" it was shown how clusters that occur in the orientation data are defined. In the last section, the techniques for estimating the mean value and measure of dispersion for the data that follow the hemispherical normal distribution were reviewed. This section addresses the problem of the confidence interval for the mean.

Since the mean of a random sample rarely equals the mean of the population from which the sample is drawn, it is desirable to construct a confidence interval around the sample mean, which gives a measure of how close the sample mean is to the true population mean. For univariate data, the formulas for the confidence limits, which define the boundaries of the confidence interval, are available for several parametric distributions (Krumbein and Graybill, 5, ch. 6, table 6.7). The process of constructing confidence intervals around the mean of bivariate orientation data, however, becomes more complex. Fisher (2) derives the following formula for computing the radius c (or the vertex angle) of the cone of confidence for the mean of the spherical normal distribution in the case where $k \geq 3$:

$$\cos c = 1 + \frac{N-|R|}{|R|} \left[\left(\frac{1}{P} \right)^{1/(N-1)} - 1 \right] \quad (14)$$

In equation 14 N is the number of data points in the cluster, $|R|$ is the length of the resultant vector as given in equation 3, and P is the probability level.

It can be shown, by starting with the hemispherical normal distribution and following Fisher's arguments for the spherical normal distribution, that equation 14 also holds for the hemispherical normal distribution when $k \geq 6$. The application of equation 14 to actual examples is shown in the next section.

The radius c of the cone of confidence can be resolved to give the confidence limits for the dip ($\pm \hat{\phi}_c$) and the azimuth of dip ($\pm \hat{\theta}_c$) by the following relations:

$$\hat{\phi}_c = c,$$

and

$$\sin \hat{\theta}_c = \sin c / \sin \hat{\phi}, \text{ for } \hat{\phi} > 0. \quad (15)$$

When the χ^2 test, described in the next section, shows the inapplicability of the hemispherical normal distribution, a cone of confidence for the population mean will not be available. It may then be determined if the dips and azimuths of the fractures follow any known distribution, and confidence intervals may be constructed for the means of these two variables separately. An alternate approach, if no known distributions can be fitted, would be to apply the methods to nonparametric statistics for obtaining confidence intervals for the population medians; which are better measures of central tendency in this case.

Fit of Observations to Arnold's Hemispherical Normal Distribution

To compare the data in each cluster with the hemispherical normal distribution given in equation 7, the χ^2 goodness-of-fit test, indicated by the following general formula, will be used:

$$\chi^2 = \sum \frac{N_c (f_o - f_e)^2}{f_e} , \quad (16)$$

where f_o and f_e are the observed and expected frequencies, respectively, and N_c is the total number of classes chosen.

To complete the test, the value of χ^2 obtained in equation 16 is compared with the theoretical χ^2 value (6, table 4), which depends on the degrees of freedom (D.F.) for the case under examination. D.F. is given by

$$\text{D.F.} = N_c - 1 - N_p , \quad (17)$$

where N_p = number of unknown parameters to be estimated. In this case, each data point i has only two parameters, ψ_i and α_i , its angular distance from, and its azimuthal angle about, the mean direction ($\hat{\phi}$, $\hat{\theta}$), respectively. Thus, for the hemispherical normal distribution, $N_p = 2$ and $\text{D.F.} = N_c - 3$. Equation 6 defines ψ_i . The value of α_i is determined by proceeding in the following manner:

Rotate the x-y plane (while keeping the z-axis fixed) such that the mean has 0° azimuth. The transformed coordinates for point i are

$$x'_i = x_i \cos \hat{\theta} + y_i \sin \hat{\theta}$$

and

$$y'_i = -x_i \sin \hat{\theta} + y_i \cos \hat{\theta} . \quad (18)$$

Next, rotate the pole to the mean; that is, rotate the z-x' plane through angle $\hat{\phi}$ while keeping y' fixed. The new coordinates are given by

$$x''_i = x'_i \cos \hat{\phi} - z_i \sin \hat{\phi}$$

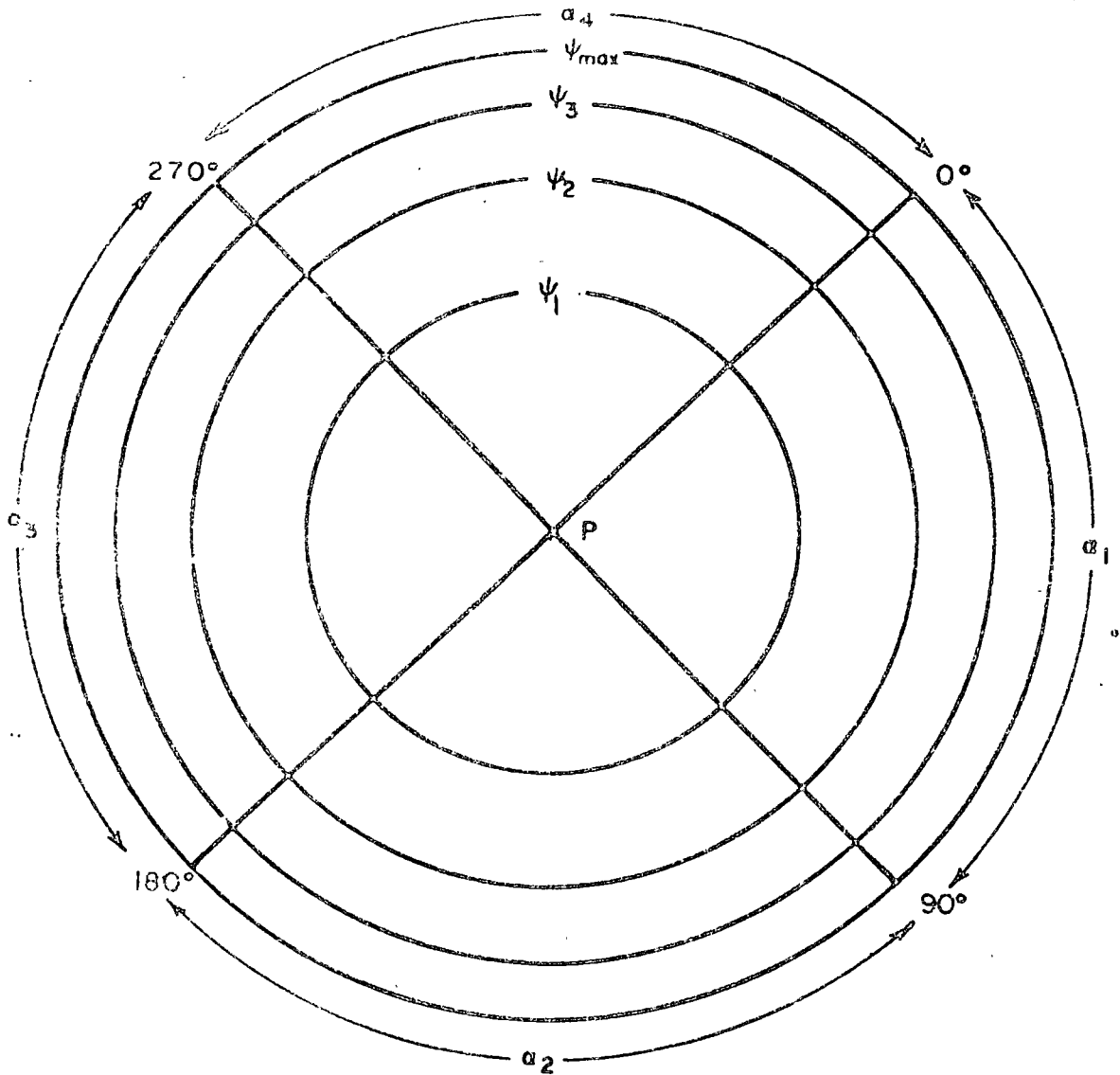
and

$$z'_i = x'_i \sin \hat{\phi} - z_i \cos \hat{\phi} . \quad (19)$$

The azimuthal angle, α_i , of observation i about the new mean direction ($\hat{\phi} = 0$, $\hat{\theta} = 0$) is then given by

$$\alpha_i = \tan^{-1} \frac{y'_i}{x''_i} . \quad (20)$$

Regarding the choice of the number of classes (N_c) to be used in the χ^2 test, there is a wide divergence of opinion in the statistical literature. A lower limit of 16 is chosen here for N_c , such that $N_\alpha = N_\psi = 4$, where $N_c = N_\psi \cdot N_\alpha$, N_ψ = number of annuli or number of ψ -classes (fig. 6), and N_α = number of sectors in each annulus. Keeping N_α constant, N_ψ is varied to a maximum value of 8 such that the upper limit of N_c is 32. It is assumed



- ψ_i = Angular distance of the outer boundary of the i th annulus from the pole P (that is, the mean) = $\cos^{-1} \left[1 - \frac{i}{N_\psi} (1 - \cos \psi_{\max}) \right]$
 α_i = Range of i th azimuthal division = 90° , $1 \leq i \leq 4$
 N_ψ = Number of ψ -annuli required ($4 \leq N_\psi \leq 8$)
 N_a = Number of azimuthal divisions = 4
 N_c = Number of classes = $N_\psi - N_a$

FIGURE 6. - Scheme of Division of Cluster Data Into N_c Classes.

that $N_a = 4$ provides an adequate measure of the azimuthal dispersion. For $N_\psi > 4$, it is required that the expected frequency should be at least one in each of the four sectors of all ψ -annuli, except the last. Note that the neglect

in accounting for the theoretical frequency in the last ψ -annulus will result in a slightly increased sensitivity of the χ^2 test.

Now the probability that a direction will be observed which makes an angle ψ_0 or more with the mean orientation vector can be written (by using equation 12 for $k \geq 6$) as

$$P(\psi > \psi_0) = e^{-k(1 - \cos \psi_0)}. \quad (21)$$

For a given distribution, the expected frequency in any ψ -interval can be found by using equation 21. For example, in the interval $[\psi_1, \psi_2]$,

$$f(\psi_1, \psi_2) = N \left[e^{-k(1 - \cos \psi_1)} - e^{-k(1 - \cos \psi_2)} \right]. \quad (22)$$

The expected frequency for each sector in this interval is then given by

$$f_0 = \frac{f(\psi_1, \psi_2)}{N_\alpha}. \quad (23)$$

The observed frequency, f_0 , for each of the N_0 classes is obtained by actual counting of the data points falling within the class limits. The process of comparing data in a cluster with the hemispherical normal distribution is carried out in the subroutine SECTOR (appendix A, fig. A-3).

APPLICATION OF ANALYSIS TO EXAMPLES

Based on the foregoing development, a given sample of orientations will be analyzed as follows:

1. Joint sets or clusters are delineated by calculating densities in all of the 100 equal-area patches (density of a patch equals the number of joint-normal intersections plotting in it) covering the hemisphere and by collecting points in those adjacent patches which show densities exceeding the threshold density indicated by the Poisson distribution test.

2. Multiple clusters in the data are handled by an efficient computer program (for an estimate of the computing time, see appendix A) which combines antipodal clusters (with near 90° dip).

3. The mean value of attitudes is computed for each cluster, and the spatial distribution of points in a cluster is shown in a level plot by constructing a planar projection after rotating the sphere to bring the mean to the pole of the sphere.

4. The data in each cluster are compared with Arnold's hemispherical normal distribution by applying the chi-square test to the bivariate data points. For a hemispherical normal distribution, Fisher's theory is used to construct confidence intervals around the cluster mean which will contain the population mean with a given level of confidence.

The method of analysis presented in the previous sections is incorporated in the computer program PATCH, which is listed in appendix B. The method can be applied to axial data originating from the observation of the attitudes of bedding planes, microfractures, joints, faults, lineations, and crystal and fold axes. The potential of the technique for analysis of axial data is illustrated below by applying it to three examples; the results are summarized in table 1. In these analyses the value $P = 0.05$ has been consistently used, corresponding to a level of confidence of 95 percent.

TABLE 1. - Statistical analysis of clusters in orientation data from three examples by the computer program PATCH

	Example 1, A-axes of glacial till pebbles ¹		Example 2, coal cleats ²		Example 3, porphyry copper fractures ³	
	1	1	2	1	2	3
Cluster number.....	1	1	2	1	2	3
Number of points in cluster..	77	69	55	57	77	7
Mean azimuth of dip.....degrees..	287.65	24.69	118.84	248.62	348.25	120.31
Mean dip.....do....	1.44	89.88	87.04	83.88	80.74	22.70
Measure of dispersion...k..	17.23	108.96	70.93	23.08	22.37	215.89
Radius of cone of confidence.....degrees..	-	1.65	-	3.95	-	-
Chi-square value.....	38.006	8.435	24.288	13.610	44.719	24.805
Theoretical chi-square value.....	22.351	22.351	22.351	22.351	32.663	22.351
Degrees of freedom.....	13	13	13	13	21	13
Confidence intervals (for hemispherical normal distribution), degrees:						
Azimuth of dip.....	-	±1.65	-	±3.98	-	-
Dip.....	-	±1.65	-	±3.95	-	-

¹100 observations; Poisson cutoff level 3.000 percent.

²135 observations; Poisson cutoff level 2.222 percent.

³286 observations; Poisson cutoff level 2.098 percent.

Example 1.--A-Axes of Glacial Till Pebbles

The orientations of the A-axes of glacial till pebbles were measured by Krumbein (4) and have been listed by Arnold (1). Krumbein analyzed the 100 observations by treating them as univariates of either the azimuth or the dip and defined a single preferred orientation for this data with a mean azimuth of 268.5° and a mean dip of 24°. The data are listed in table 2, and the polar equal area projection of this data is shown in figure 7.

TABLE 2. - A - AXES OF GLACIAL TILL
PEBBLES. KRUMBEIN (4).

A	D	A	D	A	D	A	D	A	D	A	D	A	D
8	68	11	42	12	22	20	72	23	24	26	12	32	59
32	33	34	12	35	5	38	18	39	1	48	28	49	18
62	21	66	1	73	17	75	23	80	26	84	15	84	8
84	70	85	26	85	18	86	7	87	16	89	19	89	4
92	8	94	35	96	21	96	7	101	10	103	45	105	80
109	20	110	35	112	19	114	9	115	20	122	36	126	20
129	44	132	40	137	43	139	15	141	51	141	21	155	21
159	5	175	1	179	42	182	34	182	35	206	8	222	2
302	23	309	16	311	26	311	13	311	5	315	40	317	20
321	9	276	5	278	18	282	13	292	22	293	10	293	5
295	37	300	40	262	58	263	12	264	19	264	8	264	21
267	6	271	20	211	11	242	60	243	33	246	28	249	21
251	5	253	9	253	2	256	18	224	33	231	38	231	8
232	30	233	18	233	6	236	18	238	10	326	23	322	0
343	30	344	58										

A = AZIMUTH OF DIP

U = DIP

The analysis of these observations by the program PATCH defined only one cluster (cluster 1), which encompasses a major portion of the data. However, the χ^2 value for this cluster (table 1) indicates that the distribution does not follow the hemispherical normal distribution. The asymmetric form of this distribution is illustrated in figure 8, which shows the level plots of concentrations around the cluster mean. The output from PATCH will still show values of the measure of dispersion, k, and the radius of the cone of confidence, c, but these two values are not accepted because the distribution apparently does not follow Arnold's hemispherical normal distribution.

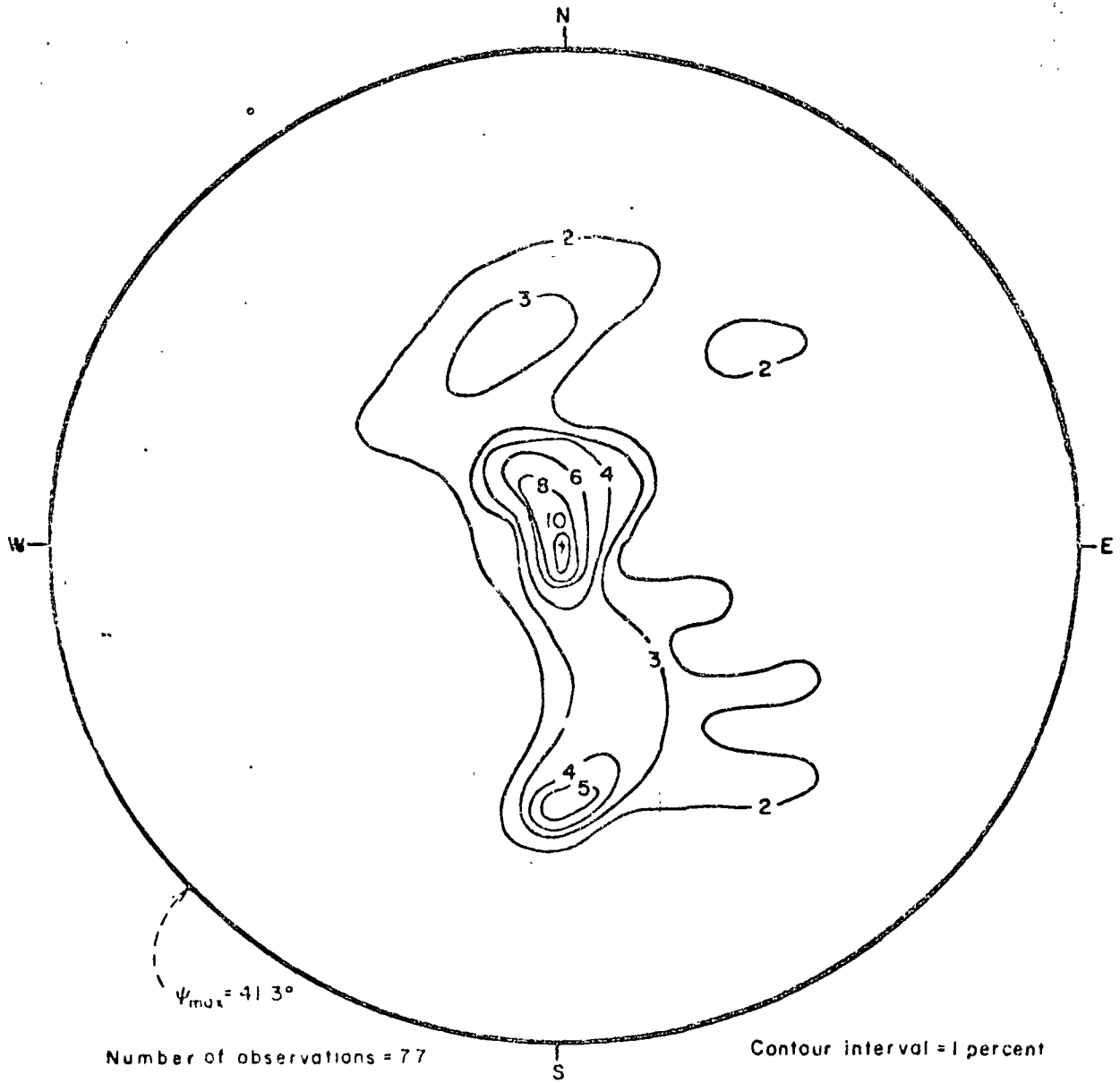


FIGURE 8. - Level Plot of Cluster 1 of A-Axes of Glacial Till Pebbles. Diagram boundary is ψ_{\max}° from the cluster mean (that is, the pole).

Example 2.--Coal Cleat Orientations

Jeran and Mashey (3) collected and analyzed 135 observations of coal cleat attitudes; these observations are listed in table 3. The equal-area projection of these axes is shown in figure 9 which illustrates two joint sets in the data. The analysis by PATCH defines the two joint sets as clusters 1 and 2. The data in cluster 1 follow the hemispherical normal distribution, whereas cluster 2 fails the χ^2 test (table 1). Since the clusters are very compact and their mean dips are nearly vertical, the visual estimates of their mean orientations⁸ by Jeran and Mashey (3) agree closely with the computations by PATCH. Level plots for the two clusters are shown in figures 10 and 11, and the output of PATCH for this example is listed in appendix C.

TABLE 3. - COAL CLEATS.
JERAN AND MASHEY (3).

A	D	A	D	A	D	A	D	A	D	A	D	A	D
12	90	14	88	15	90	15	84	15	82	17	89	19	87
19	89	19	90	20	90	20	90	21	90	22	80	23	87
24	88	24	86	24	84	24	89	24	84	24	83	24	87
24	87	25	88	25	85	26	89	27	86	27	86	29	87
30	87	30	87	30	87	31	87	32	85	32	90	32	84
33	87	33	88	40	85	103	84	103	90	105	85	106	83
108	89	109	90	110	90	111	81	111	81	111	86	112	89
112	93	114	88	115	84	115	88	117	90	117	85	118	80
118	81	119	84	119	83	119	83	119	90	120	84	120	84
120	80	121	87	121	83	121	83	122	84	124	87	124	84
125	85	125	90	128	87	129	87	129	83	130	88	132	88
132	82	132	89	143	82	150	90	190	88	193	90	196	84
197	84	197	88	198	84	200	88	200	83	201	90	203	80
203	85	203	85	204	88	205	86	206	88	206	90	206	86
208	83	207	86	207	90	208	87	208	86	209	85	210	90
211	87	211	85	212	80	212	87	215	86	216	88	219	90
221	89	248	90	283	90	286	90	290	90	292	85	292	87
297	89	298	86	305	86	306	86	307	84	309	90	315	90
315	80	316	90	324	87	329	85	350	90	30	79	33	75
104	75	328	76										

A - AZIMUTH OF DIP
U = DIP

⁸Cluster 1: azimuth of dip = 25°, dip = 90°; cluster 2: azimuth of dip = 299°, dip = 88°.

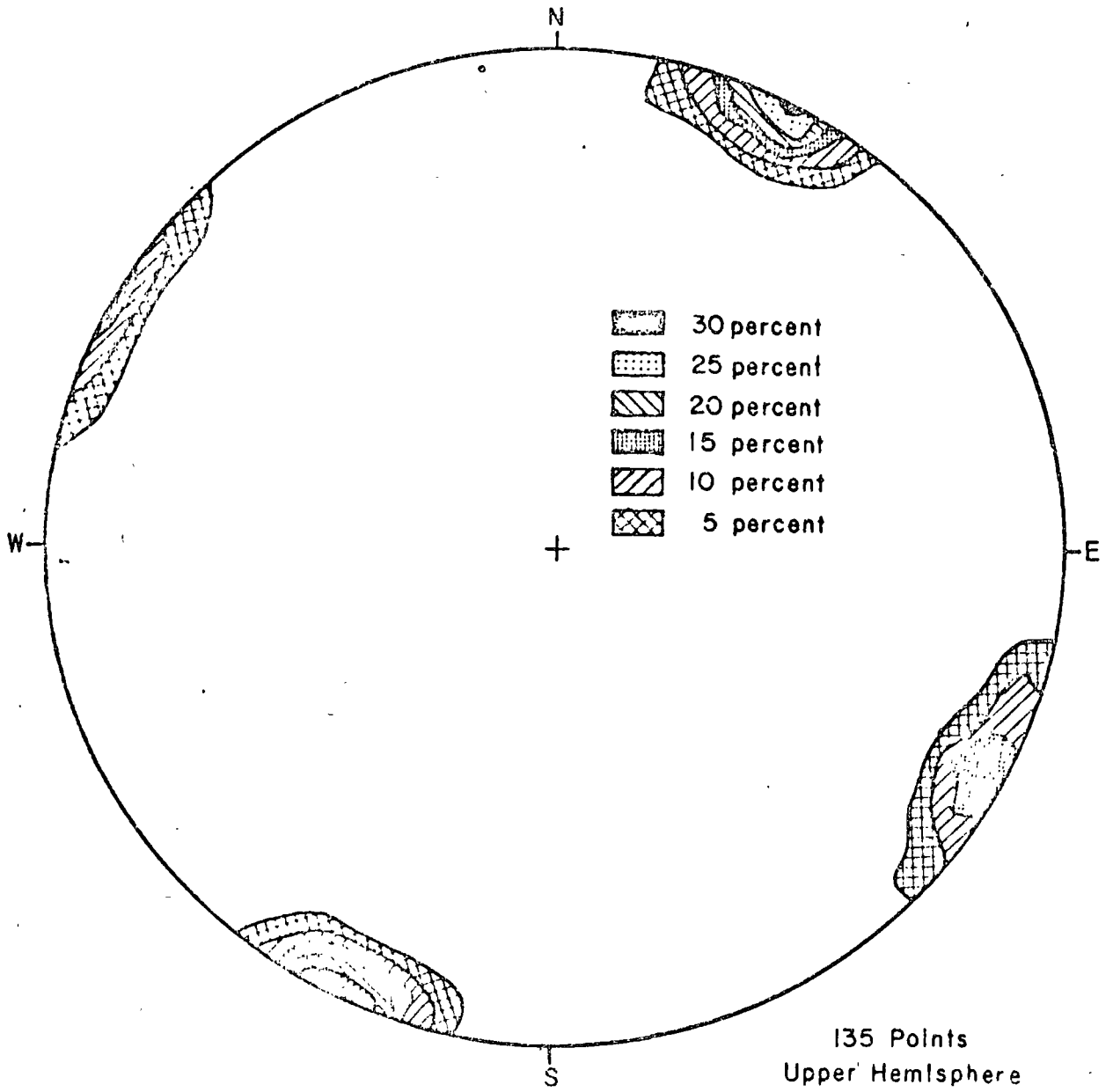


FIGURE 9. - Polar Equal Area Projection of Coal Cleats (3).

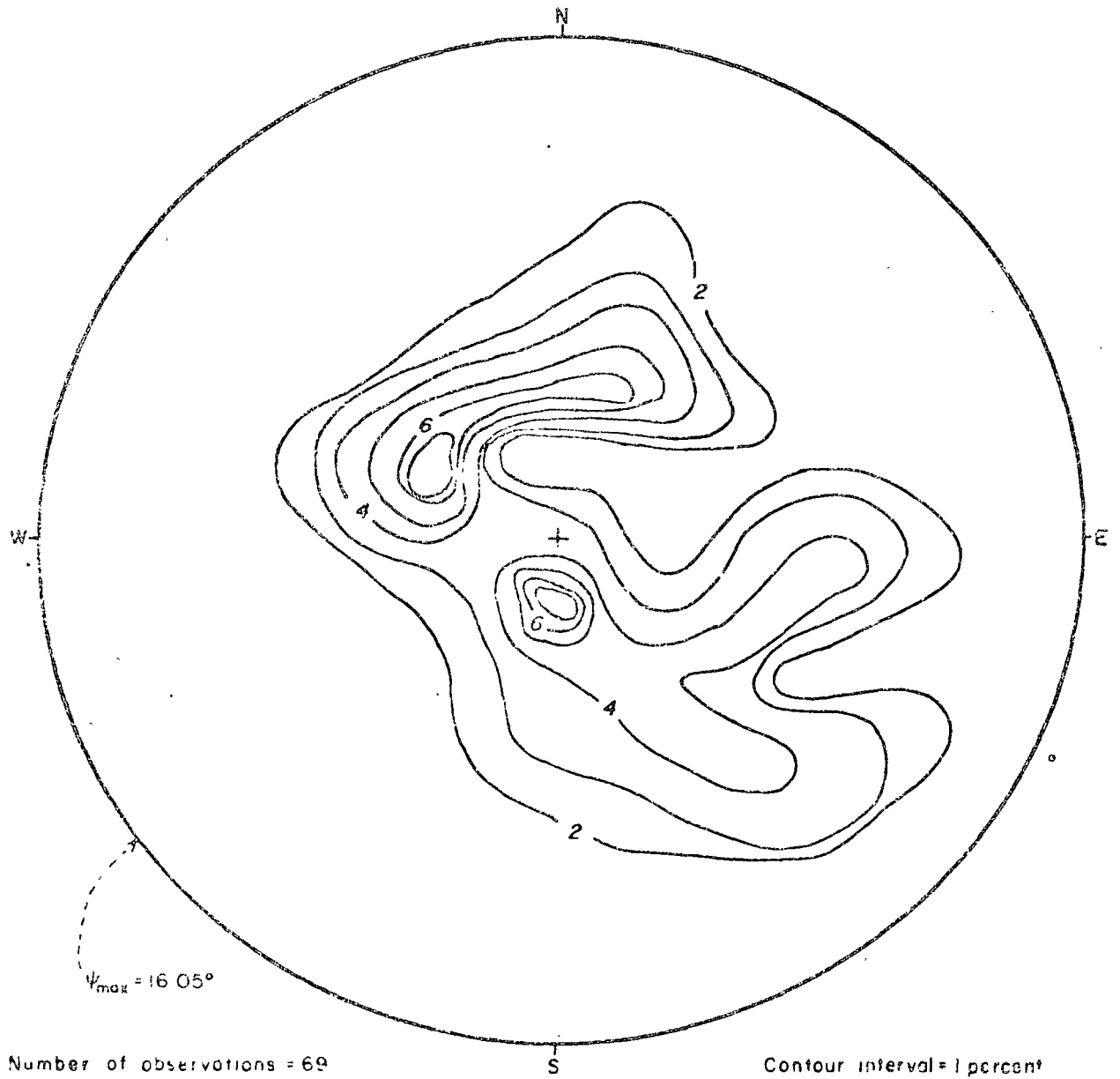


FIGURE 10. - Level Plot of Cluster 1 of Coal Cleat Data. Diagram boundary is Ψ_{\max}° from the cluster mean (that is, the pole).

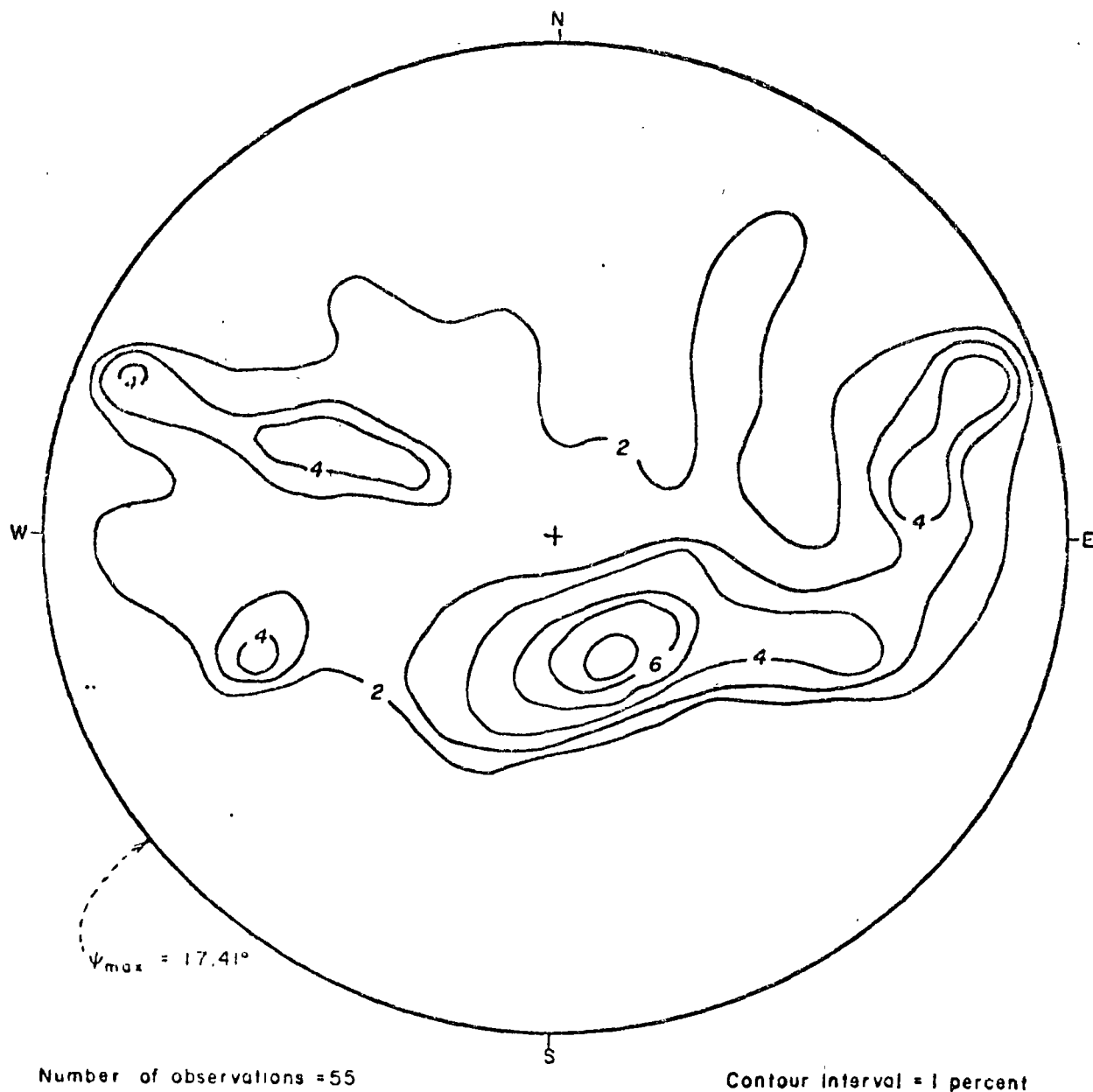


FIGURE 11. - Level Plot of Cluster 2 of Coal Cleat Data. Diagram boundary is ψ_{\max}° from the cluster mean (that is, the pole).

Example 3.--Porphyry Copper Fracture Attitudes

The third example analyzed involves 286 fracture orientations (table 4) which were collected from the walls of two mutually perpendicular drifts on the 2015 level in the San Manuel copper mine, Arizona. The polar equal-area projection of these orientations (fig. 12) fails to produce a distinct picture of the spread of the data points. However, when the cluster analysis technique is applied, a strong basis is provided (table 1) for defining a major orthogonal joint system in the site. Cluster 1 is found to conform to the hemispherical normal distribution, whereas clusters 2 and 3 fail the χ^2 test. The level plots for the three clusters are depicted in figures 13-15.

TABLE 6. - PORPHYRY COPPER FRACTURES
 SAN MANUEL MINE, ARIZ.

A	D	A	D	A	D	A	D	A	D	A	D	A	D
186	83	255	50	255	65	345	87	255	87	325	86	342	85
270	57	242	83	62	83	127	23	355	80	232	82	240	85
75	20	7	90	60	37	62	26	202	75	15	90	83	42
250	87	360	77	244	81	275	35	245	79	314	88	252	87
357	76	9	56	352	80	265	73	30	80	240	77	136	87
218	65	274	87	225	67	355	90	230	55	248	70	343	85
235	53	50	90	249	30	45	87	356	85	244	58	244	65
248	82	55	87	356	87	230	86	266	86	252	86	255	82
260	55	12	84	220	62	232	60	327	80	210	80	255	77
218	78	216	33	8	70	84	80	175	87	345	87	232	82
234	82	247	32	28	58	53	87	350	83	105	32	360	88
37	45	57	24	167	86	6	70	24	87	345	88	240	87
360	70	338	44	217	67	260	20	162	88	77	18	327	80
132	6	220	86	343	60	30	34	150	87	230	85	41	87
350	85	250	77	228	80	13	90	210	47	255	68	247	78
181	73	220	65	177	46	147	85	342	89	251	78	355	75
153	16	355	84	214	18	57	87	163	85	45	83	85	80
180	0	110	82	24	90	7	15	140	87	50	90	342	80
218	63	190	7	10	66	237	87	345	85	70	20	16	34
13	82	247	75	314	80	66	80	354	75	33	20	81	32
8	67	143	57	260	45	67	87	15	87	126	31	250	87
346	86	243	74	81	13	251	86	182	86	25	21	245	78
330	80	20	85	326	20	44	90	326	90	264	80	133	35
302	78	141	40	111	18	186	83	86	86	90	65	36	88
155	81	275	82	158	22	165	46	347	78	149	60	291	80
13	85	192	43	332	82	321	80	346	70	176	43	287	90
154	60	250	40	257	86	354	75	129	25	116	86	115	25
121	20	135	40	257	80	167	30	217	65	341	70	360	70
85	12	315	70	295	90	336	82	270	74	119	32	205	36
344	76	11	90	118	37	270	88	126	20	14	87	106	44
104	85	143	65	77	58	101	80	141	86	167	57	93	86
328	88	341	40	177	36	314	70	226	90	133	20	351	75
157	24	354	87	270	90	230	50	147	70	145	25	353	70
276	73	44	75	327	83	297	88	47	28	308	27	233	60
337	70	292	57	344	70	266	65	344	70	291	45	268	65
10	88	328	90	337	70	270	66	355	60	254	25	350	85
281	60	247	22	147	85	270	85	150	83	247	63	328	60
285	42	347	62	353	95	285	75	334	86	277	66	192	77
313	87	276	64	346	74	73	83	297	65	356	74	328	78
313	58	304	74	13	63	263	63	247	65	74	90	270	75
304	52	334	72	83	52	360	65	306	53	350	90		

A = AZIMUTH OF DIP
 D = DIP

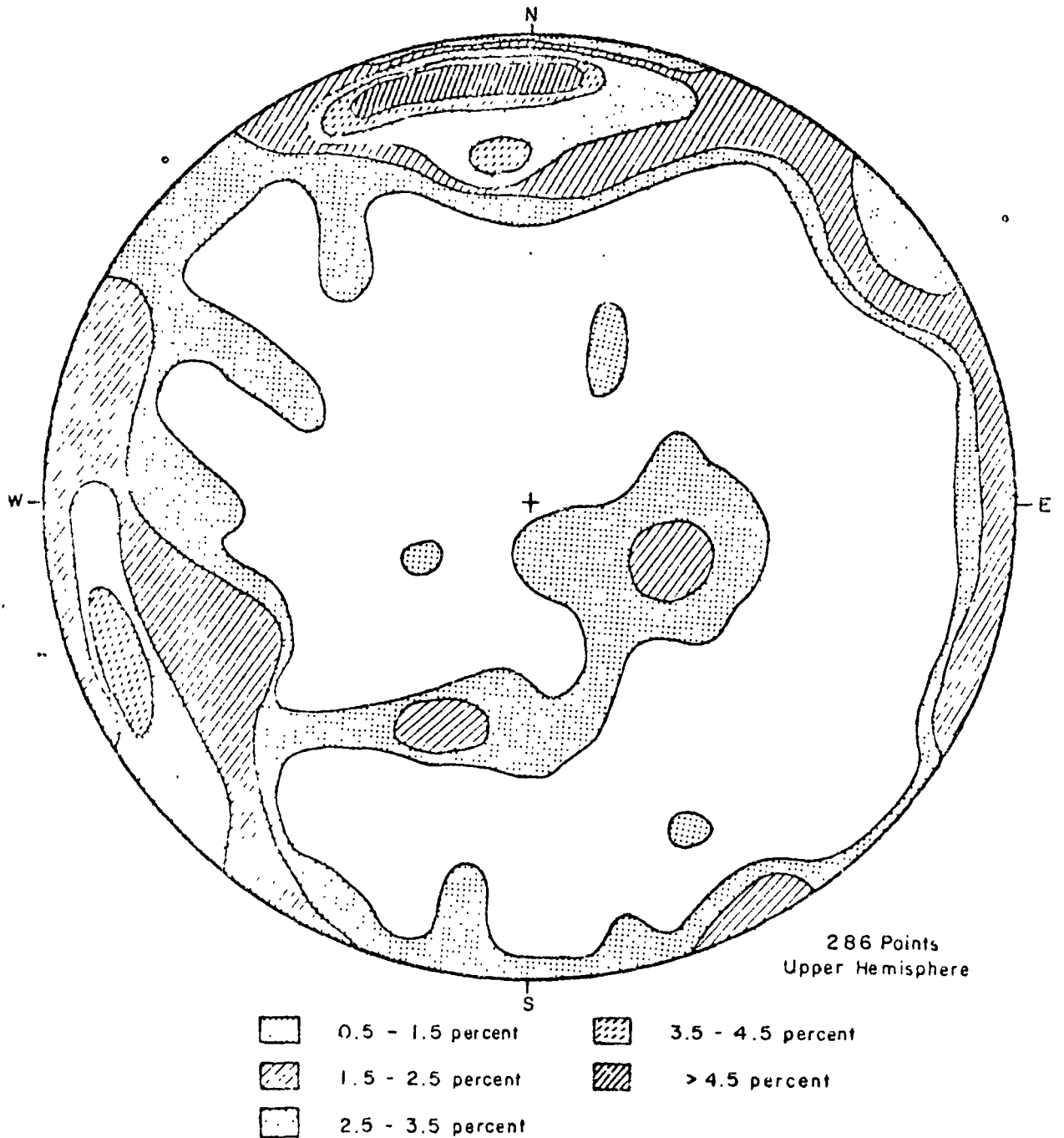


FIGURE 12. - Polar Equal Area Projection of Porphyry Copper Fractures in Panel 22, Level 2015, San Manuel Mine, Arizona.

SUMMARY

In this approach of analyzing orientation data, the surface of the upper hemisphere is divided into 100 equal-area patches, and the points (intersections of joint normals with the hemisphere) falling within each patch are

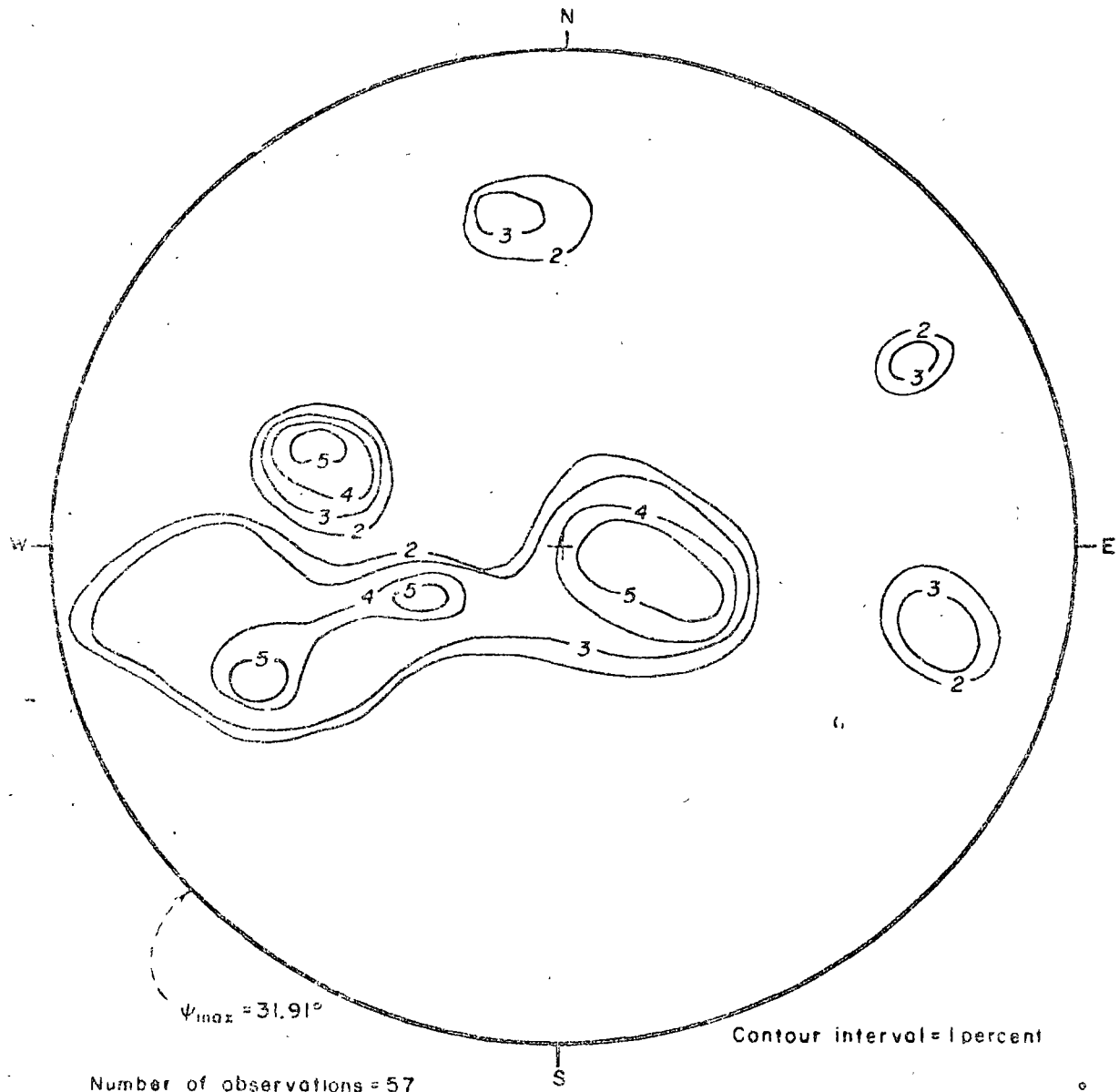
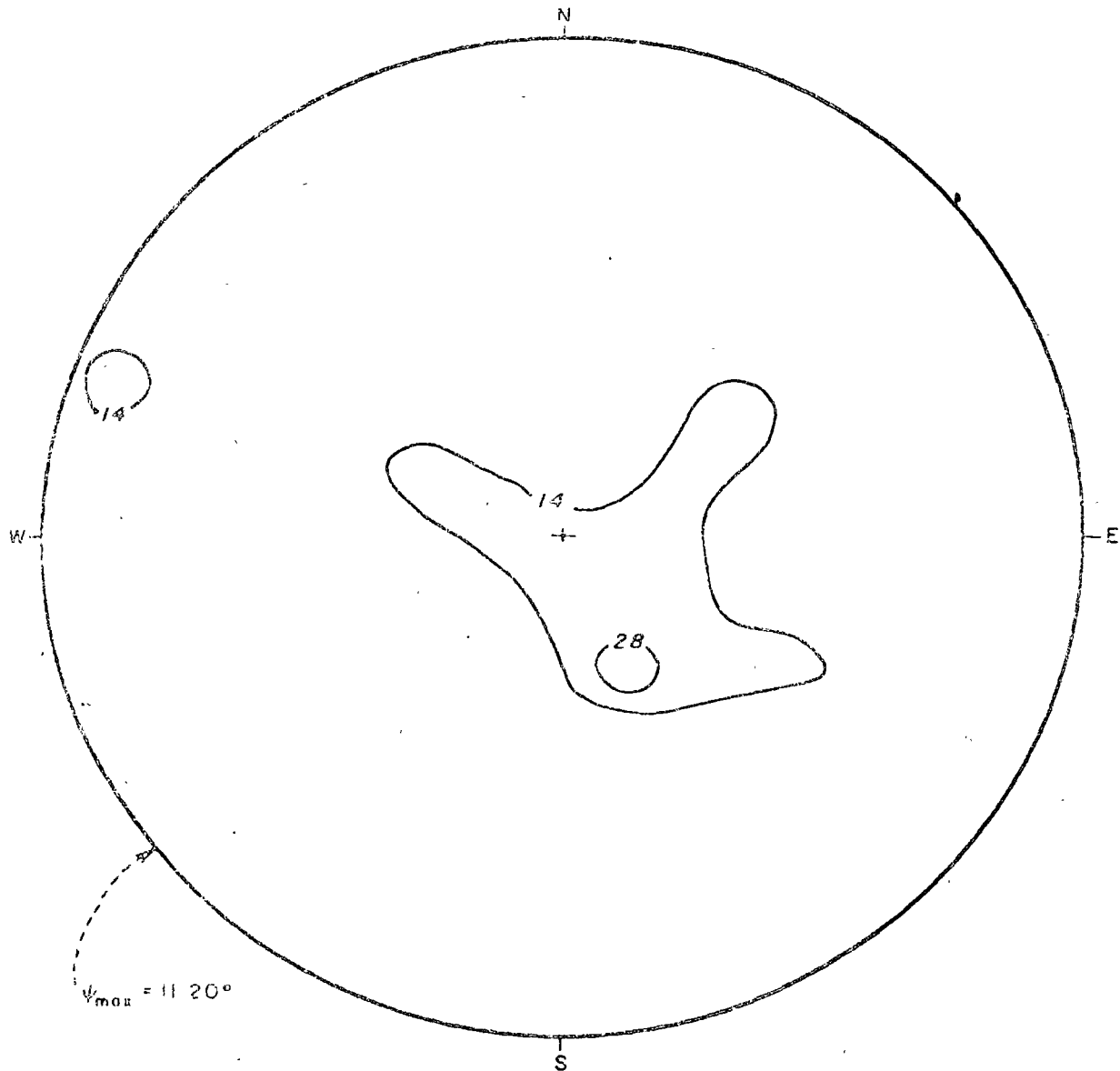


FIGURE 13. - Level Plot of Cluster 1 of Porphyry Copper Fractures, San Manuel Mine, Arizona. Diagram boundary is ψ_{\max}° from the cluster mean (that is, the pole).

counted. The distribution of the data points is then obtained in terms of significant concentrations, or clusters, whose mean attitudes are computed. A computer program is coded to treat multiple clusters in the sample and to combine antipodal clusters (with near 90° mean dip) into single clusters.

In using the Poisson distribution for obtaining significant concentrations of data points, a probability level of $P = 0.05$ was used. The use of a slightly different probability level may, however, result in defining slightly different clusters because of the "discrete" nature of the Poisson distribution.



Number of observations = 7

Contour interval = 14 percent

FIGURE 15. - Level Plot of Cluster 3 of Porphyry Copper Fractures, San Manuel Mine, Arizona.
Diagram boundary is ψ_{max}° from the cluster mean (that is, the pole).

For data in a cluster following the hemispherical normal distribution, a confidence interval (around the sample mean) is assigned such that for a given level of confidence, the population mean will not fall outside this interval. It should be possible for the engineer to project these confidence intervals into confidence intervals around the results of the structural analyses.

The method of analysis can be applied for determining the mean orientations of planar geologic discontinuities, lineations, and crystal and fold axes. The potential of the technique is illustrated by applying it to three sets of field data.

The computer program PATCH performs an efficient analysis of orientation data. The saving in computation time (as compared with some existing programs) is a function of the total number of observations and increases rapidly with the increase in this number. The output from PATCH includes a polar plot of point concentrations for a cluster while considering the cluster mean to be situated at the pole. These plots illustrate more closely the spatial distribution of points in a cluster than do the usual projections of the entire sample.

REFERENCES⁹

1. Arnold, K. J., On Spherical Probability Distributions. Ph.D. Thesis, M.I.T., 1941, 42 pp.
2. Fisher, R. A. Dispersion on a Sphere. Proc. Roy. Soc., London, sec. A, v. 217, May 1953, pp. 295-305.
3. Jeran, P. W., and J. R. Mashey. A Computer Program for the Stereographic Analysis of Coal Fractures and Cleats. BuMines Inf. Circ. 8454, 1970, 34 pp.
4. Krumbein, W. C. Preferred Orientations of Pebbles in Sedimentary Deposits. J. Geol., v. 47, 1939, pp. 673-706.
5. Krumbein, W. C., and F. A. Graybill. An Introduction to Statistical Models in Geology. McGraw-Hill Book Co., Inc., New York, 1965, 475 pp.
6. Li, J. C. R. Statistical Inference. Edwards Bros., Ann Arbor, Mich., v. 1, 1964, 658 pp.
7. Muller, Leopold. Untersuchungen Uber Statistische Kluf tmessung (Investigations of the Statistical Measurement of Fractures). Geologie und Banwesen, v. 5, No. 4, December 1933, p. 232.
8. Pincus, H. J. The Analysis of Aggregates of Orientation Data in the Earth Sciences. J. Geol., v. 61, 1953, pp. 482-509.
9. Stauffer, M. R. An Empirical Statistical Study of Three-Dimensional Fabric Diagrams as Used in Structural Analysis. Can. J. Earth Sci., v. 3, No. 4, 1966, pp. 473-498.
10. Watson, G. S., and E. Irving. Statistical Methods in Rock Magnetism. Monthly Notices of the Royal Astro. Soc., Geophys. Supp., v. 7, No. 6, November 1957, pp. 289-300.

⁹Titles enclosed in parentheses are translations from the language in which the item was originally published.

BIBLIOGRAPHY

1. Bingham, C. Distributions on a Sphere and on the Projective Plane. Ph.D. Thesis, Yale Univ., 1964, 93 pp.
2. Bucher, W. H. The Stereographic Projection, A Handy Tool for the Practical Geologist. *J. Geol.*, v. 52, 1944, pp. 191-212.
3. Cadigan, R. A. A Method for Determining the Randomness of Regionally Distributed Quantitative Geologic Data. *J. Sed. Pet.*, v. 32, No. 4, 1962, pp. 813-818.
4. Chayes, F. Application of the Coefficient of Correlation to Fabric Diagrams. *Am. Geophys. Union Trans.*, v. 27, 1946, p. 400.
5. _____. Discussion: Effect of Change of Origin on Mean and Variance of Two-Dimensional Fabrics. *Am. J. Sci.*, v. 252, 1954, pp. 567-570.
6. _____. Statistical Analysis of Three-Dimensional Fabric Diagrams, in *Structural Petrology of Deformed Rocks*. Ed. by M. W. Fairbairn. Addison-Wesley Press, Cambridge, Mass., 1949, 344 pp.
7. Cochran, W. G. *Sampling Techniques*. John Wiley & Sons, Inc., New York, 1963, 413 pp.
8. Cox, A., and R. R. Doell. Review of Paleomagnetism. *Bull. Geol. Soc. America*, v. 71, 1960, pp. 645-768.
9. Curray, J. R. The Analysis of Two-Dimensional Orientation Data. *J. Geol.*, v. 64, 1956, pp. 117-131.
10. Denness, B. A Method of Contouring Polar Diagrams Using Curvilinear Counting Cells. *Geol. Mag.*, v. 107, No. 1, January 1970, pp. 61-65.
11. Dennison, J. M. *Analysis of Geologic Structures*. W. W. Norton & Co., Inc., New York, 1968, 209 pp.
12. _____. Graphical Aids for Determining Reliability of Sample Means and An Adequate Sample Size. *J. Sed. Pet.*, v. 32, No. 4, 1962, pp. 743-750.
13. Dodd, J. Robert, J. A. Cain, and J. E. Bugh. Apparently Significant Contour Patterns Demonstrated With Random Data. *J. Geol. Educ.*, v. 13, No. 4, 1965, pp. 109-112.
14. Donn, W. L., and J. A. Shiner. *Graphic Methods in Structural Geology*. Appleton-Century-Crofts, Inc., New York, 1958, 180 pp.
15. Durand, D., and J. A. Greenwood. Modifications of the Rayleigh Test for Uniformity in Analysis of Two-Dimensional Orientation Data. *J. Geol.*, v. 66, No. 3, 1958, pp. 229-238.

16. Fisher, R. A. The Mathematical Distributions Used in the Common Tests of Significance. *Econometrica*, v. 3, 1935, pp. 353-365.
17. _____. The Significance of Deviations From Expectation in a Poisson Series. *Biometrics*, v. 6, No. 1, 1950, pp. 17-24.
18. _____. *Statistical Methods for Research Workers*. Hafner Pub. Co., New York, 12th ed., 1954, 351 pp.
19. Flinn, D. On Tests of Significance of Preferred Orientation in Three-Dimensional Fabric Diagrams. *J. Geol.*, v. 66, 1958, pp. 526-539.
20. Fox, W. T. Fortran IV Program for Vector Trend Analysis of Directional Data. *Kansas Geol. Sur. Computer Contribution No. 11*, 1967, 36 pp.
21. Griffiths, J. C., and M. A. Rosenfield. A Further Test of Dimensional Orientation of Quartz Grains in Bradford Sand. *Am. J. Sci.*, v. 251, 1953, pp. 192-214.
22. Cumbel, E. J., J. A. Greenwood, and D. Durand. The Circular Normal Distribution Theory and Tables. *J. Am. Stat. Assoc.*, v. 48, 1953, p. 131.
23. Hopwood, T. Derivation of a Coefficient of Degree of Preferred Orientation From Contoured Fabric Diagrams. *Bull. Geol. Soc. Am.*, v. 79, November 1968, pp. 1651-1654.
24. Irving, E. *Paleomagnetism*. J. Wiley & Sons, Inc., New York, 1964, 399 pp.
25. Jones, M. L., and G. E. Eddy. A Computer Program for Statistical Analysis of Two-Dimensional Orientation Data--Some Geologic Applications. *Geol. Soc. Am. Abs. with Programs*, pt. 4, Southeastern sec., 1969, p. 39.
26. Jones, Thomas A. Statistical Analysis of Orientation Data. *J. Sed. Pet.*, v. 38, No. 1, 1968, pp. 61-67.
27. Kelley, J. C. Least Squares Analysis of Tectonite Fabric Data. *Bull. Geol. Soc. America*, v. 79, 1968, pp. 223-240.
28. Firschmayer, M., and J. G. Dennis. Information From Joint Diagrams. *Felsmechanik und Ingenieurgeologie*, v. 4, No. 1, 1966, pp. 36-40.
29. Knopf, E. B. Petrofabrics in Structural Geology. Paper in Behavior of Materials in the Earth's Crust (2d Ann. Symp. Rock Mech). *Colo. Sch. Mines Quart.*, v. 52, 1957, pp. 99-111.
30. Koch, G. S., Jr., and R. F. Link. *Statistical Analysis of Geological Data*. John Wiley & Sons, Inc., New York, 2 v., 1970, 375 pp.

31. Krumbein, W. C. The Geological Population as a Framework for Analyzing Numerical Data in Geology. *Liverpool and Manchester Geol. J.*, v. 2, 1960, p. 341.
32. _____. Some Problems in Applying Statistics to Geology. *Applied Statistics*, v. 9, No. 2, 1960, pp. 82-91.
33. Krumbein, W. C., and R. L. Miller. Design of Experiments for Statistical Analysis of Geological Data. *J. Geol.*, v. 66, 1953, pp. 510-522.
34. Loudon, T. Computer Analysis of Orientation Data in Structural Geology. Tech. Rept. 13, ONR Task 389-135, Contract Nonr 1228(26), Office of Naval Research, Geography Branch, Northwestern University, Evanston, Ill., 1964, 76 pp.
35. Manning, J. C. Application of Statistical Estimation and Hypothesis Testing to Geologic Data. *J. Geol.*, v. 62, 1953, pp. 544-556.
36. Mellis, Otto. Gefugediagramme in Stereographischer Projektion (Structure Diagram in Stereographic Projection). *Zeitschr. Min. Pet. Mitt.*, v. 53, 1942, pp. 330-353.
37. Miller, R. L., and J. S. Kahn. *Statistical Analysis in the Geological Sciences*. John Wiley & Sons, Inc., New York, 1962, 483 pp.
38. Molina, E. C. *The Poisson Exponential Binomial Limit*. D. Van Nostrand Co., New York, 1947, 92 pp.
39. Ondrick, C. W., and J. C. Griffiths. Fortran IV Computer Program for Fitting Observed Count Data to Discrete Distribution Models of Binomial, Poisson, and Negative Binomial. *Kansas Geol. Survey Computer Contribution 44*, 1969, 20 pp.
40. Parks, James M. Cluster Analysis Applied to Multivariate Geologic Problems. *J. Geol.*, v. 74, No. 5, pt. 2, 1966, pp. 703-715.
41. _____. Cluster Analysis, Multivariate Facies Maps. *Bull. Am. Assoc. Petrol. Geol.*, v. 53, No. 3, 1969, p. 735.
42. _____. Computerized Trigonometric Method for Rotation of Structurally Tilted Sedimentary Directional Features. *Bull. Geol. Soc. America*, v. 81, 1970, pp. 537-540.
43. Phillips, F. C. *The Use of Stereographic Projection in Structural Geology*. Edward Arnold Ltd., London, 1954, 86 pp.
44. Pincus, H. J. Some Methods for Operating on Orientation Data. *Bull. Geol. Soc. America*, v. 63, 1952, pp. 431-434.
45. _____. Some Vector and Arithmetic Operations on Two-Dimensional Orientation Variates, With Applications to Geologic Data. *J. Geol.*, v. 64, No. 6, November 1956, pp. 533-557.

46. Pincus, H. J. Statistical Methods Applied to the Study of Rock Fractures. Bull. Geol. Soc. America, v. 62, 1951, pp. 81-130.
47. Ramsay, J. G. Folding and Fracturing of Rocks. McGraw-Hill Book Co., Inc., New York, 1967, 568 pp.
48. Rodgers, J. Use of Equal-Area or Other Projections in the Statistical Treatment of Joints. Bull. Geol. Soc. America, v. 63, 1952, pp. 427-430.
49. Selby, B. Girdle Distributions on a Sphere. Biometrika, v. 51, 1964, pp. 381-392.
50. Smart, W. M. Combination of Observations. Cambridge Univ. Press, 1958, pp. 166-188.
51. Sison, F. S. Geological Data Processing. Harper & Row, New York, 1966, 284 pp.
52. Spencer, A. B., and P. S. Clabaugh. Computer Program for Fabric Diagrams. Am. J. Sci., v. 265, 1967, pp. 166-172.
53. Spreen, W. C., and N. E. Manos. Probabilities From Limited Weather Data. Am. Geophys. Union Trans., v. 33, No. 1, 1952, pp. 21-26.
54. Steinmetz, R. Analysis of Vectorial Data. J. Sed. Pet., v. 34, No. 4, 1962, pp. 801-812.
55. Stephens, M. A. Exact and Approximate Tests for Directions. Biometrika, v. 49, 1962, pp. 463-477.
56. _____. The Statistics of Directions, The Von Mises and Fisher Distributions. Ph.D. Thesis, Univ. of Toronto, 1962, 217 pp.
57. _____. The Testing of Unit Vectors for Randomness. J. Am. Stat. Assoc., v. 59, 1964, pp. 160-167.
58. Sturges, H. A. The Choice of a Class Interval. J. Am. Stat. Assoc., v. 21, 1926, pp. 65-66.
59. Terzaghi, R. D. Sources of Error in Joint Surveys. Geotechnique, v. 15, 1965, pp. 287-304.
60. Vincenz, S. A., and J. McG. Bruckshaw. Note on the Probability Distribution of a Small Number of Vectors. Proc. Cambridge Phil. Soc. (Math. and Phys. Sci.), v. 56, pt. 1, 1960, pp. 21-26.
61. Wallace, R. E. A Stereographic Calculator. J. Geol., v. 56, 1948, pp. 488-490.

62. Watson, G. S. Analysis of Dispersion on a Sphere. Royal Astron. Soc. Monthly Notices, Geophys. Supp., v. 7, 1956, pp. 153-159.
63. _____. Equatorial Distributions on a Sphere. Biometrika, v. 52, 1965, pp. 193-201.
64. _____. More Significance Tests on the Sphere. Biometrika, v. 47, 1960, pp. 87-91.
65. _____. The Statistics of Orientation Data. J. Geol., v. 74, No. 5, 1966, pp. 786-797.
66. _____. A Test for Randomness of Directions. Royal Astron. Soc. Monthly Notices, Geophys. Supp., v. 7, 1956, pp. 160-163.
67. Watson, G. S., and E. J. Williams. On the Construction of the Significance Tests on the Circle and the Sphere. Biometrika, v. 43, 1956, pp. 344-352.
68. Wheeler, S., and G. S. Watson. A Distribution-Free Two Sample Test on a Circle. Biometrika, v. 57, 1964, pp. 256-257.
69. Whitten, E. H. T. Sequential Multivariate Regression Methods and Scalars in the Study of Fold-Geometry Variability. J. Geol., v. 74, No. 5, pt. 2, 1966, pp. 744-763.
70. Wilks, S. S. Statistical Inference in Geology. Ch. in the Earth Sciences, Problems and Progress in Current Research, ed. by J. W. Donnelly. Univ. of Chicago Press, Chicago, Ill., 1963, pp. 105-136.
71. Winchell, H. A New Method of Interpretation of Petrofabric Diagrams. Am. Mineralogist, v. 22, 1937, pp. 15-36.

APPENDIX A.--COMPUTER FORMULATION AND INPUT INSTRUCTIONS

The program PATCH is written in Fortran IV. The flow charts for the main program and subroutines are given in figures A-1, A-2, and A-3 at the end of this appendix.

PATCH provides a more sophisticated analysis of directional data with a substantial saving of time (as compared with some existing programs) for problems involving large sample size. The tabulation below compares computer time used by PATCH and SNAP (3)¹ for problems involving 135 and 951 observations. These problems were run on a CDC 6400² computer for the purpose of this comparison.

<u>Program</u>	<u>Number of data points</u>	<u>Time, sec</u>
SNAP.....	135	28
PATCH.....	135	29
SNAP.....	951	142
PATCH.....	951	54

Main Program

Sorts data into patches and computes density of each patch. Calls SPRPAC and POLARC subroutines (3) to plot data and patch densities. Defines clusters and calls KLUSTR to perform statistical analysis.

CLUP

Determines if a cluster containing patches in band J, $1 \leq J \leq 8$, contains patches in band J + 1.

PCTPLT

Plots LEVEL (J) or FLEVEL (J) at the projected midpoint of patch J.

SORTA

Sorts data into patches.

KLUSTR

Computes the resultant, R, and the precision, K, of each cluster and calls SECTOR if $K > 6$.

COMBIN

Combines antipodal clusters.

¹Underlined numbers in parentheses refer to items in the list of references.

²Reference to specific equipment is made to facilitate understanding and does not imply endorsement by the Bureau of Mines.

SPRPAC

Calculates page coordinates (IX, IY) of each observation.

POLARC

Prints "*" at the center and at every 10° interval around the boundary of the output graph. Places N, E, S, W at 0°, 90°, 180°, 270°, respectively, and prints assembled page.

SORT

Arranges points in increasing order of dip or azimuth.

Input Instructions

The program requires the following data cards:

1. Header Card
2. NOBS Card
3. Observation Cards
4. ABCDEF Card

Header Card

Contains a suitable heading for the output punched in 12A6 format.

NOBS Card

The total number of observations is punched in I5 format.

Observation Cards

The observed attitudes are punched (eight observations per card) in 16F5.0 format, the azimuth of dip preceding the dip (both quantities being in degrees).

ABCDEF Card

Indicates end of data. Any number of cases can be run, but this card must be the last card of the last case.

Glossary of Frequently Used Variables

DIP.....	Dip of observation.
AZ.....	Azimuth of observation.
NOBS.....	Number of observations.
SL, SM, SN.....	Direction cosines of observation.
LPAGE.....	Page array, stores output from POLARC and SPRPAG.
LEVEL.....	Density of patches.
DANG.....	Dip angles of band boundaries.
IBND.....	Number of patches in each band.
LPATCH.....	Number of observations in each patch.
CLUSTER(KJ,IJ).....	Patches (KJ) in cluster IJ.
IPCH(J).....	Cluster in which patch J lies (if any).
CU1, CU2.....	Azimuth and dip of observation lying in a cluster.
PCT.....	Poisson random cutoff level.
SFREQ.....	Actual sector frequency.
TFREQ.....	Theoretical sector frequency.
KBAND(J).....	Band in which patch J lies.

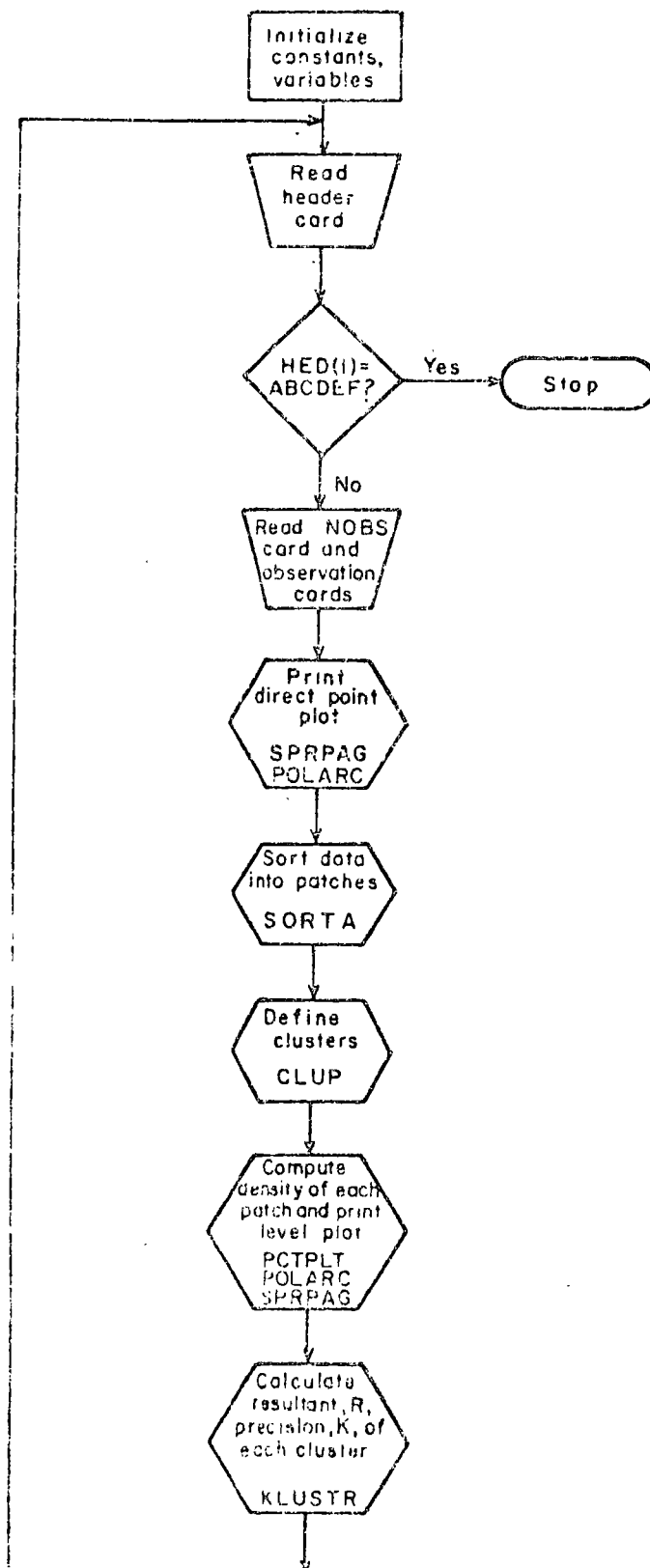


FIGURE A-1. - PATCH Main Program Flow Chart.

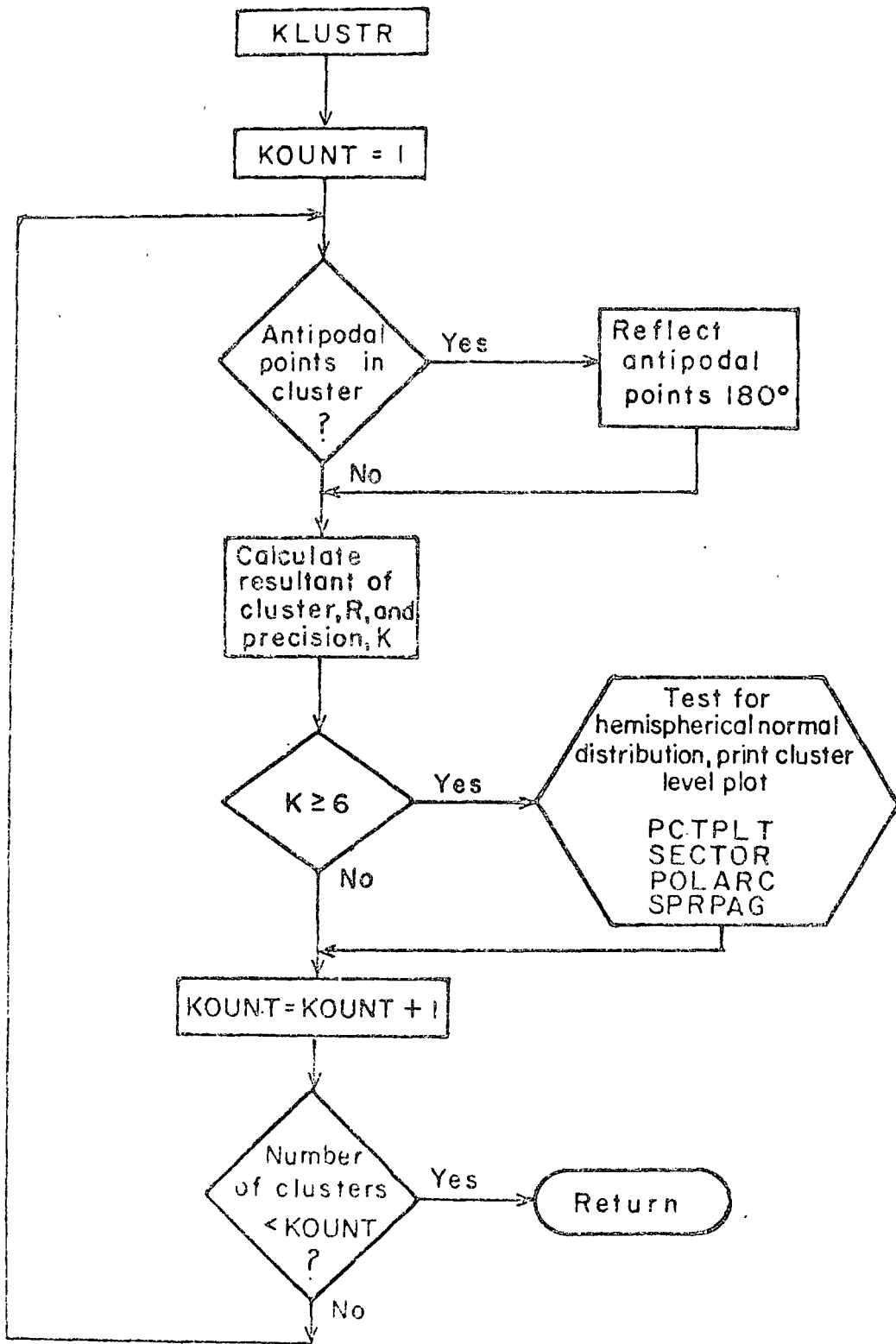


FIGURE A-2. - KLUSTER Flow Chart.

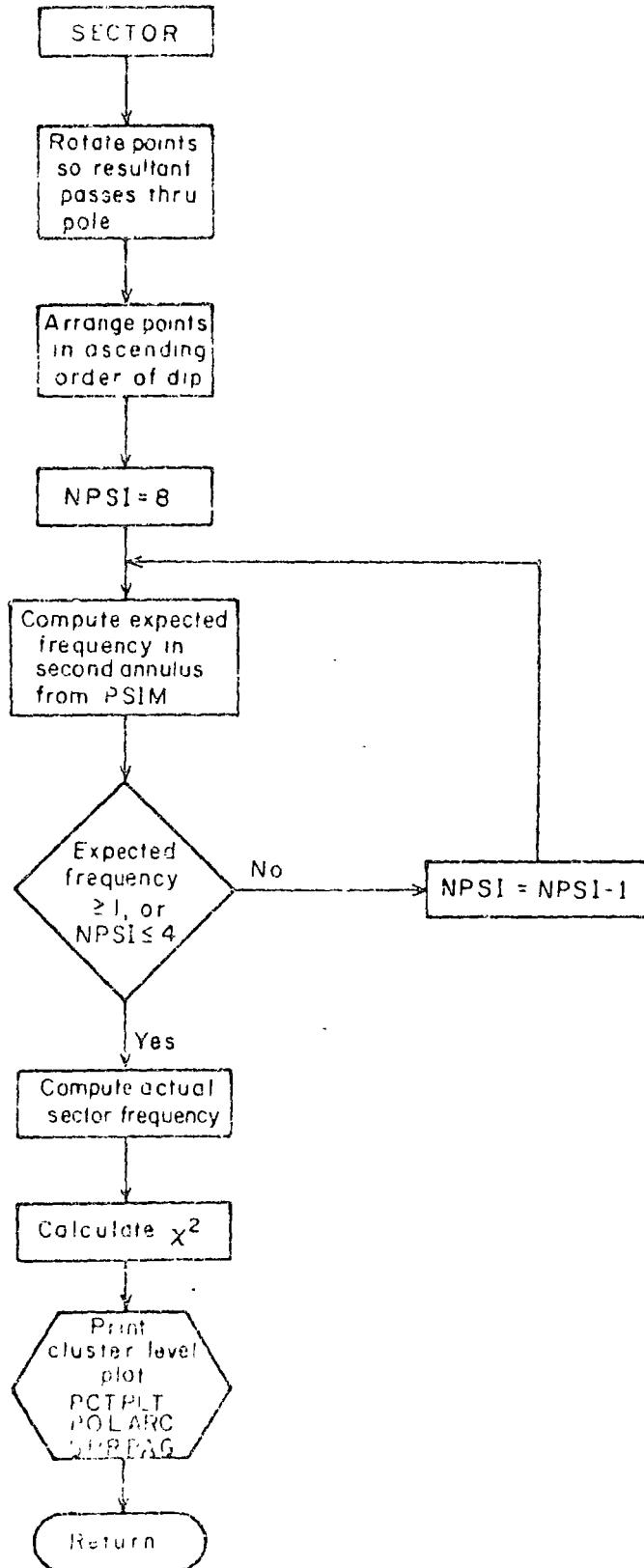


FIGURE A-3. - SECTOR Flow Chart.

APPENDIX B.--PROGRAM LISTING

```

PROGRAM PATCH(INPUT,OUTPUT,TAPES=INPUT,TAPE=OUTPUT)
C***** PATCH ANALYZES FRACTURE ORIENTATION DATA BY DEFINING CLUSTERS ON
C THE HEMISPHERE

COMMON /RLK/AZ(1000),DIP(1000),CU(900),CU2(900),SL(1000),
1 SM(1000),SN(1000),KBAND(100),NB,IBND(9),DANG(10),LPATCH(100),
2 LEVEL(100),IPTM(100),CLUSTR(50,10),LPAGE(121,73),NX,NY,NYMID,
3 NXMID,PI,DEGRAU,RADEG,Q90,XPINCH,YPINCH,RADIUS,PCT,LCOM,KJ,IJ,
4 IJPR,P,T,KOU,H,ACONV,YCONV,XK,POS(100)
DIMENSION HED(12)
INTEGER CLUSTR
REAL KANG,RIANG,LEVEL
C***** BAND DATA
C
DATA IBND/14,16,15,14,13,10,8,5,1/,KBAND/18,1,16,2,15,3,14,4,13,5,
1 10,6,8,7,5,8,1,9/,LPLUS/1H,/,LBLANK/1H,/,ASTH/1H,/,DANG/93,0,79,6
2 ,70,1,60,7,50,9,40,5,30,7,19,9,8,1,-1,0/,NB/9/,PI/3,141592,5/
DATA POS/1,2,3,4,5,6,7,8,9,10,11,12,13,14,15,16,
1 17,18,1,2,3,4,5,6,7,8,9,10,11,12,13,14,15,16,
2 1,2,3,4,5,6,7,8,9,10,11,12,13,14,15,1,2,3,4,
3 5,6,7,8,9,10,11,12,13,14,1,2,3,4,5,6,7,8,9,
4 10,11,12,13,1,2,3,4,5,6,7,8,9,10,1,2,3,4,5,
5 6,7,8,1,2,3,4,5,1,0/
DEGRAU=PI/180.
RADEG=1.0/DEGRAU
XPINCH=10.
YPINCH=6.0
Q90=90.
RADIUS=4.0
NT=RADIUS*XPINCH*0.5
NX=2*NT*1
NY=2*NT*1
NYMID=NY/2*1
NXMID=NX/2*1
NXMID1=NXMID-1
NYMID1=NYMID-1
ACONV=Q90/NXMID1
YCONV=1.0/NYMID1
XCONV=1.0/YCONV
8000 READ(5,3333) HED
3333 FORMAT(12A6)
IF(HED(1).EQ.6)GAMCDEF) STOP
READ(5,3334) NOBS,(AZ(I),DIP(I),I=1,NOBS)
3334 FORMAT(7F(16F5.0))
DO 6000 JM=50
J50=J*50
IPTM(J)=0
IPTM(J50)=0
GO 6000 K=1,10
CLUSTR(J,K)=0
6000 CONTINUE

```

```

C***** COMPUTE POISSON RANDOM CUTOFF PERCENT

      FN=FLOAT(NOBS)
      A=FN*0.01
      EFAC=EXP(-A)
      SUM=EFAC
      FAC=1.0
      DO 876 N=1,1000
      FIN=N
      FAC=FAC*A/FIN
      FNUM=EFAC*FAC
      SUM=SUM+FNUM
      TEST=1.0-SUM
      IF (TEST<0.05) 875,876,876
876  CONTINUE
875  PCT=FIN/FN

C***** SORT DATA INTO PATCHES
      CALL SORTA(NOBS,4Z,DIP,LPATCH)

C***** COMPUTE LEVEL (DENSITY) IN EACH PATCH

      LEVEL(1)=FLOAT(LPATCH(1))/FN
      DO 876 KUK=2,100
      LEVEL(KUK)=FLOAT(LPATCH(KUK)-LPATCH(KUK-1))/FN
876  CONTINUE
      FPCT=100.*PCT
      WRITE(6,3481) MED,FPCT,NOBS
3681  FORMAT(11H,30X,12A6//1X,25HPOISSON RANDOM CUT-OFF IS, F7.3,1X,
1 7HPERCENT,18X,11HLEVEL ARRAY,1X,9HTHERE ARE,15,1X,21MPUNIS IN TH
2E SAMPLE.)
      DO 3683 J49=1,50
      J50=J49+50
3683  PRINT 3482, J49,LEVEL(J49),J50,LEVEL(J50)
3682  FORMAT(52X,2(I3,F9.5,2X))
      DO 209 KL=1,73
      DO 209 JL=1,121
209  LPAGE(JL,KL)=LBLANK
      DO 200 J=1,NOBS
      CALL SPRD2(IX,IY,DIP(J),AZ(J))
200  LPAGE(IX,IY)=LPLUS
      WRITE(6,212)
212  FORMAT(1H,45X,40HEQUAL AREA PROJECTION OF OBSERVATIONS TO/
1 58X,16HUPPER HEMISPHERE///)
      CALL POLARC
      WRITE(6,4000) NOBS
4000  FORMAT(///36X,9HTHERE ARE,15,1X,27HOBSERVATIONS IN THE SAMPLE.)
      CALL PCTPLT(LEVEL)
      PRINT 213
213  FORMAT(1H1,63X,10HLEVEL PLOT,///)
      CALL POLARC
      WRITE(6,4001)
4001  FORMAT(1/32X,75HTHE UPPER HEMISPHERE IS DIVIDED INTO 100 PATCHES OF
1 EQUAL AREA. THE DENSITY/43X,64HOF EACH PATCH IS PRINTED AT THE PR
PROJECTED MIDPOINT OF THE PATCH.)

```

C***** DEFINE CLUSTERS

```

      KJ=1
      JQ=1
      I=1
      IJ=1
      LCOM=1
      IJPR=0
      DO 101 N=1,100
      IF (IPTH(N) .NE. 0) GO TO 101
      IF (LEVEL(I) - PCT) 101,102,102
102  IF (N=1) 103,103,104
104  JQ=N-1
      IF (LEVEL(JQ) - PCT) 105,106,106
105  IF (IJPR .NE. 0) GO TO 777
      IF (CLUSTH(1,1) .NE. 0) IJ=IJ+1
      GO TO 778
777  IJ=IJPR
      IJPR=0
778  CONTINUE
      KJ=1
      GO TO 103
106  IF (LCOM .EQ. 0) GO TO 107
      GO TO 103
107  KJ=MJ
103  LCOM=1
      I=KBAND(N)
      KSUM=0
      DO 7001 LIJ=1,I
7001  KSUM=KSUM+IBND(LIJ)
      CLUSTH(KJ,IJ)=N
      IPTH(N)=IJ
      KJ=KJ+1
      IF (N .EQ. 100) GO TO 101
      K2=KSUM-IBND(I)+1
      IQQA=IPTH(K2)
      IF (N .EQ. KSUM .AND. IQQA .NE. 0 .AND. IQQA .NE. IJ)
1  CALL COMBIN(IQQA)
      IF (LEVEL(N+1) .GT. PCT .AND. IPTH(N+1) .NE. 0 .AND. (IPTH(N+1) .NE.
1  IJ) CALL COMBIN(IPTH(N+1))
      IF (I .EQ. 8) GO TO 3698
      I1=I+1
      IQR3=POS(N)
      CALL CLCP(I,IQR3,11)
      KJ1=KJ-1
      DO 70 IPP=1,KJ1
      K2=CLUSTH(IPP,IJ)
      IBC=KBAND(K2)
      IF (IBC .EQ. 8) GO TO 3698
      IBC1=IBC+1
      IQMC=POS(K2)
      CALL CLCP(IBC,IQMC,IBC1)
      KJ1=KJ-1
70  CONTINUE
      MJ=KJ
      GO TO 101

```

```

3498 IF (LEVEL(100) .LT. PCT) GO TO 101
      IF (IPTH(100) .NE. 0) GO TO 9000
      CLUSTR(KJ,IJ)=100
      IPTH(100)=IJ
      KJ=KJ+1
      MJ=KJ
      GO TO 101
9000 IF (IPTH(100) .NE. IJ) GO TO 3697
      GO TO 101
3697 CALL COMBIN(IPTH(100))
      MJ=KJ
101  CONTINUE

```

C***** COMBINE ANTIPODAL CLUSTERS

```

      DO 8762 K=1,9
      J=K+9
      IJ=IPTH(J)
      IF (IPTH(K) .EQ. 0 .OR. IPTH(J) .EQ. IPTH(K)) GO TO 8762
      IF (IPTH(J) .NE. 0) CALL COMBIN(IPTH(K))
8762 CONTINUE
      CALL KLUSTR
      GO TO 8000
      END

```

SUBROUTINE KLUSTR

C***** PERFORM STATISTICAL CALCULATIONS FOR EACH CLUSTER

```

      INTEGER CLUSTR
      COMMON /BLK/AZ(1000),DIP(1000),CU1(900),CU2(900),SL(1000),
1 SM(1000),SN(1000),KBAND(100),NB,IBND(9),DANG(10),LPATCH(100),
2 LEVEL(100),IPTM(100),CLUSTR(50,10),LPAGE(121,73),NX,INY,NYMID,
3 NXMID,PI,NEGRAD,RADEG,Q90,XPINCH,YPINCH,RADIUS,PCT,LCOM,KJ,IJ,
4 IJPR,P,T,KOU,R,XCONV,YCONV,XK,POS(100)
      DIMENSION KPATCH(100),FLEVEL(100)
      DATA LPLUS/1H+/,
      DATA PLSMS/2H+==/,
      DATA BLANK/1H /
      KOUNT=1
      DO 92 JS=1,10
      IF (CLUSTR(1,JS) .EQ. 0) GO TO 92
      JR=1
      SXL=0.
      SKM=0.
      SXN=0.
      CL=0.05
      KOU = 0
      DO 677 JK=1,100
      IF (CLUSTR(JK,JS) .EQ. 0) GO TO 678
      N=CLUSTR(JK,JS)
      N1=LPATCH(N)
      IF (N .EQ. 1) KS=1
      IF (N .GT. 1 .AND. LPATCH(N-1) .EQ. 0) KS=1
      IF (N .GT. 1 .AND. LPATCH(N-1) .NE. 0) KS=LPATCH(N-1)*1.
      DO 26 III=KS,N1
      KOU = KOU + 1
      CU1(JR)=AZ(III)
      CU2(JR)=DIP(III)
      CALL SPRPAG(IX,IY,CU2(JR),CU1(JR))
      LPAGE(IX,IY)=LPLUS
      JR=JR+1
26 CONTINUE
677 CONTINUE
678 CONTINUE
      IF (KOU .LE. 2) GO TO 93
      IF (KOUNT .EQ. 1) GO TO 4003
      .PRINT(16,907) KOUNT
907 FORMAT(11H1, //,30X,14HCLUSTER NUMBER,15)
      KOUNT=KOUNT+1
      GO TO 40
4003 WRITE(6,4002)
4002 FORMAT(11H1,45X,32HSTATISTICAL ANALYSIS OF CLUSTERS//
1 //30X,14HCLUSTER NUMBER 1)
      KOUNT=KOUNT+1
      GO TO 40
93 DO 94 J=1,73
      DO 94 K=1,121
94 LPAGE(K,J)=BLANK
      GO TO 92

```

```

40 AKOU = KOU
   PRINT 4
4  FORMAT(35X,3HNUM,5X,9HAZIMUTH ,11HINCLINATION,5X,14L,10A,3HM,10X,
11HN/)

C  DETERMINE IF CLUSTER CONTAINS ANTIPODAL POINTS. REFLECT ANTIPODAL
C  POINTS 180 DEGREES.

   IF(CU2(1) .LT. 80.) GO TO 1000
   KOU1=KOU-1
   DIS=0.
   DO 9999 J=1,KOU1
   FJ=CU1(J)
   J1=J+1
   DO 9999 K=J1,KOU
   FK1=CU1(K)
   FMAX=AMAX1(FJ,FK1)
   FMIN=AMIN1(FJ,FK1)
   ADIS=AMIN1((FMAX-FMIN),(360.-FMAX+FMIN))
   IF(DIS .LT. ADIS) DIS=ADIS
9999 CONTINUE
   IF(DIS .LE. 150.) GO TO 1000
9998 CALL SORT(1,1,KOU)
   DIS=AMIN1(CU1(KOU)-CU1(1),360.-CU1(KOU)+CU1(1))
   IF(DIS - 45.) 1:1,4001
1  A=CU1(1)+90.
   B=A+180.
   IST2=0
   JQ=1
   DO 11 J=1,KOU
   IF(J .GT. 1) JQ=J-1
   IF(CU1(J) .GT. A .AND. CU1(JQ) .LE. A) IST1=JQ
   IF(CU1(J) .GT. B .AND. CU1(JQ) .LE. B) IST2=J
   IF(IST2 .NE. 0) GO TO 12
11 CONTINUE
12 DO 5 J=1,IST1
   CU2(J)=180.-CU2(J)
   IF(CU1(J) .GT. 180.) GO TO 8000
   CU1(J)=CU1(J)+180.
   GO TO 5
8000 CU1(J)=CU1(J)-180.
5  CONTINUE
   DO 5 J=IST2,KOU
   CU2(J)=180.-CU2(J)
   IF(CU1(J) .LT. 180.) GO TO 8001
   CU1(J)=CU1(J)-180.
   GO TO 6
8001 CU1(J)=CU1(J)+180.
6  CONTINUE
   GO TO 1000
4001 IST1=0
   A=CU1(1)+90.
   JQ=1
   DO 4000 J=1,KOU
   IF(J .GT. 1) JQ=J-1
   IF(CU1(J) .GT. A .AND. CU1(JQ) .LE. A) IST1=J

```

```

      IF(IIST) .NE. 0) GO TO 9
4000 CONTINUE
      DO 13 J=1ST1,KOU
      CU2(J)=180.-CU2(J)
      IF(CU1(J) .LT. 180.) GO TO 8002
      CU1(J)=CU1(J)-180.
      GO TO 13
8002 CU1(J)=CU1(J)+180.
      13 CONTINUE

```

C COMPUTE DIRECTION COSINES FOR EACH OBSERVATION

```

1000 DO 1001 J=1,KOU
      DP=CU2(J)*DEGRAD
      AT=CU1(J)*DEGRAD
      SL(J)=SIN(DP)*COS(AT)
      SM(J)=SIN(DP)*SIN(AT)
      SN(J)=COS(DP)
      SXL=SXL+SL(J)
      SXM=SXM+SM(J)
      SXN=SXN+SN(J)
      WRITE(6,3) J, CU1(J), CU2(J), SL(J), SM(J), SN(J)
      3 FORMAT(30X, I8, F12.2, F11.2, 3F11.4)
1001 CONTINUE

```

C CALCULATE STATISTICAL PARAMETERS

```

37 PRINT 38, SXL, SXM, SXN
38 FORMAT(33X, 6HTOTALS, 22X, 3F11.4)
43 HSQ = SXL*SXL + SXM*SXM + SXN*SXN
      H = SQRT(HSQ)
      PRINT 44, KOU
44 FORMAT(/3X, 10HNUMBER OBS, I6)
      PRINT 45, R
45 FORMAT(/3X, 3HM =, F10.3)
      IF(SXM .EQ. 0. .OR. SXL .EQ. 0.) GO TO 9393
      T=ATAN2(SXM, SXL)*RADEG
      GO TO 9394
9393 IF(SXL .EQ. 0.) T=90.*(2.-SXM/ABS(SXM))
      IF(SXM .EQ. 0.) T=-90.*(SXL/ABS(SXL)-1.)*90.
9394 CONTINUE
      IF (T.LT.0.0) T=T+360.
      P=ACOS (SXN/H)*RADEG
      IF(AKOU .FU. R) GO TO 7000
      AK=AKOU/(XKOU-R)
      GO TO 7093
7000 CONTINUE
      A=0.0
      AK=4999999.999
      GO TO 7094
7093 CONTINUE
      COSA= 1. - (1./AK)*(1./CL*(1./(XKOU-1.)) - 1.)
      A=ACOS (COSA)*RADEG
7094 P1=P
      11=T
      IF(P .GT. 90.) GO TO 1002

```

```

GO TO 1002
1002 P1=180.-P
      T1=T-180.
      IF (T1 .LT. 0.) T1=T1+360.
1003 CONTINUE
      IF (XK .LT. 6.) GO TO 5003
      WRITE(6,4R) T1,P1,XK,A
40  FORMAT(/27X,26H*** CLUSTER STATISTICS ***/,30X)
1   10MT, AZIMUTH,17X,F7.2,1X,3HDEG/,30X)
2   14MP, INCLINATION,13X,F7.2,1X,3HDEG/,30X)
3   12MK, PRECISION,15X,F7.2/,30X)
4   27MA, RADIUS OF CONE OF CONFID, F7.2,1X,3HDEG/)

C COMPUTE CONFIDENCE LIMITS FOR AZIMUTH AND DIP
5006 IF (P1-A) =010,5011,5012
5010 ATVM=360.
      GO TO 5013
5011 ATVM=180.
      GO TO 5013
5012 AU=A*DEGRAD
      PD=P1*DEGRAD
      P2D=90.*DEGRAD
      ATVM=ASIN ( SIN(AU)*SIN(P2D)/SIN(PD) ) *RADEG
5013 UPVM=A
      WRITE(6,5009) PLSMS,DPVR,PLSMS,ATVM
5009 FORMAT(29X,13H CONF. LIMITS/29X,4H DIP,1X,A2,1X,F6.2/29X,3H AZ,1X,
1  A2,1X,F6.2)
      GO TO 5014
5003 WRITE(6,5004) T1,P1,XK
5004 FORMAT(/27X,26H*** CLUSTER STATISTICS ***/,30X)
1   10MT, AZIMUTH,17X,F7.2,1X,3HDEG/,30X)
2   14MP, INCLINATION,13X,F7.2,1X,3HDEG/30X)
3   12MK, PRECISION,15X,F7.2)
5014 KOUNT1=KOUNT-1
      WRITE(6,5005) KOUNT1
5005 FORMAT(1H),45X,34HPOINTS BELONGING TO CLUSTER NUMBER,15//)
      CALL POLAPC
      IF (XK .GT. 0. .AND. XKOU .NE. R) CALL SECTON
92 CONTINUE
      RETURN
      END

```

SUBROUTINE SECTOR

C***** SECTOR TESTS FOR BIVARIATE-NORMAL DISTRIBUTION OF DATA

```

COMMON /BLK/AZ(1000),DIP(1000),CU1(900),CU2(900),SL(1000),
1 SM(1000),SN(1000),KBAND(100),NB,IBND(9),DANG(10),LPATCH(100),
2 LEVEL(100),IPTH(100),CLUSTER(50,10),LPAGE(121,73),NX,NY,NYMID,
3 NXMID,PI,DEGRAD,RADEG,Q90,XPINCH,YPINCH,RADIUS,PCT,LCOM,KJ,IJ,
4 IJPR,P,T,KOU,R,XCONV,YCONV,XK,POS(100)
DIMENSION SFREQ(9,4),TFREQ(9),KPATCH(100),FLEVEL(100),SANG(5)
INTEGER 0
DATA SANG/=-1.,1.,5707966,3.14159270,4.7123891,6.28318560/
DATA PI2/1.5707963/
DO 5001 JM=1,100
KPATCH(JM)=0
5001 FLEVEL(JM)=0.0
SXL=0.0
SXM=0.0
SXN=0.0
A=DEGRAD
A1=RADEG
AZL=SIN(A*P)*COS(A*T)
AZM=SIN(A*P)*SIN(A*T)
AZN=COS(A*P)
91 WRITE(6,3004)AZL,AZM,AZN
3004 FORMAT(30H DIRECTION COSINES OF THE MEAN/4X,3HL =,F8.4,3X,3HM =,
1 F8.4,3X,3HN =,F8.4)

C ROTATE MEAN TO POLE AND COMPUTE DIP + AZ OF OBS WRT MEAN

TA=T*A
PA=P*A
DO 8000 J=1,KOU
XPR=SL(J)*COS(TA)+SM(J)*SIN(TA)
YPR=-SL(J)*SIN(TA)+SM(J)*COS(TA)
ZPR=SN(J)
Z1=ZPR*COS(PA)+XPR*SIN(PA)
X1=-ZPR*SIN(PA)+XPR*COS(PA)
Y1=YPR
CU2(J)=ACOS(SL(J)*AZL+SM(J)*AZM+SN(J)*AZN)*A1
IF(X1.EQ.0..OR.Y1.EQ.0.)GO TO 9393
CU1(J)=ATAN2(Y1,X1)*A1
GO TO 9394
9393 IF(X1.EQ.0.)CU1(J)=90.*(2.-Y1/ABS(Y1))
IF(Y1.EQ.0.)CU1(J)=-((X1/ABS(X1)-1.)*90.
9394 CONTINUE
IF(CU1(J).LT.0.)CU1(J)=CU1(J)+360.
8000 CONTINUE

C ARRANGE POINTS IN INCREASING SEQUENCE OF SEMI-ANG(J) WITH MEAN

CALL SORT(2,1,KOU)
C COMPUTE EXPECTED FREQUENCY IN 2ND ANNULUS FOR PSI MAX.
PSI=CU2(KOU)*A
FN=FLOAT(KOU)

```

```

NPSI=9
NCHI=4
CPSI=COS(PSI)
90 NPSI=NPSI-1
DELSI=(1.-CPSI)/FLOAT(NPSI)
DIAU=CPSI*DELSI
DIAI=UIAO*DELSI
FXFRE=FN*(EXP(-XK*(1.-DIAI)) - EXP(-XK*(1.-DIAO)))
IF((EXFRE/FLOAT(NCHI)).GE.1. .OR. NPSI .LE. 4) GO TO 100
GO TO 90

C COMPUTE ACTUAL FREQUENCIES IN SECTORS

100 DO 69 J=1,NPSI
DO 69 K=1,NCHI
69 CFREQ(J,K)=0.
DO 888 JJ=1,KOU
CU1(JJ)=CU1(JJ)*A
CU2(JJ)=COS(CU2(JJ)*A)
888 CONTINUE
C COMPUTE THEORETICAL FREQUENCY IN NPSI RINGS AROUND MEAN
DO 71 J=1,NPSI
DEL1=1.-FLOAT(J-1)*DELSI
DEL2=DEL1-DELSI
71 TFREQ(J)=FN*(EXP(-XK*(1.-DEL1)) - EXP(-XK*(1.-DEL2)))
-- WRITE(6,920)
920 FORMAT(1H1.5H RING,AX.7H SECTOR,AX.1AH ACT SECTOR FREQ,5X.1AH THEO
1R SECT FREQ//)
DO 2 J=1,NPSI
RANG=1.-FLOAT(J-1)*DELSI
RANG1=RANG-DELSI
IF(J .EQ. 1) RANG=1.01
IF(J .EQ. NPSI) RANG1=RANG1-0.01
DO 2 K=1,NCHI
K1=K+1
DO 2 L=1,KOU
AT=CU1(L)
DP=CU2(L)
IF(AT .GT. SANG(K) .AND. AT .LE. SANG(K1) .AND. DP .LT. RANG .AND.
1 DP .GE. RANG1) SFREQ(J,K)=SFREQ(J,K)+1
2 CONTINUE

C COMPUTE CHI SQUARE VALUE FOR SECTORS

SUM=0.
DO 110 J=1,NPSI
TEST=TFREQ(J)/FLOAT(NCHI)
DO 110 K=1,NCHI
SUM=SUM+(SFREQ(J,K)-TEST)**2/TEST
110 WRITE(6,930) J,K,SFREQ(J,K),TEST
930 FORMAT(15,10X,15,2F20.7)
KFREE=(NPSI*NCHI)-3
AN=FLOAT(KFREE)
AA=2./(9.*AN)
CH95=AN*(1.-AA+1.645*SQRT(AA))**3
AA=ACOS(CU2(KOU))*A1

```

52

```
WRITE(6,3010) KERFE,SUM,CH95,AA
3010 FORMAT(//,15H DEG. FREEDOM =, 13,13H CHI SQUARE =,F10.3/,
1 17H TH. CHI SQ. 95 =,F10.3/,10H PSI MAX =,F10.3,1X,4HDEG.)
```

C CLUSTER LEVEL PLOT

```
PSIA=PSI*A1
DO 3000 J=1,KOU
CU1(J)=CU1(J)*A1
3000 CU2(J)=ACOS(CU2(J)*A1)*90./PSIA
CALL SORTA(KOU,CU1,CU2,KPATCH)
FLEVEL(1)=FLOAT(KPATCH(1))/FN
DO 8764 KUK=2,100
FLEVEL(KUK)=FLOAT(KPATCH(KUK)-KPATCH(KUK-1))/FN
8764 CONTINUE
CALL PCTPLT(FLEVEL)
WRITE(6,3032)
3032 FORMAT(1H1,//,60X,19HCLUSTER LEVEL PLOT/52X,34HWITH MEAN AT POLE AN
10 THE BOUNDARY/55X,2AHAT PSI MAX DEGREES FROM POLE//)
CALL POLARC
RETURN
END
```

SUBROUTINE SORTA(NOBS,A,D,IPATCH)

C***** SORTS DATA INTO PATCHES

```

COMMON /HLK/AZ(1000),DIP(1000),CU1(900),CU2(900),SL(1000),
1 SM(1000),SN(1000),KBAND(100),NB,IBND(9),DANG(10),LPATCH(100),
2 LEVEL(100),IPTH(100),CLUSTR(50,10),LPAGE(121,73),NA,NY,NYMID,
3 NXMID,PI,DEGRAD,RADEG,Q90,XPINCH,YPINCH,RAIUS,PCT,LCOM,KJ,IJ,
4 IJPR,P,T,KOU,R,XCUNV,YCONV,XK,POS(100)
DIMENSION A(NOBS),D(NOBS),IPATCH(100)
DO 9 I=1,100
9 IPATCH(I)=0

```

C***** ARRANGE DATA IN DECREASING ORDER OF DIP

```

NOBS1=NOBS-1
DO 7 I=1,NOBS1
II=I+1
DO 7 J=II,NOBS
IF(D(I) .GE. D(J)) GO TO 7
TMP=D(I)
D(I) = D(J)
D(J) = TMP
TMP=A(J)
A(J)=A(I)
A(I)=TMP
7 CONTINUE

```

C

C***** ARRANGE THE POINTS IN EACH BAND IN INCREASING ORDER OF AZIMUTH

```

M=1
DO 93 L=1,NB
IF(M .EQ. NOBS) GO TO 8888
94 CONTINUE
DO 92 J=M,NOBS1
J1=J+1
IF(D(J) .GE. DANG(L+1)) GO TO 8884
8885 M=J
GO TO 93
8884 DO 90 K=J1,NOBS
IF(D(K) .GE. DANG(L+1)) GO TO 8886
8887 M=J+1
GO TO 94
8886 IF(A(J) .LT. A(K)) GO TO 90
TMP=A(J)
A(J)=A(K)
A(K)=TMP
TMP=D(J)
D(J)=D(K)
D(K)=TMP
90 CONTINUE
M=M+1
92 CONTINUE
93 CONTINUE

```

8888 CONTINUE

C00000 DETERMINE WHICH PATCHES CONTAIN DATA

```

      II=0
      LP=0
      KK=0
      IOP=1
      DO 87 J=1,NB
      II=II+KK
      IBJ=IBND(J)
      DO 87 K=1,IBJ
      IF(LP .EQ. NOBS) GO TO 88
      KK=K
      KANG=FLOAT(K)*360./FLOAT(IBND(J))
      IF(K .EQ. IBND(J)) KANG=360.5
      DO 86 L=IOP,NOBS
      IF(A(L) .GT. KANG .OR. D(L) .LT. DANG(J+1)) GO TO 79
      LP=LP+1
      IF(LP .NE. NOBS) GO TO 86
79  IPATCH(II+K)=LP
      IOP=LP+1
      L=II+K+1
      GO TO 87
86  CONTINUE
87  CONTINUE
88  IF(L .EQ. 101) RETURN
      GO 89 J=L+100
89  IPATCH(J)=NOBS
      RETURN & END

```

SUBROUTINE CLUP(LI, LB, I9)

C***** DETERMINES IF A CLUSTER CONTAINING PATCHES IN BAND NUMBER J
 C***** CONTAINS PATCHES IN BAND NUMBER J*1, 1 S J S 8:

```

COMMON /BLK/AZ(1000),DIP(1000),CU1(900),CU2(900),SL(1000),
1 SM(1000),SN(1000),KBAND(100),NB,IBND(9),DANG(10),LPATCH(100),
2 LEVEL(100),IPTH(100),CLUSTR(50,10),LPAGE(121,73),NAX,NY,NYMID,
3 NAMID,PI,ZFRHL,RAUEG,Q90,XPINCH,YPINCH,RAIUS,PCT,LCON,KJ,I,
4 IJPR,P,T,KOU,K,ACONV,YCONV,AK,POS(100)
DIMENSION L(3)
REAL LEVEL
INTEGER CLUSTR
II=LI $ IJ=LB $ IC=I9 $ I91=I9-1
A=(360./FLOAT(1800/(II))) * FLOAT(18)
ISUM=0
DO 12 I=1,I91
12 ISUM=ISUM+IBND(I)
IJJ=IBND(I9)
DO 9 NQ=1,IJJ
IQ=NQ
Z=FLOAT(NQ)*360./FLOAT(1800/(IC))
IF(Z .GE. A) GO TO 10
9 CONTINUE
10 LA=ISUM-IQ-1
IG=ISUM-IJND(I9)
IF(IQ .EQ. IJJ) GO TO 87
IF(IQ - 11 81,84,81
87 L(1)=IG-1 $ L(2)=IG $ L(3)=ISUM*1
GO TO 85
81 L(1)=LA $ L(2)=LA*1 $ L(3)=LA*2
GO TO 84
84 L(1)=IG $ L(2)=ISUM*1 $ L(3)=ISUM*2
85 DO 85 J=1,3
LJ=L(J)
IF(LEVEL(LJ) .LT. PCT .OR. IPTH(LJ) .EQ. IJ) GO TO 89
IF(IPTH(LJ) .NE. 0) GO TO 4
IPTH(LJ) = IJ
CLUSTR(KJ,IJ)=LJ
KJ=KJ*1
IF(LJ .EQ. 100) RETURN
GO TO 85
4 CALL COMBIN(IPTH(LJ))
IF(LJ .EQ. 100) RETURN
85 CONTINUE
RETURN
END
```

```

SUBROUTINE SPRPAG(IX,IY,DIN,AZN)
C SPRPAG * * * * *
C GIVEN HEMISPHERE COORDINATES (DIN,AZN), SPRPAG RETURNS NEAREST
C PAGE COORDINATES (IX,IY). IF OUTSIDE PAGE, MOVE IX OR IY TO
C CLOSEST POINT ON EDGE OF PAGE
COMMON /PLK/AZ(1000),DIP(1000),CU1(900),CU2(900),SL(1000),
1 SM(1000),SN(1000),KBAND(100),NB,IBND(9),DANG(10),LFATCH(100),
2 LEVEL(100),IPTM(100),CLSTR(50,10),LPAGE(121,73),NX,NY,NYMID,
3 NXMID,PI,DEGRAU,HADEG,090,XPINCH,YPINCH,RADIUS,PCT,LCOM,KJ,IJ,
4 IJPR,P,T,KOU,R,XCONV,YCONV,XK,POS(100)
ANGLR=AZN*DEGRAU
C THE NEXT 3 STATEMENTS PERFORM EQUAL-AREA PROJECTION
100 XYT=127.2798*SIN(DEGRAD*DIN/2.0)
JDUM=XYT*SIN(ANGLR)*XCONV*0.5
JDUM=XYT*COS(ANGLR)*YCONV*0.5
200 IX=NXMID+JDUM
C BRING X INDEX IN RANGE IF IT IS OUTSIDE:
IF(IX.LT.1) IX=1
IF(IX.GT.NX) IX=NX
IY=NYMID+JDUM
C BRING Y INDEX IN RANGE IF IT IS OUTSIDE:
IF(IY.LT.1) IY=1
IF(IY.GT.NY) IY=NY
RETURN
END

```

```

SUBROUTINE POLARC
C POLARC * * * * *
C DRAWS AND LABELS AXES AND CIRCLE SURROUNDING OUTPUT GRAPH.
C PLACES AN AAA AT EVERY 10 DEGREES AROUND CIRCLE CIRCUMFERENCE WITH
C N°E, S°W AT 0, 90, 180, 270 DEGREES RESPECTIVELY.
C * * CALLS= SPRPAG * * * * *
C * * * * *
COMMON /BLK/AZ(1000),DIP(1000),CU1(900),CU2(900),SL(1000),
1 SM(1000),SN(1000),KBAND(100),NB,IBND(9),DANG(10),LPATCH(100),
2 LEVEL(100),IPTM(100),CLSTR(50,10),LPAGE(121,73),NX,NY,NYMID,
3 NXMID,PI,REFRAU,RADEG,Q90,XPINCH,YPINCH,RADIUS,PCT,LCOM,KJ,IJ,
4 IJPR,P,T,KOU,R,ACONV,YCONV,XK,POS(100)
DIMENSION LNUMS(10),LDIR(4)
DATA LNUMS/1H0,1H1,1H2,1H3,1H4,1H5,1H6,1H7,1H8,1H9/
DATA LASTER/1H0,1H1,1H2,1H3,1H4,1H5,1H6,1H7,1H8,1H9/
DATA LBLANK/1H /
NXI=NX-1
ANGL=0.0
DO 200 J=1,36
CALL SPRPAG(IX,IY,Q90,ANGL)
LPAGE(IX,IY)=LASTER
200 ANGL=ANGL+10.
LPAGE(NXMID,NYMID)=LASTER
C LABEL N°S,E°W AT APPROPRIATE POSITIONS
600 LPAGE(NXMID,NY)=LDIR(1)
LPAGE(NXMID,1)=LDIR(2)
LPAGE(NX,NYMID)=LDIR(3)
LPAGE(1,NYMID)=LDIR(4)
C PRINT THE COMPLETE ASSEMBLED PAGE IMAGE ROW BY ROW
C * *NOTE** THE INDEX K MUST GO BACKWARDS BECAUSE THE ASSUMED
C COORDINATE ORIGIN IS AT LOWER LEFT HAND CORNER OF PAGE
DO 700 J=1,NY
K=NY-J+1
700 WRITE(6,2000) (LPAGE(I,K),I=1,NX)
2000 FORMAT(27X,90A1)
DO 199 J1=1,73
DO 199 J2=1,121
199 LPAGE(J2,J1)=LBLANK
RETURN
END

```

SUBROUTINE COMBIN(K)

C***** COMBINE ANTIPODAL CLUSTERS IN BAND 1

```

      INTEGER CLUSTR
      COMMON /BLK/AZ(1000),DIP(1000),CU1(900),CU2(900),SL(1000),
1  SM(1000),SN(1000),KBAND(100),NB,IBND(9),DANG(10),LPATCH(100),
2  LEVEL(100),IPTH(100),CLUSTR(50,10),LPAGE(121,73),NX,NY,NYMID,
3  NXMID,PI,DEGRAD,RADEG,Q90,XPINCH,YPINCH,RADIUS,PCT,LCOM,KJ,IJ,
4  IJPR,P,T,KOU,R,ACONV,YCONV,XK,POS(100)
      DO 1 L=1,100
      M=L
      IF(CLUSTR(L,IJ) .EQ. 0) GO TO 2
1  CONTINUE
2  DO 3 N=1,100
      J=N
      IF(CLUSTR(N,K) .EQ. 0) GO TO 4
3  CONTINUE
4  IS=J
      M1=M-1
      DO 5 LR=1,M1
      CLUSTR(IS,K)=CLUSTR(L,IJ)
      ICJ=CLUSTR(L,IJ)
      IPTH(ICJ)=K
      IS=IS+1
5  CONTINUE
      IJPR=IJ
      DO 6 LR=1,M
6  CLUSTR(LR,IJ)=0
      IJ=K
      KJ=M+J-1
      LCOM=0
      RETURN
      END

```

SUBROUTINE SORT(IA,IB,IC)

C***** SORTS DATA IN EITHER INCREASING ORDER OF AZIMUTH OR INCREASING
 C***** ORDER OF DIP.

```

COMMON /BLK/AZ(1000),DIP(1000),CU1(900),CU2(900),SL(1000),
1 SM(1000),SN(1000),KBAND(100),NB,IBND(9),DANG(10),LPATCH(100),
2 LEVEL(100),IPTH(100),CLUSTR(50,10),LPAGE(121,73),NX,NY,NYMID,
3 NAMID,PI,DEGRAD,RADEG,Q90,XPINCH,YPINCH,RADIUS,PCT,LCOM,KJ,IJ,
& IJPR,P,T,KOU,R,XCONV,YCONV,XK,POS(100)
  IC1=IC-1
  IF(IA .EQ. 1) GO TO 2
  DO 1 K=IB,IC1
  K1=K+1
  DO 1 J=K1,IC
  IF(CU2(K) .LE. CU2(J)) GO TO 1
  TMP=CU2(K)
  CU2(K)=CU2(J)
  CU2(J)=TMP
  TMP=CU1(J)
  CU1(J)=CU1(K)
  CU1(K)=TMP
1 CONTINUE
  RETURN
2 DO 3 K=IB,IC1
  K1=K+1
  DO 3 J=K1,IC
  IF(CU1(K) .LE. CU1(J)) GO TO 3
  TMP=CU1(K)
  CU1(K)=CU1(J)
  CU1(J)=TMP
  TMP=CU2(K)
  CU2(K)=CU2(J)
  CU2(J)=TMP
3 CONTINUE
  RETURN
  END

```

SUBROUTINE PCTPLT(RLEVEL)

C**** PLOTS EITHER LEVEL(J) OR FLEVEL(J) AT THE PROJECTED MIDPOINT OF
 C**** PATCH NUMBER J.

```

COMMON /RLK/AZ(1000),DIP(1000),CU1(900),CU2(900),SL(1000),
1 SM(1000),SN(1000),KBAND(100),NB,IBND(9),DANG(10),LPATCH(100),
2 LEVEL(100),IPTM(100),CLSTR(50,10),LPAGE(121,73),NX,INY,NYMID,
3 NAMID,PI,RFGRAD,RADEG,090,XPINCH,YPINCH,RADIUS,PCT,LCOM,KJ,IJ,
4 IJPR,P,T,KOU,R,XCONV,YCONV,XK,POS(100)
INTEGER O
DIMENSION RLEVEL(100),NUM1(10),NUM(10)
DATA NUM1/1H,1M1,1M2,1M3,1M4,1M5,1M6,1M7,1M8,1M9/,
1 NUM/1M0,1M1,1M2,1M3,1M4,1M5,1M6,1M7,1M8,1M9/,LDUT/1H,/
DO 1 J=1,100
  IBJ=KBAND(J)
  AZN=(POS(J)-0.5)*360./FLOAT(IBND(IBJ))
  IBJ1=IBJ+1
  DIN=(DANG(IBJ)+DANG(IBJ1))/2.
  CALL SPRPAG(IX,IY,DIN,AZN)
  IF(DIN .LT. 91.) GO TO 3033
  IF(AZN .LT. 180.) IX=IX-2
  IF(AZN .GT. 180.) IX=IX+2
3033 CONTINUE
  IF(J .EQ. 100) IY=IY-1
  K=RLEVEL(J)*10000.+5.
  M=K/1000
  N=(K-(M*1000))/100
  O=(K-M*1000-N*100)/10
  LPAGE(IX-2,IY)=NUM1(M+1)
  LPAGE(IX-1,IY)=NUM(N+1)
  IF(M .EQ. 0) LPAGE(IX-1,IY)=NUM1(N+1)
  LPAGE(IX,IY)=LDUT
  LPAGE(IX+1,IY)=NUM(O+1)
  IF(M .EQ. 0 .AND. N .EQ. 0 .AND. O .EQ. 0) GO TO 2
  GO TO 1
2 LPAGE(IX-2,IY)=NUM1(1)
  LPAGE(IX-1,IY)=NUM1(1)
  LPAGE(IX+1,IY)=NUM1(1)
1 CONTINUE
RETURN
END
```

APPENDIX C.--COMPUTER OUTPUT FOR AN EXAMPLE PROBLEM

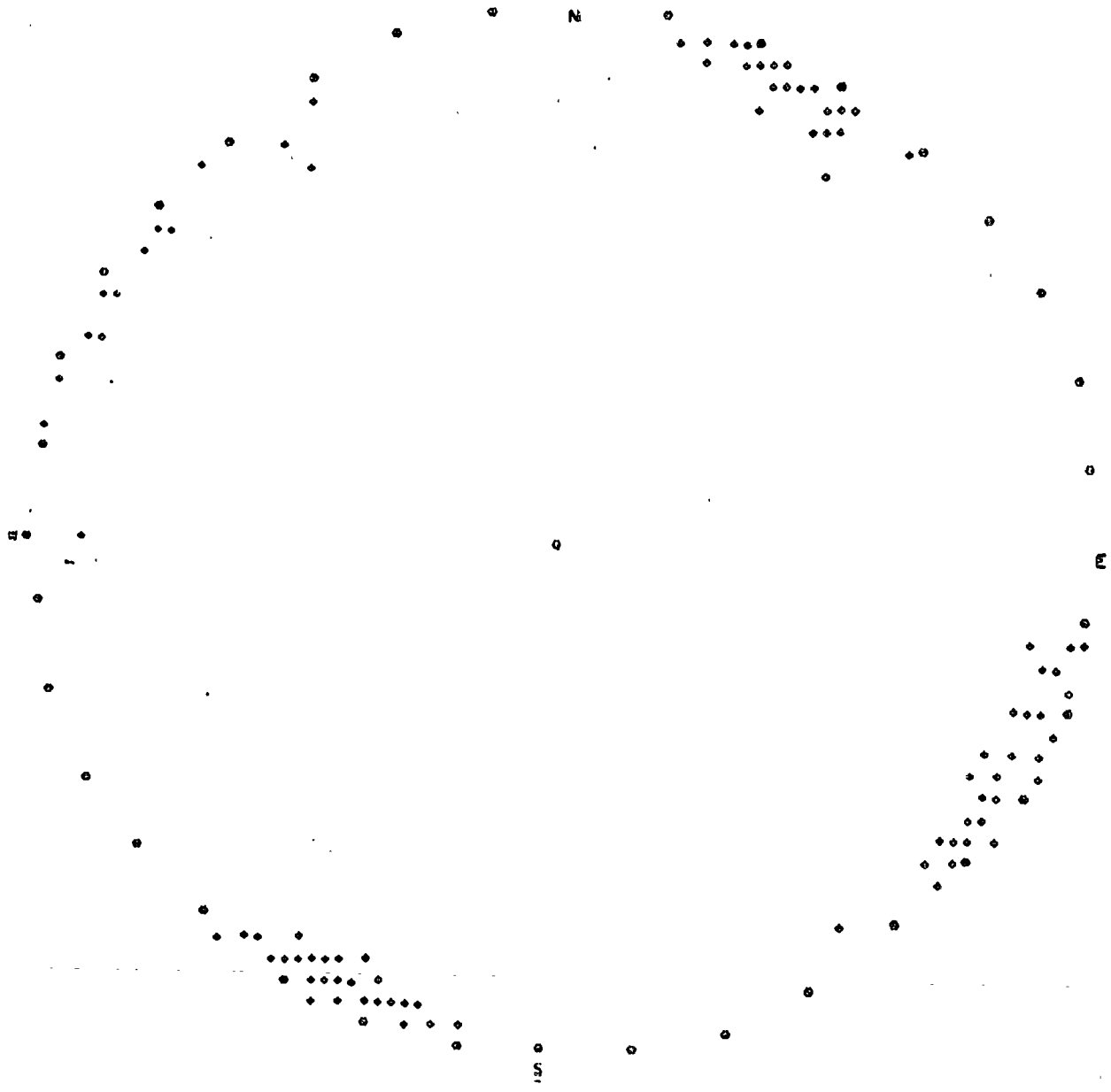
JERAN-MASHEY COAL CLEFT DATA

POISSON RANDOM CUT-OFF IS 2.222 PERCENT
THERE ARE 135 POINTS IN THE SAMPLE.

LEVEL ARRAY

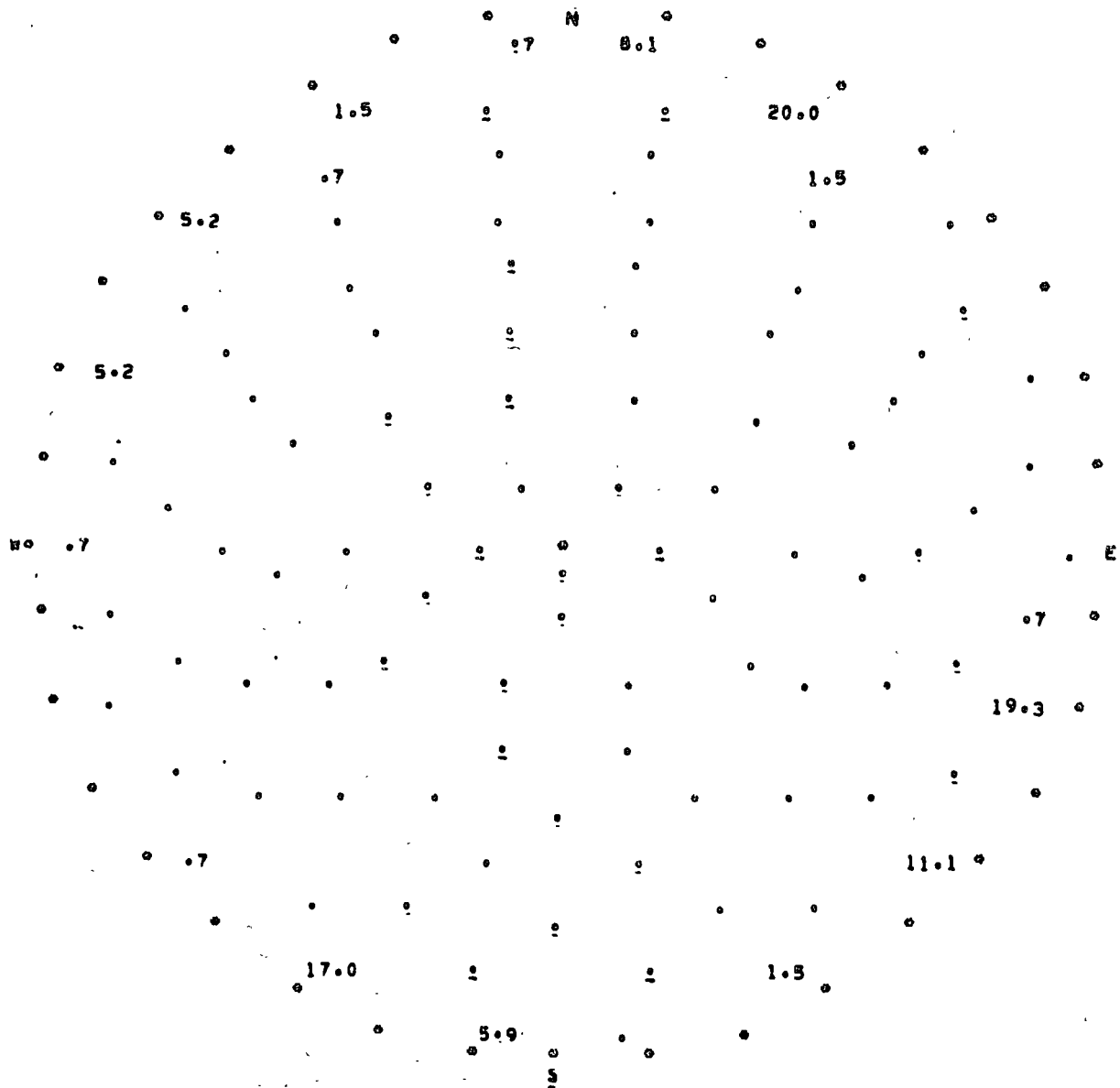
1	.08148	51	0.00000
2	.20000	52	0.00000
3	0.00000	53	0.00000
4	0.00000	54	0.00000
5	0.00000	55	0.00000
6	.19259	56	0.00000
7	.11111	57	0.00000
8	.01481	58	0.00000
9	0.00000	59	0.00000
10	.05926	60	0.00000
11	.17037	61	0.00000
12	.00741	62	0.00000
13	0.00000	63	0.00000
14	.00741	64	0.00000
15	.05185	65	0.00000
16	.05185	66	0.00000
17	.01481	67	0.00000
18	.00741	68	0.00000
19	0.00000	69	0.00000
20	.01481	70	0.00000
21	0.00000	71	0.00000
22	0.00000	72	0.00000
23	.00741	73	0.00000
24	0.00000	74	0.00000
25	0.00000	75	0.00000
26	0.00000	76	0.00000
27	0.00000	77	0.00000
28	0.00000	78	0.00000
29	0.00000	79	0.00000
30	0.00000	80	0.00000
31	0.00000	81	0.00000
32	0.00000	82	0.00000
33	.00741	83	0.00000
34	0.00000	84	0.00000
35	0.00000	85	0.00000
36	0.00000	86	0.00000
37	0.00000	87	0.00000
38	0.00000	88	0.00000
39	0.00000	89	0.00000
40	0.00000	90	0.00000
41	0.00000	91	0.00000
42	0.00000	92	0.00000
43	0.00000	93	0.00000
44	0.00000	94	0.00000
45	0.00000	95	0.00000
46	0.00000	96	0.00000
47	0.00000	97	0.00000
48	0.00000	98	0.00000
49	0.00000	99	0.00000
50	0.00000	100	0.00000

EQUAL AREA PROJECTION OF OBSERVATIONS TO
UPPER HEMISPHERE



THERE ARE 135 OBSERVATIONS IN THE SAMPLE.

LEVEL PLOT



THE UPPER HEMISPHERE IS DIVIDED INTO 100 PATCHES OF EQUAL AREA. THE DENSITY OF EACH PATCH IS PRINTED AT THE PROJECTED MIDPOINT OF THE PATCH.

STATISTICAL ANALYSIS OF CLUSTERS

CLUSTER NUMBER 1

NUM	AZIMUTH	INCLINATION	L	M	N
1	12.00	90.00	.9781	.2079	.0000
2	14.00	88.00	.9697	.2418	.0349
3	15.00	82.00	.9565	.2563	.1392
4	15.00	86.00	.9636	.2582	.0698
5	15.00	90.00	.9659	.2588	.0000
6	17.00	89.00	.9562	.2923	.0175
7	19.00	87.00	.9442	.3251	.0523
8	19.00	89.00	.9454	.3255	.0175
9	19.00	90.00	.9455	.3256	.0000
10	20.00	90.00	.9397	.3420	.0000
11	20.00	90.00	.9397	.3420	.0000
12	21.00	90.00	.9336	.3584	.0000
13	22.00	80.00	.9131	.3689	.1736
14	23.00	87.00	.9192	.3902	.0523
15	24.00	83.00	.9067	.4037	.1219
16	24.00	84.00	.9085	.4045	.1045
17	24.00	86.00	.9113	.4057	.0698
18	24.00	86.00	.9113	.4057	.0698
19	24.00	87.00	.9123	.4062	.0523
20	24.00	87.00	.9123	.4062	.0523
21	24.00	88.00	.9130	.4065	.0349
22	24.00	89.00	.9134	.4067	.0175
23	25.00	85.00	.9029	.4210	.0872
24	25.00	88.00	.9058	.4224	.0349
25	26.00	89.00	.8987	.4383	.0175
26	27.00	86.00	.8888	.4529	.0698
27	27.00	86.00	.8888	.4529	.0698
28	29.00	82.00	.8661	.4801	.1392
29	30.00	82.00	.8576	.4951	.1392
30	30.00	87.00	.8648	.4993	.0523
31	30.00	87.00	.8648	.4993	.0523
32	31.00	87.00	.8560	.5143	.0523
33	32.00	84.00	.8434	.5270	.1045
34	32.00	85.00	.8448	.5279	.0872
35	32.00	90.00	.8480	.5299	.0000
36	33.00	87.00	.8375	.5439	.0523
37	33.00	88.00	.8382	.5443	.0349
38	40.00	85.00	.7631	.4403	.0872
39	10.00	92.00	.9842	.1735	.0349
40	13.00	90.00	.9744	.2250	.0000
41	16.00	96.00	.9560	.2741	.1045
42	17.00	94.00	.9540	.2917	.0698
43	17.00	92.00	.9557	.2922	.0349
44	18.00	96.00	.9458	.3073	.1045
45	20.00	97.00	.9327	.3395	.1219
46	20.00	92.00	.9391	.3418	.0349
47	21.00	90.00	.9336	.3584	.0000
48	23.00	100.00	.9065	.3848	.1736
49	23.00	95.00	.9170	.3892	.0872
50	23.00	95.00	.9170	.3892	.0872
51	24.00	92.00	.9130	.4065	.0349
52	25.00	94.00	.9041	.4216	.0698

53	26.00	97.00	.8921	.6351	-.1219
54	26.00	94.00	.8966	.4373	-.0698
55	26.00	92.00	.8982	.4381	-.0349
56	26.00	90.00	.8989	.4384	.0000
57	27.00	94.00	.8888	.4529	-.0698
58	27.00	90.00	.8910	.4540	.0000
59	28.00	98.00	.8744	.4649	-.1392
60	28.00	94.00	.8808	.4683	-.0698
61	29.00	95.00	.8713	.4830	-.0872
62	30.00	90.00	.8660	.5000	.0000
63	31.00	95.00	.8539	.5131	-.0872
64	31.00	93.00	.8560	.5143	-.0523
65	32.00	100.00	.8352	.5219	-.1736
66	32.00	93.00	.8469	.5292	-.0523
67	35.00	94.00	.8172	.5722	-.0698
68	36.00	92.00	.8085	.5874	-.0349
69	39.00	90.00	.7771	.6293	.0000
TOTALS			62.1147	28.5614	.1399

NUMBER OBS 69

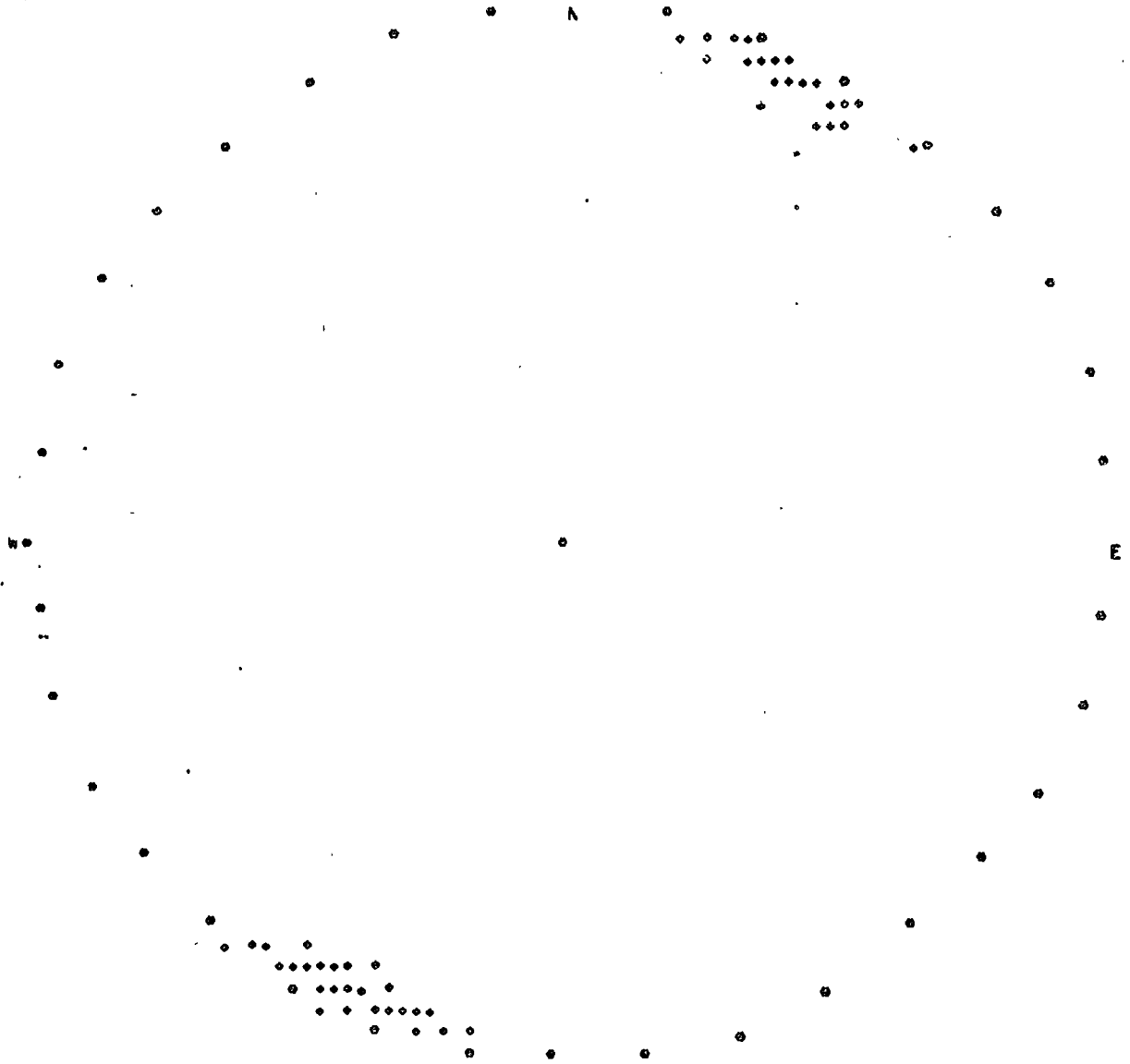
R = .68.367

*** CLUSTER STATISTICS ***

T, AZIMUTH 24.64 DEG
P, INCLINATION 89.80 DEG
K, PRECISION 108.96
A, RADIUS OF CONE OF CONFID 1.65 DEG

CONF. LIMITS
DIP +- 1.65
AZ +- 1.65

POINTS BELONGING TO CLUSTER NUMBER 1



DIRECTION COSINES OF THE MEAN
L = .9086 M = .4178 N = .0020

RING	SECTOR	ACT SECTOR FREQ	THEOR SECT FREQ
1	1	13.000	11.282
1	2	8.000	11.282
1	3	12.000	11.282
1	4	10.000	11.282
2	1	3.000	3.903
2	2	6.000	3.903
2	3	3.000	3.903
2	4	6.000	3.903
3	1	2.000	1.350
3	2	0.000	1.350
3	3	1.000	1.350
3	4	2.000	1.350
4	1	1.000	.467
4	2	1.000	.467
4	3	0.000	.467
4	4	1.000	.467

DEG. FREEDOM = 13

CHI SQUARE = 8.435

TH. CHI SQ. 95% = 22.351

PSI MAX = 16.047 DEG.

CLUSTER NUMBER NUM	2 AZIMUTH	INCLINATION	L	M	N
1	103.00	86.00	-.2244	.9720	.0698
2	103.00	90.00	-.2250	.9744	.0000
3	105.00	85.00	-.2578	.9623	.0872
4	106.00	83.00	-.2736	.9541	.1219
5	108.00	89.00	-.3090	.9509	.0175
6	109.00	90.00	-.3256	.9455	.0000
7	110.00	90.00	-.3420	.9397	.0000
8	111.00	81.00	-.3540	.9221	.1564
9	111.00	81.00	-.3540	.9221	.1564
10	111.00	86.00	-.3575	.9313	.0698
11	112.00	83.00	-.3718	.9203	.1219
12	112.00	89.00	-.3745	.9270	.0175
13	114.00	88.00	-.4065	.9130	.0349
14	115.00	84.00	-.4203	.9013	.1045
15	115.00	88.00	-.4224	.9058	.0349
16	117.00	85.00	-.4523	.8876	.0872
17	117.00	90.00	-.4540	.8910	.0000
18	118.00	80.00	-.4623	.8695	.1736
19	118.00	81.00	-.4637	.8721	.1564
20	119.00	83.00	-.4812	.8681	.1219
21	119.00	83.00	-.4812	.8681	.1219
22	119.00	84.00	-.4822	.8698	.1045
23	119.00	90.00	-.4848	.8746	.0000
24	120.00	80.00	-.4924	.8529	.1736
25	120.00	84.00	-.4973	.8613	.1045
26	120.00	86.00	-.4988	.8639	.0698
27	121.00	83.00	-.5112	.8508	.1219
28	121.00	83.00	-.5112	.8508	.1219
29	121.00	87.00	-.5143	.8560	.0523
30	122.00	84.00	-.5270	.8434	.1045
31	124.00	84.00	-.5561	.8245	.1045
32	124.00	87.00	-.5584	.8279	.0523
33	125.00	85.00	-.5714	.8160	.0872
34	125.00	90.00	-.5736	.8192	.0000
35	128.00	83.00	-.6111	.7821	.1219
36	128.00	87.00	-.6148	.7869	.0523
37	129.00	83.00	-.6246	.7714	.1219
38	130.00	88.00	-.6424	.7656	.0349
39	132.00	82.00	-.6626	.7359	.1392
40	132.00	88.00	-.6687	.7427	.0349
41	132.00	89.00	-.6690	.7430	.0175
42	103.00	90.00	-.2250	.9744	.0000
43	106.00	90.00	-.2756	.9613	.0000
44	110.00	90.00	-.3420	.9397	.0000
45	112.00	95.00	-.3732	.9237	-.0872
46	112.00	93.00	-.3741	.9259	-.0523
47	117.00	91.00	-.4539	.8909	-.0175
48	118.00	94.00	-.4683	.8808	-.0698
49	125.00	94.00	-.5722	.8172	-.0698
50	126.00	94.00	-.5864	.8070	-.0698
51	127.00	96.00	-.5985	.7943	-.1045
52	129.00	90.00	-.6293	.7771	.0000
53	135.00	90.00	-.7071	.7071	.0000
54	135.00	90.00	-.7071	.7071	.0000
55	136.00	90.00	-.7193	.6947	.0000
TOTALS			-26.1170	47.4379	2.8023

NUMBER ORS 55

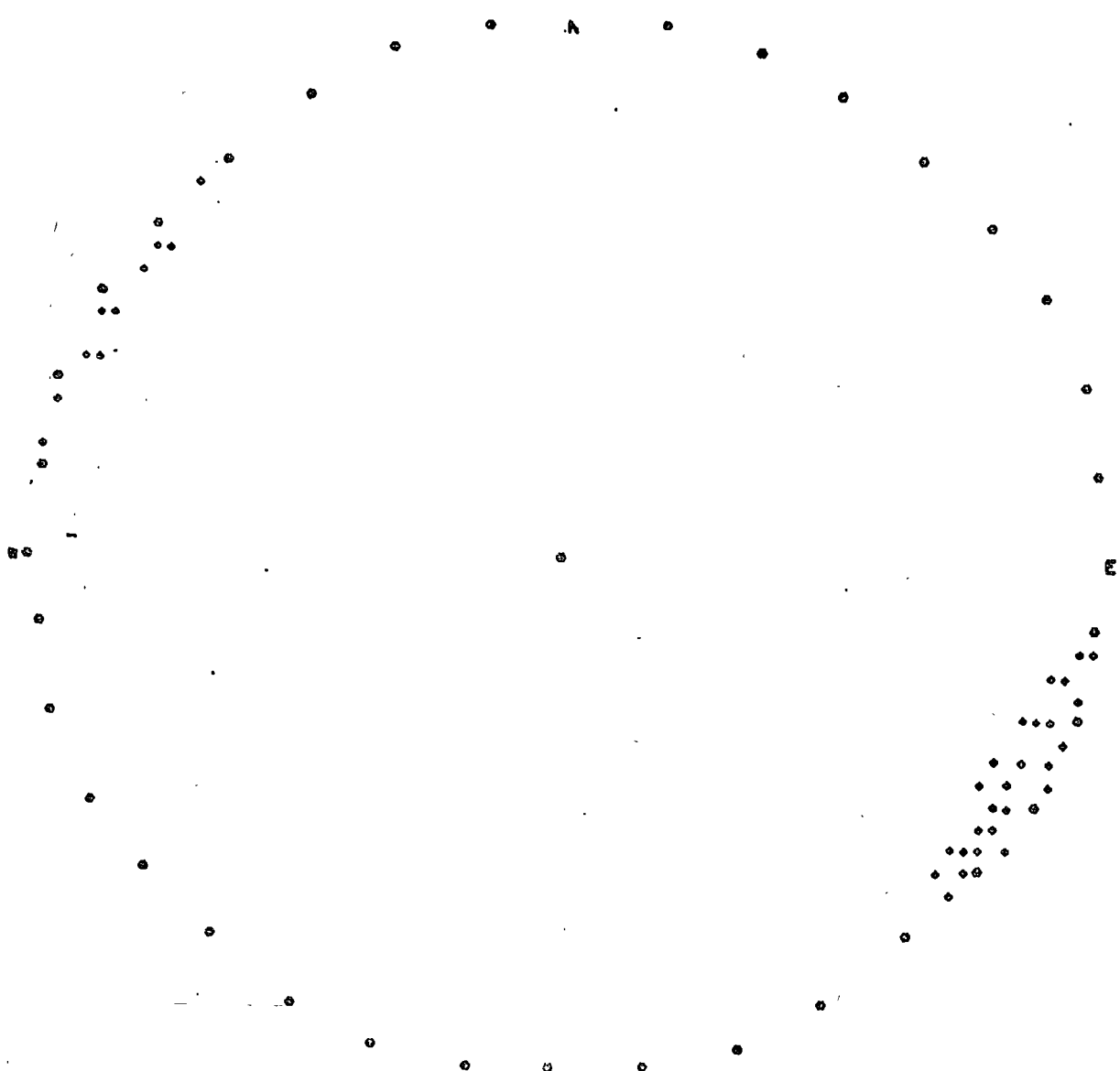
R = 54.225

*** CLUSTER STATISTICS ***

T: AZIMUTH 118.84 DEG
 P: INCLINATION 87.04 DEG
 K: PRECISION 70.93
 A: RADIUS OF CONE OF CONFID 2.30 DEG

CONF. LIMITS
 DIP +- 2.30
 AZ +- 2.30

POINTS BELONGING TO CLUSTER NUMBER 2



DIRECTION COSINES OF THE MEAN
L = -.4816 M = .8748 N = .0517

RING	SECTOR	ACT SECTOR FREQ	THEOR SECT FREQ
1	1	2.000	7.668
1	2	13.000	7.668
1	3	6.000	7.668
1	4	6.000	7.668
2	1	5.000	3.394
2	2	3.000	3.394
2	3	2.000	3.394
2	4	6.000	3.394
3	1	2.000	1.506
3	2	1.000	1.506
3	3	2.000	1.506
3	4	1.000	1.506
4	1	3.000	.668
4	2	0.000	.668
4	3	1.000	.668
4	4	2.000	.668

DEG. FREEDOM = 13
 CHI SQUARE = 24.288
 TH. CHI SQ. 95 = 22.351
 PSI MAX = 17.411 DEG.



centro de educación continua
división de estudios superiores
facultad de ingeniería, unam



MECANICA DE ROCAS APLICADA A LA MINERIA

INFLUENCE OF ROCK FRACTURES AND BLOCK BOUNDARY
WEAKENING ON CAVABILITY

M. A. MAHTAB AND J. D. DIXON

ABRIL, 1978.

Influence of Rock Fractures and Block Boundary Weakening on Cavability

by M. A. Mahtab and J. D. Dixon

The results of a parametric study of the influence of natural features (stress field, rock strength, and strength and orientation of fractures) as well as the influence of induced features (undercut span, boundary slot, and other boundary-weakening measures) on the cavability of an undercut block of ore in mining by the block-caving method are presented. The two-dimensional finite-element analysis technique was used for this study. A coarse "mesh," along with linear homogeneous assumptions for rock properties, was used to model the problem of initiation of caving in a block of ore. Interpretation of the test results suggests that weakening the "abutments" of the block as well as certain orientations of natural fractures exercise significant influence on cavability. These findings hold promise for immediate application to known situations in block-caving mines.

A host of geometric, geologic, and physical parameters are recognized to contribute to the caving performance (cavability) of rock mass in undercut mining by block caving. Bucky¹ recognized that "the ability of a block to cave or fragment is a function of its strength in tension or shear and the value of applied forces." King² related the caving characteristics of the Climax ore body to rock type as well as to fracture spacing and mineralization. King classified the cavability of rocks in the Climax ore body as very strong, moderately strong, moderately weak, and very weak. Kendrick³ concluded that "the cavability of a given ore body is based on its minimum dimension in the horizontal plane." McMahon and Kendrick⁴ related cavability of ores to modified core recovery (sometimes referred to as RQD) and the average quantity of secondary blasting. Obert et al.⁵ suggested seismic absorption as an indicator of cavability. Swaisgood et al.⁶ tabulated prominent geologic and physical features of seven selected block-cave mines. An examination of their Table 1 shows that, in five of the six "good to excellent caving" cases, the ore was jointed. In addition, some boundary-weakening measures were applied in four of the six cases.

Although there is a unanimous recognition among investigators and mine operators that rock fractures are important for successful caving of ore bodies, there has been a general lack of quantitative relationships between the characteristics of fracture systems (geometry, mechanical properties) and cavability of rock mass.

Another feature of the mechanics of caving deserves increased attention, namely that a lack of lateral confinement (for the caving block) is necessary to insure ease in caving rock masses by the block-caving mining method. Removal of lateral confinement is a measure that is commonly applied through some kind of boundary-weakening operation (for instance, corner raises in combination with long holes for presplitting). Kendrick³ gives an excellent account of induction caving through boundary weakening.

The objectives of this paper is to emphasize the influence of two critical factors in caving rock masses by the undercut (block) caving method, namely (1) the influence of low-angle (0° to 30° dip) fractures and (2) the influence of block boundary weakening.

The observations which led to an examination of the influence on cavability of several natural and induced (man-made) features are discussed in the section on "preliminary considerations." The results of a parametric study (with respect to the various features influencing cavability) of a hypothetical undercut block are presented in the section on "analysis of an example caving block." The subsequent sections of the paper present discussion of results, conclusions, and recommendations.

Preliminary Considerations

The existence of favorably inclined, closely spaced fractures having low resistance to in-plane shear stresses is important for caving ore bodies. The US Bureau of Mines (USBM) has developed procedures for sampling, mapping, and analysis of the geometry of rock fractures.^{7,8} These procedures have been applied to the analysis of the geometry of fractures in Magma Copper Co.'s San Manuel mine in Arizona.⁹ An example of the nearly orthogonal fracture system from a panel drift at the 2015 level of the San Manuel mine is shown in Fig. 1



Fig. 1—Typical nearly orthogonal fracture system in 2015 level, San Manuel mine.

M. A. MAHTAB and J. D. DIXON, Members SME, are with Acres Consulting Services Ltd., Niagara Falls, Canada and Spokane Mining Research Center, U.S. Bureau of Mines, Spokane, Wash., respectively. SME Preprint, 75AM9, AIME Annual Meeting, New York, Feb. 1975. Manuscript, Sep. 13, 1974. Discussion of this paper, submitted in duplicate prior to Jun. 15, 1976, will appear in SME Transactions, September 1976, and in AIME Transactions, 1976, Vol. 260.

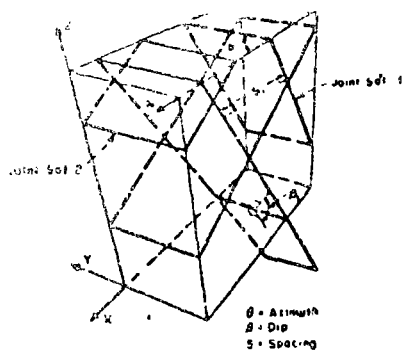


Fig. 2—Principal geometric parameters of fracture sets.

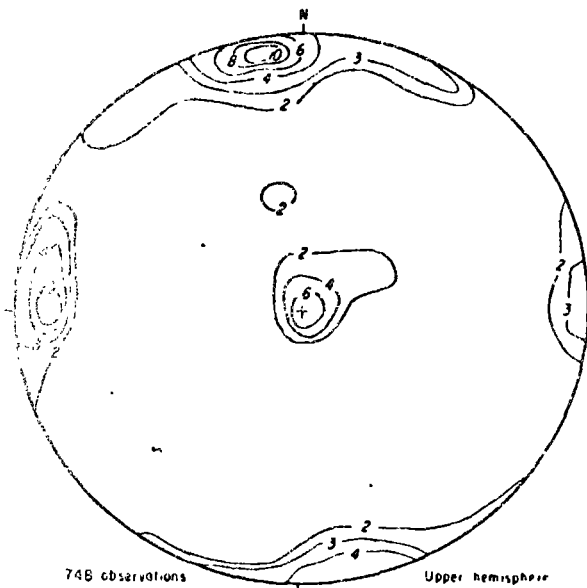


Fig. 3—Typical polar equal area projection of San Manuel fractures. The numbers on the contours represent percentages of observations.

Illustrative definitions of the principal geometric parameters of fracture sets (azimuth, dip, and spacing) are given in Fig. 2. Typical Schmidt plots of fracture orientations from a study area in San Manuel are shown in Fig. 3. These "level plots" represent the concentrations

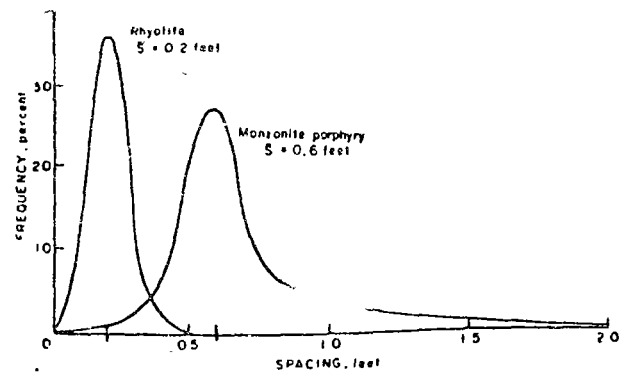


Fig. 4—Plot of spacing vs. frequency for one of three fracture sets at San Manuel mine.

of data points (normals to the fracture planes) in a polar equal-area projection of the upper hemisphere. Three nearly orthogonal sets can be seen in the figure; one is a nearly horizontal set and two are nearly vertically dipping sets). An example plot of the spacing vs. frequency of spacing for one of the three fracture sets observed in rhyolite and monzonite porphyry at the 2015 level, San Manuel, is shown in Fig. 4.

As part of a USBM study of the influence of jointing on cavability conducted in San Manuel mine, three prominent orthogonal fracture sets were delineated in two of the three principal rock types (quartz monzonite and monzonite porphyry). However, only two fracture sets, both vertical, were found to be present in the third rock type (rhyolite). The inference of this study was that the absence of the horizontal set in rhyolite contributed in part to the generally observed strong resistance of rhyolite to caving. It must be noted that the average spacing of the two vertical sets of fractures in rhyolite was smaller than the average spacing for quartz monzonite and monzonite porphyry, see Fig. 4 and Table 1, (also see Fig. 12 in Ref. 9). In addition, the RQD for rhyolite was less than 20%.

The USBM also analyzed the fracture patterns in another mine (Mine B, Table 1). Three prominent sets of fractures, all having nearly vertical dips, were delineated in a study block in this mine. The block was found too hard to cave despite some attempts to weaken the

Table 1. Observations of Some Physical and Geologic Features in Two Block-Cave Mines

	Mine*	
	A	B
Depth of Overburden, Ft	1600-1700	1400-1500
Estimated Ratio of Lateral/Vertical Rock Stresses	$\frac{1}{4}$	1
Principal Ore/Rock	<ol style="list-style-type: none"> 1. Quartz Monzonite (QM) 2. Monzonite Porphyry (MP) 3. Rhyolite (Rh) 	Similar to rock types 1 and 2 of mine A.
Fracture Orientations Strike/Dip, Degree	<ol style="list-style-type: none"> 1. N83E/87NW; N42W/89NE; N03E/22SE. 2. N60E/87NW; N20W/87SW; N23E/26SE. 3. N70E/87NW; N48W/85NE. 	3 prominent sets striking N60W, N30E, N30W and dipping nearly vertically
Fracture Spacing, Ft	<ol style="list-style-type: none"> 1. 0.6-0.7 2. 0.6-0.6 3. 0.2 	0.1-2.5 Average: 0.5
Caving Characteristics (V. Strong, Mod. Strong, Mod. Weak, & V. Weak)	<ol style="list-style-type: none"> 1. Mod Weak-V. Weak 2. V. Weak 3. V. Strong 	Mod. Strong-V. Strong
Remarks	No boundary weakening required; low lateral stress; low-angle fractures in QM & MP; Rh lacks low-angle fractures; angle of int. friction for fractures = 35°	Some boundary weakening applied; high lateral stress; absence of low-angle fractures; angle of int. friction for fractures = 35°

* Mine A represents blocks at 2015 level, San Manuel mine, Magma Copper Co., Ariz.; Mine B does not wish to be identified.

† Stress ratio at Mine A assumed to equal $\frac{p}{1-p}$, for Poisson's ratio $\nu \approx 0.2$ (Ref. 17, Table 18); stress ratio at Mine B based on one observation of horizontal stress (of 1400 psi) and assumption of 1500 psi vertical stress at 1500 ft depth.

‡ King's classification, see Ref. 2.

corners of the block. A preliminary inference of the study was that the combined effect of high lateral ground stress and a general absence of low-angle fractures (i.e., with dips less than 30°) resulted in the poor cavability of this block. The observations of the physical and geological features made by the USBM in the two aforementioned mines are summarized in Table 1. Another example of the influence of low-angle fractures on cavability can be found in the Climax ore body. A summary of the geometry of Climax fractures was presented by Kendorski¹¹ who showed that most fractures in the Climax ore body dip easterly at 40° to 60°, or shallower. Kendorski¹¹ maintains that the low-angle fractures (with close spacing) are "very important to initiating caving in a block or panel." Furthermore, "the vertical scarps at Climax's caving boundary are in the country rock [that has] a much less developed low-angle fracture pattern."

Low-angle fractures in combination with steeply dipping fractures provide brick-shaped fragments of ore and facilitate vertical movement of these fragments. The potential for vertical movement, lateral expansion, and rotation of fragments of a systematically fractured ore body (one having one vertical and one horizontal set of fractures in a two-dimensional model) is illustrated in Fig. 5, after Goodman et al.¹² (p. 648), who modeled an experiment made by Trollope.¹³

In addition to quantifying the geometric characteristics of fracture systems, it is necessary to measure the mechanical properties (strength and deformability) of fractures in order to make rational judgments as to the cavability of a given rock mass. The strength of fractures can be obtained by testing fracture specimens in a direct shear machine, and the results of these tests can be plotted as strength envelopes in the manner of Fig. 6. The simplified bilinear strength envelope of Fig. 6 derives from the experiments reported by Patton¹⁴. At low normal stresses (σ_n), the shear strength (τ) of the rough fracture (with its asperities inclined at angle i to the average joint surface) is given by

$$\tau = \tan(\phi_j + i). \quad (1)$$

However, in the range of high normal stresses when most of the asperities have been sheared off, the residual strength of the fracture is given by

$$\tau = C_j + \sigma_n \tan \phi_j \quad (2)$$

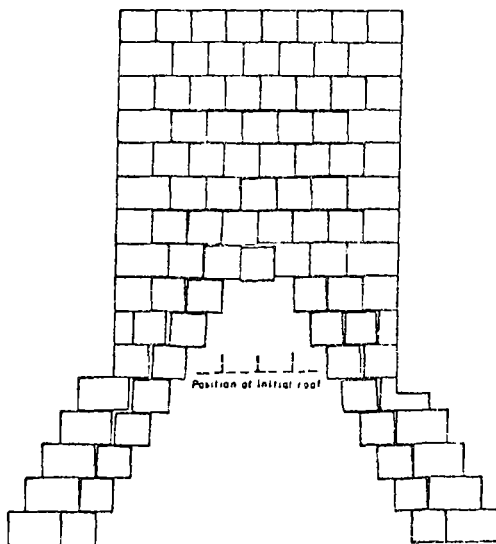


Fig. 5—Caving or collapse of initial roof in a systematically fractured medium (from Goodman et al.¹²).

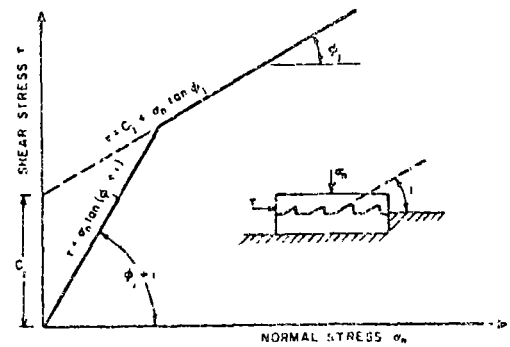


Fig. 6—Bilinear strength envelope for rough joints (from Patton¹⁴).

where ϕ_j represents the angle of residual sliding resistance (of the sheared fracture) and C_j represents the cohesion of the rough fracture. In-situ measurements of elastic modulus of fractured rock mass can be made through borehole pressure cells;¹⁵ an example plot of results is given in Fig. 7 which shows the deterioration in the rock modulus as the fracture spacing decreases. An example of this deterioration of rock modulus can be seen in presplitting, or mass boundary weakening (discussed in the next section), whereby the modulus of rock along the edges of an undercut block is reduced.

The existence of favorably inclined, closely spaced fractures having low resistance to shear is important in influencing cavability of ore bodies. However, fractures alone are not sufficient to initiate caving of an undercut block. This observation stems from the laboratory results made by Brown et al.¹⁶ on a jointed block of rock having two perpendicular sets of joints (see Fig. 8). The results of their tests, Fig. 9, show that (1) at low confining pressures, the strength of the jointed specimen is a small fraction of the strength of the intact rock with the lowest strength corresponding to the two fracture dips of 30° and 60°; and (2) at high lateral (or confining) pressure the strength of jointed specimens increases to nearly the level of strength of intact specimens subjected to the same stress conditions. These tests support the observation that a combination of favorable fracture patterns and lack of lateral confinement is necessary for ease in caving of undercut blocks of ore bodies.

Analysis of an Example Caving Block

This section will present a table of the physical and geological features influencing cavability, outline the scope of the analyses performed, introduce the method of analysis used, and present the results of the analyses.

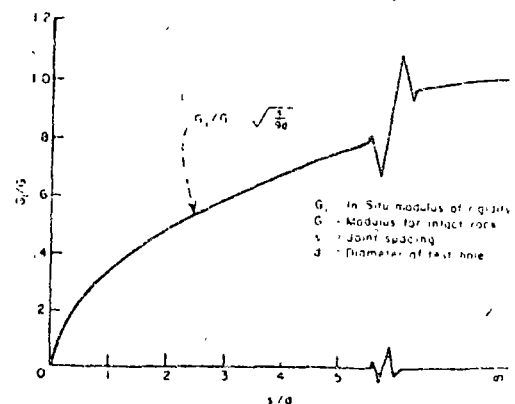


Fig. 7—Effect of spacing on in-situ modulus of fractured rock (from Panek¹⁵).

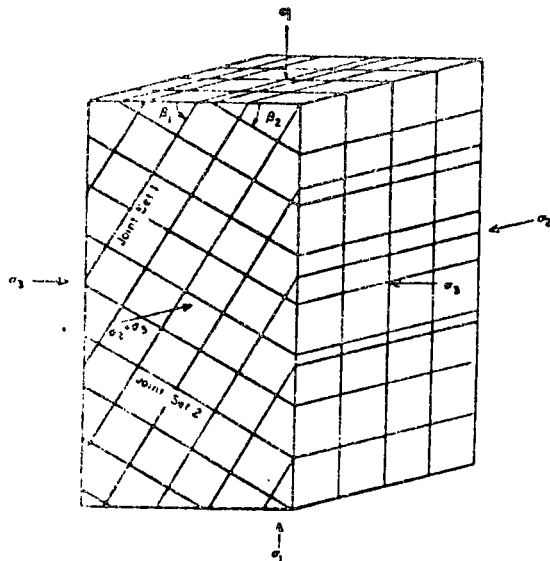


Fig. 8—Geometry of block-jointed sample for triaxial strength (from Brown and Trollope¹⁰); see Fig. 9 for results.

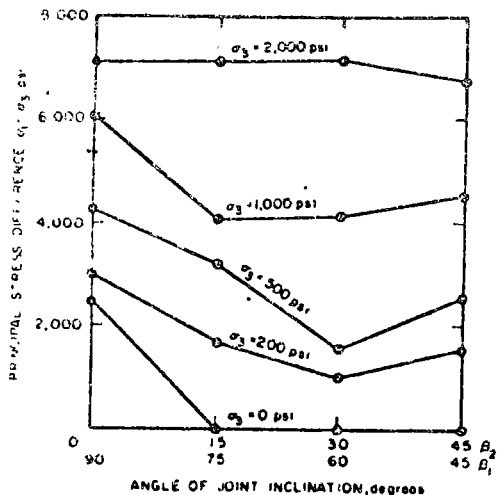


Fig. 9—Variation of peak principal stress difference with angle of joint inclination (from Brown and Trollope¹⁰).

On the basis of the observations made in the previous sections of the paper, the principal physical and geological features influencing cavability of ore bodies in an undercut mining situation can be enumerated as in Table 2.

The analyses of the influence of natural as well as induced features are restricted to the initiation of caving in an undercut block of ore. The effects on cavability of time and of procedures for drawing the caved ore are beyond the scope of the paper; considerations of support of development openings are also excluded.

Table 2. Features Influencing Cavability

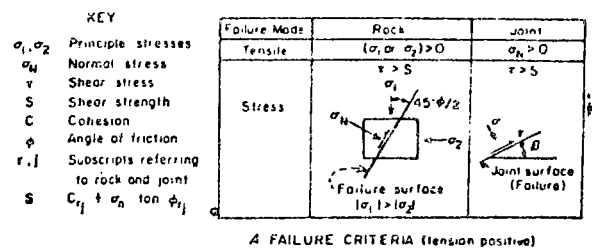
Natural Features	Induced Features
1. In-situ stress field (ratio of vertical to horizontal stress)	1. Undercut span
2. Rock strength	2. Boundary slot (vertical slots excavated at two edges of block)
3. Geometry of fractures	3. Mass boundary weakening (reduction in rock strength along two edges of block by presplitting)
4. Strength of fractures	

The precise mechanism which controls the process of caving has, as yet, not been subjected to either analytical or experimental modeling. Physical measurements made in block-caving mines have also failed to provide sufficient information to explain the caving phenomenon. Consequently, there is no definitive analysis or test which indicates whether a given block of ore will or will not cave. It is widely thought, however, that the two basic types of rock failure—by tension and by shearing—are involved in the caving process. If this concept of failure is accepted, the caving tendency of an ore block can be evaluated by examining the tensile and shear stress zones which develop above the undercut slot. This evaluation can be achieved by comparing the intensity and distribution of tensile and shear stresses with the corresponding strengths of the rock mass. This is the approach followed by the authors in making a parametric study of the influence on cavability of the various features listed in Table 2.

The analyses presented here are derived from the applied loading as well as the geometric and strength properties of rock mass in a block of ore located 1000 ft below the ground surface. A vertical stress of 165,000 psf is assumed at this depth. The design features of the block consist of widening the undercut slot, introduction of vertical boundary slots of various heights, introduction of mass boundary weakening (in a strip of rock around the boundary slot) by use of drilling and blasting holes, and hydraulic fracturing through boreholes or some other means. The geometric configuration of the hypothetical block studied herein is shown in Fig. 10 which also gives definitions of the mechanical parameters used in the various analyses.

The finite element method of analysis was used for the parametric study of the influence of the various features of Table 2 on cavability of an undercut block of ore. This method was found particularly suited to dealing with the complex geometry involved in the analyses. For each analysis condition, stresses were determined throughout the area influenced by the excavated slots. From these stresses, the distribution, orientation, and intensity of tensile and shear stresses (in the rock mass) were determined prior to locating the potential zones of tensile and shear failure.

Several simplifications were effected to reduce the difficulty and cost of obtaining results by the finite element analysis. A two-dimensional, plane strain formu-



- W Width of undercut slot
- H Height of boundary weakening slots
- h Height of undercut slot.
- W/h, aspect ratio of undercut slot
- β Joint dip angle, degrees
- w Width of mass-weakened boundary strip
- P Vertical field stress
- Q Horizontal field stress

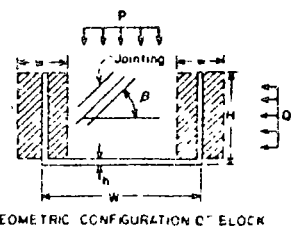


Fig. 10—Definition of Mechanical and geometrical analysis parameters.

lation was used for modeling the problem. The rock mass was considered to be homogeneous, isotropic, and linearly elastic. A coarse finite element mesh was also used to model the undercut caving configurations. Because of the use of a coarse mesh and the idealized assumptions about the properties of the rock mass, the computed stresses in the immediate neighborhood of the (geometrically acute) boundaries of the slots are not expected to be highly accurate. Note that localized stresses are of little interest in these analyses. Furthermore, the idealized conditions imposed during these analyses do provide a configuration of the problem which is suited to the parametric study described herein.

The results of the analyses are given in Fig. 11 through 17. These figures show the zones of tensile and shear failures caused by the presence in the undercut block of one or more of the features given in Table 2. The zones of tensile failure as shown in Fig. 12 and 14 to 17 were obtained by drawing dashed lines normal to the direction of tensile stresses at locations where they occurred (that is, at centers of the finite elements). Since the undercut block is symmetrical about its center line, only one half of the caving block is represented in the analysis and presentation of the results.

The zones of shear failure as indicated in Fig. 11 to 17 were determined through a more involved procedure. These zones delineate the locations in the undercut block where driving shear stresses exceeded shear strengths. The driving shear stresses were obtained from finite element analysis results. The shear strengths were determined by application of the Mohr-Coulomb failure law

$$S = C + \sigma_n \tan \phi. \quad (3)$$

The normal stress, σ_n , on the plane of shear was obtained from finite element analysis results, whereas the values of cohesion, C , and angle of friction, ϕ , were preassigned.

The zones of shear failure presented in Fig. 12 to 17 include the potential failure of intact rock as well as shear failure along fracture planes. Where failure of intact rock is involved, shear failure surface would be expected to be aligned at $\pm(45 - \phi/2)$ degrees from the direction of maximum compressive stress. Tensile fracturing would, however, occur normal to the direction of principal stresses. On fracture surfaces, shear failure would occur by sliding along the fracture, and tensile failure would occur normal to the direction of the fracture.

Unless otherwise noted, the following parameters were consistently used for the various analyses: vertical field stress = 165,000 psf; P/Q , or the ratio of vertical to horizontal field stress = 3; R , the ratio of undercut width to undercut height = 30; height of boundary slot = 120 ft; rock strength, $\phi_r = 45^\circ$, $C_r = 0$; and fracture strength, $\phi_f = 20^\circ$, $C_f = 0$.

Discussion of Results

As evidenced from Fig. 11, the effect of a reduction in lateral confinement from a P/Q of 1 (hydrostatic stress field) to a P/Q of 3 is to shift the shear zone from directly above the undercut slot to the edges (abutments) of the block. At the same time, the shape of the shear failure zone is changed and the total volume of rock affected is increased. The effect on tensile failure zone (although not shown) was also significant; the tensile failure zone occupied areas above the undercut slot (as shown in Fig. 12a).

The influence of slot width, in terms of the ratio, R , of the width and height of undercut slot, is shown in Fig. 12. Several-fold increases occurred in the volume of rock under conditions of both tensile and shear failure when R was increased from 5 to 30. The influence of an

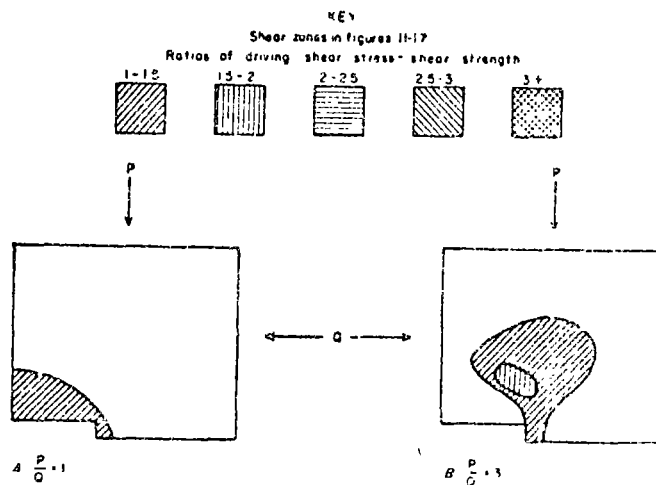


Fig. 11—Influence of lateral confinement on shear zone.

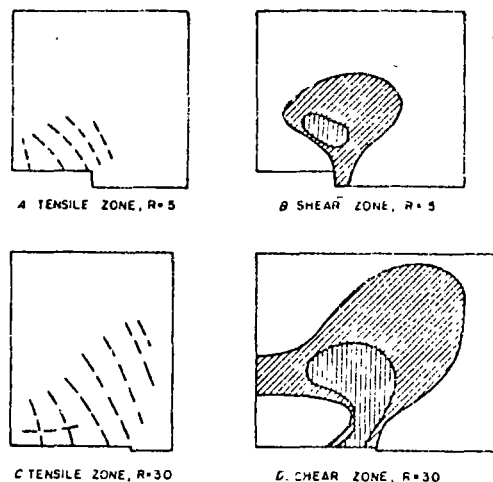


Fig. 12—Influence of undercut slot width on extent of tensile and shear zones ($R = \text{width/height of slot}$).

increase in slot width on cavability, as shown in Fig. 12, is in agreement with the conclusion of Kendrick.⁹

The influence of rock strength, in terms of the angle of internal friction ϕ_r , is consistent with engineering experience and judgment in that, as shown in Fig. 13, there is a progressive increase in the total volume of rock sheared as the value of ϕ is decreased.

A marked influence of the height, H , of the boundary slot on tensile failure zones in the undercut block is shown in Fig. 14. As mentioned earlier, the dashed lines in Fig. 14A, 14C and 14E, are drawn normal to the direction of tensile stresses in the rock elements. It may be noted that the difference in the volume of rock under tension is more dramatic between the cases $H = 0$ and $H = 120$ ft than between the cases $H = 120$ ft and $H = 200$ ft. However, no attempt was made to determine an optimum height for the boundary slot. We note that, ordinarily, intact rock is capable of withstanding some tension. However, in practically all block-caving situa-

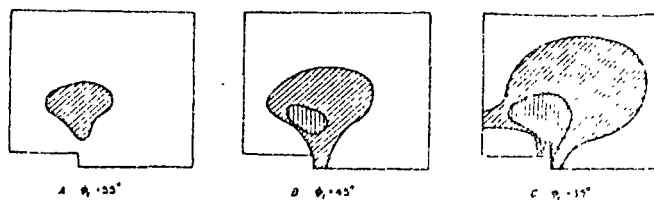


Fig. 13—Influence of rock strength on shear zones, $R = 5$.

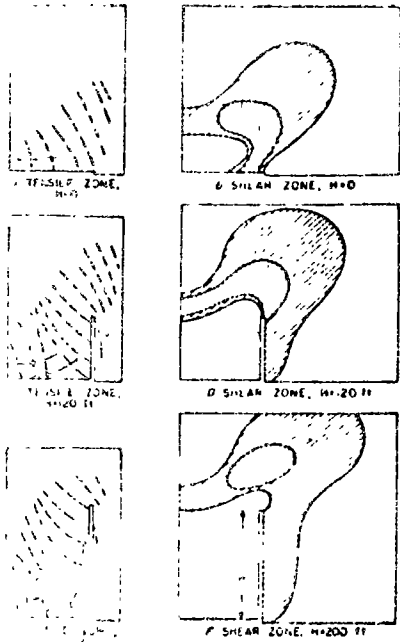


Fig. 14—Influence of height (H) of boundary slot on tensile and shear zones.

view of increased cavability. A dramatic increase occurred in the extent of both tensile and shear failure zones when the mass boundary weakening (that is, reduction in the modulus of the rock) was applied to strips of rock on both sides of the boundary slot (Figs. 15A and 15B). The increase in volume of tensile and shear zones for the case of "full" mass boundary weakening was approximately 30%. Tensile zones were further extended into the "roof" above the undercut slot. These results indicate that the caving tendency of a block of ore can be enhanced more by presplitting toward the abutments than by presplitting toward the block. In effect, the mass boundary weakening of the block abutments tends to lengthen the effective "span" of the block, which is a desirable feature in inducing caving.

The influence of orientation of fractures on the size and shape of the tensile and shear failure zones is shown in Figs. 16 and 17. Fig. 16 compares the influence of low-angle fractures (having dips of 0° , 15° , and 30°) on the failure zones. The shear zones are seen to be highly sensitive to the dip of low-angle fractures. The horizontal fractures are shown to exercise the most pro-

ductive geologic discontinuities permeate the rock mass. Therefore, the assumption made here, that fractures in rock mass cannot withstand tension, is reasonable. The influence of increasing the height of the boundary slot was less pronounced for shear failure zone than for the tensile failure zone. The shear zone, however, encompasses a larger volume of rock (with the boundaries of the zone shifted upward and farther back into the abutments of the block) as the height of the boundary slot is increased.

The influence of mass boundary weakening on development of tensile and shear failure zones is shown in Fig. 15. A comparison of no mass boundary weakening (Figs. 15E and 15F) with partial weakening toward the block (Figs. 15C and 15D) shows a significant increase in the extent of the tensile failure zone due to partial mass boundary weakening. However, the shear failure zone failed to show any improvement from the point of

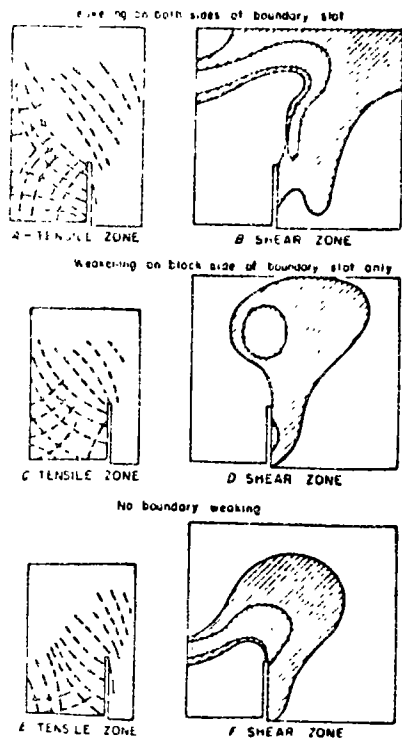


Fig. 15—Influence of mass boundary weakening on tensile and shear zones.

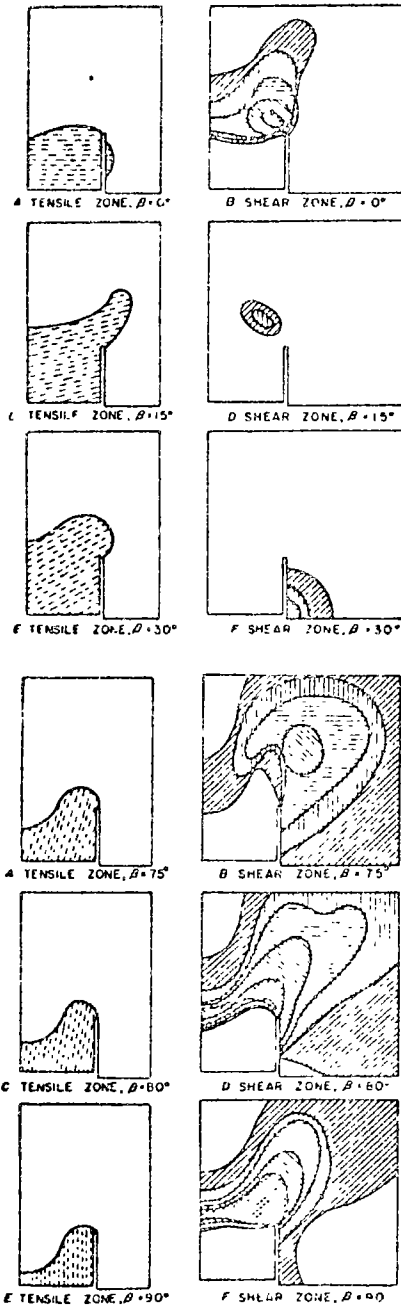


Fig. 16—Influence of low-angle fractures on tensile and shear zones.

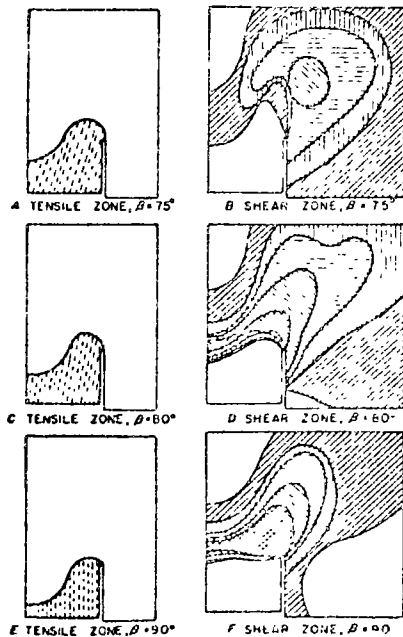


Fig. 17—Influence of nearly vertical fracture on tensile and shear zones.

nounced effect on shear failure. All low-angle fractures (Fig. 16) showed approximately the same effect on the tensile failure zone which encompassed the entire span of the undercut slot. However, the combined effect of shear and tensile failure is most pronounced for the horizontal fractures.

The influence on the failure zones developed above the undercut slot of nearly vertically dipping fractures (those having dips of 75°, 80°, and 90°) is shown in Fig. 17. The tensile zone is most pronounced for fractures dipping at 90°. The combined effect on tensile and shear zones is approximately the same for all the nearly vertical fractures.

Conclusions and Recommendations

Several steps can be taken in developing a mine to obtain optimum initial caving conditions. Natural features that exist in the ore body (stress field, rock strength, fracture orientation, and strength) can be exploited during the initiation of the caving process. If the horizontal stress field is not uniform, the cross section of the undercut slot can be oriented parallel to the minimum horizontal stress. Caving should ideally be initiated in the weakest portion of the ore body. This should provide mass boundary weakening on one side of additional blocks, thus reducing the total effort in continued caving of the ore body.

Other design features can be introduced to further optimize initial caving conditions. The introduction of a vertical boundary slot, especially in situations where the horizontal stress is a large fraction of the vertical stress, appears to be more effective than increasing the width of an undercut slot. This reduces or eliminates the horizontal stress field, a factor that greatly influences cavability. Furthermore, by introducing mass boundary weakening around the boundary slots, more favorable conditions for caving can be obtained. The most effective mass boundary weakening was created by blasting into the abutment side of the boundary slots. This effectively increased the span of the undercut slot causing greater zones of tensile stress to occur immediately above the slot and created extensive shear zones over the abutment areas of the slot where caving is normally expected to progress.

A combination of one low-angle (0° to 30° dip) set of fractures and another nearly vertical (75° to 90° dip) set of fractures is the most effective two-dimensional fracturing configuration for ease in cavability of an ore body.

In an actual three-dimensional situation, one set of low-angle fractures and two sets of nearly vertical fractures will be most effective in improving cavability.

Acknowledgments

The authors are indebted to James Swaisgood, Dames and Moore, and Douglas Bolstad and Brian Brady, Denver Mining Research Center, for their constructive reviews of the paper. Special thanks are due Sally Oslund, Michael Leidich, and David Tafoya, Denver Mining Research Center, for their assistance in computing and reducing the results of the analyses presented in this paper.

References

- ¹ Bucky, P.E., "Fundamental Considerations in Block Caving," *Quarterly of the Colorado School of Mines*, Vol. 51, No. 3, July 1956, pp. 129-146.
- ² King, R.V., "A Study of Geologic Structure at Climax in Relation to Mining and Block Caving," *Trans. AIME*, Vol. 163, 1945, pp. 145-155.
- ³ Kendrick, R., "Induction Caving of the Urad Mine," *Mining Congress Journal*, Oct. 1970, pp. 39-44.
- ⁴ McMahon, B.K., and Kendrick, R.F., "Predicting the Block Caving Behavior of Orebodies," SME-AIME Preprint No. 69-AU-51, presented at AIME Annual Meeting, Washington, D.C., Feb. 1969, 9 pp.
- ⁵ Obert, L., Munson, R., and Rich, C., "Caving Properties of the Climax Ore Body," Presented at the Annual AIME Intermountain Section Minerals Conference, Vail, Colo., Aug. 2, 1973. To be published in SME AIME Transactions.
- ⁶ Swaisgood, J.R., McMahon, B.K., and West, L.J., "Rock Mechanics in the Planning and Control of Block Caving," Joint-Meeting MMII-AIME, Tokyo, May 1972, Print No. T IIc2, 14 pp.
- ⁷ Bolstad, D.D., Alldredge, J.R., and Mahtab, M.A., "Procedures Used for Sampling Fracture Orientations in an Underground Coal Mine," RI 7763, US Bureau of Mines, 1973, 9 pp.
- ⁸ Mahtab, M.A., et al., "Analysis of Fracture Orientations for Input to Structural Models of Discontinuous Rock," RI 7669, US Bureau of Mines, 1972, 70 pp.
- ⁹ Mahtab, M.A., Bolstad, D.D., and Kendorski, F.S., "Analysis of the Geometry of Fractures in San Manuel Copper Mine, Arizona," RI 7715, US Bureau of Mines, 1973, 24 pp.
- ¹⁰ Kendorski, F.S., "Outline of Fracture Geology of the Climax Area," presented at 9th Annual Intermountain Minerals Conference, Vail, Colorado, Aug. 1973.
- ¹¹ Kendorski, F.S., Personal Communication, Aug. 5, 1974, Denver Mining Research Center, Denver, Colo.
- ¹² Goodman, R.E., Taylor, R.L., and Brekke, T.L., "A Model for the Mechanics of Jointed Rock," *Journal of Soil Mechanics and Foundations Division, American Society of Civil Engineers*, Vol. 94, No. SM3, May 1968, pp. 637-659.
- ¹³ Trollope, D.H., "The Stability of Trapezoidal Openings in Rock Masses," *Felsmechanik und Ingenieurgeologie*, Vol. 4, No. 5, 1966.
- ¹⁴ Patton, F.D., "Multiple Modes of Shear Failure in Rock," *Proceedings, 1st Congress International Society of Rock Mechanics*, Lisbon, Portugal, Vol. 1, 1966, pp. 509-513.
- ¹⁵ Panek, L.A., "Effect of Rock Fracturing on the Modulus as Determined by Borehole Dilatation Tests," *Proceedings, 2nd Congress International Society of Rock Mechanics*, Belgrade, Yugoslavia, Vol. 1, Paper 2-16, 1970, 5 pp.
- ¹⁶ Brown, E.T., and Trollope, D.H., "Strength of a Model of Jointed Rock," *Journal of Soil Mechanics and Foundations Division, American Society of Civil Engineers*, Vol. 96, No. SM2, March 1970, pp. 685-704.
- ¹⁷ Kendorski, F.S., "Influence of Jointing on Engineering Properties of San Manuel Mine Rock," MS Thesis, Dept. of Mining and Geological Engineering, Univ. of Arizona, 1971, 126 pp.





centro de educación continua
división de estudios superiores
facultad de ingeniería, unam



MECANICA DE ROCAS APLICADA A LA MINERIA

TEMA: EFECTO DEL AGUA EN LAS MASAS ROCOSAS.

Chapter 6 : Groundwater flow; permeability and pressure

Introduction

The presence of groundwater in the rock mass surrounding an open pit has a detrimental effect upon the mining programme for the following reasons:

- a) *Water pressure* reduces the stability of the slopes by reducing the shear strength of potential failure surfaces as described on pages 24 and 25. Water pressure in tension cracks or similar near vertical fissures reduces stability by increasing the forces tending to induce sliding (page 26).
- b) High *moisture content* results in an increased unit weight of the rock and hence gives rise to increased transport costs. Changes in moisture content of some rocks, particularly shales, can cause accelerated weathering with a resulting decrease in stability (page 33).
- c) *Freezing* of groundwater during winter can cause wedging in water-filled fissures due to temperature dependent volume changes in the ice. Freezing of surface water on slopes can block drainage paths resulting in a build-up of water pressure in the slope with a consequent decrease in stability.
- d) *Erosion* of both surface soils and fissure infilling occurs as a result of the velocity of flow of groundwater. This erosion can give rise to a reduction in stability and also to silting up of drainage systems.
- e) *Discharge* of groundwater into an open pit gives rise to increased operating costs because of the requirement to pump this water out and also because of the difficulties of operating heavy equipment on very wet ground.
- f) *Liquefaction* of overburden soils or waste tips can occur when water pressure within the material rises to the point where the uplift forces exceed the weight of the soil. This can occur if drainage channels are blocked or if the soil structure undergoes a sudden volume change as can happen under earthquake conditions.

Liquefaction is critically important in the design of tailings dams and waste dumps and it is dealt with in the references numbered 104 to 108 listed at the end of this chapter. It will not be considered further in this book since it does not play a significant part in controlling the stability of rock slopes.

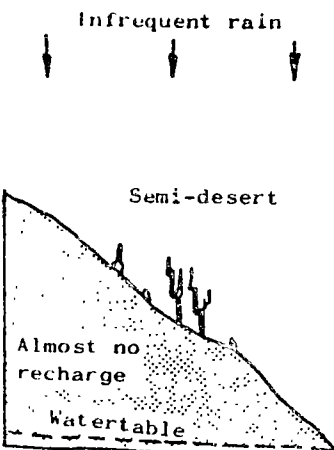
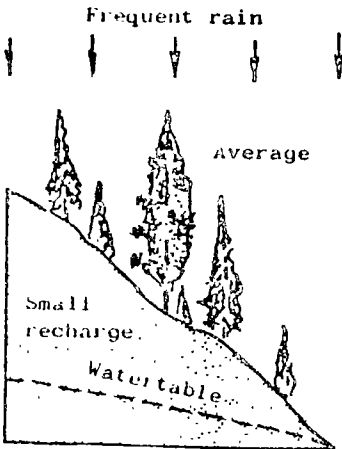
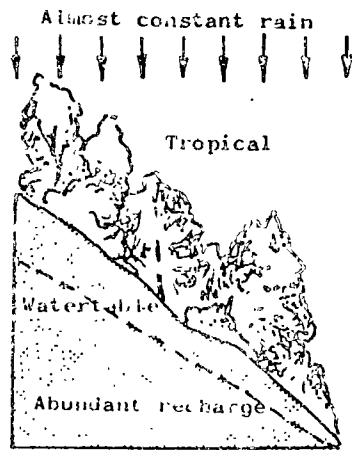
By far the most important effect of the presence of groundwater in a rock mass is the reduction in stability resulting from water pressures within the discontinuities in the rock. Methods for including these water pressures into stability calculations are dealt with in later chapters of this book. This chapter is concerned with methods for estimating or measuring these water pressures.

Groundwater flow in rock masses

There are two possible approaches to obtaining data on water pressure distributions within a rock mass:

- Deduction of the overall groundwater flow pattern from consideration of the permeability of the rock mass and sources of groundwater.
- Direct measurement of water levels in boreholes or wells or of water pressures by means of piezometers installed in boreholes.

As will be shown in this chapter, both methods abound with practical difficulties but, because of the very important influence of water pressure on slope stability, it is essential that the best possible estimates of these pressures should be available before a detailed stability analysis is attempted. Because of the large number of factors which control the groundwater flow pattern in a particular rock mass, it is only possible to highlight the general principles which may apply and to leave the reader to decide what combination of these principles is relevant to his specific problem.



The hydrologic cycle

A simplified hydrologic cycle is illustrated in Figure 48 to show some typical sources of groundwater in a rock mass. This figure is included to emphasise the fact that groundwater can and does travel considerable distances through a rock mass. Hence, just as it is important to consider the regional geology of an area when starting the design on an open pit mine, so it is important to consider the regional groundwater pattern when estimating probable groundwater distributions at a particular site.

Clearly precipitation in the catchment area of the pit is an important source of groundwater, as suggested in the sketch opposite, but other sources cannot be ignored. Groundwater movement from adjacent river systems, reservoirs or lakes can be significant, particularly if the permeability of the rock mass is highly anisotropic as suggested in Figure 49. In extreme cases, the movement of groundwater may be concentrated in open fissures or channels in the rock mass and there may be no clearly identifiable water table. The photograph reproduced in Figure 50 shows a solution channel of about 1 inch in diameter in limestone. Obviously, the hydraulic conductivity of such a channel would be so high as compared with other parts of the rock mass that the conventional picture of a groundwater flow pattern would probably be incorrect in the case of a slope in which such features occur.

These examples emphasise the extreme importance of considering the geology of the site when estimating water table levels or when interpreting water pressure measurements.

Definition of permeability

Consider a cylindrical sample of soil on rock beneath the water table in a slope as illustrated in Figure 51. The

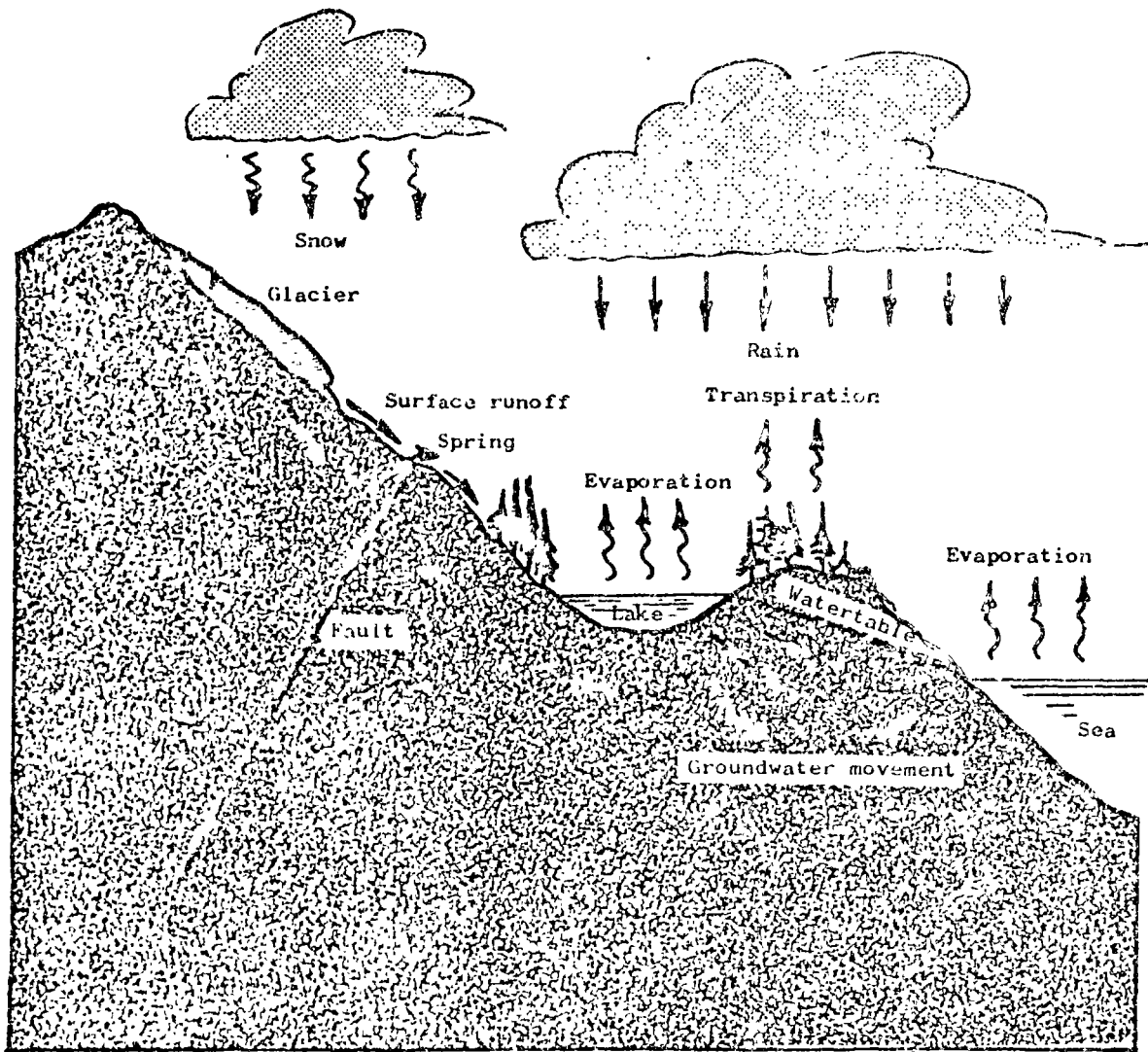


Figure 48 : Simplified representation of a hydrologic cycle showing some typical sources of groundwater .

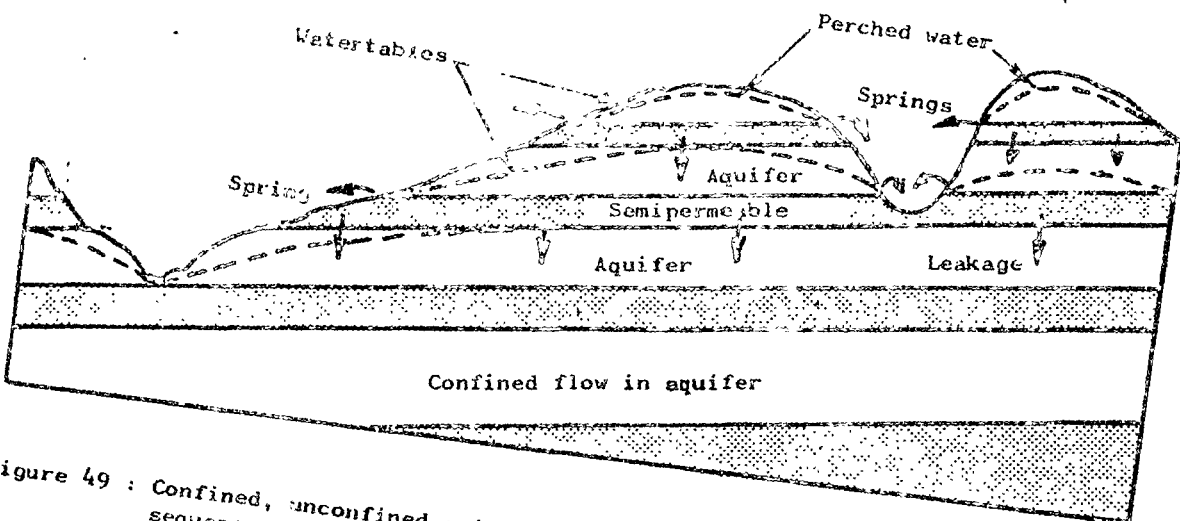


Figure 49 : Confined, unconfined and perched water in a simple stratigraphic sequence of sandstone and shale . After Davis and de Wiest 109.



Figure 50:
Solution channel in a limestone specimen. The hydraulic conductivity of such a channel would be very high as compared with the permeability of the intact rock or of other discontinuities and it would have a major influence on the groundwater flow pattern in a rock mass .

sample has a cross-sectional area of A and a length L . Water levels in boreholes at either end of this sample are at heights h_1 and h_2 above a reference datum and the quantity of water flowing through the sample in a unit of time is Q . According to Darcy's law, the coefficient of permeability of this sample is defined as ^{110,111,112}:

$$k = \frac{Q \cdot L}{A(h_1 - h_2)} = \frac{V \cdot L}{(h_1 - h_2)} \quad (21)$$

Permeability conversion table.	
To convert cm/sec to :	Multiply by
meters/min	0.600
μ /sec	10^4
ft/sec	0.0328
ft/min	1.968
ft/year	1.034×10^6
$\text{cm}^2 \cdot$	1.031×10^{-5}
Darcy \cdot	1.045×10^3

* for water at 20°C.

Where V is the discharge velocity. Substitution of dimensions for the terms in equation (21) shows that the permeability coefficient k has the same dimensions as the discharge velocity V , i.e. length per unit time. The dimension most commonly used in groundwater studies is centimetres per second and typical ranges of permeability coefficients for rock and soil are given in Table II¹¹³. Figure 51 shows that the total head h can be expressed in terms of the pressure p at the end of the sample and the height Z above a reference datum. Hence

$$h = \frac{p}{\gamma_w} + Z \quad (22)$$

where γ_w is the density of water. As shown in the figure, h is the height to which the water level rises in a borehole or standpipe.

Permeability of jointed rock

Table II shows that the permeability of intact rock is very low and hence poor drainage and low discharge would normally be expected in such material. On the other hand, if the rock is discontinuous as a result of the presence of joints, fissures or other discontinuities, the permeability can be considerably higher because these discontinuities act as channels for the water flow.

The flow of water through fissures in rock has been studied in great detail by Huitt¹¹⁴, Snow¹¹⁵, Louis¹¹⁶, Sharp¹¹⁷, Maini¹¹⁸ and others and the reader who wishes to pursue this complex subject is assured of many happy hours of reading. For the purposes of this discussion, the problem is simplified to that of the determination of the equivalent permeability of a planar array of parallel smooth cracks¹¹⁶. The permeability parallel to this array is given by:

$$k = \frac{ge^3}{12\nu \cdot b} \quad (23)$$

where g = gravitational acceleration (981 cm/sec²)

e = opening of cracks or fissures

b = spacing between cracks and

ν is the coefficient of kinematic viscosity (0.0101 cm²/sec for pure water at 20°C)

The equivalent permeability k of a parallel array of cracks with different openings is plotted in Figure 52 which shows that the permeability of a rock mass is very sensitive to the opening of discontinuities. Since this opening changes with stress, the permeability of a rock mass will therefore be sensitive to stress.

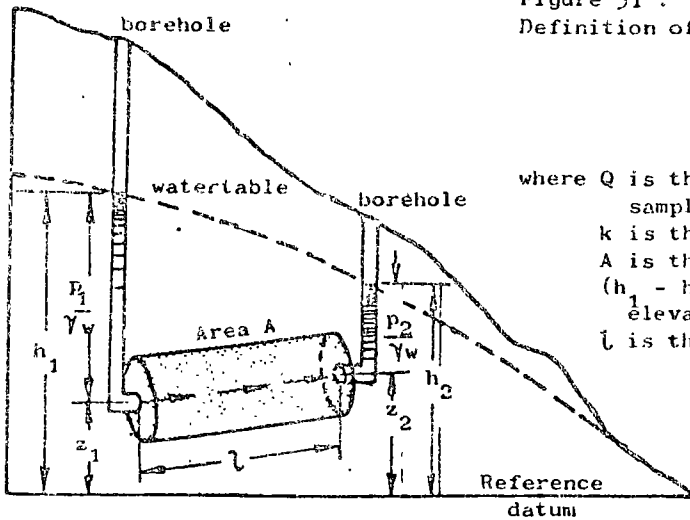


Figure 51 :
Definition of permeability in terms of Darcy's law.

$$Q = kA \frac{(h_1 - h_2)}{l}$$

where Q is the amount of water flowing through the sample in unit time,
k is the coefficient of permeability,
A is the cross-sectional area of the sample,
($h_1 - h_2$) is the difference in watertable elevation between the ends of the sample and
l is the length of the sample .

TABLE II - PERMEABILITY COEFFICIENTS FOR TYPICAL ROCKS AND SOILS

	k - cm/sec	Intact rock	Fractured rock	Soil
practically impermeable	10^{-10}	Slate		Homogeneous clay below zone of weathering
	10^{-9}	Dolomite		
	10^{-8}	Granite		
low discharge poor drainage	10^{-7}	Limestone Sandstone		Very fine sands, organic and inorganic silts, mixtures of sand and clay, glacial till, stratified clay deposits
	10^{-6}			
	10^{-5}		Clay-filled joints	
	10^{-4}			
	10^{-3}			
High discharge Free draining	10^{-2}		Jointed rock	Clean sand, clean sand and gravel mixtures
	10^{-1}			
	1.0		Open jointed rock	
	10^1		Heavily fractured rock	Clean gravel

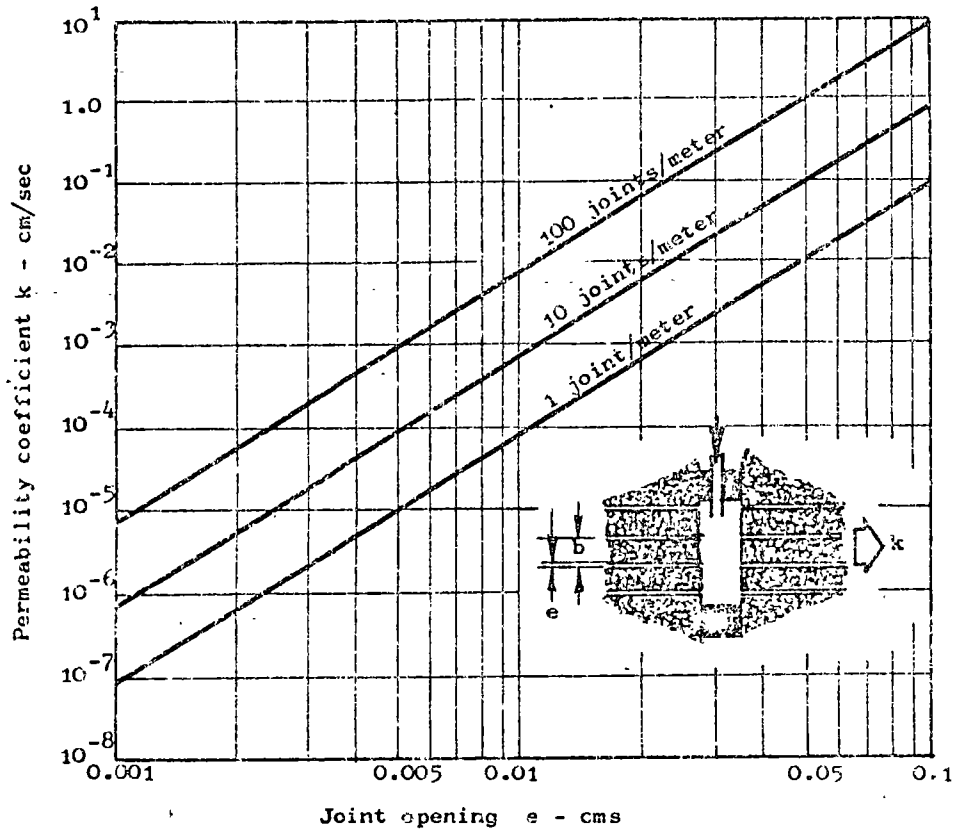


Figure 52 : Influence of joint opening e and joint spacing b on the permeability coefficient k in the direction of a set of smooth parallel joints in a rock mass.

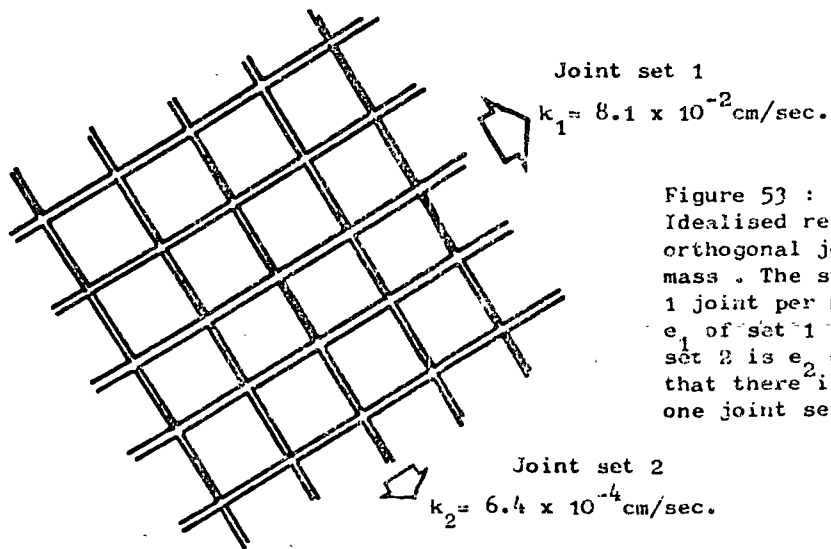


Figure 53 : Idealised representation of two orthogonal joint systems in a rock mass . The spacing of both sets is 1 joint per meter. The joint opening e_1 of set 1 is 0.10cm and the for set 2 is $e_2 = 0.02$ cm. It is assumed that there is no cross-flow from one joint set to another.

Louis¹¹⁶ points out that equation (23) only applies to laminar flow through planar parallel fissures and that it gives rise to significant errors if the flow velocity is high enough for turbulent flow to occur, if the fissure surfaces are rough or if the fissures are infilled. Louis lists no fewer than 8 equations to describe flow under various conditions. Equation (23) gives the highest equivalent permeability coefficient. The lowest equivalent permeability coefficient, for an infilled fissure system, is given by

$$k = \frac{e}{b} \cdot k_f + k_r \quad (24)$$

where k_f is the permeability coefficient of the infilling material and

k_r is the permeability coefficient of the intact rock.

(Note that k_r has been ignored in equation (23) since it will be very small as compared with the permeability of open joints).

An example of the application of equation (23) to a rock mass with two orthogonal joint systems is given in Figure 53. This shows a major joint set in which the joint opening e_1 is 0.10 cm and the spacing between joints is $b_1 = 1$ meter. The equivalent permeability k_1 parallel to these joints is $k_1 = 8.1 \times 10^{-2}$ cm/sec. The minor joint set has a spacing $b_2 = 1$ joint per meter and an opening $e_2 = 0.02$ cm. The equivalent permeability of this set is $k_2 = 6.5 \times 10^{-4}$ cm/sec, i.e. more than two orders of magnitude smaller than the equivalent permeability of the major joint set.

Clearly the groundwater flow pattern and the drainage characteristics of a rock mass in which these two joint sets occur would be significantly influenced by the orientation of the joint sets.

Flow nets

The graphical representation of groundwater flow in a rock or soil mass is known as a flow net and a typical example is illustrated in Figure 54. Several features of this flow net are worthy of consideration.

Flow lines are paths followed by the water in flowing through the saturated rock or soil.

Equipotential lines are lines joining points at which the total head h is the same. As shown in Figure 54, the water level is the same in boreholes or standpipes which terminate at points A and B on the same equipotential line.

Water pressures at points A and B are not the same since, according to equation (22), the total head h is given by the sum of the pressure head p/γ_w and the elevation Z of the measuring point above the reference datum. The *water pressure* increases with depth along an equipotential line as shown in Figure 54.

A complete discussion on the construction or computation of flow nets exceeds the scope of this book and the interested reader is referred to the comprehensive texts by Cedergrén¹¹²

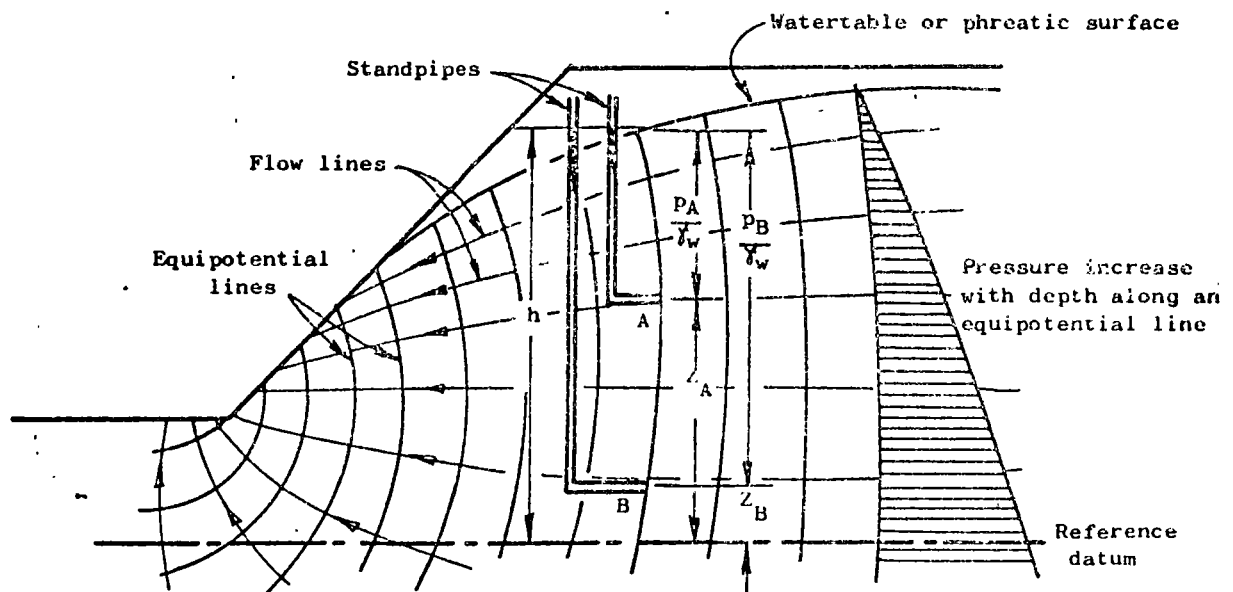


Figure 54: Two-dimensional flow net in a slope.

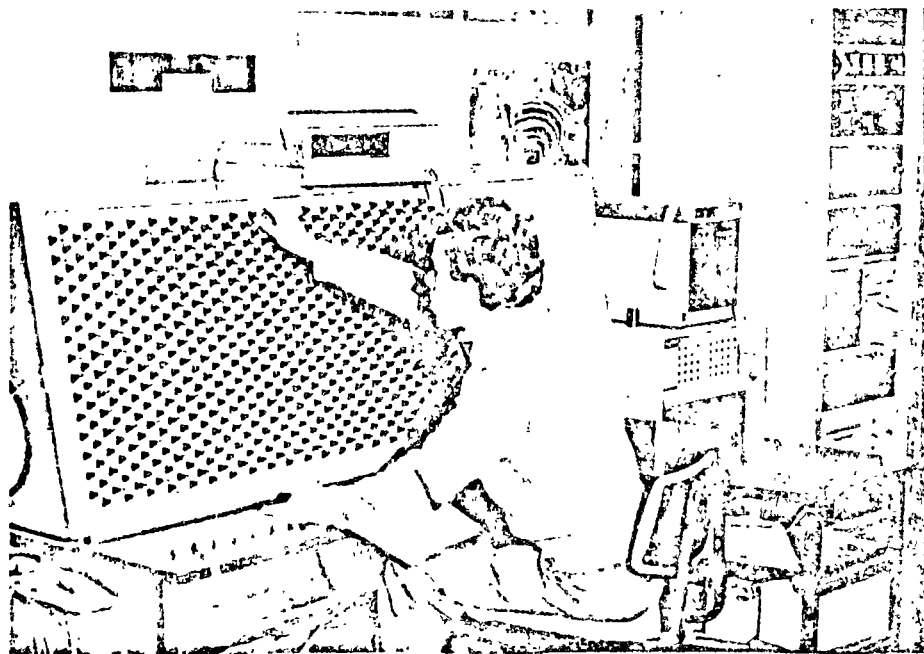


Figure 55 : Electrical analogue for the study of anisotropic groundwater flow and drainage problems 117.

and Haar¹¹⁹ for further details. Traditional graphical methods for constructing flow nets¹²⁰ have now largely been superseded by analogue^{121,122} and numerical methods¹²³.

An example of an electrical resistance analogue for the study of anisotropic seepage and drainage problems is illustrated in Figure 55. Some typical examples of equipotential distributions, determined with the aid of this analogue, are reproduced in Figure 56¹²⁴.

Field measurement of permeability

Determination of the permeability of a rock mass is necessary if estimates are required of groundwater discharge into an open pit or if an attempt is to be made to design a drainage system for the pit.

For evaluation of the stability of the pit slopes it is the *water pressure* rather than the volume of groundwater flow in the rock mass which is important. The water pressure at any point is independent of the permeability of the rock mass at that point but it does depend upon the path followed by the groundwater in arriving at that point (Figures 49 and 56). Hence, the anisotropy and the *distribution* of permeability in a rock mass is of interest in estimating the water pressure distribution in a slope.

In order to measure the permeability at a "point" in a rock mass, it is necessary to change the groundwater conditions at that point and to measure the time taken for the original conditions to be re-established or the quantity of water necessary to maintain the new conditions. These tests are most conveniently carried out in a borehole in which a section is isolated between the end of the casing and the bottom of the hole or between packers within the hole. The tests can be classified as follows:

- a) Falling head tests in which water is poured into a vertical or near vertical borehole and the time taken for the water level to fall to its original level is determined.
- b) Constant head tests in which the quantity of water which has to be poured into the borehole in order to maintain a specific water level is measured.
- c) Pumping tests or Lugeon tests in which water is pumped into or out of a borehole section between two packers and the changes induced by this pumping are measured.

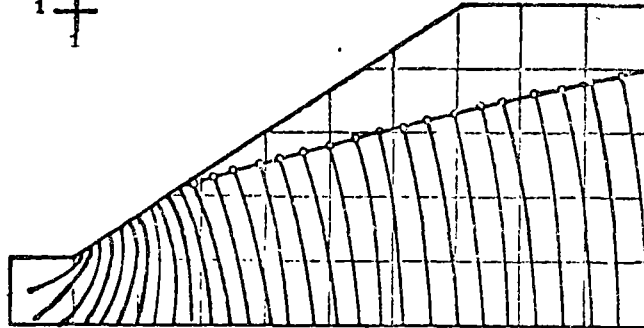
The first two types of test are suitable for measurement of the permeability of reasonably uniform soils or rock. Anisotropic permeability coefficients cannot be measured directly in these tests but, as shown in the example given below, allowance can be made for this anisotropy in the calculation of permeability. Pumping tests, although more expensive, are more suitable for permeability testing in jointed rock.

Falling head and constant head tests

A very comprehensive discussion on falling head and constant head permeability testing is given by Horslev¹²⁵ and a few of the points which are directly relevant to the present

Permeability ratio

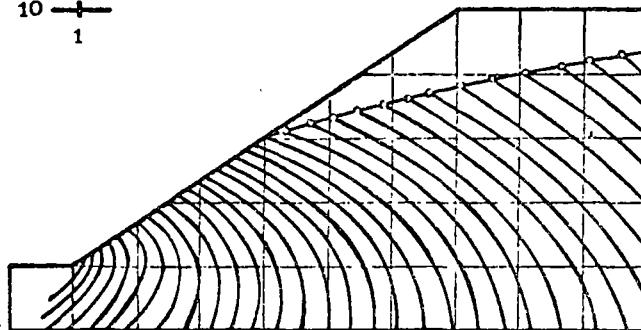
1 +
1



a) Isotropic rock slope.

Permeability ratio

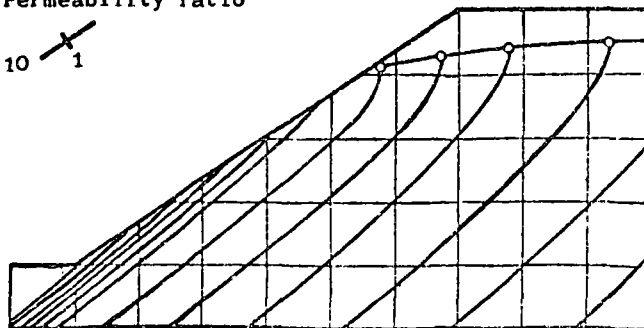
10 +
1



b) Anisotropic rock slope - horizontally bedded strata .

Permeability ratio

10 +
1



c) Anisotropic rock slope - strata dipping parallel to slope .

Figure 56 : Equipotential distributions in slopes with various permeability configurations.

discussion are summarised hereunder.

The coefficient of permeability k is calculated from falling-head and constant head tests in saturated ground (test section below water table) as follows.

$$\text{Falling head: } k = \frac{A}{F(t_2 - t_1)} \cdot \log_e \frac{H_1}{H_2} \quad (25)$$

$$\text{Constant head: } k = \frac{q}{F H_c} \quad (26)$$

where A is the cross section area of the water column.
 $A = \frac{1}{4} \pi d^2$ where d is the inside diameter of the casing in a *vertical* borehole. For an inclined hole, A must be corrected to account for the elliptical shape of the horizontal water surface in the casing.

F is a shape factor which depends upon the conditions at the bottom of the hole. Shape factors for typical situations are given in Figure 57.

H_1 and H_2 are water levels in the borehole, measured from the rest water level, at times t_1 and t_2 respectively.

q is the flow rate and

H_c is the water level, measured from the rest water level, maintained during a constant head test.

(Note that Napierian logarithms are used in these equations and that $\text{Log}_e = 2.3026 \text{Log}_{10}$)

Consider an example of a falling head test carried out in a borehole of 7.6 cm diameter with a casing of 6.0 cm diameter. The borehole is extended a distance of 100 cms beyond the end of the casing and the material in which the test is carried out is assumed to have a ratio of horizontal to vertical permeability $k_h/k_v = 5$.

The first step in this analysis is to calculate the shape factor F from the equation given for the 4th case in Figure 57. The value of $m = \sqrt{5} = 2.24$ and substituting $D = 7.6$ cm and $L = 100$ cm,

$$F = \frac{2\pi L}{\text{Log}_e (2m L/D)} = \frac{628}{\text{Log}_e 58.19} = 154$$

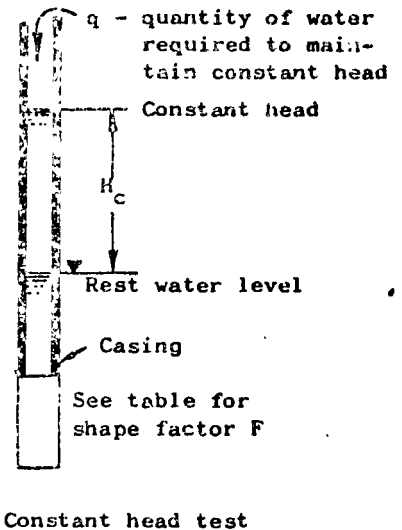
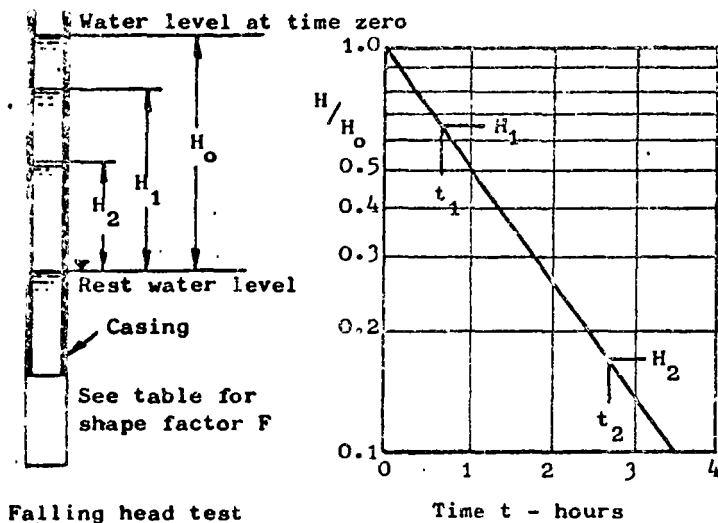
Measurement of water levels at different times for the falling head test gave the following values:

$$H_1 = 10 \text{ metres at } t_1 = 30 \text{ seconds}$$

$$H_2 = 5 \text{ metres at } t_2 = 150 \text{ seconds}$$

The cross-sectional area A of the water column is
 $A = \frac{1}{4} \pi (6)^2 = 28.3 \text{ cm}^2$.

Substituting in equation (25), the horizontal permeability k_h is given by



End conditions	Shape factor F
	$F = 2.75d$
	$F = 2.0 d$
	$F = \frac{2\pi L}{\text{Log}_e (2L/D)}$ <p>For $L > 4D$.</p>
	<p>For determination of k_h :</p> $F = \frac{2\pi L}{\text{Log}_e (2m L/D)}$ <p>where $m = (k_h/k_v)^{1/2}$, $L > 4D$.</p>
	$F = \frac{2\pi L}{\text{Log}_e (4L/D)}$ <p>For $L > 4D$.</p>

Figure 57 : Details of falling head and constant head tests for permeability measurement in soil or rock masses with shape factors for borehole end conditions .

$$k_h = \frac{28.3 \log_e 2}{154 (150-30)} = 1.06 \times 10^{-3} \text{ cm/sec.}$$

Since the ratio of horizontal to vertical permeability has been estimated, from examination of the core, as $k_h/k_v = 5$, $k_v = 2.12 \times 10^{-4}$ cm/sec.

Laboratory tests on core samples are useful in checking this ratio of horizontal to vertical permeability but, because of the disturbance to the sample, it is unlikely that the absolute values of permeability measured in the laboratory will be as reliable as those determined by the borehole tests described above. Laboratory methods for permeability testing are described in standard texts such as that by Lambe¹²⁶.

Pumping tests in boreholes

In a rock mass in which the groundwater flow is concentrated within regular joint sets, the permeability will be highly directional. If joint opening e could be measured in situ, the permeability in the direction of each joint set could be calculated directly from equation (23). Unfortunately, such measurements are not possible under field conditions and the permeability must therefore be determined by pumping tests.

A pumping test for the measurement of the permeability in the direction of a particular set of discontinuities such as joints involves drilling a borehole perpendicular to these discontinuities as shown in Figure 58. It is assumed that most of the flow is concentrated within this one joint set and that cross-flow through other joint sets, past the packers and through the intact rock surrounding the hole is negligible. A section of the borehole is isolated between packers or a single packer is used to isolate a length at the end of the hole and water is pumped into or out of this cavity.

A variety of borehole packers are available commercially¹²⁷ but the author considers that many of these packers are too short to eliminate leakage. Leakage past packers is one of the most serious sources of error in pumping tests and every effort should be made to ensure that an effective seal has been achieved before measurements are commenced. A simple, inexpensive and highly effective packer has been described by Harper and Ross-Brown¹²⁸ and the principal features are illustrated in Figure 59. This packer is manufactured from rubber hosing which is normally used in the building industry for forming voids in concrete*. It consists of inner and outer rubber tubes enclosing a diagonally braided cotton core and this arrangement allows an increase in diameter of approximately 20% when the hose is inflated. Because of its low cost and simplicity, long packers can be used and packer lengths of 10 feet (3 meters) have proved extremely effective in pumping tests in 3 inch (7.6 cm) diameter boreholes.

The permeability of the discontinuities perpendicular to the borehole is calculated as follows:

* Available in a wide range of diameters from Ductube Company Limited, Daneshill Road, Lound, Near Retford, Nottinghamshire, England.

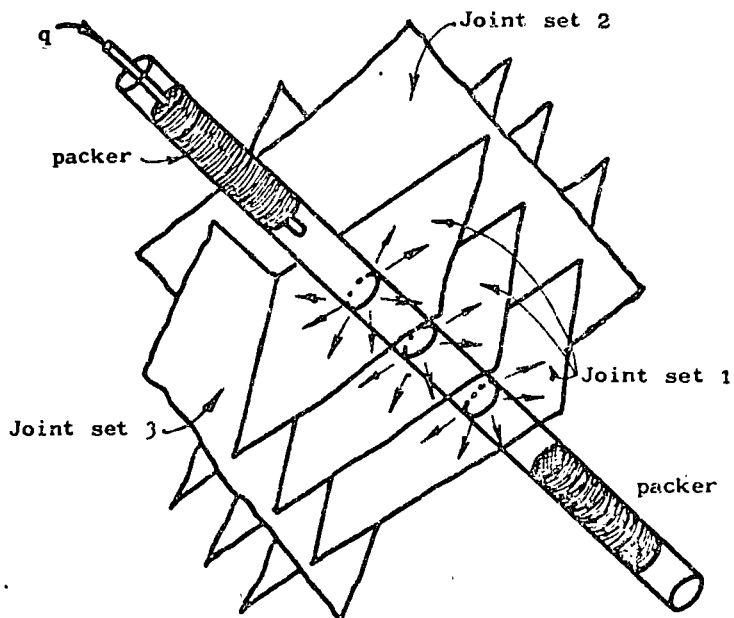


Figure 58 : Pumping test in regularly jointed rock. The borehole is drilled at right angles to the joint set in which the permeability is to be measured.

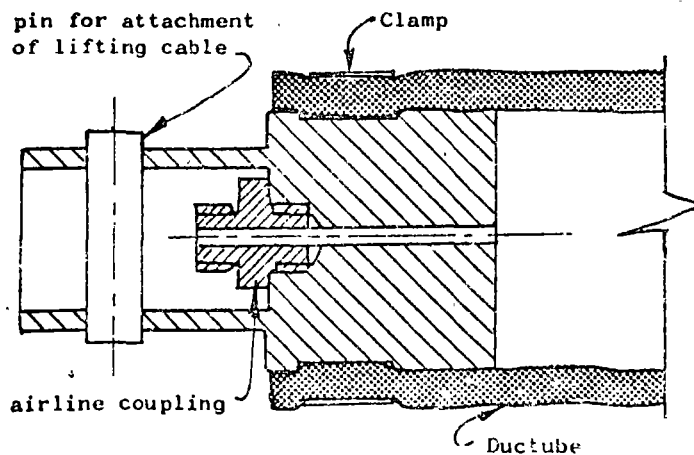


Figure 59 : Section through the end of a packer for sealing the bottom end of a pumping test cavity . The upper packer end has additional fittings for pressure inlet and piezometer cables.

$$k = \frac{q \text{ Log}_e (2 R/D)}{2 \pi L (H_1 - H_2)} \quad (27)$$

where q is pumping rate required to maintain a constant pressure in the test cavity

L is the length of the test cavity

H_1 is the total head in the test cavity

D is the borehole diameter

H_2 is the total head measured at a distance R from the borehole

The most satisfactory means of obtaining the value of H_2 is to measure it in a borehole parallel to and at a distance R from the test hole. Where a pattern of boreholes is available, as is the case on many opencast mine sites, this does not present serious problems. Techniques for water pressure measurement are dealt with in the following section of this chapter.

When only one borehole is available, an approximate solution to equation (27) can be obtained by using the shape factor F for a stratified system (Figure 57). Substituting this value into equation (26) gives

$$k = \frac{q \cdot \text{Log}_e (2^m L/D)}{2 \pi L H_c} \quad (28)$$

where, in this case, $m = (k/k_p)^{1/2}$,

k is the permeability at right angles to the borehole (the quantity required)

k_p is the permeability parallel to the borehole which, if cross flow is neglected, is equal to the permeability of the intact rock

H_c is the constant head above the original groundwater level in the borehole.

The value of the term $\text{Log}_e (2^m L/D)$ in this equation does not have a major influence upon the value of k and hence a crude estimate of m is adequate. Consider the example where $L = 4D$; the values of $\text{Log}_e (2^m L/D)$ are as follows:

k/k_p	1.0	10^2	10^4	10^6	10^8	10^{10}	10^{12}
m	1.0	10^1	10^2	10^3	10^4	10^5	10^6
$\text{Log}_e (2^m L/D)$	2.1	4.4	6.7	9.0	11.3	13.6	15.9

A reasonable value of k for most practical applications is given by assuming $k/k_p = 10^6$, $m = 10^3$ which gives

$$k = \frac{1.4q}{L H_c} \quad (29)$$

In deriving equation (29), it has been assumed that the test cavity is long and, therefore, a large number of boreholes

unities (say 100) and that the value of k represents a reasonable average permeability for the rock mass (in the direction at right angles to the borehole). When the discontinuity spacing varies along the length of the hole, water flow will be concentrated in zones of closely spaced discontinuities and the use of an average permeability value can give misleading results. Under these circumstances, it is preferable to express the permeability in terms of the permeability k_j of individual discontinuities where

$$k_j = \frac{k}{n} \quad (30)$$

n is the number of discontinuities which intersect the test cavity of length L .

The value of n can be estimated from the borehole core log and, assuming that the discontinuity opening (e in equation (23)) remains constant, the variation in permeability along the borehole can then be estimated.

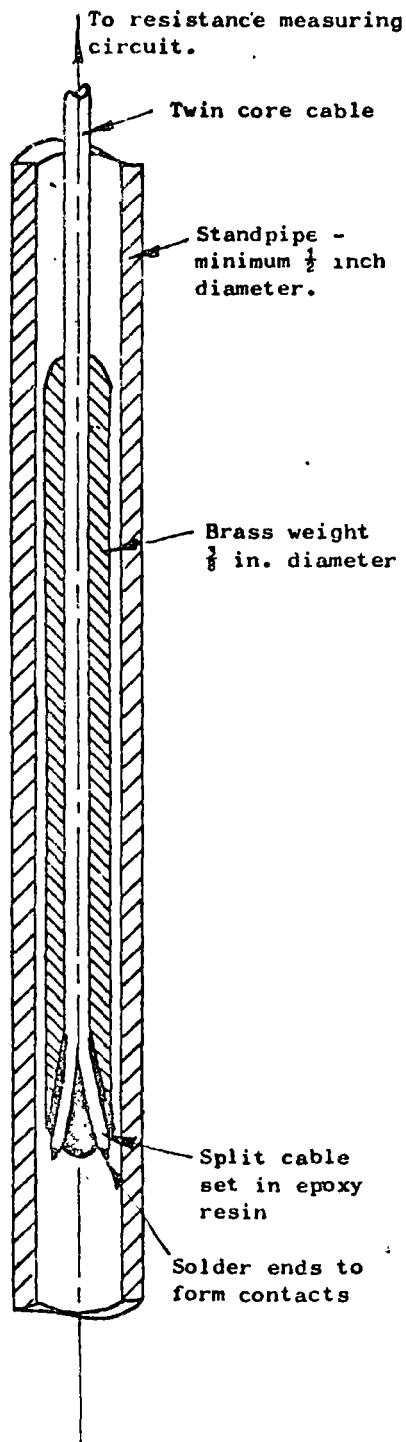
Before leaving this question of permeability testing it must be pointed out that the discussion which has been presented has been grossly simplified. This has been done deliberately since the literature dealing with this subject is copious, complex and confusing. A number of techniques, more sophisticated than those which have been described here, are available for the evaluation of permeability but the author believes that these are best left in the hands of experienced specialist consultants. The simple tests which have been described are generally adequate for open pit stability and drainage studies.

Measurement of water pressure

The importance of water pressure in relation to the stability of slopes has been emphasised in several of the previous chapters. If a reliable estimate of stability is to be obtained or if the stability of a slope is to be controlled by drainage, it is essential that water pressures within the slope should be measured. Such measurements are most conveniently carried out by *piezometers* installed in boreholes.

A variety of piezometer types are available and the choice of the type to be used for a particular installation depends upon a number of practical considerations. A detailed discussion on this matter has been given by Terzaghi and Peck¹²⁹ and only the most important considerations will be summarised here.

The most important factor to be considered in choosing a piezometer is the time lag of the complete installation. This is the time taken for the pressure in the system to reach equilibrium after a pressure change and it depends upon the permeability of the ground and the volume change associated with the pressure change. Open holes can be used for pressure measurement when the permeability is greater than 10^{-4} cm/sec but, for less permeable ground, the time lag is too long. In order to overcome this problem, a pressure measuring device or piezometer is installed in a sealed section of the borehole. The volume change within this sealed section, caused by the operation of the piezometer



A simple probe for water level detection .

should be very small in order that the response of the complete installation to pressure changes in the surrounding rock should be rapid. If a device which requires a large volume change for its operation is used, the change in pressure induced by this change in volume may give rise to significant errors in measurement.

Some of the common types of piezometer are briefly discussed hereunder.

a) Open piezometers or observation wells

As discussed above, open ended cased holes can be used to measure water pressure in rock or soil in which the permeability is greater than about 10^{-4} cm/sec. All that is required for these measurements is a device for measuring water level in the borehole. A very simple probe consisting of a pair of electrical contacts housed in a brass weight is illustrated in the sketch opposite. When the contacts touch the water, the resistance of the electrical circuit drops and this can be measured on a standard "Avometer" or similar instrument. The depth of water below the collar of the hole is measured by the length of cable and it is convenient to mark the cable off in feet or meters for this purpose. Portable water level indicators, consisting of a probe, a marked cable and a small resistance measuring instrument, are available from Soil Instruments Ltd., Townsend Land, London N.W.9 or from Soiltest Inc., 2205 Lee Street, Evanston, Illinois 60202, U.S.A.

b) Standpipe piezometers

When the permeability of the ground in which water pressure is to be measured is less than 10^{-4} cm/sec, the time lag involved in using an open hole will be unacceptable and a standpipe piezometer such as that illustrated in Figure 60 should be used. This device consists of a perforated tip which is sealed into a section of borehole as shown. A small diameter standpipe passing through the seals allows the water level to be measured by means of the same type of water level indicator as described above under open hole piezometers. Because the volume of water within the standpipe is small, the response time of this piezometer installation will be adequate for most applications likely to be encountered on an open pit mine site.

An advantage of the standpipe piezometer is that, because of the small diameter of the standpipe, a number can be installed in the same hole. Hence different sections can be sealed off along the length of the borehole and the water pressure within each section monitored. This type of installation is important when it is suspected that water flow is confined to certain layers within a rock mass.

c) Closed hydraulic piezometers

When the permeability of the ground falls below about 10^{-6} cm/sec, the time lag of open ended boreholes or standpipe piezometers becomes unacceptable. For example, approximately 5 days would be required for a typical standpipe piezometer to reach an acceptable state of equilibrium after a change in water pressure in a rock or soil mass having a permeability of 10^{-7} cm/sec.

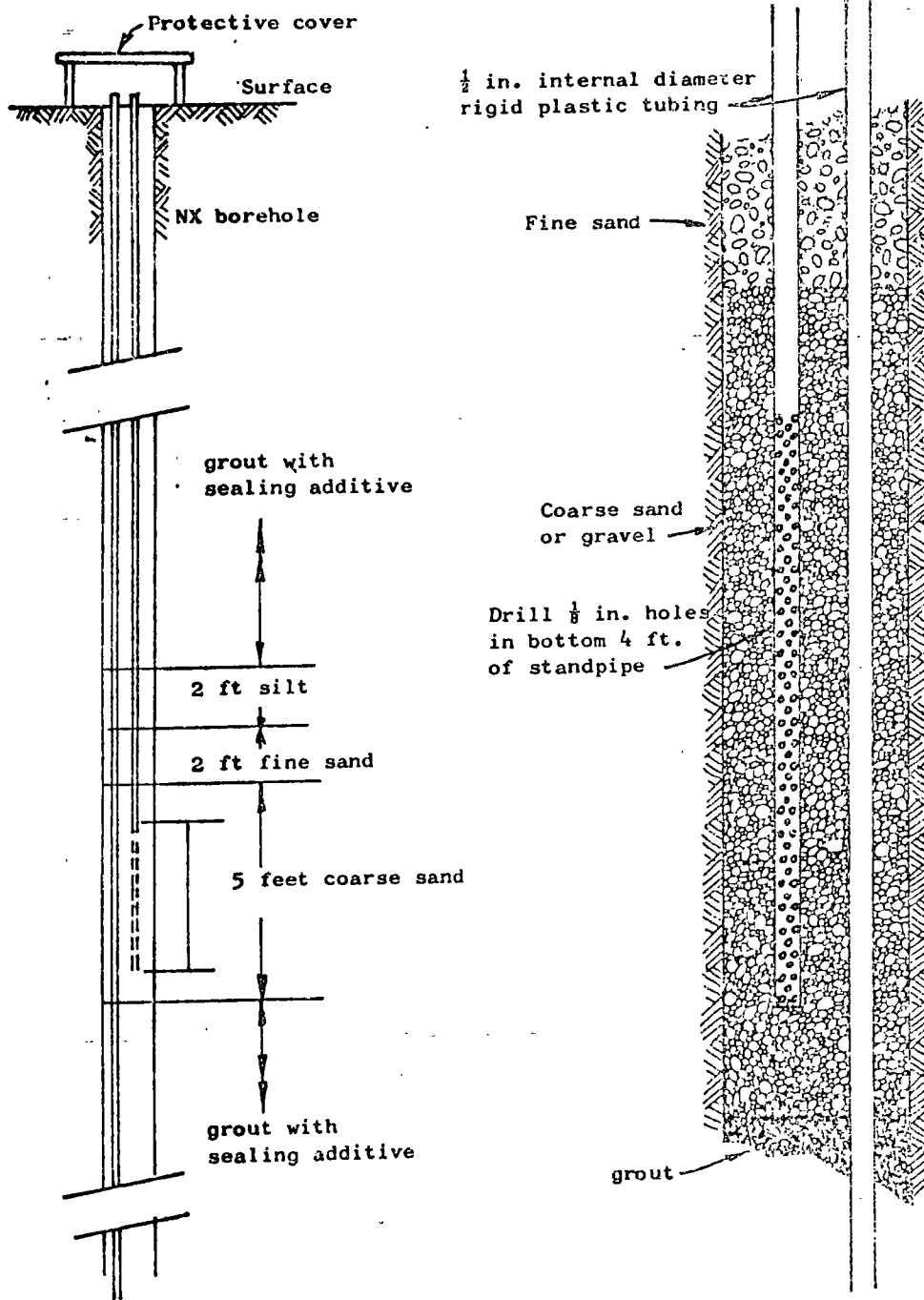


Figure 60 : Typical standpipe piezometer installation . Variations should be made to suit local conditions and to utilise local materials.

An improved time lag can be obtained by using a closed hydraulic piezometer such as that described by Bishop et al¹³⁰. This type of piezometer is completely filled with de-aired water and is suitable for measurement of small water pressures. Such piezometers are generally used for pore pressure measurement during construction of embankments or dams where they can be installed during construction and left in place.

d) Air Actuated Piezometers

A very rapid response time can be achieved by use of air actuated piezometers in which the water pressure is measured by a balancing air pressure acting against a diaphragm. As shown in Figure 61, an air valve allows air to escape when the air and water pressures on either side of the diaphragm are equal¹³¹. A commercially available air piezometer, manufactured by Soil Instruments Ltd., Townsend Lane, London N.W.9, England, is illustrated in Figure 62. Similar types of instrument are available from other suppliers and the author believes that these devices will play an increasingly important role in slope stability studies.

e) Electrically indicating piezometers

An almost instantaneous response time is obtained from piezometers in which the deflection of a diaphragm as a result of water pressure is measured electrically by means of some form of strain gauge attached to the diaphragm. A wide variety of such devices are available commercially and they are ideal for measuring the water pressure within the test cavity during a pumping test¹¹⁸. Because of their relatively high cost and because of the possibility of electrical faults, these piezometers are less satisfactory for permanent installation in boreholes.

General comments

A frequent mistake made by engineers or geologists in examining rock or soil slopes is to assume that groundwater is not present if no seepage appears on the slope face. In many cases, the seepage rate may be lower than the evaporation rate and hence the slope surface may appear completely dry and yet there may be water at significant pressure within the rock mass. Remember that it is water pressure and not rate of flow which is responsible for instability in slopes and it is essential that measurement or calculation of this water pressure should form part of the site investigation for stability studies. Drainage, which is discussed in a later chapter, is one of the most effective and most economical means available for improving the stability of open pit mine slopes. Rational design of drainage systems is only possible if the water flow pattern within the rock mass is understood and measurement of permeability and water pressure provides the key to this understanding.

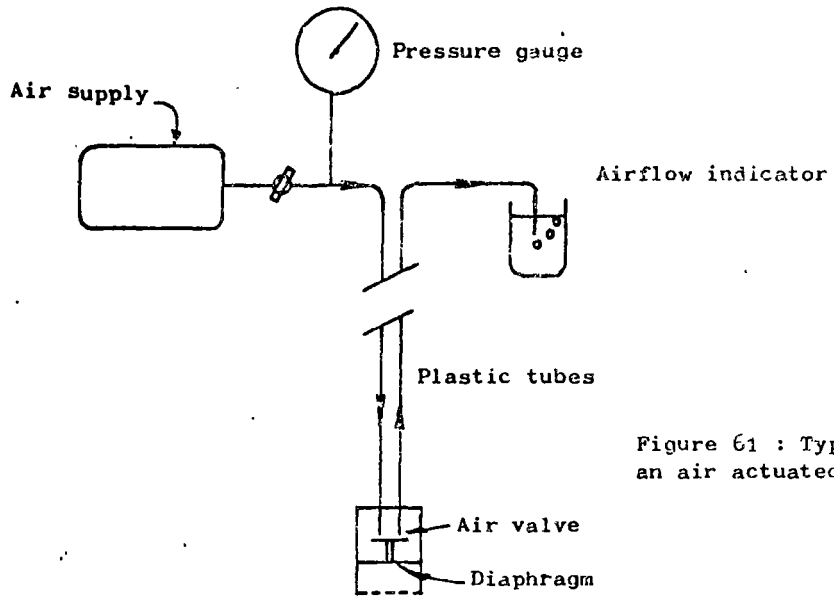


Figure 61 : Typical circuit for an air actuated piezometer .

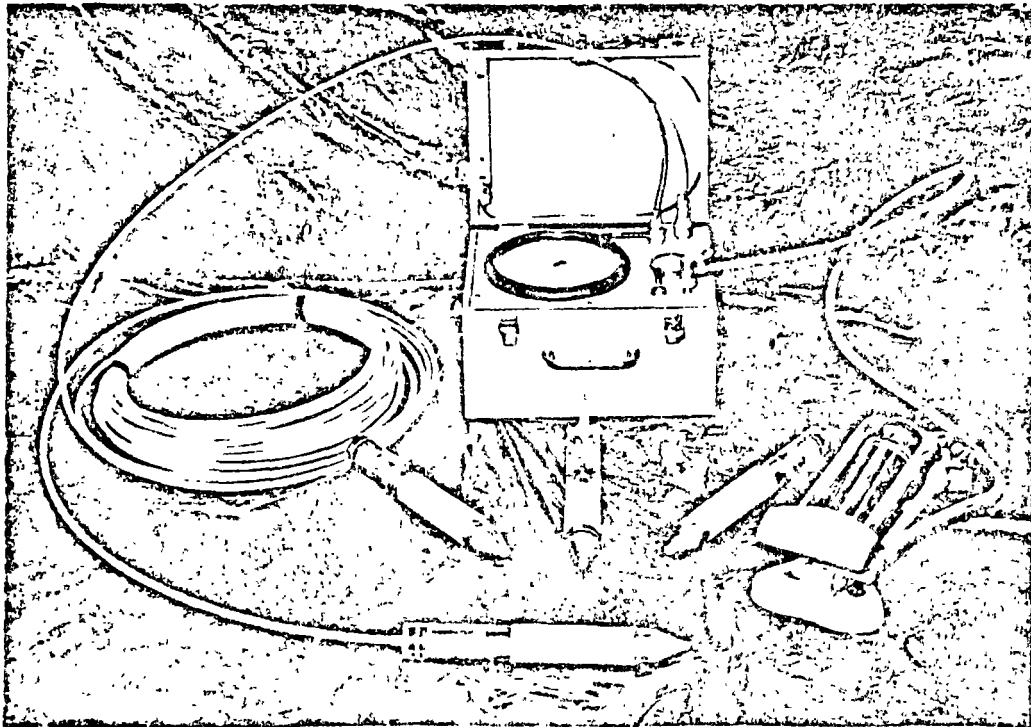


Figure 62 : Air actuated piezometer manufactured by Soil Instruments Ltd , London.

Chapter 6 references

Selected references on permeability and water pressure measurement.

104. BRAUNER, C.O. The influence and control of groundwater in open pit mining. *Proc. 5th Canadian Symposium on Rock Mechanics*, Toronto 1968.
105. DOBRY, R. and ALVAREZ, L. Seismic failures of Chilean Tailings dams. *Proc. American Society of Civil Engineers*. Vol. 93, No. SM6, 1967.
106. BRAUNER, C.O. Case studies of stability on mining projects. *Proc. 1st Symposium on Stability for Open Pit Mining*, Vancouver 1970. Published by AIME, New York 1971.
107. CASAGRANDE, L. and MACIVER, B.N. Design and construction of tailings dams. *Proc. 1st Symposium on Stability for Open Pit Mining*, Vancouver 1970. Published by AIME, New York 1971.
108. SEED, H.B. and LEE, K.L. Liquefaction of saturated sands during cyclic loading. *Journal Soil Mechanics and Foundation Div. Proc. ASCE*. Vol. 92, No. SM6, 1966, pp. 105-134.
109. DAVIS, S.N. and DE WIEST, R.J.M. *Hydrogeology*. John Wiley & Sons, New York, London 1966, 463 p.
110. MORGENSTERN, N.R. The influence of groundwater on stability. *Proc. 1st Symposium on Stability of Open Pit Mining*, Vancouver 1970. Published by AIME, New York 1971.
111. SCHEIDEGGER, A.E. *The physics of flow through porous media*. MacMillan, New York 1960.
112. CEDERGREEN, H.R. *Seepage, drainage and flow nets*. John Wiley & Sons, New York 1967.
113. DAVIS, S.N. Porosity and permeability of natural materials, in *Flow through porous media*, edited by R. de Wiest, Academic Press, London 1969, pp. 54-89.
114. HUITT, J.L. Fluid flow in simulated fracture. *Journal American Inst. Chemical Eng.* Vol. 2 1956, pp.259-264.
115. SNOW, D.T. Rock fracture spacings, openings and porosities. *Journal Soil. Mech. Foundation Div. Proc. ASCE*. Vol. 94 1968, pp. 73 - 91.
116. LOUIS, C. A study of groundwater flow in jointed rock and its influence on the stability of rock masses. Doctorate thesis, University of Karlsruhe 1967 (in German). English translation *Imperial College Rock Mechanics Research Report No. 10*, September 1969, 90 p.
117. SHARP, J.C. Fluid flow through fissured media. *Ph.D. Thesis, University of London (Imperial College)* 1970.

118. MAINI, Y.N. In situ parameters in jointed rock - their measurement and interpretation. *Ph.D. Thesis, University of London (Imperial College)* 1971.
119. HAAR, M.E. *Groundwater and Seepage*, McGraw Hill Co. Co., New York, 1962.
120. TAYLOR, D.W. *Fundamentals of Soil Mechanics*. John Wiley & Sons, New York, 1948.
121. KARPLUS, W.J. *Analog Simulation. Solution of Field Problems*. McGraw Hill Co., New York, 1968.
122. MEEHAN, R.L. and MORGENSTERN, N.R. The approximate solution of seepage problems by a simple electrical analogue method. *Civil Engineers and Public Works Review*. Vol. 63, 1968, pp.65-70.
123. ZIENKIEWICZ, O.C., MAYER, P. and CHEUNG, Y.K. Solution of anisotropic seepage by finite elements. *Journal Eng. Mech. Div., ASCE*, Vol. 92, EM1, 1966, pp.111-120.
124. SHARP, J.C., MAINI, Y.N. and HARPER, T.R. Influence of groundwater on the stability of rock masses. *Trans. Institute Mining and Metallurgy*, London. Vol. 81, Bulletin No. 782, 1972, pp.A13-A20.
125. HORSLEV, M.S. Time lag and soil permeability in groundwater measurements. *U.S. Corps of Engineers Waterways Experiment Station, Bulletin No. 36*, 1951, 50p.
126. LAMBE, T.W. *Soil testing for engineers*. John Wiley and Sons, New York, 1951.
127. MUJIR WOOD, A.M. In-situ testing for the Channel Tunnel. *Proc. Conference on in-situ investigations in soils and rocks*, London 1969. Published by The Institution of Civil Engineers, London, 1969. pp.79-86.
128. HARPER, T.R. and ROSS-BROWN, D.M. An inexpensive durable borehole packer. *Imperial College Rock Mechanics Research Report No. D24*, 1972, 5p.
129. TERZAGHI, K. and PECK, R. *Soil Mechanics in Engineering Practice*. John Wiley and Sons Inc., New York, 1967. 729p.
130. BISHOP, A.W., KENNARD, M.F. and PENMAN, A.D.M. Pore-pressure observations at Selsset dam. *Proc. Conf. on Pore Pressure and Suction in Soils*. Butterworth, London, 1960, pp.91-102.
131. WARLAM, A.A. and THOMAS, E.W. Measurement of Hydrostatic uplift pressure on Spillway weir with air piezometers. *Instruments and apparatus for soil and rock mechanics*. American Society for Testing and Materials Special Technical Publication No. 392, 1965, pp.143-151.

The angle ϕ will assume the sign of $(Z_2 - Z_3)$. As shown in figure 5C, ϕ is positive when the joint dips toward the observer.

The azimuth of dip, θ , is now given by the following formula

$$\theta = \text{azimuth of Y-axis (deg)} \pm \psi^\circ \pm 90^\circ.$$

Notice that the convention of measuring positive angles clockwise from Y-axis and from line 34 is consistently used (fig. 5C).

Solution of an Example Problem

The solution for the dip and azimuth of dip of a hypothetical joint observed in an inclined borehole will be presented in this section. The data for the problem includes

azimuth of borehole axis = 134° ,

inclination of borehole = 12° ,

diameter of borehole = 0.125 ft,

diameter of borescope = 0.0833 ft,

and $Y_1' = 0$, $Y_2' = 0.1092$, and $Y_3' = 0.1333$.

The computed values of X, Y, Z coordinates of points 1, 2, and 3 are tabulated in figure 5D. The values of ψ and ϕ obtained from equations 3 and 4 (see the computer output) are

$$\psi = -43.8^\circ,$$

and $\phi = 79.5^\circ$.

The graphical solutions for ψ and ϕ (fig. 5A, 5B) agree with the computed values. The azimuth of dip is then given by (see fig. 5C for sign convention)

$$\theta = \text{azimuth of borehole} + \psi - 90^\circ,$$

or $\theta = 0.2^\circ$.

COMPUTER PROGRAM FOR DETERMINING ATTITUDES OF JOINTS

Input Instructions

	<u>Card</u>	<u>Columns</u>	
Set 1	1	1-5	NH = Total number of holes surveyed.
Set No		6-15	DB = Diameter of borescope, ft.
Set 2	2	1-5	DEPTH = Depth of hole, ft.
		6-10	DHOLE = Diameter of hole, ft.
		11-15	HOLAZ = Azimuth of hole axis, deg.
		16-20	HDIP = Inclination of hole, deg (no sign for uphole, negative for downhole).
		21-80	Alphanumeric information about the borehole.
	3	1-5	N = Serial number of joint in this hole.
		6-10	YP(1) = Distance (right) from collar to eyepiece, ft.
		11-15	YP(2) = Distance (top) from collar to eyepiece, ft.
		16-20	YP(3) = Distance (left) from collar to eyepiece, ft.
		21-25	AXIAL = Length of tubing removed, if any, ft.
		30	NEND = 1 if N is the last joint in this hole, otherwise blank.
		31-80	REMARK = Alphanumeric information about joint: Filling, width, etc.

The total number of cards in set 2 = $n + 1$, where n = number of joints surveyed in this hole. Set 2 should be followed by additional sets of cards for each succeeding hole (total number of these sets = NH).

Program Listing

```

PROGRAM ATTITUD(TAPE5,OUTPUT,TAPE6=OUTPUT,PUNCH)
C   DETERMINATION OF DIPS AND AZIMUTHS OF DIPS OF JOINTS SURVEYED
C   WITH A BORESCOPE IN INCLINED BOREHOLES
DIMENSION YP(3),HED(10),REMARK(8),SJ(8),DJ(8)
RADN=57.2957795
READ(5,10) NH,DB
DO 100 J=1,NH
  READ(5,12) DEPTH,DHOLE,HOLAZ,HDIP,HED
  WRITE(6,14) HED,DEPTH,DHOLE,HOLAZ,HDIP
  GAMA=HDIP/RADN
  SH=DHOLE-DB/2.
  SA=SQRT(SH**2+DB**2)
  S=SIN(GAMA)
  C=COS(GAMA)
  WRITE(6,30)
40 READ(5,13) N,YP(1),YP(2),YP(3),AXIAL,NEND,REMARK
  DEPTH=DEPTH-AXIAL
  DO 41 I=1,3
41  YP(I)=DEPTH-YP(I)
     YP21=YP(2)-YP(1)
     YP31=YP(3)-YP(1)
     Y2=C**YP21-S**SH
     Y3=C**YP31
     Z2=S**YP21+C**SH
     Z3=S**YP31
     AM=Z3/Z2
     ANUM=Y3-AM**Y2
     DNUM=SA**(AM-2.)
     D34=SQRT(ANUM**2+DNUM**2)
     PSI=ACOS(ABS(ANUM)/D34)**RADN
     SPSI=(ANUM/ABS(ANUM))**(ABS(DNUM)/DNUM)
     PSI=SPSI**PSI
46  AREA2=(SA**(1.-AM)**(2.**Y2-Y3))
     IF(AREA2.EQ.0.) GO TO 47
     DIP=ATAN((Z2-Z3)**D34/AREA2)**RADN
     GO TO 48
47  IP=90.0
48  SDIP=DIP/ABS(DIP)
     DIPAZ=HOLAZ+PSI+SPSI**SDIP**90.0
     IF(DIPAZ.GT.360.) DIPAZ=DIPAZ-360.
     IF(DIPAZ.LT.0.) DIPAZ=DIPAZ+360.
     WRITE(6,42) N,YP(1),YP(2),YP(3),PSI,DIPAZ,DIP,REMARK
     NP=N-((N-1)/8)**8
     SJ(NP)=DIPAZ
     DJ(NP)=DIP
     IF(NEND.NE.0.OR.NP.EQ.8)PUNCH 43,(SJ(I),DJ(I),I=1,NP)
     IF(NEND.EQ.0)GO TO 40
     PUNCH 44,N,HED
100 CONTINUE
10  FORMAT(15,F10.2)
12  FORMAT(4F5.2,10A6)
13  FORMAT(15,4F5.2,15,10A5)
14  FORMAT(1H1,10A6,/' DEPTH OF HOLE      =,F9.2, FT'/
   1  ' HOLE DIAMETER      =,F9.4, FT'/ ' AZIMUTH OF HOLE =
   2  ',F9.1, DEG'/ ' HOLE INCLINATION =,F9.2, DEG'/)
30  FORMAT(' NO. YP(R) YP(T) YP(L) PSI DIPAZ DIP  REMARKS//)
42  FORMAT(14,3F7.4,3F6.1,4X,10A5)
43  FORMAT(16F5.0)
44  FORMAT(15,15X,10A5)
STOP
END

```

Description of Output

The output from the program includes the following:

1. The information given on card 2 of set 2 for each hole.
2. The Y' distances of points 1, 2, and 3, from the collar of the hole--YP(R), YP(T), and YP(L), respectively--for each joint.
3. The angle Ψ , the azimuth of dip, the dip, and the alphanumeric information (remarks) for each joint.
4. Punched cards with eight pairs of azimuth of dip and dip for use with PATCH program of reference 4.

A listing of the computer output for the example problem is as follows:

EXAMPLE PROBLEM GIVEN IN TEXT

DEPTH OF HOLE = 1.00 FT
 HOLE DIAMETER = .125 FT
 AZIMUTH OF HOLE = 134.0 DEG
 HOLE INCLINATION = 12.00 DEG

NO.	YP(R)	YP(T)	YP(L)	PSI	DIPAZ	DIP	REMARKS
1	0.0000	.1092	.1333	-43.8	.2	79.5	HYPOTHETICAL JOINT

SUMMARY

A new scheme for determining dips and azimuths of dips of joints surveyed with a borescope in inclined boreholes is presented. The procedures used by the Bureau for collecting and recording the borescope data are described, and a computer program based on the solution scheme is listed. The solution for an example problem is obtained by the scheme presented in the report as well as by the graphical technique for solving a three-point problem. The computer-based scheme presented here should be useful in analyzing the large quantities of data obtained from comprehensive borehole surveys. The input and output formats for the computer program listed in the report are suited to the procedures followed by the Bureau. The program can, however, be easily modified to suit any other convention.

General report for Third Congress of the International Society for Rock Mechanics, Denver, September 1974.

The Design of Rock Slopes and Foundations

by E. Hoek, Professor of Rock Mechanics, Imperial College, London

P. Londe, Technical Director, Coyne & Bellier, Paris

SUMMARY

A critical review of the present "State of the Art" of the design of surface workings in rock is presented in this report which is divided into four sections:

1. Appraisal of rock masses
2. Design methods
3. Rock slopes
4. Rock foundations

Site investigation techniques, laboratory tests, mathematical and physical models are all examined in the light of their relevance to engineering design. The use of the factor of safety as a design index is discussed and an assessment is given of the most practical approach to designing rock slopes and foundations. The influence of groundwater on the stability of surface workings is considered and the use of drainage and grouting for groundwater control is discussed. Other methods for improving stability, including the use of controlled blasting techniques and the reinforcement of the rock mass, are considered.

INTRODUCTION

For centuries building on rock has been synonymous with building safely. During the past few decades this situation has changed and the increasing size of structures such as arch dams and opencast mines has presented engineers with an entirely new set of problems. The severity of these problems and the inadequacy of existing design methods has been emphasised by several catastrophic failures which have occurred in recent years.

The solution to these problems is not simple. Design methods in rock engineering evolve slowly, largely by trial and error since the physical and mechanical laws governing the behaviour of rock masses are poorly understood. Geologists, whose contribution to the development of rock engineering is vital, also find themselves in difficulty in attempting to quantify problems which have dimensions of both scale and time which are smaller than those with which the geologist is normally concerned.

As design methods are evolved, new problems which had not been anticipated arise. New failure modes or unusual combinations of forces are recognised and the rock engineer is faced with a new set of unsolved problems. It would be a mistake to regret this state of affairs. On the contrary, even if the engineer is frustrated by his inability to solve these new problems the very fact that these problems are recognised is a step towards increased safety.

In reflecting upon the current state of development of rock mechanics, the general reporters are greatly encouraged by one particular trend which has begun to emerge during the past decade and which suggests that the subject is slowly reaching maturity. This is the trend to work towards a *balanced* design; even if all the factors which contribute towards the overall behaviour of a structure are not known with any great precision, at least the influence of each factor is considered in arriving at an assessment of the probable behaviour of that structure.

In the past one tended to find "schools" or "techniques" emphasised. There was, for example, the "Austrian" school or the "South African" school and the "photoelastic" era and, more recently, the "finite element" era. While these individual approaches made and will continue to make valuable contributions to the development of rock mechanics, they did not provide a complete or a balanced picture of the whole. Just as the medical world has long realised that there is no one approach which will solve all the problems of illness, so the rock engineer is realising that no one method will solve all the problems which he is likely to encounter. Rock is an extremely complex engineering material and designing in rock requires the application of as much science as relevant, as much experience as available and as much common sense as possible. Above all, a design must be balanced in that every factor, even those which cannot be quantified, must be considered before reaching a final decision.

Turning now to the structure of this report on surface workings. Two sub-divisions are immediately obvious:

- a) Rock slopes
- b) Rock foundations

Flow charts showing the main steps required for the designs of these two types of construction are presented in Figures 1 and 2. It will be noted that there are many common elements in these two charts, particularly those areas concerned with geological data collection, preliminary stability analysis and shear strength testing. On the other hand, deformation behaviour is a crucial design consideration for foundations but not for slopes while controlled failure is acceptable for some slopes but totally unacceptable for foundations. This report is therefore divided into four major sections which deal with the problems which are particularly important in slope design and problems which are particularly important in foundation design.

Rather than present a catalogue of all the things which we can do well, the general reporters have chosen to place the main emphasis on those things which we do badly, where our knowledge is inadequate and where research is considered necessary. Many of the statements which are presented are controversial and certain parts may even be biased. This is because the general reporters are typical working engineers who have not attempted to read all the literature, who have not understood all that they have read and who have not necessarily formed unbiased opinions upon that which they have understood. This is a report on the state of the art in rock slope and foundation engineering as seen through the eyes of these two general reporters and it is hoped that it will stimulate others to look more closely at some of the questions raised.

1. APPRAISAL OF ROCK MASSES

1.0 Introduction

The engineering appraisal of a rock mass includes:

- a *qualitative* estimate of the response of the rock mass to change in either geometry or loading. This includes an assessment of possible failure modes.
- a *quantitative* measurement of parameters used in the numerical analysis of the behaviour of the slope or foundation.

Several means have to be used:

- a) geology and hydrogeology
- b) detailed description of the structure (geometry of discontinuities, infilling, etc.) and determination of engineering identification indices.
- c) direct measurement of mechanical parameter meters for use in the analysis.
- d) monitoring the behaviour of the rock mass with changes in load or with time.

Point (a) will not be dealt with in this report which is devoted to the mechanical aspects of slope and foundation behaviour. It is stressed, however, that *geology*, with its description of the rocks, their genesis and history and the sorts of features that characterise the region, together with *hydrogeology*, with its description of the groundwater regime, are vital for a complete understanding of the site.

1.1 List of methods of appraisal

Rock mechanics offers many methods for testing samples, investigation of rock masses and monitoring rock mass behaviour. Indeed, so many methods are available that many engineers are confused by the choice, sceptical about the reliability of the results and sometimes doubtful about the meaning of these results. The purpose of this report is to propose a *selection* of techniques which the general reporters consider most useful for the engineer who wants to know the significant engineering properties of rock masses.

Each method described is particularly applicable to a specific stage in the study of rock slopes or foundations. Some methods yield only *rough qualitative indices* which provide warnings or which facilitate comparison with other sites. Other methods supply *quantitative measurements* of variables which can be used for analysis.

The categories, which are common to both slopes and foundations, which are considered here, are in-situ investigations and laboratory tests. Instrumentation, together with methods of analysis, is required to fill different roles in rock slope and in foundation engineering and will be discussed under these headings later in the report.

The methods selected as the most reliable or the most promising are:

In-situ investigation

Mapping of structures on surface outcrops in exploration adits or on borehole cores.

Graphical presentation of structural geological data.

Geophysics

"Petite sismique"

Rock quality designation (RQD)

Lugeon tests

Jacking tests

Residual stress measurements.

Laboratory tests

Compression and point load tests

Radial permeability tests

Shear tests on discontinuities

1.2 In-situ investigation

1.20 Introduction

This section is devoted to investigations carried out *on the site*. Some of these methods apply from the very first stage of the study while others can only be used when boreholes and adits are available. These methods are typical of recent developments in engineering geology.

There are tests other than those discussed here. The writers have selected only those which seem particularly relevant to the present purpose: the design of slopes and foundations as engineering structures.

1.21 Mapping of structural features

A description of the rock structure (geometry and nature of discontinuities such as faults and joints) is an essential ingredient in any analysis of rock slope stability or of foundation behaviour. The amount of detail required for different stages of the analysis depends upon whether one is designing a slope or a foundation and this difference is highlighted in Figures 1 and 2.

The rock slope engineer is frequently faced with the problem of designing miles of highway cut or open pit mine bench and it is clearly impossible to map all the structural features involved. Consequently the geological data collection is usually carried out in two stages, separated by a preliminary analysis which is intended to isolate critical slopes. Only these critical slopes are considered in detail.

On the other hand, the consequences of failure of a foundation are usually so serious that the preliminary design is carried out in much greater detail and the detailed geological data collection is required at a much earlier stage in the investigation. Since the foundation engineer is concerned with a particular site of limited extent, the amount of work is not usually excessive.

Mapping of surface outcrops of rock is one of the most reliable means of defining the structure of a rock mass. Mapping techniques such as those described by Broadbent, C.D. and Rippere, K.H. (1970) are well developed. Dangerous and inaccessible faces can be mapped by terrestrial photogrammetric methods (Ross-Brown, D.M. and Atkinson, K.B., 1972). In either case, appropriate corrections must be applied to compensate for mapping errors (Terzaghi, R.D., 1965).

These surface mapping techniques are most effective when applied to freshly exposed hard rock faces in slopes, trial excavations or in exploration adits although care must be taken to allow for blasting damage in these faces. Surface mapping is less effective when there is a considerable amount of overburden soil or vegetation overlying the site or when the surface exposures are heavily weathered and the structural pattern ill-defined. In these cases, use must be made of sub-surface exploration methods.

Exploration adits, although by far the most expensive method of sub-surface exploration, are probably the most effective. Not only do they provide a large scale sample of the rock mass but, because the geologist can gain access to the interior of the rock mass, the nature and the orientation of structural features visible within the adit can be determined with considerable precision. Site investigation methods which do not provide information on the inclination and orientation of structural features are of little value to rock engineers since this information is vital in any stability analysis. With careful planning, these adits can be used for large scale drainage tests (Sharp, J.C., 1970) and can themselves become drainage and/or grouting galleries once the construction has commenced.

Trial trenches can only be used where the depth of overburden is small but, where this method is applicable, very valuable information can be obtained supplying a continuous perception of the rock and of

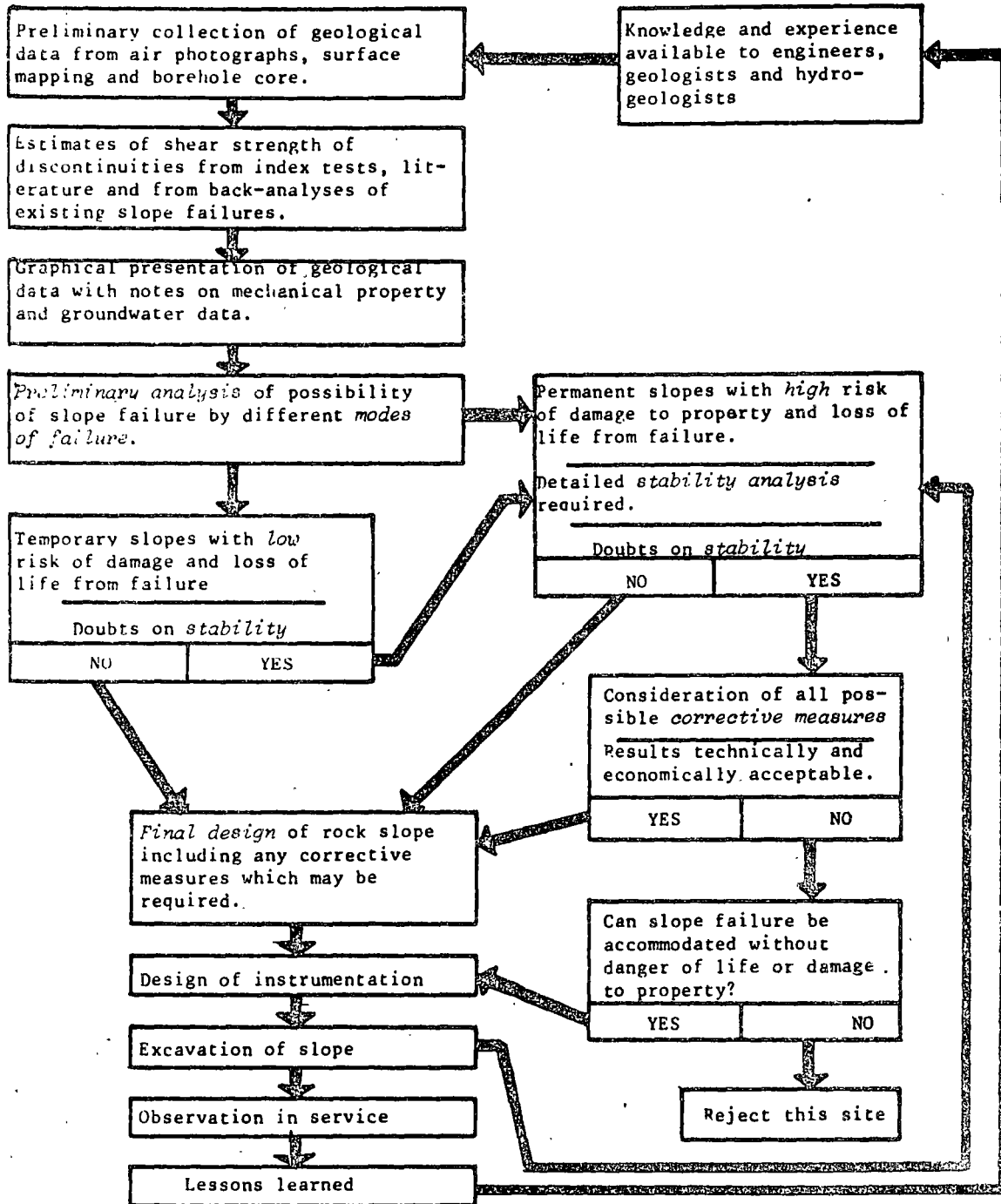


Figure 1: Rock Slope Design Flow Chart

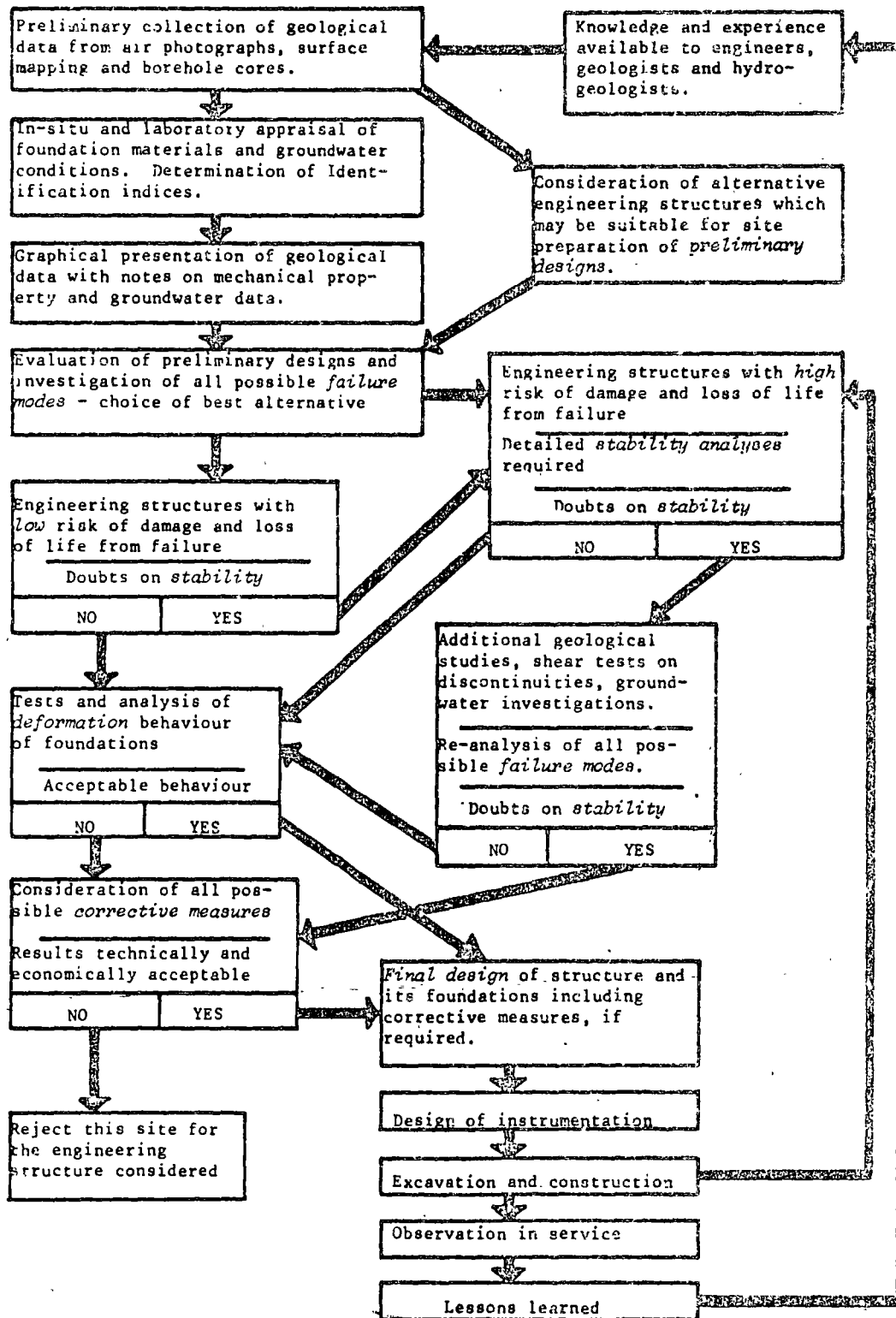


Figure 2: Foundation Design Flow Chart

its main geological features with no gaps over great lengths. Considering that excavation equipment for digging these trenches is readily available on most sites, it is surprising that so little use is made of this method for site investigations for rock slopes and foundations.

Diamond drilling is the most commonly used site investigation method for unexposed rock masses. Although diamond drilling equipment (Jeffers, J.F., 1966) and drilling methods (Rosengren, K.J., 1969) are highly developed, the results of a diamond drilling programme are frequently unsatisfactory. One of the major sources of difficulty is associated with core orientation. Unless the orientation of structural features visible on the core is known, the investment in a drilling programme will be largely wasted since the core will only be of qualitative value to the slope or foundation engineer. Methods of core orientation are available (Kempe, W.F., 1967) but, because they require careful treatment and because they introduce delays into the drilling timetable, these methods are disliked by most diamond drillers. The development of simple and reliable *core orientation systems* is a challenge to drilling equipment manufacturers and the successful development of such tools would represent a significant step forward in site investigation technology.

Of all the techniques used in site investigation, diamond drilling must surely be the one which is subjected to the most abuse. All too frequently, in order to satisfy a site investigation specification derived from some out-dated code of practice, an inexperienced driller is provided with antiquated drilling equipment and instructed to drill in a number of locations which have been chosen with little regard to local geological conditions. Payment on the basis of length of hole drilled rather than on the core recovered is also placing the emphasis incorrectly and the final result is usually of no use whatever. All core boxes should be systematically photographed, so as to keep a safe record of them. All too often the core boxes have disappeared when their examination is most required. Good colour pictures are adequate for checking important features.

Development of site investigation contract policies has simply not kept pace with development of equipment and with *the needs of the rock engineer*. This congress could benefit greatly from the presentation of a model diamond drilling contract for site investigations by an experienced geotechnical consultant who is familiar with the problems of negotiating such contracts in different parts of the world.

Sophisticated drilling techniques such as integral sampling (Rocha, M., 1967) although having great potential, are unlikely to gain wide acceptance while the quality of basic diamond drilling generally available is so poor.

Recognition of the difficulty of obtaining high quality diamond drilling has led some companies to advocate the use of *optical or television probes* for the examination of borehole walls. In theory, if such tools could be made effective and reliable, there would be no need for expensive diamond drilling and holes could be drilled with percussion equipment at low cost. Unfortunately, this theory is far from realisation and currently available borehole probes are exceedingly costly and notoriously unreliable and are

probably more expensive to use than high quality diamond drilling equipment. In the hands of specialised companies having the necessary technical expertise to maintain and to operate these units and to interpret the results, excellent results can be obtained particularly for the detection of thin soft layers which are likely to be missed by the coring. "Do-it-yourself" operations are to be avoided.

1.22 Graphical representation of structural data

The reader may consider it unusual that this topic is identified for special discussion and yet, when one considers that the graphical presentation of structural geology data is a vital link in the communications chain between the geologist and the engineer, it becomes obvious that this is not a trivial question. The graphical presentation of results which depend upon more than three parameters is a permanent source of worry for the engineer. Here we have more than ten variables, not all having the same significance, but all requiring presentation in a form which can be understood and utilised by the engineer. Further research into methods of data presentation would certainly be worth while. Improving the presentation would enable the engineer to understand the geological structure more clearly and to recognise mechanical behaviour patterns more easily. This improved presentation would also considerably ease the difficulties which occur in the dialogue between geologists and engineers.

Several methods have been proposed for presenting the three-dimensional geological structure of a site and some of these methods are briefly reviewed here.

Major features such as large faults can be drawn on a map, clearly showing their direction in space (e.g. Muller, L., 1963). Such maps are most important when considering the overall geological conditions of the site since smaller scale features which may have a more direct influence upon the stability of the site will usually be related to these major features.

One great difficulty in preparing geological maps is to recognise the *continuity or persistence* of structural features. Since a thin clay seam of large extent may be more critical than a large pocket of crushed material, the determination of continuity from outcrops and borehole intersections is an important part of this stage of the site investigation. The writers have found that *scale models* of the site (constructed from rigid plastic sheet or from rods) are extremely useful in this respect since it is possible to visualise the three-dimensional nature of the rock structure more easily (Fig.3). Duplicate models in the design and site offices will minimise misunderstanding.

Minor features such as thin joints, bedding planes etc. cannot be represented individually since there are too many of them and such features must be treated statistically in order to establish *structural patterns*. Polar diagrams, projections of a unit hemisphere, are widely used for this type of analysis (Phillips, F.C., 1971). The *equal area projection* (Fig.4a) is often preferred by structural geologists because it allows for easy plotting of the distribution frequency in space. The *stereographic or equal angle projection* (Fig.4b) is preferred by many engineers because all circles on the hemisphere remain

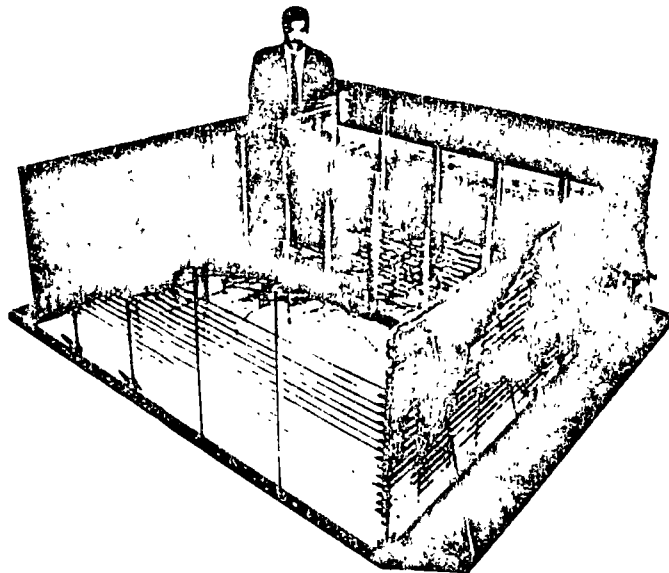


Figure 3 : Plexiglass model of the geology of a dam site.

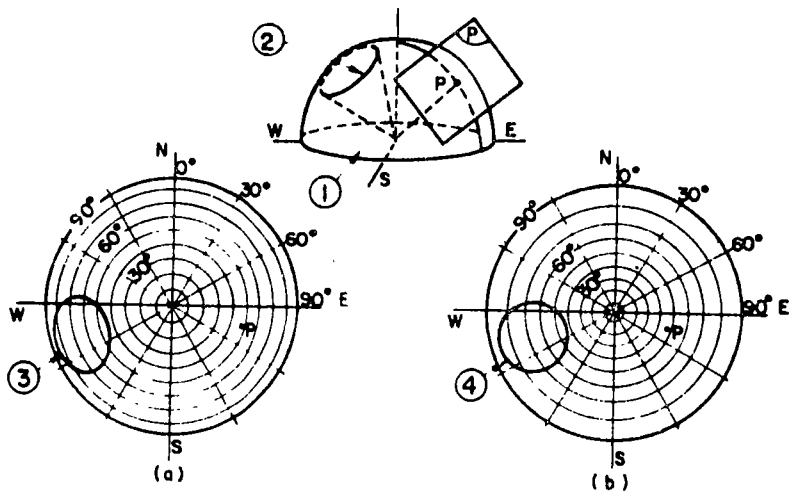


Figure 4 : Polar diagrams .

- (a) Equal area projection (Schmidt)
- (b) Equal angle projection (Wulff)
- (1) Upper hemisphere.
- (2) Circle on sphere.
- (3) Projection of circle (not circular)
- (4) Projection of circle (circular)

circles on the projection and this property allows very convenient graphical treatment of stability problems. The errors in determination of the statistical distribution of structural features can be minimised by using a special grid for counting plotted points. The writers suggest that these counting errors have been over-emphasised since there are certainly systematic errors in the data collection process due to bias resulting from the direction of outcrops and adits in relation to the direction of the structures (Terzaghi, R.D., 1965). Moreover, there are likely to be differences in the statistical results of two surveys carried out by two different teams. Hence, the writers suggest that the statistical treatment of structural patterns and the subsequent graphical stability analyses can be carried out with comparable accuracy using either equal-area or stereographic projections. The choice of which method to be used can therefore be based upon convenience and personal preference.

Use of these projections for presentation and analysis of structural data provides the engineer and the geologist with a very powerful tool. Once the user has become familiar with this tool, it is rapid, convenient and reliable to use. The general reporters wish to enter a strong plea that the use of these projections should form an essential part of any rock mechanics teaching programme.

In spite of the advantages of the methods already described, it must be pointed out that no one method of graphical presentation is entirely satisfactory because no one method can cover *all the parameters* of the problem: direction, spacing, continuity, opening, roughness and infilling of structural discontinuities. Hence, in addition to plots of structural patterns, the authors visualise the need for something similar to the grading curves used in soil mechanics. The development of such a system is a challenge to research workers in rock mechanics.

The surface roughness of structural discontinuities is a question of vital interest to rock slope and foundation engineers. The shear strength of the discontinuities and the permeability of the rock mass are significantly influenced by *dilatancy* of rough joints during shearing. This dilatancy is closely related to the shape of the surface irregularities and to the previous history of shear displacement. In other words, description of the surface roughness of joints at all scales is part of the geometric description of the rock structure, (Fecker, E. and Rengers, N., 1971). How this description can be done is a vital question for discussion.

1.23 Geophysics

Seismic refraction is a well established method used by geophysicists to measure the thickness of weathered rock or soil cover. It has proved extremely useful as a site investigation tool for rapid comparison between several sites. This method yields only a zoning of depth in terms of *longitudinal velocities*. It is well known that longitudinal velocities are not well correlated with other mechanical properties of rock. The question then raised is: can we rely upon this seismic survey for a first selection of sites?

Another development which may in time play an important part in site investigation is that of *seismic logging* of boreholes as used by the oil

industry. The advantage of these methods is that percussion drilling rather than diamond core drilling, can be used, resulting in a considerable cost reduction. Various types of logging tools are available and have shown promising results when applied to problems outside the petroleum engineering industry (Zemanek, J., 1968; Baltosser, R.W. and Lawrence, H.W., 1970). Recent investigations (Lakshmanan, J. and Allard, T., 1971) have shown that there is a good correlation between the fractured density within the rock mass and the *transverse velocity* of the seismic signals.

Finally, the recent improvements in *gravimetry* have made it possible to use this geophysical method for the detection of voids in rock formations. It has been successful since 1970, when high sensitivity gravimeters were built by Lacoste-Romberg, for localising buried quarries or karstic channels.

1.24 "Petite Sismique"

The method called Petite Sismique (Schneider, B., 1967) is entirely different in its principle of operation. Instead of one, several *seismic parameters* (particularly transverse velocity, wavelength and attenuation) are measured and shown on the card (fig. 5). Somewhat similar to a passport, which does not fully describe its holder, but identifies him sufficiently for police officers, the Petite Sismique gives the *identification* of the site and enables the differences, or similarities, with other sites to be detected. This technique has been successfully used in a number of countries and probably deserves to be used more widely. Calibration of a qualitative index of this type can only be achieved by collection and comparison of the results of many successful applications.

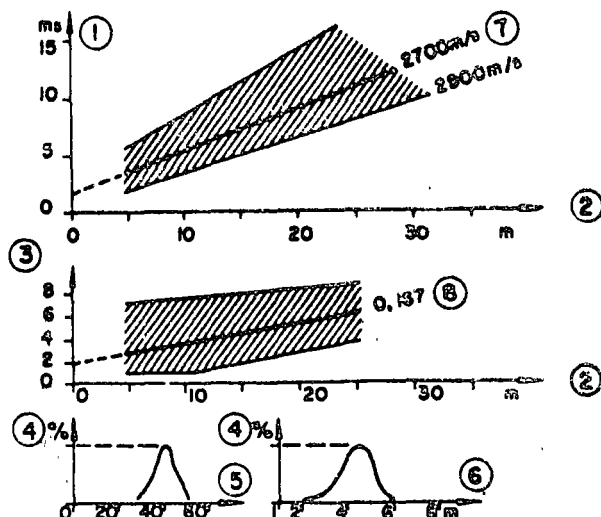


Figure 5: "Petite Sismique" card for a site. (Schneider, B., 1967)

- (1) Time for transverse wave.
- (2) Distance between shock and geophones.
- (3) Gain (dial units).
- (4) Frequency.
- (5) Schmidt sclerometer readings.
- (6) Half wave length (transverse wave)
- (7) Median velocity.
- (8) Median attenuation.

Quantitative correlations have been established between Petite Sismique parameters and other engineering parameters (e.g. Fig. 6). Considering that Petite Sismique survey requires only one engineer for a relatively short space of time, it appears to be a cheap way of getting useful information on a given rock foundation. The only condition is that there should be enough rock exposed, either in outcrops or preferably in adits.

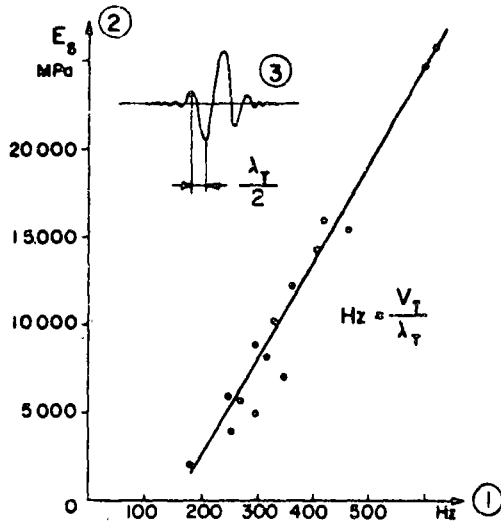


Figure 6 : Correlation between static modulus of deformation and frequency of transverse wave signal obtained by "Petite Sismique" , for various rocks.

- (1) Frequency of transverse wave signal (Hertz)
- (2) Static modulus of deformation (MPa)
- (3) Transverse wave seismogram.

1.25 Rock quality designation (RQD)

The rock quality designation (RQD) (Deere, D.H., 1968) is an index of core recovery obtained by summing the length of pieces of core longer than 10cm and dividing this length by the total length of hole. It is an index of fracture frequency and has proved very useful on many sites for estimating the depth of excavation required before good quality rock suitable for foundations is reached. One of its main advantages is its extremely low cost; the computation of RQD for hundreds of metres can be done in a few hours, either on site or from photographs of the core boxes.

The main question is whether the quality of workmanship can influence the length of individual core pieces and hence the RQD value. It is believed that, provided the drilling operations are carried out by qualified personnel using modern equipment to produce core of at least 50mm in diameter, the RQD or similar fracture frequency indices are useful guides to the mechanical characteristics of a rock mass.

The presentation of results of the successful experiences involving the use of RQD would be useful in clarifying some of the uncertainty associated with these techniques and in convincing sceptical engineers of their value.

1.26 Lugeon test

This well known test, originally proposed by Maurice Lugeon as a criterion for groutability, is widely used to estimate the permeability of rock masses. The test involves packing off a section of borehole and measuring the amount of water which can be injected into the rock mass through this section in a given period of time and at an excess pressure of 10 kg/cm² (1 M Pa).

Several authors argue that this test is invalid in rock because an excess pressure of 10 kg/cm² is sufficient to open discontinuities and to change the permeability or the hydraulic conductivity of the rock mass. Indeed, if a great deal of trouble is taken to orient the hole at right angles to the set of fissures in which permeability is to be measured, to vary the packer spacing and the pressure of injection, a great deal of information can be deduced on the spacing and the opening of discontinuities. A further refinement to the Lugeon test, involving the use of four packers instead of two, has been proposed by Louis (1970). In this test, the central section between the second and third packers is the measuring section, while the two outer sections act as flow barriers which are designed to ensure that radial flow occurs in the measuring section (Fig. 7).

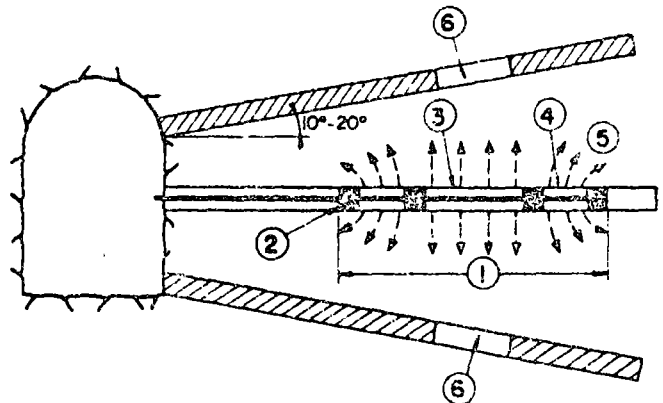


Figure 7 : Hydraulic triple probe for water tests. (Louis, C., 1970)

- (1) Probe.
- (2) Packer (0.8 m long).
- (3) Central measuring section (2 to 5 m long).
- (4) Outer flow barrier section (2 m long).
- (5) Flow lines (radial in central section).
- (6) Piezometers in lined holes.

A question that the general reporters raise is: are we really improving the Lugeon test which is extremely simple and adequate for most sites? The modifications to this test described above may give the illusion of great accuracy but this accuracy may not in fact be obtainable in a medium as complex as rock. While the reporters accept the need for the adoption of a scientific approach to the very difficult problem of water seepage in rock masses, they also feel that there is a need for a clear and unambiguous presentation of the results already achieved, so that the general reader can judge for himself whether progress is being made in this field. One question which will be discussed in more detail later in this report, but which has a bearing on the use of the Lugeon test,

is: does the flow net concept derived from the consideration of flow through porous media apply to rock masses or is it necessary to use an approach based on flow through individual discontinuities?

1.27 Jacking tests

Jack tests designed to determine the modulus of elasticity of a rock mass are more relevant to foundations than to rock slope design. Nevertheless, these tests are discussed in this common section because there are some cases in which results of jacking tests may give information on rock mass behaviour, which is useful to the rock slope designer.

Most jacking tests are interpreted in terms of the Boussinesq equations which provide a relationship between measured load and displacement and the modulus of elasticity. Since these equations are only valid for an elastic continuum, their use yields a modulus of elasticity for an "equivalent" continuous medium. Consequently, the first question which arises is: can the modulus of elasticity obtained by a jacking test be applied to the design of an engineering structure founded on a discontinuous rock mass?

Closer examination of the results of a jacking test shows that the relationship between load and deformation is generally non-linear. In other words, it is possible to infer from a given test several values of deformability depending on the magnitude and the sign (loading or unloading) of the applied load. In fact, these non-linear curves can be used as an additional identification index for the rock mass (Schneider, B., 1967). Correlations with other engineering properties have shown that various slopes of the curves (Fig.8) are indicative of the fracture frequency and the mechanical behaviour of the rock mass. These identifications indices may be useful during the preliminary site investigation. The non-linear load deformation curves obtained in jacking tests are also useful in establishing the stress limits beyond which the concept of modulus of elasticity becomes meaningless and where a foundation design based upon elastic theory could not be considered reliable.

Jacking tests are usually performed in adits where the reaction to the applied load is provided by the opposite side of the gallery. Surface tests can also be carried out if the load reaction is provided by deep anchors (Stagg, 1967). The main point of controversy in the use of these devices relates to the size of the loaded area and the magnitude of the applied load; small load area and high stress, or large load area and low stress? The second alternative is more expensive but probably closer to the conditions which will apply to the full scale structure. In fact, the crucial point of this argument is the question of what effect the scale of the structure has upon the foundation deformations. It is unlikely that this question will be resolved by theoretical discussions and what is needed is a correlation between jacking test results and the deformation of foundations measured on full scale structures. Some attempts have been made to establish such correlations (Ward and Burland, 1969) but it cannot be claimed that this question has been adequately resolved.

Borehole jacks have been developed in several countries and have the advantage of being capable of application at depth within a rock mass. The question

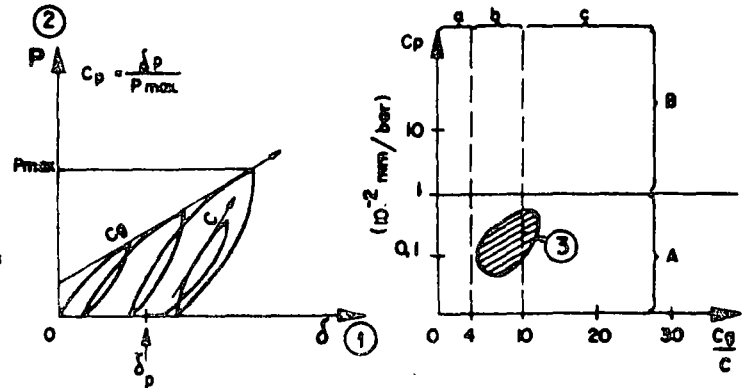
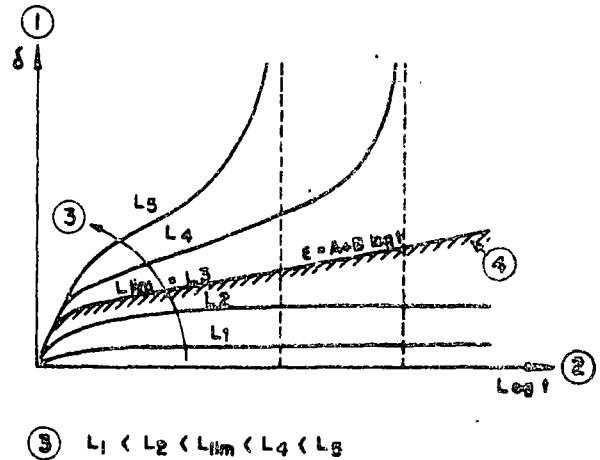


Figure 8 : The jacking test and its interpretation. (Schneider, 1967).

- (1) Displacement of plate.
- (2) Plate stress.
- (3) Points for a given site.
- C, Cg Slopes.
- Cp in 10⁻² mm per bar.
- δp irreversible displacements.
- A Zone of practically elastic deformations.
- B Zone of important irreversible deformations.
- a Zone of compact rock.
- b Zone of average rock.
- c Zone of open jointed rock.

of scale effect is even more important in this case and many engineers will remain sceptical about their use until it has been convincingly demonstrated that the results are relevant to full-scale foundation design. The walls of a borehole, however, are less disturbed than the walls of an adit excavated by blasting. This is in favour of the borehole jacks.



(5) $L_1 < L_2 < L_{lim} < L_4 < L_5$

Figure 9 : Displacement versus time - Limiting load.

- (1) Displacement.
- (2) Time (log. scale)
- (3) Limiting load ($L_{lim} = L_3$)

Many jacking tests show that deformation is *time dependent*. It is therefore interesting to investigate the effect of sustained loading, although such tests are not often carried out in situ because of the high cost and time requirement. It has been suggested that the maximum strain rate under constant load that can be accepted is that corresponding to the upper linear curve in Fig.9, in which strain is plotted against the logarithm of time. The load giving this behaviour is the maximum permissible load above which failure of the foundation will occur after a finite lapse of time. The tests can be carried out by plate loading at the rock surface, or by the use of borehole jacks. The influence of the scale of the test upon the time dependent characteristics measured is an important point requiring further investigation.

1.28 Residual stresses

Before applying a new load to a rock foundation, it may be important to know the magnitude of stresses of tectonic origin which already exist within the rock mass. A knowledge of these stresses is less important to rock slope engineers, although there may be cases where high stresses can develop near the surface, e.g. at the toe of a high cliff.

One method of stress measurement is to use a *flat jack* which is inserted into a slot cut into the rock and pressurised to restore the readings on a deformation gauge set across the slot. This method has the advantage of giving a direct measurement of the stress acting across the slot, but it has the disadvantage of being limited to shallow depth from the rock surface (Fig.10).

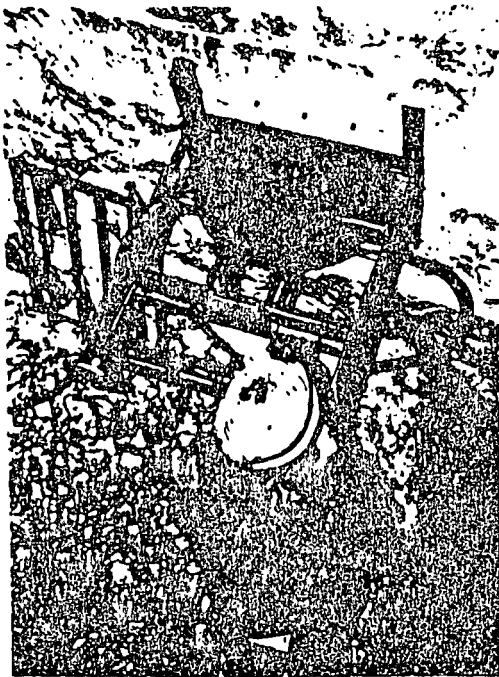


Figure 10 : Flat jack test - cutting a slot with a circular saw. (Photograph by courtesy of S.E.I.L., Paris).

An alternative method is to use electrical resistance strain gauges, or photoelastic transducers which are glued into the borehole and stress relieved by *over coring*. These methods permit the measurement of stresses at depth within the rock mass, but the interpretation of the results, particularly in an anisotropic rock system, is difficult and there are sometimes significant variations between the measurements carried out at adjacent points in the same borehole.

In view of the relative unimportance of residual stress results in the design of surface workings, it is not considered appropriate that stress measuring techniques should be discussed in greater detail in this report. It is, however, hoped that the rock engineer's ability to measure stress will be improved as a result of the research activities of those who are concerned with underground excavation design and to whom residual stress is a crucial issue.

1.3 Laboratory tests

1.30 Introduction

Only a limited number of tests which can be carried out in the laboratory are considered relevant to rock slope or foundation design. The reason is that the behaviour of the rock mass is governed by the orientation and nature of the discontinuities in the rock mass, whereas the samples sent to the laboratory generally consist of the stronger rock material. There are, however, two reasons for studying samples in the laboratory. The first is that the behaviour of the material gives a clue to some of the problems which are likely to arise on the scale of the rock mass. In fact, the rock material is often a small scale model of the rock mass because it has passed through the same tectonic and geological history and the small scale features in the material are frequently closely related to the large scale features in the rock mass. Consequently, a test on a small sample of intact rock can frequently give a useful *identification index* which can assist in the engineering appraisal of the rock mass. A second reason for laboratory testing is that of convenience, provided that it is possible to obtain samples of rock and particularly of rock containing discontinuities such as bedding planes or joints. The best place to carry out these tests is in the laboratory. It must be emphasised that the laboratory need not be located in London or Paris and that a hut or caravan on some remote site can be an effective location for laboratory type work. The term laboratory testing is used here to differentiate between those tests which are carried out on samples which have been removed from the rock mass, and those tests carried out in situ.

The tests discussed here are only a few of those which can be carried out in the laboratory in order to understand the behaviour of rock. It has been assumed that the general reporter of Theme I will cover this subject more thoroughly and that only those topics of direct relevance to the design of surface workings will be dealt with in Theme III. It may be argued that many properties other than those discussed hereunder are useful for the study of rock properties required in the design of slopes and foundations. This question is open for discussion but the tests described are considered by these general reporters to be adequate for design purposes within the framework of currently available knowledge. These tests are:

Compression tests (including point load tests)

Radial permeability

Shear strength of joints

1.31 Compression tests

The *uniaxial unconfined compression test* is a cheap and easy means for obtaining an identification index of the rock material. More elaborate tests, which are extremely numerous, have little practical value for slope and foundation design. The results of uniaxial compression tests, like all other tests on rock, invariably show a significant amount of scatter. This scatter is associated with the discontinuous nature of rock: the engineering properties being governed by discontinuities which may range from grain boundaries on a small scale to joints and faults on a large scale.

Some authors have argued that the amount of scatter associated with the uniaxial compressive test is reason enough for the test to be discarded. On the other hand, some argue that the amount of scatter gives a useful qualitative indication of some aspects of the nature of the rock mass. The general reporters suggest that the following qualitative indications may be obtained by uniaxial testing: (a) the mean value of strength allows an initial *classification* of the site, (b) the variation in strength from one zone to another gives an indication of the *heterogeneity of the site*, (c) variation in strength with the orientation of the sample gives an indication of the possible *anisotropy* of the rock mass, (d) scatter of the results of small sample tests gives an indication of the *microfracturing* of the rock as a result of previously applied tectonic stresses.

In order to minimise the time and expense involved in preparing the ends of specimens for uniaxial compression testing, it has been suggested that *point load tests* or *Brazilian tests* yield results of comparable accuracy. In these tests an unprepared piece of

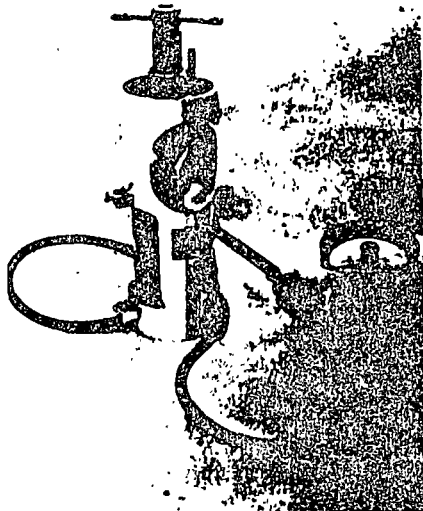


Figure 11a : Machine for point load strength determination. (Manufactured by Robertson Research)

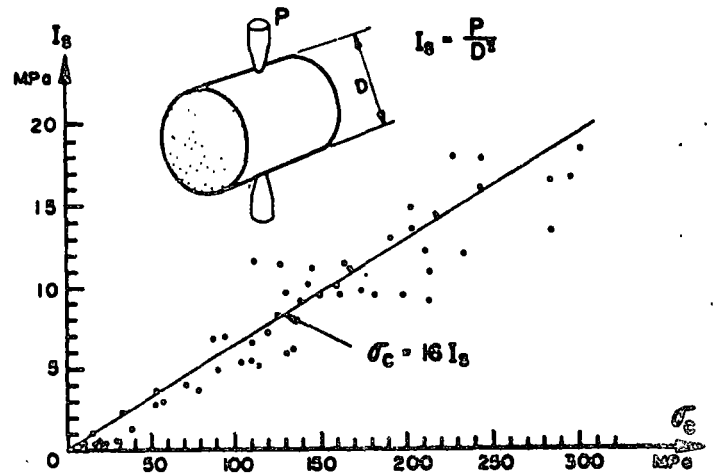


Figure 11b : Relationship between point load strength index I_s and uniaxial compressive strength σ_c .

rock core is loaded between two points (Fig.11) and the core is split as a result of tensile stresses developed across the core. This test, which is extremely cheap and quick to use during site investigations, provides results which are closely related to the strength of the rock material (D'Andreas, D.V. et al, 1965).

In addition to strength testing, measurement of the *modulus of elasticity* on cores of rock subjected to uniaxial loading is a basic means for determining this property of the rock material. This value must obviously be reduced when considering the deformation of a rock mass and the extent of this reduction is a question requiring further investigation.

1.32 Radial permeability

Radial permeability is also an indirect measure of the degree of fracture of a sample of rock material (Bernaix, J., 1967). In this test, cores with an axial hole (Figure 12) are subjected to radial percolation of water under pressure. The index measured in this test is the ratio $S = k(-1)/k(+50)$ in which $k(-1)$ is the permeability measured for convergent flow under a differential pressure of 50 bar. When S is high the rock material permeability is very sensitive to applied stresses, a phenomenon which is typical of fractured rock. The main value of this test is not for the measurement of the permeability of the rock material, which generally has little influence on the hydraulic behaviour of a rock mass, but of the degree of fracturing of the rock material. A great number of tests have shown the existence of correlations between the ratio S and the scatter of strength values, or the scale effect on strength.

The use of this simple test is therefore similar to that of the uniaxial compression test. The value obtained is, however, more clearly related to the degree of fracture of the specimen and it has little relationship to the mineral composition of the rock.

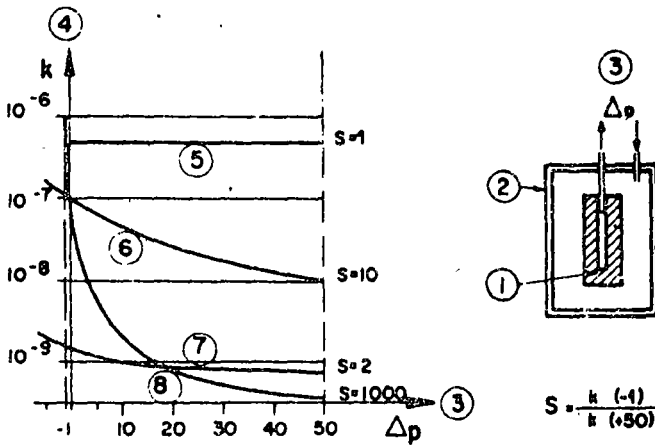


Figure 12 : Radial permeability test and curves for various values of index S (Bernaix,J., 1967)

- (1) Rock sample with axial hole.
- (2) Pressure cell.
- (3) Water pressure differential Δp (bar).
- (4) Permeability "k" (cm/s).
- (5) Oolitic limestone (no fissures).
- (6) Gneiss (average).
- (7) Gneiss (compact).
- (8) Gneiss (fissured).

1.33 Shear strength of discontinuities

Because the stresses acting on rock slopes and foundations are low, fracture of intact rock is seldom involved in the failure of these structures; their mechanical behaviour being governed by shear movement on discontinuities such as faults and joints. Consequently, determination of the shear strength of these discontinuities is a question of fundamental importance in the design of surface workings.

The surfaces of separation (stratigraphic layers such as bedding planes and geologically induced fractures such as faults and joints) have a tensile strength which is for all practical purposes zero, and a shear strength which depends on wall roughness, the infilling material and the amount of imbrication (arrangement of individual blocks). The most dangerous for stability are obviously the surfaces that are planer, smooth, filled with soft materials, of large area and not interlocked. This is the case of shear fault. Less dangerous discontinuities are those which have not been subjected to large shear displacements in the geological past and where there is some interlocking of surface roughness or cementing of the surfaces by precipitated infilling.

The difference in mechanical behaviour between these two types of surface is illustrated in Figures 13 and 14 in which shear stress is plotted against displacement and against normal stress. In the case of rough surfaces (curve A in Figure 13) interlocking of surface irregularities causes the sample to behave in an approximately linear-elastic manner for small displacements. At a given displacement, the peak shear strength of the surface is overcome as a result of over-riding or shearing through of the interlocking irregularities and a rapid drop in shear strength occurs as displacement is continued. Eventually, when

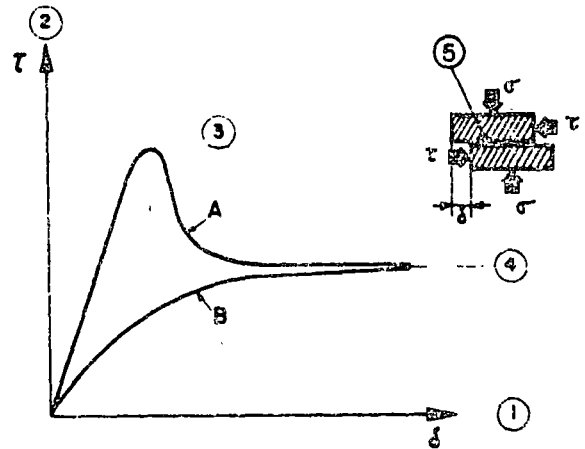


Figure 13 : Variation of shear resistance with displacement on a discontinuity.

- (1) Displacement .
- (2) Shear stress .
- (3) Peak shear strength.
- (4) Residual shear strength.
- (5) Pre-existing discontinuity.
- A Rough surface which has not been subjected to previous displacement.
- B Smooth surface which has been subjected to large displacement.

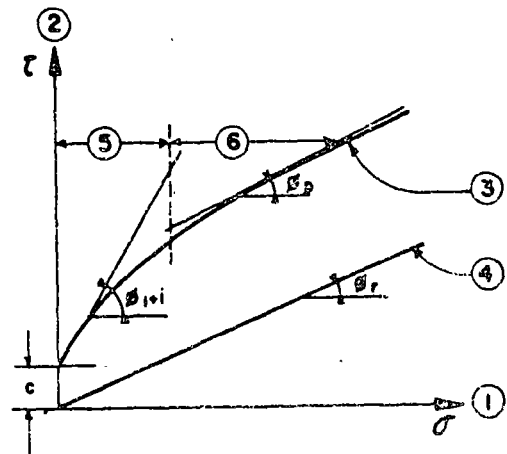


Figure 14 : Variation of shear strength with normal stress for peak and residual strength.

- (1) Normal stress.
- (2) Shear strength.
- (3) Peak strength.
- (4) Residual strength.
- (5) Dilation.
- (6) Shear.

the surfaces have been ground smooth, a residual strength value is reached.

In the case of smooth surfaces (curve B in Figure 13), the peak strength has already been exceeded during previous geological movement and the shear strength increases smoothly with displacement until the residual strength value is reached.

Considering the values of peak and residual strengths for various applied normal stress levels, the curves illustrated in Figure 14 are typical of the behaviour of rock surfaces. In the case of the peak strength behaviour, a small value of cohesion c may be present due to cementing of the surfaces. The curve relating shear strength and normal stress is generally non-linear as illustrated. This curve is steeply inclined at low normal stresses as a result of the interlocking of surface irregularities. Because of the high strength of the rock material from which these irregularities are formed, shear displacement at low normal stress takes place as a result of overriding or *dilation* in which the irregularities move over one another and the total volume of the specimen is increased. The slope of the curve at low normal stresses can be approximated by the angle $(\phi_i + i)$ where ϕ_i is the friction angle of the material surface and i is the average angle of incidence of the surface irregularities to the direction of shearing (Patton, F.O., 1966). As the normal stress increases, the dilation of the specimen is inhibited and fracturing of or shearing through the interlocking surface irregularities commences. Eventually, the shear strength of the surface is controlled entirely by the shearing through of these irregularities and the inclination of the curve approaches the peak friction angle ϕ_p of the rock material.

In the case of the smooth surface (curve B in Fig.13), the residual strength behaviour is defined by the friction angle ϕ_r and the cohesion is, for all practical purposes zero. Note that the friction angles ϕ_p and ϕ_r are not necessarily equal since the infilling material in the case of the smooth surface may have been altered by weathering.

An extremely important point which emerges from Figure 14 is that the residual strength of sheared surfaces is *not influenced by the scale of the test*. This is because the friction angle ϕ_r is a dimensionless number and, provided that there is no cohesion intercept, its value can be determined by tests on small samples (Londe, P., 1973). On the other hand, when large shear displacements have not already occurred in the geological past and when the sample displays a peak strength behaviour (curve A in Fig.13), both the cohesion c and the roughness angle i will depend on the scale of the specimen tested. The basic question which must be considered here is: can the values of cohesion and roughness angle determined in small scale laboratory tests be relied upon for the design of large engineering structures?

This question can only be answered by considering the behaviour of full scale engineering structures, such as rock slopes and Figures 15 and 16 illustrate an example of this type of analysis. In Fig.15, the results of a number of shear tests on porphyry joints are plotted and the lines A, B, C and D define the limits of scatter of the peak and residual strength values. In Fig.16, critical slope height versus slope angle relationships have been derived from the results given in Fig.15 and are compared with the slope height - slope angle relationship for nine porphyry slope failures in the Rio Tinto area. It will be noted that all the slope failures fall within the region defined by the residual strength parameters, although it should be noted that a small cohesion intercept (0.1 MPa) has been assumed for this analysis (Hoek, E., 1970). Note that, unless the small cohesion value is included,

all slopes should have failed at the residual friction angle of approximately 35° .

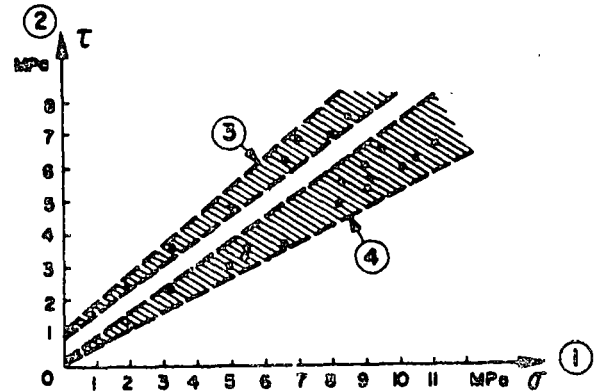


Figure 15 : Shear strength results for porphyry joints from Rio Tinto in Spain.

- (1) Normal stress (MPa)
- (2) Shear strength (MPa)
- (3) Peak strength .
- (4) Residual strength.

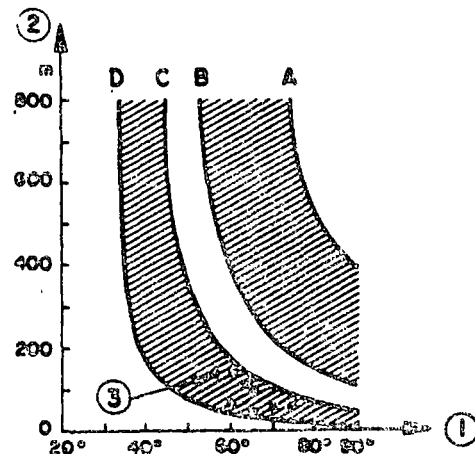


Figure 16 : Critical slope height versus slope angle relationships derived from figure 15, compared with mine slope failures in porphyry.

- (1) Slope angle (degrees).
- (2) Slope height (meters).
- (3) Slope failures.

In Figure 17, values of cohesion and friction angle have been plotted from the results of a number of analyses, similar to that discussed above. Many of these results have been determined from relatively short term failures in small slopes and, included in the diagram, an arrow gives a qualitative indication of the influence of time and scale of the structure. This is a question which obviously requires a great deal of research and discussion but, as a result of their own experience, the reporters propose the following general rules:

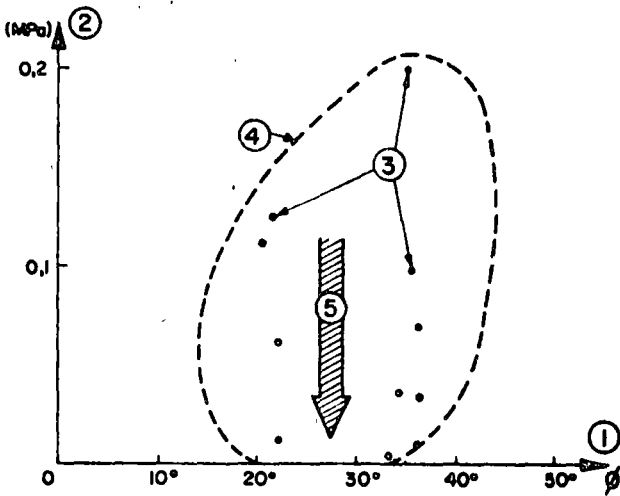


Figure 17 : Relationship between cohesion and friction angle determined by back-analysis of slope failures.

- (1) Friction angle ϕ (degrees).
- (2) Cohesion (Megapascals)
(1 MPa = 10 Kg/cm² = 142 lb/in²)
- (3) Each point corresponds to an observed slope failure.
- (4) Boundary of suggested range of values which can be used for slope design.
- (5) Influence of time and size.

- a) When a very large structure such as an arch dam or major building foundation is being designed for conditions of long term stability (more than 100 years), it is recommended that the design based on zero cohesion and a residual friction angle ϕ_r , which can be determined in small scale laboratory tests.
- b) Where temporary rock structures of limited size are being designed, it is permissible to allow some cohesion and non-linearity of the shear strength versus normal stress curve, provided that these values are checked against typical values obtained from back analysis of failures in similar materials.

The general reporters regard it as irresponsible engineering practice to attempt to calculate the value of cohesion from the intact strength of small scale rock samples.

Several different types of direct shear machines have been designed and two typical designs are illustrated in Figure 18 and 19. The machine shown in Fig 18 is capable of testing relatively large specimens (approximately 400mm x 600mm) while the small machine shown in Fig.19 is designed for testing pieces of core or small hand samples. Friction angles measured in either of these types of machines tend to compare very well and, since the reporters do not advocate the determination of cohesion by laboratory testing, it makes little practical difference which one is used. The only reason for using the large one is when one has to test a thick joint.

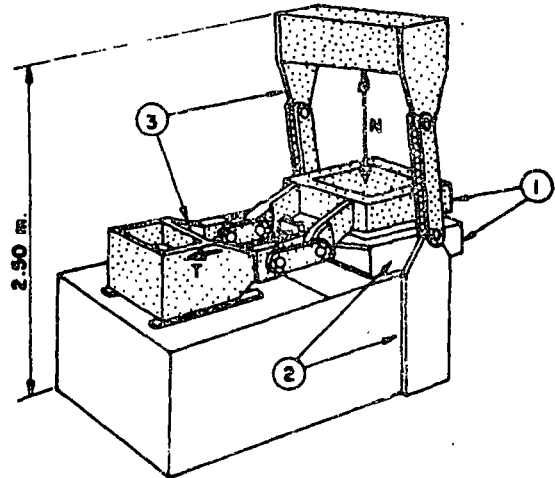


Figure 18 : Direct shear apparatus for testing rock joints in the laboratory (Londe,P., 1973)

- N Normal force.
- T Shear force.
- (1) Upper and lower parts of shear box.
- (2) Fixed parts.
- (3) Moving parts.

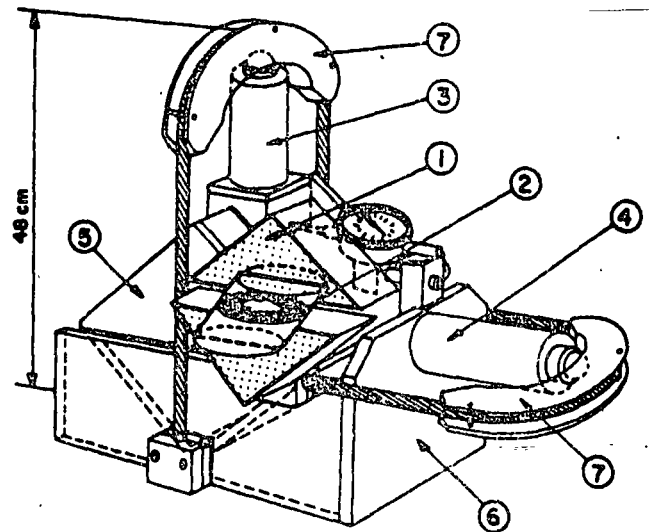


Figure 19 : Portable shear machine for use in site laboratories. Weight 400 N (Hoek,E and Bray,J., 1973)

- (1) Concrete or plaster cast specimen mount.
- (2) Shear surface.
- (3) Normal load jack.
- (4) Shear load jack.
- (5) Upper shear box.
- (6) Lower shear box.
- (7) Rope load equaliser.

In order to estimate cohesion from large scale shear tests, many authors have reported the results of shear tests carried out in situ. In these tests, the specimen is cut free from the surrounding rock mass, with the exception of one side which is left attached.

Shear and normal loads are generally applied by means of flat jacks or hydraulic ram jacks and, because of the large size of the equipment required, these tests are extremely expensive. These general reporters do not recommend in situ shear testing except under very special circumstances. Many readers may wish to disagree with this recommendation and the reporters would welcome a general discussion on this topic.

2. DESIGN METHODS

2.1 Introduction

Before going on to discuss the design of rock slopes and foundations, it is necessary to consider the general question of how a design in rock should be approached. Having accumulated data on the geometry of the rock structure, the mechanical properties of the rock mass and the groundwater conditions, how is this information to be processed in order to arrive at an assessment of whether the overall design will be satisfactory?

Considering the large number of parameters which are involved in defining the behaviour of a rock mass, the fact that their measured values will be widely scattered and their inter-relationships ill-defined, it is clear that a precise assessment of the performance of the rock mass is not possible. In addition, it must be kept in mind that different criteria will have to be satisfied, depending upon the purpose of the rock structure. Hence, a safe slope may be regarded as one which remains standing for the duration of its working life while a foundation may be regarded as inadequate because of differential movements of relatively small magnitude which can induce failure in a structure such as a concrete dam.

In spite of these difficulties, it is, nevertheless, clearly necessary that some form of *quantitative* assessment of the performance of the rock slope or foundation should be attempted. The following chapter gives a brief review of the methods which can be used together with comments on the usefulness and limitation of each of the methods. Detailed discussions on the application of some of these methods to the design of rock slopes and foundations are given later in this report.

The following topics will be discussed in this chapter:

- Model studies
- Mathematical models
- Limit equilibrium methods
- Mechanical effects of water pressure
- Factor of Safety.

2.1 Model studies

Mechanical and civil engineers have made extensive use of models as design tools for many years. Hence, a complex component for an aeroplane, a car or a bridge can be made up at low cost as a reduced scale model and tested to destruction. Because the materials used are man-made and their behaviour is well known, precise model laws can be used for the interpretation of the results of such model tests. Consequently, such models are valid and valuable design tools.

Because of the difficulties involved in studying the behaviour of fullscale rock structures, it is not surprising that many attempts have been made to use models in much the same way as they are used in other branches of engineering. Two distinct types of physical models must be considered:

- a) *Phenomenological Models* which are designed to study general behaviour pattern
- b) *Design Models* which are intended to provide quantitative information.

Models which are built up of simple bricks of plaster, cement, wood or any other material to represent a rock mass can provide extremely valuable information on *behaviour patterns* in such discontinuous systems. Such models have revealed previously unrecognised failure modes or have confirmed hypotheses built up by careful field observation. Note that these models are essentially *geometrical models* and that no serious attempt is usually made to simulate all the mechanical properties of the rock mass. Model studies of this type (Maury, V., 1970, Barton, N.R., 1970, Krstanovic D., 1967, Goodman, R.E., 1972) have proved invaluable as *research tools* and the writers strongly recommend the use of simple models to assist students and design engineers in understanding the basic behaviour patterns in discontinuous rock masses.

On the other hand, models which are intended to provide quantitative design information are not favoured by these general reporters. Even if it were possible to satisfy all the similitude requirements, the amount of time required and the cost of constructing a detailed *design model* is such that it is most unlikely that more than one model will be built for any particular problem. Such a model, if well made, may create an illusion of great accuracy and may encourage the designer to accept a single set of results without considering other failure modes and behaviour patterns. Hence, while value of models as research and educational tools is not questioned, their use as design tools is not recommended since their use defeats the basic object of a good design - to consider all possible combinations of parameters and to arrive at a *balanced judgement*. A "precise" answer based upon an inadequate set of assumptions is of no use to the design engineer.

2.2 Mathematical models

Two types of mathematical model are relevant to this discussion:

- a. Finite element models
- b. Dynamic relaxation models

Recent developments in both finite element (Goodman, R.E. and Dubois, J., 1972) and dynamic relaxation models (Cundall, P., 1971) have extended the methods to make it possible to deal with *discontinuous systems* and *simple three-dimensional problems*. Although the mechanical properties of all the elements in a discontinuous rock mass are difficult to represent and although the capacity of present computers limits the size of problem which can be dealt with, the writers are confident that further development of these techniques will provide engineers of the future with very powerful tools. Compared with physical models, these mathematical models will be both cheaper and

GENERAL REPORT

quicker to operate. Their one outstanding advantage is the possibility, at small additional cost, to vary each of the parameters involved in order to check the *sensitivity* of the design to these variations.

In spite of general optimism about the development of these tools, there are still serious barriers to their effective use as design methods. These barriers involve the difficulty of supplying adequate *input data* for a meaningful analysis. Consider a relatively simple stability problem involving a rock mass with three intersecting sets of discontinuities and subjected to water seepage. The input data required for a mathematical model of this problem are:

- 3 values for friction angles
- 3 values for cohesion
- 3 values for hydraulic conductivity
- 3 values of compression modulus
- 3 values for shear modulus
- 3 values for dilatancy coefficient

A total of 18 variables, each having a range within which its values can be scattered. In addition, the hydraulic boundary conditions (generally very poorly known) have to be defined.

The simple question which must, therefore, be considered is - can input data be obtained for real problems which will permit a meaningful mathematical model to be used for design purposes? The answer, in the case of typical problems encountered by the design engineer, is no. Consequently, the conclusion must be that these mathematical models are extremely useful research tools but must be used with caution if applied to real problems.

2.3 Limit equilibrium methods

The most important failure modes in rock masses which are subjected to low loads (i.e. surface workings) are associated with movement on preexisting discontinuity surfaces (faults, bedding planes, joints etc.). If failure of the intact rock material and deformations within the rock mass are ignored, a simplified mathematical model of the failure process in a rock mass can be constructed. In this model it is assumed that sliding of blocks of material occurs when a condition of *limiting equilibrium* is reached, i.e. when the driving forces due to gravity and water pressure are exactly balanced by the resisting forces due to friction and cohesion. Because deformation of the rock mass is not considered, large blocks, which are assumed to remain intact, can be considered and the force system can be simplified to a few total forces acting at specific points on the surface of the blocks. The problem of a wedge of rock resting on three intersecting discontinuities can now be solved on the basis of:

- 3 values for friction
- 3 values for cohesion
- 3 values for forces due to water pressure

A total of nine variables. As discussed in section 1.33, a critical structure is normally designed on the basis of zero cohesion and hence this number of variables can be reduced to 6 for such cases.

Graphical and analytical limit equilibrium solutions to a variety of rock stability problems have been published (Wittke, W., 1965, Londe, P., 1965, John, K., 1968, Londe, P. et al, 1969 and 1970, Hendron et al, 1971, Hoek et al, 1973). These methods are the most widely accepted and commonly used *design tools* in

surface rock engineering because they are simple and quick to apply and because they permit a rapid assessment of the influence of variations in all the parameters involved in the solution. The graphical methods are particularly useful for *field applications* and can play an important part in the progressive design of site investigations - each step in the investigation being designed to check specific features which the analysis has shown to be important.

This approach has, of course, some limitations. The conditions of limiting equilibrium are assessed without taking the deformations of the rock mass into account. If the rock mass is to act as a foundation, these unknown deformations may be unacceptably large and it is therefore necessary to carry out additional work (Fig. 2) to check this deformation behaviour. The assumption that the sliding mass remains intact may also be unrealistic and practical observations suggest that the breaking up of a block of rock during the early stages of sliding will have a significant influence upon the behaviour of a slope. In some cases, improved drainage due to opening up of fractures may be sufficient to stabilise the slope.

Are these limitations serious enough to overcome the advantages of the method? The answer seems to depend upon which point of view is taken. The responsible engineer should be concerned with the detection of factors important in controlling the stability of his particular site rather than with "accurate" computations. Once these factors have been identified, realistic practical decisions can then be taken on the steps which are necessary to ensure that the rock mass will behave in a reasonably predictable manner. On the other hand, the research scientist is concerned with understanding the full picture, hopefully in order that he may be able to evolve better design methods. Consequently, he may feel that the assumptions upon which the limit equilibrium methods are based are unacceptable and that the more comprehensive treatment provided by mathematical models is preferable.

The general reports feel that both points of view are valid and the development of these and other methods is necessary provided that the final aim of designing safe rock structures is kept clearly in mind.

2.4 Mechanical effects of water pressure

2.40 Introduction

A rock mass is seldom dry. Water seeps through fissures as soon as a hydraulic gradient develops, either from rainfall or from water present in a dam or from the creation of an excavation below the water table.

Only the *mechanical effects* of water seepage will be considered here, that is the influence of fissure *water pressure* upon stability - an influence which is unusually important and is sometimes the governing factor in a slope or foundation design.

In order to determine the pattern of water forces developed by the flow of water in a rock mass, the designer has to know or to make assumptions on the flow conditions. This is an extremely difficult problem.

Firstly, the answer depends upon the geometry of the structural discontinuities in the rock mass and, as pointed out in section 1.21, this geometry is difficult to ascertain. Secondly, it depends upon the boundary conditions of the hydraulic field (including

time - transient or steady state seepage). Thirdly, changes in fissure opening as a result of deformation (some of which are due to the water pressure itself) can significantly influence the hydraulic conductivity of the rock mass. Fourthly, there is a marked scale effect in hydraulic conductivity measurements.

No general solutions which will allow all these conditions to be considered are yet available. There are, however, some simplified models which are very useful to the designer in that they enable him to appreciate the possible influence of water pressures on the stability of rock masses and, also, provide guidance on appropriate corrective actions.

2.41 Forces developed by water seepage

The water flowing in fissures in a rock mass has a hydraulic head at each point and this allows us to extend, to these systems, the concept of *potential gradient* used in the hydraulics of porous media. The forces developed by seepage flow are body forces applied to the intact rock and are proportional to the potential gradient. These forces have to be added to the forces generated by buoyancy.

The *hydraulic conductivity* of a rock mass is governed by the discontinuities which have a much higher "permeability" than the rock material. Because of the inherently anisotropic nature of the rock mass, the hydraulic conductivity is *anisotropic* and the forces due to water pressure have preferred directions. In some cases, these forces are detrimental to stability since they have magnitudes approaching that of other forces (such as weight of the rock mass or the thrust from a structure) and act in unfavourable directions (such as towards the free faces of the rock mass).

The concept of a *conductivity tensor* to represent both magnitude and direction of hydraulic conductivity in a rock mass is an interesting research topic (Maini, Y.N.T., 1971) but it cannot be claimed that it is a practical design tool. Consequently, the only approach available to the design engineer is to consider a number of simplified models of possible flow behaviour in order to obtain a qualitative assessment of the influence of the forces developed by water flow in a rock mass. Hence, schematic flow nets which allow for the anisotropic nature of the rock can be used to estimate the magnitude of water pressures which can be used in stability analyses (Sharp, J.C., Hoek, E., Brawner, C.O., 1972). It is important that the method of stability analysis should allow a wide range of possible forces due to water pressure to be considered in order that the sensitivity of the design to these variations can be assessed (Londe, P. et al 1969 and 1970).

A disadvantage of using flow nets for assessing water forces is that they assume a static flow situation. In fact, forces due to water pressure may change in magnitude and direction due to deformation of the rock mass and, under some circumstances, the forces due to water pressure may disappear due to increased permeability resulting from deformation while, in other cases where a large supply of water is available from a reservoir, the forces may persist due to the greater flow volumes. Consequently, the concept of water *energy* is probably necessary for a full understanding of the response of a rock mass

to water flow. An interesting question for discussion is whether it is possible to introduce this concept into a practical stability analysis.

A considerable amount of attention has been devoted to defining the type of water flow in rock masses - whether it is laminar or turbulent. Research studies have shown that the type of flow has relatively little influence upon the forces which are developed but that the quantity of flow can be significantly different from that predicted by simple models, (Louis, C., 1970, Sharp, J.C., 1971, Jouanna, P., 1972).

2.42 The planar fissure model

Several authors have shown, by theory or by experiment, that in a rock mass where all the discontinuities are planar and of constant opening from node to node, the modulus of deformation of the rock mass is very low as compared with the modulus of deformation of the rock material. Obviously, in such a system, the opening of the discontinuities will change significantly with applied load.

Applying the laws of hydraulics, linear or otherwise, to this behaviour may produce extremely spectacular changes in hydraulic conductivity for moderate variations in stress (Serafim, J.L. and Del Campo, A., 1965, Londe, P. and Sabarly, F., 1966). These changes could result in the completed engineering structure having a behaviour pattern entirely different from that predicted from site investigations carried out on an unloaded rock mass. The application of this model to engineering design has two important consequences. Firstly, any stability analysis must include extreme water pressure conditions resulting from stress changes and, secondly, the design of remedial measures should take this extreme behaviour into account.

A discussion on the validity of this model would be useful since it has a great practical significance, particularly for foundation design.

2.43 The preferential channel model

Practical observations of the flow of water from discontinuities exposed in adits shows that, in some rock types, water flows through *preferential channels* which are usually located within the planes of the discontinuities (Sabarly, E et al, 1970).

Examination of a model where all water seepage occurs through such preferential channels leads to an important conclusion: in this case, drainage will not have a significant influence upon the flow conditions except where a drain happens to intersect a channel. Consequently, drainage will not be effective as a corrective measure for improving stability. This conclusion has very serious implications since drainage is an essential feature in the design of many foundations and slopes.

Whatever one's personal opinion on this model, it seems important to answer the following questions:

- a) How can the seepage of water which takes place through channels in a rock mass be detected?
- b) Can the "permeability" of a rock mass with preferential channels be controlled by

routing?

- c) Is it possible to drain such a rock mass, possibly by different drainage systems?

While it is unlikely that an actual rock mass will correspond to either the planar fissure model or to the preferential channel model, these models do represent extreme situations which the designer has to consider as "the most unfavourable mechanical possibilities which could be expected" (Terzaghi, K., 1929). This is a basic principle of rock design when the safety of a large structure is involved.

2.5 Comments on the use of a Factor of Safety

One of the most controversial questions in rock engineering is concerned with the use of the factor of safety concept. Is the factor of safety of a slope or a foundation meaningful or is it, as some writers have suggested, a totally misleading and useless concept?

The factor of safety for a rock slope may be defined as the ratio of the total force available to resist failure to the total driving force tending to induce failure. In the case of a foundation, the factor of safety may be considered as the ratio of the amount of deformation anticipated as a result of movements within the rock mass to the allowable deformation of the structure.

In the case of a rock structure in which a large number of ill-defined parameters interact in a complex manner, the calculation of safety is a much less satisfactory process.

Should the entire concept be rejected? Are there alternative methods which are more acceptable?

One possible approach which has been discussed by several authors is the *probabilistic analysis* of variables leading to a concept of safety in terms of a given probability of failure. This definition of safety is, in itself, a problem since many clients find it extremely difficult to accept an admission by the consulting or design engineer that there is a possibility however small, of failure. A factor of safety of 1.5 or 2.0 may be regarded as acceptable because it represents a familiar situation which experience suggests will be safe while a probability of failure of 1 in 100,000, which may mean precisely the same thing, will be treated with suspicion.

If the probabilistic approach was inherently superior to the factor of safety approach, this problem of definition could be overcome in time since it is basically a question of education. A more serious difficulty, however, is the difficulty of dealing with the large number of variables involved in the problem. Some mathematicians may be confident that these problems can be solved by probabilistic methods, but most engineers are certainly not convinced that these methods are reliable - even if they can understand the mathematical jargon which tends to be used to excess.

These general reporters feel that probabilistic methods have a great deal of merit and that further developments and a greater familiarity with the techniques will eventually result in these methods

gaining wider acceptance as practical design tools. The present conclusion, however, is that probabilistic methods are not yet sufficiently developed for general application in rock engineering.

In the absence of acceptable probabilistic methods and as an alternative to the use of a single value for the factor of safety in an engineering design, an approach which is frequently used is to analyze the *sensitivity of the design to changes in significant parameters*. There are several methods available for doing such a sensitivity analysis and two examples are given below:

- a) For the condition of *limiting equilibrium*, calculate the value of one of the important parameters required to satisfy the conditions being studied for a range of values of the other parameters involved. Hence, the value of cohesion required to satisfy the condition of limiting equilibrium in a slope problem can be calculated for a range of friction angles and groundwater conditions. An example of this type of analysis is given in section 3.3.
- b) By varying each significant parameter in turn while keeping the values of other parameters constant, the *sensitivity of the factor of safety* to variations in each parameter can be evaluated. The rate of change of factor of safety probably has more significance in engineering design than the value of the factor safety itself because this rate of change is indicative of the importance of each parameter and of whether the behaviour of the structure can be controlled by artificially inducing changes in these parameters.

Graphical presentation of the results of these *sensitivity analyses* is of the utmost importance since it is only when the variations which have been computed are clearly displayed that they can form the basis of sound engineering decision making. The computer, with its ability to check a large number of variations rapidly and to display the results of these computations in various graphical forms has a very important part in this type of analysis.

The conclusion of this section is that the concept of factor of safety is not easily used in rock engineering but that the rate of change of factor of safety is probably the most reliable indicator of engineering behaviour which is currently available. This subject certainly deserves a wide and open discussion and it may well form the theme for a future Congress.

3. ROCK SLOPES

3.0 Introduction

This chapter is devoted to the application of rock mechanics to rock slope engineering.

The rock slope engineer is primarily concerned with ensuring that a slope will not fail or that, if failure is allowable, it should occur in a predictable manner. Except when a slope is also to act as a foundation, the deformation of the rock mass into which the slope is cut is of secondary importance.

In contrast to the foundation engineer, who is generally concerned with a specific site of limited extent, the slope engineer may be involved in designing many kilometers of highway cuttings or the overall slopes of an open pit mine. Since neither the time scale nor the economics of such a project allows a detailed investigation of each slope, it is essential that the slope engineer should work to a system which allows him to eliminate stable slopes at a very early stage of his investigations and to concentrate his attention onto those slopes which are critical.

Figure 1 shows that very crude stability analyses should be carried out at an extremely early stage of a project when only the most rudimentary geological data is available. These analyses should permit the engineer to differentiate between those slopes which are obviously stable and those in which some risk of failure exists. They should also be used as an aid to the planning of site investigations to ensure that a maximum amount of relevant information is obtained at minimum cost. More detailed types of analyses, applied only to critical slopes, are only justified when detailed information on the structural geology, the groundwater conditions and the mechanical properties of the rock mass is available. Such analyses should permit a consideration of the widest possible range of conditions rather than being confined to the production of a "precise" answer for a particular set of assumptions.

Having established that a given slope is potentially unstable, the designer has then to consider whether its stability can be improved by changes in geometry, by drainage or by reinforcing the rock mass. In some special circumstances, particularly in mining, an economical solution may be to accept the risk of failure and to make provision to predict and to accommodate this failure with the minimum of risk of loss of life or damage to property.

The following topic will be discussed in this chapter:

- Recognition of slope failure modes
- Simple slope design charts
- Influence of water pressure on stability
- Design of critical slopes
- Increasing the stability of slopes
- Prediction of slope failure

3.1 Recognition of slope failure modes

The importance of structural geology in controlling the stability of a rock slope has already been emphasised and the first stage in any stability analysis involves a recognition of the most likely failure modes for a particular combination of geological features.

Without doubt, the most effective means of recognising these different failure modes is to examine a graphical presentation of all the relevant structural geology data together with the proposed slope geometry with the aim of detecting patterns which are representative of the different types of failure. A convenient presentation is to use a large topographic map of the site and to plot the geological data on small diameter stereonets (equal-area or equal angle spherical projections) which are pasted onto the map at the observation points (positions of boreholes

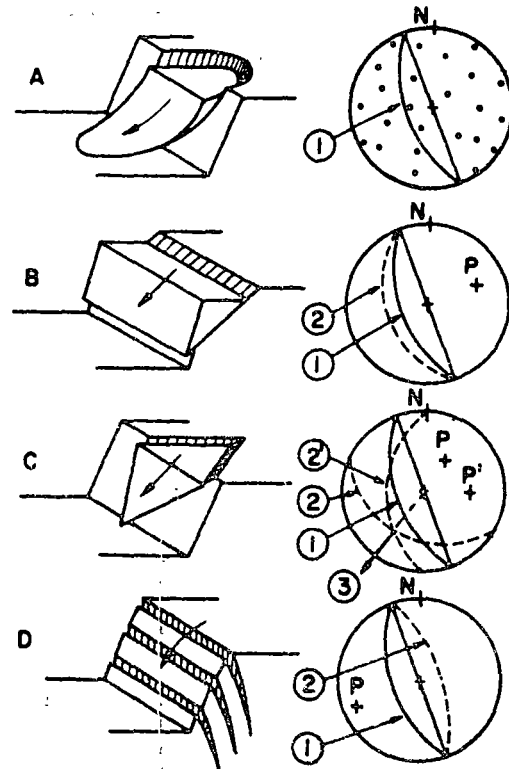


Figure 20 : Recognition diagram for different types of slope failure. (Lower hemisphere equal area projection).

- A Circular failure in soil, waste rock or heavily fractured rock with no identifiable structural pattern.
 - B Plane failure in highly ordered structure, e.g. slate.
 - C Wedge failure involving sliding along the line of intersection of two planes.
 - D Toppling failure in hard rock with steeply dipping discontinuities.
- (1) Slope face.
 (2), (2') Discontinuity planes.
 P, P' Poles of planes.
 (3) Direction of sliding.

or outcrops). The proposed slope geometry can then be overlaid on these plots to check the likelihood of different types of failure. Recognition diagrams for four important types of slope failure are presented in Figure 20 and, once the designer has become familiar with these diagrams, the recognition of potential failure is relatively simple.

An essential feature of this early consideration of stability is that the designer should attempt to keep an entirely open mind, being prepared to consider all possible types of slope failure, including those which he knows that he will be unable to analyse. The early recognition of a potential failure will allow remedial measures to be carried out at the design and construction stage. Such measures are invariably cheaper and more effective than corrective measures which have to be taken in the case of a slope which is found to be unstable during an advanced stage of the construction.

It must, however, be made clear that not all potential slope failures can be recognised before construction commences since critical geological features may not be exposed or may have been missed during preliminary site investigations. The designer must, therefore make provision for both time and finances to deal with *unexpected problems* which may arise during construction. He should also ensure that facilities are available at short notice for the implementation of any remedial measures which may be required.

3.2 Simple slope design charts

Ever since Taylor published his simple slope design charts in 1937 (Taylor, D.W., 1948), soil engineers have made use of these and of more elaborate charts for the preliminary analysis of circular failure in soil slopes. These charts have proved to be invaluable aids to the designer in that they permit a rapid assessment of stability under conditions where a detailed analysis would not be justified. Can such charts be used for rock slopes in which failure is controlled by pre-existing discontinuities?

Since it is only possible to graph a limited number of variables, the first step in producing a meaningful rock slope design chart is to consider whether there are a few variables which are so important that, by setting all other variables to zero and considering only these few, a reasonable approximation to the answer can be obtained. In the case of a rock slope design, this process can best be illustrated by means of a practical example.

Figure 21 illustrates the geometry of a rock slope containing a wedge separated from the rock mass by three intersecting discontinuities - one tension crack and two planes on which sliding can occur. This type of problem has been analysed in detail by Hoek, E., Bray, J.W. and Boyd, J.M. (1973) and the proportions of the different forces acting on a particular wedge are given in the pie-chart in Figure 21.

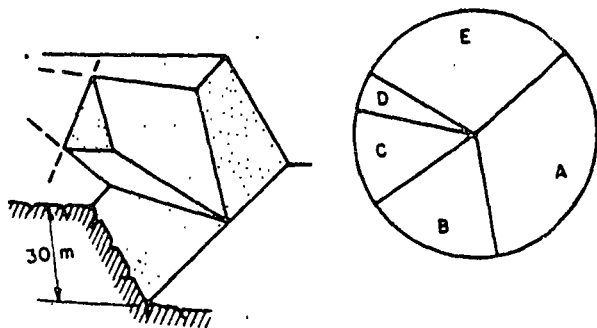


Figure 21 : Contribution of different forces to the stability of a wedge separated from the rock mass by three intersecting discontinuities.

Resisting forces :

A Friction on sliding planes	33%
B Resistance due to cohesion	19%

Disturbing forces :

C Uplift forces due to water pressure on sliding planes	13%
D Force due to water pressure in tension crack	5%
E Component of wedge weight acting down line of intersection	30%

Note that the two items, A (frictional resistance on the sliding surfaces) and E (component of the weight of the wedge acting down the line of intersection) contribute 63% of the total of all the forces acting on the wedge. Both of these items depend upon the geometry of the wedge and it can be shown that only six variables (the dips and dip directions and the angles of friction of the two planes on which sliding takes place) are necessary completely to define A and E (Hoek, E., 1973). A set of simple charts have been prepared by combining these variables into groups and these charts may be used to improve upon the assessment of stability provided by the recognition diagrams illustrated in Figure 20. An example of the use of these charts is presented in Figure 22.

Note that the factor of safety derived from these charts is independent of the height or the angle of the slope face. This is because the only strength parameters involved in the calculation are the friction angles which, as pointed out in section 1.33, are independent of the dimensions of the sample. Although these calculations are based upon a very much simplified set of assumptions, and do not therefore provide absolute values, they have made possible the production of a very useful design index for rock slope engineers. An interesting question is - are there other simple relationships of this type which could be utilised in deriving simple design charts for other modes?

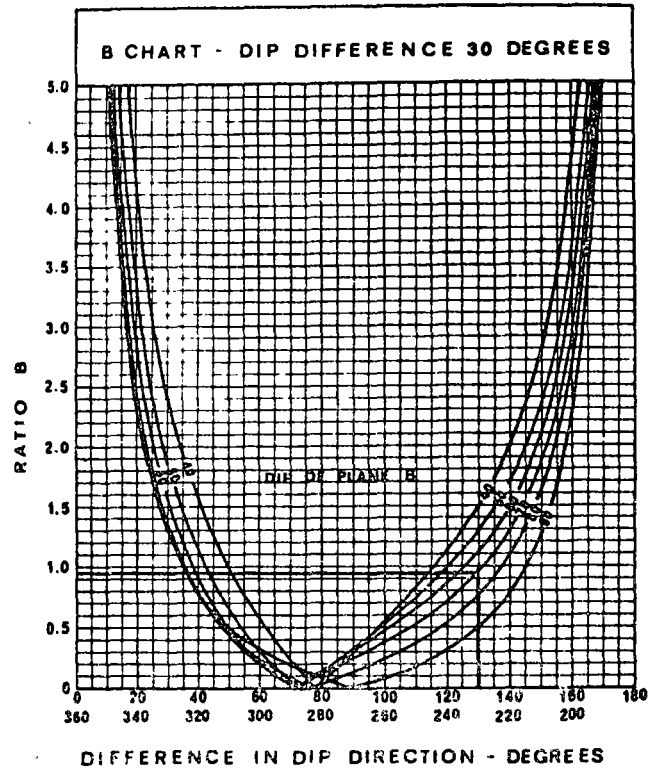
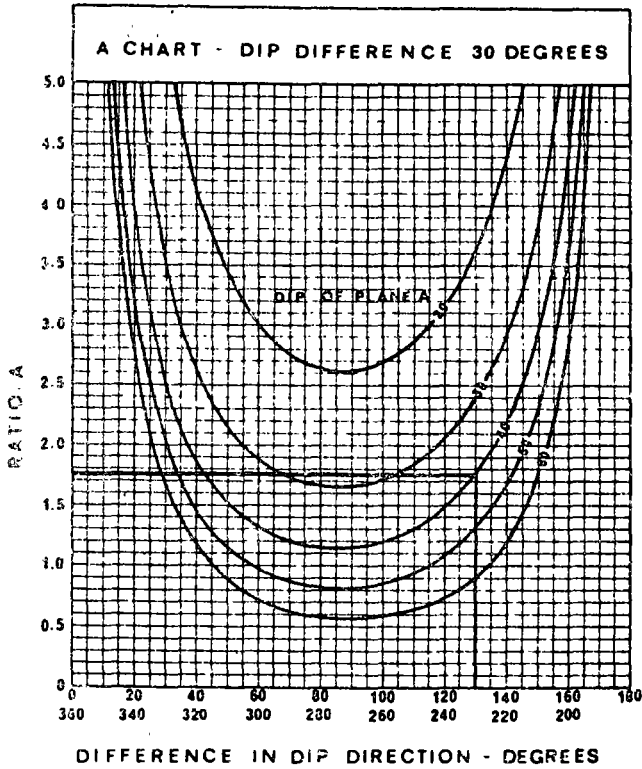
3.3 Influence of water pressure

Figure 21 shows that, for the example considered, water pressure in the tension crack and on the planes along which sliding occurs contribute 18% of the total of the forces acting on the wedge. For steeper slopes with very deep filled tension cracks, this proportion can rise as high as 50%. A consideration of the influence of water pressure upon the stability of a slope is obviously of major importance but how should this influence be evaluated?

The difficulties of adequately defining the water flow pattern in a rock mass have already been discussed (section 2.4) and the reader will appreciate that a precise calculation of the influence of water pressure upon slope stability is not possible. However, in view of its importance, the only reasonable approach is to base the calculation upon the worst set of conditions which can be anticipated and to use the results of these calculations as an aid to judging the consequences of probable groundwater conditions in the rock mass under consideration.

An example of such a calculation is presented in Figure 23 in which the shear strength (friction and cohesion) required for limited equilibrium in a 25 meter slope, in which two-dimensional plane failure occurs, is plotted for a number of different assumptions. The dotted line included in this figure surrounds the shear strength values obtained from the back-analysis of a number of slope failures (Figure 17) and this type of composite plot assists the slope designer in judging how important various changes are in relationship to the shear strength available.

In this example, relatively low shear strength values are required to ensure the stability of a dry slope. Note that the presence of a tension crack (line 2) does not significantly reduce the stability of the



Example of determination of factor of safety for dry cohesionless slope with potential wedge failure.

	Dip	Dip direction	Friction angle	Tan ϕ
Plane A	40°	105°	20°	0.364
Plane B	70°	235°	30°	0.577
Difference	30°	130°		

From charts : A = 1.75 and B = 0.95,

Factor of Safety $F = A \cdot \tan \phi_A + B \cdot \tan \phi_B = 1.75 \times 0.364 + 0.95 \times 0.577 = 1.18$.

Figure 22 : Example of simple wedge failure charts for slope design .

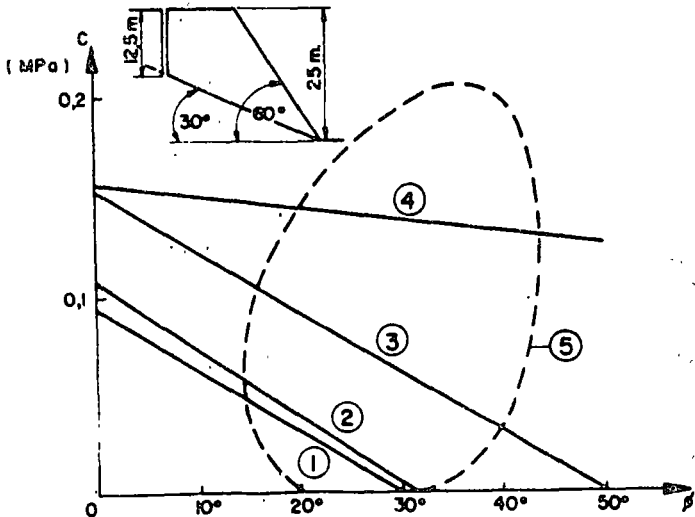


Figure 23 : Shear strength mobilised for various conditions of two-dimensional plane failure.

- (1) Dry slope with no tension crack.
- (2) Dry slope with tension crack.
- (3) Slope with water-filled tension crack.
- (4) Slope with water-filled tension crack and water pressure on failure surface.
- (5) Boundary of zone of observed slope failures (see Figure 17).

slope provided that there is no water present. When the tension crack becomes water-filled under conditions of heavy rain or due to poor control of surface drainage, a significant increase in shear strength is required to maintain stability (line 3). The most severe conditions which could occur in very heavy and prolonged rain which could result in the slope

becoming completely saturated (line 4) would almost certainly produce failure in this slope. While the conditions giving rise to line 4 may be very rare, their inclusion in the calculations give a clear indication of the *sensitivity of the slope to water pressure*. An example of a slope which failed with considerable violence due to the filling of a deep tension crack during heavy rain has been analysed by Roberts and Hoek (Roberts, D. and Hoek, E., 1973). In this case, the factor of safety of the slope was found to reduce from approximately 1.9 for a dry slope to about 0.8 for a saturated slope. Although these values themselves may not be accurate, their difference and the understanding of the mechanism which leads to this difference is important and this analysis enabled the designers to implement simple drainage measures to prevent the recurrence of these extreme conditions.

Some indications on the drainage measures which can be applied to a rock slope will be given in a later section of this chapter.

3.4 Design of critical slopes

A large proportion of the total number of slopes which the average engineer will be called upon to design can be dealt with by means of the simple techniques already described. Occasionally, however, a situation may arise in which obvious and inexpensive steps such as minor changes in slope geometry or simple drainage measures cannot be applied. Under these circumstances, the slope designer may be faced with a critical problem in which it is essential that a more detailed evaluation of the stability of the slope and of the effectiveness of more elaborate corrective measures should be undertaken.

The first and most important step in this analysis is the acquisition of reliable data on the structural geology, the mechanical properties of the rock mass and the possible variation in groundwater conditions. Unless such data is obtained, any subsequent calculation will not only be a waste of time but may even be misleading since it may generate a false sense of security in the designer who has been through the calculations but who may have failed to account for some critical factor in the slope. The collection of this data may involve the drilling of additional boreholes, the testing of samples to establish the shear strength of the discontinuities and the carrying out of pumping tests and the installation of piezometers to detect changes in groundwater conditions. Whenever possible, *existing slope failures* in the same rock types in the area should be carefully studied and an attempt made to deduce the shear strength which was mobilised in these failures. (Natural slope failures may give misleading values because of the very long time scale involved in such failures and back-analysis should therefore be confined to excavated slopes).

Once this data has been obtained, a detailed analysis of the stability of the slope and of the effectiveness of remedial measures can then be carried out by means of techniques which permit the inclusion of all the relevant variables in the analysis. Such techniques have been described by Londe, Vigier and Vormeringer (1970), Hendron, Cording and Aiyer (1971) and Hoek, Bray and Boyd (1973). Because of the complex inter-relationships between the large number of variables involved in these problems, the calculations are generally carried out with the assistance

of computers.

It must be emphasised that, in spite of the versatility of these types of calculations, they are still based upon simplified models of the actual failure processes which take place in the slope. The designer should, therefore, beware of falling into the trap of relying too heavily upon the results of such analyses which should be used to assist but not to replace the judgement of the engineer. These analyses show, in the same way as do less elaborate methods the sensitivity of the slope to the various assumptions which have been made.

3.5 Increasing the stability of slopes

There are four basic methods for increasing the stability of rock slopes:

- a) Changing the slope geometry
- b) Drainage of groundwater in the slope
- c) Reinforcement of the rock mass
- d) Control of blasting

3.5.1 Changing the slope geometry

Changing the geometry of the slope generally means reducing the slope height or reducing the angle of the slope and, when it is possible to implement this remedial measure, it is generally the cheapest means of improving the stability of the slope. It is however, not always the most effective measure since reducing the height or the angle of the slope not only reduces the driving force tending to induce failure but it also reduces the normal stress and hence the frictional force resisting sliding. Consequently, before implementing this measure, it is essential to check whether it will be effective. As a general rule, very steep slopes can most effectively be stabilised by reducing their height while relatively flat high slopes can be stabilised by reducing the slope angle, provided that the stability is not controlled by major geological structures such as faults.

In addition to the slope height and the slope angle, the geometry of the slope as seen in plan has a significant influence upon stability. Correct alignment of the slope face with respect to the dip directions of the major structural features in the rock mass will reduce the number of these features which will "daylight" in the slope and hence improve the stability of the slope. Relatively small changes in the position or alignment of the slope face can result in considerable improvements in stability and this should be regarded as both a design and a remedial measure. Whenever possible, the creation of "noses" in slopes should be avoided since slopes which are convex and in which a number of features daylight are inherently less stable than concave slopes where good lateral restraint is provided by the curvature of the face.

One major advantage which changing the slope geometry has over other methods of improving the stability of slopes is that its effects are *permanent*. This is because the improvement in stability is achieved by a more effective utilisation of the inherent properties of the rock mass and by making permanent changes to the force system in the slope. This force system can also be changed by drainage and by reinforcement but these changes may be reversed if

the drains become blocked or if the load carrying capacity of the reinforcement is reduced. Consequently when methods other than changing the slope geometry are used to improve stability, it is essential that these remedial measures be *maintained* and that a check should be made at least once a year (preferably just before the wettest season) to ensure that these measures are still effective.

2.52 Slope drainage

From the discussion on the influence of water pressure on the stability of slopes (section 3.3), it will be clear that the presence of groundwater in the rock mass into which a slope has been cut is always detrimental to stability. It follows that drainage of this groundwater will always improve stability but the questions which concern the slope engineer are - how much improvement can be achieved by drainage and how much will it cost?

The simplest and cheapest form of groundwater control is to minimise the amount of water which can collect in pools on the top of the slope. Simple calculations show that water which can enter open tension cracks from the top of the slope is very dangerous since it has the potential for generating high water pressures within the slope. There is no excuse for allowing water to collect on the top of a slope and good engineering practice requires that these areas should be graded to encourage the free run-off of surface water and that surface drains, when they are installed, should be properly maintained to ensure that they remain effective. Where tension cracks are visible in the tops of critical slopes in areas of high rainfall intensity, it is advisable to fill these cracks with porous material such as gravel and then to seal the top of the crack with impervious material such as clay. This will prevent direct entry of surface water, particularly during heavy rain, but will allow water already in the rock mass to drain freely towards the slope face.

Percussion drilled horizontal boreholes can be very effective in draining a rock mass but very few quantitative design guides can be given for the spacing of these holes since their effectiveness depends almost entirely upon whether or not they have intersected water-bearing fissures. In heavily fractured rock, the holes may be regularly spaced since the permeability of the rock mass will be reasonably uniform. In rock masses with widely spaced fissures, the holes should be drilled to intersect those fissures which are believed to be heavily water-bearing. Generally, the holes should be drilled a horizontal distance into the slope approximately equal to the height of the slope. The main advantage of this method of slope drainage is that it is cheap to install and to operate since the water drains under gravity and pumping is not generally required.

Vertical boreholes, drilled from the surface and fitted with down-hole pumps, have the advantage that they can be operative before the slope is excavated and can be used to improve the stability of slopes which are only required to remain stable during a limited period. Permanent drainage by pumped vertical boreholes is expensive and is liable to become ineffective at the most critical times due to pump or power failure.

Drainage galleries, while certainly the most expensive form of drainage, are probably the most effective means of controlling the groundwater in a critical slope. These galleries have the advantage of exposing a large number of fissures within the rock mass through which water can drain freely by gravity. When additional drainage paths are required, these can be created by drilling from within the gallery. While it is difficult to justify the construction of a gallery for drainage only, it is frequently possible to reduce the cost of this measure by careful planning. Hence, an exploration adit can become a drainage gallery at a later stage in a project or existing underground excavations, particularly in mines, can be utilised provided that care is taken to remove the water which accumulates in these excavations.

3.53 Reinforcement of slopes

Improving the stability of rock slopes by artificially reinforcing the rock mass is generally only economically feasible for relatively small slopes or for stabilising blocks of limited size on slopes. This is because the forces which have to be applied by the rockbolts or cables may be as high as 20% of the total weight of the rock which is potentially unstable. The installation of reinforcement in a slope in which instability is already evident is the least effective form of reinforcement since much of the strength of the rock mass will already have been lost due to the opening up of fractures and displacements along discontinuities. On the other hand, if reinforcement is used as part of the design system and is installed during construction of the slope so that dilation of the rock mass is inhibited, the effectiveness of the reinforcement is greatly enhanced. A more detailed discussion on the reinforcement of rock masses is given in section 4.45 of this report.

3.54 Control of blasting

A final question which must be mentioned in this section is that of the control of blasting during excavation of a slope. While this may not generally be regarded as a means for improving the stability of slopes, there is no doubt that the damage due to blasting has a very significant influence upon stability. Experience suggests that a slope which has been created by carefully controlled blasting may be stable at an angle which is 5 to 10 degrees steeper than a slope which has been subjected to the heavy blasting which is now common in open pit mining. The aim, therefore, should be to minimise the damage to the rock mass which is to form the final slope and this can generally be achieved by the use of presplitting or smooth blasting techniques (Langefors, U. and Kilhstrom, B., 1963). The use of these methods is now fairly common in civil engineering but they have not gained wide acceptance in mining because of the relatively high cost of drilling which is involved. Although the actual drilling cost is high, it is believed that the total cost of creating and maintaining a slope by the use of controlled blasting, accounting for the smaller volumes which have to be excavated and the reduction of slope maintenance, will be lower than the cost of an equivalent slope excavated by normal heavy blasting. A comparison of such costs recorded on actual projects would be of great interest to slope engineers and the general reporters suggest that this comparison would form an excellent topic for a short research project.

3.6 Prediction of slope failure

When all efforts to stabilise a slope have failed and it is clear that failure is inevitable, it is sometimes necessary to attempt to predict the behaviour of the slope in order that men and equipment may be moved past it before it fails. One of the best known case histories of slope failure prediction is that of the spectacularly accurate prediction of the date on which a very large failure occurred at the Chuquicamata mine in Chile (Kennedy, B.A. and Niermayer K.E., 1970). Figure 24 shows the plot of surface displacement versus time on which this prediction was based and this curve is typical of several examples of slope behaviour prior to failure which have been observed.

Generally, the first obvious sign of instability is the formation of one or more tension cracks on the top of the slope. These tension cracks may occur several years before the failure takes place but model studies (Barton, N., 1971) have shown that these tension cracks are the first manifestation of deep-seated shear movement in the rock mass and that they must be regarded as warnings of instability. Simple measurements of the opening of tension cracks with time can give valuable information on the behaviour of the slope and it will generally be found that the rate of opening increases with time. When the measurements are carried out with sufficient frequency and accuracy, a close correlation between opening of the tension crack and recorded rainfall on the site will frequently be found.

Opening of tension cracks will generally be followed by slumping of the crest of the slope and by bulging of the toe of the slope. Because the movement of the rock mass is controlled by pre-existing discontinuities, these changes may be less obvious than those which occur in soil slopes. Sometimes the movement of an unstable block of rock may be oblique to the face of the slope and it may be difficult to detect these subsequent movements without measurement of a number of points on the surface of the slope

Because of the complexity of the movement pattern which takes place in a rock slope, the installation of sub-surface measuring devices such as boreholes extensometers may not be effective since it may be extremely difficult to interpret the results. It is also usually both dangerous and difficult to install these devices and to keep them effective for the life of the slope.

The most successful slope monitoring systems which have been used to date are those based upon simple survey type measurements of the movement of targets placed on the surface of slopes. These measurements may be by normal triangulations or they may utilise one of the electro-optical distance measuring devices which are now commercially available (St. John, C.M. and Thomas, T.L., 1972) The latest developments in stereophotogrammetry are also promising (Ross-Brown, D.M. and Atkinson, K.B., 1972).

No means for quantitative evaluation of the results of such measurements are currently available and, in view of the large number of parameters involved, may never be available. However, experience suggests that the accelerating displacement curve reproduced in Figure 24 is typical of slope failure

and that it gives as good an indication as any which is likely to be available in the foreseeable future of the likely failure date.

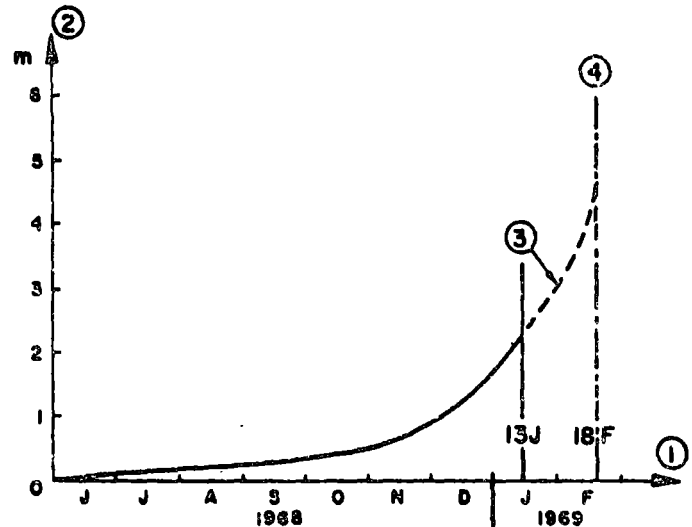


Figure 24 : Plot of displacement of fastest moving target on the face of the Chuquicamata mine (Chile). The failure, involving approximately 12 million tons of material, occurred on 18th February 1969.

- (1) Date.
- (2) Displacement in meters.
- (3) Extrapolation of data collected up to 13th January 1969.
- (4) Predicted failure date.

4. ROCK FOUNDATIONS

4.0 Introduction

This chapter is devoted to specific applications of rock mechanics to rock foundation engineering.

The flow chart shown in Figure 2 illustrates the main steps of the appraisal, design, construction and monitoring of the rock foundation of a large engineering structure. This chart, of course, is very crude as compared with the actual approach, which entails much knowledge and judgement and subtle relationships between several fields of engineering, geology, science and craftsmanship.

For the sake of clarity, this chapter has been divided into five categories of problems:

- a) Resistance to failure, i.e. safety as regards rupture
- b) Deformations, and their effects on the stresses in the foundation rock and the structure
- c) Mechanical effects of water seepage through the fissures of the rock mass.
- d) Corrective action that the designer can take
- e) Monitoring of the foundation rock.

Rock mechanics offers a number of tools to help solve these problems. As already stated in the Introduction to this general report, although the design analysis is very crude, owing to our limited knowledge, the rock mechanics approach leads to a correct understanding of the basic or possible behaviour patterns. This is vital for the foundation designer, whose main concern is *not to compute accurately but to judge soundly*.

4.1 Structure of rock foundations

The designer's main concern is to prevent failure of the foundations as it represents the worst possible case.

The methods of assessing stability, involving potential appraisal, determination of possible failure modes and analysis of the conditions of limiting equilibrium (Fig.25), have already been dealt with in chapters 1 and 2 of this report. Although it is not necessary to repeat these methods in this chapter, it is necessary to emphasise that the consideration of the *resistance to failure* of a foundation must always precede the study of foundation *deformations*, since all subsequent calculations are only relevant when it has been demonstrated, beyond reasonable doubt, that the foundation will not fail.

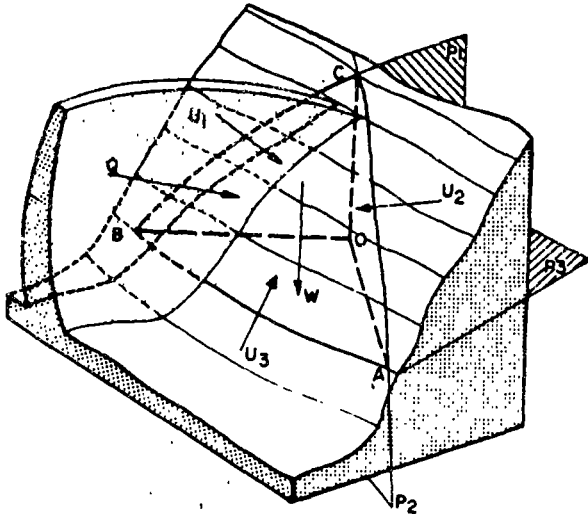


Figure 25 : Stability of a tetrahedral rock volume.
(Londe, P., 1973)

- OABC Tetrahedron.
- P_1, P_2, P_3 Geological surfaces of separation.
- U_1, U_2, U_3 Water pressure forces.
- W Weight.
- Q Thrust of dam .

4.2 Deformation of rock foundations

4.20 Introduction

In considering the deformation of rock foundations, it is necessary to differentiate between deformations *within the rock mass* and *surface*

displacements. The first category is useful for understanding the intrinsic behaviour of the foundation whereas the second is adequate for analysing the engineering structure built on the rock. The rock mass is comparable, in that respect, to an *equivalent continuous* medium which has the same surface deflections.

On the other hand, the deformation within the rock mass cannot be determined without considering the actual *discontinuous* medium, or at least a representative model of it. Because of the contribution of the surfaces of separation, the deformations within a discontinuous rock mass under low confining stresses, will be significantly different from those in a continuous medium. This will be the case for surface workings. In the case of underground workings the confining stresses are higher and, once the discontinuities within the rock mass have been forced into intimate contact, the deformation behaviour will approximate to that of the continuous medium.

The theory of elasticity is satisfactory for the analysis of deflections of the equivalent continuous medium, at least as a first approximation, provided that the irreversible part of the first loading cycle (due to closing of the fissures) is considered separately.

Determination of the deformations within a discontinuous rock mass requires the use of mathematical or small scale models.

4.21 Determination of elastic parameters

The equivalent continuous medium can be defined by Young's modulus and Poisson's ratio, giving the same displacements at the surface as those of the actual site. Since the deformations within the rock mass are different from those in a continuous medium, this approach is necessarily a rough approximation. In practice, however, it is reasonable to assume an elastic behaviour for most rock foundations, the only restrictions being to use an appropriate elastic modulus for the stress range under consideration. Comparisons between the results of analyses and measurement of foundation deformations on many dams have shown this approximation to be valid. Such comparisons are not generally available for other types of surface structure.

How can the equivalent elastic parameters be determined at the design stage? Jacking tests are almost the only practical means available for such determinations and yet the interpretation of the results of such tests is open to question. In section 1.27, the influences of *scale* and of *duration of loading* upon the results of a jacking test were queried. Even if these questions are ignored, many *different moduli* can be derived from the non-linear curves obtained from a jacking test. Although it has been proposed that these results are useful identification indices for the rock mass, the question which must now be considered is: can they provide numerical parameters for use in a deformation analysis?

Experience suggests that, provided a large number of tests are carried out in situ, the mean value and the scatter found from such tests allows a reasonable estimate of full scale deformability. It seems likely that, in a rock mass, the small samples are models of

larger samples, themselves models of still larger blocks, this series being closely related to what has been called, in section 1.22, the "grading curve" of the rock mass. If this concept is valid, it would explain why the scale effect does not result in extremely low moduli for very large dimensions and also the fact that scale effect does not appear to have too significant an influence on jacking tests.

For the analysis of the foundation behaviour of the Auburn dam, the U.S. Bureau of Reclamation has worked out a method aimed at reducing the number of in-situ jacking tests required. The principle is to combine the two components of deformability of the mass (a) the modulus measured on cores and (b) the surfaces of separation (spacing, thickness, infilling). This "analytical" method has to be calibrated on each site (Von Thun and Tarbox, 1971)

There are cases where the jacking test has given lower values than the moduli worked out from the overall behaviour of the completed structures. This was the case at the Vouglans dam where plate tests (28cm diameter) gave an average modulus of 16,000 MPa, whereas the dam loading gave 30,000 MPa (Groupe de Travail, CFCB, 1967). Several explanations are, of course, possible for this "reverse" scale effect: fissures under the jack plate, higher test stresses and, most important perhaps, the fact that the Boussinesq and Vogt solutions used to derive the moduli do not apply to the discontinuous system. The concept of the equivalent continuous medium is therefore possibly responsible for the discrepancy.

A final remark concerns Poisson's ratio, which is assumed, not measured. This concept is probably far from applicable to a rock mass where, not only do the lateral deformations of intact laboratory specimens show wide variations, but the presence of discontinuities will have a significant influence upon the lateral deformation behaviour of the rock mass.

The discussion is therefore open. How shall we measure the deformability of a rock foundation for design purposes? Jacking tests, either on the surface or in boreholes, appear to be the only practical means currently available, even if their results have to be treated with caution. Is it possible to improve the test procedure and our comprehension of the tests?

4.22 Influence of rock deformation on engineering structures

Whereas permissible displacements of rock slopes are usually large, those of a foundation are extremely small, owing to the damage which they can induce in the engineering structure.

This structure is sensitive to two separate effects:

- a) The absolute magnitude of the deformations
- b) The relative displacements, from one zone to another of the foundation area.

Effect b) is generally more detrimental than effect a). Hundreds of dams have been designed using the Trial Load Method of analysis which required an assumption on the ratio EC/ER between the modulus of the concrete and that of the rock mass. It has been

checked that, provided this ratio is nearly constant over the whole foundation area, its influence on the maximum stresses in a high arch dam is slight. For example, a variation from 1 to 5 may result in an alteration of the critical stresses by 20% (some are increased, others are decreased). This means that great accuracy in measuring ER is not required, at least for this part of the design, and that the scale effect is not such a serious drawback to the determination of deformability. In low or rigid structures, the influence of EC/ER is much more marked but, fortunately the stresses are seldom critical in such cases.

On the other hand, however, local variations of EC/ER have a strong influence on stresses in the vicinity. For instance, an arch dam can span a fault zone of several meters in thickness with practically no change in the stress pattern, except locally where special arrangements must be made. Should a zone of softer (or harder) rock be much wider than the thickness of the dam, the problem is more serious. Finally, when a major part of the bank has a modulus different from the remainder, it results in mechanical asymmetry which is much more important on the stress pattern than geometrical asymmetry.

The difficulties met in determining the deformability of a rock mass are therefore, at least partly, offset even for an indeterminate structure by two favourable conditions:

- a) It is not necessary to measure the rock modulus with any great accuracy
- b) Relative variations, resulting from heterogeneity are probably obtained with adequate accuracy, from small scale tests.

Can these conditions be relied upon? This question certainly warrants further discussion.

4.23 Irreversible deformations

Jacking tests as well as monitoring of rock foundations have shown that a part of the first deformation is irreversible, especially near the ground surface. This is due to the closing of fissures and to some local minute shear failures. The equivalent modulus for the first loading is therefore lower than the modulus which applies to the further loading cycles. This behaviour is what could be called *strain hardening*, as in metals, with the difference that in rock it develops from the beginning of loading instead of beyond a threshold. This point is vital for the structure, because the low modulus at the first loading may create the most critical conditions. The problem is all the more serious as this irreversible displacement is extremely difficult to estimate from small jacking tests. Furthermore, it is not the same over the whole foundation area and hence the elastic heterogeneity of the foundation is exaggerated.

A major point is therefore to establish whether the designer can obtain the irreversible part of the foundation displacement from jacking, or other tests. Is a measurement or estimate of the scale effect possible as it would most probably be very large? The stress used in the test has undoubtedly a governing influence on the irreversible deformations, as would be expected in a strain hardening phenomenon.

4.24 Influence of rock deformations on instrumentat instrumentation

When a fixed reference point is required for geodetic measurements or for anchoring an inverted pendulum, it has to be at a distance increasing with the magnitude of load applied to the rock foundation. Dams with thrusts amounting to millions of kilo newtons and influenced by billions of kilo newtons of water weight, are particularly interesting. What is the distance required to obtain fixed points? This computation is seldom made.

It was however carried out recently, using elastic theory, and published in the form of charts for different types of loading (Mladvenovitch, V., 1970). It is realised that the engineering structure displaces the supporting medium far and deep; much farther and deeper than commonly reckoned. For instance, an inverted pendulum should be anchored at a depth of about 100m, so as to give a reasonable measurement for the displacement of the base of a dam 100m. high (Fig.26).

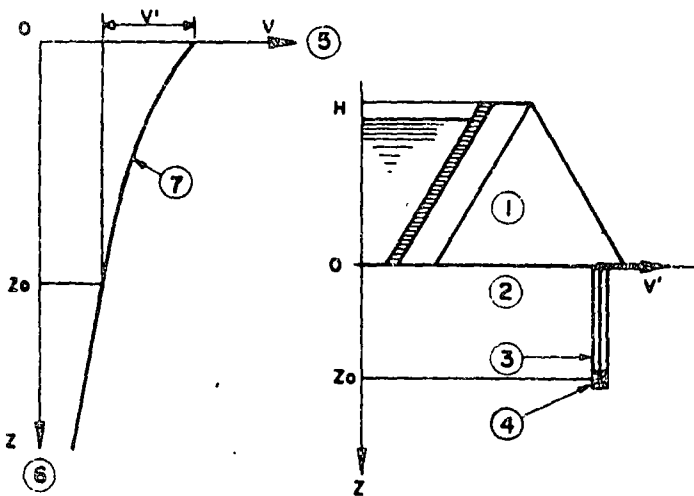


Figure 26 : Example of influence of depth of anchorage of inverted pendulum on measured relative displacement.

- (1) Multiple-arch dam . Cross section.
- (2) Rock foundation (continuous elastic medium)
- (3) Inverted pendulum.
- (4) Anchor point at depth Z_0 .
- (5) Horizontal displacement V .
- (6) Depth.
- (7) Actual curve $V(\%)$.
- V' Measured displacement.

4.25 Deformations within the rock mass

All the preceding comments concerning the surface of the rock mass could, more or less, be dealt with by assuming an equivalent continuous medium. This assumption is not valid inside the mass, where the stress and strain patterns are governed by the discontinuous nature of the medium. For instance, the transmission in depth of a compressive stress field applied at the surface will differ drastically

from the continuous solution and close the fissures in much narrower bands and at a greater depth than shown by Boussinesq's equations (Fig.27). Although several eminent authors have tackled this difficult problem their results do not lead to a convenient tool for the designers, owing to the extreme complexity of the data. The models, both physical and mathematical, are the same as those discussed in paragraphs 2.1 and 2.2. The discussion and comments would also be the same.

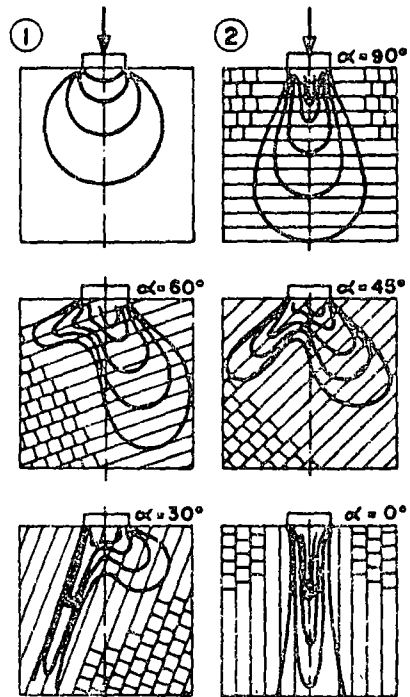


Figure 27 : Distribution of stresses in a jointed rock mass of varying bedding dips under an applied external normal load (Gaziev and Eriikhan , 1971).

- (1) Continuous medium.
- (2) Series of discontinuous rock masses (α = angle between bedding planes and load).

Fortunately the design can generally be carried out on the basis of *qualitative reasoning*. It is not always necessary to compute to arrive at a sound engineering answer. The main concept to remember is that compressions applied at the surface of fissured rock, act along deep and narrow bands within the rock mass, closing fissures, and that conversely tensions applied at the surface open fissures only in the close vicinity of the applied load.

This effect is of fundamental importance in the hydraulic regime of seepage, and therefore on the resulting water pressures.

More instrumentation is required to investigate these mechanisms which, for the time being, are mostly theoretical. Meanwhile the designers have to make allowance for them in order to avoid the danger-

ous conditions they could create, should they really fully develop.

4.26 Special case of deep excavations

Some heavy engineering structures, particularly large dams and tall buildings with many basement levels required the excavation of deep cuts into overburden and sometimes the rock below. The applied forces during the excavation process are therefore a system *unloading* the rock foundation, before re-loading with the structure. The analysis of the foundation rock deformations in this case is extremely difficult, and has very little to do with the results of small scale jacking tests, where the unloading stage cannot be simulated. It would be extremely interesting to discuss the point of how to forecast the behaviour of a rock formation during a cycle of unloading followed by re-loading. The problem is not simple, and includes the considering of pre-existing residual stresses.

There has been a case of a sound limestone bed, 10m thick, lying horizontally over a softer formation, in which the application of a load of 2,000,000kn by a tall building, and, elsewhere, the unloading up to 10,000,000kn by a deep excavation, resulted in punch-shear failure through the whole thickness of the bed.

4.3 Mechanical effects of water seepage

This topic has been discussed in section 2.4 and the details will not be repeated here. It must, however, be emphasised that the control of water pressure is of fundamental importance in the design of rock foundations which are required to support large engineering structures. It is the dominant factor in the case of dams.

4.4 Foundation treatment methods

4.40 Introduction

The engineer can improve the properties of a rock foundation by three different categories of corrective action:

- Reducing deformations
- Increasing strength
- Controlling the hydraulic forces

All these means are not equally efficient at a given foundation site. Moreover, their effect is not always clearly understood, owing to the inadequacy of knowledge still prevailing in several fields of rock mechanics. There is therefore a part of guesswork in many decisions taken about foundation treatment. There are a number of rock foundations where no corrective action whatsoever has been taken, and there are others, like at El Atazar dam, where practically every possible type of corrective action has been taken (Guerreiro and Serafim, 1970).

The purpose of this section is to make comments and speculate on some usual or less usual methods so as to promote discussion and, with a little luck, improvements of our present techniques. The means of corrective action dealt with are:

- Consolidation grouting
- Presplitting
- Excavation and concreting of joints and faults

Surface strengthening

Reinforcement with steel

Curtain grouting and drainage

4.41 Consolidation grouting

It is possible to increase the stiffness of a rock mass by injecting cement grout in the open cracks. This treatment, conventionally applied in the near foundation zone of practically all large structures, has two main effects: the first is to reduce the *irreversible* part of the deformation, and the other is to increase the *modulus of elasticity*. This result can be achieved however only if the cracks are open, and if they are *groutable*.

The first condition is often met near the ground surface, where the lack of confinement leads to a loosening of the blocks (Snow, D.T., 1968). The opening of the fissures near the surface is clearly indicated by the high hydraulic conductivities generally measured in the upper sections of water tests.

This necessary condition is not, however, sufficient. It is also required that the grout should penetrate the fissures at the moderate pressures permissible near the surface. For *cement grout* the minimum groutable opening is about 0.2mm. It should be remembered that such an opening corresponds to a high hydraulic conductivity. For instance, 0.2mm cracks at 1 metre spacing give a permeability in their direction of about 50 Lugeon units. The tentative conclusion is that consolidation grouting with cement is probably useless in rock zones where the water tests have given less than say 50 Lugeon units.

In rocks with fine cracks *chemical grouts* can be used: silica gels or synthetic resins. The resins are restricted to extremely rare cases, owing to their cost (Price, D.G. and Plaisted, A.C., 1970).

Attempts were sometimes made to *jet out* the soft filling materials before grouting. The process is difficult and requires great skill. Usually, series of holes are used for injecting air and water, with or without chemicals such as bicarbonate, while some other holes act as outlets for the eroded materials. It seems that the high cost and always doubtful results of the operation hinder its development.

The *efficiency* of consolidation grouting has not often been checked. There are a few cases in literature, mentioning either an increase of modulus measured in jacking tests performed before and after the treatment, or an increase of seismic velocity. But in most cases the question remains: what is the real gain of stiffness obtained? Another point is: *how to check* the result? This latter aspect is important contractually for the acceptance of the works by the owner.

It seems, however, that the main result is to reduce the deformation heterogeneity over the foundation area, the zones with wide open cracks being equivalent, after treatment, to the other zones. That is probably why the treatment is very generally applied, even if not properly understood.

4.42 Presplitting

Another possible action to reduce the deformabil-

ity of the foundation is to open the excavation by presplitting. It greatly reduces the tendency for the blocks near the bottom of the excavation to become loose under the action of shock waves. The result is again, a lower irreversible deformation and a higher modulus. The theory of presplitting has been attempted in a continuous medium. The mechanism in a fissured, therefore discontinuous, medium is not well understood and spacing of holes together with their explosive loads are still empirical. Practice has shown the great advantages of the process, widely used at present. Consolidation grouting is still required, as presplitting does not correct the natural heterogeneity of deformability of the rock mass.

4.43 Excavation and concreting of joints and faults

The presence of major joints or faults in the foundation of a large engineering structure is not a counter-indication although it gives rise to occasional severe difficulties. There are very few dam sites for instance with no major geological feature crossing the foundation area.

When the filling materials are soft, or when there are open voids, the common practice is to fill them with concrete, either by hand or by injection, after the necessary excavations have been done.

It is not always reckoned necessary to treat the whole surface of the joint. The concreting of a rectangular network of galleries and shafts within the plane of the huge vertical joint called "Julie la Rousse" in the Monteynard arch dam right abutment is an example of successful *partial treatment* (Faivre D'Arcier, G. and Conte, J., 1964). The more thorough filling of several faults in Nagawado dam abutments (Fig.28) used 20,000 cubic metres of concrete (Fujii, T., 1970). The excavation of the soil and broken rock material was done with a high pressure water jet (10 MPa) for fear that explosives would shake and disturb the foundation granite. There may be some other applications of this excavation method for "dental work" of that nature.

The problems raised by replacing soft materials in the foundation with concrete are different depending upon the nature of the stresses to be transmitted, but in all cases the most difficult point to answer is: what area of the fault or joint has to be concreted? The answer depends upon the assumptions made on the distribution of stresses within the rock mass, a very doubtful field of rock mechanics.

On the other hand, when considering shear strength the fact that concrete has usually a higher modulus than fissured rock may induce local concentration of higher shear stresses and *progressive failure*. That is why small concrete key ways, as sometimes contemplated across shear zones, are of doubtful efficiency. This question deserves further study. In any event such corrective action should always be contemplated with a serious monitoring of the treated zone. The foundation treatment of the Carei highway bridge, France (Fig.29) is composed of concrete shafts, excavated down to a bed that cannot slide into the valley. A difficult question is: what would be the load on the piles in case of movements of a higher bed of the rock formation?

4.44 Surface strengthening

Action at the rock surface is possible by means of concrete buttresses, struts, shotcrete and gunite. Although the forces supported by these elements are slight as compared with the total forces involved in the equilibrium of the rock mass, practical experience has proved that this type of corrective action is often adequate.

The progressive loosening of fissured rock starts at the free surface. Its cause may be either the stress relief due to excavation or the slow alteration of the matrix, or more often, the softening of the materials filling the joints. Slight opening of the joints goes with imperceptible rotations and sliding of rock blocks, large enough, however, to reduce very appreciably the strength and stiffness of the rock mass as a whole, even at depth.

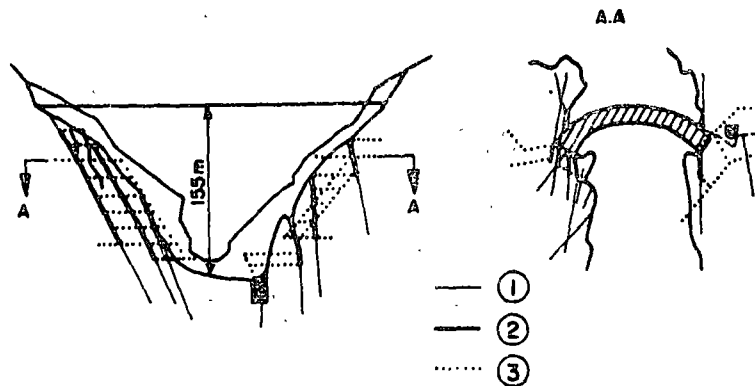


Figure 28 : Nagawado Arch-dam concreted faults . (Fujii, 1970)

- (1) Fault.
- (2) Concreted excavation in fault.
- (3) Adit.

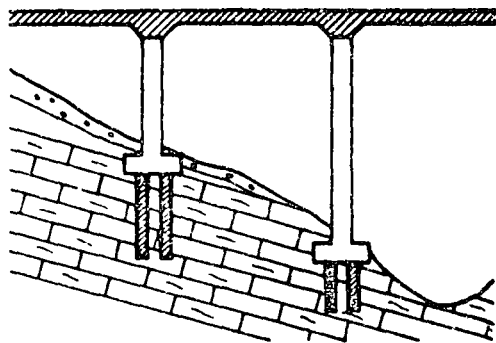


Figure 29 : Concreted shafts under Careil bridge piers (France).

A shotcrete or gunite layer applied immediately after the opening of the excavation obviously provides superficial protection against weathering. As the projected material moulds itself around all the irregularities and penetrates into cracks, even of minute size, it develops a spectacular increase of the stiffness of the "skin" of the rock mass. It is, sometimes, however, argued that the efficiency of shotcrete or gunite is more doubtful on a surface which is not concave, and even, in some places, sharply convex. The role of a reinforcing mesh, even light, is then probably essential. Again, the point is to apply a resisting force across all joints where they daylight at the surface so as to prevent their first displacement from starting. Experience shows that this force can be extremely small. It is interesting to mention that the protective lining is so flexible that it can follow the general displacement of the rock mass without breaking, therefore keeping its full efficiency.

Rigid buttresses or struts look stronger than thin linings and the forces are able to withstand can be computed. Is this the reason why some designers trust them more? It should be remembered, however, that in surface workings as in underground workings, the forces are all the higher as the support is more rigid. The main point in modern techniques is to avoid the progressive deterioration of the compactness of the rock mass, originating always at the free surface. There is therefore a weakness in strengthening by localised rigid units: the surface left unsupported between units is not protected at all (Fig.30), unless it is covered by a layer of gunite.

The discussion is open on the relative merits of flexible continuous protection and rigid discrete supports. One of the factors to be considered is obviously the deformability of the rock mass proper, the geological structure and also the sequence of the works.

The theory of the mechanism of surface strengthening has yet to be developed. Engineers are unable to put forward a quantitative analysis of the interaction between rock loads and surface protection. They are therefore unable to prove the design arrangements. There are, however, a number of successful applications.

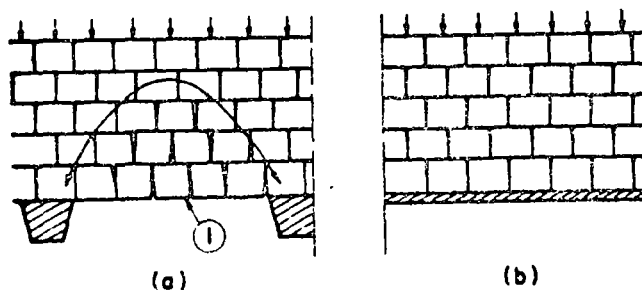


Figure 30 : Comparison of surface strengthening of a discontinuous rock mass .

- (a) with buttresses.
- (b) with shotcrete.

(1) Zone of loosening of rock blocks.

4.45 Reinforcement with steel

Rock is a material with practically no tensile strength and often low shear strength, owing to its numerous surfaces of separation. The idea of reinforcing it with steel bars, as is done for concrete, is therefore very logical. The two principles used in concrete are also used in rock: "passive" steel as in reinforced concrete, "active" steel as in prestressed concrete (Fig.31).

Two main reasons however preclude any complete analogy with reinforced or prestressed concrete:

- a) The rock mass is a discontinuous medium with a mechanical behaviour drastically different from that of concrete.
- b) The steel cannot generally be installed in rock masses either at the optimum location or at the optimum time.

In fact, the choice between passive and active steel is still open to discussion because the theory has not yet been developed.

The prestressing solution results in a clearer conception of the forces. Each bar or cable is equivalent to a given and well known applied load. It can be introduced into any mathematical or physical model. Of course this applied load has several effects. In the first place it can reduce, by vectorial addition, the effect of other applied loads which are detrimental to stability. In the second place, it can increase the friction resistance of joints by adding a normal compressive stress to the existing stress. It is also possible to introduce a high enough compression to avoid the development of tension, i.e. opening of cracks. One may even claim that prestressing reduces the irreversible part of foundation displacement by closing some open cracks.

The method, however, has some drawbacks. Although the total loads that can be practically applied are still very small as compared with the forces present

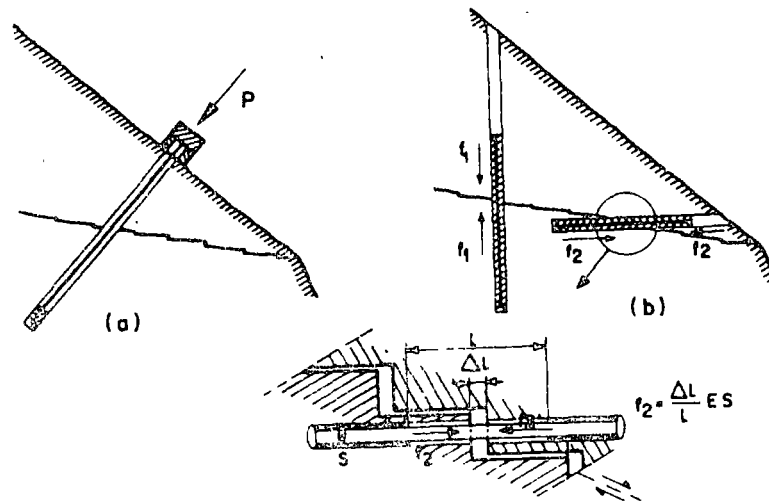


Figure 31 : Reinforcement with steel . Sketches .

(a) Prestressed cable.

(b) "Passive" anchor bars.

in the rock mass, the stresses near the anchor zones are high, approaching the compressive or shear strength of the rock. In addition, there is always the threat of failure of high tensile steel wires by *stress corrosion*, particularly in rocks where the chemical composition of water might be much more unfavourable than in concrete. The process has, however, proved very successful in some cases such as the surface strengthening of the banks at Vajont Dam, or the tightening of treated fault zones in the Nagawado dam abutments.

Ordinary reinforcement bars embedded over their whole length have been used more often. Although the mechanism of their action is more difficult to understand, they have proved successful in many cases. The principal is to introduce into the rock mass additional tensile and shear resistance at the surfaces of separation crossed by the steel. The maximum available force is determined by the steel cross section but the stress actually developed is not known.

It has been argued that passive steel can contribute a stabilising force only after rock has deformed, i.e. after failure. This is true but the rock strain necessary to mobilise the steel reaction is extremely small owing, first, to the fact that all deformation is concentrated within the thickness of the joints and second to the fact that the steel is perfectly embedded in its hole. This point is vital for the proper functioning of the reinforcement. A joint opening of 0.2mm, for instance, would have to open only 10^{-4} mm. more to develop a stress of 100MPa (permissible stress of mild steel). Should the bond fail over a certain length on both sides, the opening of the joint will remain an extremely small fraction of a millimeter.

The theory of the reinforcement is however not yet available. It seems that there are two distinct

cases to consider.

In the first case, steel is used for stabilising a possible failure by sliding on one or two single, smooth geological features such as bedding planes or faults. The computation can be done assuming that the strain will be limited to a low value due to the reinforcement, and allowing a certain shear strength to develop. With joints exhibiting peak strength, it may be possible to keep a part of this peak strength. The question is: how to compute this available cohesion? There is no answer yet, although one might feel that it could be given by a close examination of the process of progressive failure.

In the second case, steel can be used in an imbricated rock mass, or for stabilising shear surfaces with some degree of roughness. In this case, shear strain is accompanied by dilatancy. The joint crossed by reinforcement opens up and puts the steel under tension as soon as a shear failure starts. Another way of looking at the mechanism is to consider the intrinsic curve of a rough joint. If irregularities are arranged in a random pattern, their angles vary and are higher for smaller irregularities and one obtains a curve, with a very steep slope near the origin (Fig.14). This means that for low normal stresses the angle of friction is much higher than usually assumed. The consequence is that, with the low normal stress developed in the steel bar by a slight dilatancy of the joint, a relatively high shear strength is available. The effect of the reinforcement is therefore to translate the intrinsic curve as a whole towards the left resulting in an appreciable cohesion. At the same time, the interlocking action of the steel, which, with a moderate force, prevents the smallest irregularities of the joint from slipping, probably results in increased stiffness. The reinforcement might therefore be visualised as a means of improving the modulus of deformation of the rock foundation. The results

obtained with mine rock bolts (Leonet, O., et al, 1971) tend to show that embedded bars are better than free, anchored bars.

A difficult problem is raised by the anchoring of main cables of large suspension bridges, which apply shear and tensile loads of high magnitude to the rock mass. At Tancarville bridge, France (Fig. 32), the load was 160,000 kilo newtons. It was anchored in chalk. All possible failure surfaces were investigated, in terms of the structural data, and grouting together with placement of "passive" reinforcing bars was done.

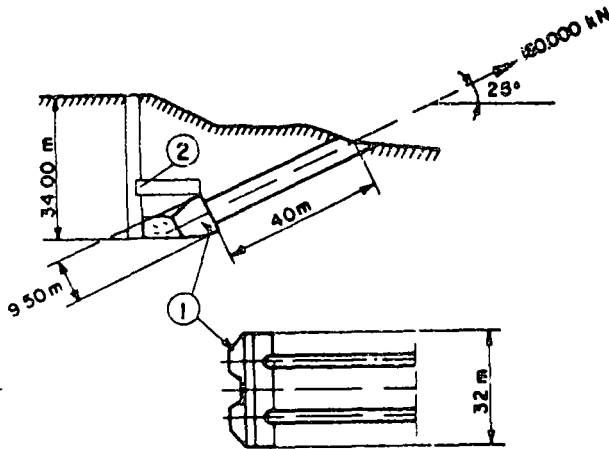


Figure 32 : Anchorage of Tancarville suspension bridge, Right bank (Esquillan , 1961).

- (1) Concreted key excavated in rock.
- (2) Shafts and adits.

In the cases where millions of newtons are required, the use of prestressing would lead to serious problems of stress concentration, whereas ordinary reinforcement, in adits backfilled with concrete, is a cheap and straightforward operation.

The extension of this concept plus a better understanding of the mechanical behaviour would lead to a new material for the design of foundations: *reinforced rock*. It is fully realised that much has to be studied yet and that several statements in the foregoing are controversial, but it is considered that the prospects are promising enough to stimulate at least a lively discussion.

4.46 Curtain grouting and drainage

When the decision is made to act on seepage forces the two main tools are grouting and drainage. They are complementary, although sometimes only one is used. In the past, say before 1960, most of the rock foundations were only grouted when water seepage was an obvious nuisance (particularly to reduce loss of water from reservoirs). It is interesting to note that, until recently, rock foundations of dams had deep grout curtains, and only gravity dams had drainage curtains, usually very shallow and practically limited to the rock-concrete contact. After the

effect of water seepage on the stability of foundations was better understood, that is practically after the Malpasset Dam abutment failure, drainage was considered the best action in most cases. It is at any rate the only efficient treatment in rock of low hydraulic conductivity, such as all rock with fine fissures.

In paragraph 2.4, comments were made on the basic understanding we have acquired at present, of water seepage in fissured rock and of forces that it develops. Even if this knowledge is still qualitative, it is adequate for directing the engineer's work. As it often happens in foundation engineering the main point is not to have a perfect technique of analysis but rather a sound understanding of the possible mechanisms. There is, however, a limitation: what is the effectiveness of any corrective measure? The danger is believing that the action is efficient while in fact it may not be. Grout curtains, with one or several lines of holes, aim at plugging the water paths by grout. An ideal grout curtain would support the whole water pressure on one face, no water remaining on the other side. Unfortunately, there are several reasons which prevent grout curtains from acting in this perfect way. First the limitations given in paragraph 4.41 are still valid: cement grout does not penetrate thin fissures, and does not remove sandy fillings. The use of chemicals and the jetting out of fissures is generally too expensive for the purpose. Even more as the efficiency of a thin curtain is extremely sensitive to a minor and local defect. This point, strongly made by Prof. A. Casagrande at the First Rankine Lecture - 1961, was then questioned by several authors but is now commonly accepted.

Fortunately in finely fissured rocks, where a grout curtain is not valid, *drainage* is a suitable alternative. It fully controls the hydraulic potential on the downstream side. In other words it achieves exactly what was required from the grout curtain, the only difference being that *the drainage increases the amount of leakage, whilst the grouting reduces it*. This is without any consequence in most rocks where the hydraulic conductivity is low. Conversely, if the conductivity is high grouting has to be carried out, should it be only as a consolidation treatment.

To summarise it can be stated that, for fissured rocks:

- a) of low permeability (say less than 5 Lugeon units), drainage is generally essential, whereas grouting is useless,
- b) of high permeability (say more than 50 Lugeon units), grouting is required for controlling water leakage whereas drainage is not necessary.
- c) for medium permeability, drainage is always useful, its cost is low, and the decision on whether to carry out a grout curtain can be made on the basis of economics (permissible water loss or cost of pumping leakage).

The theory of change of conductivity of rock *under stress*, as discussed in paragraph 2.42, leads to other considerations (W. Ter-Minassian et al, 1967) which have a particular significance in dam foundations, but may also have to be considered in other

cases. The fact that the stresses applied by the engineering structure act at depth and might render the rock extremely tight if it is finely fissured makes the limitations of the grout curtain mentioned above still more pronounced. It also helps to locate the drains in a zone of the foundation where they are not "masked" by the watertight barrier due to stresses. In the case of arch dams they should be directed in an upstream direction.

This theory, although checked in the few cases where the foundation rock was adequately instrumented for the purpose, is still controversial. It would be extremely useful to the profession to know of cases where the behaviour of water seepage has confirmed or invalidated this model. On the other hand, it is likely that in the future, more *drainage tests* than grouting tests will be carried out at the design stage. This would be a normal trend as "drainability" might be a vital part of the design of a large structure foundation (Pena, H. et al, 1970).

Another important point, made in paragraph 2.43 is whether the drainage can be effective in a rock formation where water flows through preferential channels. As a single line of drains gives no protection in this case, it may be necessary to contemplate a uniform distribution of drains through the whole rock mass. This mechanism has to be studied in more detail. It is a vital subject of investigation, because a number of foundations protected with a conventional drainage curtain are *perhaps* not drained at all. Of course many rocks probably have not the ideal plane fissure flow type nor the equally ideal preferential channel flow type. A number of recent observations however have shown that the preferential channel flow is frequent and the governing factor for the efficiency of drainage is the proportion of flow drained: as soon as channels are present the ratio between water discharge via channels and discharge via fissures is very high. The result is that a drain which does not intersect a channel does not significantly alter the flow net and the corresponding pressures.

For all the previous reasons, the effect of drainage, often vital for the stability of the foundation, should be monitored. *Piezometers* are therefore considered as an integral part of the drainage design. They would also detect the ageing of the system, as it is well known that drains have to be maintained against clogging by fine grains of soil or chemical deposits. Only piezometers can give warning in time that drains have to be reamed out or new drains have to be drilled.

4.5 Monitoring of rock foundations

4.50 Introduction

It was realised, rather recently, by civil engineers that instrumentation and monitoring of the foundations of major works was a vital part of design. However, before 1960 hardly any rock foundations were monitored. It is generally considered at present that monitoring of the foundations is at least as important as monitoring of structure. The French word for instrumentation is "auscultation" from the medical term meaning an investigation through specific sounds or noises. As in the medical field, it is not necessary to assume that the patient is ill before

practising "auscultation". As a matter of fact, the role of instrumentation, as a medicine, is twofold: research into the normal behaviour and early detection of any significant divergence from it. The information obtained is all the more valuable, the earlier readings are started. When possible, instrumentation should be installed before the structure is built.

Finally, instruments left within the rock mass should be robust and the reading operations should be simple since the conditions on a site are far different from those in a laboratory. The methods discussed here do not cover all available instrumentation, but are reckoned to be the most reliable and suitable for rock foundations.

4.51 Geodetic measurements

Two types of measurements, based on geodesy, are commonly performed: displacements in directions x, y, z by *triangulation*, and displacements in the vertical direction z only, by *levelling*. The sensitivity of levelling is ten times more (0.1mm at 50m distance) than that of triangulation.

Recent developments in electro-optical distance measured devices (Penman, A.R., 1971, Thomas, T.L. and St. John, C., 1972) have added an important factor of rapid and accurate measurement of distance to geodetic measurements. A combination of these new methods and traditional optical survey methods provides the engineer with a powerful set of monitoring techniques.

The main drawback in all these methods, however, is the possibility, which has often been observed, of unstable reference points. The *small displacements* to be measured in a rock foundation may be exceeded by errors from reference base movements. The latter movements may come from elastic deformations of the ground under applied loads and also from erratic displacements of the surface layers where the monuments are founded.

It is therefore suggested that geodetic measurements should not be relied upon for the detection of the small displacements which are associated with the normal behaviour of an engineering structure. They can however, provide a means of detecting large displacements which are indicative of abnormal behaviour.

4.52 Inverted pendulums

In foundation rocks, pendulums are usually of the inverted type: the wire is anchored at the bottom of a shaft and kept in a vertical position by a ring float at the upper part (Fig.33). Normal pendulums can be used however when placed between adits like in Monteynard dam abutments. The sensitivity is about 0.05mm in x and y directions.

Inverted pendulums are probably the most accurate instruments that one can place in a rock foundation. They give a very reliable value of the horizontal displacement vector provided the fixed point is really fixed. What should therefore be the depth of the shaft? That is a question still to be answered. It depends of course on the loads applied to the foundation, but also on the geological structure of this foundation. Recent computations (Mladyenovitch, V., 1970) have shown that most of the pendulums now in

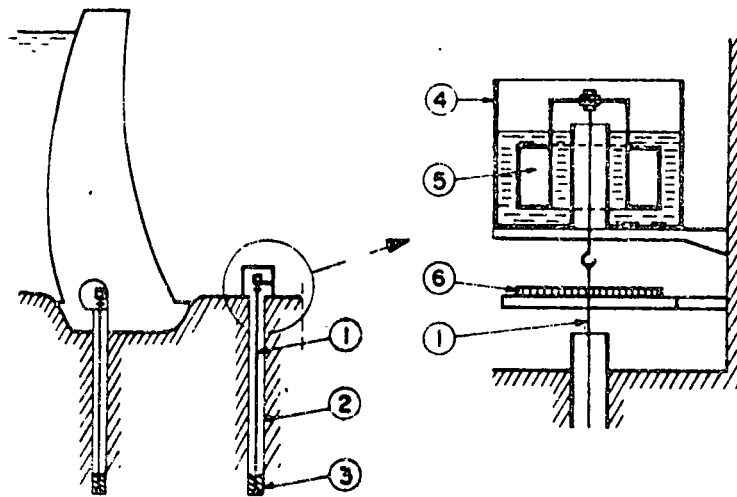


Figure 33 : Inverted pendulum in foundation rock (Electricite de France).

- (1) Stainless steel wire.
- (2) Large diameter borehole.
- (3) Anchor zone.
- (4) Ring-shaped tank.
- (5) Ring-shaped float.
- (6) Reading scale.

operation are not anchored deep enough to give a good approximation of the absolute displacement (see section 4.24). In spite of this drawback they would however *detect* very early deviation from normal behaviour. A mention should be made also of the difficulty of drilling deep, straight vertical holes to be sure that the wire does not come into contact with the walls at any level.

4.53 Wires in boreholes

The relative displacement along the pendulum wire itself could be measured, but in practice, special wires, not necessarily vertical, are used for this purpose. The main difficulty is to eliminate length variations due to stress and temperature. Invar wires have to be used for years to calibrate the geodetic base lengths and the technology is the same, except that the wires are installed in adits or boreholes. The systems have been used for many years in mines but the development of the method is recent for rock foundations. It is now common to install eight wires of different lengths in the same hole (Fig.34).

The main difficulties for the installation of this valuable device are:

- a) Drilling straight holes, particularly when they are long and near the horizontal, and executed from a narrow adit.
- b) Avoiding possible friction along the walls by an adequate tension.
- c) Avoiding creep of the wire due to too high a tension.

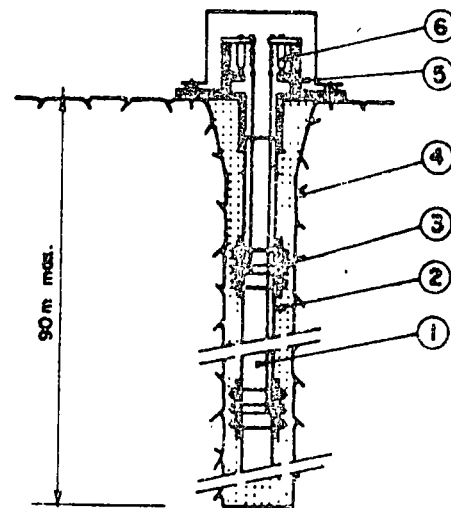


Figure 34 : Borehole "Elongameter"
(Manufactured by TELEMAT)

- (1) Stainless steel wire (8 wires).
- (2) Watertight PVC casing (50mm diameter).
- (3) Anchor ring for wire no. 1.
- (4) Borehole (75 mm diameter).
- (5) Measuring head.
- (6) Vibrating wire device.

- d) Anchoring correctly the different wires of different lengths

According to the local conditions and length of wire the sensitivity varies: it is approximately 0.1mm for a range of 5cm.

Although a definite improvement, this multiple wire device is still discontinuous; the fissures cannot be localised exactly within each section between anchor points. The ideal would be a long extensometer, able to measure the strain over its whole length (Bernaix, J., 1969).

4.54 Clinometers

Two types of clinometers are used in rock foundations: *fixed instruments*, and sliding cells *lowered into boreholes*.

The first type is extremely accurate. The vibrating wire clinometers for instance give a sensitivity of $5 \cdot 10^{-6}$ radians, and they give the direction α and γ of the variation of slope. A number of them are installed in adits, shafts or underground chambers, to detect any possible anomaly of deformation.

The second type, using boreholes lined with a plastic casing equipped with guiding grooves is very commonly in soil. Its lower accuracy is due to the imperfection of the guides, deformation of the hole, and inaccuracy in positioning the cell at the same place for each series of readings. It is therefore not a good device for measuring the real deformation of a rock mass by integration of elementary slope variations. It is however useful to detect any possible shear zone or surface along the borehole. The only drawback is that beyond a certain shear strain the measuring cell will jam in the hole and not give any further information on the section below.

The *chain deflectometer* (Muller, G and Muller, L., 1970) is an instrument of intermediate type; although removable from the borehole for repair or calibration, it is left homed-in for several series of measurements

4.55 Geophysics

Monitoring by geophysics has been attempted several times. Although not often applied, these methods are perhaps worth developing, and it would be interesting to gather the experiences, positive or negative, obtained on rock foundations. It is tempting to use geophysical methods as they act somewhat like radiology in medicine: they "look" inside a large body of rock.

Electric conductivity could bring valuable information on changes of permeability, but above all on alteration or dissolution of rock owing to the resulting change in ion content.

Seismic refraction or transmission between fixed points could detect a possible change in fissure openings, in other words, in stresses. The investigations made in the foundation of Gage 2 Dam in France (Faurox et al, 1968) are encouraging. It would be interesting to know whether other experiments have been attempted, and what are the most significant seismic parameters: velocity, length, attenuation of

waves? which waves? For instance, at Gage 2 dam, the variations between empty reservoir and full reservoir conditions, were 20% for the wave velocity and 90% for attenuation of energy.

Finally *microseismic* recording by highly sensitive seismographs of minute shocks originated in the foundation may detect either a normal adaption to the new stress field, or the onset of failure. This method of micro-seismic measurement, mainly used in monitoring rock slopes, could probably be used in foundations as well, provided it is interpreted with great skill; otherwise there might be needless concern at quite normal developments.

4.56 Piezometers and drains

The drains, which are usually installed in foundations, at least when the hydraulic gradients could develop forces detrimental to stability (e.g. in dam foundations), are not only efficient corrective measures (see 4.46) but also useful monitoring instruments. The increase in discharge, or the drying out, of a drain obviously has a meaning. However, no interpretation is possible without the second term of the flow net, i.e. the hydraulic potential. That is why all designers now agree on the absolute need for *piezometric measurements together with drain discharge readings*. The whole is what has been called in French "auscultation hydraulique". It seems that it is a powerful means of detection of any rearrangement of strains in the rock foundation. As a slight deformation of the rock mass entails a much larger deformation of the fissures, which in turn result in spectacular changes in hydraulic conductivity, it is claimed that the slightest modification of rock strains should react on the flow net, i.e. on the piezometer readings and drain flow rates.

Although this behaviour has been observed in a few cases, it is of utmost importance to gather further confirmation, because it would give a powerful means of warning, probably *before* any anomaly is detectable by other instruments.

It should be remembered, however, that the theory of sensitivity of flow net to fissure width variation does not hold when the flow is concentrated along channel-like paths. This point, discussed in 2.4 has to be considered seriously for the interpretation of "hydraulic instrumentation."

A mention should be made here about the reliability of piezometric measurements.

The piezometer tips are either too short, giving only a local value difficult to use, or too long, giving a wrong "mean" value by permitting circulation of water between levels at different potentials. The *continuous borehole piezometer* (Fig.35) worked out in France (Groupe de Travail CFGE, 1970) is an important step towards proper piezometric readings: a complete log of pressure is possible for the whole length of the borehole, which, in addition, does not allow circulation of water, thanks to a rubber membrane.

Finally, drain holes could also be used to perform Lugeon tests, at constant locations during the operation of the structure (Louis, C., 1971). Tests of this nature are not often done, although they deserve to be, to enable a better understanding of foundation rock behaviour.

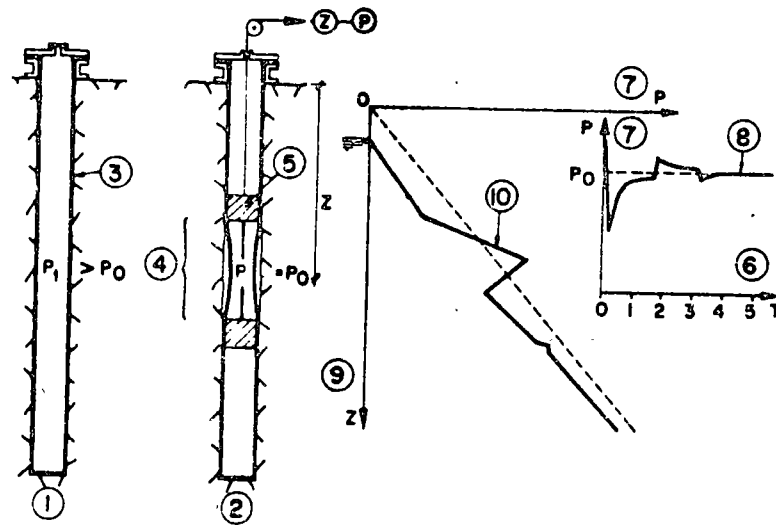


Figure 35 : Continuous borehole piezometer (Groupe de Travail du CFGB , 1970)

- (1) Borehole with rubber membrane under pressure ($P_1 > P_0$).
- (2) Borehole during measurement at depth Z ($P = P_0$).
- (3) Rubber membrane.
- (4) Measuring probe.
- (5) Packe..
- (6) Time in minutes.
- (7) Water pressure inside probe.
- (8) Curve of pressure vs. time at depth Z .
- (9) Depth.
- (10) "log" of water pressure.

ACKNOWLEDGEMENTS

The authors wish to express their sincere appreciation to the following persons who provided much valuable assistance in discussion on various parts of this report:

M. Pierre Habib of the laboratoire de Mecanique des Solides of the Ecole Polytechnique and Chairman of the French Committee for Rock Mechanics,

M. Marc Panet of the Laboratoire Central des Ponts et Chaussees.

M. Pierre Duffaut from Electricite de France,

M. Claude Louis of the Bureau de Recherches Geologiques et Minieres,

Dr. John Bray of the Rock Mechanics Centre at Imperial College, London.

Thanks are also due to the secretarial and drawing office staff who have worked with the authors to produce this report within extremely tight time schedules.

LIST OF REFERENCES

- BAI TOSSER, R.W. and LAURENCE, H.W. Application of well logging techniques to Metallic Mineral Mining. *Geophysics* Vol.35 pp 143 - 152, 1970
- BARTON, N.R. A model study of the behaviour of steep excavated slopes, *Ph.D.Thesis*, Imperial College, London, 1970.
- BERNAIX, J. "Etude Géotechnique de la Roche de Malpasset". Dunod ed., Paris (1967).
- BERNAIX, J. "Une nouvelle méthode de mesure des déformations d'un massif rocheux: l'extensomètre intégral à bande magnétique", *Colloque de Géotechnique des Comités Français de Mécanique des Sols et de Mécanique des Roches*, Toulouse (Mars 1969)
- BROADBENT, C.D. and RIPPERL, K.H. Fracture studies at the Kimberley pit. *Proc.Symposium on Planning Open Pit Mines*, Johannesburg, 1970. Publisher A.A.Balkema, Amsterdam. pp.171-179, 1971
- CUNDALE, P.A. A computer model for simulating progressive large-scale movements in block rock systems *Rock Fracture Symposium of ISRM*, Nancy, France, 1971.
- D'ANDREA, D.V., FISHER, R.L., and FOGELSON, D.E. "Prediction of compressive strength from other rock properties", U.S. Bureau of Mines Report of Investigations 6702 (1965)
- DEERE, D.U. "Geologic Consideration", in K.G.Stagg and O.C.Zienkiewicz (eds) *Rock Mechanics in Engineering Practice*, New York (1968).
- FAIVRE D'ARCIER, G. and CONTE, J. "La consolidation des appuis du barrage de Monteynard" *ICOLD.8th International Congress*, Edinburgh. Report Q28-R19 (1964)
- FAUROUX, G., GARNIER, J.C. and LAKSHMANAN, J. "Observation des variations de contraintes dans le rocher de fondation du barrage du Gage 2 par auscultation dynamique", *International Symposium of Rock Mechanics*, Madrid (1968)
- FECKER, E. and RENGERS, N. "Measurement of large scale roughness of rock planes by means of profilograph and geological compass" *Rock Fracture, Symposium of ISRM*, Nancy. Report I - 18 (1971)
- FUJII, T. "Fault Treatment at Nagawado dam," *ICOLD.10th International Congress*, Montreal, Report Q37-R59 (1970).
- GAZIEV, and ERLIKHAM, S.A. "Stresses and strains in anisotropic rock foundation (model studies)", *Rock Fracture, Symposium of ISRM*, Nancy. Report II-I (1971).
- GOODMAN, R.E. Geological investigations to evaluate stability. *Proc. 2nd Conference on Stability in Open Pit Mining*. Vancouver 1971 (In Press)
- GOODMAN, R.E. and DUBOIS, J. "Duplication of Dilatancy in Analysis of Jointed Rocks", *Proceedings of ASCE*, Vol.98, SM4, paper 8853 (April, 1972)
- GRUPE DE TRAVAIL DU CFGB. "Essais et calculs de mécanique des roches appliqués à l'étude de la sécurité des appuis d'un barrage voute - Exemple de Vouglans," *ICOLD. 9th International Congress*, Istanbul Q32 - R49 (1967).
- GRUPE DE TRAVAIL DU CFGB "Quelques développements récents des moyens d'auscultation du massif rocheux", *ICOLD. 10th International Congress*, Montreal. Q38 - R49 (1970)
- GUERRERO, R. and SERAFIM, J.L. "Problems relating to the foundation of Fl Atazar dam", *ICOLD.10th International Congress*, Q37 - R59 (1970)
- HENDON, A.J., CORDING, E.J. and AIYER, A.K. Analytical and graphical methods for the analysis of slopes in rock masses. *U.S. Army Engineering Nuclear Cratering Group*. Tech. Report No.36, 168p, 1971.
- HOEK, E., BRAY, J.W. and BOYD, J.M. The stability of a rock slope containing a wedge resting on two intersecting discontinuities *Quarterly Journal of Engineering Geology*, Vol 6. No.1, 1973.
- HOEK, E. and BRAY, J.W. *Rock Slope Engineering*, Inst. Mining and Metall., London 1973.
- HOEK, E., Methods for the rapid assessment of the stability of three-dimensional rock slopes. *Quarterly Journal of Engineering Geology*, Vol 6, No.2, 1973.
- JEFFERS, J.P. Core barrels designed for maximum core recovery and drilling performance *Proc. Diamond Drilling Symposium*, Adelaide, 1969.
- JOHN, K.W. Graphical stability analyses of slopes in jointed rock, *Proceeding of ASCE*, vol.94, SM2, paper 5865 (March 1968)
- JOUANNA, P. Effet des sollicitations mécaniques sur les écoulements dans certains milieux fissurés *Ph.D. Thesis* Toulouse University - France - 1972.
- KEMPE, U.F. Core orientation, *Proc.12th Exploration Drilling Symposium*, Univ. Minnesota, 1967.
- KENNEDY, B.A. and NIEMEYER, K.E. Slope monitoring systems used in the prediction of a major slope failure at the Chuquicamata mine, Chile. *Proc. Symposium on Planning Open Pit Mines*, Johannesburg, 1970
- KRSMANOVIC, D. and MILIC, S. Model experiments on pressure distribution in some cases of a discontinuum, *Rock Mechanics and Engineering Geology*, suppl. 1 (1964)
- KRSMANOVIC, D. Contribution to the study of the failure problem in rock mass, *Proc.Geotechnical Conference Oslo* Vol.1. 1967.
- LAKSHMANAN, J. and ALI, P. Le carottage sismique, *Rock Fracture, Symposium of ISRM*, Nancy. Report I-20 (1971).
- LANCEFORS, U. and KIHLSSTROM, B. *Rock Blasting* Wiley & Sons, New York, 404p. 1963.
- LECHAT, P., MONTJOIE, A. and LEMOINE, Y. Apport des études sismiques à l'étude de la fracturation du rocher dans le cas d'un site de barrage, *Rock Fracture, Symposium of ISRM*, Nancy, Vol.2 (1971).
- LEONET, O., SINOÛ, P. and TINCELIN, F. Etude du comportement d'un toit en fonction de différents modes de boulonnage, *Rock Fracture, Symposium of ISRM*, Nancy. Report III - 6 (1971)
- LONDE, P. Une méthode d'analyse à trois dimensions de la stabilité d'une rive rocheuse, *Annales des Ponts et Chaussées*, No.1, pp.37-60 (Janv.1965)

- LONDE, P. and SABARLY, F. La distribution des permeabilites dans la fondation des barrages voutes en fonction de champ de contrainte, *ISRM 1st International Congress*, Lisbon. Report 8-6 (1966)
- LONDE, P., VIGIER, G. and VORMERINGER, R. Stability of rock slopes, a three dimensional study, *Proceedings of ASCE*, vol. 95, SM 1, paper 6363 (January 1969)
- LONDE, P. Three dimensional analysis of rock foundation stability, *Water Power*, pp. 317-319 (Sept. 1970)
- LONDE, P., VIGIER, G. and VORMERINGER, R. Stability of rock slopes, graphical methods, *Proceedings of ASCE*, vol 96, SM 4, paper 7435 (July 1970)
- LONDE, P. The mechanics of rock slopes and foundations. *Quarterly Journal of Engineering Geology*. Vol 6, No.1, 1973.
- LUGEON, M. Barrages et Geologie. Dunod ed., Paris (1933)
- LOUIS, C. A study of groundwater flow in jointed rock and its influence on the stability of rock masses, *Ph.D Thesis*. University of Karlsruhe, English translation, Imperial College, London (1969)
- LOUIS, C. Ecoulement à trois dimensions dans les roches fissurées, *Revue de l'Industrie Minerale*, Special issue, pp. 73-93 (July 1970)
- LOUIS, C. Hydraulic Triple Probe to determine the directional hydraulic conductivity of porous or jointed rock, *Imperial College*, Report D 12, London, 1970.
- LOUIS, C. and MAINI, Y.N.T. Determination of in-situ hydraulic parameters in jointed rock, *ISRM 2nd International Congress*, Belgrad. Report 1/32 (1970).
- LOUIS, C. Influence de l'état de contrainte sur les écoulements dans les roches. Discussion of "Theme Barrage". *Revue de l'Industrie Minerale*, Special issue, pp. 152-154 (July 1971).
- MAINI, Y.N.T. In-situ hydraulic parameters in jointed rock. Their measurement and interpretation, *Ph.D Thesis*, Imperial Collge, London (1971).
- MAURY, V. Les milieux stratifies, Dunod ed., Paris (1969).
- MAURY, V. and DUFFAUT, P. Stress distribution model analysis in a two families discontinuity medium, *ISRM 2nd International Congress*, Belgrade. Report 8/19, (1970).
- MIADYENOVITCH, V. Deplacements à l'intérieur d'un massif dus aux charges réparties sur sa surface, *Revue de l'Industrie Minerale*, (July 1970).
- MULLER, L. Der Felsbau, F.Enke ed., Stuttgart (1963)
- MULLER, G. and MULLER, L. Monitoring of dams with measuring instruments, *ICOLD. 10th International Congress*, Montreal. Q38-R54 (1970).
- PATTON, F.D. Multiple modes of shear failure in rock, *ISRM 1st International Congress*, Lisbon. Report 3-47 (1966)
- PENA, H., GRADOR, J., BARBDETTE, R. and PAUTRE, A. Injection, drainage et auscultation hydraulique dans les fondations du barrage de Rapel (Chili) *ICOLD, 10th International Congress*, Montreal. Q37-R36 (1970).
- PENMAN, A.D.M. and CHARLES, J.A. Measuring movements of engineering structures *Proc. 13th International Congress of Surveyors*, Weisbaden, Paper 605.4., 1971.
- PHILLIPS, F.G. *The use of stereographic projections in Structural Geology*. Edward Arnold, London, IIIrd Edition, 1971.
- PRICE, D.G. and PLAISTED, A.C. Epoxy resins in rock slopes stabilisation works *Rock Fracture, Symposium of ISRM*, Nancy. Report III-9 (1971)
- ROBERTS, D. and HOEK, E. A study of the stability of a disused limestone quarry in the Mendip Hills, England. *Proc. 32nd Conference on Stability in Open Pit Mining*, Vancouver, 1971 (in press).
- ROCHA, M. A method of integral sampling of rock masses. *Rock Mechanics*. Vol 3, No.1, pp. 1-12, 1967.
- ROSENGREN, K.J. Diamond drilling for structural purposes at Mount Isa. *Proc. Australian Diamond Drilling Association Symposium*, Surfer's Paradise November 1969.
- ROSS-BROWN, D.M. and ATKINSON, K.B. Terrestrial photogrammetry in open pits *Trans. Inst. Min. Metall* London, Vol. 81, pp. A205-214, 1972.
- SABARLY, F. Les injections et les drainages de fondations de barrages en roches peu permeables *Geotechnique*, Vol. 18/2, pp. 229-40 (Juin 1968)
- SABARLY, F., PAUTRE, A. and LONDE, P. Quelques reflexions sur la drainabilité des massifs rocheux, *ISRM 2nd International Congress*, Belgrad. Report 6-12 (1970)
- SCHNEIDER, B. Moyens nouveaux de reconnaissance des massifs rocheux, *Annales de l'I.T.B.T.P.*, Paris (July, August 1967).
- SERAFIM, J.L. and DEL CAMPO, A. Interstitial pressures on rock foundation of dams, *Proceedings of A.S.C.E.*, Vol. 91, SM5, paper 4484 (1965).
- SHARP, J.C., HOEK, E. and BRAUNER, C.O. Influence of groundwater on the stability of rock masses. *Trans. Inst. Mining and Metall.*, London, Vol. 81, 1972.
- SNOU, D.T. Fracture deformation and changes of permeability and storage upon changes of fluids pressure, *Colorado School of Mines*, Pt. A, 63 (1968).
- SNOW, D.T. Rock fracture spacings, openings and porosities, *Proceedings of ASCE*, Vol. 94, SM 1 (1968). (b).
- ST. JOHN, C.M. and THOMAS, T.L. The NPL Mekometer and its application to mine surveying and rock mechanics. *Trans. Inst. Min. Metall.*, Vol. 79. No. 761. 1970.
- STAGG, K.G. In situ tests on the rock mass. *Rock Mechanics in Engineering Practice*. Ed. Stagg K.G. and Zienciewicz, O.C., Wiley, New York, 1965.
- TAYLOR, D.W. *Fundamentals of Soil Mechanics*. Wiley, New York. 700 p. 1948.
- TER-MINASSIAN, W., SABARLY, F. et LONDE, P. Comment proteger les barrages voutes contre la pression de l'eau dans les appuis. *ICOLD 9th International Congress*, Istanbul, Q.32-R.12 (1967)
- TERZAGHI, Ch. Effect of Minor Geologic Details on the Safety of Dams. *The American Institute of*

Mining and Metallurgical Engineers Inc. - (1929)

TERZAGHI, R.D. Sources of error in joint surveys,
Geotechnique, Vol.15 (1965)

VON THUN, J.L. and TARBOX, G.S. Deformation moduli
determined by joint shear index and shear catalog
Rock Fracture, Symposium of ISRM, Nancy. Report
11-23 (1971)

WARD, W.H. and BURLAND, J.B. Assessment of the deforma-
tion properties of jointed rock in the mass.
International Symposium on Rock Mechanics, Madrid,
1968.

WITKE, W. A numerical method of calculating the
stability of loaded and not loaded rock slopes
(in German) *Rock Mechanics and Engineering
Geology*, Vol.30, suppl.11 (1965)

ZEMANEK, J. The borehole televiewer - a new logging
concept for fracture location and other types
of borehole inspection. *Society of Petroleum
Engineers*. Sept. 1968.

Drakensberg pumped storage scheme : rock engineering aspects

J. B. BOWCOCK Partner, Gibb, Hawkins & Partners, Johannesburg.

J. M. BOYD Senior Geotechnical Engineer, Golder Associates, Maidenhead, U.K.

E. HOEK Principal, Golder Associates, U.K.

J. C. SHARP Principal, Golder Associates, U.K.

SYNOPSIS: The Drakensberg Pumped Storage Scheme is a multi-purpose project being undertaken jointly by the Electricity Supply Commission and the Department of Water Affairs. The Scheme involves three major underground excavations for the pumping and generating plant and associated subsidiary equipment. There is in addition an extensive series of inter-connecting tunnels to act as waterways and access. The general approach to the rock engineering aspects of the Scheme are described and details are given of the project feasibility considerations and subsequent exploratory geological and geotechnical work. The geological programme is outlined and details are given of the rock mechanics investigations involving sample and in-situ testing and evaluation of rock reinforcement and pneumatically applied concrete. The testing of an enlargement to the full cross sectional dimensions of the future machine hall and of a full scale penstock test chamber to determine the feasibility of concrete lined pressure tunnels are described. The inter-relationship of investigation, testing, analysis and design are considered in the Paper.

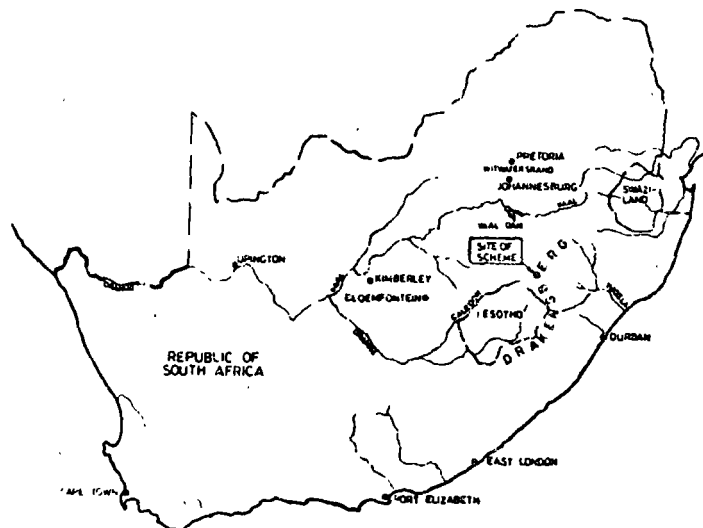
INTRODUCTION

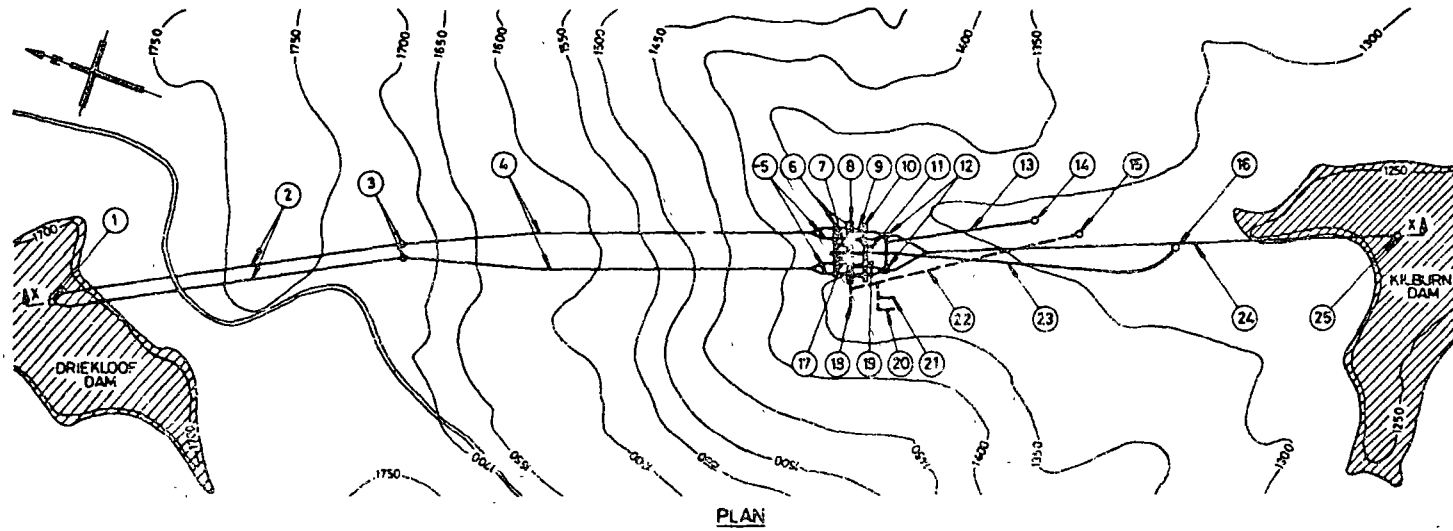
1. Engineering Description of the Works

The principal source of water for Johannesburg and other centres in the Witwatersrand for both industrial and domestic purposes has traditionally been the westward flowing Vaal river (Figure 1). However this source is no longer

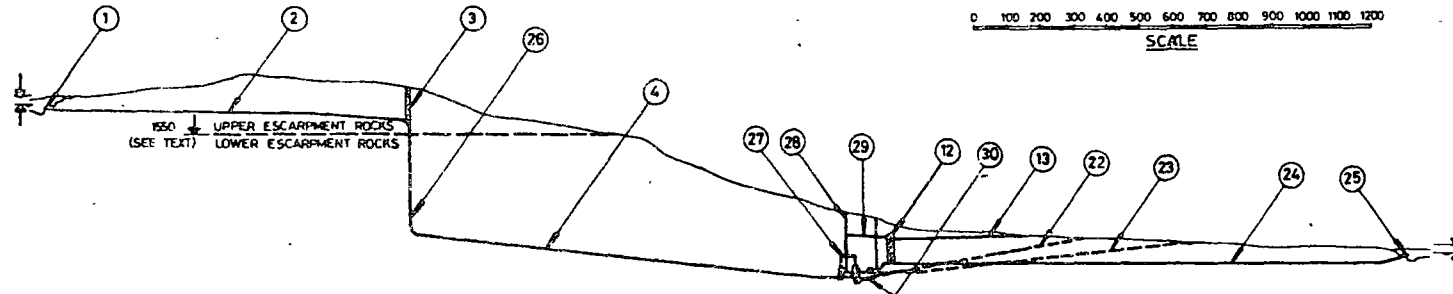
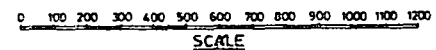
sufficient to provide an assured supply to meet the demands of this rapidly growing area. As a result, the Department of Water Affairs has proceeded with a scheme to abstract water from the upper regions of the eastward flowing Tugela river and to pump this over the Drakensberg escarpment into the Vaal catchment.

FIGURE 1
LOCATION PLAN





- ① HEADRACE TUNNEL INTAKE
- ② HEADRACE TUNNELS 2Nº
- ③ SURGE SHAFTS 2Nº
- ④ PRESSURE TUNNELS 2Nº
- ⑤ PENSTOCKS 4Nº
- ⑥ VALVE HALL
- ⑦ CONTROL BLOCK
- ⑧ MACHINE HALL
- ⑨ BUSBAR TUNNELS 4Nº
- ⑩ TRANSFORMER HALL
- ⑪ BUSBAR SHAFT
- ⑫ SURGE CHAMBERS 2Nº
- ⑬ AUX ACCESS TUNNEL AND LINK TUNNEL
- ⑭ AUXILIARY ACCESS TUNNEL PORTAL
- ⑮ EXPLORATORY ADIT PORTAL
- ⑯ MAIN ACCESS TUNNEL PORTAL
- ⑰ AMENITIES BLOCK
- ⑱ MACHINE HALL TEST ENLARGEMENT
- ⑲ BUSBAR SHAFT
- ⑳ PLATE BEARING TEST ADIT
- ㉑ PENSTOCK TEST CHAMBER
- ㉒ EXPLORATORY ADIT
- ㉓ MAIN ACCESS TUNNEL
- ㉔ TAILRACE TUNNEL
- ㉕ TAILRACE TUNNEL PORTAL
- ㉖ PRESSURE SHAFTS 2Nº
- ㉗ VENTILATION TUNNEL
- ㉘ LIFT SHAFT
- ㉙ DISCHARGE SLUCEWAY
- ㉚ DRAFT TUBES 4Nº
- EXPLORATORY CONTRACT
- † PRELIMINARY CONTRACT
- EXPLORATORY WORKS



SECTION X-X

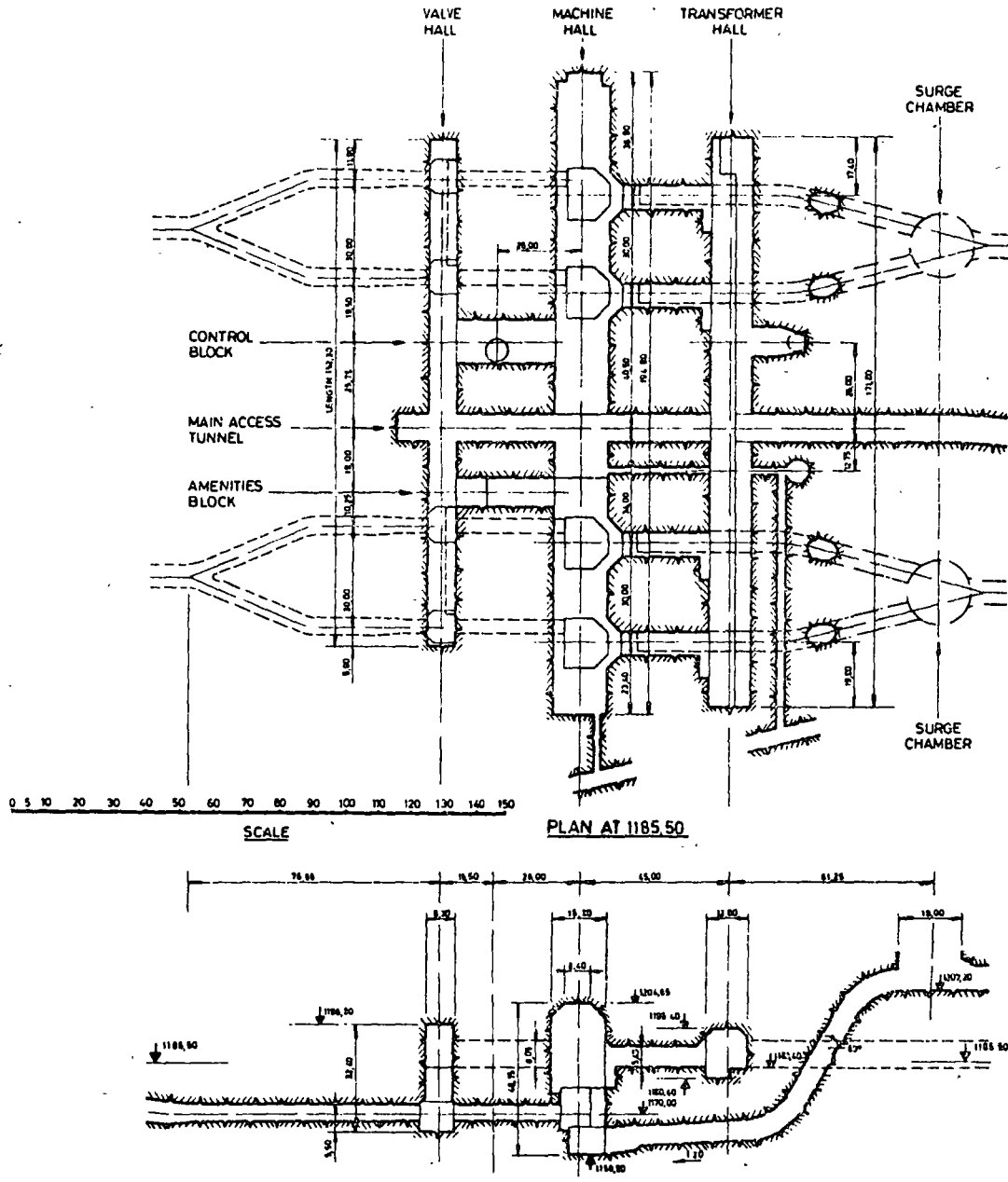
LONGITUDINAL PLAN AND SECTION OF WORKS

The first phase of this scheme was completed in 1974 and water is now being pumped over the escarpment from a pumping station at Jagersrust.

The predicted demand for water from the Vaal catchment would have made it necessary to duplicate this pumping scheme by 1980. However, as an alternative, studies were carried out into the possibility of developing a pumped storage scheme in the vicinity of the first pumping station which could be used both for pumping water into the Vaal for water supply purposes and for storing electricity. These studies

were undertaken jointly by the Department of Water Affairs and the Electricity Supply Commission (Escom) as a result of which it was decided to proceed with the Drakensberg Pumped Storage Scheme (1).

Escom will use the Drakensberg Scheme primarily to store surplus off-peak energy from thermal power stations. For water supply purposes the Department will draw water from the upper reservoir (Driekloof).



TYPICAL CROSS-SECTION ON A WATERWAY
 FIGURE 3
 PLAN AND SECTION OF POWER STATION

The pumping head will be approximately 500 m, one of the highest in the world for this type of scheme.

The Scheme, which is now in the early stages of construction, is located approximately 5 kilometres to the north of the existing Jagersrust pump station. The principal engineering structures include an underground power station to contain four reversible pump-turbines each driving a 250 MW reversible motor-generator, associated tunnels and shafts, surge chambers and access tunnels (Figures 2 and 3). These works will be carried out under contract to Escom. In addition, the Scheme involves the construction of two major embankment dams at Kilburn and at Driekloof and extensive open excavations. These excavations and dams are not discussed further in this paper.

An initial study of the rock mechanics aspects of the Scheme was made by the Council for Scientific and Industrial Research (CSIR). After this study Escom appointed Gibb Hawkins and Partners as its consulting engineers for the design and site supervision of the excavation, stabilization and lining of the underground works. Gibb Hawkins and Partners in turn appointed Golder Associates of the United Kingdom as their specialist advisers for the rock engineering aspects of the Scheme.

Two exploratory contracts were awarded by Escom at the beginning of 1975. The first contract involved excavation of an exploratory adit and an exploratory shaft with inter-connecting headings in the area of the future machine hall. In addition provision was made in this contract for excavation of a test enlargement to the full span of the machine hall and construction of a trial length of concrete lined pressure tunnel. The second contract was for exploratory drilling both from the surface and from underground.

In August 1975 a preliminary contract was awarded for the excavation of the tailrace tunnel and main access tunnel (headrace and tailrace refer to the generating mode). Further contracts will be awarded by Escom for the remainder of the underground work.

This paper describes the rock engineering aspects of the Scheme including investigation, testing and design phases. Particular emphasis is placed on the power station excavations. Following a brief summary of geological and groundwater conditions, the main rock engineering aspects are discussed. At the time of writing (July 1976) the exploratory works are still in progress and full results are therefore not available.

2. Summary of Geological and Groundwater Conditions

2.1 Geology

The underground works lie mainly beneath the south facing slopes of the Drakensberg escarpment between elevation 1730 m at the top of the surge shafts and elevation 1214 m at the invert of the tailrace portal (Figure 2).

The Scheme is sited mainly within rocks of the Beaufort Series of the Karroo System. Fossil and stratigraphic evidence indicates a continental depositional environment. Lateral facies variations are common and therefore the boundaries of lithological units are frequently diachronous.

A distinct division of rock types in the vicinity of the Scheme occurs below a prominent sandstone horizon which outcrops at approximately elevation 1550 m (Figure 2).

Below the marker horizon the rocks are primarily sandstones, siltstones and mudstones from the Middle and Lower Beaufort Series. Siltstones and mudstones from these horizons vary in colour from greenish or bluish grey to dark grey.

Above the marker the rocks consist mainly of interbedded sandstones, siltstones and mudstones of the Upper Beaufort Series, the mudstones and siltstones of which have respectively a distinctive reddish-brown and greyish-green colouration.

In addition to the rock types mentioned above there are also occasional thin carbonaceous seams predominantly in those rocks below the marker horizon. Carbonaceous seams are usually thin, poorly developed fossil leaf remains within dark mudstones.

Dolerite sills and dykes are also present. The dykes are typically near-vertical, from one to three metres thick, and often bounded by slickensided, serpentinitised shear zones. A major sill having an upper elevation of 1133 m and over 70 m thick has been found beneath the proposed machine hall.

The strata within the Site area are essentially horizontal and bedding forms the dominant structural feature. Bedding plane spacing has been found to vary from less than 5 mm up to 500 mm. Frequently cross bedding and other sedimentary structures occur within the lithological units.

Joint surveys have been carried out both on surface exposures and in underground adits. The surveys show three statistically significant near-vertical jointing trends striking at approximately 120° , 160° and 190° . In interpreting the significance of the jointing it should be remembered that the major axes of the main halls are east-west, the axes of the tailrace and pressure tunnels are approximately north-south. (All directions in this paper are with respect to magnetic north, $19^{\circ}04'$ west of grid north).

Faults are usually associated with dolerite dykes although displacements are generally limited to a few metres.

2.2 Groundwater

Borehole permeability tests carried out over the area of the Scheme show a range of permeability from 10^{-6} m/s to 10^{-9} m/s. In general, the sedimentary units are relatively impermeable. Permeable fractured zones up to 2 m thick have been found at dyke margins.

Piezometers were installed in selective boreholes to determine existing groundwater conditions, seasonal variations and the influence of tunnel excavation on groundwater pressures.

The presence of low permeability mudstone and siltstone seams gives rise in general to a preferred groundwater flow direction parallel to the bedding within the more permeable units. The dykes and dyke margins modify this general flow pattern by dividing the rock mass into a series of reservoirs. Significant changes in piezometric head across dykes have been observed.

The groundwater table is generally close to surface. Significant departures from hydrostatic conditions with depth are expected in the vicinity of the escarpment.

ROCK ENGINEERING ASPECTS OF THE SCHEME

1. General Approach

The underground excavations required for a hydro-electric scheme such as the Drakensberg project have to be designed to satisfy a number of hydraulic, mechanical and electrical requirements. These requirements impose certain constraints upon the size, shape, depth below surface and orientation of the various excavations which make up the underground complex. Within these constraints, rock engineering principles are applied to check the feasibility of the proposed layout (basic consideration of excavation size, spacing and geology). Further, they are used to design the detailed shapes, excavation sequences and support systems which are necessary to ensure that the excavations remain stable throughout the life of the project.

The scope of the investigation, testing and design processes depends largely upon the characteristics of the rock mass and the nature of the in-situ stress field. These factors will determine the degree of stability inherent in the roof, sidewalls and inter-sections of the excavations and the necessary reinforcement to maintain required stability conditions permanently.

During feasibility studies for a project, only the most general type of geological information is usually available. At this stage, the potential behaviour characteristics of the rock mass are identified in very broad, general terms. Precedent and experience from other similar schemes are principal factors.

Such experience is related to the rock mass and excavation geometry by means of geomechanical classifications (2 and 3). Geomechanical classifications can be used to distinguish between different potential failure modes which may range from structurally controlled roof falls in jointed hard rock masses, to failure of intact rock material under stress in more homogeneous, weaker rock masses.

The potential behaviour and possible support requirements for the underground excavations are then estimated.

During the exploratory phase the available geological information becomes more detailed and a final specific design is formulated. At this stage, the mechanical behaviour of the rock mass is considered in terms of the most dominant characteristics and the investigation, testing and design processes are related to these specific parameters.

2. Project Feasibility Stage

As previously mentioned, the earliest studies on the rock mechanics aspects of the Drakensberg project were carried out by the CSIR and were based upon the use of a geomechanics classification system (2). These studies suggested that stable roof spans would be limited by the poor quality, horizontally bedded rock mass in which the major underground excavations would probably be located. Other schemes with similar rock conditions to Drakensberg were appraised. Table 1 gives the general rock mass characteristics and machine hall sizes for the Drakensberg, Poatina and Portage Mountain hydro-electric projects.

Based upon comparisons with the Poatina scheme in Tasmania (4), the use of a trapezoidal roof arch with a total span limited to 20 m was considered. In order to minimise the effective overall height of the Drakensberg excavation and thus ensure greater inherent stability of the sidewalls, each of the four pump-turbines was planned to be located in individual pits separated by adequate rock pillars.

TABLE I

Project Name	Machine Hall		Rock Condition
	Dimensions LxWxH (metres)	Depth (metres)	
Drakensberg (Natal RSA)	193 x 16,3 x 45	150	Horizontal series of sandstones and siltstones and mudstones
Poatina (Tasmania, Australia)	92 x 13,7 x 26	152	Horizontally bedded mudstone. Horizontal stress approximately twice vertical.
Portage Mountain (B.C. Canada)	271 x 20,4 x 44	61	Interbedded sandstone, shale and coal measures dipping 15°. Horizontal stress approximately twice vertical.

Following a detailed appraisal of the CSIR recommendations several major points emerged which affected the layout of the scheme and the scope of the subsequent exploratory works. These were as follows :-

- (1) In accordance with the CSIR's recommendations, the pump-turbines would be located in a machine hall of the minimum possible cross-sectional dimensions. This would be achieved by separating components such as transformers and valves within separate halls, which would be located far enough from the machine hall to minimise interaction of the stress fields surrounding these excavations. Similarly, the downstream surge chambers were to be located as far away from the other major excavations as possible.
- (2) The initial design of the roof of the machine hall would be based upon a trapezoidal section (similar to that used at Poatina). The purpose of this shape is to limit the roof span in the horizontally bedded sequence by means of haunches. In order to check the validity of this concept to the rock mass conditions at Drakensberg and to permit the evolution of a rational roof support system, based upon the use of tensioned reinforcement and pneumatically applied concrete (PAC), it was proposed that a machine hall test enlargement should be excavated during the exploratory phase of the project. This test excavation would be carefully excavated in stages, monitored and the results used to ascertain the optimum roof shape and support system.

- (3) In order to take advantage of potential cost savings of using concrete instead of steel lining for the lower portion of the penstocks, it was proposed that a penstock test chamber should be constructed during the exploratory contract.

This chamber, which would be lined in the same manner as the lower portion of the penstocks would be fully instrumented and tested to the full hydraulic head of the Scheme to check the interaction of the lining and the surrounding rock mass with respect to deformation and leakage.

In addition to the specific test openings mentioned above, a comprehensive geological and geotechnical investigation and testing programme were developed to determine conditions throughout the Scheme.

3. Exploratory Stage

3.1 Introduction

The purpose and scope of the various elements of the exploratory programme were established initially in terms of the design objectives. Adequate flexibility was built into each element to allow progressive refinement during the exploratory phase.

The following main factors were considered:-

- (1) Geology
- (2) Groundwater
- (3) Mechanical characteristics of the rock mass
 - (i) Sample testing
 - (ii) In-situ testing
- (4) Rock reinforcement testing
- (5) Evaluation of exploratory works.

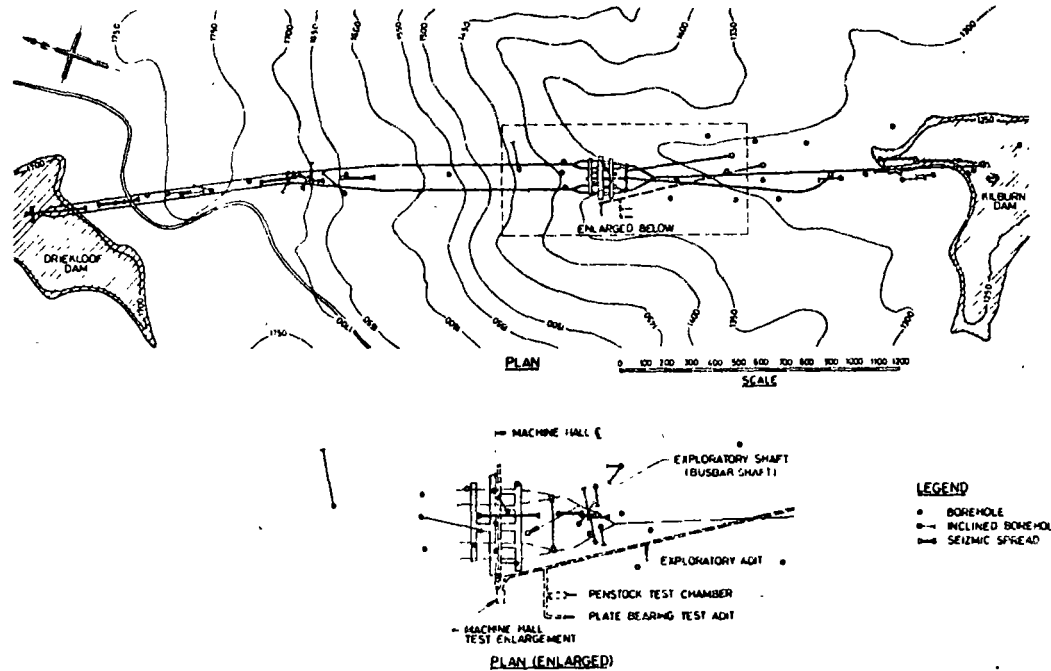
These studies together with the machine hall test enlargement and the penstock test chamber are described in the following section of the paper.

The geological and groundwater conditions have been summarised earlier in this paper. The broad scope of the investigations are described in the following section for completeness.

The investigation and testing programmes were carried out to satisfy the following two main requirements :-

- (1) Classification of stability/support conditions in tunnels and minor openings
- (2) Specific design of major halls, blocks and intersections.

For the first requirement, extensive use has been made of simple index tests on core to supplement geological data. For the second requirement more elaborate tests have been carried out at a representative scale and at locations relevant to the major works.



3.2 Geological Investigations

Figure 4 shows the locations of boreholes which were drilled primarily during the exploratory contract to investigate both the general geological conditions over the entire alignment and the detailed conditions in the vicinity of the major excavations. The rocks were classified according to argillaceous content as illustrated on Figure 5.

Most of the boreholes were drilled with 54 mm diameter double tube coring equipment. The core was generally wrapped in aluminium foil and waxed immediately upon extrusion from the barrel in order to minimise deterioration due to weathering prior to testing. Permeability testing was carried out in representative boreholes.

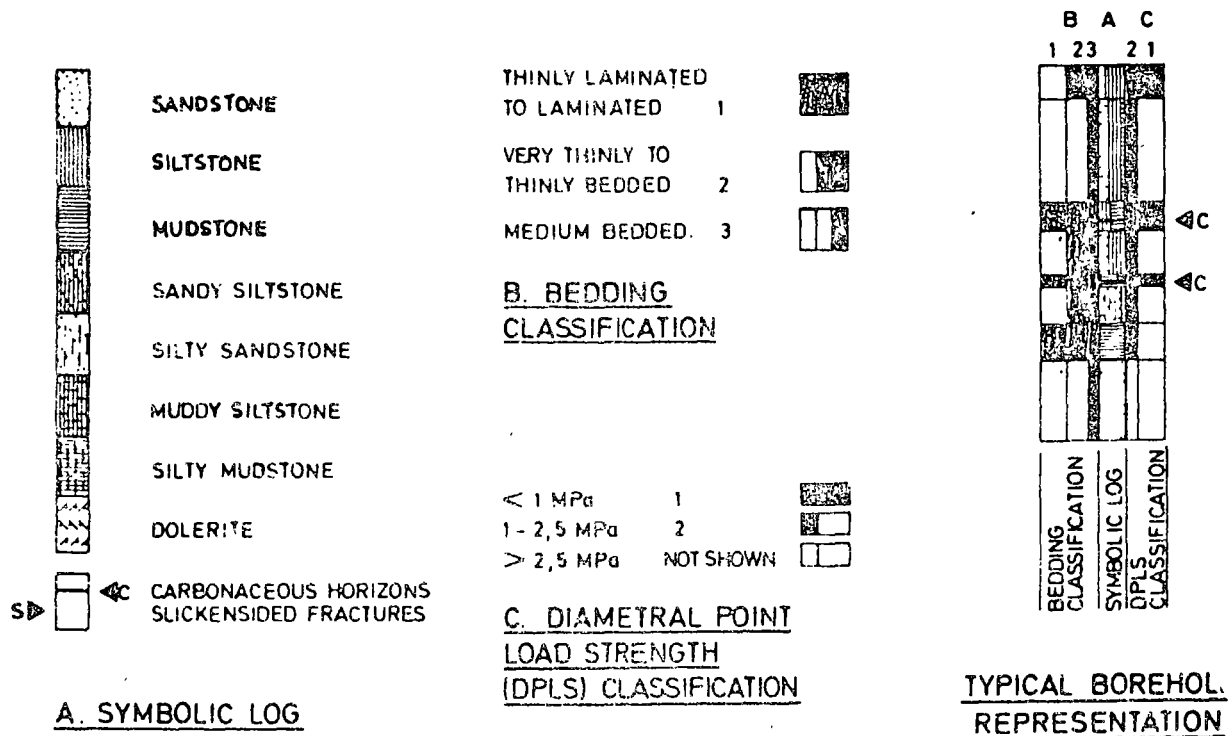


FIGURE 5

GENERAL ROCK CLASSIFICATION SCHEME FOR TUNNEL ROOF CONDITIONS

Detailed geological logging was carried out on all core. An example of a typical geological log is given in Figure 6. An expanded scale of logging was used in the vicinity of the major cavern roofs.

High quality colour photography of all core prior to testing was carried out in order to provide a permanent record.

Geophysical investigations were carried out along traverses as indicated in Figure 4 to check the depth of surface weathering and to identify anomolous zones between borehole locations. Surface reflection, refraction, up-hole and cross-hole shooting seismic techniques as well as magnetometer surveys were used. The measured seismic velocities were high for the rock types encountered (except in anomolous zones), an indication of the relatively unfractured nature of the in-situ rock mass. Magnetometer surveys proved to be

useful in the location and mapping of dykes along tunnel alignments.

3.3 Sample Testing

Tests on core samples were carried out for two main purposes :-

- (1) To provide representative 'intact' strength and modulus values for the various rock types
- (2) To provide index values for classification of stability/support conditions in tunnels and minor openings.

Small scale sample test results were not used as a basis for design of the major openings.

Early studies of various types of index tests indicated that the Point Load Index for core loaded diametrically (parallel to bedding) gave the most representative mechanical index for roof stability conditions.

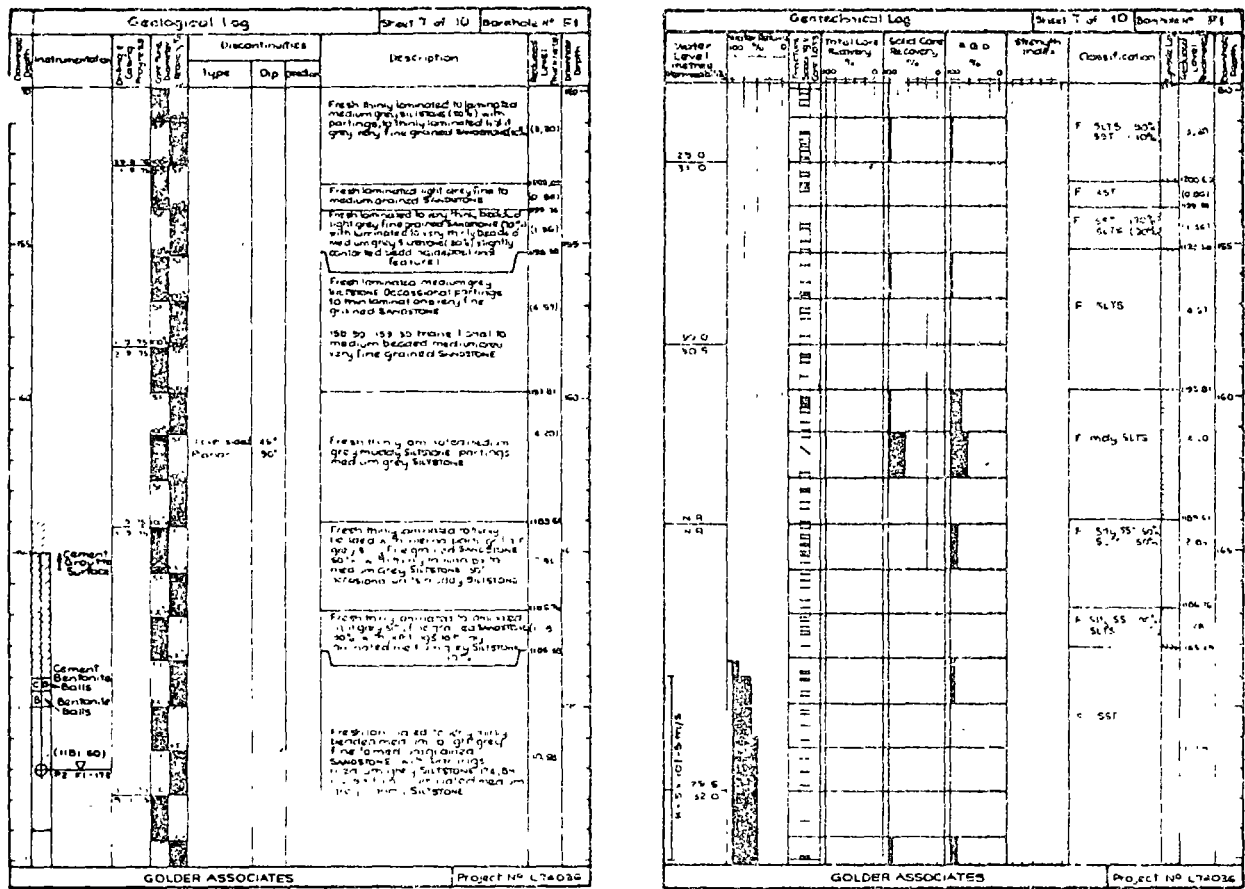


FIGURE 6

TYPICAL GEOLOGICAL AND GEOTECHNICAL LOGS

This test was therefore carried out as a general index test for the entire works and also incorporated into a Roof Stability Index for tunnel (limited span) sections. Correlation with lithology and actual roof conditions in the tunnels allowed three classes of diametral point load strength values to be defined (Figure 5).

The susceptibility of the siltstones and mudstones to deterioration on exposure was studied using the Slake Durability Test. A series of visual tests, using dye penetrants on samples subjected to various wetting and drying cycles, was also carried out.

Uniaxial compression testing of cores with modulus measurement using mechanical calipers was carried out on a large number of representative specimens. Results from such tests were correlated with lithology, inclination of bedding to the core axis and other parameters. Expected lower values of strength for increase in argillaceous content and at critical inclinations of the bedding to the core axis were determined. The sample preparation and testing techniques used were relatively simple and the results should be considered as 'index' values rather than absolute parameters.

A series of carefully controlled uniaxial compression tests on selected core samples from the various lithological groups was also carried out to determine laboratory values of strength, modulus and Poisson's ratio. Modulus and Poisson's ratio measurements were made using strain gauge techniques.

Shear testing of mudstone samples and specific bedding planes and joints was also carried out.

3.4 In-Situ Testing

The objective of the in-situ testing programme was to provide definitive design data for the major underground openings. The following tests were carried out :-

- (1) Measurement of the in-situ stress field
- (2) Measurement of rock mass moduli for strata within which the major caverns would be excavated
- (3) Measurement of rock mass moduli for strata surrounding the penstock test chamber.

(a) In-situ Stress Determination

Measurements of in-situ stresses are necessary in order to determine likely stresses and displacements induced in the rock as a result of excavation. All such measurements were therefore concentrated in the vicinity of the power station. The objective of the tests was to provide average stress values in the vicinity of the main halls and in particular ratios of principal stresses.

It was recognised that stress measurements in the rock mass at Drakensberg would be difficult owing to the weak nature of the rock and the relatively limited depth below surface of the excavations. The CSIR triaxial strain cell overcoring method was considered to be the most suitable. The disturbed nature of the excavation surfaces did not favour the use of flat jacks (stress relieving slots) and bored raises were not available for larger scale overcoring methods.

Following an initial test to check equipment operation, a two stage testing programme was drawn up and carried out by the CSIR. The scope of the second stage was based on the first stage results.

Only two measurements out of a possible total of ten yielded correlatable results from the first stage testing. The other tests were discounted due to flooding, lack of gauge adhesion or breakage of the overcored section. Preliminary results indicated the minor principal stress to be vertical and slightly greater than the overburden stress. The ratio of horizontal to vertical stresses (horizontal stresses about equal) was approximately 2,5 to 1.

The second stage of tests has been carried out but results are not yet available.

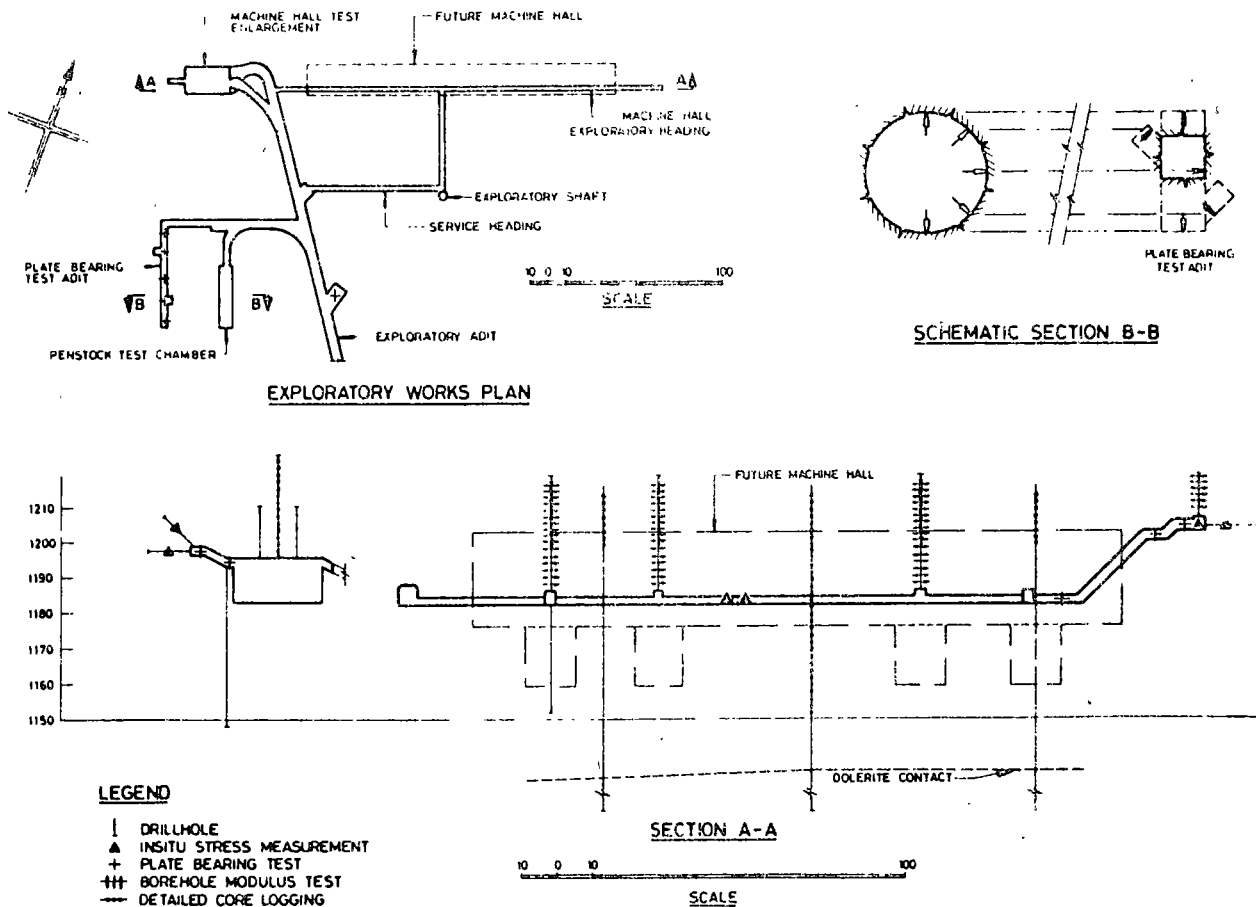


FIGURE 7
TEST LOCATIONS

(b) Rock Mass Modulus Determination - Power Station

Rock mass moduli in the vicinity of the power station were determined by Plate Bearing Tests at representative locations together with Borehole Modulus Tests (Goodman Jack) in a number of boreholes in the roof and walls at the proposed machine hall location.

Plate Bearing Tests were carried out in exploratory headings at locations shown on Figure 7. The locations corresponded to the roof strata encountered in the machine hall test enlargement and the proposed machine hall roof (the machine hall test enlargement was excavated prior to a final decision on the machine hall elevation). The test equipment is shown typically on Figure 8. A loaded area of $1,00\text{m}^2$ with a corresponding contact stress of up to $4,5\text{ MPa}$ was used. The maximum stress was determined following consideration of the stress changes induced during excavation.

Tests were carried out parallel and normal to the bedding. Rock mass displacements were measured relative to the loading plate on the loading axis. Three point extensometers were used at depths up to 6 m. Several loading cycles were carried out (generally 5) and a short term creep test was carried out at the maximum loading.

A typical test result is shown on Figure 9. The influence of rock relaxation at limited depths is clearly indicated. Modulus values are corrected to allow for the confining effect of the heading using results from a three dimensional boundary integral equation method study (5).

Borehole modulus tests using a Goodman Jack were carried out in vertical boreholes into the proposed machine hall roof strata. The boreholes were spaced along the length of the proposed machine hall as illustrated on Figure 7. Tests were carried out on representative strata identified during detailed logging. Other tests were also carried out in the vicinity of the larger scale Plate Bearing Tests to compare the results obtained from each type of test. In addition, borehole jacking tests were carried out in horizontal holes in both a horizontal and vertical sense on selected strata to determine modulus anisotropy.

(c) Rock Mass Modulus Determination - Penstock Test Chamber

Plate Bearing Tests were carried out in a special test adit alongside the penstock test chamber to determine the rock mass modulus at various points around the chamber. The tests were carried out on strata representative of those exposed in the chamber excavation. All tests were radial to the surface as indicated on Figure 7.

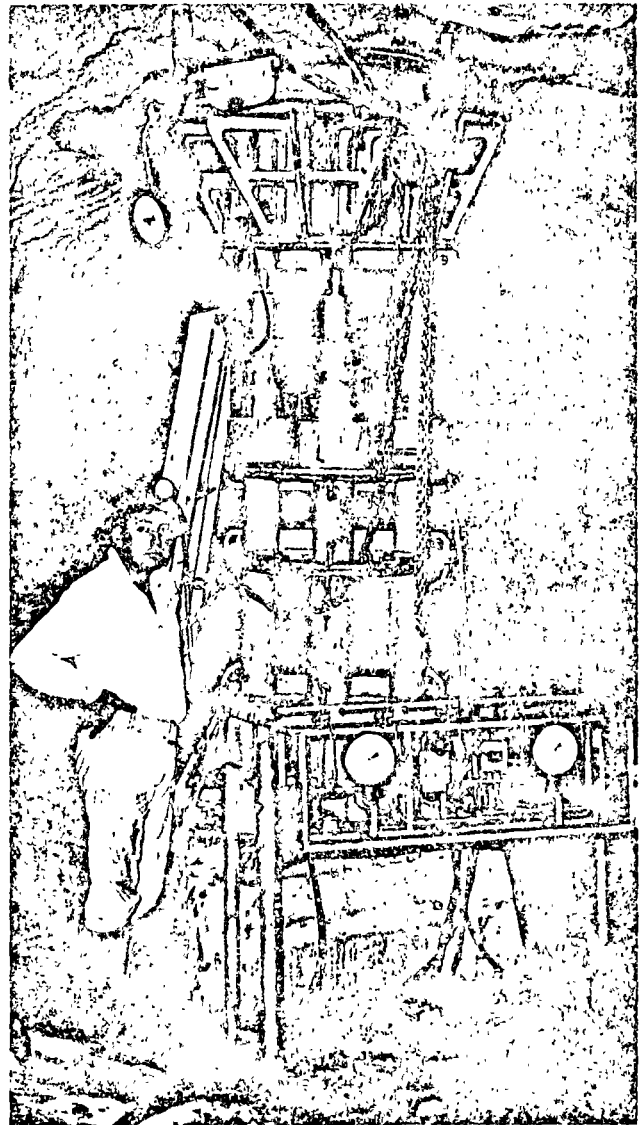


FIGURE 8
PLATE BEARING TEST EQUIPMENT

Tests were carried out using a plate area of $0,5\text{ m}^2$ and contact stresses up to $9,0\text{ MPa}$. Such stresses are representative of the induced stress (pressure) changes in the penstocks during operation.

The test normal to the invert of the penstock test chamber was repeated following grouting of the rock mass. The grouting process was designed to simulate as closely as possible the actual grouting technique around the lining of the test chamber.

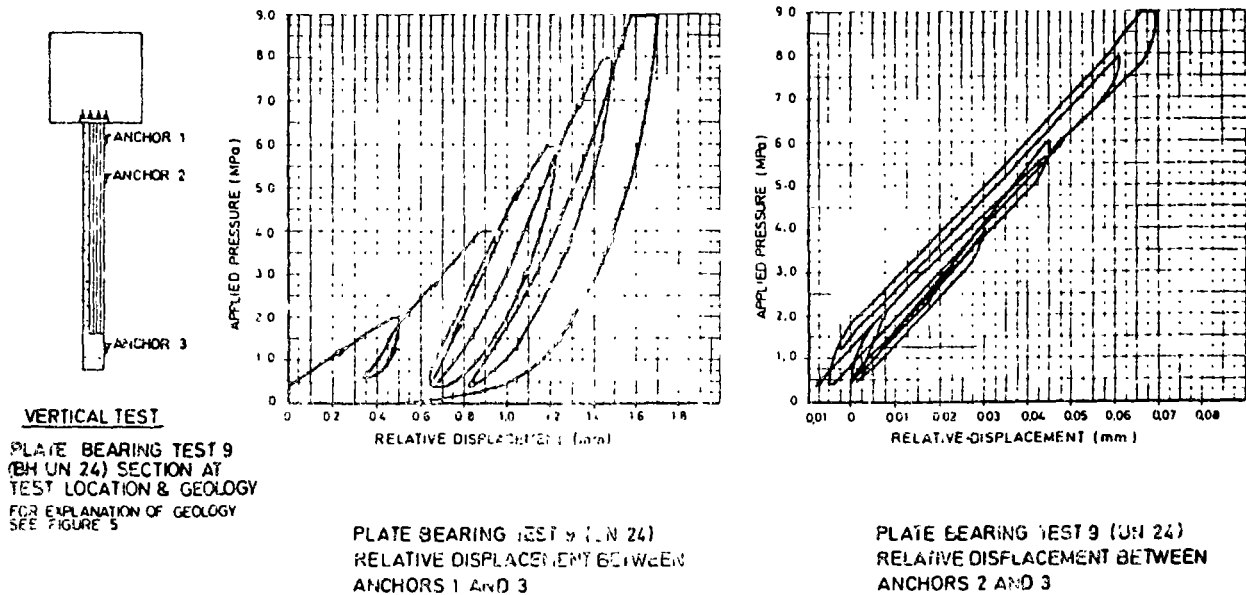


FIGURE 9

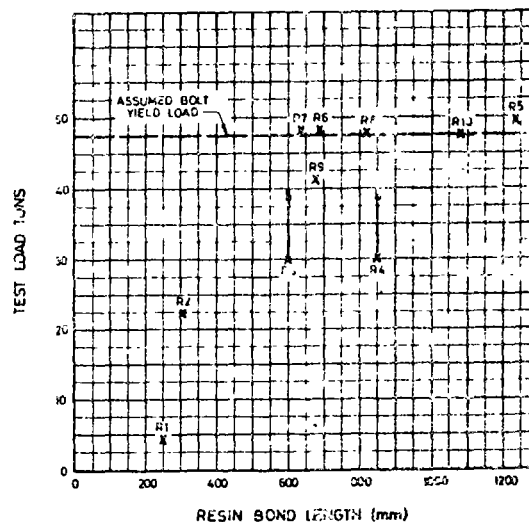
TYPICAL PLATE BEARING TEST RESULTS

3.5 Rock Reinforcement and Crane Beam Anchor Testing

The performance of rock reinforcement was tested in relation to the various rock strata where reinforcement will be required.

Of particular importance was establishing anchorage criteria in the weaker rock units. Pull-out tests were conducted on resin and mechanical anchorages using various types of reinforcement bar.

As expected the performance of mechanical anchorages in the weaker rock units was poor. Resin anchorage systems were, in general, highly satisfactory and optimum lengths for various reinforcement loads were determined. Typical results are shown on Figure 10.



KEY

■ MAX TEST LOAD
 R# TEST NUMBER

ROCK REINFORCEMENT TEST RESULTS

Specific tests were carried out on the type of reinforcement proposed for the main halls. It is intended that resin anchored bolts with adequate or continuous (threadbar) nut adjustment will be used. Secondary bonding of the free length after completion of final tensioning will be effected probably using cement grout.

It is intended that the crane beams in the machine and valve halls will be supported by stressed rock anchors, each with a working load of 90 tons. Tests will be carried out to determine the anchorage characteristics of the rock strata in which the anchors will finally be located. A cement grouted anchorage will be used. During the tests each anchor will be fully loaded and unloaded several times and in addition short term creep tests on anchorages of varying length will be carried out.

3.6 Evaluation of PAC (Pneumatically Applied Concrete)

As currently proposed all excavations will be permanently lined with mesh reinforced PAC other than where a placed concrete lining is required for hydraulic or internal structural reasons. The PAC lining will be applied generally in two stages with mesh reinforcement being placed after the initial PAC application. Currently PAC as used in the exploratory contract and preliminary contract works has been evaluated.

PAC spalling has been recorded and the results related to the particular rock strata/bedding weakness. Only limited trials using mesh reinforcement have been carried out. The following conclusions involving the use of PAC for the permanent lining of rock strata such as encountered at Drakensberg are as follows :-

- (1) The rock surface should be sound (controlled blasting and adequate scaling) and inspection immediately prior to PAC application is required
- (2) Specialised PAC mixing and application equipment capable of spraying PAC at a specified distance from the face are required. This implies equipment with considerable nozzle/operator reach for the main halls
- (3) Only trained operatives with adequate experience should be used
- (4) Adequate pinning back of mesh to the first PAC layer to ensure minimal clearance is required.

Since the process of PAC application is highly dependent upon the method used, final trials will be carried out after the main contract award.

4. Machine Hall Test Enlargement

The purpose of the machine hall test enlargement (MHTE) can be summarised as follows :-

- (1) To confirm that the roof span required for the main halls is feasible
- (2) To demonstrate that haunches (required to limit the span) can be effectively excavated and reinforced
- (3) To determine the necessary level of reinforcement for the roof span.

In order to develop a realistic loading condition for the roof span, the effect of sidewall excavation was simulated by excavating slots to a depth equal to about half the final sidewall height. The principal stages of excavation are shown on Figure 11.

The influence of excavation to the full cross-section on the stresses in the roof strata will be determined by a staged stress analysis using both the results of monitoring from the actual test excavation and the results from the in-situ stress measurements and rock mass properties.

The elevation of the MHTE was chosen such that the haunches and roof were positioned in the weakest possible strata (as determined from the drilling from surface) for the 15 m range in possible level for the proposed machine hall. This level was only finally selected in July 1976, based on the required setting for the pump-turbines. The axis of the MHTE is parallel to the proposed machine hall.

The length of the MHTE (approximately 1.5 times the span) was chosen to allow for a central 10 m section which would be relatively unaffected by end constraints.

The excavation sequence for the test enlargement was slightly more complex than that for the proposed machine hall (5 slices instead of 3) because of the need to install crown instrumentation prior to significant rock deformation.

Reinforcement/support was provided by two means :-

- (1) Rock bolts estimated on the basis of precedent and simple numerical analyses
- (2) Temporary hydraulic props along the centreline of the enlargement (5 x 100 ton capacity).

The purpose of the temporary props was to provide a calibrated stiff support along the centreline as well as a temporary support during excavation. Prior to increasing the span at a given stage the props were set to a nominal load (10 ton) and the increase in load with span monitored.

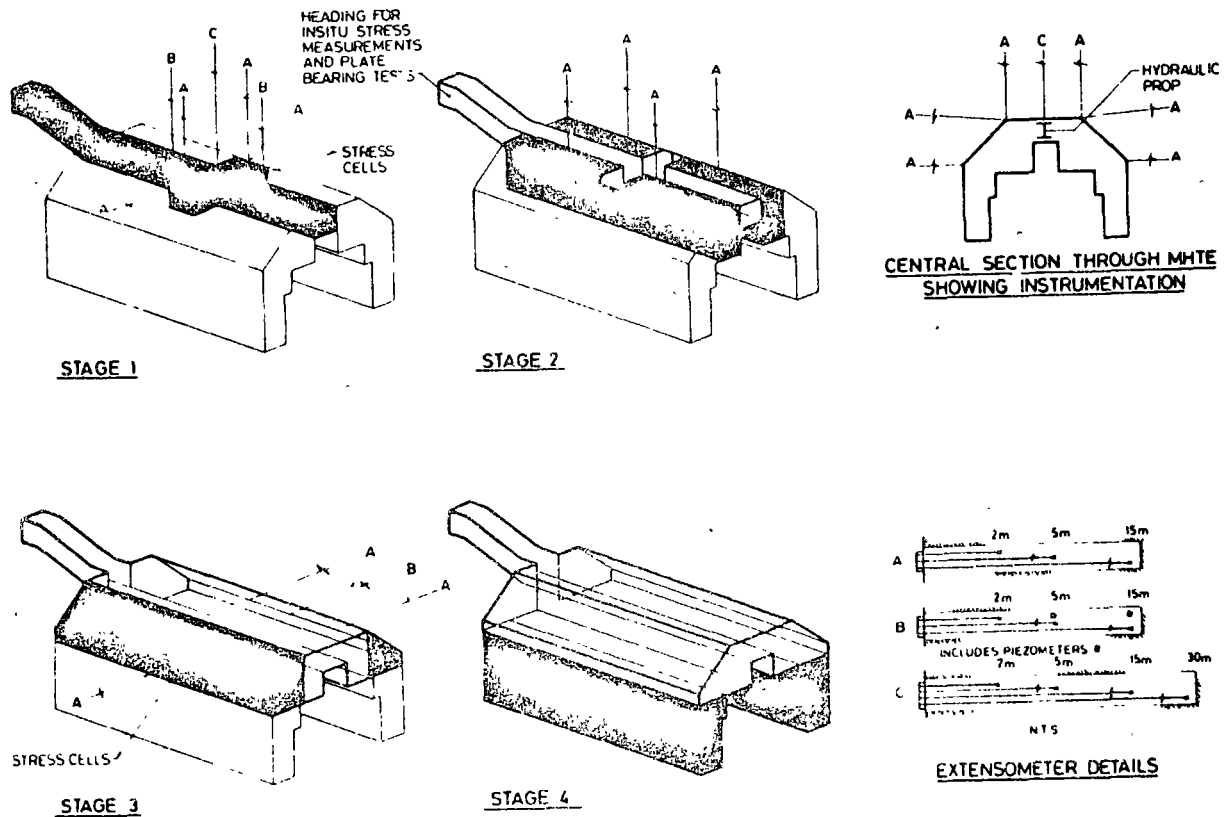


FIGURE 11
MACHINE HALL TEST ENLARGEMENT : STAGE EXCAVATION

The load carried by the props was then distributed to the primary reinforcement as an installed 'calibrated' load and the props subsequently unloaded. It was thus possible to observe potential support requirements under acceptable displacement conditions (as monitored by the extensometers). Unfortunately the excavation of Stage 2 (Figure 11) caused considerable damage to the pillar supporting the props and the stiffness of the pillar was significantly reduced. Following an evaluation of this condition, additional load was placed in the primary reinforcement for safety reasons.

The instrumentation comprised the following types :-

- (1) Displacement monitoring (multi-point rod extensometers, convergence measurements, precise levelling)
- (2) Stress change monitoring (embedded mercury filled stress cells)
- (3) Piezometric monitoring
- (4) Load monitoring in reinforcement and central support jacks.

The instrumentation was primarily located on three sections; a central section and sections spaced 5 m either side. Typical layouts are shown on Figure 11.

Displacement monitoring using the extensometers proved to be reliable except where blasting damage occurred. Typically a resolution of 0,01 mm was achieved and both elastic and irrecoverable deformations were monitored. The monitoring results at each stage were compared with displacement data predicted prior to excavation from finite element analyses.

A typical plot of displacement versus time/ excavation stages is shown on Figure 12. Both closure measurements and precise levelling were an order of magnitude less accurate than the tensometers.

Stresses monitored during the excavation stages were very sensitive to changes in excavation geometry and could be usefully correlated with the displacement records (Figure 12).

Piezometric monitoring in the roof strata indicated relatively high pressures (up to 15 m head) relatively close to the excavation face. These measurements further indicated the low transverse permeability of the siltstones. Consideration of likely loadings due to groundwater pressures on roof strata will be made during the design stage.

Load monitoring in primary reinforcement has yielded few results to date (end Stage 3) as deformations have been small since the reinforcement was installed (Figure 12). Significant load increases (of the order of 40 tons) were observed in some support props during Stage 3 excavation. These load increases occurred where the pillar was relatively undamaged and were used in assessing Stage 3 primary reinforcement loads. At all stages of the development a continual evaluation of displacement, stress and load changes was carried out.

At the time of writing Stage 4 (sidewall) excavation remains to be completed.

Penstock Test Chamber

The penstock test chamber has been constructed to check the suitability of concrete as a lining for the pressure tunnels. The chamber has been located in an area representative of the weaker rock conditions expected along its alignment. Attention was given in the choice of site to locating the chamber in strata having a considerable modulus variation over the height of the chamber.

A principal objective of the test was to determine the relative behaviour of the concrete lining, grouted rock and surrounding rock mass to demonstrate that an effective transfer of stress into the rock will occur under acceptable deformations and leakage.

The chamber was concreted in three bays approximately 10 m long having a finished internal diameter of 5,5 m and a nominal lining thickness of 0,6 m. The three bays are separated by conventional waterstops. Each end of the chamber is terminated by a concrete plug.

The central bay is considered to be representative of tunnel operating conditions and contains all the instrumentation. The instrumentation is arranged on 5 sections as illustrated on Figure 13 with particular emphasis on monitoring the

central section.

The principal instrumentation can be summarised as follows :-

- (1) Diametral changes across the tunnel section monitored by means of internal closure measurements
- (2) Radial deformation of the lining, grouted rock and surrounding rock mass monitored by means of multi-point bore-hole extensometers which are tied in with the diametral closure measurement (1)
- (3) Strains in the lining measured by means of embedded and surface vibrating wire gauges (radial and tangential strains monitored)
- (4) Stresses across the lining/rock interface monitored by means of mercury filled embedded stress cells (radial and tangential stresses monitored)
- (5) Water pressures behind the lining and in the surrounding rock mass monitored by means of hydraulic piezometers.

Remote read-out of instrumentation under high fluid pressures (up to 7,5 MPa) necessitated special developments particularly of remote sensing elements. Temperatures are monitored at various points in the test zone and invar rods/wires are used for reference displacement monitoring. Stress cells are designed to allow for compensation from within the chamber.

As previously discussed a series of plate bearing tests was carried out to determine radial modulus conditions within the rock mass as well as the effect of grouting.

High pressure grouting behind the chamber lining will be monitored by means of the installed instrumentation. Particular attention will be paid to uniformity of deformations and stresses indicating that a complete grout ring has been established. Residual stresses induced in the lining will be carefully monitored.

The chamber pressurization programme has not yet been finalised. It is intended however to pressurize in stages and carry out tests at constant pressure as well as under cyclic conditions.

A theoretical study of likely deformations/stresses will be finalised prior to commencement of testing. The test chamber is located at a shallower depth than the proposed pressure tunnel alignments. It will thus be a valid acceptance test from overall pressure/rock cover considerations.

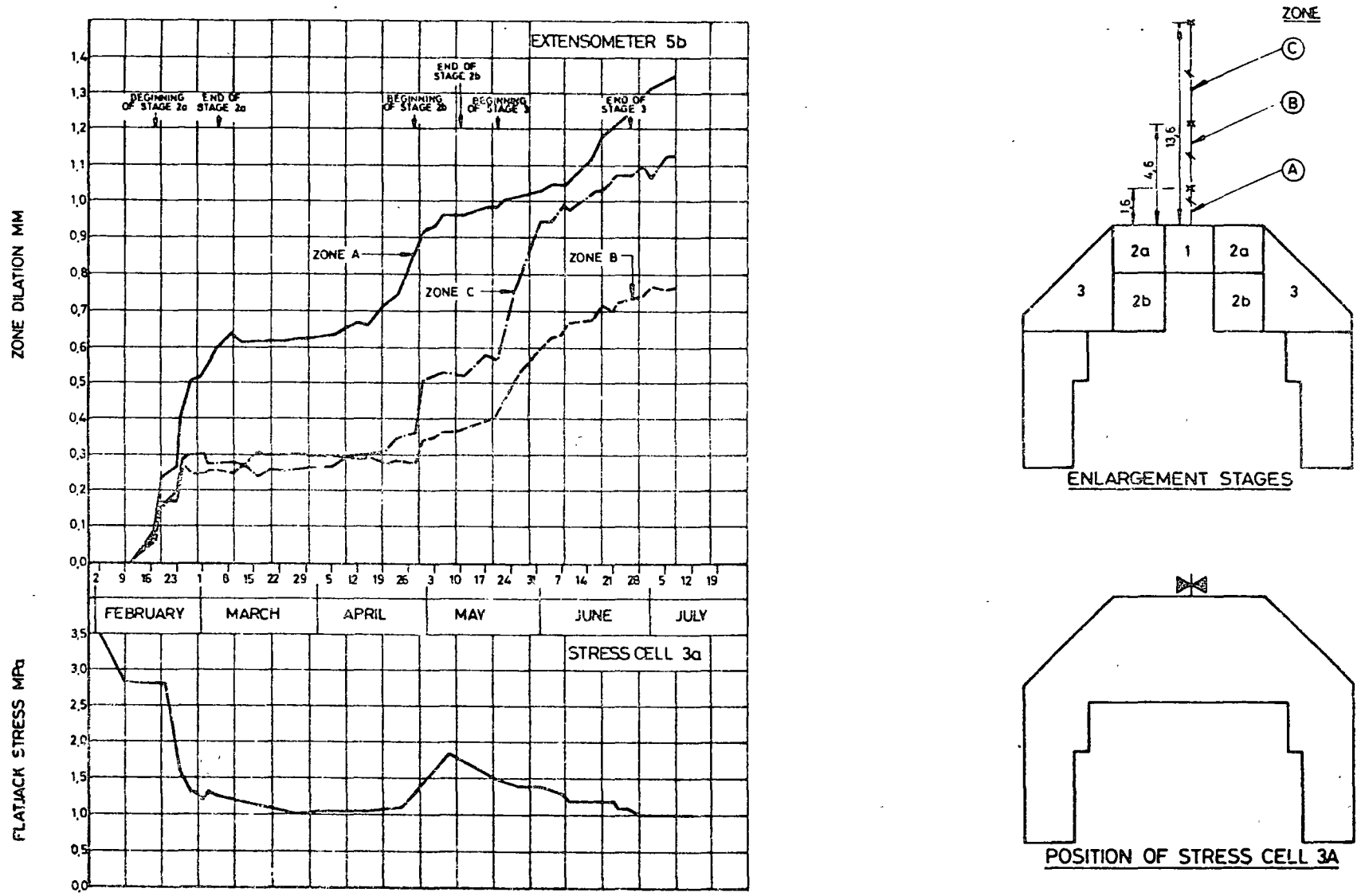
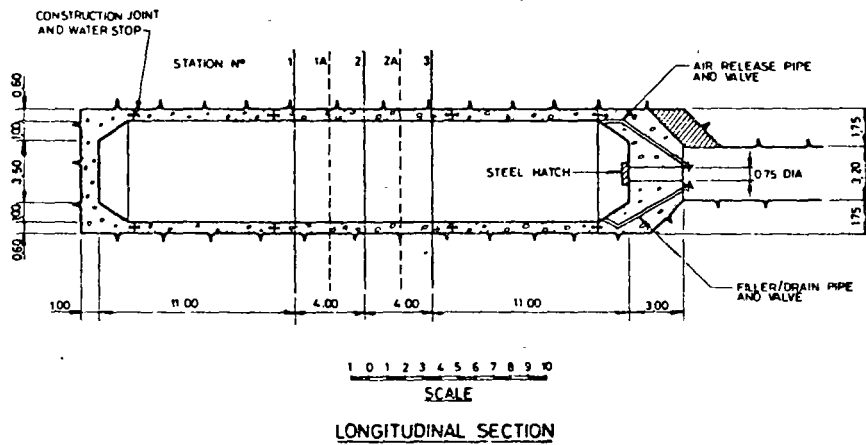


FIGURE 12
TYPICAL ROOF DISPLACEMENT AND STRESS CHANGE CHARACTERISTICS - MACHINE HALL TEST ENLARGEMENT



LEGEND

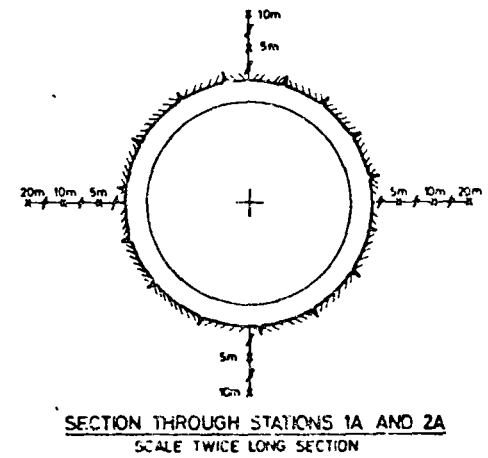
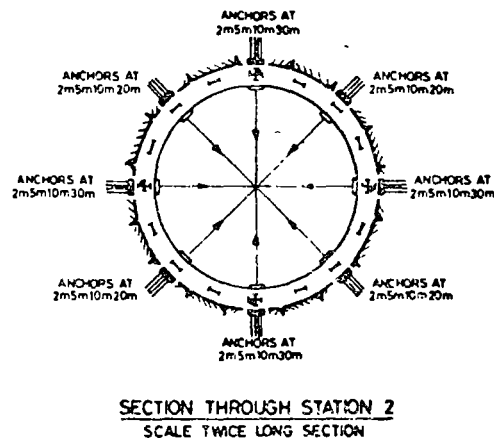
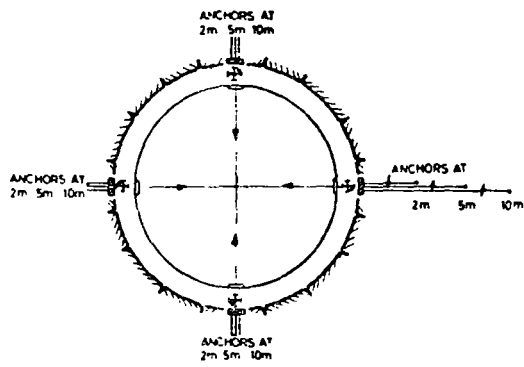
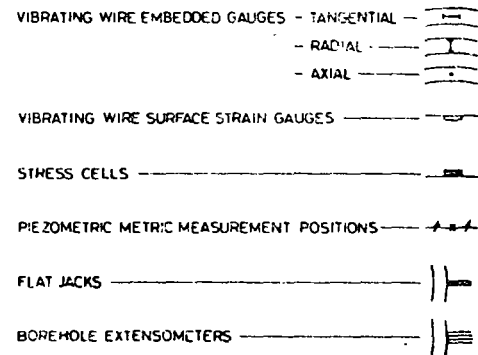


FIGURE 13
 PENSTOCK TEST CHAMBER



FIGURE 14
PENSTOCK TEST CHAMBER - EXCAVATION OF UPPER BENCH

6. Proposed Design Studies

The design process for the excavation and reinforcement requirements of the main underground works was initially considered during the formulation of the investigation and testing programme which was consequently arranged to provide relevant parameters for the design requirements.

As already outlined, considerable attention has been paid to testing rock conditions at a representative scale. Both the machine hall test enlargement and penstock test chamber are full scale tests. The information obtained from the investigation and testing stages will be used primarily to extrapolate observed underground conditions to the overall station layout using recognised stress analyses techniques and a structural evaluation of the rock mass. Optimisation of the detailed underground layout and rock reinforcement with respect to localised geological conditions will then be carried out.

Principal design aspects are as follows :-

- (1) Excavation method to achieve specified profiles
- (2) Shape and precise elevation of major roof spans taking into account predominant bedding features, haunch geometry and geology
- (3) Reinforcement of major roof spans including haunches
- (4) Reinforcement of sidewalls
- (5) Excavation sequence for main halls
- (6) Excavation sequence, shape and reinforcement of major intersections

- (7) Reinforcement of minor galleries and tunnels in the vicinity of the main works
- (8) Excavation sequence, shape and reinforcement of surge chambers
- (9) Penstock linings (both steel and concrete)
- (10) Drainage of the rock mass in the vicinity of the penstocks and upstream wall of the valve hall
- (11) Rock reinforcement details (inclination, timing, installation, tensioning, secondary grouting, corrosion protection)
- (12) Crane beam anchors (installation, tensioning, grouting, corrosion protection)
- (13) PAC and mesh reinforced PAC.

Principal methods of analysis are as follows :-

- (1) Two and three dimensional stress and deformation analyses (finite element and boundary integral equation methods)
- (2) Kinematic check of prevailing geological structure to identify potential failure modes caused by movement of blocks of rock
- (3) Analysis of structurally controlled failures taking into account rock stresses and reinforcement loadings (production of detailed reinforcement requirements and likely rock deformations).

A final design will be evolved from the results of the full scale tests, an evaluation of the rock mass characteristics and an analysis of the final station layout in terms of the measured parameters.

The inter-relationship of investigation, testing, analysis and design for the underground works at Drakensberg is summarised on Table II.

TABLE II
INTERRELATIONSHIP OF INVESTIGATION - TESTING - ANALYSIS - DESIGN

KEY ○ - MINOR INFLUENCE ⊙ - MAJOR INFLUENCE	GEOLOGY GROUNDWATER		SAMPLE TESTING					IN SITU TESTING					FULL SCALE TESTS		ANALYSIS				
	GEOLOGICAL INVESTIGATIONS	PERMEABILITY MEASUREMENTS	LOW PRESSURE MEASUREMENTS	POINT LOAD INDEX TEST	UNIAxIAL COMPRESSIVE STRENGTH TESTS	MODULUS DETERMINATION	SHEAR TESTING	DURABILITY TESTING	INSITU STRESS MEASUREMENTS	ROCK MASS MODULUS FLAKE BEARING TEST	ROCK MASS MODULUS BOREHOLE JACKING TEST	ROCK REINFORCEMENT TESTING	CRANE KAIL ANCHOR TESTS	PAC EVALUATION	MACHINE HALL TEST ENLARGEMENT	PENSTOCK TEST CHAMBER	STRESS/DEFORMATION ANALYSIS	KINEMATIC CHECK	STABILITY ANALYSES REINFORCEMENT DESIGN
DESIGN																			
EXCAVATION METHOD/PROFILE	○							○						○	⊙				
SHAPE/ELEVATION MAJOR ROOF SPANS	⊙			○	○	○	○		⊙	⊙	○			⊙			⊙	⊙	⊙
REINFORCEMENT MAJOR ROOF SPANS AND HAUNCHES	⊙	○	○	○	○	○	○		⊙	⊙	○	⊙	○	⊙	⊙		⊙	⊙	⊙
REINFORCEMENT OF SIDEWALLS	⊙	○	○	○	○	○	○		⊙	⊙	○	⊙	○	⊙	⊙		⊙	⊙	⊙
EXCAVATION SEQUENCE FOR MAIN HALLS	⊙							○	○	○	⊙	○	⊙	⊙	⊙		⊙	○	⊙
EXCAVATION SEQUENCE SHAPE AND REINFORCEMENT INTERSECTIONS	⊙			○	○	○	○		⊙	⊙			⊙	⊙			⊙	⊙	⊙
REINFORCEMENT OF TUNNELS IN VICINITY OF MAIN WORKS	⊙	○	○	⊙	○	○	○	○											
EXCAVATION SEQUENCE SHAPE AND REINFORCEMENT SURGE CHAMBERS	⊙		○	○	○	○	○	⊙	⊙	○	⊙		○	○			○	⊙	⊙
PENSTOCK LININGS	⊙	⊙	⊙	⊙	○	○	○	○	⊙	⊙	○		○		⊙	○	○	○	○
DRAINAGE OF PENSTOCK AND UPSTREAM WALLS OF HALLS	⊙	⊙	⊙					○	○				○	○	⊙	○			
ROCK REINFORCEMENT DETAILS	⊙					○	○	○		○	⊙		○	⊙	○				
CRANE BEAM ANCHORS	⊙					○	○	○			○	⊙							
PAC AND MESH REINFORCED PAC	⊙		⊙	○		○	⊙	○	○	○	○		○	⊙	○				

CONCLUSIONS

The determination of rock mass properties at Drakensberg in relation to the design of underground excavations has been reviewed. The investigation methods and testing techniques have been outlined and the reasons for their selection given.

The particular role of full scale testing has been highlighted. The relevance of testing at other scales, both in-situ and on a sample scale, has also been discussed in relation to the final design process.

The current status of the investigation/testing works precludes the reporting of detailed results at this stage. A full evaluation of all data is expected by early in 1977.

ACKNOWLEDGEMENTS

The authors wish to thank the Electricity Supply Commission for permission to publish this paper and Gibb Hawkins and Partners and Golder Associates for the material which has been used in its preparation. They also wish to acknowledge the extensive contribution of their many colleagues whose work is reported here.

REFERENCES

- SECRETARY FOR WATER AFFAIRS (1974-1975) Report on the Proposed Second Phase of the Tugela-Vaal Government Water Project with the Drakensberg Pumped Storage Scheme Development.
- BIENIAWSKI, Z.T. (1973) Engineering classification of jointed rock masses. Trans. S.Afr. Instn. Civil Engrs, vol. 15, no. 12, December 1973, pp 335-344.
- BARTON, N; LIEN, R; LUNDE, J. (1974) Analysis of rock mass quality and support practice in tunnelling and a guide for estimating support requirements. Norwegian geotechnical institute internal report 54206.
- ENDERSBEE, L.A. and HOFTO, E.O. Civil engineering design and studies in rock mechanics for Poatina underground power station, Tasmania. J. Australian Inst. Engrs. vol. 35, September 1963, pp 187-206
- HOCKING, G; BROWN, E.T; WATSON, J.O. (1976) Three dimensional elastic stress analysis of underground openings by the boundary integral equation method, 3rd Symposium on Engineering Applications of Solid mechanics, Toronto, June 1976.

STRUCTURALLY CONTROLLED INSTABILITY IN UNDERGROUND EXCAVATIONS

by

Dr Evert Hoek, Principal,
Golder Associates Ltd.,
224 W 8th Avenue,
Vancouver, BC., Canada.

ABSTRACT

Structurally controlled instability is one of the major factors to be considered in relation to the design of underground excavations in hard, jointed rock masses. This instability may take the form of gravity falls of wedges or blocks from the roof of the excavation or the sliding along planes or lines of intersection of planes in the roof and sidewalls.

This paper describes a number of simple checks for falling or sliding using stereographic plots of structural data obtained from borehole core or pilot tunnel mapping. These simple kinematic checks are used to identify problem areas which can then be analysed in greater detail using stereographic techniques or computerised vector analyses. The dimensions and hence the weight of each block or wedge which can fall or slide can be calculated and a reinforcing system can then be designed to prevent instability.

These considerations lead to a number of general conclusions on the optimum orientation of underground excavations in relation to the structure of the rock mass in which they are located. The sequence of excavation is also important, particularly when large spans or the intersections between large excavations are being created, and the timely installation of reinforcing elements to prevent the development of instability at each excavation stage is discussed.

INTRODUCTION

An example of the role of structural discontinuities in controlling the stability of an underground excavation is illustrated in figure 1 which shows a tunnel in a slate quarry in the United Kingdom. This tunnel was constructed approximately 100 years ago without any form of rock support or reinforcement and the tunnel shape has stabilised to conform with the structural pattern in the rock mass.

In most modern rock excavations, close control of the excavation profile is required and the degree of over-break apparent in figure 1 is unacceptable. Consequently, potentially unstable blocks or wedges must be identified and dealt with, either by adjustments to the excavation location or profile or by reinforcement or support of the rock mass.

The basic information required for an evaluation of the structural stability of an excavation is the orientation, inclination, spacing and characteristics of discontinuities such as faults, joints and bedding planes in the rock mass. This information can be obtained from oriented diamond drill core or from the mapping of surface outcrops or pilot tunnels. The data are most conveniently assembled and presented



Figure 1 : A tunnel in slate showing the influence of structural discontinuities upon excavation stability.

on plotting grids prepared by spherical projection. Space does not permit a full discussion on these techniques and the reader is referred to comprehensive descriptions by Phillips (1971), Goodman (1976) and Hoek and Bray (1977).

Throughout this paper, the stereographic or equal angle projection is used for the presentation and analysis of structural data. This projection has been chosen in preference to the equal area projection because it affords a more convenient means for constructing the intersection figures required for stability analyses.

KINEMATIC CHECKS

Two simple kinematic checks for falling or sliding wedges are illustrated in figure 2.

Gravity falls from the excavation roof can occur when the apex A of a wedge of rock falls within the base B-C, as illustrated in the left hand sketch in figure 2a. Stereographically, this condition is satisfied if the centre of the stereonet falls within the closed figure formed by the intersection of at least three great circles representing discontinuities in the rock mass.

Sliding of wedges in the excavation roof can occur when the apex A falls outside the base B-C provided that at least one of the planes bounding the wedge dips at a steeper angle than the angle of friction. Figure 2b shows that this condition is satisfied when one of the three great circles representing the planes touches or falls within the dashed circle defined by the angle of friction ϕ . The same kinematic check applies to the sliding of wedges from the excavation sidewalls.

In regularly jointed rock masses, 'mirror-image' wedges occur in the floor and opposite sidewall as illustrated by the vertically hatched areas in figure 2b. Sliding of mirror-image sidewall wedges can occur if the stereonet centre falls within the intersection figure as illustrated in figure 2a.

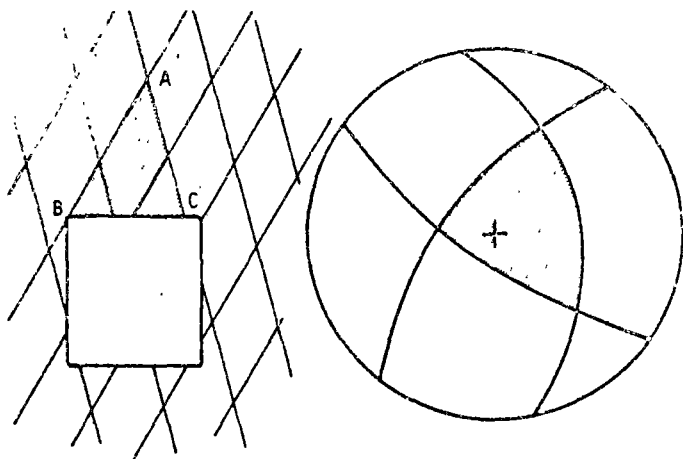


Figure 2a : Kinematic check for gravity falls from the roof of an excavation .

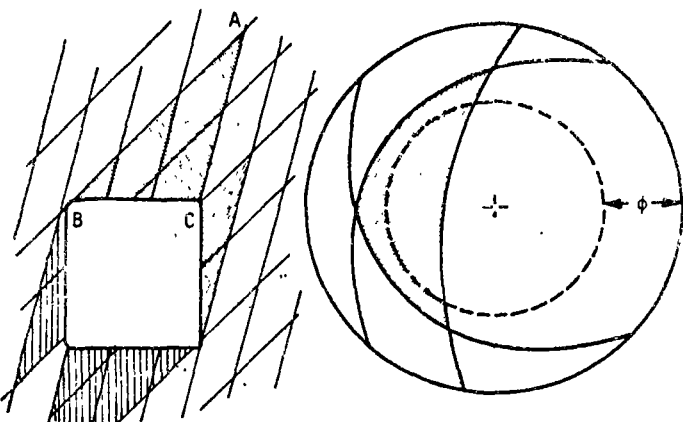


Figure 2b : Kinematic check for the sliding of wedges from the roof or sidewalls of an excavation.

The kinematic checks illustrated in figure 2 can be used during the preliminary evaluation of structural data obtained from core logging or exploratory tunnel mapping. They will give an indication of problem areas which can then be investigated in greater detail. The kinematic checks give no information on the possible size of falling or sliding wedges and, since this information is required for the design of support systems, a more detailed form of analysis is necessary. This analysis is described below.

DETAILED WEDGE ANALYSIS

Figure 3 gives the constructions required to find the maximum size of wedges which can fall or slide from the roof or sidewalls of a square tunnel running due east-west.

A lower hemisphere stereographic projection of three planes is given in figure 3a. These planes are represented by the three great circles marked A, B and C. The strike lines, marked a, b and c, are plotted as are the lines of intersection ab , ac , bc .

Since the lower hemisphere projection has been used, it is convenient to view the wedge in the roof of the excavation in the same direction, i.e. from the apex to the base of from the interior of the rock mass into the tunnel. A plan view of the wedge is given in figure 3b and the construction of this view is carried out as follows :

The strike lines a, b and c in the stereographic projection are equivalent to traces of the discontinuity planes in the horizontal tunnel roof and the directions of these traces can be determined directly from the strike lines. Starting at the northern sidewall, the trace a is drawn across the full span of the tunnel, parallel to the strike line a. From the intersection of the trace with the northern sidewall, the trace b is drawn parallel to the strike line b and, similarly, the trace c is drawn from the intersection of trace a and the southern sidewall. The intersection of traces b and c determines the plan shape of the largest wedge which can form for this particular combination of discontinuities in this tunnel.

In order to find the position of the apex of the wedge, draw the lines of intersection from the corners of the plan view of the wedge, parallel to the lines of intersection ab , ac and bc in the stereographic projection. The vertical height h_p of the wedge is found by taking a section through the apex of the wedge, parallel to the tunnel alignment. The apparent dips α and ξ of the traces of the planes in the vertical plane running parallel to the tunnel axis, due east-west, are used to define the height of the wedge as shown. The volume of the wedge is given by the product of the base area of the true plan view and one third of the height h_p .

Construction of the sidewall wedge shown in figure 3c is slightly more complicated as apparent dips α , β and ξ have to be used to define the intersection figure in the sidewall and because projected views of the lines of intersection are required to locate the apex of the wedge.

Starting at the roof of the tunnel, the traces a' and a'' are drawn at the apparent dip angles α and ξ , determined from the stereographic projection. From the intersection of the trace a'' and

CRITERIA ANALYSIS OF UNDERGROUND WEDGES

In spite of the apparent complexity of the construction given in figure 3, the example considered is possibly one of the simplest which could occur. In many real situations the underground excavation designer may be faced with five or six strongly developed sets of discontinuities intersecting an inclined tunnel with a curved roof profile. The stereographic analysis of potential instability in such cases can become so complex and tedious that even the most enthusiastic structural geologist would soon become discouraged. The most difficult problem of all occurs at the intersection of two underground tunnels when additional free faces are created and rock stability has to be considered very carefully.

In order to overcome these problems, Golder Associates has developed a set of computer programs which are used for the design of major underground excavations in hard jointed rock masses. These programs can be used for initial kinematic checks or for complete stability analyses of specific geological features. For example, from detailed geological maps of a pilot tunnel, structural features can be projected onto the final excavation profile and wedges which can fall or slide identified. With such advance warning, the installation of reinforcement at each excavation stage can be designed to provide complete support for the roof and sidewalls of the final excavation.

INFLUENCE OF IN SITU STRESS

When the height h_r or h_b of a wedge is less than the span of the excavation or the height of the sidewall, it is unlikely that the stability of the wedge could be influenced significantly by the in situ stress in the rock mass. However, when the apex angle of the wedge becomes acute, the normal stresses acting across the potential failure planes should be considered in the stability analysis.

Consider the extreme example of the sliding of a block between two parallel discontinuities as illustrated in figure 5. The condition of limiting equilibrium for the block of rock of weight W can be written as :

$$\sigma_n = \frac{W}{2h_b} \left(\frac{\sin \xi}{\tan \phi} - \cos \xi \right)$$

where σ_n is the average normal stress acting across the discontinuities and

ϕ is the angle of friction of the discontinuity surfaces.

When the average normal stress σ_n is less than the right hand side of the equation, the block will be unstable and reinforcement would have to be provided in order to restore its stability. If the average normal stress is higher than the right hand side of the equation, the amount of reinforcement can be reduced or eliminated, depending upon the factor of safety which is required.

The magnitude of the average normal stress σ_n has to be computed from the measured in situ stress field and the stress redistribution associated with the creation of the excavation. If this stress is to be relied upon to provide support, care should be taken to check that this stress could not be reduced by the creation of other excavations close to that being considered.

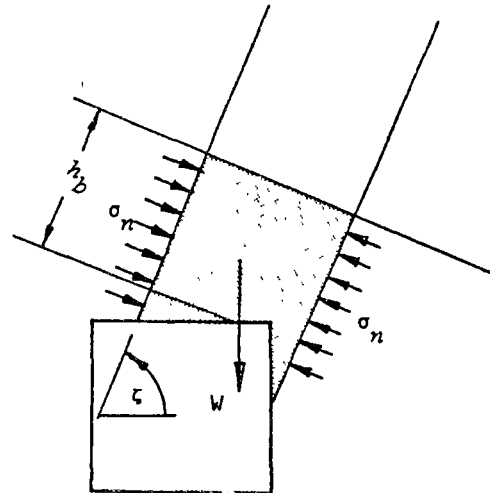


Figure 5 : Influence of in situ stress on the stability of a block in the roof of an excavation.

ORIENTATION OF UNDERGROUND EXCAVATIONS

When the designer has a choice of the orientation of an underground excavation, consideration should be given to the selection of this orientation to give the smallest number of roof and sidewall instability problems. When only one major discontinuity, such as a fault, is present in the rock mass, the optimum orientation is obtained by placing the smallest plan dimension of the excavation parallel to the strike of the discontinuity. In the case of a tunnel, this means that the tunnel should be aligned normal to the strike of the discontinuity.

When several sets of discontinuities are present in the rock mass, the choice becomes rather more difficult. One obvious orientation to avoid is to align a tunnel parallel to the line of intersection of two important discontinuities as shown in figure 6. However, this may be only one of many possible forms of instability in a heavily jointed rock mass and it may be necessary to conduct a sensitivity study on the structural data in order to arrive at an optimum orientation.

SEQUENCE OF EXCAVATION AND SUPPORT INSTALLATION

It will be obvious from the examples considered in this paper that the dimensions of wedges which can form in the roof and sidewalls of excavations depend upon the span of the roof and the height of the sidewall. If such potential wedges have been recognised at an early stage of excavation, the subsequent excavation sequence can be designed to permit the sequential installation of reinforcing bolts or cables. Hence, the pilot tunnel can be used as access for the installation of the first reinforcement which should have sufficient capacity to support any blocks or wedges which would be unstable at the next excavation stage. Once the next stage has been excavated, additional reinforcing can be installed to secure the exposed faces and to provide support for subsequent stages.

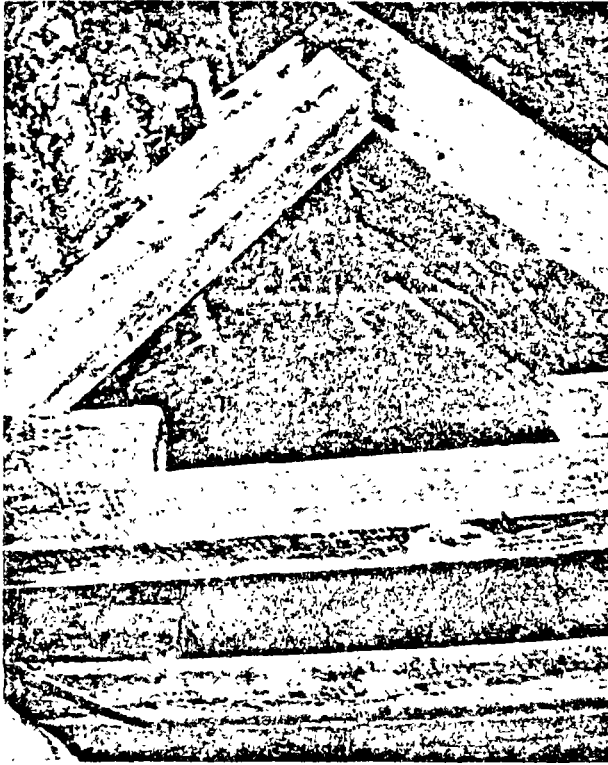


Figure 6 : "Cathedral" failure in the roof of a tunnel aligned parallel to the line of intersection of two well developed discontinuities.

3. Phillips, F.C. *The use of Stereographic Projection in Structural Geology*. Edward Arnold, London, Third edition 1971, 89 pages.

CONCLUSION

In most publications dealing with the design of underground excavations, the emphasis is usually placed on instability due to stress in the rock mass. While stress-induced instability is important, it is not the only form of instability which must be considered and the treatment of structurally controlled stability problems has been reviewed in this paper. Early recognition of potential instability caused by the intersection of discontinuities in the rock mass is important if effective remedial measures are to be designed. Simple kinematics checks can be used to identify potential problem areas.

Where wedges of significant size are likely to be exposed in the roof or sidewalls of an excavation, determination of the size and weight of these wedges is necessary in order that the length, capacity and direction of reinforcing bolts or cables can be established. Such detailed analyses can be carried out with the aid of the stereographic projection method outlined in this paper or by a computer analysis of the interaction of the excavation shapes and the structural discontinuities in the rock mass.

REFERENCES

1. Goodman, R.E. *Methods of Geological Engineering in Discontinuous Rocks*. West Publishing Company, St. Paul, 1976, 472 pages.
2. Hoek, E. and Bray, J.W. *Rock Slope Engineering*. Revised Second Edition, The Institution of Mining and Metallurgy, London, 1977, 402 pages.



INTERNATIONAL ROAD FEDERATION
FEDERATION ROUTIERE INTERNATIONALE
国际道路联盟

VIIIth IRF WORLD MEETING



DESIGN, CONSTRUCTION AND MAINTEN- ANCE OF ROCK SLOPES ON HIGHWAY PROJECTS

C. O. Brawner
Principal Partner, Golder Associates Ltd
Evert Hoek
Principal Partner, Golder Associates Ltd

Canada

1977 October 16-21, Tokyo, Japan
16-21 Octobre, Tokyo, Japon

DESIGN, CONSTRUCTION AND MAINTENANCE OF ROCK SLOPES ON HIGHWAY PROJECTS

C. O. Brawner
Principal Partner, Golder Associates Ltd
Evert Hoek
Principal Partner, Golder Associates Ltd

Canada

The most important factors which contribute to the instability of rock slopes on highway projects are:

- (a) Adverse geological discontinuities in the rock mass in which the slope is cut.
- (b) High ground water pressures in the rock mass.
- (c) Damage to the rock mass caused by blasting.

The design of a rock slope depends upon the early recognition and interpretation of these factors. The paper describes the techniques which may be used in both the feasibility and the final design stages of highway projects. The use of air photographs, field mapping and diamond drilling in geological interpretation is considered together with field and laboratory tests to determine rock strength and ground water parameters required for stability analyses.

Emphasis is placed on the design of blasting patterns for the excavation of rock slopes to minimize damage to the rock mass behind the slope face.

Even when the factors listed above have been recognized and incorporated into a slope design, it may be impossible or uneconomic to design a stable slope which depends only upon the strength of the rock mass. In such situations, remedial measures must be considered and these include the provision of drainage to relieve ground water pressures, the use of anchored cables or bolts which apply restraining forces to critical portions of the rock mass and the application of surface layers to protect the exposed rock mass against deterioration caused by moisture and temperature changes.

HIGHWAY SITE SELECTION

The primary consideration in siting a highway is the location of population or industry centres to be served by that highway. Once the overall route has been established there is usually a considerable amount of flexibility in the detailed route to be followed from one centre to the next and it is in the selection of this detailed routing that geotechnical considerations can be of major importance.

An examination of air photographs of potential highway routes by a trained observer will establish the location of such features as old landslides which should be avoided, if at all possible, in routing the new highway. Detailed regional geological maps exist for many parts of the world and these will usually indicate the broad range of rock types and structural geological features which would be encountered on a particular route. Full use should be made of such maps and an engineering geologist would normally be able to identify general areas where potential slope stability problems could exist and which should be avoided if possible.

Having established two or three possible routes on the basis of air photography examination and a consideration of the regional geology of the area, field surveys of these potential routes are then required. Initially, these surveys can be carried out by engineering geologists or geologists with a sound understanding of rock and soil slope behaviour and the survey results can be presented in general descriptive terms. Features which should be noted are:

- (a) Steep-sided valleys in hard jointed rock where formation of a highway cutting could induce instability higher up the slope.
- (b) Areas where existing instability has been noted from air photograph examination or where such instability is evident from the ground.
- (c) The general surface water flow characteristics of the

area and particularly any seeps or springs which could indicate sub-surface water flow which will have an adverse influence upon stability.

(d) The presence of clays, particularly active clays such as montmorillonites, in joint fillings and in slope debris. These materials have very low strength characteristics and will generally indicate the need for careful consideration of slope stability conditions.

(e) The presence of material such as shales, mudstones and claystones which are prone to deteriorate when exposed to the atmosphere and which require special treatment in slopes.

(f) The presence of faults or of particularly well developed jointing which could play a dominant role in slope behaviour.

The final choice of the highway route can generally be made on completion of these field surveys and it is evident that, other factors permitting, the route with the smallest number of potential slope problems should be chosen. In hilly or mountainous regions, the optimum route may still include a number of potentially unstable rock slopes. The remainder of this paper is devoted to the detection, analysis, and treatment of such slopes.

COMMON TYPES OF SLOPE FAILURE

Several common types of slope instability are illustrated in Figure 1 and each of these failure types is discussed briefly below.

(a) Circular failure occurs in soils and soft rocks and also in rock masses which have been very heavily disturbed by glacial or tectonic activity. The failure surface is approximately hemi-spherical in shape and movement is characterized by a slumping of the crest of the slope and a bulging of the toe of the slope. Where ground water is present in the slope, the failure can occur quite suddenly and the failed material can move a considerable horizontal distance from its original position. Under certain extreme conditions, the failure can take the form of a flow slide which has many of the characteristics of an avalanche and can move large distances at high speeds.

Many large landslides have the overall appearance of circular failures although, in many cases, portions of the failure surface will follow pre-existing weakness planes such as faults or bedding surfaces.

(b) Plane failures occur in slopes cut in rock masses with very strongly developed structural features such as faults, bedding planes and joints. When one of these structural features, which is very much weaker than the intact rock material, is exposed in the face of the cut slope and is inclined at an angle greater than about 30° into the cutting, sliding can occur on this plane. Shear tests on the weak material can be performed to determine the approximate critical angle for stability.

(c) Wedge failures are a more complex form of rock slope failure in rock masses with strongly developed structural features. In this case sliding takes place along the line of intersection to two discontinuity surfaces. Figure 2 illustrates a wedge failure in a rock slope.

(d) Toppling failure can occur in slopes in which steeply dipping discontinuities separate the rock mass into a series of columns. This type of failure has only been described in geotechnical literature in the past decade. The authors have found that it is a surprisingly common failure mode. Recognition of potential toppling conditions in a rock mass is important if effective remedial measures are to be applied to a slope cut in this rock.

(e) Ravelling of heavily jointed rock is generally a

gradual process which occurs as a result of gradual weathering of weak portions of the rock mass or because of freeze/thaw conditions in cold wet climates.

(f) Weak seams of shale or mudstone tend to weather more rapidly than surrounding rocks such as sandstone and this can give rise to undercutting of blocks of the harder overlying rocks as illustrated in Figure 1f. Recognition of this potential weathering problem is important since freshly exposed shale or mudstone may appear to be good sound rock and the instability due to undercutting

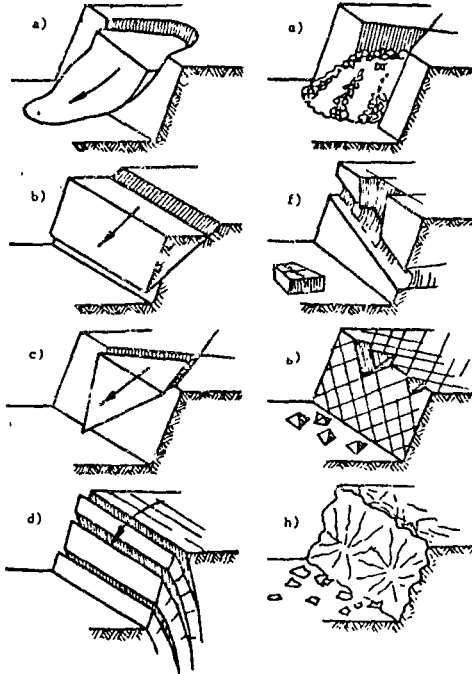


Figure 1: Common types of rock slope instability.

- a) Circular failure in soils and very disturbed and altered rock.
- b) Plane failure on through-going planar discontinuities.
- c) Wedge failure along the line of intersection of two discontinuities.
- d) Toppling failure in steep slopes in rock with steeply dipping discontinuities.
- e) Raveling of heavily jointed and disturbed rock.
- f) Undercutting of blocks on slope due to weathering of weak seams.
- g) Rockfalls from heavily jointed rock masses.
- h) Rockfalls from slope faces damaged by heavy blasting.



Figure 2: Wedge failure in a hard rock slope involving sliding along the line of intersection of two discontinuity planes.

may take several years to develop.

(g) Rockfalls from heavily jointed rock masses are akin to the raveling process discussed in (e) above. Freeze-thaw conditions and deterioration of joint in-filling materials can result in individual blocks becoming detached and falling with very little warning. Scaling of loose blocks can be an effective remedial measure.

(h) Slope instability induced by excessively heavy blasting is a man-made problem brought about by an inadequate understanding of the process of rock fragmentation resulting from the detonation of a contained explosive charge. Figures 3 and 4 illustrate two extreme cases of this fragmentation. In the rock slope shown in Figure 3, serious fractures have been induced by very heavy blasting and it will be noted that these fractures follow a random curving pattern, ignoring the natural fracture planes in the rock mass. On the other hand, Figure 4 shows a rock face created by controlled blasting techniques and it will be seen that there are no loose unstable pieces in this face. The amount of explosives used in the closely spaced holes should be the minimum required to develop the tension crack which will form the final slope face. Favourable results in average rock will usually be obtained with the use of about 0.7 Kg of explosive per square meter of rock face.



Figure 3: Damage to a rock face by excessively heavy blasting giving rise to rockfall instability.

Figure 4: Clean stable rock face created by pre-split blasting techniques.

SITE INVESTIGATION FOR ROCK SLOPE DESIGN

If preliminary field surveys have established that one or more of the failure modes illustrated in Figure 1 are likely to be encountered along a chosen highway route, detailed investigations of areas of potential instability are required to establish the seriousness of the problem and to provide the basis for the design of remedial measures. These site investigations should include geological mapping of structural features in rock outcrops, detailed logging of diamond drill core to detect variations in rock strength conditions and to determine attitude of structural features in the rock mass, rock strength tests, particularly of weakness planes and clay-filled discontinuities, and the observation of ground water conditions. These latter observations, involving the installation of piezometers in diamond drilled boreholes, are very important since the presence of water in a rock slope is always detrimental to stability and the reduction of water pressure by drainage is one of the most effective and economical remedial measures.

A detailed discussion on site investigation techniques exceeds the scope of this paper and the reader is referred to the text book by Hoek and Bray¹ which describes the techniques which should be used and the interpretation of the results of the investigations described above. These investigations and the subsequent interpretation and analysis of results should always be carried out by an engineering geologist or geotechnical engineer since serious and expensive errors can be made if the information is misinterpreted by someone lacking adequate training or experience.

ANALYSES AND DESIGN

Hoek and Bray¹ have reviewed the graphical and mathematical techniques which are available for the analysis of the failure types illustrated in Figures 1a to d. They

have also discussed the influence of blasting on the stability of rock slopes (Figure 1h). See also *The Modern Techniques of Rock Blasting* by Langefors and Kihlstrom². Most of these techniques are relatively simple and have been found, from experience in many practical applications, to give a reliable basis for the design of rock slopes.

No analytical techniques are available for the types of failure illustrated in Figures 1e to g and the successful design of slopes in which these problems occur depends upon experience and an awareness of the range of remedial measures which are available for dealing with these failure processes.

Normal rock excavation practice has generally been to specify that new slopes in rock be cut to 1/4 to 1 and that shallow, 'V' type ditches be used. These slopes were not designed according to the strength or quality of the rock. With the knowledge that now exists in rock mechanics, the stable slope angle can be determined with reasonable success and at reasonable cost.

Where the rock strength or where the geologic structure is favourable, rock cuts should be designed and constructed with vertical slopes (Figure 5). This will re-

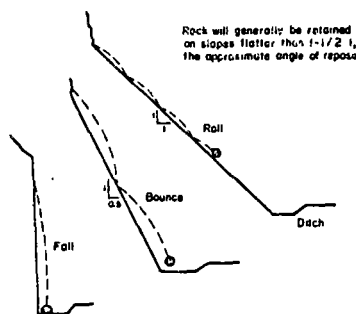


Figure 5: Provided the rock strength and geologic structure is favourable, vertical slopes should be considered using controlled blasting. (Drawing modified from Ritchie³).

duce quantities, allow wider ditches to be used and result in rockfalls dropping vertically into the inner ditch instead of bouncing or rolling onto the highway (Brawner⁴).

Where geologic structural weaknesses dip out of the slope at a steep angle the slope should be excavated to this angle (Brawner⁵).

Controlled blasting using pre-split or cushion blasting should be specified for the excavation of all rock slopes where the geologic structure is oriented favourably for stability. The rock in the slope will be subjected to less damage due to seismic acceleration forces which, if large, can break rock and open joints for tens of feet back from the slope face. With controlled blasting, slopes can be excavated steeper and the slopes will ravel less, requiring much less maintenance over the years.

The design must specify the magnitude of the blasting in the main area of any cut be kept to a reasonable minimum by the use of delays. Normally not more than 500 pounds of explosive per delay should be detonated at one time.

MAINTENANCE

More problems generally exist with stability of rock slopes that were constructed decades ago rather than on recent construction. This is generally a result of hazardous construction procedures that have been used in the past.

The most important maintenance techniques that are effective are summarized in the following text.

(a) Scaling the Rock Face.

Where the rock is jointed with random orientation or a limited number of blocks appear to be unstable these blocks can be removed by scaling. A geologic appraisal is recommended to locate rocks that require scaling. Scaling is normally not recommended where very blocky rock exists or where the rock dips out of the slope. Scaling can be performed using hand or hydraulic tools. If explosives are used, care must be taken to ensure vibration does not

loosen more rocks than planned.

(b) Flattening the Slope.

Where excessive rockfalls occur or where the joints or bedding dips out of the slope, the slope can be flattened. A uniform slope may be used or the cut can be benched. The bench should be wide enough to clean since falling rock from above may bounce from a debris filled bench onto the road.

(c) Slope Drainage.

The most common method is to drill horizontal drain holes into the slope on 5 to 10 meter centers for distances of at least 10 meters and not more than 0.25 times the slope height. If the holes collapse, perforated plastic pipe should be installed. If ice glaciers develop the drains must be insulated or heated with heating cables. A track mounted percussion unit can be used for rapid installation. The drains are particularly effective in soft rock. A typical drain is shown in Figure 6.



Figure 6: Horizontal drain installed to reduce the water pressure in a rock slope.

(d) Surface Stabilization and Shotcrete.

Concrete can be sprayed on the rock face to increase resistance to raveling, to reduce weathering, and to seal exposed joints. The procedure is particularly applicable to blocky slopes. The rock must be clean and wetted prior to application. A thickness of only 4 to 6 cm. is required for long term stability. Where large blocks exist with joints far apart the shotcrete need not cover the entire surface of the intact rock but need only extend 20 to 25 cm. beyond the cracks. Far more shotcrete than is actually needed is frequently applied by the contractor at considerable unnecessary expense. Frequent drain openings are required so that water pressure does not build up behind the shotcrete. Figure 7 shows a typical portable shotcrete plant and application.

Where the rock is extremely blocky or the zone of weathering is considerable, wire mesh can be pegged to the rock, followed by the application of shotcrete.

(e) Rock Support with Rock Bolts or Cables.

Rocks which provide key support to blocks higher in the slope can be stabilized by the installation of rock bolts. To develop long term stability, they should al-



Figure 7: Portable shotcrete plant (left). Field application to stabilize rock slope (right).

ways be tensioned and fully grouted. The tensioning increases the shear strength along the joint and the grouting resists stress relaxation and minimizes the probability of corrosion. The installation should be designed to develop a specific load capacity. In soft rock, bolts may be used in combination with shotcrete and wire mesh. Figure 8 shows rock bolts being installed.

Where the rock joints dip out of the slope at a moderately steep angle, short steel dowels can be grouted in place in front of the rock face to provide support.

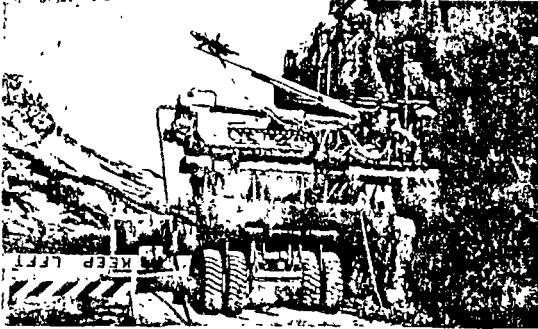


Figure 8: Installation of rock bolts.

(f) Concrete Support Buttresses. Where large blocks of rock overhang a slope or where excavation may undermine a large volume of rock, a concrete buttress can be constructed to provide support. See Figure 9. The buttress must be capable of taking the full load of the rock above. Usually the buttress should be keyed into the rock with steel dowels.



Figure 9: Concrete buttress to support rock.

(g) Special Ditch Design. Highway ditches can often be economically excavated with sufficient depth and a steep roadside slope to catch the majority of the rock which may fall into the ditch. On less important roads, this procedure is reasonable.

(h) Catch Walls. Where it would be expensive to develop deep ditches the construction of catch walls can be effective to control rolling rock. The slope side of the wall must be vertical to reduce the potential of the rock rolling up and over the wall. Concrete walls are rigid and frequently crack and break when hit by large rocks. Gabion walls are more resilient to impact, and less expensive than concrete walls, see Figure 10.



Figure 10: Rock filled gabion wall constructed to catch rolling rock.

(i) Wire Mesh Blankets. Where blocky rock is prevalent in the slope and raveling is a problem, wire mesh draped over the slope can be effective in controlling rockfall, see Figure 11. The blocks roll down behind the wire mesh and drop into the ditch where they are removed with maintenance equipment.



Figure 11: Wire mesh draped over a blocky rock slope.

(j) Rock Sheds. In very rocky mountain areas where rock tends to roll or fall from a considerable height, it may be necessary to construct rock sheds to carry the rock over the highway. Figure 12 shows both concrete and timber sheds.



Figure 12: Concrete and timber rock sheds.

RECORDS OF ROCKFALLS AND SLIDES

In areas where rockfalls occur, records should be maintained which record every serious fall which requires maintenance clean-up. At such time as funds are available to improve stability, the records will show the location where the most frequent and most serious falls occur. Stabilization of these areas can then be developed on a rational priority basis.

REFERENCES

1. HOEK, E. and BRAY, J.W. Rock Slope Engineering. Revised second edition. Published by the Institution of Mining and Metallurgy, London, 1977.
2. LANGEFORS, V. and KIHLMSTROM, B., "The Modern Techniques of Rock Blasting" John Wiley and Sons, 1967.
3. RITCHIE, A.M., "The Evaluation of Rockfall and its Control", Highway Record, Vol. 17, 1963.
4. BRAUNER, C.O., "Rock Slope Stability on Railway Projects", American Railway Engineering Association, Chicago, 1975.
5. BRAUNER, C.O., "Rock Slope Stability in Highway Construction", Canadian Good Roads Assn., 1967.

ESTABILIDAD DE TALUDES EXCAVADOS EN ROCA

Carlos A. Soto

El siguiente artículo ha sido reproducido de la revista técnica MINERALES, publicación oficial del Instituto de Ingenieros de Minas de Chile, Vol. XXX, No. 131, 1975.

El artículo constituye una recopilación de información (ver referencias) acerca de los principios básicos que gobiernan la estabilidad de taludes en roca. Se discuten aspectos económicos y de seguridad, propiedades mecánicas fundamentales de la roca y sus modos clásicos de falla, factores que influyen en la estabilidad, principios de los métodos de estabilización mediante reforzamiento, etc.

El objetivo último de este artículo ha sido discutir brevemente los principios básicos enunciados y, al mismo tiempo, ayudar a definir la naturaleza de aquellos problemas cuyo estudio y solución requiere el uso de servicios especializados.

En esa fecha, el autor ocupaba el cargo de Ingeniero Investigador en el Centro de Investigación Minera y Metalúrgica (C.I.M.M.), en Santiago de Chile. El artículo fue publicado poco después que el autor concluyera sus estudios de post-grado en Mecánica de Rocas en la Escuela Real de Minas (Royal School of Mines), Colegio Imperial de Ciencia y Tecnología (Imperial College of Science and Technology) Londres, bajo la supervisión del Dr. Evert Hoek, quien entonces era Profesor de Mecánica de Rocas en la Universidad de Londres. Desde 1975 a la fecha presente, el Sr. Soto ha mantenido el cargo de Ingeniero de Mecánica de Rocas y Estabilidad en Golder Associates, Vancouver, Canadá. Esta empresa es un grupo internacional de ingenieros consultores geotécnicos y de minas.

I. INTRODUCCION

Durante los últimos años el estudio de los problemas relativos a taludes excavados en roca ha adquirido una progresiva importancia, por la necesidad de excavar taludes de grandes dimensiones requeridos tanto en proyectos de ingeniería de minas como civil (diseño de minas a rajo abierto, carreteras excavadas en roca, etc.).

Enfatizando la incidencia de este campo en la industria minera, es necesario mencionar que sus problemas específicos deben abordarse tratando de compatibilizar dos requerimientos conflictivos: costo mínimo de extracción de mineral, y seguridad razonable en la operación de la mina. En efecto, grandes sumas de dinero pueden ahorrarse aumentando el ángulo de un talud al disminuir la cantidad de material estéril extraído para obtener una cierta cantidad de mineral, pero si el ángulo es excesivo puede inducirse una falla o derrumbe con pérdidas considerables de vidas y equipos comprometiendo la operación futura de una mina.

Un diseño de talud óptimo será entonces un compromiso entre un talud suficientemente abrupto como para ser aceptable en lo económico, y uno cuyo ángulo es lo suficientemente pequeño como para ser seguro.

Actualmente para hacer económicamente factible una operación minera a rajo abierto es ineludible sacrificar una parte de la seguridad máxima en favor del beneficio económico. Determinar en qué medida esto puede hacerse es una cuestión tan importante como difícil.

Otro aspecto que complica el problema proviene de reconocer que la masa rocosa involucrada en cada talud es única, y por lo tanto no existen soluciones de rutina que garanticen la respuesta adecuada en todos los casos. Así, la solución de un problema práctico individual debe construirse a partir de la información específica acerca de la geología del lugar, resistencia de la masa rocosa, observaciones sobre el agua subterránea, y una buena dosis de sentido común de ingeniería. La proporción en que se mezclan estos ingredientes varía según el caso, tal como también lo hace el tipo de herramienta o técnica disponible para construir una solución.

*Investigador del Centro de Investigación Minera y Metalúrgica (CIMM).

II. CONSIDERACIONES ECONOMICAS Y DE PLANIFICACION

La influencia que ejerce el ángulo del talud en el diseño y economía de una mina a rajo abierto resulta obvia. Ahora bien, dado que los beneficios económicos obtenidos al diseñar un talud relativamente abrupto pueden ser anulados por las pérdidas causadas por un gran derrumbe o deslizamiento del talud, una evaluación de la estabilidad de los taludes finales de la mina es de importancia fundamental en la planificación de la operación.

Sin embargo el ángulo de los taludes finales no es lo único importante desde un punto de vista económico: también es posible obtener grandes beneficios por medio de taludes abruptos en las fases iniciales de la explotación.

Por otra parte, debe reconocerse que la estabilidad no es lo único que determina los ángulos de talud óptimos a usar en un caso práctico. Así, por ejemplo, influyen las características de los grandes equipos mineros que no pueden ser operados en bermas demasiado angostas. Además, la pendiente de los caminos de transporte debe mantenerse dentro de ciertos límites determinados por las condiciones de operación óptimas de camiones y trenes, lo que generalmente conduce a la necesidad de diseñar taludes de ángulo menor.

Dentro del problema global de considerar la estabilidad del talud como un todo no debe perderse de vista el otro problema, de menor alcance físico pero no menos importante, como es el de la estabilidad de bancos individuales. Esto es fundamental desde el punto de vista de la operación diaria. Así por ejemplo, un derrumbe en un banco por el cual pasa la principal vía de transporte o en el cual se encuentra una instalación importante, producirá serios tropiezos en el programa de explotación. Estos problemas relativamente pequeños, que ocurren con escasa o ninguna advertencia, ciertamente que también pueden producir pérdidas de vidas y daño a los equipos.

III. PRINCIPIOS BASICOS EN LA FALLA DE TALUDES

En el diseño óptimo de taludes excavados en roca se intenta determinar el ángulo de talud más apropiado como función de la altura del mismo. Para hacer esto, es necesario asumir un modo de comportamiento de la masa rocosa. Una gran

parte del trabajo de investigación en este campo se ha hecho postulando que la masa rocosa se comporta como un medio elástico continuo. Sin embargo, al tratar de obtener resultados prácticos este enfoque tiene grandes limitaciones, principalmente debido a que nuestro conocimiento de las propiedades mecánicas de las masas rocosas es todavía muy limitado.

Mucho más realista entonces resulta el enfoque contrario, que considera que, en términos generales el comportamiento de una masa rocosa está dominado por discontinuidades: planos de fallas, fracturas, planos de estratificación, etc. La masa rocosa es así un medio discontinuo, cuyas propiedades mecánicas revelan una resistencia considerablemente menor que la de la roca intacta o sana. Este enfoque es el más utilizado en el diseño práctico de taludes excavados en roca.

Debe destacarse, sin embargo, la importancia que la mecánica del medio continuo ha tenido en la investigación. Por ejemplo, de desplazamientos globales de la masa rocosa, o en esquemas de flujo del agua subterránea, en donde se pueden aplicar ciertos métodos numéricos tales como la técnica de elementos finitos.

1 Relación entre la altura máxima y el ángulo de un talud

Aun cuando la estabilidad de una masa rocosa puede estar enteramente dominada por discontinuidades geológicas, también hay situaciones en que la orientación e inclinación de estas discontinuidades es tal que un deslizamiento simple de bloques, tajadas o cuñas no es posible. El proceso de falla o derrumbe de tales taludes consistiría entonces en una combinación entre el movimiento según esas discontinuidades, y la falla del material intacto o roca sana.

En tales casos, es posible esperar que taludes más altos y abruptos que los de una situación promedio puedan ser estables. De hecho esto ha sido confirmado de manera general por la evidencia práctica recogida en un gran número de minas a rajo abierto.

Esto puede ilustrarse en el gráfico de la Fig. 1, que muestra una relación típica (obviamente no exacta para cada caso) entre la altura máxima y el ángulo de taludes en "roca dura", que para tales condiciones aun son estables (según Kley y Luiton¹, y Ross-Brown²).

2 El rol de las discontinuidades en los procesos de falla

La inclinación de las superficies de discontinuidad en las cuales puede ocurrir un deslizamiento puede llegar a tener una influencia dramática en la estabilidad de un determinado talud. Esta situación se ilustra en la Fig. 2, que muestra la variación

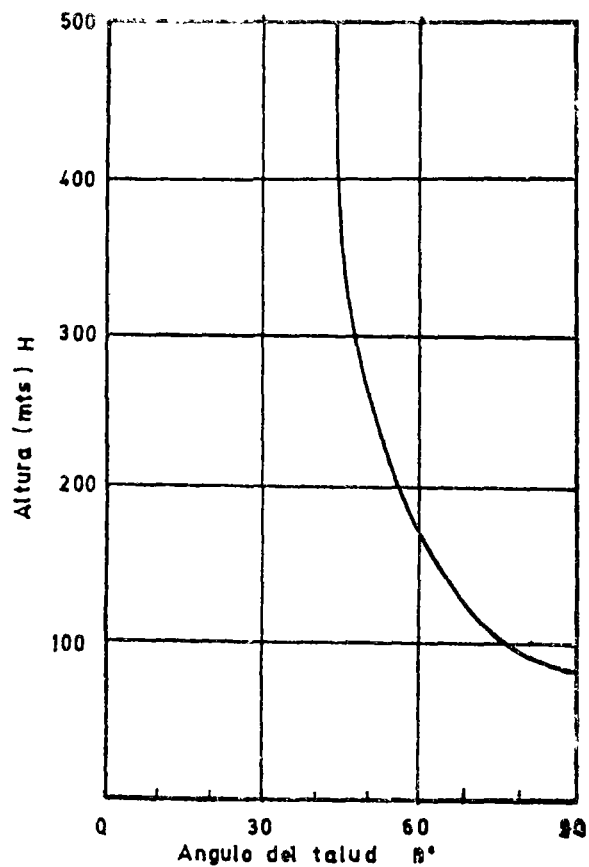


Figura 1

de la altura crítica de un talud vertical en función del ángulo de inclinación de una discontinuidad plana, para taludes secos y saturados según datos de Hoek^{3, 5}.

Este gráfico muestra que, por ejemplo, cuando la inclinación de la discontinuidad es de 50° con respecto a la horizontal en ambas curvas la altura crítica de un talud disminuye a aproximadamente la cuarta parte de la altura crítica del caso en que la discontinuidad es vertical u horizontal. La detección de estos rasgos geológicos es entonces de fundamental importancia en los estudios de estabilidad. La Fig. 2 es válida sólo para un caso específico; ella depende de los parámetros de resistencia en la discontinuidad, y de la densidad de la roca.

3 Propiedades mecánicas fundamentales

Las propiedades mecánicas más importantes en relación al análisis de la estabilidad de taludes son el ángulo de fricción, la cohesión y la densidad de las masas rocosas.

Para la definición de fricción y cohesión podemos recurrir a la Fig. 3, que ilustra la variación de la resistencia al cizalle o corte τ , con la fatiga normal σ . τ es entonces la fuerza por unidad de

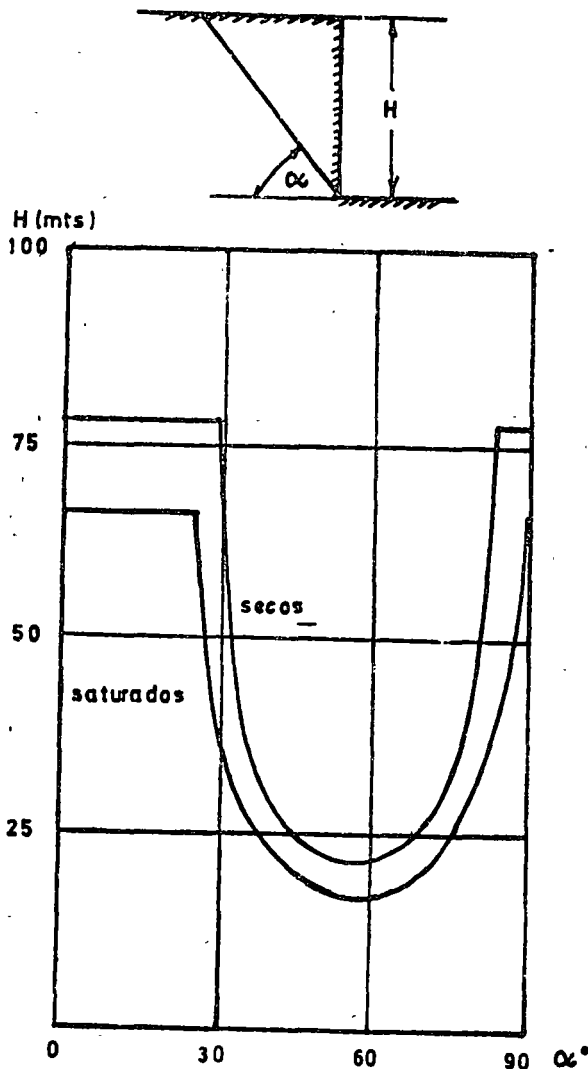


Figura 2

área requerida para producir el deslizamiento a lo largo de una discontinuidad en presencia de σ (fuerza normal por unidad de área), según se muestra en la misma figura.

Este gráfico es sólo una relación aproximada, dado que en la mayoría de los casos prácticos la dependencia que aquí se ilustra como lineal es más bien curva. La pendiente de esta línea es el ángulo de fricción ϕ , mientras que la cohesión τ es el valor de la resistencia de cizalle cuando la fatiga normal σ es nula. Este es el caso, por ejemplo, cuando la superficie de discontinuidad se encuentra cementada, en donde se requiere un τ finito con $\sigma = 0$ para producir deslizamiento.

En consecuencia, la relación entre τ y σ está dada por:

$$\tau = c + \sigma \operatorname{tg} \phi \quad [1]$$

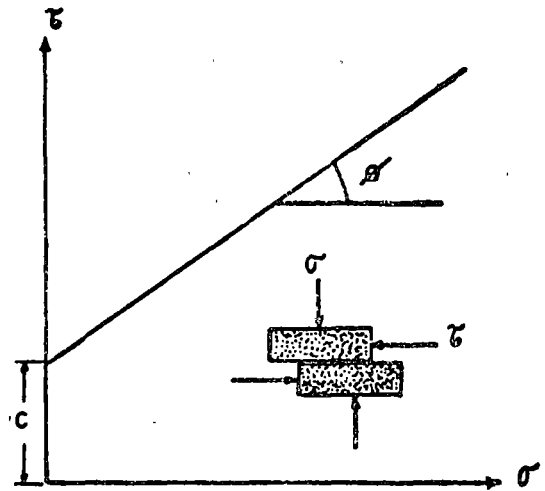


Figura 3

4. Deslizamiento debido a carga gravitacional

En orden a ilustrar el mecanismo de deslizamiento simple consideramos un bloque de peso W que descansa en una superficie inclinada de ángulo α con respecto a la horizontal según la Fig. 4.

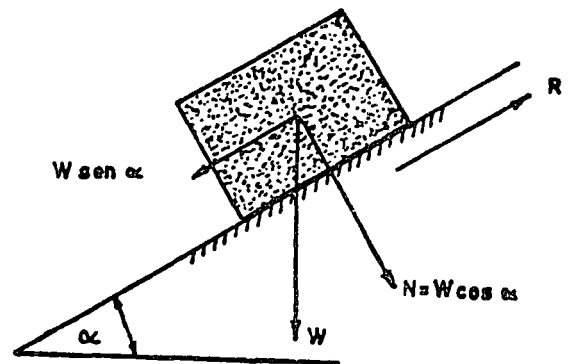


Figura 4

La fatiga normal, esto es la fuerza por unidad de área que actúa en forma perpendicular a la superficie de deslizamiento, está dada por:

$$\sigma = \frac{N}{A} = \frac{W \cos \alpha}{A} \quad [2]$$

donde A es el área basal del bloque.

La resistencia al cizalle o corte será entonces, de [1] y [2]:

$$\tau = c + \frac{W \cos \alpha}{A} \operatorname{tg} \phi \quad [3]$$

y la fuerza resistente que se opone al deslizamiento está dada por :

$$R = \tau A = c A + W \cos \alpha \operatorname{tg} \phi \quad [4]$$

Cuando el bloque se encuentre a punto de empezar a deslizar, decimos que se ha alcanzado la condición de "Equilibrio Límite". En dicha condición, la fuerza perturbadora (que induce el deslizamiento) es igual a la fuerza resistente, o

$$W \operatorname{sen} \alpha = c A + W \cos \alpha \operatorname{tg} \phi \quad [5]$$

Si la cohesión c es nula, la condición de equilibrio límite se transforma en:

$$\alpha = \phi \quad [6]$$

5. Presión de poros y fatiga efectiva

Dependiendo de una serie de factores tales como el régimen del escurrimiento de aguas superficiales y napas subterráneas, los poros o cavidades existentes entre los granos de un determinado material que pueden contener agua a presión. Esta presión de agua, μ , llamada también presión intersticial o de poros, actúa en todas direcciones. En particular lo hace en dirección contraria a la fatiga normal actuante entre las caras opuestas de una cavidad o una discontinuidad en la masa rocosa.

Esta última situación se indica de manera esquemática en la Fig. 5, que muestra el efecto de la presión de agua μ en una muestra de roca que es sometida a cizalle, según una superficie de falla.

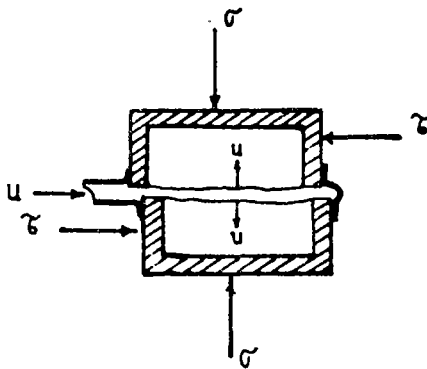


Figura 5

La fatiga normal σ (fatiga total) que actúa en la superficie de falla se reduce a la fatiga efectiva $(\sigma - \mu)$, que es la que efectivamente actúa normal a la superficie. En consecuencia, la relación [1] se transforma en:

$$\tau = c + (\sigma - \mu) \operatorname{tg} \phi \quad [7]$$

Vemos entonces que la presencia de μ produce una disminución de la resistencia al deslizamiento. En relación al ángulo de fricción ϕ y la cohesión c debe notarse que:

— En la mayoría de las rocas duras, así como en muchos suelos arenosos y gravas, c y ϕ no cambian con la presión de agua μ ; la disminución de resistencia al cizalle τ se debe casi enteramente a μ (disminución de la fatiga normal de σ a $\sigma - \mu$). En consecuencia, lo fundamental es la presión de agua μ , y no el contenido de agua o humedad.

— En rocas blandas y arcillas, c y ϕ a su vez varían con el contenido de agua lo cual, además del efecto directo de μ , produce una disminución adicional en la resistencia τ .

6. Efecto de la presión de agua en una grieta de tensión

Podemos estudiar este problema utilizando el mismo análisis elemental del caso de un bloque que descansa en un plano inclinado, según la Fig. 6. Este bloque se encuentra separado de la masa rocosa mediante una grieta de tensión, que a su vez está llena de agua.

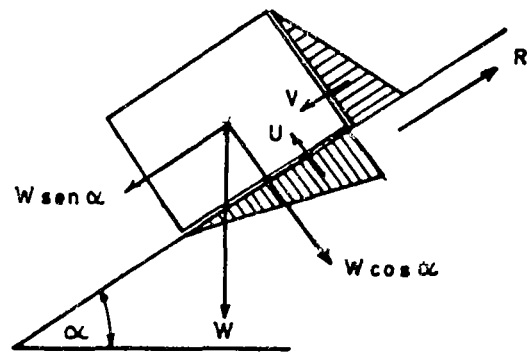


Figura 6

La presión de agua dentro de la grieta de tensión aumenta linealmente con la profundidad. En otras palabras, es una distribución hidrostática de presiones, tal como se indica en la figura anterior. Si como es una hipótesis habitual, la presión hidrostática del fondo de la grieta puede transmitirse hacia la base del bloque, dicha presión se disipa a su vez a lo largo del plano inclinado hasta anularse en contacto con la presión atmosférica. En la base del bloque tenemos entonces una nueva distribución lineal de presiones de agua.

Las fuerzas totales resultantes de estas dos distribuciones de presiones son U y V , como se indica en la Fig. 6. La condición de equilibrio límite puede escribirse en este caso:

$$W \operatorname{sen} \alpha + V = c A + (W \cos \alpha - U) \operatorname{tg} \phi \quad [8]$$

Ambas fuerzas, U y V , reducen la estabilidad,

puesto que U disminuye la fuerza resistente y V aumenta la fuerza perturbadora que induce al deslizamiento.

7. Estabilización mediante reforzamiento

Uno de los métodos artificiales más efectivos para estabilizar bloques o cuñas localizados sobre discontinuidades de deslizamiento potencial es el uso de pernos o cables de anclaje tensionados.

Continuando con la mecánica elemental de deslizamiento de un bloque, consideremos el efecto que sobre él ejerce un perno de anclaje cuya dirección hace un ángulo β con respecto al plano de eventual deslizamiento, tal como se esquematiza en la Fig. 7.

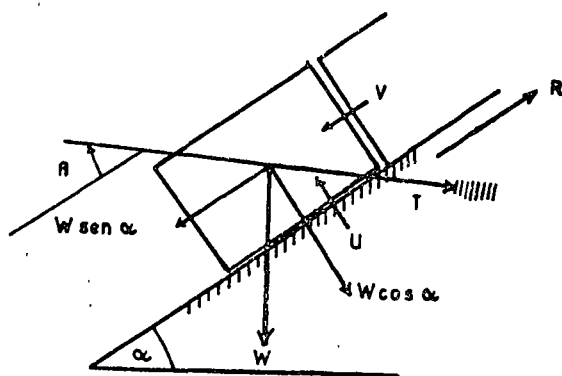


Figura 7

El perno de anclaje ha sido tensado hasta aplicar una fuerza T , y asumimos que las fuerzas U y V previamente discutidas también están presentes. La condición de equilibrio límite se escribe entonces:

$$W \sin \alpha + V - T \cos \beta = cA + (W \cos \alpha - U + T \sin \beta) \tan \phi \quad [9]$$

En consecuencia, la tensión aplicada por el perno produce un doble beneficio: reduce la fuerza perturbadora en $T \cos \beta$ y al mismo tiempo aumenta la fuerza resistente en $T \sin \beta \tan \phi$.

La orientación óptima del perno de anclaje, β , será aquella que requiere una tensión T mínima. Derivando la ecuación [9] con respecto a β se encuentra que:

$$\beta \text{ óptimo} = \phi \quad [10]$$

8. El factor de seguridad

Todo el análisis previo de estabilidad se ha basado en la condición de equilibrio límite. Esto sugiere la necesidad de definir un índice o factor que entregue una idea de la estabilidad de un talud bajo otras condiciones, además de la defi-

nida como equilibrio límite. Puede definirse así un factor de seguridad, F , como la razón entre la fuerza total que se opone al deslizamiento (resistente) y la fuerza total que lo induce (perturbadora).

En el caso del bloque ilustrado en la Fig. 7, sometido a las fuerzas W , U , V y T , el factor de seguridad será:

$$F = \frac{cA + (W \cos \alpha - U + T \sin \beta) \tan \phi}{W \sin \alpha + V - T \cos \beta} \quad [11]$$

La condición de equilibrio límite está representada entonces por $F = 1$ y teóricamente cualquier talud cuyo factor de seguridad sea mayor que la unidad será estable. Esto plantea problemas vitales que se discuten brevemente a continuación.

Una primera cuestión fundamental es determinar qué valor de F puede considerarse aceptable en un caso práctico. Dada la incertidumbre que hay, primero en la elección de un modelo para representar un proceso físico (por ejemplo, el deslizamiento simple de nuestro bloque), y segundo en la información entregada al modelo (ángulo de fricción, cohesión, densidad, etc.), debe reconocerse que el valor calculado para F no tiene un sentido absoluto.

Por esta razón, muchos autores, McMahon⁴, entre otros, han sugerido la necesidad de un enfoque probabilístico para evaluar la seguridad de un talud en base a la variación de cada uno de los parámetros que controlan la estabilidad. Sin embargo, esto está aún lejos de ser una operación rutinaria, principalmente debido a las dificultades para obtener una información completa que permita efectuar un análisis estadístico consistente para todos los parámetros involucrados.

Lo más adecuado es, por ahora, efectuar un análisis de sensibilidad para detectar la influencia de cada variable sobre la estabilidad del talud, a partir de un amplio rango de condiciones. Esto permite obtener, no factores de valor absoluto, sino que relativos y con precisión razonable. Tal información, junto a una dosis de buen sentido, generalmente permiten efectuar un diseño adecuado y con significado práctico.

9. Falla rotacional o de volteo

El factor de seguridad que se ha discutido recién tiene como limitación estar basado en la falla por deslizamiento del bloque solamente y no considera por tanto la falla por rotación o volteo. La condición elemental para este último modo de falla, en el caso de un bloque que descansa sobre un plano inclinado, se muestra en la Fig. 8.

El bloque caerá por volteo cuando la inclinación del plano, α , sea tal que el vector peso del

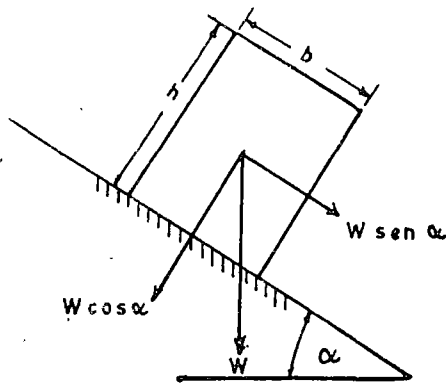


Figura 8

bloque, W , pase por fuera de la base del mismo. Esto ocurre cuando:

$$\operatorname{tg} \alpha > \frac{b}{h} \quad [12]$$

Considerando la influencia que este modo de falla idealizado puede tener en problemas reales, lo que de hecho ocurre es una falla por volteo de estructuras columnares que se hayan formado debido a una particular geología estructural. El comportamiento real es sin duda mucho más complejo, incluyendo desplazamientos en cualquier discontinuidad y acomodación de bloques.

El uso de cables o pernos de anclaje también es muy adecuado para reforzar taludes en este tipo de terrenos, uniendo mediante ello varias columnas para producir unidades estructurales de mayores dimensiones, que pueden ser más estables.

IV. FALLA SEGUN UNA DISCONTINUIDAD PLANA

La falla según un plano de discontinuidad es un fenómeno de ocurrencia relativamente raro en taludes excavados en roca debido a que sólo en ciertas ocasiones se cumplen todas las condiciones geométricas requeridas para tal modo de falla. Según se verá en la próxima sección, la falla tipo cuña es un caso más general, cuyo análisis admitiría a la falla plana como un caso especial.

Sin embargo, no se debe desconocer que la falla plana ocurre en ocasiones, especialmente cuando existe un control preponderante por parte de una discontinuidad estructural. Además, este tipo de análisis es particularmente útil para demostrar la sensibilidad del talud ante cambios en la resistencia al cizalle o en las condiciones del agua subterránea. Dicha sensibilidad no es obvia, ni mucho menos, en otros tipos de análisis más complejos.

1. Condiciones geométricas

Las siguientes condiciones deben cumplirse para

que el deslizamiento ocurra según un plano individual:

- El plano de deslizamiento debe tener un rumbo paralelo, o dentro de $\pm 20^\circ$, con respecto al de la cara del talud;
- El plano de deslizamiento debe asomar en la cara del talud, es decir su buzamiento o inclinación debe ser menor que el ángulo del talud. En la Fig. 9, esta condición se expresa como $\alpha < \beta$;

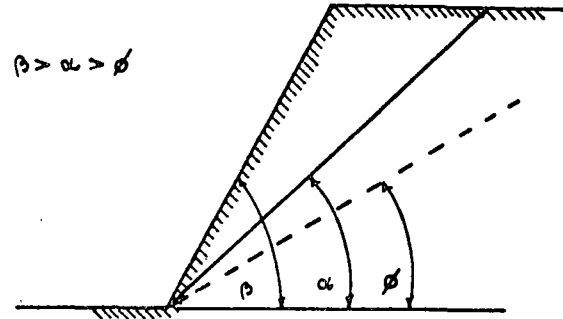


Figura 9

- La inclinación del plano de falla debe ser mayor que el ángulo de fricción en ese plano, esto es $\alpha > \phi$, en Fig. 9. Comparar con la condición de equilibrio límite en ausencia de cohesión, $\alpha = \phi$, según ecuación [6]. En definitiva entonces, se requiere $\beta > \alpha > \phi$, y
- Para que el plano de deslizamiento no tenga una extensión ilimitada, debe haber superficies de desprendimiento laterales cuya resistencia al deslizamiento sea despreciable, las que se indican en la Fig. 10. Tales superficies no se requieren en el caso de la "nariz" de un talud, donde un plano de falla tendría una extensión finita.

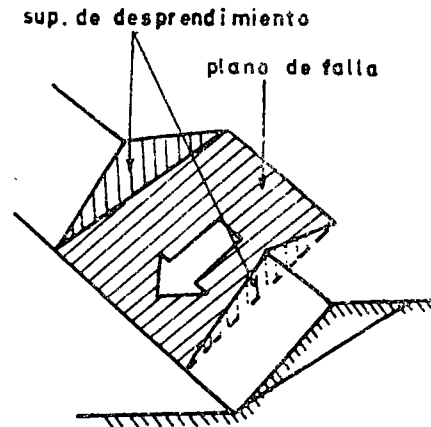


Figura 10

2. Postulados del análisis

Con relación a la Fig. 11, el análisis de la falla plana de un talud se efectúa asumiendo lo siguiente:

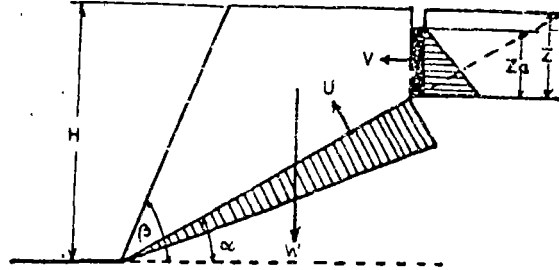


Figura 11

- Existe una grieta de tensión de profundidad Z en la superficie superior del talud, cuyo rumbo es paralelo al de la cara del talud;
- La grieta de tensión es vertical, y está llena de agua en una profundidad Z_a ;
- El agua entra a la superficie de deslizamiento por el fondo de la grieta de tensión y escurre escapando a presión atmosférica en la cara del talud. Las distribuciones de presión se indican en la misma Fig. 11;
- Todas las fuerzas presentes (W , U , V) actúan a través del centro de gravedad de la masa que desliza, es decir, no hay momentos que tiendan a producir rotación;
- La resistencia al cizalle en la superficie de deslizamiento se define en términos de cohesión y fricción, según la ecuación [1], esto es: $\tau = c + \sigma \operatorname{tg} \phi$, y
- El análisis es bidimensional, es decir, se aplica a una tajada del talud de grosor unitario.

El factor de seguridad de este talud se define en forma similar a la deducción de la ecuación [11], excepto que T no está presente y V es ahora horizontal, puesto que la grieta de tensión es vertical. Es decir,

$$F = \frac{cA + (W \cos \alpha - U - V \sin \alpha) \operatorname{tg} \phi}{W \sin \alpha + V \cos \alpha} \quad [13]$$

En este caso, A es el área de la superficie de deslizamiento. En 2 dimensiones es la longitud desde el fondo de la grieta al pie del talud, según Fig. 11. El peso de la masa deslizante es W . A y W se calculan a partir de la geometría indicada y la densidad de la masa rocosa. Además, la fuerza total ejercida por una distribución de presión de agua es igual al área de la distribución (triángulos), obteniéndose:

$$V = \frac{1}{2} \gamma_a Z_a^2 \quad [14]$$

$$U = \frac{1}{2} \gamma_a Z_a A \quad [15]$$

donde γ_a es la densidad del agua.

El factor de seguridad recién definido puede aplicarse a diversos casos particulares, ya sea en que U , V , o c estén ausentes. Para el caso de un talud seco sostenido por fricción solamente, la ecuación [13] da:

$$F = \frac{\operatorname{tg} \phi}{\operatorname{tg} \alpha} \quad [16]$$

expresión que es consistente con la condición de equilibrio límite, ecuación [6], en nuestro previo análisis elemental de un bloque.

V. FALLA TIPO CUÑA

Este tipo de falla, más frecuente que la anterior, se puede originar cuando existe al menos 2 planos de discontinuidad preponderantes que al intersectarse producen una cuña que puede deslizarse hacia afuera del talud, como lo indica la Fig. 12. Este es el caso cuando los planos de discontinuidad tienen rumbos bastante diferentes (fuera de $\pm 20^\circ$) al de la cara del talud.

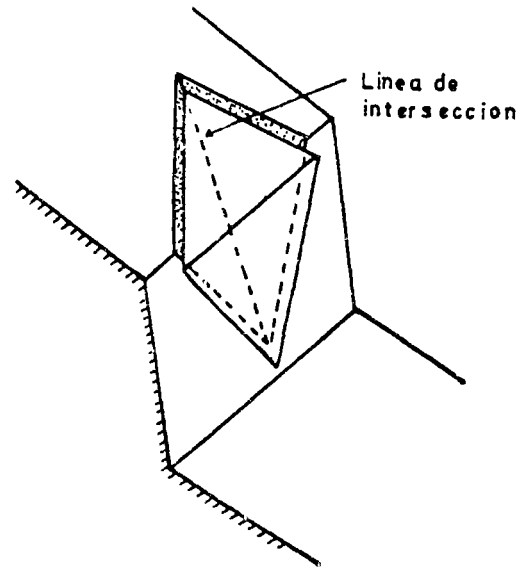


Figura 12

En el análisis [5] simple que sigue asumimos que el ángulo de fricción es el mismo en ambos planos, y que no hay cohesión (una hipótesis conservadora). La Fig. 13a muestra una sección vertical que pasa por la línea de intersección de ambos planos. La condición requerida para que el deslizamiento ocurra es:

$$\beta_1 > \alpha_1 > \phi \quad [17]$$

en donde β_i y α_i son el ángulo del talud y la inclinación de la línea de intersección medidos en esa particular sección, y ϕ es el ángulo de fricción. Nótese la semejanza entre la expresión [17] y la condición para falla plana discutida en la sección IV-1. En la misma figura se indican las componentes del peso W en direcciones normal y paralela a la línea de intersección.

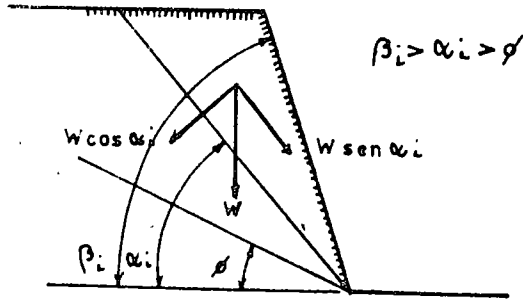


Figura 13 a

Considerando una sección perpendicular a la línea de intersección de ambos planos, Fig. 13b, podemos calcular el factor de seguridad en función de las fuerzas o reacciones normales a cada plano, R_A y R_B , y la fuerza $W \cos \alpha_i$, esto es:

$$F = \frac{(R_A + R_B) \operatorname{tg} \phi}{W \cos \alpha_i} \quad [18]$$

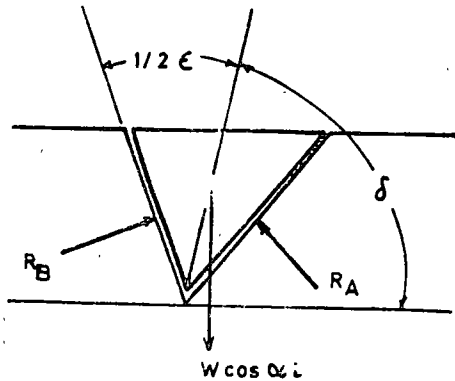


Figura 13 b

Debemos obtener entonces R_A y R_B en función de W y la geometría de la cuña (ángulo de volteo δ y ángulo de la cuña ϵ).

Resolviendo para las fuerzas horizontales se tiene:

$$\begin{aligned} R_A \operatorname{sen}(\delta - \frac{1}{2} \epsilon) &= R_B \operatorname{sen} [180 - (\delta + \frac{1}{2} \epsilon)] \\ &= R_B \operatorname{sen} (\delta + \frac{1}{2} \epsilon) \end{aligned} \quad [19]$$

y para las fuerzas verticales:

$$R_A \cos(\delta - \frac{1}{2} \epsilon) - R_B \cos(\delta + \frac{1}{2} \epsilon) = W \cos \alpha_i \quad [20]$$

de donde:

$$R_A + R_B = \frac{W \cos \alpha_i \operatorname{sen} \delta}{\operatorname{sen} \frac{1}{2} \epsilon} \quad [21]$$

y finalmente:

$$F = \frac{\operatorname{sen} \delta}{\operatorname{sen} \frac{1}{2} \epsilon} \cdot \frac{\operatorname{tg} \phi}{\operatorname{tg} \alpha_i} \quad [22]$$

Comparando esta expresión con [16], vemos que ella es de la forma:

$$F_c = K \cdot F_p \quad [23]$$

donde F_c es el factor de seguridad de la cuña, F_p el de una eventual falla plana de un talud cuyo ángulo es β_i , y en que la discontinuidad tiene un buzamiento o manteo α_i . El coeficiente K es en general mayor que la unidad, puesto que de la Figura 13b vemos que $\delta > \frac{1}{2} \epsilon$. Es decir, $F_c > F_p$, y así el efecto de cuña ha aumentado el factor de seguridad comparado con esa hipotética falla plana.

Las expresiones [22] y [23] muestran además que la falla plana puede considerarse como un caso particular de la falla de una cuña. En efecto, la falla plana puede describirse como la de una cuña cuyos dos planos coinciden, esto es: $\epsilon = 180^\circ$. Si además $\delta = \frac{1}{2} \epsilon = 90^\circ$, entonces $K = 1$, y $F_c = F_p$.

Por último, debe mencionarse que los ángulos δ y ϵ se determinan mediante proyección estereográfica, una descripción de lo cual cae fuera del alcance de este artículo. Autores como Phillips⁶, presentan un excelente tratamiento de tales técnicas. Existen abacos⁷ para determinar el coeficiente K que facilitan el cálculo iterativo y cartas de diseño simple muy expeditas.

El modelo presentado aquí es simple y particular, para ilustrar los principios básicos, pero la presente edición de MINERALES contiene otro artículo que presenta una técnica más general y sofisticada para el análisis de cuñas.

VI. FALLA CIRCULAR:

Los taludes excavados en roca son susceptibles de experimentar, principalmente, procesos de falla de los tipos previamente discutidos, con un fuerte control de la geología estructural. Sin embargo, existen otros problemas en el área minera que involucran la presencia de materiales menos resistentes, tales como suelos de sobrecarga y botaderos de lastre, en donde no existen estructuras dominantes, y la superficie de falla busca libremente el camino de menor resistencia a través del talud.

Se ha observado que en tales circunstancias la superficie de falla se acerca a una forma circular, según la práctica aceptada en Mecánica de Suelos

aplicada a taludes. En este campo hay una muy completa literatura disponible (Terzaghi⁷, Bishop⁸, etc), a la cual debería dirigirse el lector interesado. Baste señalar aquí que tal comportamiento puede encontrarse en la roca fragmentada que forma un botadero de lastre o de ripios, suelos de sobrecarga en un talud, o incluso en ciertos taludes excavados en roca altamente alterada o meteorizada que hayan perdido un control estructural definido.

VII. OBSERVACIONES FINALES:

En un campo tan amplio como son los taludes excavados en roca, el propósito de este trabajo ha sido plantear los principios fundamentales que rigen su comportamiento mediante modelos simples y elementales. Estos permiten ilustrar la influencia de los principales parámetros en la estabilidad de un talud, la cual resulta mucho menos obvia en los análisis más complejos.

El factor de seguridad, F , debe utilizarse de preferencia para estudios de sensibilidad, como se ha mencionado. El problema de definir un valor aceptable de F para que un talud sea estable, por ejemplo entre 1.3 a 2.0, es función de la confianza que inspiran el modelo de análisis utilizado y la información que se le entrega. Cuando después de un análisis simple persiste una considerable duda, lo más razonable será recurrir a

técnicas más complejas y/o a los servicios especializados que puedan estar disponibles.

REFERENCIAS

1. Kley, R. J. y Lutton, R. J. Engineering properties of nuclear craters: a study of selected rock excavations as related to large nuclear craters. Report us Army Engineers, Nº PNE 5010, 1967.
2. Ross-Brown, D. R. Slope design in open cast mines. Ph. D. Thesis, London University.
3. Hoek, E., The influence of structure upon the stability of rock slopes. Proc. 1st Symposium on Stability in Open Pit Mining, Vancouver 1970. AIME, New York, 1971, págs. 49-63.
4. McMahon, B. K., A statistical method for the design of rock slopes. Proc. 1st Australia-New Zealand Conference of Geomechanics, Melbourne, August 1971.
5. Hoek, E. y Bray, J. W., Rock Slope Engineering. The Institution of Mining and Metallurgy, London 1974.
6. Phillips, F. C., The use of stereographic projections in structural geology. Edward Arnold, London. Third edition (paperback) 1971.
7. Terzaghi, K., Theoretical Soil Mechanics. Wiley, New York, 1943.
8. Bishop, A. W., The use of the slip circle in the stability analysis of earth slopes, Geotechnique, Vol. 5, 1955.

